# Investigations into the Generation and Pleiotropic Reactivity Modes of the Nitrile Imine 1,3-Dipole

**Keith Livingstone**

**June 2020**

# Investigations into the Generation and Pleiotropic Reactivity Modes of the Nitrile Imine 1,3-Dipole
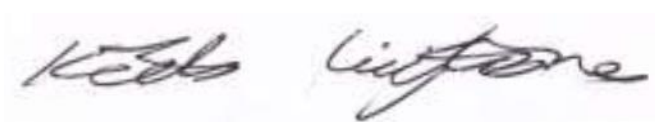
Keith Livingstone

April 2020

A report submitted to the Department of Pure and Applied Chemistry, University of Strathclyde, Glasgow, in fulfilment of the requirements for the degree of Doctor of Philosophy.

I certify that this report has been written by myself. Any help I have received in my research work and the preparation of the report itself has been acknowledged. In addition, I certify that all information sources and literature used are indicated in the report.

This thesis is a result of the author's original research. It has been composed by the author and has not been previously submitted for examination which has led to the award of a degree.

Signed:

Keith Livingstone

June 2020

# Abstract

The nitrile imine 1,3-dipole is a versatile intermediate with a diverse range of applications from chemical biology to materials chemistry. In the 60 years since its initial discovery, this system has been found to undergo 1,3-dipolar cycloaddition with numerous dipolarophiles, while also engaging with various conventional heteroatomic nucleophiles through an electrophilic addition mechanism. This pleiotropic reactivity profile makes the nitrile imine an especially unique motif within 1,3-dipole chemistry.

The research detailed within this thesis relates to the manipulation of the nitrile imine 1,3-dipole and its role in the discovery of novel chemical transformations and works towards methods of harnessing its complex reactivity profile with the ultimate goal of improving the understanding of the species in its continued application within ligation chemistry. As an initial investigation, a novel approach towards the popular 2,5-tetrazole nitrile imine precursor was developed. Employing robust Suzuki-hydrogenation methodology previously established within our laboratory, this protocol demonstrates a facile means of accessing a broad palette of 2,5-diaryl tetrazoles for application as a source of nitrile imines (*Scheme 0.1*).
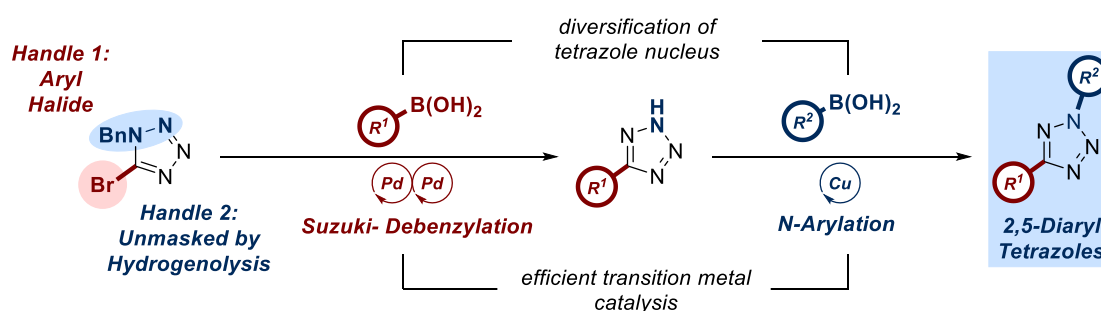
*Scheme 0.1: The development of a novel route towards 2,5-diaryltetrazoles employing Suzuki-debenzylation methodology*

With efficient access to the 1,3-dipole demonstrated, the extensive reactivity of the nitrile imine was investigated through its combination with arylboronic acids. Drawing mechanistic inspiration from the Petasis-Mannich reaction, a novel and metal-free approach towards C-C bond formation was developed, forming an array of aryl ketone hydrazone compounds (*Scheme 0.2*). The scope of the procedure was further expanded through the introduction of hydrazonyl chlorides as an alternative source of the nitrile imine. Exemplification of the transformation was accomplished through the metal-free synthesis of hypolipidemic agent fenofibrate, the adaption of the methodology to incorporate the nitrile oxide 1,3-dipole, and the integration of 2,5-tetrazole photolysis within a flow-chemistry manifold.
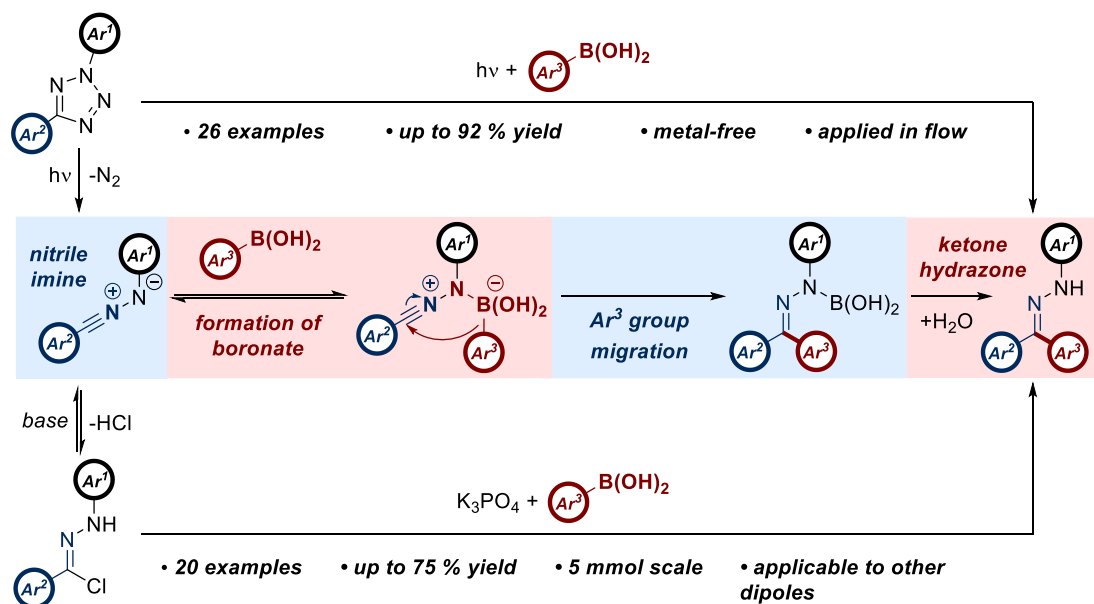
*Scheme 0.2: The development of a metal-free C-C bond-formation through the combination of nitrile imines and arylboronic acids*

Finally, following extensive experience with the promiscuous reaction profile of nitrile imines, a series of competition experiments were undertaken to develop a comprehensive guide to the relative reactivity of the pleiotropic dipole (*Scheme 0.3*). The study investigated numerous potential substrates, spanning a selection of biomolecular residues, potent nucleophiles and bespoke dipolarophiles. Particular attention was paid to common NI bioorthogonal ligation agents that have been previously reported. Based on this, a definitive roadmap of NI reactivity was developed towards the more informed application of the versatile dipole within the field of chemical biology.
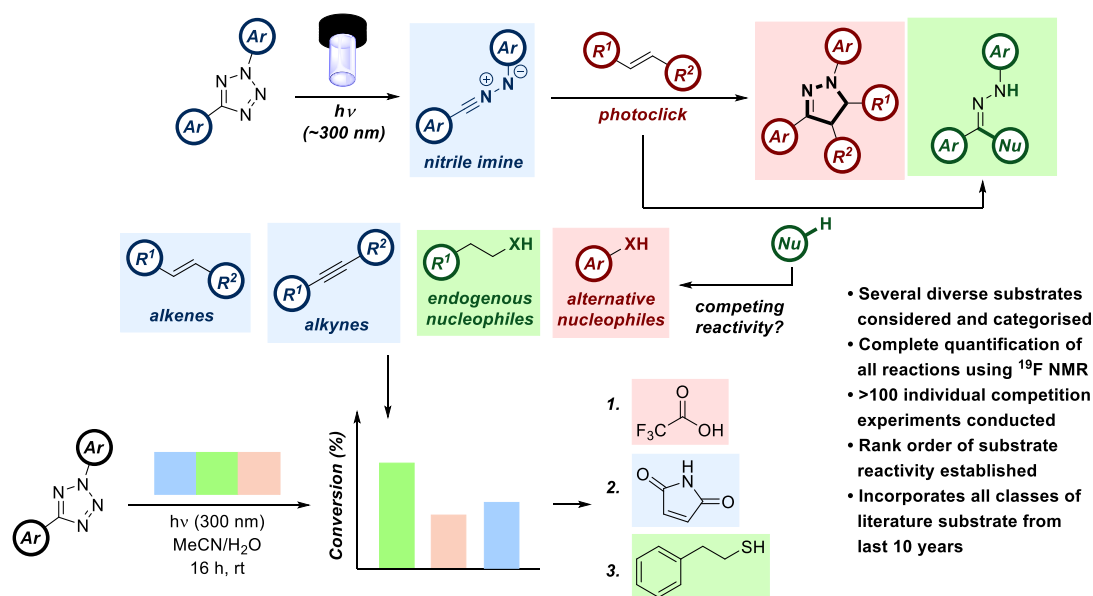


*Scheme 0.3: Quantitative investigations into the reactivity profile of the nitrile imine 1,3-dipole*

# Preface

Some of the original research conducted as part of this thesis has been published. The sections involved and their corresponding publications are listed below.

Chapter 1.   C. Jamieson and K. Livingstone, *The Nitrile Imine 1,3-Dipole*, Springer, Cham, 2020.

Chapter 2.   K. Livingstone, S. Bertrand and C. Jamieson, *J. Org. Chem.*, 2020, **85**, 7413–7423.

Chapter 3.   K. Livingstone, S. Bertrand, J. Mowat and C. Jamieson, *Chem. Sci.*, 2019, **10**, 10412–10416; K. Livingstone, S. Bertrand, A. R. Kennedy and C. Jamieson, *Chem. Eur. J.*, 2020, **26**, 10591–10597.

# Acknowledgements

First and foremost, I would like to thank my supervisor Dr. Craig Jamieson for his invaluable input, guidance and advice throughout my PhD and all the years before that. Thank you for meeting me on that very snowy January afternoon in 2013, it's been quite a journey since then!

I also wish to acknowledge all of the people I have had the opportunity to share a lab with over the past 4 years. Firstly, to Emma, Frankie, Mathias, Adam, Kirsty M, Kirsty W, Jen C, Meghan and Jenna- you all made the CJAM group a great place to be, and it was pleasure to have been able to spend the time with you all. To Mo and Nicola, thank you for all your patience and helpfulness when I was a clueless summer placement student asking a question every minute. I have never learned as much about lab life as I did from both of you over those few months. To Peter, I have never met someone who lives up to their middle name quite as well, and thank you for the endless would-you-rathers during our time working together. To Chris M, my fellow tuba player and peanut hater, thank you for all the fun times, and I hope you've learned all of the flags of the world by now. To Graeme, I'm sorry for all the stress you had to go through with SIPBS, but I'm very glad that it landed you in the fumehood next to me! Thanks for all the chats, pints, and game nights over the past couple of years. To Chris R, my favourite money-saving expert/caricaturist, thanks for taking over Peter's would-you-rather mantle and for many fun chats. I'll miss our drunken walks back to Dennistoun at two in the morning! To Gemma, thanks for having the decency to laugh at all my jokes over the past year, I'm sorry that we don't get to share a lab together for longer. Keep up the squash, you'll have Ross running scared in no time!

Further thanks go to the other students, academics and staff throughout the department for creating such a great atmosphere in the Thomas Graham. In particular I'd like to thank Conor, Paul, Adele, Giorgia, Guiseppe, Norman, Andrew, Kenny, Krystian, David, Nikki and Mhairi for the many nights out, nights in, pub quizzes and games of squash and basketball. A life of chemistry would be really boring without all those fun moments in between, and thank you for sharing them with me. I am also grateful to have been able to spend my time at Strathclyde along with Raymond Chung, and I'd like to thank him for all the fun memories, many long conversations and great advice over the years. I would also like to acknowledge the help of Craig Irving, who consistently goes above and beyond to give every student as much help (and cake!) as he can. Certain parts of this thesis would never have been possible without Craig's input.

I'd also like to extend my gratitude to my friends and colleagues at GSK Stevenage that I met during the course of my PhD. In particular, I'd like to thank my industrial supervisor Dr.

# List of Abbreviations

| | |
|---|---|
| 18-crown-6 | 1,4,7,10,13,16-hexaoxacyclooctadecane |
| 2-MeTHF | 2-methyltetrahydrofuran |
| acac | Acetoacetate |
| Ac | Acetyl |
| AmPhos | Di-*tert*-butyl(4-dimethylaminophenyl)phosphine |
| AMU | Atomic mass unit |
| API | Active pharmaceutical ingredient |
| $BAr^F_4$ | Tetrakis[3,5-bis(trifluoromethyl)phenyl]borate |
| BEMP | 2-*tert*-Butylimino-2-diethylamino-1,3-dimethylperhydro-1,3,2-diazaphosphorine |
| BLG | β-lactoglobulin |
| Boc | *tert*-Butyloxycarbonyl |
| BODIPY | Boron-dipyrromethene |
| BRD | Bromodomain-containing protein |
| BrettPhos | 2-(Dicyclohexylphosphino)3,6-dimethoxy-2',4',6'-tri*iso*propyl-1,1'-biphenyl |
| CCDC | Cambridge Crystallographic Data Centre |
| COD | Cyclooctadiene |
| CPME | Cyclopentyl methyl ether |
| CTAB | Cetyltrimethylammonium bromide |
| Cys | Cysteine |
| DABCO | 1,4-diazabicyclo[2.2.2]octane |
| dba | Dibenzylideneacetone |
| DBU | 1,8-Diazabicyclo[5.4.0]undec-7-ene |
| DCE | Dichloroethane |
| DCM | Dichloromethane |
| DFT | Density functional theory |
| DIC | Di*iso*propylcarbodiimide |
| DIPEA | *N*,*N*'-diisopropylethylamine |
| DMA | *N*,*N*'-dimethylaniline |
| DMAP | 4-Dimethylaminopyridine |
| DMF | *N*,*N*'-dimethylformamide |
| DMSO | Dimethylsulfoxide |
| DNA | Deoxyribonucleic acid |
| DoE | Design of experiments |

| | |
|---|---|
| dppf | 1,1'-Bis(diphenylphosphino)ferrocene |
| dr | Diastereomeric ratio |
| DTBPF | 1,1'-Bis(di-*tert*-butylphosphino)ferrocene |
| ee | Enantiomeric excess |
| EM | Electromagnetic |
| EPA | Ether-isopentane-enthanol |
| Et | Ethyl |
| FMO | Frontier molecular orbital theory |
| Fmoc | Fluorenylmethyloxycarbonyl |
| Fmoc-Gly-OH | *N*-(9-Fluorenylmethoxycarbonyl)-*L*-glycine |
| Fmoc-Leu-OH | *N*-(9-Fluorenylmethoxycarbonyl)-*L*-leucine |
| Fmoc-Phe-OH | *N*-(9-Fluorenylmethoxycarbonyl)-*L*-phenylalanine |
| Fmoc-Tyr(O$^t$Bu)-OH | *N*-(9-Fluorenylmethoxycarbonyl)-*O*-*tert*-butyl-*L*-tyrosine |
| FTIR | Fourier-transformed infra-red spectroscopy |
| HATU | 1-[Bis(dimethylamino)methylene]-1*H*-1,2,3-triazolo[4,5-*b*]pyridinium 3-oxide hexafluorophosphate |
| HMDS | *bis*(trimethylsilyl)amide |
| HOMO | Highest occupied molecular orbital |
| HPLC | High-performance liquid chromatography |
| HRMS | High resolution mass spectrometry |
| IMes | 1,3-Dimesitylimidazol-2-ylidene |
| IR | Infra-red |
| ISC | Intersystem crossing |
| k$_{rel}$ | Relative reaction rate |
| LCMS | Liquid chromatography-mass spectrometry |
| L-E | Leu-enkaphalin |
| LRMS | Low resolution mass spectrometry |
| LUMO | Lowest unoccupied molecular orbital |
| *m*/*z* | Mass divided by charge number of ion |
| MCR | Multi-Component Reaction |
| Me | methyl |
| mGlu 2 | metabotropic glutamate 2 |
| MMT | (Monomethoxy)-triphenylmethyl |
| MS | Molecular sieve |
| NBS | *N*-bromosuccinimide |

| | |
|---|---|
| NCS | *N*-chlorosuccinimide |
| NI | Nitrile imine |
| nm | Nanometres |
| NMM | *N*-methylmorpholine |
| NMR | Nuclear magnetic resonance |
| NMSSC | National mass spectrometry service centre |
| NO | Nitrile oxide |
| OAc | Acetate |
| O$^{i}$Pr | *iso*propoxide |
| PBM | Petasis Borono-Mannich |
| PBS | Phosphate-buffered saline |
| Pd G1 | Palladium(II) phenethylamine chloride precatalyst |
| Pd G2 | Aminobiphenyl palladium(II) chloride precatalyst |
| Pd G3 | Aminobiphenyl palladium(II) methanesulfonate precatalyst |
| Pd G4 | *N*-methylaminobiphenyl palladium(II) methanesulfonate precatalyst |
| Pd/C | Palladium on charcoal |
| PEG | Polyethylene glycol |
| Ph | Phenyl |
| Pin | Pinacol |
| PPARα | Peroxisome proliferator-activated receptor alpha |
| PVC | Poly(vinylchloride) |
| Py | Pyridine |
| QY | Quantum yield |
| RockPhos | 2-Di(*tert*-butyl)phosphino-2',4',6'-triisopropyl-3-methoxy-6-methylbiphenyl, |
| RuPhos | 2-Dicyclohexylphosphino-2,6-diisopropoxybiphenyl |
| S$_{E}$Ar | Electrophilic aromatic substitution |
| SPhos | 2-Dicyclohexylphosphino-2',6'-dimethoxybiphenyl |
| SPPS | Solid-phase peptide synthesis |
| T$_1$ | Longitudinal relaxation |
| T$_2$ | Transverse relaxation |
| TBAB | Tetrabutylammonium bromide |
| TBAF | Tetrabutylammonium fluoride |

| | |
|---|---|
| $^{t}$BuXPhos | 2-Di-*tert*-butylphosphino-2,'4',6'-tri*iso*propylbiphenyl |
| tetrakis | Tetrakis(triphenylphosphine)palladium(0) |
| TFA | Trifluoroacetic acid |
| THF | Tetrahydrofuran |
| TIPS | Tri*iso*propylsilane |
| TLC | Thin-layer chromatography |
| TMS | Trimethylsilyl |
| TPA | Triphenyl acetate |
| Triflic | Trifluoromethanesulfonic |
| Trityl/Trt | Triphenylmethyl |
| Trp | Tryptophan |
| UV | Ultraviolet |
| UV-Vis | Ultraviolet-visible light |
| XPhos | 2-Dicyclohexylphosphino-2',4',6'-tri*iso*propylbiphenyl |
| $\lambda_{max}$ | Wavelength of maximum absorbtion |

# Contents

# 1 Nitrile Imines

The generation of nitrile imines (NIs) can be traced back to the beginning of the 20th century, although these reports lacked both characterisation and application of the highly reactive species. The first synthetically tractable report came from Huisgen in 1959.[1] This initial study was remarkably comprehensive, documenting multiple approaches towards the generation of the NI, and detailing its reactivity with a number of dipolarophiles and nucleophiles. Huisgen dominated the area for much of the next decade and provided invaluable insights into the reactivity, kinetics and chemoselectivity of NIs through a number of publications.[1–18]

Interest in the applications of NIs was more sparse over the next few decades, with the majority of publications focusing instead on the mechanism of their formation, or reactivity with different substrates. Recently, however, NI chemistry has enjoyed a renaissance throughout the literature, with a raft of applications identified in the synthesis of active pharmaceutical ingredients (APIs), in bioorthogonal conjugation, and in materials chemistry over the past fifteen years.[19–21]

## 1.1 Properties

### 1.1.1 Resonance Forms

NIs are members of the nitrillium betaine family of 1,3-dipoles, which possess the general formula outlined in *Figure 1.1*.[22] These are isoelectronic with the allyl anion, with 4 π electrons shared across three atoms. The inherent reactivity of 1,3-dipoles comes from the incomplete octet of the neutral terminus, which gives rise to a number of potential resonance forms. The contribution of each of these canonical forms is highly important in governing the reactivity of the species.



*Figure 1.1: The general structure of the nitrillium betaines*

Two resonance forms can be viewed as the dominant contributors to NI structure: the propargylic and allenic forms (*Figure 1.2*). From a geometric perspective, the propargylic structure can be described as planar (with respect to the N-C-R bond axis), while the allenic form is slightly "bent".[23] NIs are often referred to as "floppy" molecules, with a low interconversion energy barrier between the two isomers.[24–26]
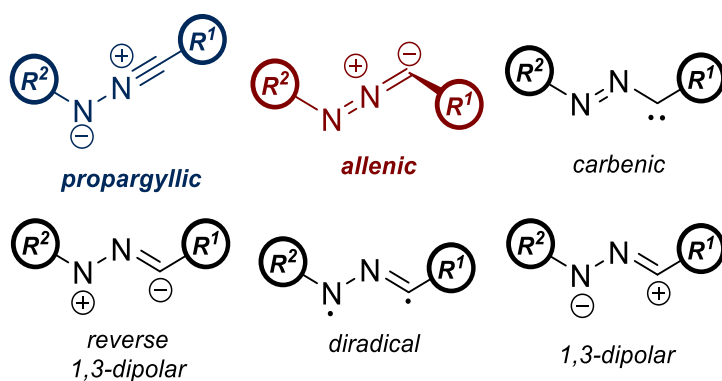
*Figure 1.2: The six potential resonance forms of NIs*

Which of these two resonance forms predominates depends significantly on the substituents on both termini of the NI.[27] One of the most important factors is the electronegativity of the terminal nitrogen atom. Increased electronegativity favours the linear, propargylic structure, forming a more electrophilic dipole with a low energy lowest unoccupied molecular orbital (LUMO), and *vice versa* in the case of the allenic form.[28,29]

More recently, attention has turned to the importance of the contribution of the carbenic resonance form. Computational studies have indicated that substitution of the *C*-terminus of the NI with a heteroatom such as nitrogen or oxygen could increase the carbenic character to up to 20% of the overall resonance contribution.[30,31] This has been partially confirmed experimentally, with 5-amino NI shown *via* infra-red (IR) spectroscopy to exhibit the lowest C-N bond order of any NI ever recorded.[31]

### 1.1.2 Characterisation of NIs

A number of spectroscopic techniques have been employed in an effort to suitably characterise NIs. As expected in a nitrillium betaine 1,3-dipole, the inherent reactivity of the species is a major stumbling block in this process.

Following on from their initial application,[1] any preliminary evidence of the existence of an NI intermediate was indirect,[10] with the first direct detection of an NI reported in 1973, using ultraviolet-visible light (UV-Vis) spectroscopy at cryogenic temperatures.[32]

Multiple approaches towards the spectroscopic characterisation of NIs were reported throughout the 1980s. The UV-Vis spectra of diphenyl NI and derivatives were reported independently by both Holm and Heimgartner, employing 12 K matrix isolation and immobilisation using ether-isopentane-ethanol (EPA) or poly(vinylchloride) (PVC) glass.[33–35] The IR spectra were also disclosed in these same reports. The palette of diaryl NIs characterised using this technique increased towards the middle of the decade, with over 20 UV-Vis and IR spectra reported.[36–39] The utility of this approach was significantly bolstered

with the application of "flash" photolysis, enabling the direct capture of the UV-Vis spectrum of an NI at room temperature.[40,41]

Other spectroscopic approaches were also developed, principally using high temperature gas phase techniques.[42] This enabled analysis through mass spectrometry, photoelectron spectroscopy, or IR *via* immobilisation of the NI on a KBr disc.[24,43] Modern-day advances in IR technology have recently seen the re-emergence of this approach as the most valuable analytical technique in the characterisation of reactive NIs.[27,31,44]

[14]N nuclear magnetic resonance (NMR) spectroscopy has also been shown to be a feasible approach, although a limitation of this technique is that the NI requires enhanced stability relative to other spectroscopic methods.[45] More recently, photocrystallography was also employed as a means of characterising diaryl NIs.[46]

### 1.1.3  Spectroscopic Properties

NI UV-Vis spectra are dominated by a large absorption around 240-275 nm (heteroatom-substituted NIs) or 370-465 nm (diaryl NIs).[32–36,38,40,41,43,47] This is postulated to originate from a $\pi$-$\pi$* transition, with, in the case of diaryl NIs, an extremely large extinction coefficient leading to a very broad signal.[40] Electron-rich species on the *N*-terminus of the NI and electron-deficient species on the *C*-terminus further increase absorption wavelength.[40]

IR spectroscopy is one of the most valuable techniques in determining whether a specific NI will adopt an allenic or propargylic structure, as the most prominent peak of the spectrum corresponds to the C-N anti-symmetric stretch, with the stretching frequency increasing with increasing bond order. All NIs with a C-N stretch frequency below 2100 cm$^{-1}$ are almost entirely allenic (C-N bond order of 2), while those with a stretch frequency above 2200 cm$^{-1}$ are likely to primarily exist as the propargylic resonance form. Those with a value between 2100 cm$^{-1}$ and 2200 cm$^{-1}$ exhibit both allenic and propargylic character.[48] Most diaryl, or even monoaryl NI species have been shown to possess a predominantly propargylic structure through this technique (C-N stretch typically ranges from 2215-2250 cm$^{-1}$).[35,37,39,43] The addition of any conjugative functional group onto either of the aromatic rings, electron donating or withdrawing, will lower the bond order of the C-N bond and will lower the stretching frequency accordingly.[39] NIs substituted by heteroatoms typically adopt allenic or mixed resonance forms, with C-N stretch values between 1990 and 2170 cm$^{-1}$.[27,30,31,48–52]

There has been considerably less focus on the characterisation of NIs by NMR spectroscopy in comparison to other methods, likely due to the relatively specialised conditions required making the stability of the compound a necessity. In the specific cases where NI NMR spectra have been examined, ^{13}C resonances have been observed between 45 and 70 ppm.[25,45] This is complicated by large longitudinal relaxation ($T_1$) values and small transverse

relaxation ($T_2$) values, which can lead to extremely broad and undetectable peaks.[45] [14]N NMR spectroscopy is a viable alternative, which generates a signal for the α-N at around -215 - -170 ppm.[45]



*UV-Vis*
**R[1]** - $\lambda_{max}$ ↑ with ↑ electron-withdrawing property
**R[2]** - $\lambda_{max}$ ↑ with ↑ electron-donating property

*NMR*
**N$_\alpha$** - *characteristic sharp signal -215 - -170 ppm*

*IR*
**C-N bond** - *antisymmetric stretch around 2250-2000 cm$^{-1}$*
- *frequency ↑ with ↑ in bond order*
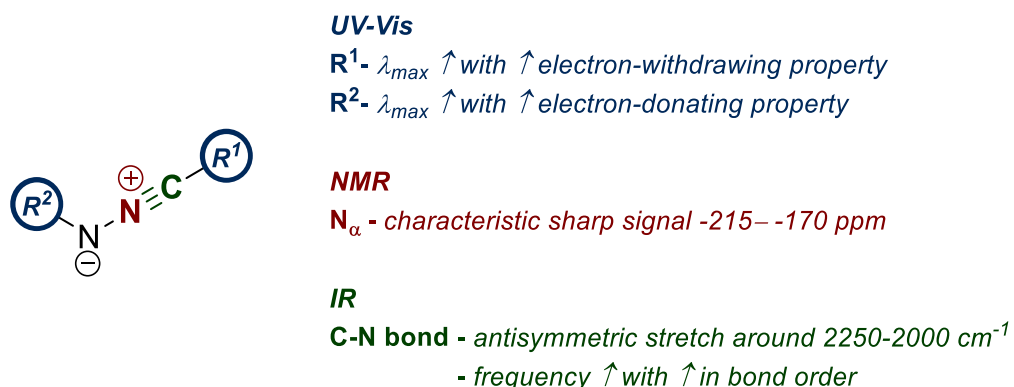
*Figure 1.3: A summary of the spectroscopic characteristics of NIs*

## 1.2 The Generation of Nitrile Imine Derivatives

As most forms of the NI moiety are unstable under standard conditions, they must typically be generated *in situ* by an appropriate precursor. This is possible through a range of chemical transformations, each with their own advantages and disadvantages. Examples of each are provided in the subsequent sections.

### 1.2.1 *Hydrazonyl Halides*

The most common NI precursor is the hydrazonyl halide, or a derivative thereof.[53] The NI is typically generated from this precursor through treatment with a base, as shown in *Scheme 1.1*, causing deprotonation and subsequent elimination of the halide.[54]
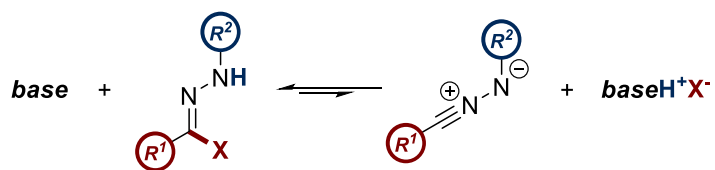


*Scheme 1.1: The generation of NIs using hydrazonyl halides*

The generation of NIs from hydrazonyl chlorides was first noted in Huisgen's original 1959 report, as an alternative to the thermolysis of 2,5-disubstituted tetrazoles (*Section 1.2.3*).[1] Treatment of diphenyl hydrazonyl chloride with triethylamine in the presence of dicyclopentadiene yielded the expected pyrazoline in an 83 % yield (*Scheme 1.2*). The liberation of the NI in this manner was later shown to be a reversible process through a combination of kinetic and isotope labelling studies.[10] Hydrazonyl chlorides were able to act as a "depot" of the NI, which was slowly consumed at a rate dependent on the reactivity of the dipolarophile partner of the cycloaddition.
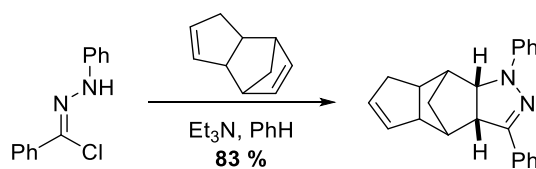
*Scheme 1.2: The first example of NI generation using hydrazonyl halides*

Further mechanistic work has since shown that NI formation from hydrazonyl halides is in competition with the formation of the analogous carbonium cation (*Scheme 1.3*).[55] Unsurprisingly, the relative formation of either intermediate is highly dependent upon pH, with the NI dipole formation becoming increasingly favourable with increasing pH. The $pK_a$ of the hydrazonyl halide therefore has a significant impact on the rate of NI generation, as the deprotonation of the species is the rate determining step of the reaction.[56] Reactivity may also be modified through variation of the *C* and *N*-substituents, and through careful selection of the halide or psuedohalide leaving group. For example, increased reactivity has been exemplified through the exchange of a hydrazonyl bromide with a hydrazonyl iodide, due to the lower $pK_b$ of the iodide anion.[57]



| R | $pK_a$ |
|---|---|
| Me | 9.64 |
| F | 9.42 |
| NO$_2$ | ~8 |
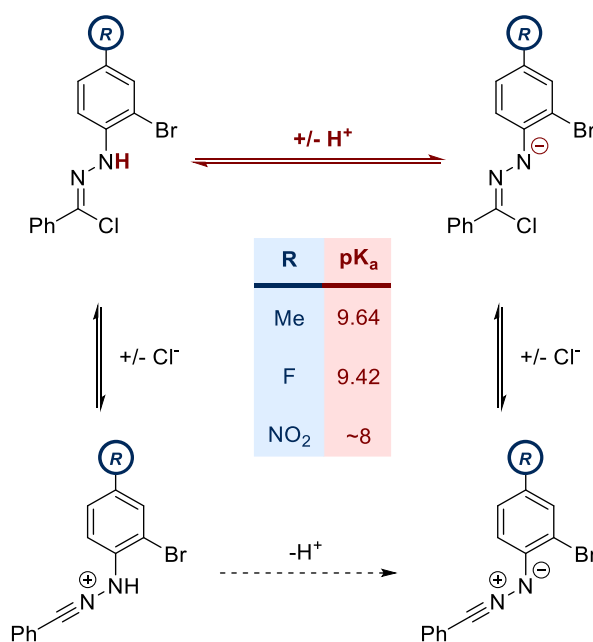
*Scheme 1.3:The pKa of the hydrazonyl halide can be influenced by substituent*

The selection of base can also prove important when generating NI species using hydrazonyl halides. Silver(I) carbonate in particular has been proposed to facilitate NI formation through an alternative mechanism to that of a more conventional base, such as triethylamine.[58] Whereas triethylamine has been shown to initiate reaction through the deprotonation of the hydrazonyl halide, the silver(I) cation is believed to initially generate the carbonium ion, which then forms the NI through deprotonation by the carbonate anion (*Scheme 1.4*).[59] The driving force behind this process is the formation of the insoluble AgCl salt.[60] This may also influence the rate of NI reactivity, as the solubility of the salt generated upon NI formation

has a significant impact on the balance of the equilibrium between these products and the starting hydrazonyl halide.
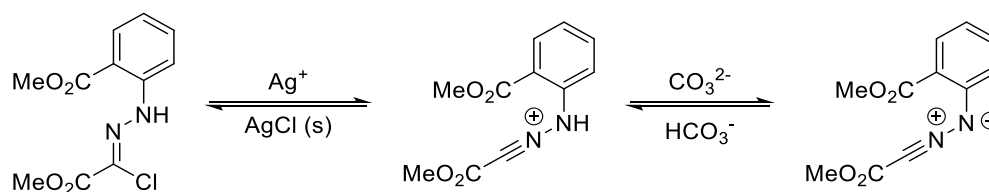


*Scheme 1.4: The use of silver salts in the generation of NIs*

Numerous examples exist in the literature documenting the successful application of both organic and inorganic bases within this reaction. For example, inorganic bases are competent in the generation of NIs in aqueous media, as evidenced in the first reported example of NI cycloaddition under such conditions (*Scheme 1.5*).[61]
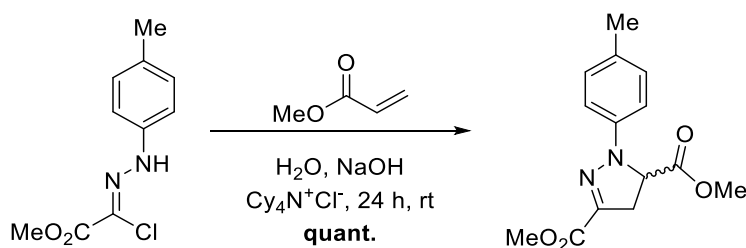


*Scheme 1.5: The first example of NI cycloaddition under aqueous conditions*

The presence of a halide counter-ion itself in the reaction mixture can also have a significant impact upon the reactivity of the NI. Recent examples in the literature have shown that when generating NIs through irreversible means (*Section 1.2.3*), performing the reaction in phosphate-buffered saline (PBS) can lower the reactivity, by trapping some of the dipole as the corresponding hydrazonyl chloride (*Scheme 1.6*). This is accomplished by the chloride anion within the buffer.[62]
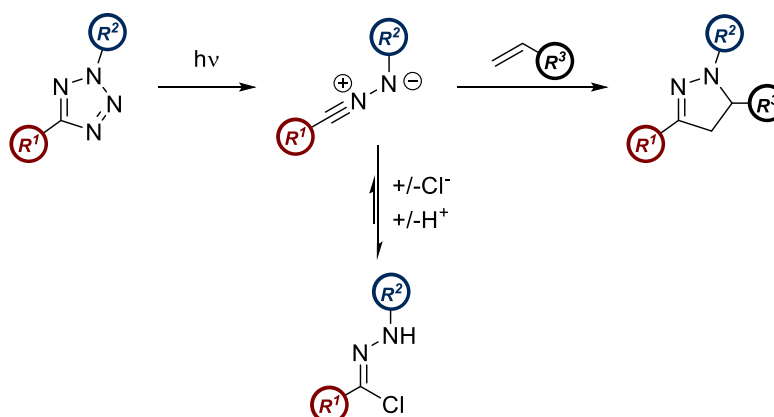


*Scheme 1.6: The trapping of an NI dipole via the presence of chloride anions in an aqueous reaction mixture*

As discussed previously, hydrazonyl halides are ubiquitous within the literature as a robust means of generating NIs, with numerous examples including microwave and solvent-free

approaches.[63,64] The most conventional means of synthesising these precursors is through halogenation with an electrophilic halogen source,[65] although hydrazonyl chlorides may also be accessed through the treatment of the relevant hydrazide species with a chlorinating agent such as $POCl_3$ (*Scheme 1.7*).[66] The hydrazonyl iodide can be generated *via* a Finkelstein reaction of the relevant hydrazonyl bromide analogue.[57]
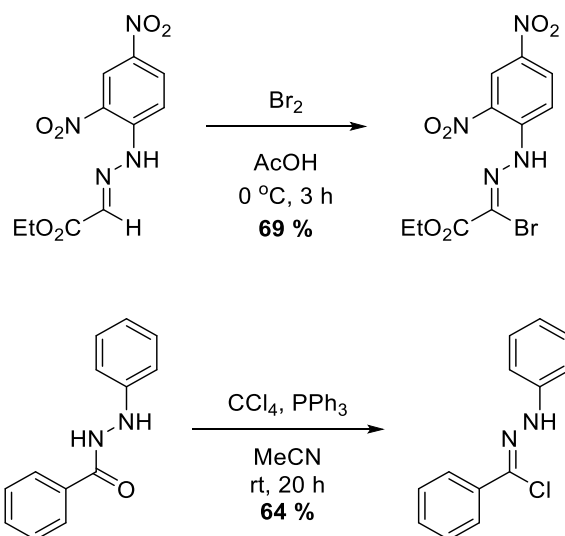


*Scheme 1.7: Exemplar methods of synthesising hydrazonyl chlorides*

Hydrazonyl halides are mildly unstable to atmospheric conditions, and are severe skin irritants.[67] As such, it is also common to generate these species *in situ* (*Scheme 1.8*).[67,68] Indeed, this can be taken a step further, beginning with the aldehyde and generating the hydrazone, hydrazonyl bromide and NI *in situ* prior to isolation of the product.[69]
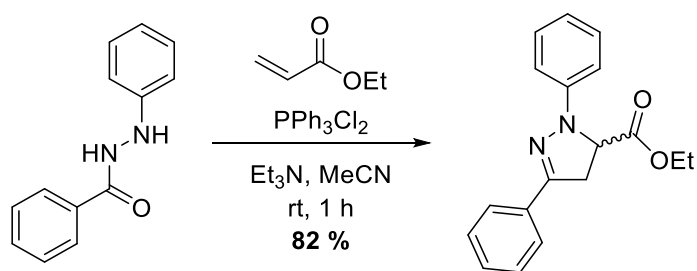


*Scheme 1.8: The in situ generation and consumption of the hydrazonyl halide*

## 1.2.2 Hydrazones

In addition to generation through the halogenated derivatives, NIs can also be accessed directly from the corresponding aldehyde hydrazones through an oxidative process (*i.e. via* loss of $H_2$ rather than HX). This is typically accomplished using heavy metal salts, such as lead(IV) or mercury(II) acetate,[70,71] with the proposed mechanism shown in *Scheme 1.9*. Hypervalent iodine can also generate NIs directly from hydrazones, and is believed to proceed *via* a similar mechanism.[72,73]
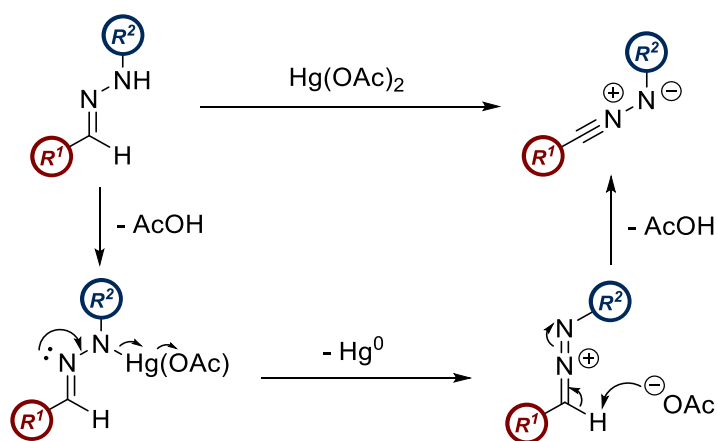
*Scheme 1.9: The mechanism of NI formation using heavy metal acetates*

One drawback in this approach to NI formation is the use of acetate as the counterion. As will be discussed below (*Section 1.3.2.4*), carboxylate moieties are known to rapidly react with NIs.[12] This often impacts the yield of the intended reaction when heavy metal acetates are used in their generation.

Oxidation of hydrazones can also be employed when the hydrazone is generated *in situ*, as evidenced by a report from 2014, where no intermediates are isolated in between the starting aldehyde material and the cycloadduct of the NI (*Scheme 1.10*).[74] Mercury(II) acetate is again used to generate the NI.
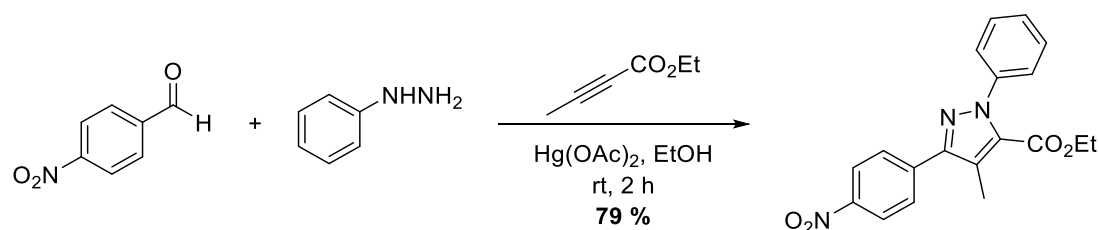


*Scheme 1.10: The generation and consumption of hydrazones in situ by mercury(II) acetate*

## 1.2.3 Tetrazoles

Excluding hydrazonyl chlorides, tetrazoles are the most common precursor to the NI dipole in the literature.[62] Tetrazoles form NIs through the expulsion of the *N*-3 and *N*-4 atoms of the heterocycle as nitrogen gas.[75] This may be initiated through either thermal or photochemical means. In both cases, only the 2,5-disubstituted regioisomer of the tetrazole is relevant. While the 1,5-disubstituted species may also expel nitrogen when heated or exposed to ultraviolet (UV) light, it does not form the NI during its decomposition pathway.[76]

The thermal degradation of 2,5-disubstituted tetrazoles was the first ever approach reported to yield NIs, again by Huisgen in 1959 (*Scheme 1.11*).[1] The method was viewed as particularly useful as no exogenous reagents were required, merely the tetrazole and the reaction partner. However, one downside was (and indeed, remains) the temperature required

in tetrazole thermolysis. In the case of 2,5-diphenyl NI, the most prevalent example of the species within the literature, temperatures in excess of 160 °C are required to facilitate decomposition.[12] While the substituent of the *C*-aromatic ring was shown to be interchangeable, exchange of the *N*-phenyl ring for a methyl group increased the thermolysis temperature to over 200 °C. This represented a drawback in the applications of tetrazole thermolysis, due to the prerequisite that the reaction product must be stable to such high temperatures itself.
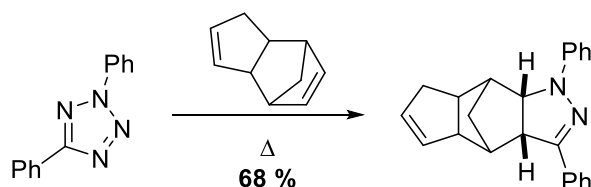


*Scheme 1.11: The original example of NI 1,3-dipolar cycloaddition via tetrazole thermolysis*

The rate of thermolysis is highly dependent on the *C* and *N* substituents of the respective NI, and this has been studied by a handful of research groups.[77–80] Rate of NI formation is most simply measured by iteratively incorporating electron donating and electron withdrawing groups into both aromatic rings of 2,5-diphenyl tetrazole. Curiously, it has been shown that electron-donating groups on the *C*-aryl ring can facilitate more rapid decomposition, while electron-withdrawing groups on the *N*-aryl ring have the same effect.[77,78,80] This implies that cleavage of the *N*-2-*N*-3 and *C*-5-*N*-4 bonds is not symmetrical, suggesting that there must be residual charges present at the transition state of the thermolysis of 2,5-diaryl tetrazoles.[77] Hammett plots of this reaction generated by Baldwin suggested that the influence of substitution of the *N*-aromatic ring is around 5-times that of the *C*-aryl ring, leading to the hypothesis that the *N*-2-*N*-3 bond is the first to be broken, likely during the rate-determining step of the process (*Graph 1.1*).[78]

The photolysis of 2,5-disubstituted tetrazoles was first documented nearly a decade after the thermolysis of the species (*Scheme 1.12*).[10] This method had the advantage of no longer requiring extremely high temperatures to form the NI. However, in the case of most 2,5-diaryl tetrazole species, the wavelength of light required was around 250-300 nm, well into the UV-B range of the electromagnetic (EM) spectrum.[81] This required the use of high-power mercury lamps that remain an uncommon laboratory accessory, and as such applications of this transformation were limited for many years.
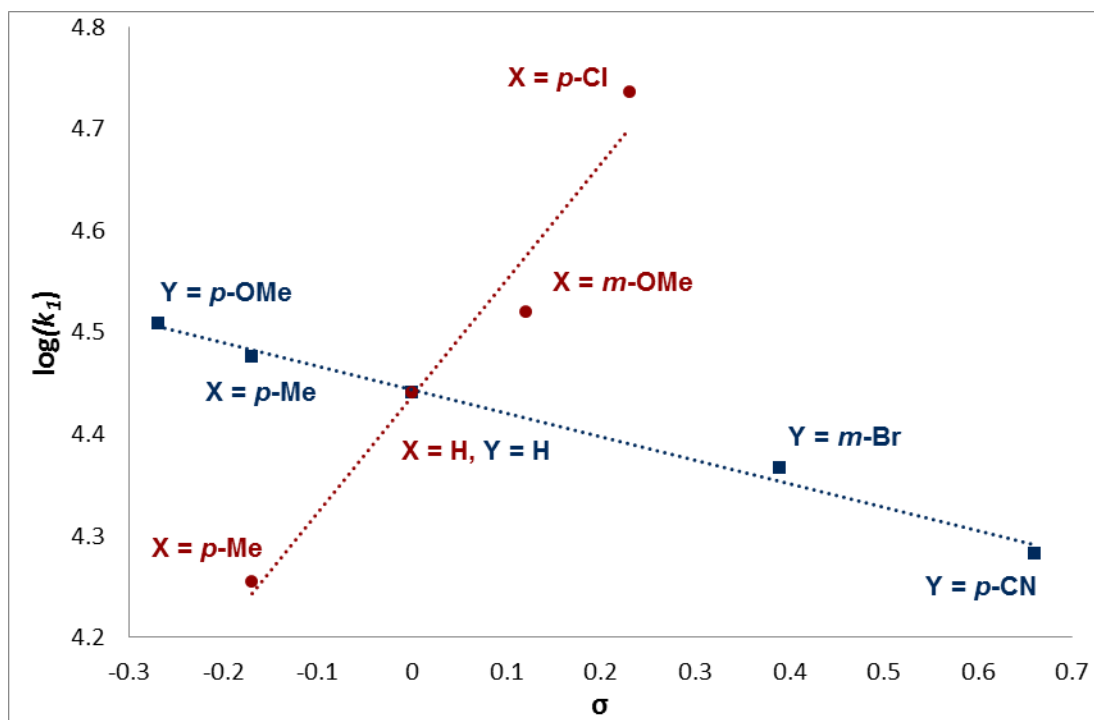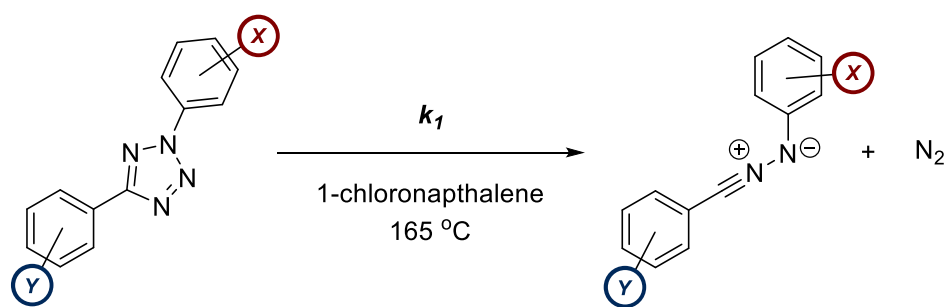
Graph 1.1: The correlation between the electronic properties of both aryl rings and rate of NI generation

In 2007, Lin re-visited the procedure in a report which documented the cycloaddition of some NIs with various dipolarophiles. The dipole was accessed using 2,5-diaryl tetrazoles and a hand-held 300 nm UV lamp commonly used for the analysis of thin-layer chromatography (TLC) plates (*Scheme 1.13*).[82]
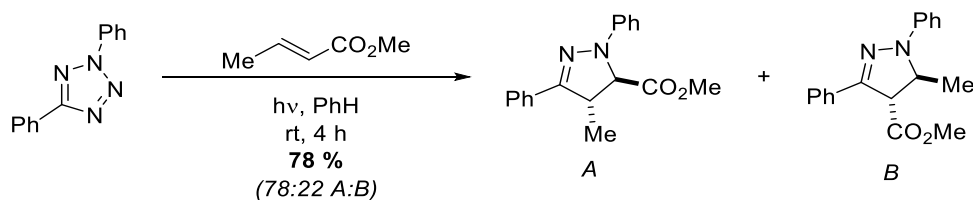


Scheme 1.12: The original example of NI 1,3-dipolar cycloaddition when using photolysis of a tetrazole as an NI source

From this report, photolysis of 2,5-diaryl tetrazoles quickly gathered momentum as a popular approach for NI generation in both bioorthogonal and materials chemistry (discussed further in *Section 1.4*).[21,62] The method was particularly attractive due to the traceless, user-activated method of NI formation in which no exogenous reagents were required.
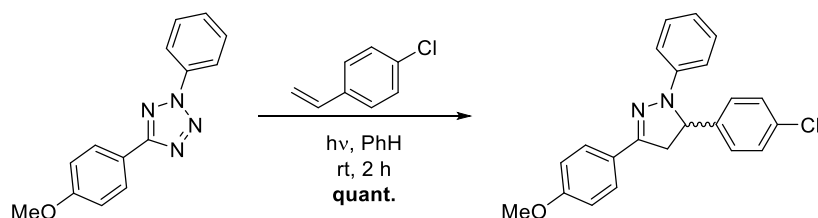
*Scheme 1.13: An example from Lin's 2007 publication on the photolysis of 2,5-diaryl tetrazoles*

One particularly active area of research was the development of novel tetrazoles with increased wavelength of maximum absorbtion ($\lambda_{max}$) values. When considering 2,5-diphenyl tetrazole, the prerequisite of a UV-B light source undoubtedly hindered its application, due to the likelihood of causing cellular damage through reactivity with deoxyribonucleic acid (DNA).[83] Some of the first reports to address this issue modified the substituents of both termini of the tetrazole. The use of heteroatomic substituents were shown to generate a "push-pull" system of electron flow, which raised the $\lambda_{max}$ into the lower energy UV-A range.[84]

Subsequent efforts were dedicated to extending the conjugation of the tetrazole $\pi$-electron system. Analogues substituted by naphthalenes, thiophenes and pyrenes were all found to furnish the relevant NI upon exposure to UV-A light.[85–87] In both the thiophene and pyrene derivates, NI formation was observed at wavelengths of over 400 nm, the visible region of the spectrum.

Other modifications demonstrated that further extension of the operational wavelength was possible. The use of two-photon excitation generated a naphthalene-based NI from the corresponding tetrazole using a 700 nm laser.[88] A summary of these efforts is outlined in *Scheme 1.14*.

One additional advantage of the availability of numerous tetrazole species that generate NIs at different wavelengths of light is their potential application in "$\lambda$-orthogonal" chemistry, whereby two photolabile moieties may be selectively activated in the presence of one another using two different wavelengths of light.[89,90] This technique can even be applied to two different tetrazole species (*Scheme 1.15*).[91]

11
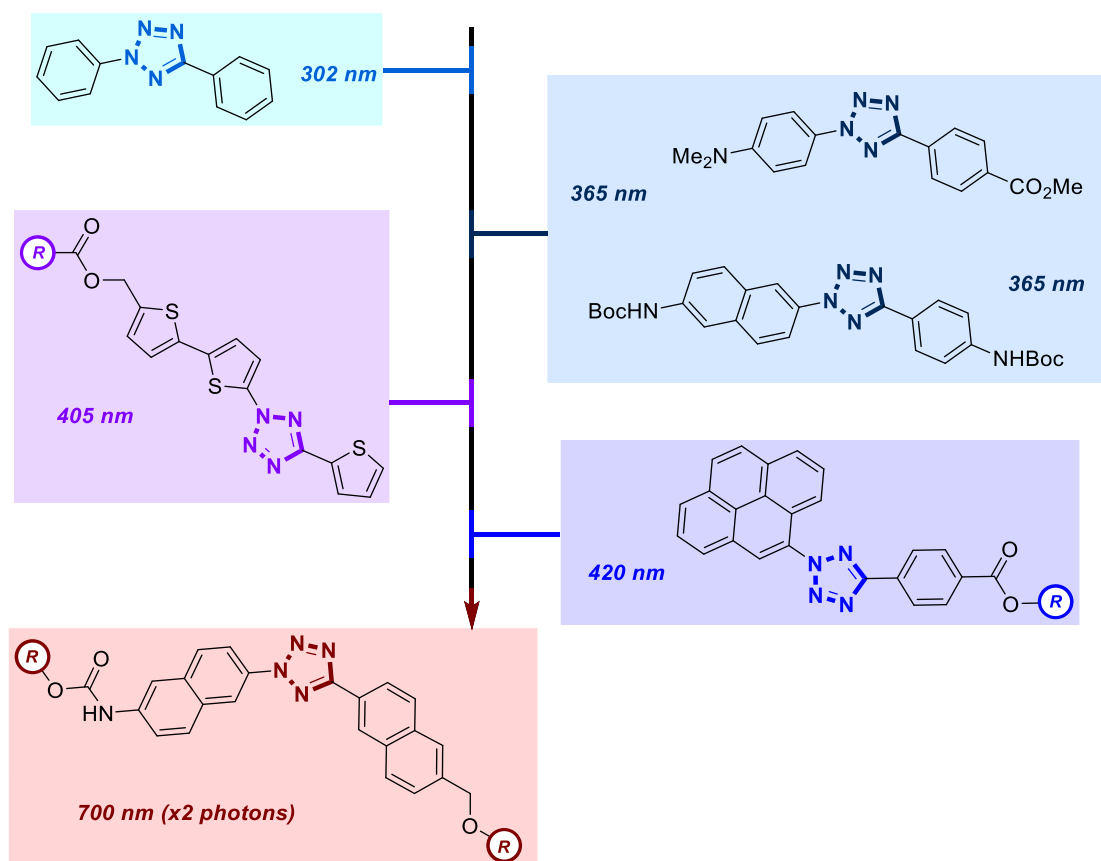
*Scheme 1.14: The progressive increase in the wavelength required in the photolysis of different species of 2,5-tetrazoles*

In comparison to the other methods of NI generation, there was surprising lack of mechanistic discussion into the photolysis of tetrazoles in the years following its discovery. Fifteen years after Huisgen's initial report, Padwa documented the quantum yields (QYs) of a number of diaryl tetrazoles, proposing that the photodecomposition of the species originated from a forbidden n-π* transition to the first excited singlet state.[92]

Further measurements of tetrazole QYs followed.[93] In comparison to other photochemical reactions, the QYs were generally good, indicating an efficient photolytic procedure. Solvent polarity, concentration, and even the substituents of the *C*-aryl ring did not significantly alter this QY, with only substitution of the *N*-aryl ring found to have any significant impact. Analogous to Baldwin's results in the thermolytic studies of tetrazole cleavage, electron-withdrawing groups were found to improve QY.[93] This again suggests that the photolysis of 2,5-disubstituted tetrazoles is non-symmetrical. Furthermore, the lack of an effect on the QY by substitution of the *C*-aryl ring indicated a similar finding to the thermolysis study- the *N*-2-*N*-3 bond was broken first in the rate determining step of the process.
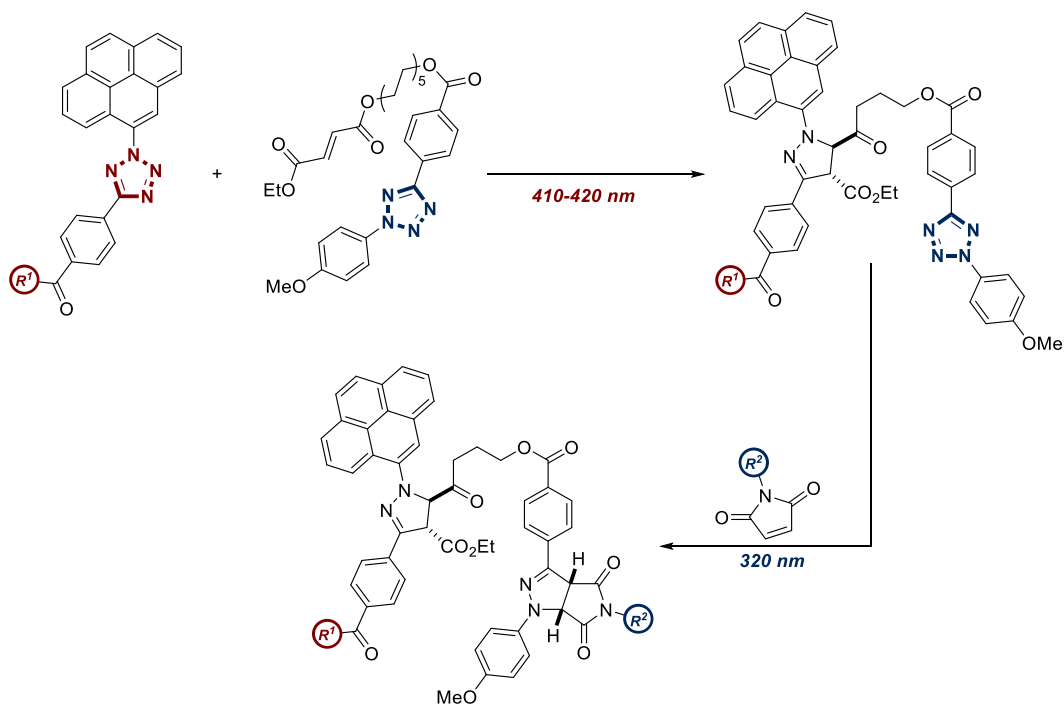
*Scheme 1.15: The selective photolysis of one tetrazole moiety in the presence of another based on differing λmax values*

A significant advancement towards the elucidation of the mechanism was made in 2017, by the Barner-Kowollik group.[94,95] Using recently developed computational methods in combination with experimental evidence, an alternative mechanism of photochemical NI formation was proposed, shown in *Scheme 1.16*. Firstly, the excitation of the starting tetrazole was identified as a π-π* transition to the first excited single state, $S_1$. The highest occupied molecular orbital (HOMO) in question was shown to be positioned around both the tetrazole heterocycle and the *N*-aryl ring, justifying the previous experimental evidence that *N*-aryl properties had such a significant impact on QY. Secondly, the NI itself was found to be formed *via* the first triplet state, $T_1$, of the tetrazole, meaning intersystem crossing (ISC) from $S_1$ to $T_1$ was necessary. Once in the triplet state, tetrazole decomposition was expected to proceed through a diradical intermediate, forming the NI upon returning to the ground state through a conical intersection.

This mechanistic interpretation had implications relating to specific tetrazole substrates. While excitation of the tetrazole to the $S_1$ state may be guaranteed through an appropriate light source, two other factors determine the QY of the corresponding NI: the favourability of ISC and the favourability of any competing relaxation processes.

Firstly, for ISC to occur, the $S_1$ and a $T_n$ state must be as near to degenerate as possible. This can be influenced to an extent, whereby the use of a higher energy wavelength may excite the tetrazole to a higher state of vibrational energy in addition to excitation to the singlet state, however computational approaches are still necessary to derive the numerical values of the relevant triplet energy levels. A second prerequisite is a similarity in tetrazole

conformation in the $S_1$ and $T_n$ states. Any differences correspond to an unfavourable energy penalty which will decrease the likelihood of ISC in relation to other competing processes. Unfortunately, the conformation of both excited species is another property specific to the individual tetrazole that can only be derived through computational means.
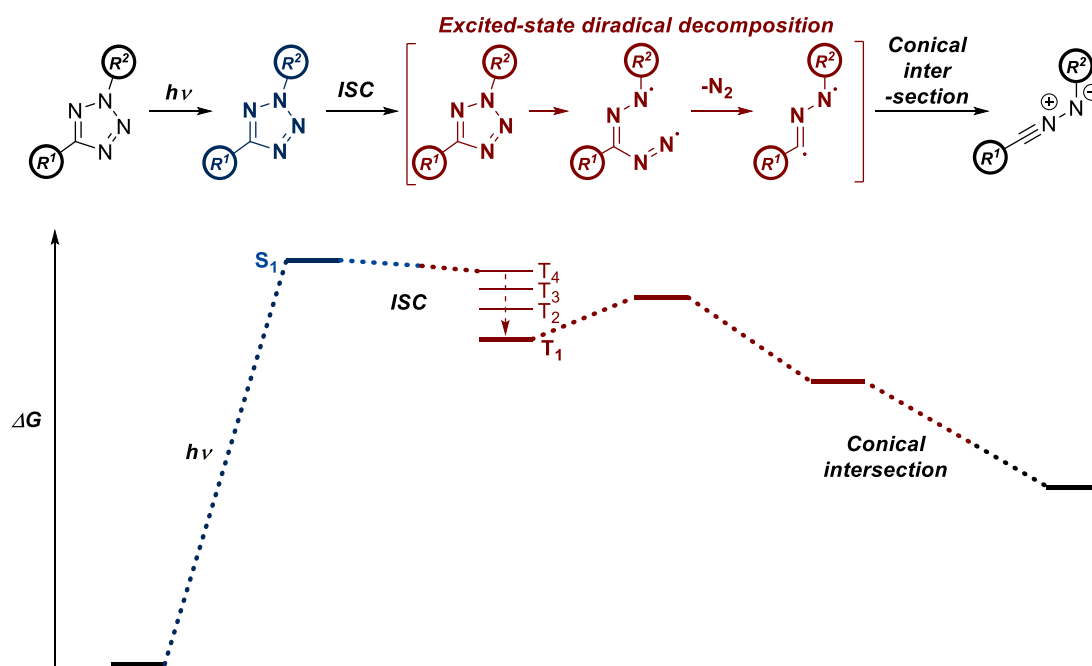


*Scheme 1.16: The mechanism of NI generation via photolysis of 2,5-tetrazoles*

When considering competing pathways to ISC, the non-radiative relaxation pathway known as charge recombination was found to be of particular importance.[96] The favourability of this process increases with increasing charge separation between the excited $S_1$ state and the ground state, and the extent of charge separation affected upon the molecule following irradiation will determine whether this pathway is dominant. As with the other properties discussed above, charge recombination is inherent to individual molecules.

To summarise, the exact QY through which a 2-5-substituted tetrazole will generate the corresponding NI is non-trivial, and requires empirical experimental determination or advanced computational calculations on a case-by-case basis to elucidate whether dipole formation is possible (*Scheme 1.17*). Fortunately, cases whereby the corresponding NIs fail to form entirely appear to be limited to only a handful of tetrazoles, containing nitro moieties and dimethylamino functional groups.[82,94] The vast majority tetrazoles reported in the literature generate the relevant NI in good QYs.
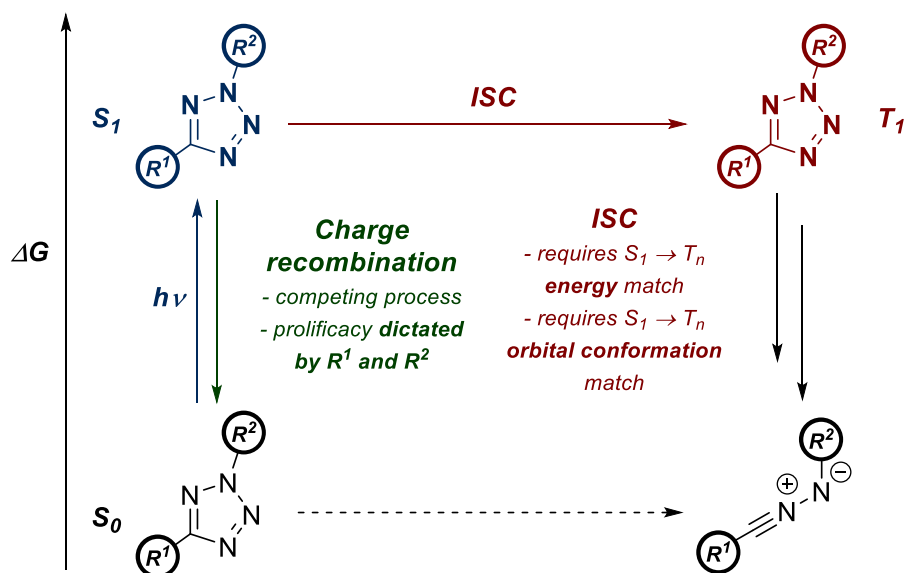
*Scheme 1.17: Both charge recombination potential and ISC ability must be considered when elucidating the QY of a 2,5-tetrazole*

### 1.2.4   Sydnones

Sydnones are mesoionic compounds typically represented as a cationic oxadiazole species with an exocyclic anionic oxygen atom.[97] Due to the zwitterionic nature of sydnones, they have been known for some time to participate in 1,3-dipolar cycloadditions.[98] Reaction of a sydnone with a dipolarophile will initially lead to a fused 5,5 ring system, which upon cycloreversion furnishes $CO_2$ gas and the pyrazoline/pyrazole product (*Scheme 1.18*)[99]
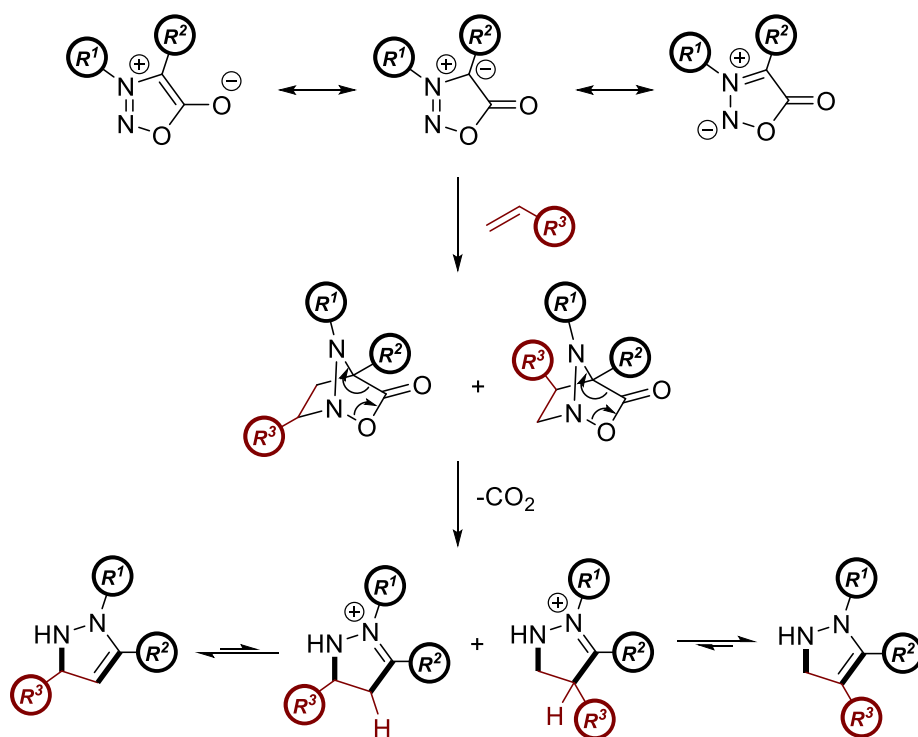


*Scheme 1.18: The general tautomeric forms of sydnones and their reactivity with dipolarophiles*

While also applicable to the synthesis of pyrazoles and pyrazolines, thermal sydnone cycloadditions do not proceed through an NI intermediate. However, photolysis of arylsydnone derivates activates an alternative mechanistic pathway by which the sydnone expels $CO_2$ prior to any cycloaddition, generating the relevant NI.[100] This transformation is thought to occur through initial formation of an unstable diazirine species, followed by further isomerisation to furnish the dipole (*Scheme 1.19*). [101,102]
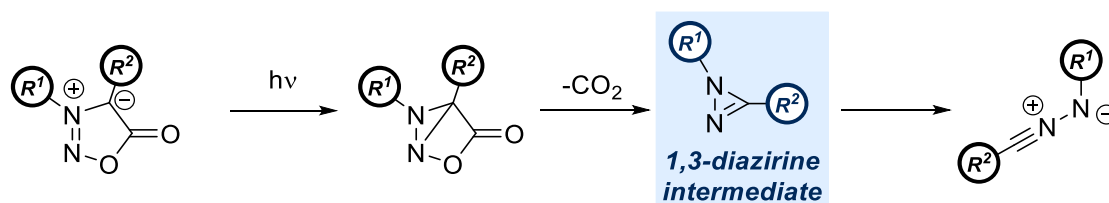


*Scheme 1.19: The hypothesised mechanism of NI formation via sydnone photolysis*

Applications of sydnones as NI sources are known, although limited in comparison to both hydrazones and tetrazoles. One reason is the relative inefficiency of the process. The QYs of diaryl sydnones are around ten times lower than the corresponding tetrazoles.[41]

## 1.3    The Reactivity of Nitrile Imines

NIs exhibit a broad scope of reactivity with several different substrates. The inherent property of 1,3-dipoles to undergo 1,3-dipolar cycloaddition with olefins and alkynes is shared by NIs, but reactions with various nucleophiles are also well-documented.

### 1.3.1    1,3-Dipolar Cycloaddition

The cycloaddition of a 1,3-dipole with an appropriate dipolarophile, typically a carbon-carbon double- or triple-bond, is a powerful reaction that is broadly applicable in organic synthesis. NIs have been widely characterised to undergo this transformation with numerous different dipolarophiles.

### 1.3.1.1 Regioselectivity

Cycloaddition between an NI and a non-symmetric dipolarophile can theoretically generate both the 4-substituted and 5-substituted pyrazoline/pyrazole adduct, and classification of the regioisomeric preferences of different dipolarophiles has been thoroughly investigated.

Generally, intermolecular NI cycloadditions favour the regioisomer with the most sterically-encumbered substituent in the 5-position of the resulting heterocycle. Extensive investigations by Huisgen have shown that the *N*-terminus of the NI is much more tolerant of steric bulk, partially justifying this trend (*Scheme 1.20*).[5–7,16] However, it should be noted that 4-substitued regioisomers are still known in many cases, and the outcomes of these cycloadditions often generate unexpected regioisomeric mixtures.[103]

The electronics of regioselectivity are slightly more complex. Initial attempts to rationalise a general trend utilised frontier molecular orbital theory (FMO), through calculations of the relative electron density of the corresponding HOMO and LUMO orbitals at each reaction centre.[104–107] This approach relies on the theory that HOMO and LUMO orbitals of similar sizes are more likely to interact, due to more efficient overlap, favouring one regioisomer over the other. This original application of FMO suggested that 5-substituted heterocycles were favoured in the majority of cases, with the exception of highly electron-withdrawing groups yielding either regioisomeric mixtures or 4-substituted products.[105]
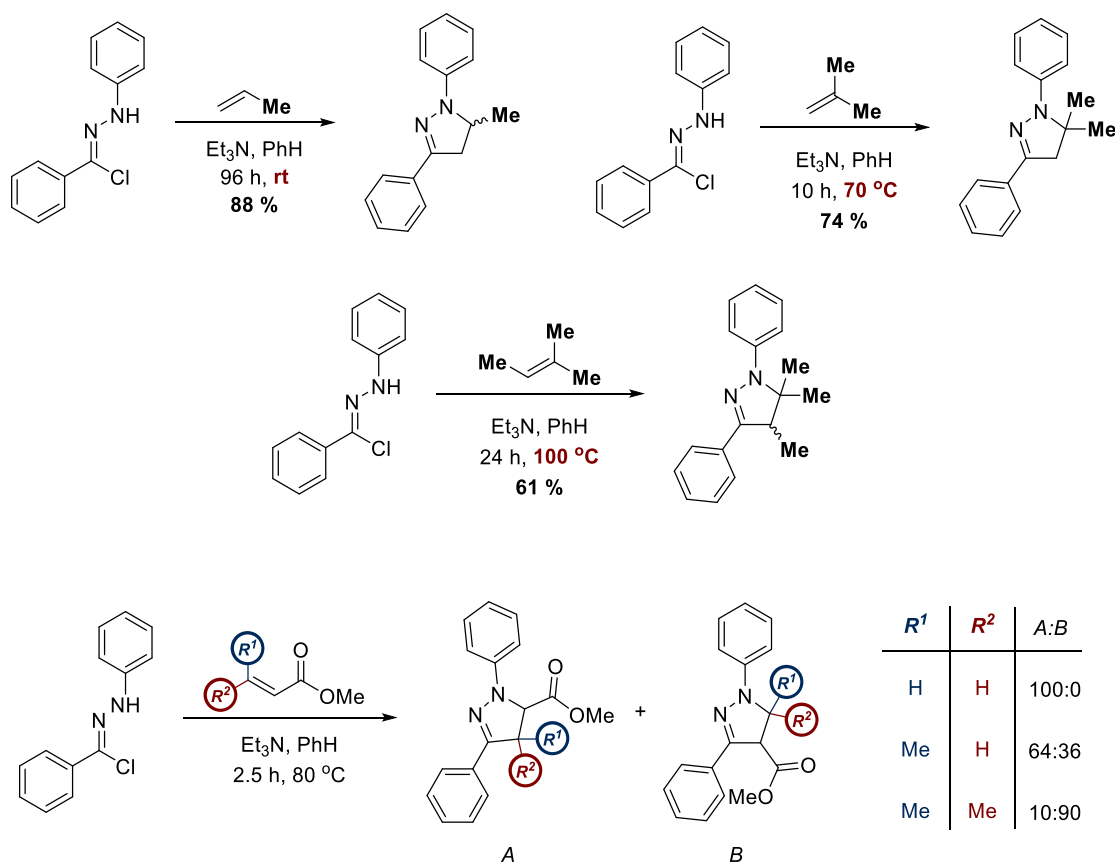


Scheme 1.20: While more forcing reaction conditions are required for NI cycloaddition with increasing steric bulk, regioselectivity consistently favours the 5-substituted regioisomer

While this technique is commonly used in the literature to predict or account for NI regioselectivity, it is not universal, nor quantitative. More recent approaches have employed density functional theory (DFT) as a tool to understand the regioselectivity of NI cycloadditions.[108,109] The application of concepts such as hard-soft acid-base theory, molecular electron density theory, relative electrophilicity and Fukui functions within these higher levels of theory have enabled a much more accurate understanding of NI regioselectivity, including quantitative predictions in some instances.[110,111]

However, despite these significant advances, regioselectivty in NI cycloadditions remains difficult to predict or rationalise. While the vast majority of cases of mono-substituted

alkenes and alkynes yield the 5-substituted product [112], there are numerous exceptions, hindering the development of a general set of rules. While FMO[113,114] and DFT[115,116] calculations have both aided in rationalising unexpected results, neither have demonstrated satisfactory levels of accuracy in their broader prediction methods.

One curious exception to this unpredictable regioselectivity is the use of enamines as dipolarophiles. Vicinal enamines exhibit exclusive regioselectivity for the 4-substituted pyrazoline product, apparently in contrast to the combined steric and electronic influences that direct most other functional groups to the 5-position.[7,117] This is discussed in more detail in *Section 1.3.2.5*.

### 1.3.1.2 Rate of Reaction

The rate of reaction of NIs with dipolarophiles can be significantly influenced by both electronic and steric effects, and is rationalised very effectively by FMO theory.[105] In this context, NIs are considered to be "type II" dipoles, meaning that interactions between both the HOMO of the dipole and the LUMO of the dipolarophile *and* the interactions of the LUMO of the dipole and the HOMO of the dipolarophile may have an impact on reaction rate.[118] Consequently, any form of substitution of the dipolarophile, electron-donating or electron-withdrawing, will increase reaction rate, with ethene the least reactive olefin species in NI cycloadditions. Indeed, all alkenes with no form of conjugative electronic activation are very poor substrates, requiring large excesses or forcing conditions to generate the desired product.[5] This trend was first proposed by Sustmann in 1971, and confirmed experimentally by Tomaschewski in the early 1990s using diphenyl NI, where it was shown that a plot of substituent ionisation potential versus reaction rate generated a characteristic parabolic curve, with an unsubstituted olefin as the point of inflection (*Graph 1.2*).[118,119]

Substitution of the NI dipole can alter this reactivity profile significantly. In particular, the NI can be transformed into a pseudo type I dipole *via* the attachment of electron-donating groups. This occurs by raising the LUMO energy of the dipole to the point where LUMO-dipole-HOMO-dipolarophile interactions are no longer significant. Unsurprisingly, this further increases the reactivity of the NI with electron-deficient dipolarophiles, while neutralising the reactivity of electron-rich dipolarophiles.[119–121] This approach requires the substitution of the *N*-terminus of the NI, as substitution of the *C*-terminus is less effective in raising the orbital energy.[121]

*Graph 1.2: The relative reaction rates of different dipolarophiles in NI 1,3-dipolar cycloaddition reactions with diphenyl NI*

The relief of ring strain can also have a beneficial impact on reaction rate. Numerous examples in the literature document increases of 20 to 50-fold when using strained cyclic systems relative to their linear analogues.[8,122,123] Of particular note are the rapid cycloaddition rates of cyclooctenes and spiro[2.3]hex-1-ene, both of which offer substantial enhancement even relative to other strained systems.[122,123]. A more hydrophilic strained cyclopropenyl system, azaspiro[2.3]hex-1-ene, has also recently been reported (*Figure 1.4*).[124]



*Figure 1.4: Two examples of strained dipolarophiles designed to increase the rate of NI cycloaddition*

Increased steric bulk has a detrimental effect on reaction rate, and while disubstituted alkenes are typically competent substrates, trisubstituted olefins react much more slowly.[5–8]

Tetrasubstituted systems will not normally undergo cycloaddition, with only certain substrates compatible *via* substantial electronic activation (*Scheme 1.21*).[8]
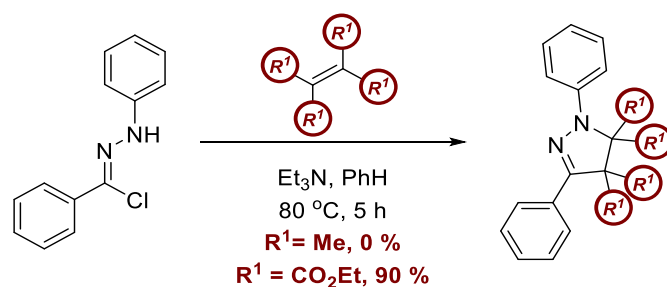


*Scheme 1.21: Electronic activation can have a substantial impact on conversions in NI cycloadditions*

Several additional effects should also be considered when evaluating the rate of NI cycloaddition. For instance, *trans* alkenes are much more competent substrates than the corresponding *cis* isomers, and are also typically several orders of magnitude more reactive than the analogous alkyne (*Scheme 1.22*).[5] The exact origins of these effects remain unclear, but may be partially explained by the efficiency of orbital overlap during the respective transition states.
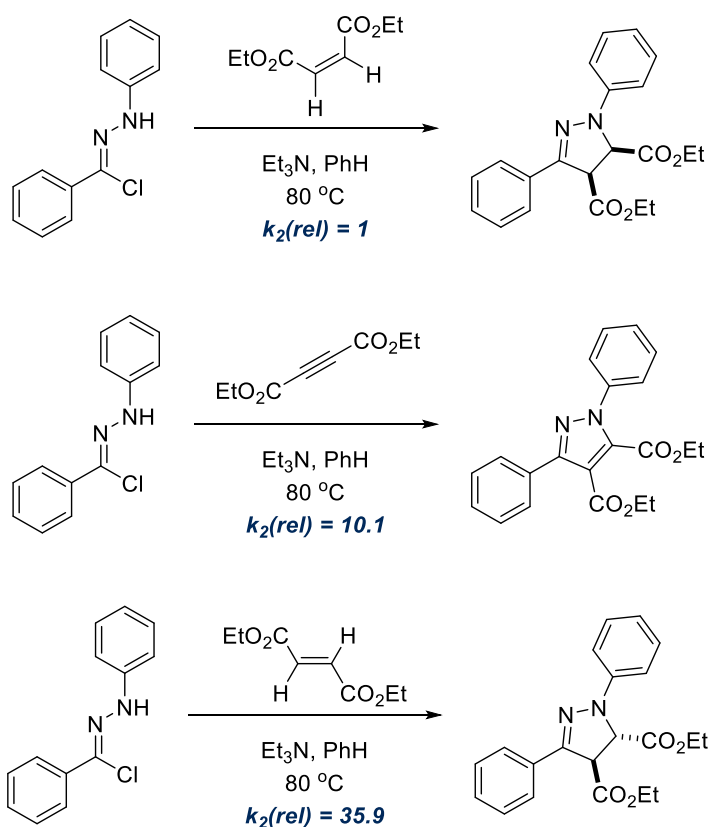


*Scheme 1.22: The relative reaction rates of NI 1,3-dipolar cycloaddition with 3 similar substrates*

The influence of entropy on cycloaddition rate should also be noted. Competition experiments have determined that intramolecular cycloadditions between NIs and electronically neutral alkenes have similar reaction rates to intermolecular cycloadditions

with electronically activated alkenes.[92] This can be rationalised by considering the highly ordered transition state of a cycloaddition reaction, meaning that the high entropy penalty required for the intermolecular process cannot always be fully negated by electronic activation of the substrate.

When using a reversible source of NI, the rate of dipole generation can also impact the rate of cycloaddition. In the case of hydrazonyl chlorides, both increasing pH and decreasing chloride concentration have a positive impact on reaction rate.[125]

### 1.3.1.3 Carbon-Carbon Double Bonds

NIs were first shown to undergo 1,3-dipolar cycloaddition with alkenes by Huisgen in his initial report, yielding the expected pyrazoline from diphenyl NI and dicyclopentene (*Scheme 1.11*).[1] This scope was expanded considerably in 1962, when Huisgen outlined the reactivity of NIs with a comprehensive library of dipolarophiles.[16]

In the decades that have followed, numerous research groups have demonstrated that 1,3-dipolar cycloaddition between NIs and alkenes is a facile and robust reaction, applicable to a broad palette of compounds. Examples range from relatively unreactive unconjugated alkenes,[5,92] through aryl and vinyl olefins,[6,126,127] and to highly activated species such as α-β unsaturated carbonyls and vinyl sulfoxides (*Scheme 1.23*).[7,128,129]
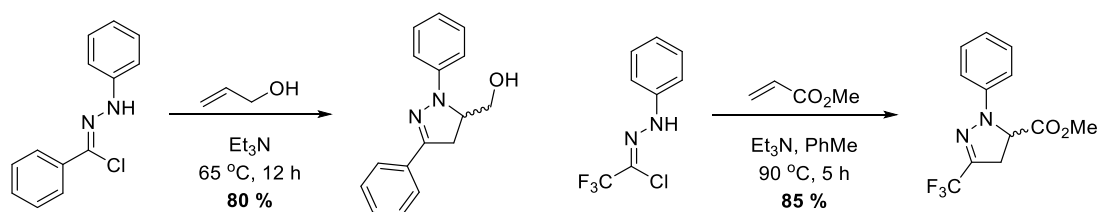


Scheme 1.23: A brief example of known NI cycloadditions

In addition to these intermolecular cycloadditions, intramolecular reports are equally prevalent. This was first exemplified by Zecchi in 1977, 3 years after the same author had performed the reaction using an alkyne intramolecular dipolarophile (*Scheme 1.24*).[130,131] While more synthetically challenging to install both the dipolarophile and dipole precursor within the same molecule, intramolecular cycloaddition has multiple advantages over intermolecular cycloaddition. Depending on the attachment of the "tether" between the reagents, the regioselectivity rules discussed above may be overridden. Furthermore, cyclisation of a single molecule negates the significant entropy penalty encountered during the highly ordered transition state of a 1,3-dipolar cycloaddition. This means that unactivated dipolarophiles that may have otherwise required vast excesses or extremely high temperatures can instead be cyclised in good yields using milder conditions.[92]
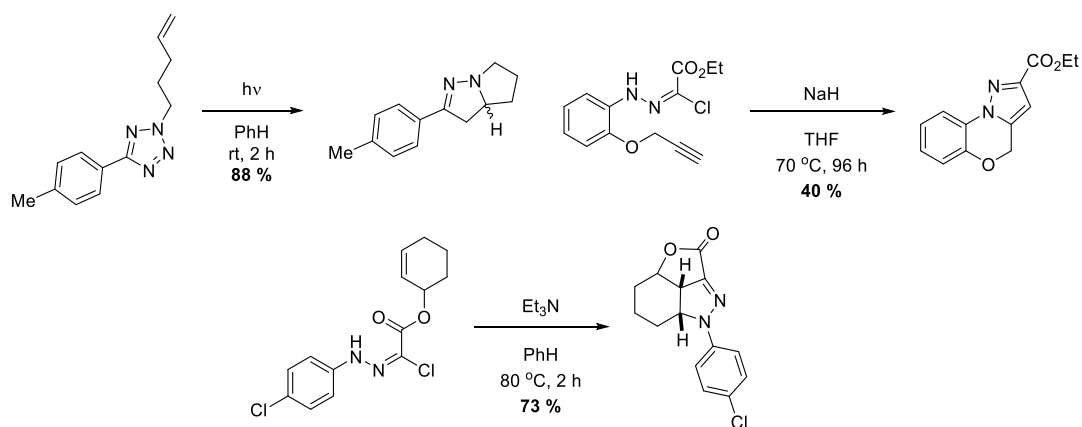
*Scheme 1.24: The intramolecular cycloadditions of NIs*

Multiple NI precursors have been employed in the synthesis of pyrazolines. Hydrazonyl halides are the most common in both intermolecular and intramolecular examples,[127,132–134] however there are also numerous examples involving the photolysis and thermolysis of tetrazoles.[1,135–137] Examples of sydnone photolysis also exist, but are less common.[138,139]

One additional point of complexity to consider in NI-alkene cycloaddition is the formation of up to two contiguous stereocentres. Engineering a stereoselective 1,3-dipolar cycloaddition is extremely challenging, as regio-, diastereo- and enantioselectivity must all be carefully controlled. Nevertheless, multiple examples of both diastereoselective and even enantioselective NI cycloadditions exist.

The simplest method of generating stereoselectivity is *via* substrate control, with the presence of a chiral centre elsewhere in the molecule. This was initially exemplified in 1998 using both Fischer carbene complexes and simple carbohydrates as directing groups in separate NI cycloadditions (*Scheme 1.25*).[140,141] These procedures and others have demonstrated impressive diastereomeric ratio (dr) values.[142,143]
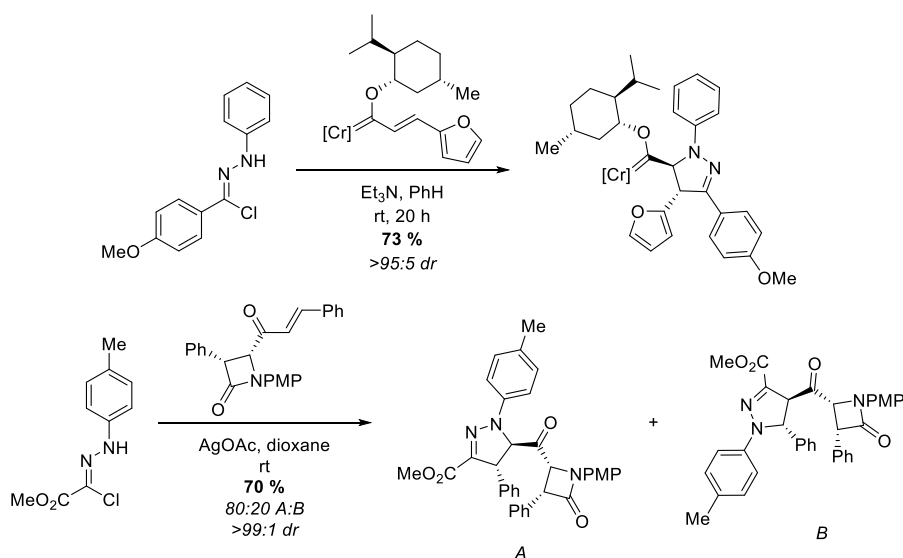


*Scheme 1.25: Diastereoselectivity via substrate control in the NI cycloaddition*

The first intramolecular example was published in 1999, with stereo-induction *via* a chiral ester vinylic to the dipolarophile.[144] While low levels of diastereoselectivity were achieved, stereochemical induction through an existing chiral centre is significantly more challenging in intramolecular examples than intermolecular examples. Regardless, numerous reports exist with chiral directing groups adjacent to both the dipolarophile,[145–147] and the NI precursor (*Scheme 1.26*).[148]
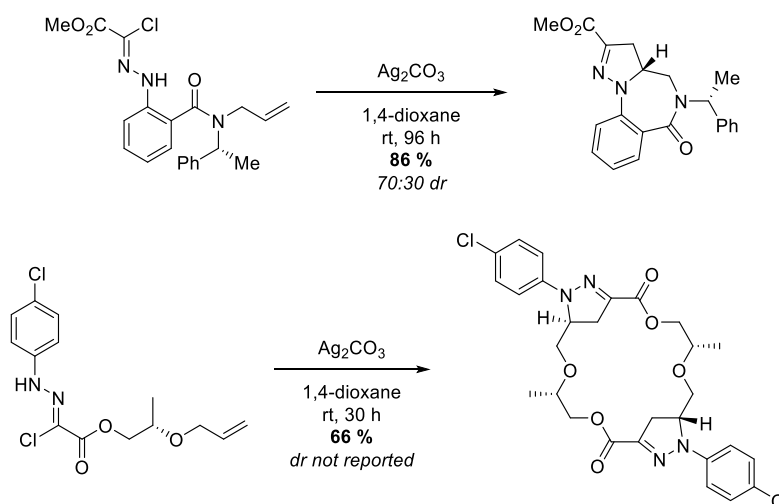


*Scheme 1.26: Preparation of enantiopure cycloadducts via substrate control*

Enantioselective examples of NI cycloaddition are less common and cannot be generated by chiral directing groups alone. Instead, a Lewis acid catalyst and chiral ligand must be employed, as was first documented by Sibi in 2005, where a simple diaryl NI was shown to cyclise enantioselectively with a dipolarophile containing an oxazolidinone moiety (*Scheme 1.27*).[149,150] Stereochemical induction was accomplished through the use of magnesium triflate as a Lewis acid in conjunction with a bespoke chiral ligand. Mechanistically, the oxazolidinone functioned as a directing group, complexing with the Lewis acid and establishing the regioselectivity. Enantioselectivity was achieved *via* coordination of the chiral ligand, shielding one face of the dipolarophile and leaving only one orientation from which the NI may undergo cycloaddition. This was a versatile transformation and proceeded with >99 % enantiomeric excess (ee) in almost all cases.
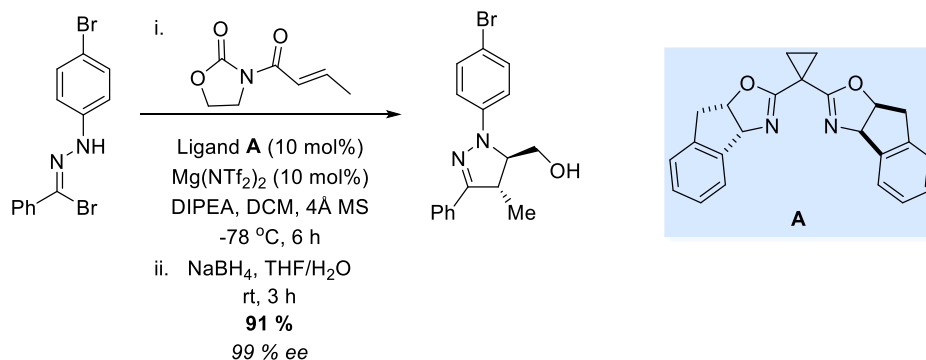


*Scheme 1.27: Enantioselective NI 1,3-dipolar cycloaddition facilitated by a chiral ligand and Lewis acid*

23

Further examples of enantioselective NI cyclisation have since followed, but all rely on the same general approach of stereo-induction through a Lewis acid and chiral ligand (*Scheme 1.28*).[151,152] It is essential that the dipolarophile also contains an appropriate directing group for coordination to the Lewis acid, either as part of the substrate or as a removable auxiliary group.
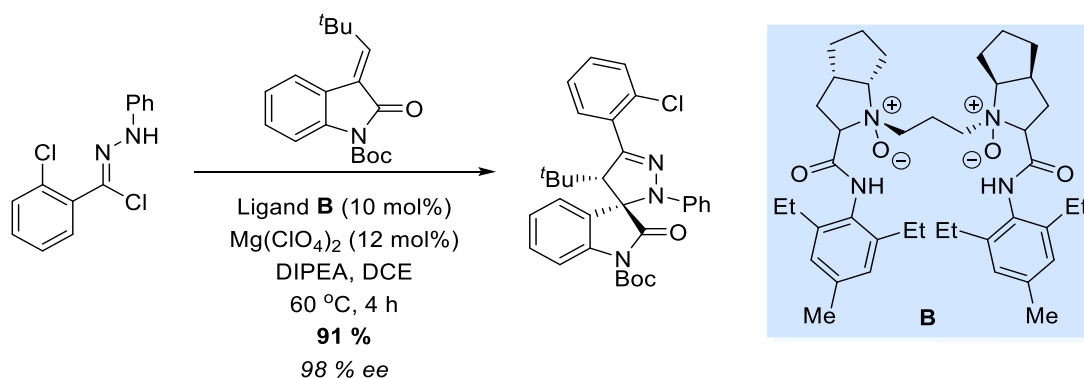


*Scheme 1.28: A further example of enantioselective 1,3-dipolar cycloaddition using an NI*

### 1.3.1.4 Carbon-Carbon Triple Bonds

NIs may also undergo 1,3-dipolar cycloaddition with alkynyl functionalities, furnishing pyrazoles. This was first demonstrated in 1962, with the scope later expanding significantly (*Scheme 1.29*).[6,7,16]
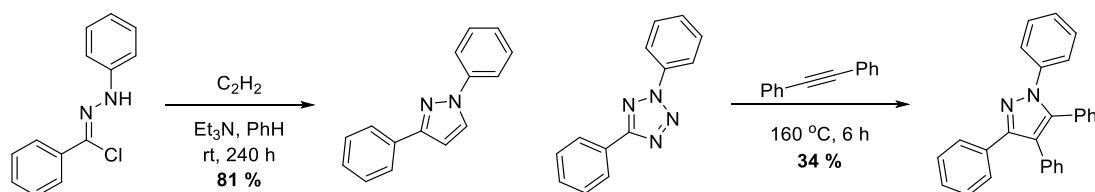


*Scheme 1.29: Initial examples of NI cycloaddition with alkynes*

Alkynes are less reactive towards NIs than the analogous *trans*-alkenes, by a factor of 12-14.[8] Most literature examples which involve alkyne cycloaddition are intramolecular, employ electronically-activated substrates, or require extremely forcing conditions (*Scheme 1.30*).[130,132,153–155] An accessible approach towards NI cycloaddition with acetylene itself was recently developed by Ananikov, through the generation of the gas *in situ* from $CaC_2$ and water.[156]
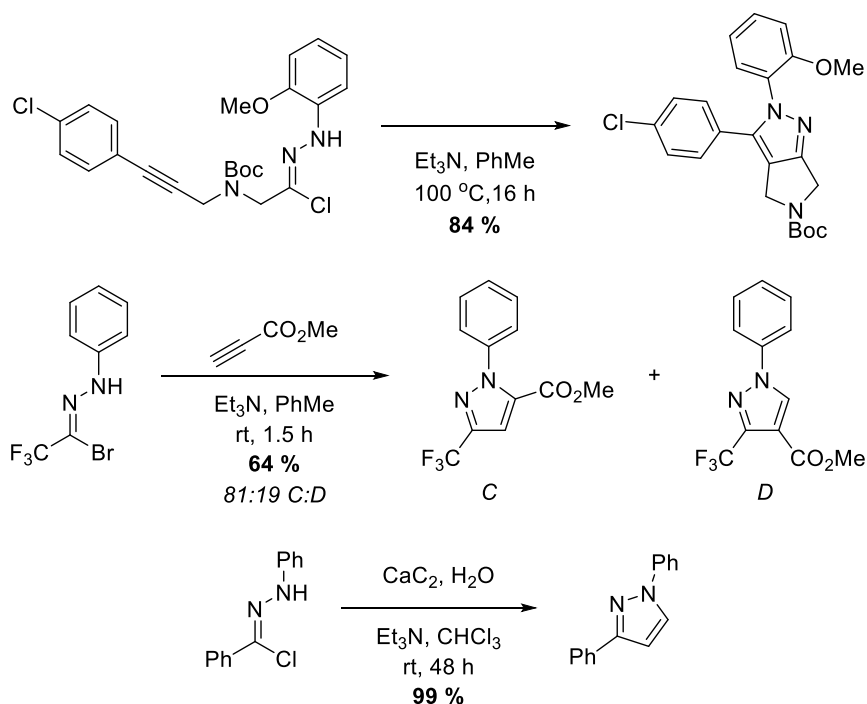
*Scheme 1.30: Further examples of the cycloaddition of acetylenes with NIs*

Benzynes have also been shown by Moses to be a competent dipolarophile, providing facile access to a range of indazoles (*Scheme 1.31*).[157] The extremely reactive nature of this highly strained intermediate presents challenges in the optimisation of such a transformation.[158] Precedent indicates that the use of a hydrazonyl halide as the NI source is required, enabling an appropriate base to form both the NI and benzyne from their relevant precursors at similar rates.
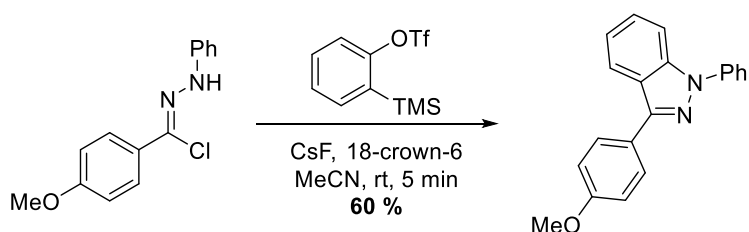


*Scheme 1.31: The cycloaddition of NIs and benzynes*

The reaction of terminal alkynes with NIs is also open to an alternative mode of reactivity. The enhanced acidity of the alkyne proton facilitates the potential nucleophilic attack of the corresponding anion at the neutral terminus of the NI (*Scheme 1.32*).[159] This complicates the use of these species, however, the process could likely be avoided through selection of an appropriate base. It should be noted that this unexpected product was later found to spontaneously cyclise to afford the desired pyrazole.
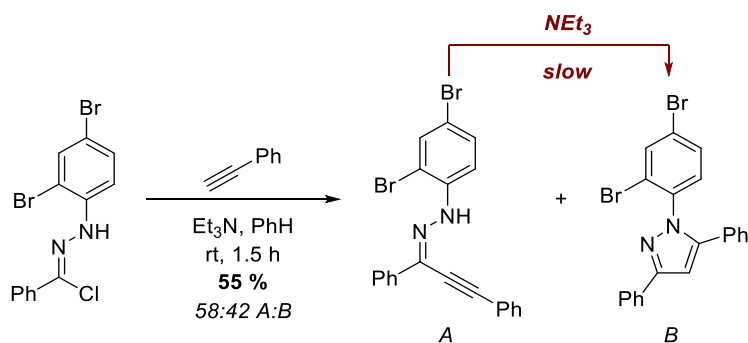
*Scheme 1.32: The formation of an unexpected alkyne-NI adduct prior to pyrazole formation*

### 1.3.2    Nucleophiles

Although not as prolific as 1,3-dipolar cycloaddition, NIs react with various nucleophiles by the general mechanism shown in *Scheme 1.33*. The primary product of all reactions is the general motif shown, with the formation of a carbon-heteroatom bond at the *C*-terminus of the NI, and protonation of the *N*-terminus. The structure may undergo further intramolecular rearrangement in some cases, but this is the primary product of all nucleophilic addition reactions of NIs.
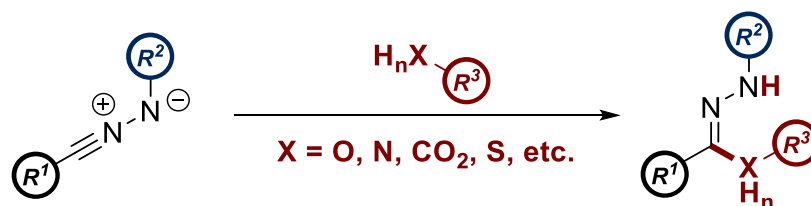


*Scheme 1.33: The general reaction mechanism by which nucleophiles react with NIs*

It was believed that the rate of reactivity of NIs with these nucleophilic species was many times lower than that of dipolarophiles. Recent publications, however, have demonstrated that certain functional groups may compromise the orthogonality of the NI-alkene cycloaddition.[160,161]

### 1.3.2.1 Alcohols

Alcohols may react with NIs to generate the corresponding hydrazonyl ester. This reactivity was exemplified in Huisgen's initial publication in 1959, however the species isolated was in fact a diphenyl hydrazide (*Scheme 1.34*).[1] Huisgen proposed that migration of the aryl group was driven by the formation of a thermodynamically favourable amide bond.[12]
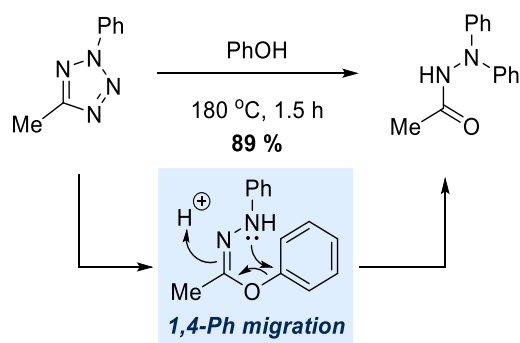
*Scheme 1.34: Huisgen's initial report into the reaction of phenol with an NI*

Later studies demonstrated that isolation of the primary adduct is also possible, and that hydrazide formation requires substantial heating (*Scheme 1.35*).[162] Work from Tomaschewski also argued against a purely intramolecular mechanism of rearrangement, as heating the primary product in different alcohols gave mixtures of final products.[162]
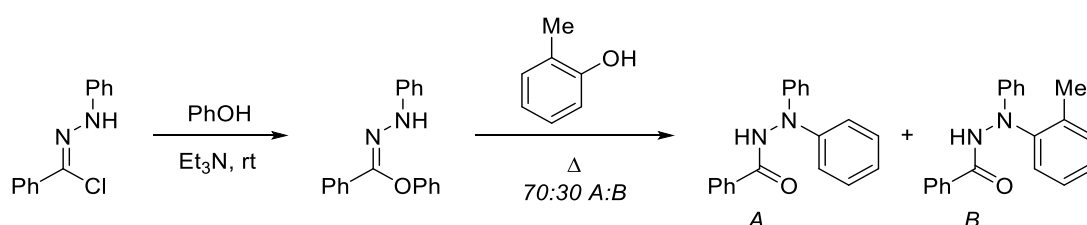


*Scheme 1.35: Further mechanistic insight into the reaction of NIs with alcohols*

The reactivity of alcohols with NIs is very low in comparison to other nucleophiles and dipolarophiles, and is almost always less efficient.[160] All literature examples of this transformation require the presence of vast excesses of the alcohol, and the adducts are only likely to be observed through the use of a solvent such as water, methanol or phenol.[163,164]

### 1.3.2.2 Amines

As with alcohols, amines will add to NIs in the manner outlined above, as was also exemplified in 1959, with an expanded study reported 2 years later (*Scheme 1.36*).[1,12] The primary product of this addition is more stable than the alcohol adduct, and hence no spontaneous rearrangements were observed.
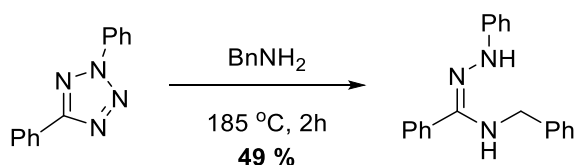


*Scheme 1.36: Huisgen's initial work in the use of amines as NI nucleophiles*

As may be anticipated when considering the relative nucleophilicities, nitrogen-based nucleophiles are considerably more reactive towards NI dipoles than alcohols.[160] This

27

negates the requirement for superstoichiometric quantities of the amine within the reaction mixture, meaning this procedure has seen more extensive application.

The most frequent adaption has been in the synthesis of five, six and seven-membered heterocycles.[165–173] This is typically accomplished through the use of a nitrogenous nucleophile containing a pendant acid or ester group, with spontaneous lactamisation occurring upon formation of the primary addition product.[171,172] Further examples can be found where the use of a coupling agent is necessary to facilitate lactamisation, while others have utilised a cyanamide moiety in the formation of cyclic guanidine derivatives (*Scheme 1.37*).[167–169,174]
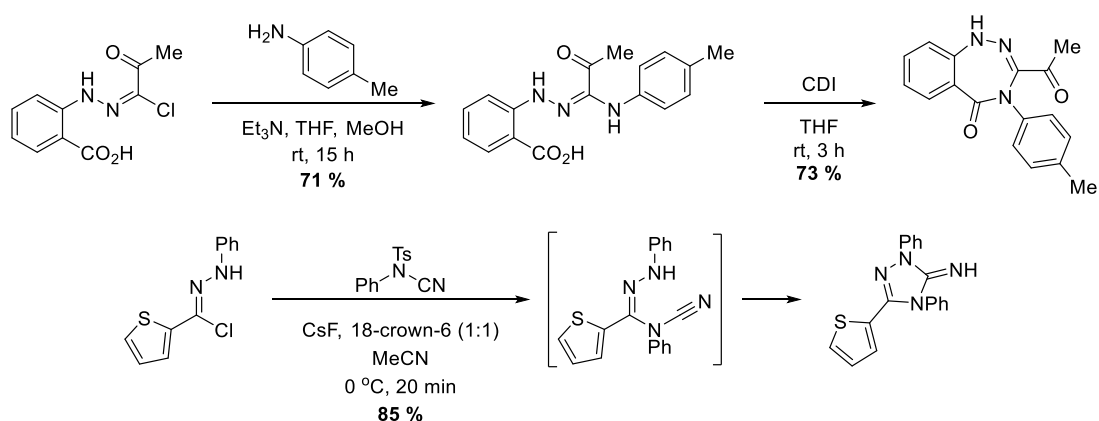


*Scheme 1.37: Two examples of the cyclisation of primary products of nucleophilic amine addition*

### 1.3.2.3 Thiols

Thiols react with NIs through the classic addition mechanism outlined above to yield α-mercaptohydrazones. This was first discovered by Huisgen in 1959 using diphenyl NI and thiophenol, and further elucidated by the same author in 1961 (*Scheme 1.38*).[1,12]
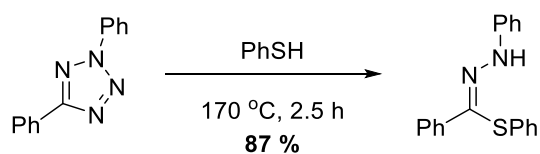


*Scheme 1.38: Huisgen's initial example of thiol as a NI nucleophile*

The reactivity of thiols with NIs is analogous to amines. While facile, the reaction does not furnish a product of particular synthetic value. Consequently, the main application of this reaction is in the synthesis of sulfur-containing heterocycles. Employing a similar strategy as above, a pendant carboxylic acid or ester typically serves as a means of cyclisation after the nucleophilic addition of the thiol (*Scheme 1.39*).[171,175–178]
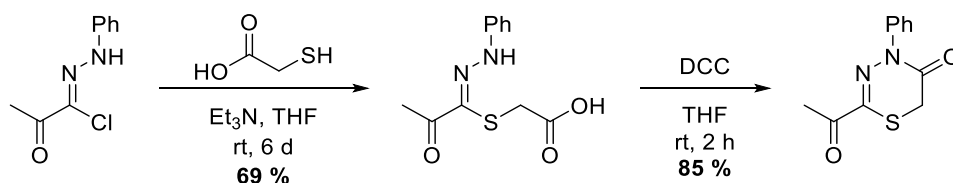
*Scheme 1.39: The application of thiol nucleophilicity in the synthesis of sulfur-containing heterocycles*

The addition of thiols to NIs is highly efficient and has been responsible for the generation of multiple unexpected by-products. This is typically observed in attempted 1,3-dipolar cycloadditions using sulfur containing-substrates (*Scheme 1.40*).[161,179,180] In some instances, control experiments indicated that the desired cycloaddition products were formed when exchanging the sulfur for an oxygen atom.[179] Thiols can also out-compete both amines and carboxylic acids in reactions with NIs.[160,176] However, more recent studies have suggested that the order of reactivity of NIs can be established as acids > thiols >> amines.[161]
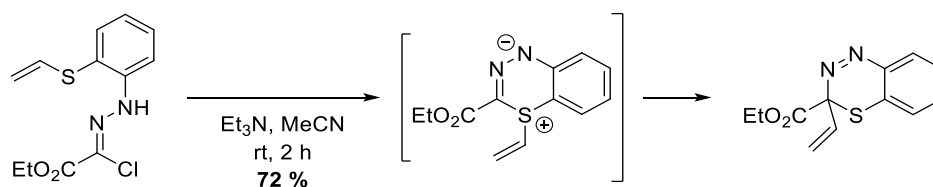


*Scheme 1.40: The high reactivity of sulfides with NIs can often lead to unexpected rearrangement products when attempting a 1,3-dipolar cycloaddition*

### 1.3.2.4 Carboxylic Acids

First reported in 1961,[12] the reaction of carboxylic acids and NIs serves as another example where the primary nucleophilic adduct was not isolated as part of the initial study, with a *bis*-hydrazide formed in 83% yield (*Scheme 1.41*). Huisgen proposed a similar mechanism to that of the alcohol rearrangement, with a 1,4-acyl shift furnishing a stable product with two amide bonds.
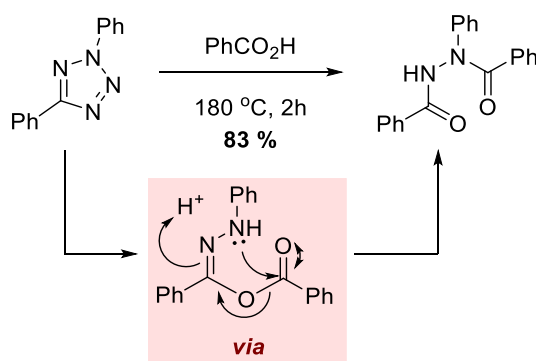


*Scheme 1.41: The first example of carboxylic acids acting as an NI nucleophile and the hypothesised mechanism of their addition*

However, unlike the reaction between an NI and an alcohol, the reactivity of a carboxylic acid is extremely favourable, and can outcompete both dipolarophiles and other nucleophiles.[161] In the reaction between diphenyl NI and acetic acid, low-temperature

spectroscopic techniques show the formation of the primary nucleophilic adduct at -135 °C, with rearrangement to the *bis*-hydrazide occurring at around -70 °C (*Scheme 1.42*).[34,181] In contrast to other nucleophiles, it is likely that deprotonation of the acid by the NI occurs prior to addition to the electrophilic centre. This may account for the increased reactivity of the carboxylate relative to other neutral species.
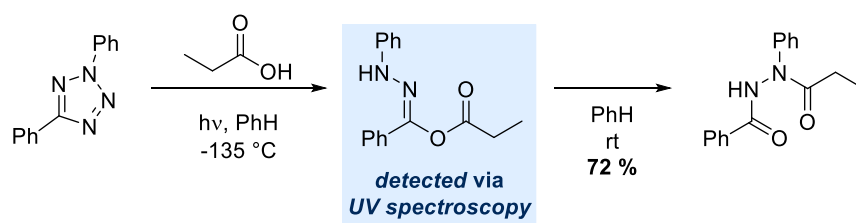


*Scheme 1.42: Further mechanistic insight into the reaction of NIs and carboxylic acids*

Despite this unprecedented and efficient reactivity, very few publications exploited this reaction between the 1960s and 2010s. Most reports noting the formation of these products mention them only as a side product, either through the use of an acetate buffer or acetic acid as a reaction solvent, or as an alternative method of NI trapping.[163,164,181] Only in recent years has the reactivity of NIs with carboxylic acids been reassessed.[161,182] Additional applications have since emerged both as a photoaffinity label in biochemistry, and as a ligating agent in materials chemistry (*Sections 1.4.1.2* and *1.4.2.3*).[183–185]

### 1.3.2.5 Enamines and Enol Ethers

The reactivity of NIs with enamines was first discovered in 1967.[7] They represent intriguing substrates, as they can be treated as either a dipolarophile or a nucleophile. In his initial report, Huisgen isolated the pyrazoles that would be expected by a 1,3-dipolar cycloaddition followed by elimination (*Scheme 1.43*). The enamines were also shown to react very efficiently, again consistent with a cycloaddition. As a type II dipole, both the LUMO and the HOMO of the NI are available for mixing with the complementary orbital of the dipolarophile.[104] The highly electron-donating effect of an enamine would raise the HOMO of the dipolarophile significantly, facilitating better overlap with the LUMO of the NI and improving reactivity.
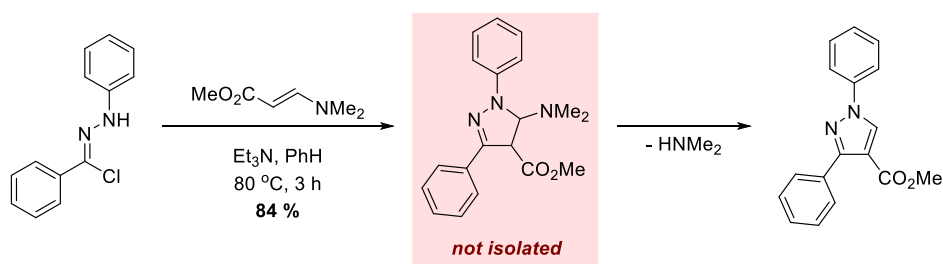


*Scheme 1.43: Enamine dipolarophiles exhibit absolute regioselectivity in NI dipolar cycloadditions*

While all of the above evidence was indicative of a 1,3-dipolar cycloaddition mechanism, some curiosities remained. It was possible that the assumed pyrazoline was itself the secondary product of the reaction, with an initial hydrazone being formed by the nucleophilic attack of the enamine onto the *C*-terminus of the NI (*Scheme 1.44*). Quenching of the generated iminium by the *N*-terminus would yield the same product. Furthermore, the use of an enamine had some peculiar influences on the regiochemistry of the reaction. In contrast to most other dipolarophiles, enamine substrates generate a single regioisomer, yielding 5-aminopyrazolines. This anomaly could indicate a sequential nucleophilic addition/cyclisation mechanism, as opposed to a 1,3-dipolar cycloaddition.
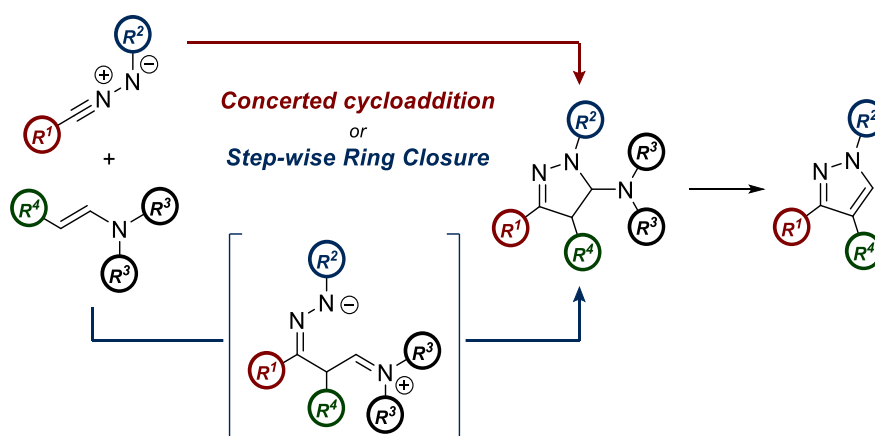


*Scheme 1.44: The two potential modes of cyclisation proposed for enamine dipolarophiles*

This issue is further complicated when exploring further literature (*Scheme 1.45*). A number of publications document the use of enamines as NI nucleophiles, isolating the corresponding hydrazonyl adduct.[186–190] However, others highlight the formation of pyrazolines or pyrazoles exclusively, with no mention of any isolated intermediates.[19,57,191–194] The mechanism of this transformation has recently been examined computationally, with the transition state being reported as an asynchronous cycloaddition.[117] While the reaction may not be fully synchronous, the absence of an energy minimum between the starting materials and product is indicative of a 1,3-dipolar cycloaddition. However, the isolation of a range of nucleophilic adducts in the literature suggests that the true reactivity of enamines with NIs may be substrate dependent.
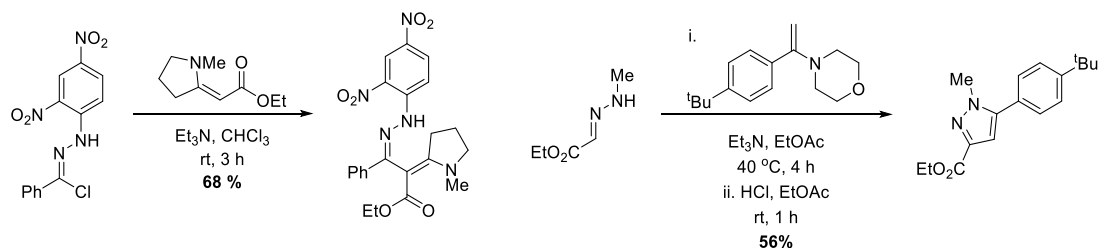


*Scheme 1.45: Two different reactivity profiles of enamines and NIs have both been widely reported throughout the literature*

Regardless of mechanism, the enamine system remains the only directing group within NI cycloaddition chemistry with exclusive selectivity for the 5-position of the pyrazoline, a valuable attribute in synthetic applications. Additionally, the corresponding ammonium species can be treated as an excellent leaving group in many of the pyrazoline products. These two characteristics, combined with the facile nature of the reaction, has made this transformation an excellent method for the regiospecific preparation of pyrazoles. This is typically accomplished through the use of a simple enamine as a directing group, which is eliminated from the product after treatment with an acid or base (*Scheme 1.46*). Examples from the literature have utilised morpholine,[19,191,192] piperazine[193] and dimethylamine[190] as directing groups.
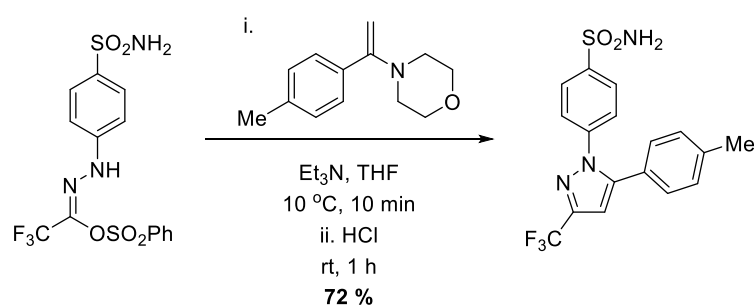


*Scheme 1.46: A further example of enamines as a NI cycloaddition directing group*

Recent work by Jasinski has also capitalised on the remarkable regioselectivity of these systems through the use of enol ethers as dipolarophiles (*Scheme 1.47*).[195] As with enamines, elimination of the "directing group" following cycloaddition leads to the isolation of the aromatic pyrazole with complete regioselectivity.
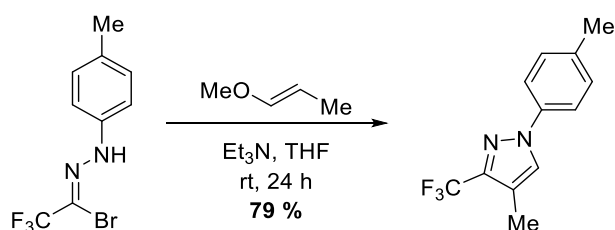


*Scheme 1.47: The application of enol ethers in the regioselective synthesis of pyrazoles*

### 1.3.3 Dimerisation

In the absence of an appropriate dipolarophile or nucleophile, two equivalents of NI may react with one another, leading to dimerisation products. The reaction conditions can prove extremely important in dictating the exact product, with NIs able to yield either a 1,2,4,5-dihydrotetrazine or a 1,2,3-triazole, with compelling evidence for the formation of both species reported.

There are two initial modes of NI dimerisation, with two equivalents combining in either a "head-to-tail" or "head-to-head" manner. Both processes yield dihydrotetrazines: the 1,2,4,5-

analogue in the case of the former and the 1,2,3,4-analogue in the case of the latter (*Scheme 1.48*). However, the 1,2,3,4-dihydrotetrazine species may undergo cycloreversion to generate a *bis*-azoethylene. This compound can undergo either thermal or photochemical ring closure, generating one equivalent of the 1,2,3-triazole and the corresponding nitrene.[196,197]
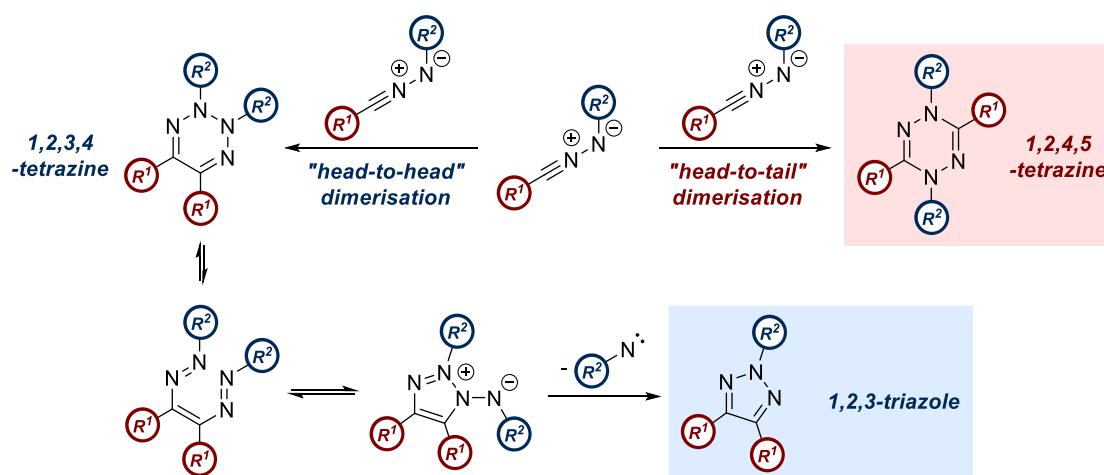


*Scheme 1.48: The two modes of dimerisation observed in NI chemistry*

As previously mentioned, the nature of the species formed depends entirely upon the reaction conditions, which are likely derived from the source of NI (*Scheme 1.49*). For example, under the thermal conditions employed when using hydrazonyl halides or tetrazole thermoylsis, the 1,2,4,5-dihydrotetrazine dimer forms exclusively.[4,12,198–200] Further study has suggested that this species is quite stable, and is unlikely to regenerate NIs under typical reaction conditions.[201]
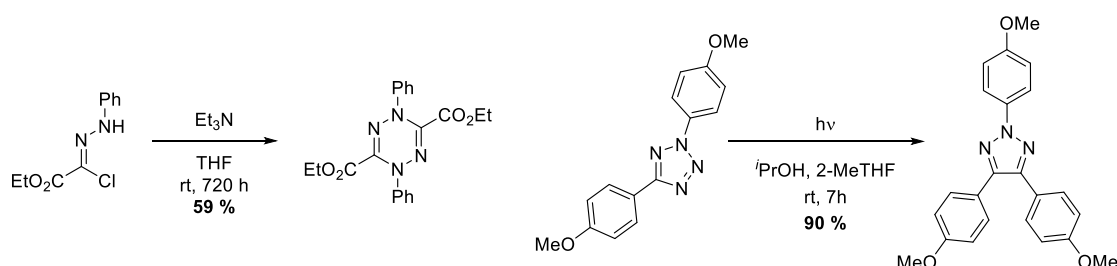


*Scheme 1.49: Examples of NI dimerisation*

Conversely, photochemical generation of the NI from tetrazoles or sydnones overwhelmingly favours the formation of 1,2,3-triazoles.[75,102,201–205] The intermediate *bis*-azoethylene is commonly isolated in smaller amounts, perhaps as expulsion of the nitrene to facilitate triazole formation may require slightly more forcing conditions than the initial photolysis.[196,197,202]

The exact nature of this difference in reactivity remains relatively under-explored, with a number of reports failing to account for the preference of either pathway. Control experiments have shown the formation of the 1,2,4,5-dihydrotetrazine to be irreversible

under photochemical conditions, meaning an alternative explanation is required to account for the complete selectivity for the formation of the 1,2,3,4-dihydrotetrazine.[201] The issue is complicated by the fact that the formation of 1,2,3-triazole is feasible in the absence of UV light, meaning its limited formation relative to 1,2,4,5-tetrazine under thermal conditions is also unexplained.

### 1.3.4 Decomposition

In the absence of an appropriate reaction partner and at sufficient dilutions to inhibit dimerisation, NIs will decompose to yield a number of simpler constituents. This is only applicable to irreversible methods of NI generation, such as 2,5-tetrazoles or sydnones, as species such as hydrazonyl chlorides will maintain an equilibrium between the NI and the precursor until the reaction is quenched.

The principal product of NI decomposition is the corresponding carbodiimide isomer. This can be generated thermally,[204] but can also be accelerated through photolysis of the NI.[36,206,207] The exact nature of this rearrangement was presumed for many years to proceed *via* a diazirine intermediate,[36,207] which was finally confirmed by Nunes in 2014 in a report that fully detailed the decomposition pathway of NIs (*Scheme 1.50*).[44] Initial isomerisation to the diazirine may be followed by two competing degradation pathways. The more dominant of these is further rearrangement into the carbodiimide, however formation of the corresponding nitrile of the *C*-terminal substituent is also possible. The *N*-terminal substituent is expelled as a nitrene in this instance, generating the corresponding aniline. This degradation pathway has been shown to be active in a number of NI species.[31,44,206,208]
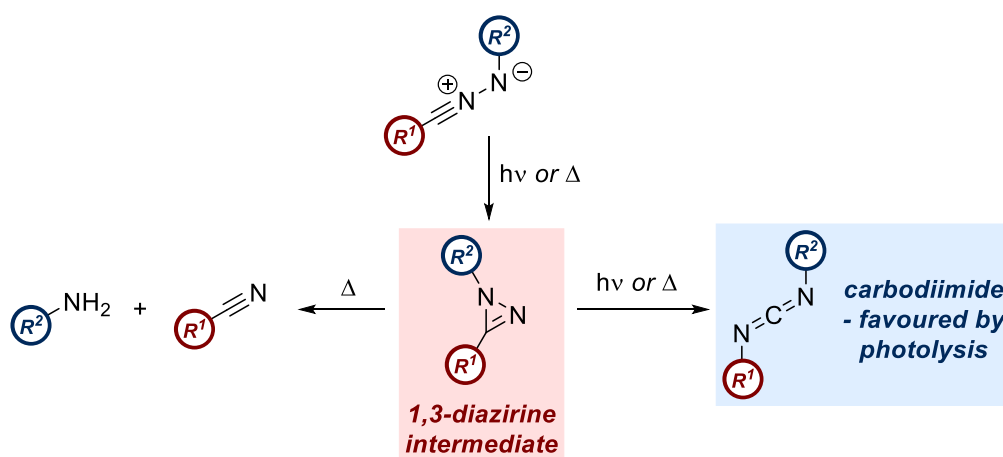


Scheme 1.50: Decomposition pathways of the NI in the absence of a suitable reaction partner

## 1.4 Applications of Nitrile Imine Derivatives

Given the range of processes in which NI species participate, it is unsurprising that several different fields have developed a raft of applications of the dipole. While naturally finding widespread use within general synthetic chemistry, [19,135,191,193,209–211] NIs are most prolific in

bioorthogonal and materials science. The applications of the latter two fields will be covered in this section, owing to their increasing presence within recent scientific literature.

## 1.4.1 Bioorthogonal Chemistry

The facile and often quantitative nature of 1,3-dipolar cycloadditions are well documented, often falling under the moniker of "click" chemistry.[212] The cycloaddition between NIs and alkenes specifically has long been considered orthogonal, and consequently NI cycloadditions have enjoyed widespread application over the past decade as a bioorthogonal labelling tool.[62,213–215] Photolysis of a 2,5-diaryl tetrazole is typically the preferred source of the dipole within this manifold, due to the traceless nature of the reaction. As this represents a photochemical, high yielding transformation between two non-endogenous functional handles with minimal by-product formation, the term "photoclick" is commonly used to describe the procedure.[216]

### 1.4.1.1 Protein Ligation

Lin introduced the concept of protein conjugation through NI cycloaddition in 2008.[217] A 2,5-tetrazole was incorporated into lysozyme and green fluorescent protein through simple amidation chemistry, before the formation of a pyrazoline adduct *via* treatment of the proteins with acrylamide following liberation of the NI. Later the same year, Lin employed the 2,5-tetrazole as the ligating agent. Incorporation of *O*-allyltyrosine into Z-domain protein furnished the augmented dipolarophile, which was rapidly modified when exposed to the relevant NI (*Scheme 1.51*).[216] One of the immediately apparent advantages of photoclick chemistry was that the pyrazoline products were intrinsically fluorescent, and as a consequence this represented self-reporting ligation methodology.
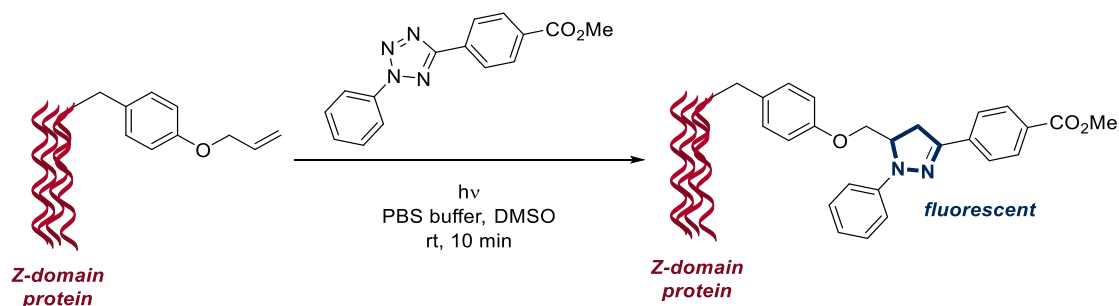


*Scheme 1.51: Incorporation of a dipolarophile within a protein and its subsequent ligation using NI chemistry*

Subsequent reports have since further optimised this procedure through the modification of both partners. Firstly, the reactivity of the NI itself may be enhanced through careful control of the energy levels of its molecular orbitals. For example, when using an allyltyrosine-modified protein as a dipolarophile, appropriate modification of the NI functional groups may afford up to a 200-fold increase in cycloaddition rate by raising the HOMO energy of the dipole (*Graph 1.3*).[121]
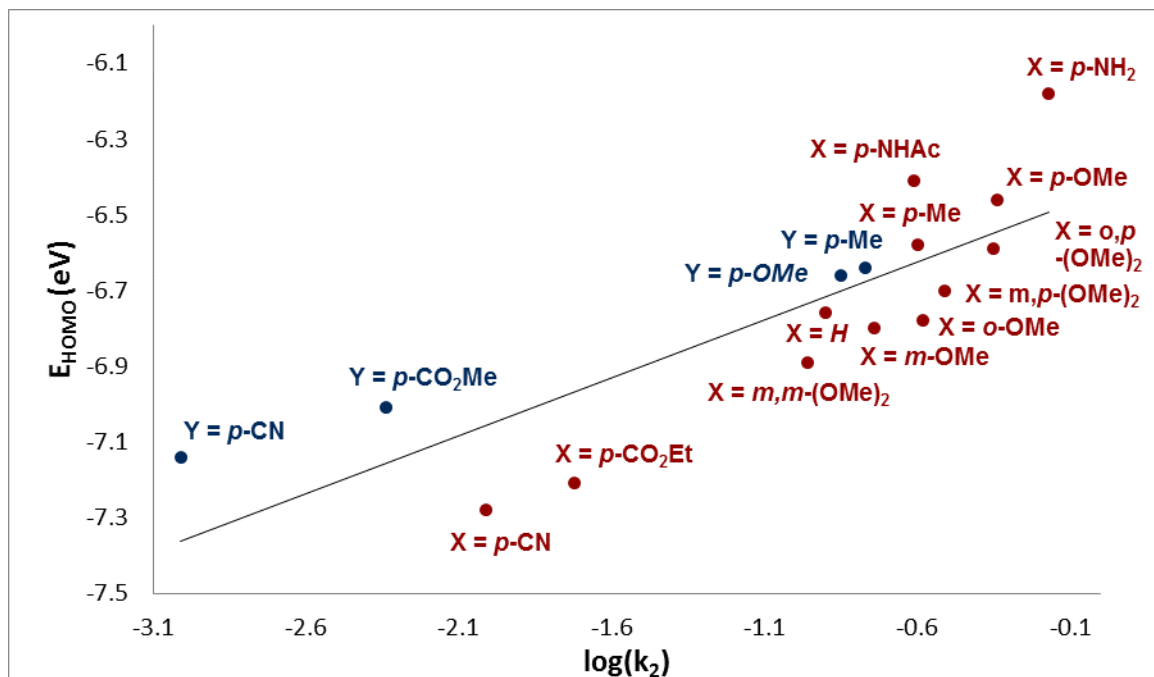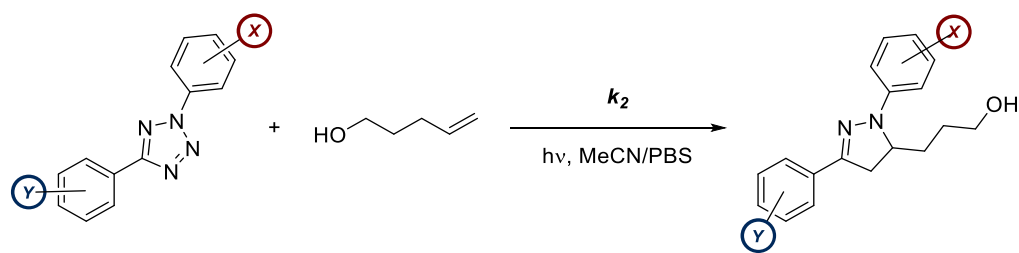
*Graph 1.3: The increase in cycloaddition rate observed when raising the HOMO of the NI*

The reactivity of the dipolarophile may also be improved, mainly through the approaches discussed in *Section 1.3.1.2*. The additional challenge in this context is enhancing reactivity while maintaining facile incorporation of the moiety into a biomolecular scaffold. The synthesis of both tetrazole and alkene-containing amino acid structures is relatively simple, with approaches towards both ubiquitous in the literature.[123,218–220] For alkenes, this normally involves simple, one step procedures, such as the allylation of tyrosine or the amidation of lysine with acrylic acid.[216,219] The design of tetrazole-containing scaffolds are slightly more complex and require multiple transformations, but remain relatively straightforward (*Scheme 1.52*).[220]
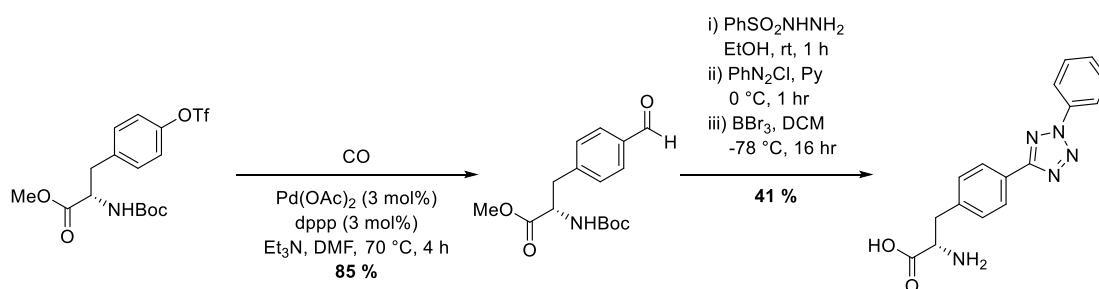


*Scheme 1.52: An example synthesis of an artificial amino acid containing a 2,5-diaryl tetrazole*

36

Following the re-emergence of research into the reactivity of NIs towards nucleophilic additions (*Section 1.3.2*), more recent studies from Lin have investigated methods of shielding NIs from nucleophilic attack. Substitution of the *ortho* positions of the *C*-aryl ring of an NI has subsequently been shown to preserve cycloaddition reactivity, while sterically occluding the *C*-terminus from nucleophilic attack by endogenous residues (*Scheme 1.53*).[221,222]
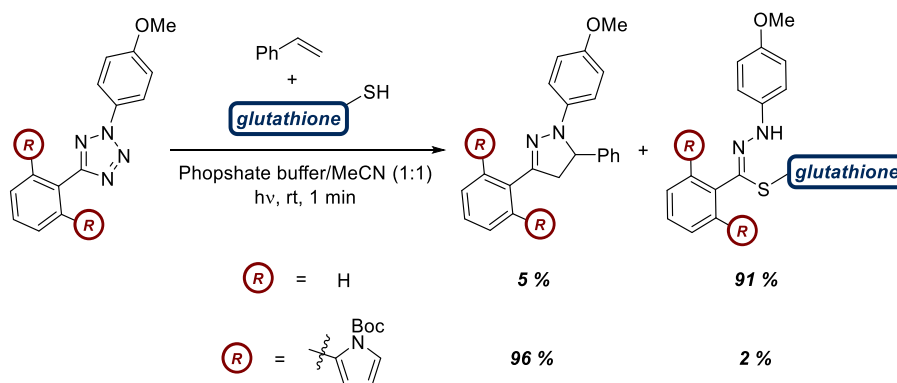


*Scheme 1.53: Steric encumbrance of the NI C-terminus may enhance reactivity with dipolarophiles relative to nucleophiles*

In 2018, Yu reported the application of diaryl sydnones as an alternative NI source for bioorthogonal ligation (*Scheme 1.54*).[223] This shares similar advantages to the use of 2,5-tetrazoles, such as user-defined light activation and no requirement for endogenous reagents, however it also shares the same shortcomings, with wavelengths of 311 nm required for effective ligation. More recent reports have alleviated this concern through successful use of the technique in live cells with 405 nm light, paving the way for further application of this methodology.[224]
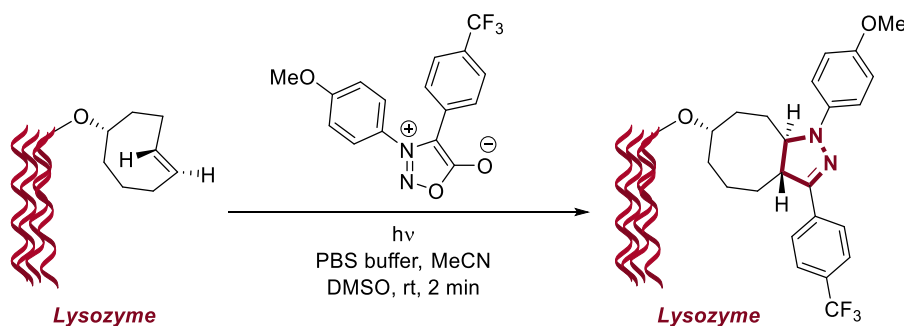


*Scheme 1.54: The application of diaryl sydnones in NI ligation chemistry*

### 1.4.1.2 Bioconjugative Reactions

The reactivity of the NI dipole with carboxylic acids has recently found widespread application in the field of bioconjugative chemistry, for example in the design of photo-affinity probes. Within the last 4 years, 2,5-tetrazoles have been incorporated into photo-affinity probes of bromodomain-containing proteins BRD2-4 and kinases such as protein

kinase A, among others.[161,182,183] In all of these reports, the NI was found to combine with an acidic amino acid moiety in close proximity to the active site. A direct comparison of tetrazole photolysis with other known light-activated photo-affinity probes also found that the NI afforded a substantial increase in ligation propensity (*Scheme 1.55*).[183]
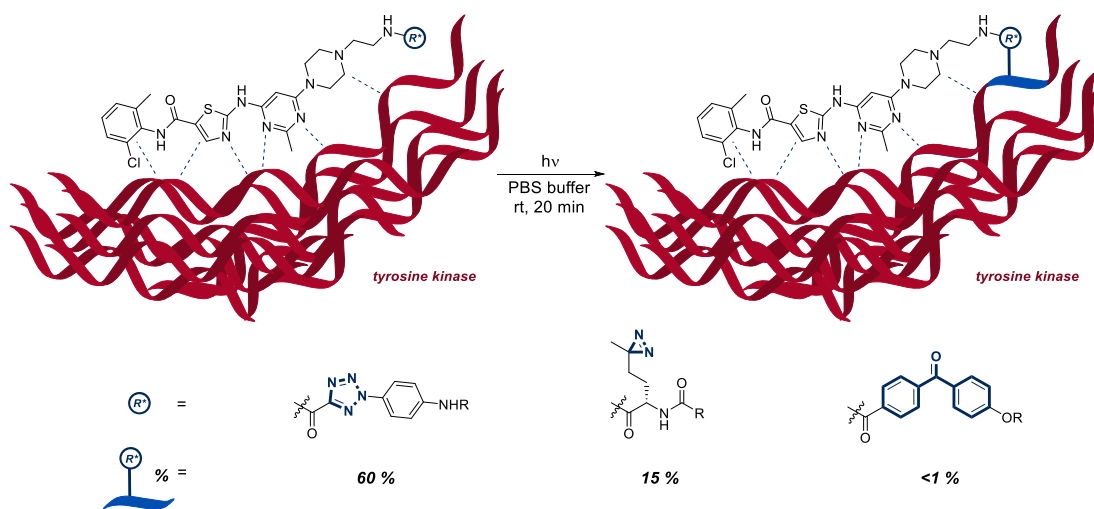


*Scheme 1.55: A comparison of the proficiency of an NI as a photoaffinity label*

In 2017, Lin reported the first genetic incorporation of a 2,5-tetrazole into biomolecules for applications in protein cross-linking.[225,226] This methodology is attractive as a probe for further investigation of dynamic protein interactions in living systems (*Scheme 1.56*). This approach was exemplified in living cells with the cross-linking of a mutant form of growth factor receptor-bound protein 2 and the epidermal growth factor receptor. Again, an NI-carboxylic acid interaction was found to be responsible for this reactivity.
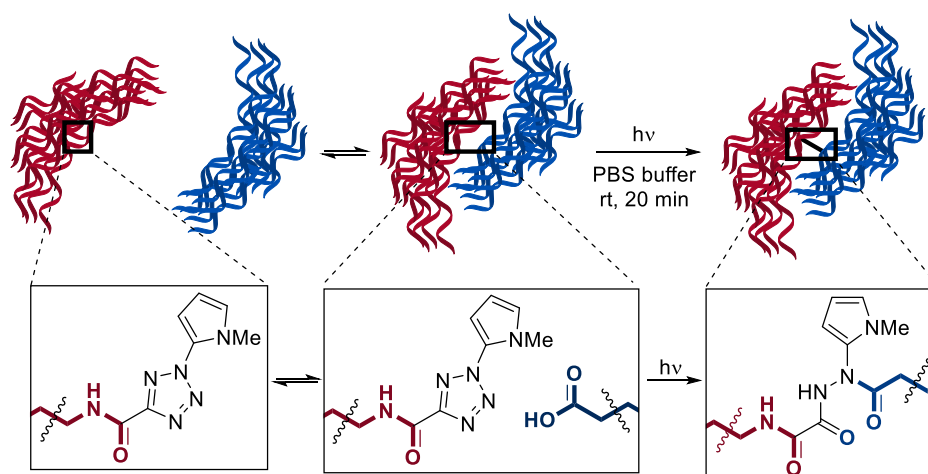


*Scheme 1.56: The cross-linking of proteins using NI-carboxylic acid bioconjugation methodology*

This broad reactivity profile has also found application in phenotypic screening, where incorporation of an NI precursor within a bioactive molecule may facilitate the identification of the protein with which the compound exhibits an effect. This was first employed by Ding and Li in 2017, in the implication of numerous proteins as potential targets of two small

molecules exhibiting antiproliferative effects in cancer cell lines.[227] Degradation studies of the ligated targets identified an aspartate residue as a suspected conjugation site of the NI.

### 1.4.1.3 Chemosensors

An additional biocompatible application of NI cycloaddition is in the detection or visualisation of analytes within living systems, for example, *via* turn-on fluorescent imaging. In most cases, these probes are activated through photochemical "uncaging" of a chromophore, however photolytic generation of the NI will lead directly to the synthesis of a fluorescent pyrazoline due to the proximity of a dipolarophilic alkene. This was first exemplified in 2011 following the attachment of such a system to a taxol-based molecule with a known binding affinity for microtubules.[228] Photolytic activation generated up to an 112-fold increase in fluorescence (*Scheme 1.57*).
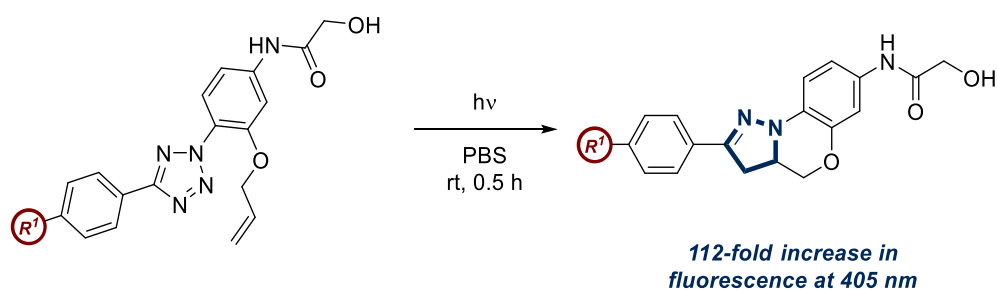


Scheme 1.57: An intramolecular cycloaddition of a light-generated NI that may be performed in vitro, yielding a highly fluorescent pyrazoline

In this seminal report, the fluorescent reporting moiety was formed through an intramolecular process (in other words, independent of the analyte), but more recent examples have targeted pyrazoline formation through direct reaction with the biomolecule of interest. The accumulation of the *bis*-carboxylate species known as fumarate can often be indicative of the poor regulation of metabolism, a common characteristic of some cancers. Investigations by Meier elucidated that 1,3-dipolar cycloaddition between an NI and fumarate can also form highly fluorescent pyrazolines, representing a quantitative evaluation of fumarate levels *via* an *off→on* chemical probe (*Scheme 1.58*).[229,230] While initial studies employing hydrazonyl chlorides observed a near 100-fold increase in fluorescence in the presence of excess fumarate, this was driven to a 400-fold increase when 2,5-tetrazoles were applied.[230]

Lin also exemplified the self-reporting properties of the NI-fumarate cycloaddition using 2,5-tetrazoles augmented with a boron-dipyrromethene (BODIPY) chromophore.[231] In contrast to the cycloadducts employed in earlier reports, the BODIPY-pyrazolines do not exhibit a fluorophore, as the fluorescence of the BODIPY moiety is quenched by the pyrazoline, and *vice versa*. The starting 2,5-tetrazole, however, is highly fluorescent in the

absence of the pyrazoline, making this an example of an *on→off* chemical probe (*Scheme 1.58*).
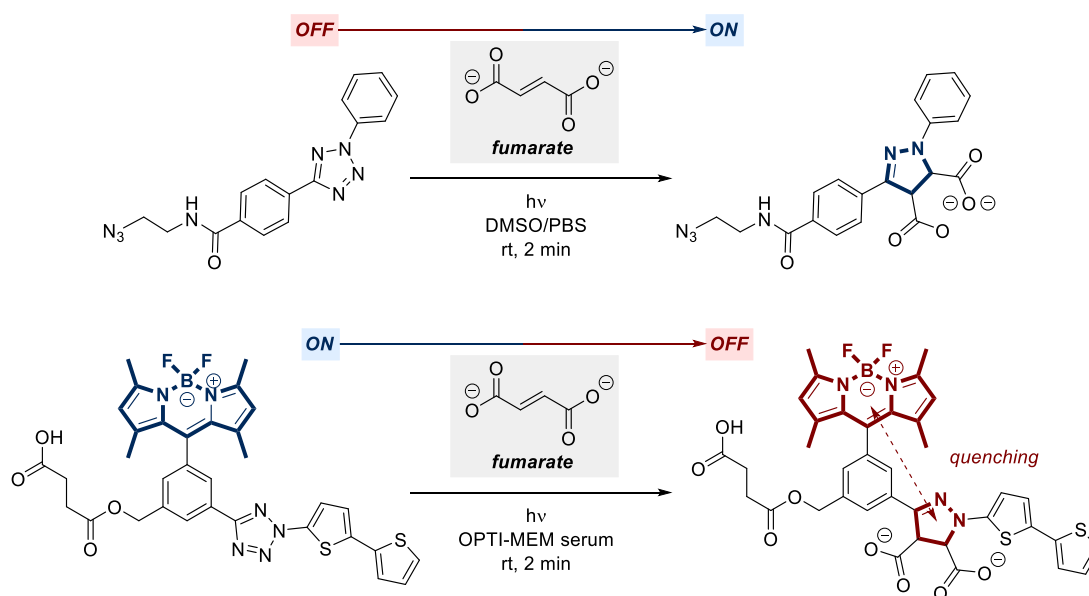


*Scheme 1.58: The application of NIs in the detection of the oncometabolite fumarate*

## 1.4.2  Materials Chemistry

The NI dipole is also prevalent within materials chemistry. As before, most examples involve the introduction of photo-labile 2,5-tetrazoles as the preferred NI precursor, which is particularly convenient when selective NI generation is required (for example, in surface patterning). 1,3-Dipolar cycloaddition is the most common reactivity profile exemplified, due to its high yields and fast reaction times. However, in direct analogy with other fields, the introduction of carboxylic acid ligation agents has recently risen to prominence.

### 1.4.2.1 Polymer Synthesis

The first example of polymerisation using NIs emerged in 1966, from Stille.[199] The monomers applied were of an "A-A", "B-B" format, with reaction of *bis*-hydrazonyl chlorides and *bis*-acetylenes forming pyrazole-linked products (*Scheme 1.59*). A similar publication later that year expanded this scope to include *bis*-olefins as the "B-B" component, which generated fluorescent pyrazoline-linked polymers.[232]
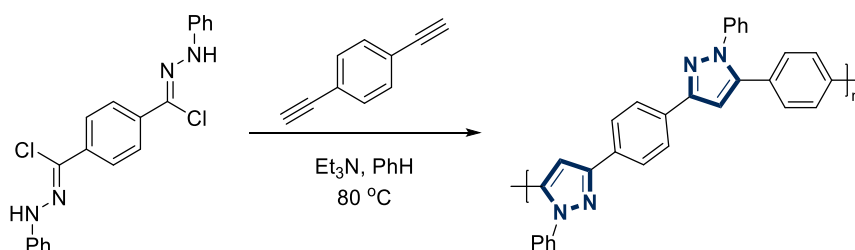


*Scheme 1.59: Stille's initial report into the use of NIs in polymerisation reactions*

A significant development in NI polymerisation chemistry was the application of tetrazoles as an NI source, due to the lack of exogenous reagents required to generate the dipole. Repeating the above using a *bis*-2,5-tetrazole in conjunction with a *bis*-dipolarophile afforded the desired polymers through simple thermolysis (*Scheme 1.60*).[200,233] The photolytic generation of a similar polymer has also recently been exemplified.[234]
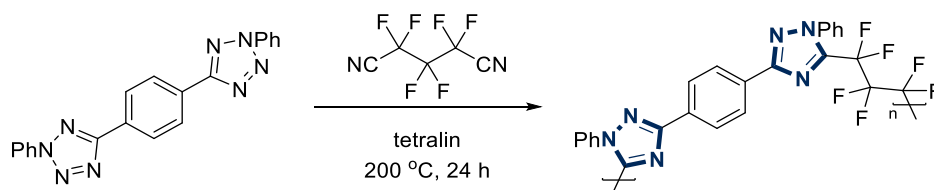


Scheme 1.60: 2,5-tetrazoles can also be used as NI sources in polymerisation reactions

NI polymers of the "A-B" monomer type are also well established. These were again introduced by Stille in 1969, in the polymerisation of a tetrazole with a pendant alkynyl functionality, and in a further example using an olefin.[235] While these polymers were accessed *via* thermolysis of the tetrazole, literature precedent also exists for the generation of a pyrazoline-linked polymer using UV light (*Scheme 1.61*).[236] Control of reaction concentration is of particular importance, as many NI-based monomers of the A-B type have the ability to react intramolecularly.
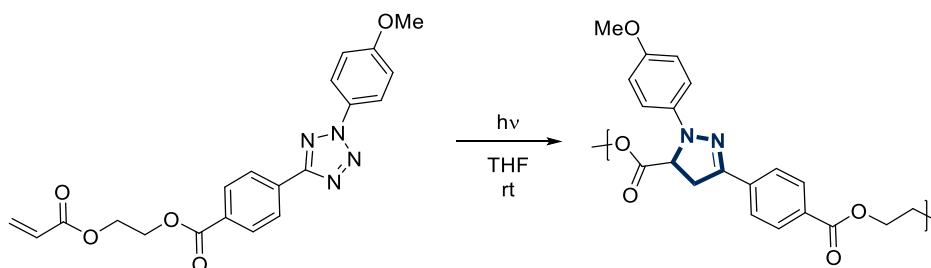


Scheme 1.61: NI polymerisation using a monomer of the A-B type

NI chemistry can also be applied in extending the chain length of existing polymers. For example, modification of nitrilebutadiene rubber with a terminal tetrazole enables their dimerisation when photolysed in the presence of a *bis*-maleimide linker (*Scheme 1.62*).[237] This enables controlled linear growth while minimising cross-linking, facilitating access to high molecular weight polymers with low dispersity values. This has also been applied in the synthesis of copolymers, through the introduction of a second pair of orthogonal functional handles.[238]
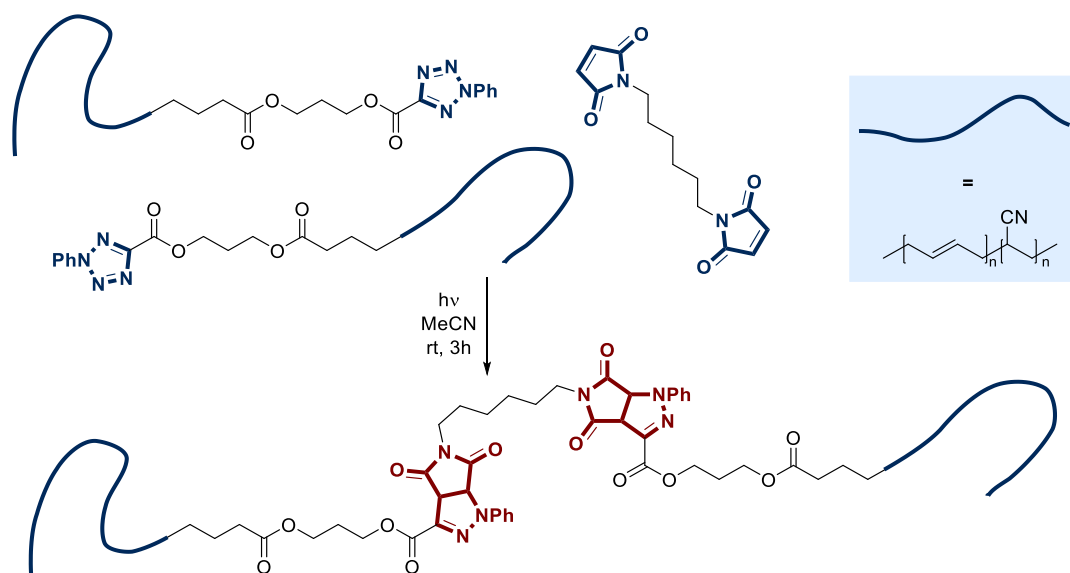
*Scheme 1.62: The synthesis of extended linear polymers using NI cycloaddition*

### 1.4.2.2 Polymer Cross-Linking

In the examples discussed above, NI chemistry was employed during the polymerisation process. However, these reagents are also useful in the cross-linking of polymer chains when generated after the polymerisation process has been completed. This first requires incorporation of a NI precursor into the monomer side-chain, and polymer synthesis through an alternative approach, such as free-radical polymerisation.[239] Cross-linking in polymers is important as it can drastically alter the properties of the product. Control over the process is similarly crucial, in order to influence the extent of alterations made to the polymer. Photolytic NI generation is extremely convenient as the use of a focused light source can afford exquisite control over the sites of reaction.

The simplest method of NI-induced cross-linking involves the synthesis of a co-polymer that incorporates both a 2,5-tetrazole and a dipolarophile such as acrylonitrile or butadiene (*Scheme 1.63*). Initial examples from Stille showed that cross-linking could be induced through heating of the material to temperatures in excess of 160 °C.[240] This "activation" temperature may be influenced through the modification of functional groups present around the tetrazole, with substitution of the *N*-aryl ring influencing the decomposition threshold by as much as 60 °C.[241]

In 1994, Darkow reported that UV irradiation of similar polymers could also be used to yield the cross-linked products.[242,243] This affords more control over the localisation of the reaction, however cross-linking was less efficient when using thicker samples due to the relative opacity of the product.[242]

| R* | Ph | (4-Cl)Ph | (4-OMe)Ph | Me |
|---|---|---|---|---|
| **Decomposition Temperature (°C)** | 210 | 160 | 220 | 250 |
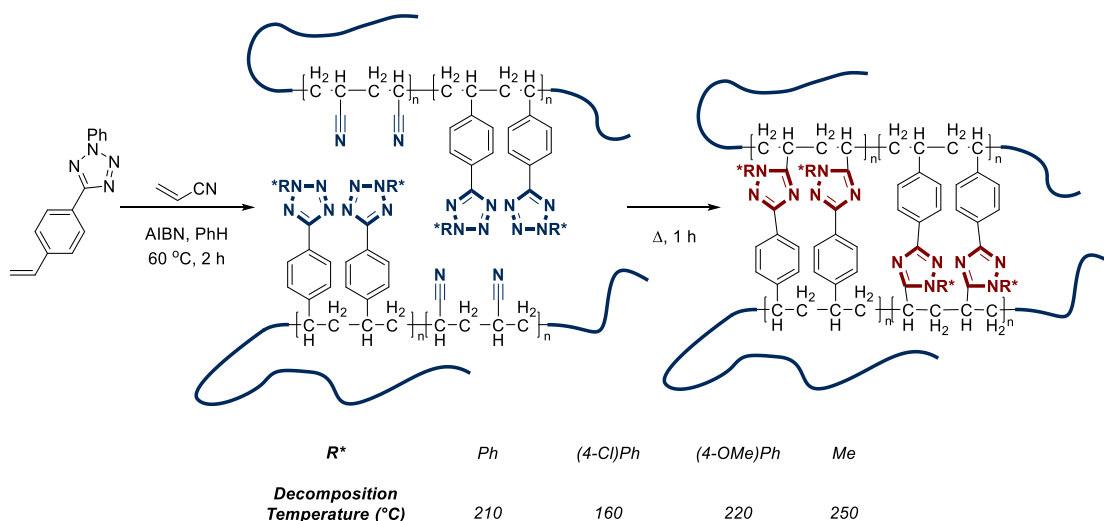
*Scheme 1.63:The preparation of a polymer containing an NI precursor and its subsequent cross-linking*

While incorporation of a tetrazole into the polymer backbone is a simple method of ensuring efficient NI coverage, the properties of the polymer are undoubtedly compromised by the necessity of having the same functional group present in at least one of the monomers. This problem is exacerbated by the inclusion of a dipolarophile within the polymer. Recent examples of NI-induced cross-linking from Meier, Barner-Kowollik and Bowman have reintroduced the concept of adding a cross-linking agent to the reaction.[244,245] The polymer is first synthesised or modified to include a tetrazole or an alkene, before a dimeric structure of the other reaction partner is added under UV irradiation (*Scheme 1.64*). This has greatly expanded the utility of NIs as a cross-linking agent and can be applied in the modification of many common polymers, such as cellulose.[245] The use of a disulfide-linked *bis*-NI as the cross-linking agent also enables retroactive degradation of the linkers through treatment with a reducing agent.

While modes of reactivity including nitrile cycloaddition and NI dimerisation have been shown to induce cross-linking,[240,243] the formation of pyrazoline cross-linkers has the additional benefit of generating fluorescent functional groups. The extent of cross-linking may therefore be quantified by monitoring the fluorescence intensity of the product. Linear polystyrene, functionalised with a tetrazole moiety on both termini, may form a dense cross-linked network when photolysed in the presence of a trimeric maleimide species.[246] Degradation of this polymer and measurement of the fluorescence spectrum can then inform on the success of the initial photochemical cycloaddition (*Scheme 1.65*).
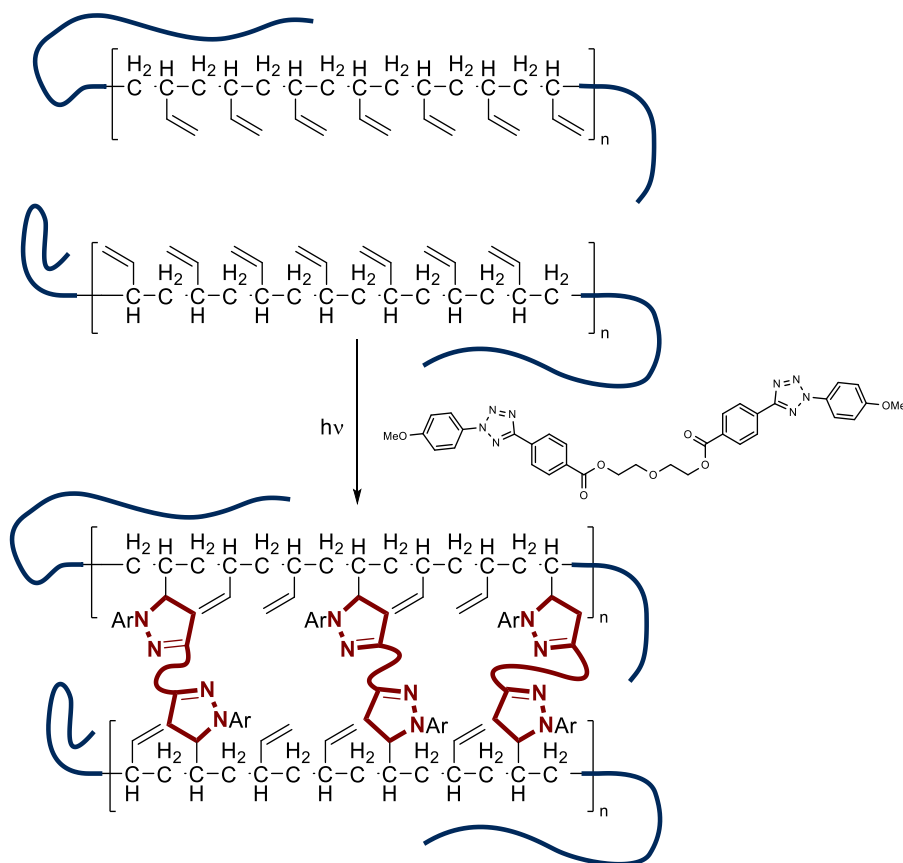
*Scheme 1.64:The light-activated cross-linking of a butadiene polymer using a bis-NI cross-linking agent*

### 1.4.2.3 Surface Chemistry

Surface chemistry, at the interface of small molecule and macromolecular research, is a diverse field with broad applications throughout materials science. During the past ten years, the NI dipole has become a popular ligation agent in this area.[21] This approach to surface modification is attractive owing to its orthogonality and high reactivity, with the additional benefit that the NI may be generated using only UV light. The most straightforward example is in the immobilisation of a polymer onto the surface of an organic or inorganic network. This was first exemplified in two independent publications from Barner-Kowollik and Nallani and Liedberg in 2011.[247,248] The former modified a silicon wafer and a sample of cellulose with a 2,5-tetrazole moiety, which were exposed to UV light in the presence of a poly(methyl)acrylate derivative capped with a maleimide dipolarophile (*Scheme 1.66*). The liberated NI rapidly formed the desired cycloadduct, attaching the polymer to the surface. Nallani and Liedberg demonstrated similar reactivity in the ligation of the horseradish peroxidase enzyme to the surface of a polymersome, a synthetic replica of liposomes.[249]
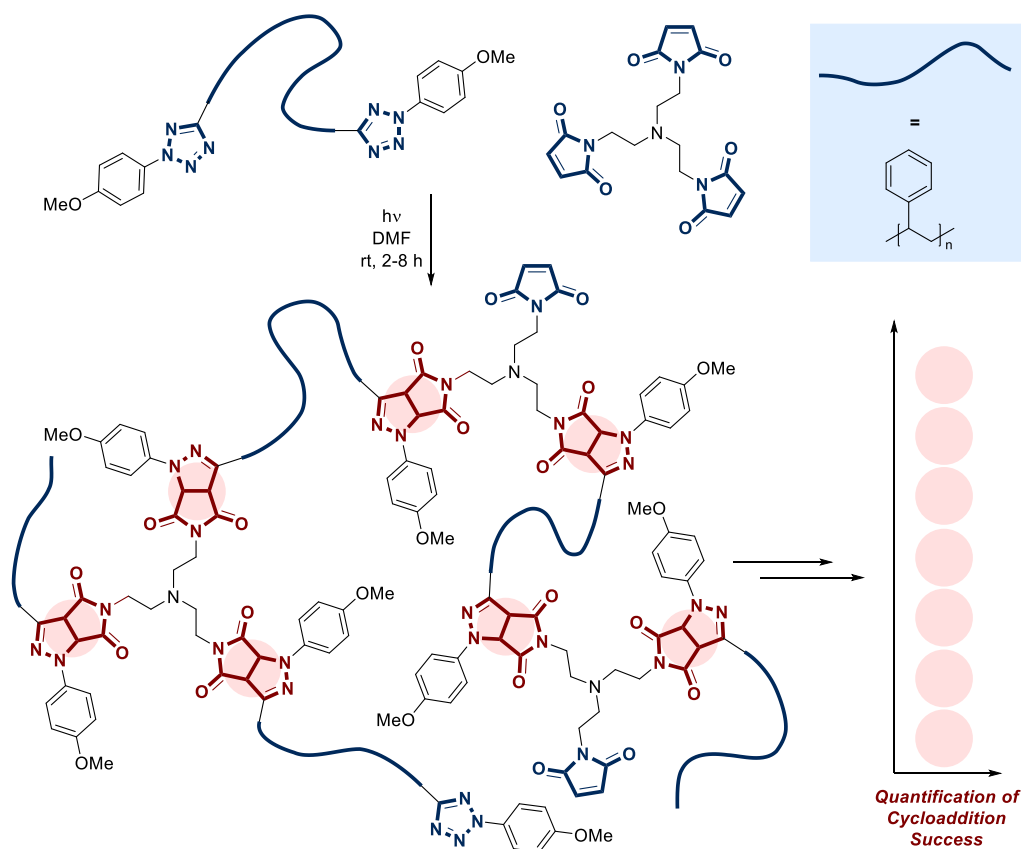
*Scheme 1.65: Quantitative analysis of the efficiency of NI cycloaddition in polymer cross-linking*

The photochemical activation of 2,5-tetrazoles is once again a highly favourable property in this field. The use of a template, or shadow mask, that permits controlled irradiation of the surface can allow for accurate "patterning" of the surface with the NI reaction product. This was demonstrated during the development of bespoke non-fouling brushes, with ligation of a poly(methyl)acrylate monomer onto a silicon wafer, again employing NI-maleimide cycloaddition chemistry.[250] The use of a templated shadow-mask rendered the 2,5-tetrazole inert in the regions of the surface obstructed from the light source, enabling controlled surface-patterning (*Scheme 1.67*).

An alternative method of surface patterning was disclosed by Ravoo in 2016.[251,252] Microcontact chemistry involves the selective application of reagents only to certain areas of the surface, using a specially designed stamp coated in the required compound.[253] A reaction will occur only in the areas of the surface where the stamp made direct contact with the environment. In the case of NI cycloadditions, a tetrazole-doped silicon wafer was shown to undergo pattern-specific reactivity with several dipolarophiles, which were administered to the surface *via* microcontact printing (*Scheme 1.68*).
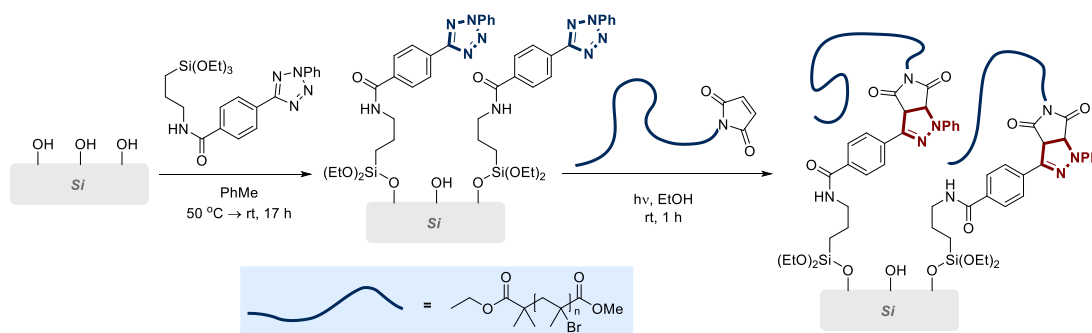
*Scheme 1.66: The attachment of a poly(methyl)acrylate derivative to a silicon wafer using NI chemistry*

The modification of surfaces can yield materials with unusual properties and numerous potential applications. One of the first examples of this involving NI chemistry was the functionalisation of a cellulose paper sheet with a hydrophobic polymer based on methyl methacrylate, with the hydrophobic properties of the polymer translated to the sheet.[248] Another early example was the ligation of silicon wafers with short polymers containing a diazo moiety. The facile $E \rightarrow Z$ isomerisation of this motif upon exposure to light created the first example of a light-responsive surface engineered through NI chemistry (*Scheme 1.69*).[254]



*Scheme 1.67: The photo-patterning of a surface through the application of NI cycloaddition and a shadow-mask*

*Scheme 1.68: The application of NI chemistry and microcontact printing in the patterning of surfaces*

Recodable surfaces have also been exemplified in NI-mediated surface modification. This chemistry relies on reversible bonding interactions between a surface and a coordinating group. While NIs themselves do not possess the appropriate properties, they are often used as ligating agents for the installation of the reversible reaction partners. One example from 2015 capitalised on the host-guest binding properties of cyclodextrin, anchoring this carbohydrate onto a polydopamine surface through a NI cycloaddition using a shadow-mask (*Scheme 1.70*).[255] The resulting pattern was visualised through treatment of the surface with a rhodamine dye, modified by an adamantyl moiety to coordinate with the cyclodextrin. This interaction may then be reversed by washing the material with an excess of a cyclodextrin solution.



*Scheme 1.69: Surface labelling can be applied in the synthesis of photoresponsive surfaces using NI cycloaddition*

Surface modification using alternative NI reaction partners have also been disclosed, with most employing carboxylic acids in very recent reports. Zetterlund/Barner-Kowollik and Ravoo have both independently reported this application within the past two years, in the augmentation of tetrazole-functionalised nanoparticles and silicon wafers, respectively.[252,256] One earlier report from 2016, also from Ravoo, documented the application of thiols as an NI ligation agent in the immobilisation of biotin and triethyleneglycol on the surface of a silicon wafer.[251]



*Scheme 1.70: The ligation of cyclodextrins to surfaces using NIs, and its application in reversible host-guest chemistry*

## 1.5    Conclusions and Outlook

In the six decades following the initial synthetic report on the introduction of NIs, a number of publications have exploited the unique properties of this valuable species. The 2007

rediscovery of the benefits of 2,5-diaryl tetrazole photolysis in particular has revitalised the field,[82] with a number of new and exciting applications of the dipole emerging, relative to the limited literature activity of the 1980s and 1990s. Of additional significance is the recent reevaluation of carboxylic acids and thiols as NI reaction partners.[161] While initially stimulating the development of additional applications of NIs exploiting this reactivity,[183,184] it has also prompted a reassessment of the orthogonality of "tetrazole photoclick chemistry", which has led to the development of much improved NI and alkenyl functional handles within this field.[124,222]

Looking towards the future applications of this dipole, it is likely that the photolysis of 2,5-tetrazoles will become the most commonplace method of NI generation owing to the exceptional value of this approach to the fields of ligation chemistry. Further investigation into the true orthogonality of the NI towards either 1,3-dipolar cycloaddition or nucleophilic trapping is certainly necessary, but likely to be overlooked in a discipline dominated by an application-driven philosophy.

## 1.6    Overarching Aims

Consequently, the original research documented in the subsequent chapters of this thesis is driven by the central theme of simplifying the application of NI derivatives in ligation chemistry through an increased understanding of their generation and reactivity. This will commence through the investigation of an alternative synthesis of 2,5-diaryl tetrazoles, which are forecast to become the most popular method of NI generation in the years to come. Current approaches towards these heterocycles are generally robust, however, are incompatible with an array-type synthesis that focuses on rapid construction of a library of different tetrazoles. This shortcoming will be addressed through the application of Suzuki-hydrogenolysis methodology in the diversification of a key tetrazole motif.

With efficient access to a diverse palette of NIs enabled, subsequent studies are devoted to further understanding the reactivity of the NI, and its application in the development of novel C-C bond formations. The interaction of this 1,3-dipole with aryl boronic acids has never been investigated, however mechanistic interpretation of the Petasis-Mannich reaction reveals potential similarities between the two transformations. This represents an opportunity for the development of a metal-free, light-activated method of C-C bond formation, requiring only a tetrazole and boronic acid, with no exogenous reagents. Furthermore, the introduction of hydrazonyl halides as an alternative NI source could facilitate the extension of the methodology into similar 1,3-dipolar systems, such as the nitrile oxides.

The final chapter in this thesis is dedicated to further understanding the relative reactivity of the NI dipole with various substrates. As mentioned above, it is likely that the application of

the NI in ligation chemistry will continue with limited investigation into the reactivity of the dipole with alkenes relative to its reactivity with native functionalities such as carboxylic acids or thiols. The development of a complete framework of individual competition experiments will establish a rank order of substrate reactivity with the NI, enabling more informed application of the dipole within bioorthogonal sciences.
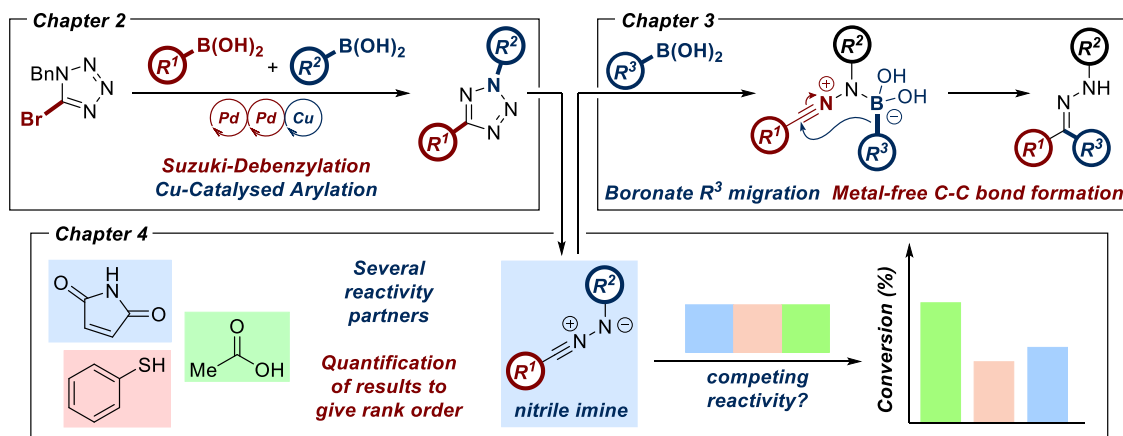


Scheme 1.71: A summary of the overall objectives of this thesis

# 2    A Modular Protocol for the Synthesis of 2,5-Diaryl Tetrazoles

As discussed above, future application of the NI 1,3-dipole will most likely rely on the photolysis of 2,5-diaryl tetrazoles as the primary precursor. Consequently, it is crucial to develop robust protocols for the synthesis of these valuable NI sources. This chapter describes the development of novel, modular methodology to enable facile and rapid access to a library of 2,5-diaryl tetrazoles.

## 2.1    Introduction

### 2.1.1    Current Methods of 2,5-Tetrazole Synthesis

The retrosynthesis of the tetrazole motif can be considered from two different approaches. The first is the construction of the heterocycle with a single aromatic ring, either *N* or *C*-linked, already present. The second aryl group is then introduced in a separate modification following tetrazole synthesis. This enables more efficient modification of the substituents augmenting the tetrazole, which influence its $\lambda_{max}$ value and hence reactivity (discussed in *Section 1.2.3*). The second approach involves direct construction of the tetrazole with both aryl rings in place. This has the obvious advantage of affording direct access to the desired compound and is the most common technique employed in the literature.

Despite the numerous advanced and modern applications of 2,5-diaryl tetrazoles, the vast majority of publications employ some derivitisation of the Kakehi tetrazole synthesis, developed in 1976 (*Scheme 2.1*).[257,258] This involves the electrocyclisation of an aryl diazonium salt with an aryl sufonylhydrazone, normally employing a vast excess of base such as pyridine. The regioselectivity of this cyclisation can be attributed to the enhanced steric encumbrance in the transition state of the 1,5-regioisomer. The sulfonyl hydrazone moiety is accessed *via* the condensation of benzenesulfonyl hydrazide with a benzaldehyde derivative, allowing for an extremely broad scope.

An alternative to the Kakehi synthesis emerged in 2015, using aryl diazonium salts and aryl amidines (*Scheme 2.2*).[259] While this reaction appears to also constitute an electrocyclisation, it was shown to first proceed through nucleophilic attack of the diazonium species by the amidine, followed by oxidative ring-closure facilitated by the addition of iodine and potassium iodide. Due to the symmetry of the amidine, regioselectivty is not an issue, however the scope is slightly limited by the availability of this reactant.
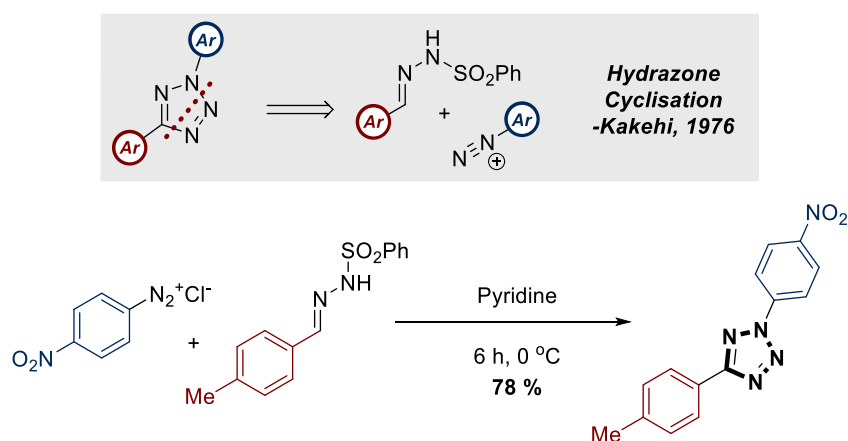
*Scheme 2.1: The Kakehi tetrazole synthesis*

Numerous approaches have been developed for the attachment of an *N*-aryl ring in the 2-position of *C*-arylated tetrazoles. Initial reports involved the application of hypervalent heavy elements, such as bismuth and iodine (*Scheme 2.3*).[260,261] While this became a widely studied approach, the reactions were not atom economical, and often required the use of palladium and copper co-catalysts.[261–263]
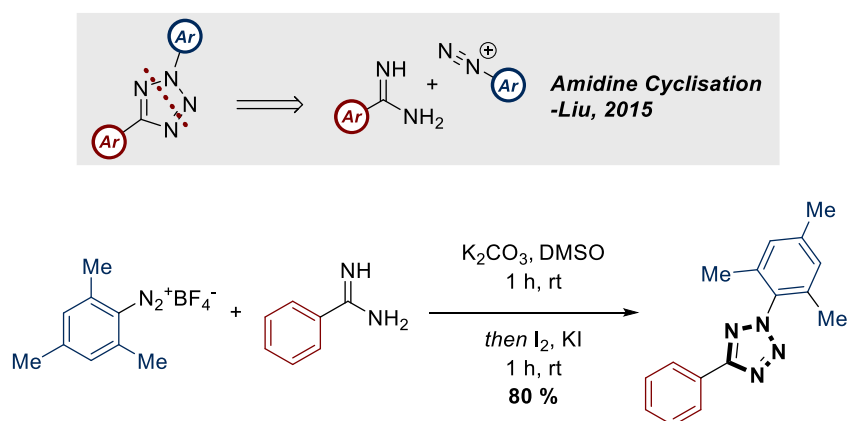


*Scheme 2.2: The synthesis of 2,5-diaryl tetrazoles through the combination of aryldiazonium salts and amidines*

More recently, copper-catalysed Chan-Lam-type coupling between 5-substituted 1*H*-tetrazoles and aryl boronic acids has emerged as a more accessible route towards 2,5-diaryl tetrazoles (*Scheme 2.4*).[264–267] The use of a copper(I) salt in the presence of an oxygen atmosphere facilitates a remarkably efficient process that can safely generate the product in excellent yields. The regioselectivity of this reaction and those above are derived from steric considerations in the transition state, rather than electronics.

One disadvantage of *N*-arylation is the prerequisite of using 5-aryl tetrazoles. Fortunately, the synthesis of this moiety is extensively documented, and is typically achieved *via* the 1,3-dipolar cycloaddition of an aryl nitrile and hydrazoic acid.[268] While $HN_3$ is an extremely hazardous, highly toxic species, it is typically generated *in situ* through treatment of an azide salt with a Bronsted or Lewis acid.
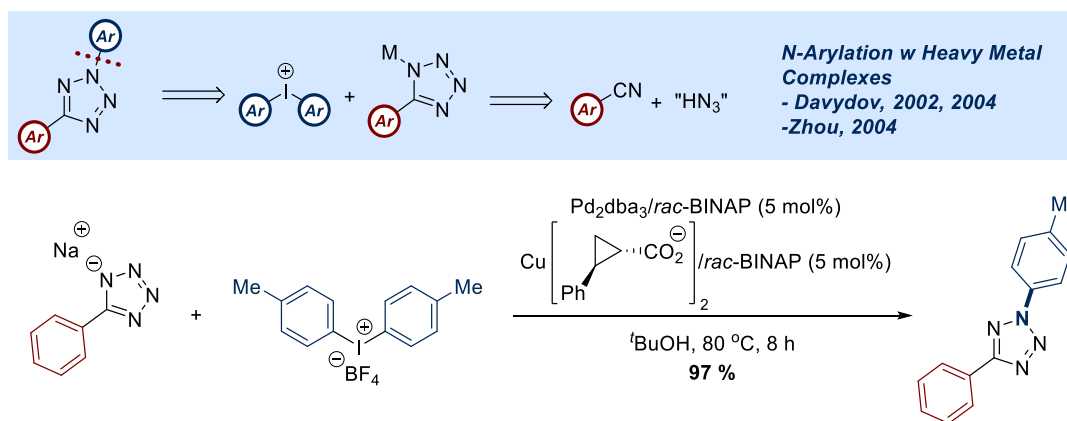
*Scheme 2.3: N-arylation of tetrazoles using hypervalent iodine species*

In contrast to the *N*-arylation of tetrazoles, arylation of the 5-position is a very uncommon transformation. The formation of an $sp^2$-$sp^2$ carbon-carbon bond typically falls within the domain of palladium-catalysed cross-coupling, but while 5-bromo and 5-metallated tetrazoles are known to undergo such reactions, this has only ever been documented using the 1,5-regioisomer.[269,270]
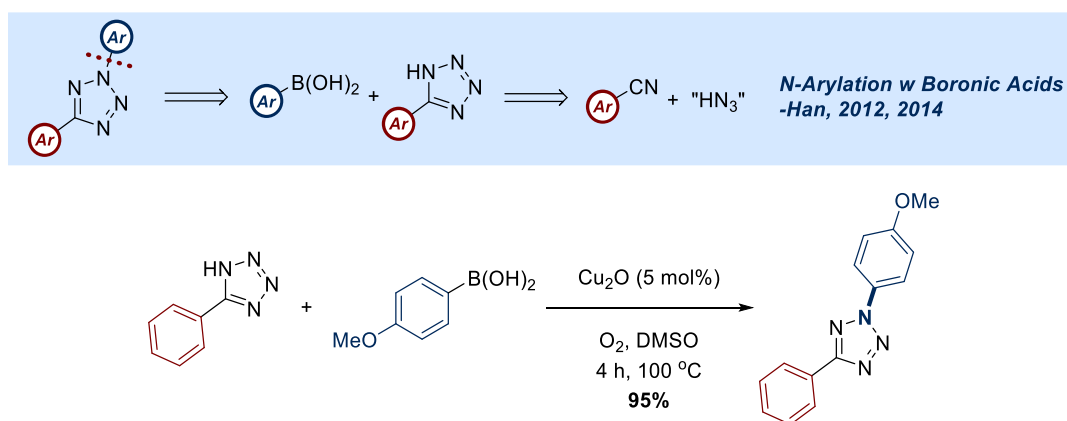


*Scheme 2.4: Copper-catalysed N-arylation of 5-substituted tetrazoles using boronic acids*

This highlights the principal problem with this approach: the steric bulk of the 5-position is required to ensure regioselective modification of the 2-position, hence the efficient synthesis of a *C*-5 unsubstituted 2-aryl tetrazole is challenging. However, one example was reported in 2016 involving the cycloaddition of diazonium salts and TMS-diazomethane (*Scheme 2.5*).[271] Silyl deprotection and subsequent bromination afforded access to an electrophilic cross-coupling partner for *C*-arylation, although no such reaction was conducted.

## 2.1.2 The Benefits of a Modular Approach to Tetrazole Synthesis

One of the most attractive aspects of employing 2,5-diaryl tetrazoles as an NI source is that the substituents of both aryl rings offer remarkably sensitive tuning of several key properties, including wavelength of NI liberation, and the HOMO/LUMO energy levels of the resulting dipole (*Scheme 1.14* and *Graph 1.3*). It is logical that when using 2,5-diaryl tetrazoles as a

source of NI, it will be necessary to synthesise a small library to ascertain which tetrazole possesses optimal properties for the application at hand. However, this is at odds with the methods of 2,5-diaryl tetrazole synthesis currently available. While methods of *N*-aryl ring modification are ubiquitous, all require the prior synthesis of a *C*-aryl tetrazole *via* cycloadditions using highly toxic hydrazoic acid, and modifications of the *C*-aryl ring remain completely underdeveloped.
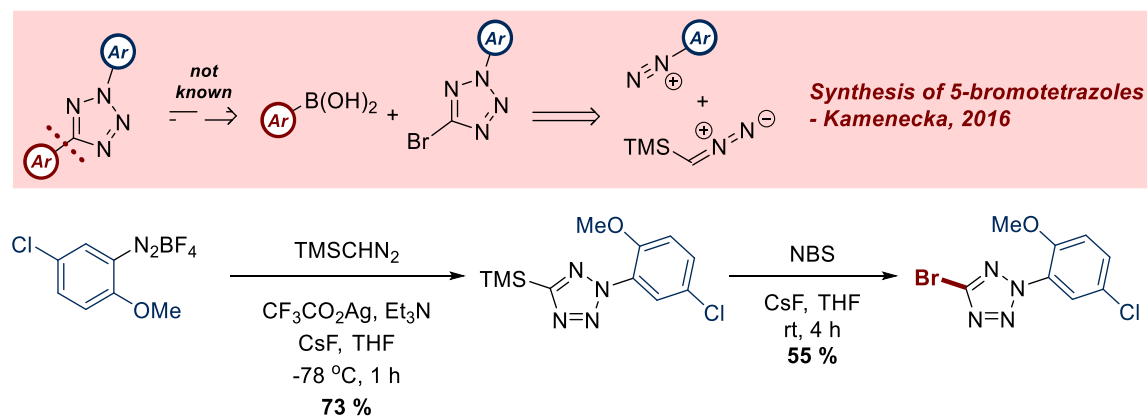


*Scheme 2.5: The synthesis of 5-bromo-2-aryltetrazoles*

The existing synthetic approaches also suffer from other shortcomings. The Kakehi synthesis in particular, while robust and well-precedented, is undermined by the use of an explosive starting material, large quantities of corrosive and pungent solvent, low reaction yields and laborious purification techniques. More broadly, the use of explosive starting materials is a ubiquitous problem within this field, with all current synthetic routes employing extremely hazardous and explosive reagents such as diazonium salts, azides, and diazomethane.

To facilitate simple and rapid access to a library of 2,5-diaryl tetrazoles, a new approach must be devised. This philosophy must centre upon the use of a common intermediate with two principal characteristics (*Figure 2.1*). Firstly, it must already contain the tetrazole heterocycle, as this would avoid repeated introduction of explosive and toxic reagents. Ideally, a single large-scale synthesis of the intermediate would suffice for the generation of numerous 2,5-diaryl derivatives. Secondly, the tetrazole must incorporate two chemically orthogonal functional handles, to allow for facile and, importantly, regioselective *N*-2 and *C*-5 arylation.
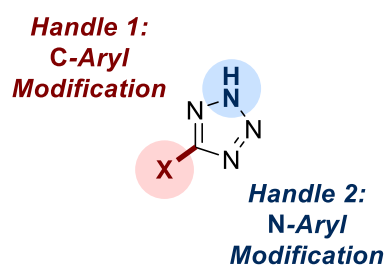


*Figure 2.1: The ideal hypothetical synthon for the modular synthesis of a library of tetrazoles*

## 2.2 Aims

It is proposed that the optimal realistic equivalent of the desired tetrazolyl synthon would be 1-benzyl-5-bromotetrazole. Previous literature precedent has documented the large-scale synthesis of this precursor, which will be replicated to obtain gram-scale quantities of this motif.[269]

The main aims of the project will incorporate our laboratory's previous experience in the development of a one-pot Suzuki-hydrogenation protocol.[272] This will facilitate simultaneous modification of the *C*-5 position of the tetrazole with a variety of boronic acids, and concomitant deprotection of the *N*-1 position. Tautomerisation of the free 5-aryl tetrazole would then facilitate regioselective functionalisation of the *N*-2 position using established methods.[264,265]

Consequently, the project will commence with the independent optimisation of the Suzuki and hydrogenolysis reactions before combining both into a one-pot protocol. Particular attention will be paid to the practicality of the approach, minimising purification steps (*Scheme 2.6*).

Following optimisation, the scope of 5-aryl tetrazoles accessible *via* this procedure will be explored, employing a diverse palette of boronic acids. The methodology will be further exemplified through the utilisation of known *N*-2 coupling approaches to synthesise a broad library of 2,5-diaryl tetrazoles.
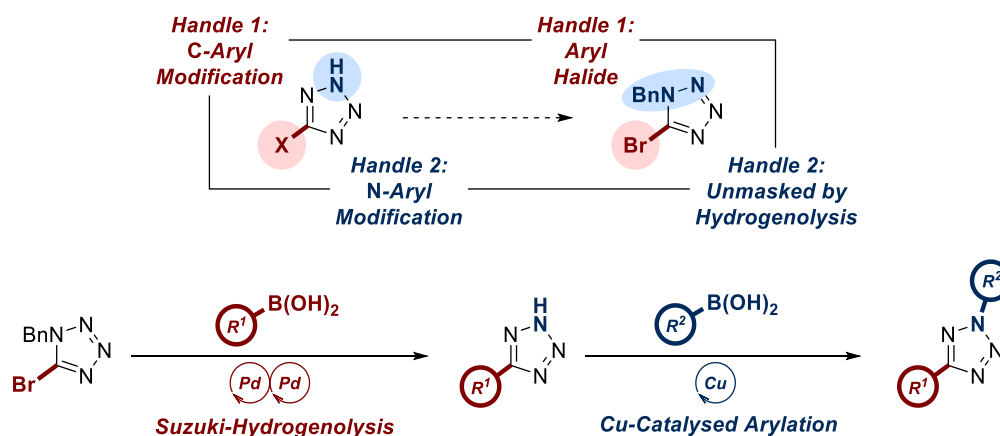


Scheme 2.6: The overall reaction scheme intended to furnish a novel, modular approach to 2,5-diaryl tetrazoles

## 2.3 Results and Discussion

### 2.3.1 Synthesis of 1-Benzyl-5-Bromotetrazole

To begin the development of the methodology, gram-scale synthesis of the desired starting material was first established. Retrosynthesis of 1-benzyl-5-bromotetrazole identified bromination of the electron-rich *C*-5 position as an appropriate final step, leaving the

construction of 1-benzyltetrazole as the only obstacle. As mentioned above, synthesis of the tetrazole moiety itself requires a cycloaddition between diazonium salts and hydrazones, or nitriles and hydroazoic acid. Fortunately, previous literature precedent had identified that the reaction of benzylisocyanide with hydrazoic acid would furnish the desired product in excellent yields (*Scheme 2.7*).[269] Furthermore, it was shown to perform very well on scales of up to 30 g, ideal for the synthesis of the core starting material throughout the project.



*Scheme 2.7: The literature conditions originally identified for the synthesis of 1-benzyltetrazole*

Due to safety concerns, the *in situ* generation of hydrazoic acid using a Bronsted acid such as acetic acid was deemed too hazardous. Consequently, it was decided to synthesise benzylisocyanide separately, before employing the less explosive trimethylsilylazide (*Scheme 2.8*).[273]



*Scheme 2.8: The reported [3+2] cycloaddition of benzylisocyanide and TMS-azide*

Synthesis of benzylisocyanide (**2.3**) was conducted *via* the formylation of benzylamine and subsequent dehydration using POCl$_3$, with both steps proceeding in acceptable yields (*Scheme 2.9*). However, the pungent odour of the benzylisonitrile product was an undesirable characteristic in the intended gram-scale syntheses to follow, and the route was abandoned.



*Scheme 2.9: The synthesis of benzylisocyanide (**2.3**)*

When considering alternative approaches, it was proposed that the synthesis of the heterocycle may be avoided entirely through the benzylation of 1*H*-tetrazole itself. This would facilitate the synthesis of the desired intermediate using readily available starting materials without necessitating the handling of any explosive or toxic reagents. An initial attempt employing triethylamine afforded the product in acceptable yield, while the introduction of caesium carbonate improved conversion further, allowing facile access to significant quantities of 1-benzyltetrazole (**2.5**) (*Scheme 2.10*). While the yield was diminished due to the presence of both regioisomers, this was not problematic as the

eventual removal of the benzyl protecting group should render both regioisomers compatible. However, to simplify the subsequent optimisation, only the 1-benzyl regioisomer **2.5** was taken forward. The bromination of this compound was then accomplished through the application of *N*-bromosuccinimide (NBS), which proceeded in excellent yield (*Scheme 2.11*).
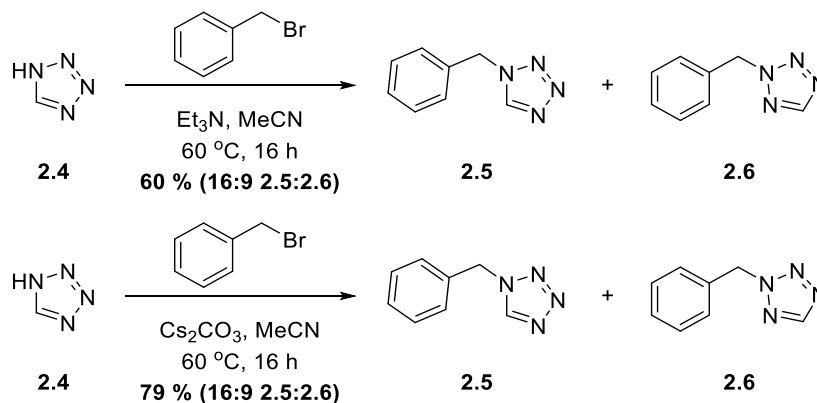


*Scheme 2.10: The benzylation of 1H-tetrazole employing either triethylamine or caesium carbonate*
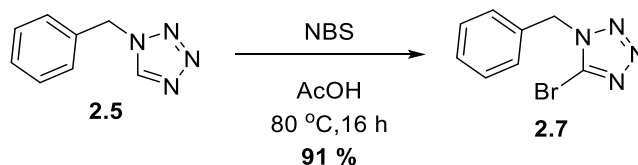


*Scheme 2.11: The bromination of 1-benzyl tetrazole to furnish **2.7***

### 2.3.2 Optimisation of Reaction Conditions

As discussed in *Section 2.2*, the Suzuki and hydrogenolysis stages of the reaction were optimised individually to maximise the conversion of the protocol. This would also highlight any incompatibility upon the combination of both procedures.

#### 2.3.2.1 Optimisation of Suzuki Reaction

The optimisation of the Suzuki reaction commenced with the identification of pre-existing conditions, employing 3 mol% Pd(PPh$_3$)$_4$ (tetrakis) as the Pd catalyst.[274] While a convenient starting point, it was desirable to identify an alternative catalyst due to the well-reported instability of this complex. Furthermore, previous studies have shown that the triphenylphosphine motif is capable of poisoning Pd/C catalysts, an undesirable attribute for any eventual one-pot investigation.[272]

Initial screening was therefore undertaken using six palladium(II) precatalysts. Precatalysts represent a versatile alternative to classical sources of Pd(0), owing to their relatively inert properties prior to treatment with a base, when the active catalyst species is liberated.[275] These compounds are also employed as a pre-formed metal-ligand complex, simplifying the overall practicality of a reaction that often requires the separate addition of a catalyst and

ligand. The six precatalysts were screened alongside two different solvents and bases (*Graph 2.1*), with both toluene and potassium carbonate included due to their prolificacy within previous literature examples.[274] Phenylboronic acid, as the simplest possible aryl substrate, was employed as the coupling partner.
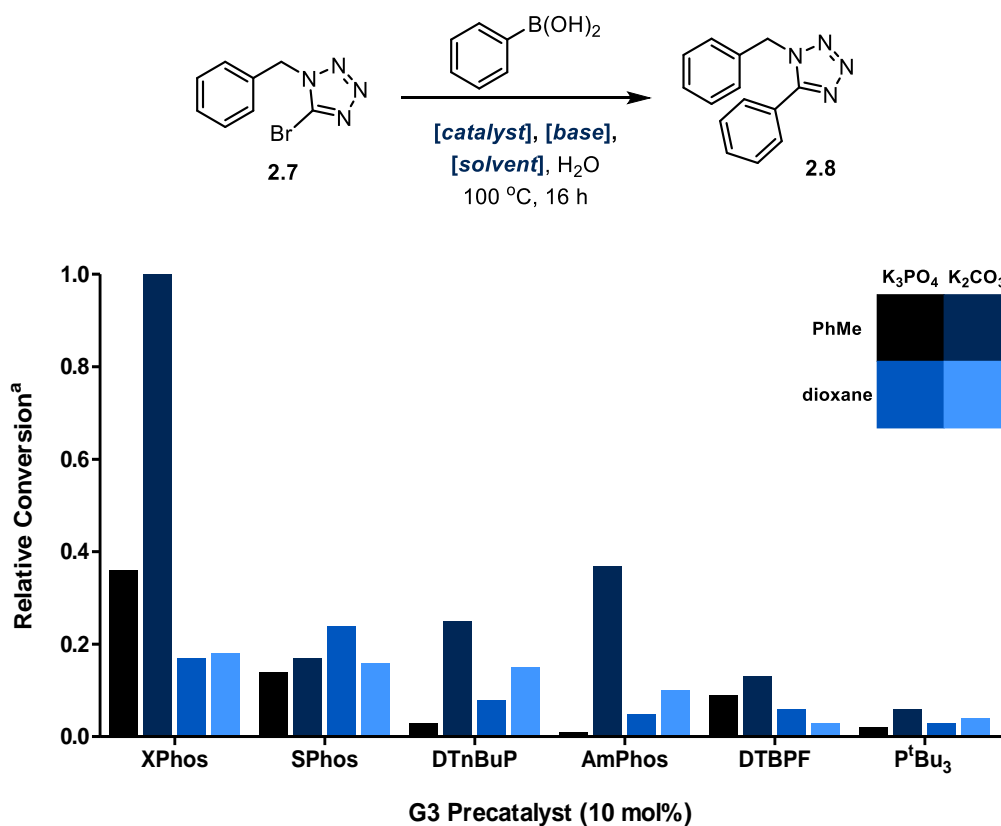


Graph 2.1: Initial catalyst screening identified XPhos Pd G3 as a suitable candidate for further study
[a]Conversion was determined by HPLC with reference to an internal standard
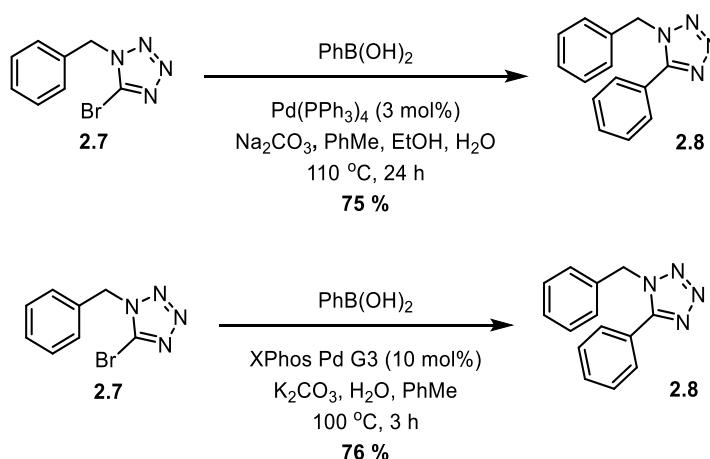


Scheme 2.12: A direct comparison of the previously reported literature conditions, and those identified from a screen of modern precatalysts

The results of this initial screen immediately identified a relatively superior set of conditions, with a combination of XPhos Pd G3, toluene and potassium carbonate affording **2.8** with conversion values almost three times greater than the second-best conditions. The

identification of toluene and carbonate was unsurprising, given their application in the previous literature report.[274] Indeed, a larger scale replication of these newly identified conditions and of the established literature conditions gratifyingly yielded comparable conversions of the product, with XPhos requiring a much shorter reaction time (*Scheme 2.12*).

To further enhance the efficiency of the newly identified conditions, initial follow-up screening sought to establish whether different generations of the XPhos precatalyst would improve conversion (*Table 2.1*). However, this was found have no significant impact on yield. The introduction of XPhos as a separate ligand was found to be detrimental to conversion, despite the addition of superstoichiometric portions of XPhos relative to $Pd(OAc)_2$ to facilitate palladium(0) generation.[276]

*Table 2.1: Investigation of the formation of **2.8** employing different generations of XPhos precatalysts*
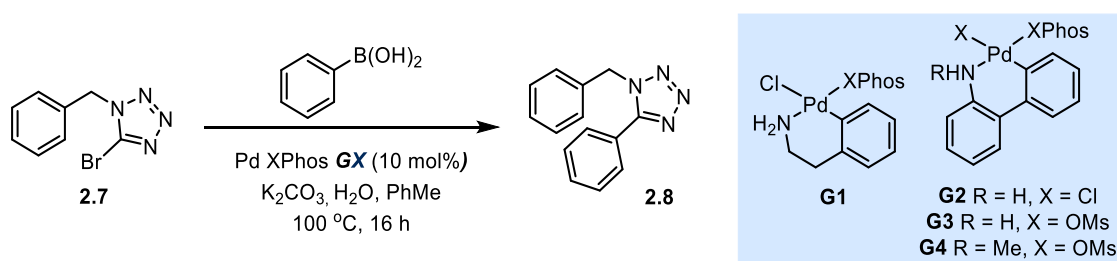


| Entry | (Pre)catalyst | Conversion (%)[a] |
|:-----:|:-------------:|:-----------------:|
| 1 | XPhos + Pd(OAc)$_2$ | **50** |
| 2 | XPhos Pd G1 | **65** |
| 3 | XPhos Pd G2 | **66** |
| 4 | XPhos Pd G3 | **63** |
| 5 | XPhos Pd G4 | **70** |

[a]Conversion values determined by LCMS with reference to caffeine as an internal standard.

The isolated yields of Suzuki reactions are often compromised by water-promoted protodeboronation or oxidation of the boronic acid.[277] To address this potential shortcoming, the stoichiometry of water was examined. It was found that significantly reducing the stoichiometry from one hundred equivalents to only five had a negligible impact upon conversion (*Table 2.2*). While this improved the efficiency of the process, it was unfortunately unsuccessful in improving conversion to **2.8**.

Prior to further optimisation using phenylboronic acid, it was deemed appropriate to investigate the applicability of additional substrates. It was reasoned that identifying any potential limitations of the methodology at this early stage would facilitate a more informed

approach towards further improving the conditions. Consequently, three additional boronic acids were selected and subjected to the high-throuput screening conditions outlined in *Graph 2.1*. 4-methoxyphenylboronic acid, 4-fluorophenylboronic acid, and 4-cyanophenylboronic acid were selected to represent a range of electron-donating and withdrawing substituents in order to highlight any weaknesses in the methodology. The poor performance of potassium phosphate and 1,4-dioxane in the initial screen led to their replacement with caesium carbonate and acetonitrile, respectively (*Graph 2.2*).

*Table 2.2: Water stoichiometry was found to have a limited impact on reaction conversion*
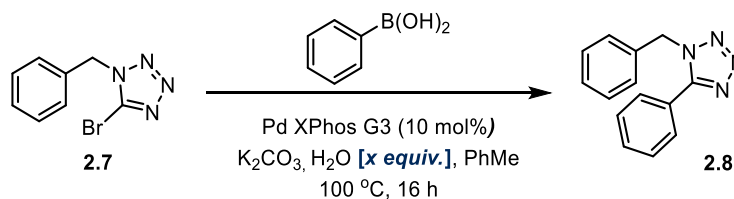


| Entry | Water Stoichiometry (equivs) | Conversion (%)[a] |
|-------|------------------------------|-------------------|
| 1 | 1 | 64 |
| 2 | 5 | 73 |
| 3 | 10 | 76 |
| 4 | 20 | 75 |
| 5 | 50 | 70 |

[a]Conversion values determined by LCMS with reference to caffeine as an internal standard.

Interrogation of the resulting data immediately highlighted the superiority of XPhos and SPhos relative to the other precatalysts. DTnBuP also exhibited promising conversions, however this was not consistent over all substrates. Toluene was again identified as the favourable solvent, with acetonitrile furnishing substantially diminished yields. Both potassium and caesium proved to be acceptable counterions for the carbonate base, with very little discrepancy between the species. The outcome of this study was the confirmation of XPhos and potassium carbonate in toluene as the best combination of reaction conditions identified thus far.

While relative conversion values are beneficial in identifying optimal conditions within a defined data set, such results provide no context of the overall conversion of the reaction. Consequently, all three new boronic acids were exposed to the identified conditions at an increased scale, and isolated yields were obtained (*Scheme 2.13*). This quickly highlighted that while the reaction was applicable to electron-rich and neutral boronic acids, electron-deficient species afforded extremely poor conversions.
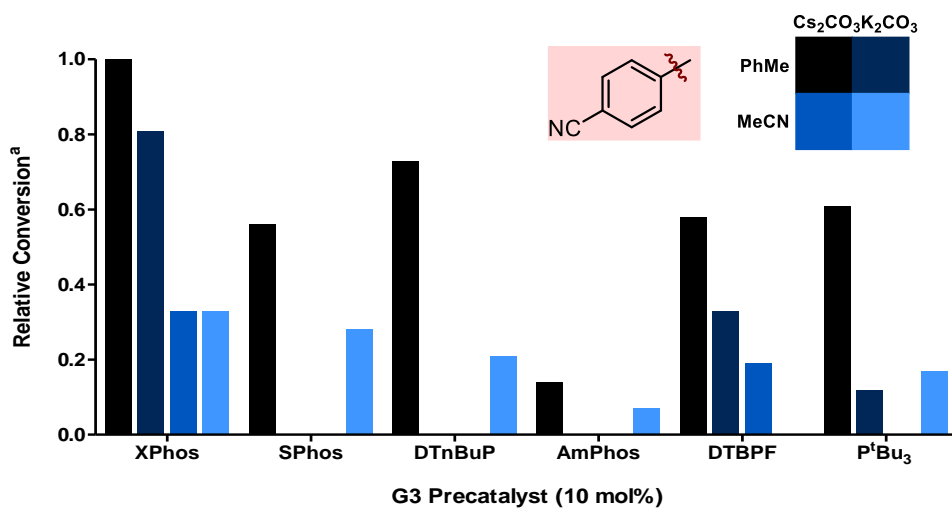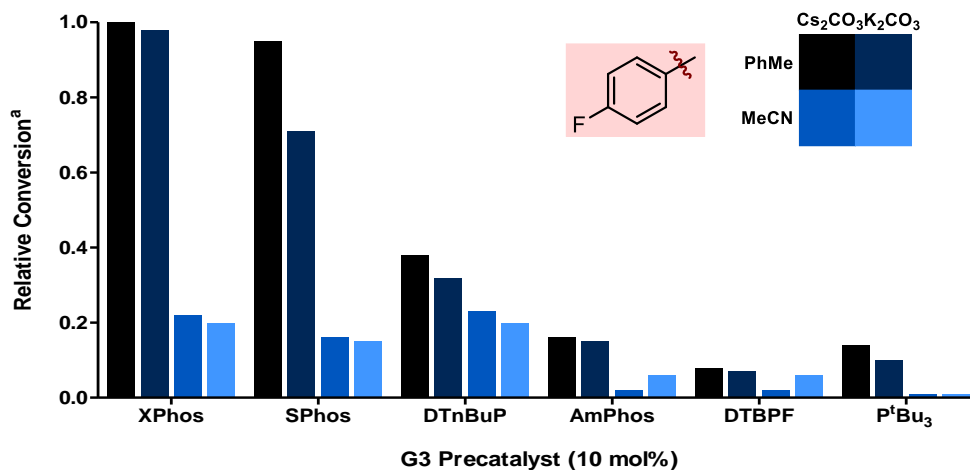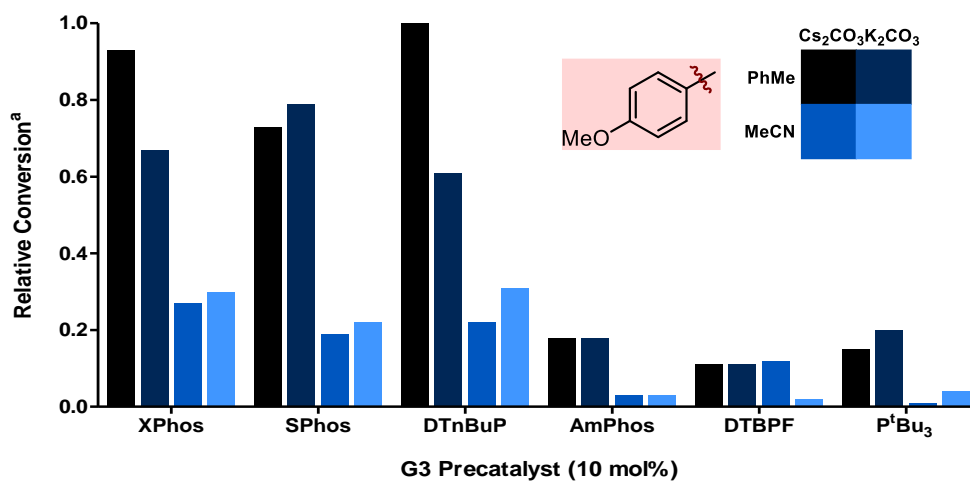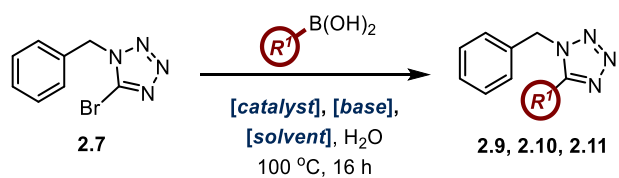
*Graph 2.2: Investigation of additional boronic acid substrates in combination with six Pd precatalysts*
*[a]Conversion was determined by HPLC with reference to an internal standard*
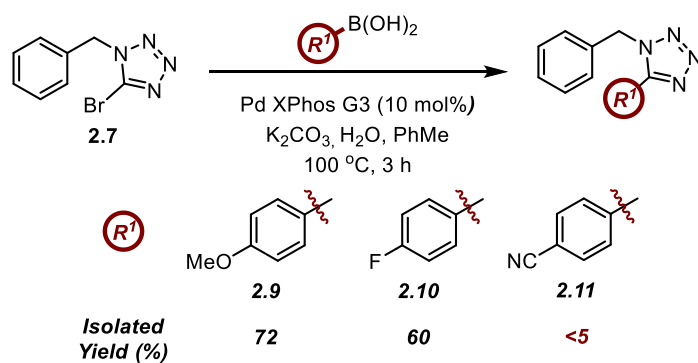
Scheme 2.13: The isolated yields of benzyl tetrazoles **2.9** to **2.11**

It was determined that further investigation of the shortcomings of the reaction with electron-deficient boronic acids was necessary prior to the continuation of the optimisation. A targeted high-throughput screen was designed examining two electron-deficient aryl boronic acids and their corresponding pinacol ester derivatives. The primary aims of this experiment were two-fold. Firstly, it was considered that the poor performance of 4-cyanophenylboronic acid previously may represent a substrate-specific issue, as opposed to the incompatibility of all electron-deficient motifs. Nitriles are competent transition metal ligands, which may inhibit the catalyst.[278] The incorporation of 4-(trifluoromethyl)phenylboronic acid was intended to assess this possibility. The inclusion of the pinacol esters of both boronic acids hoped to elucidate whether more controlled release of the boronic acid may afford greater control over the desired C-C bond formation. The inclusion of alternative base and solvent combinations in potassium phosphate and *n*-butanol were intended to further modulate the rate of boronic acid liberation (*Graph 2.3*).

While conversions remained slightly lower than desired, it was apparent that the incompatibility of 4-cyanophenylboronic acid was not shared by all electron-deficient species. Despite possessing a similar Hammet $\sigma_p$ value,[279] the trifluoromethyl motif did not inhibit the procedure in the same manner. Gratifyingly, this result was replicated upon scale-up of the reaction (*Scheme 2.14*). Unfortunately, boronic acid pinacol esters were poor substrates, while toluene was again shown to be the optimal reaction solvent. Caesium carbonate was adopted as a base for the remainder of the study, owing to the marginally better conversion values obtained relative to potassium carbonate.

With the apparent identification of the optimal discrete variables, efforts were made to reduce the catalyst loading. While 10 mol% often represents an acceptable turnover rate in cross-coupling chemistry, it was deemed unsuitable in this instance. Given that similar yields were obtained in the application of only 3 mol% of tetrakis earlier in the project, it would not be justifiable to employ XPhos Pd G3 at such high loadings. Furthermore, the significant cost and limited abundance of palladium necessitates that every effort is made to reduce the quantity consumed whenever possible. Disappointingly, initial attempts to decrease the

catalyst loading resulted in a substantial decrease in conversion below 5 mol% loading (*Table 2.3*).
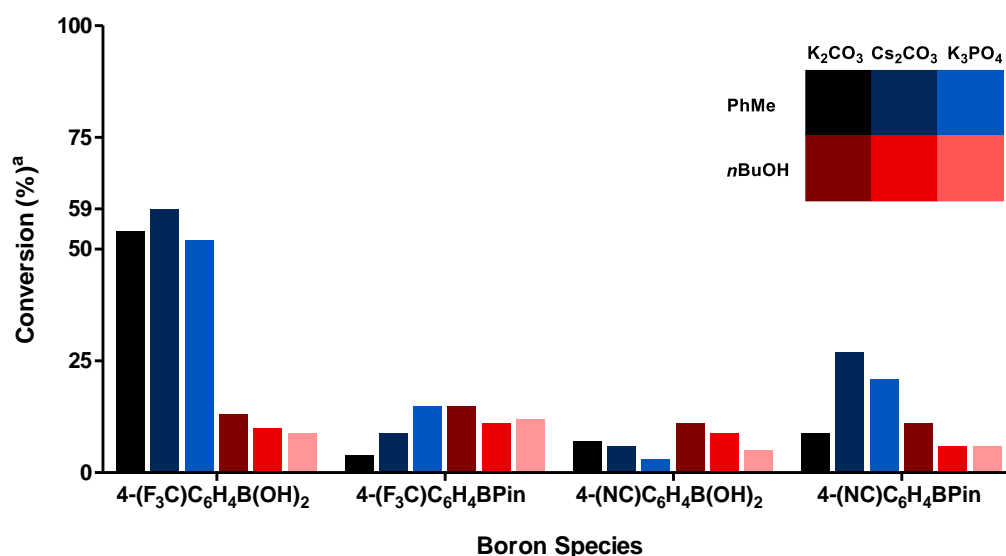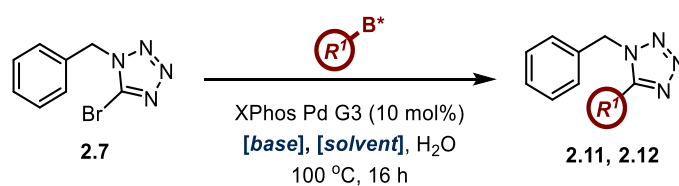


*Graph 2.3: An additional screen of electron-deficient boron species indicated that some substrates were compatible with the conditions, while Cs₂CO₃ represented a minor improvement over K₂CO₃. ᵃConversion was determined by LCMS with reference to caffeine as an internal standard*
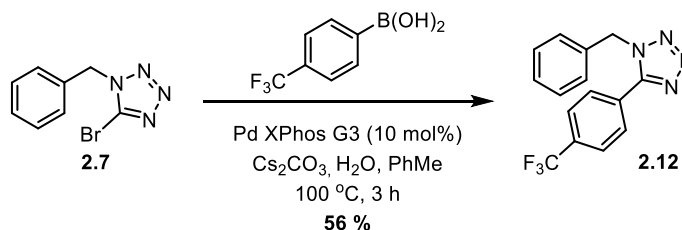


*Scheme 2.14: The isolation of tetrazole 2.12*

This represented a significant set-back in the optimisation campaign, and all efforts were subsequently redirected towards reducing catalyst loading. It was proposed that small alterations to the structure of XPhos may facilitate more efficient catalyst turnover, given the comparable yields obtained by SPhos in earlier screening reactions (*Graph 2.2*). To explore this theory, a selection of bulky, biaryl, monodentate phosphine ligands were investigated.[280,281] The boron species selected for this screen were those employed in *Graph 2.3*. This was intended to enable facile identification of any significant improvement in conversion by interrogating the most challenging palette of substrates. Tetrakis and XPhos were also both included to enable a direct comparison with the other catalysts.
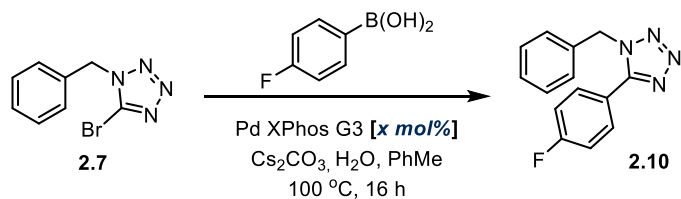
| Entry | Catalyst Loading (mol%) | Conversion (%)[a] |
|:-----:|:-----------------------:|:-----------------:|
| 1 | 10 | **52** |
| 2 | 5 | **47** |
| 3 | 2.5 | **14** |
| 4 | 1 | **6** |
| 5 | 0.5 | **3** |

[a]Conversion values determined by LCMS with reference to caffeine as an internal standard.

Despite the introduction of four alternative bulky biaryl ligands, XPhos remained by far superior (*Graph 2.4*). Interestingly, XPhos also comfortably outperformed tetrakis within this small library of substrates, further emphasising the utility of this species. Retaining XPhos as the ligand, alternative palladium sources were then investigated as a final attempt to increase reaction yield at a loading of 5 mol%. Unfortunately, all other palladium species failed to achieve the conversion values of XPhos Pd G3 (*Table 2.4*).
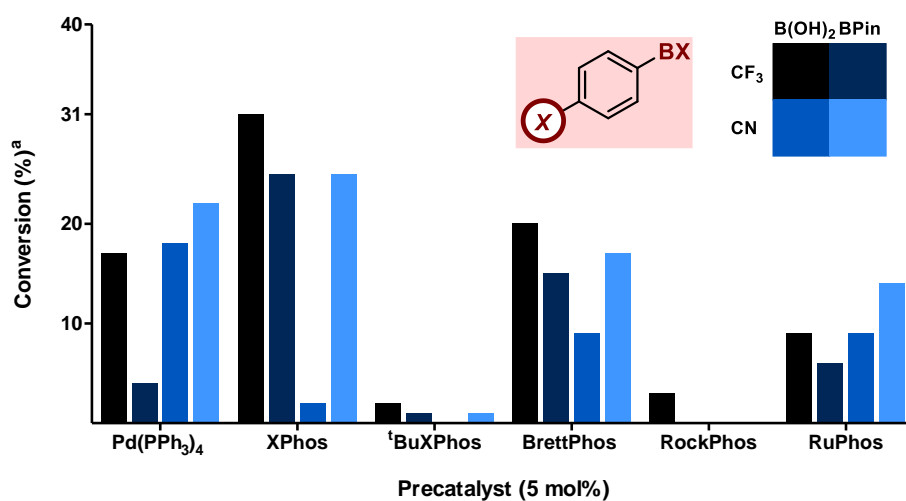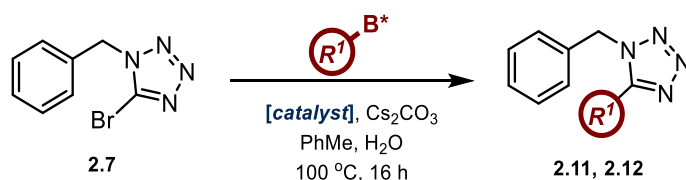


*Graph 2.4: An investigation into alternative ligands for the Suzuki coupling of **2.7** and organoboron species*
*[a]Conversion was determined by LCMS with reference to caffeine as an internal standard*

*Table 2.4: Investigations into the impact of palladium source on the cross-coupling of **2.7** and 4-(trifluoromethyl)phenylboronic acid*
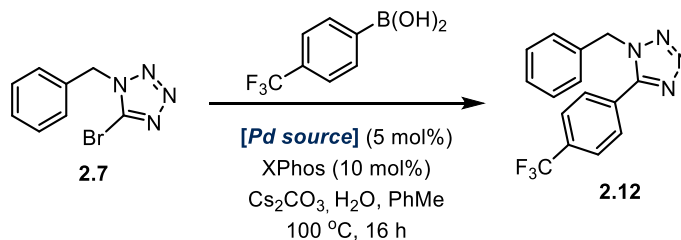


| Entry | Palladium Source | Conversion (%)[a] |
|:-----:|:----------------:|:-----------------:|
| 1 | XPhos Pd G3 | 48 |
| 2 | $PdCl_2$ | 3 |
| 3 | $Pd(OAc)_2$ | 7 |
| 4 | $Pd(PPh_3)_2Cl_2$ | 0 |
| 5 | $Pd(dppf)Cl_2$ | 20 |
| 6 | $Pd_2(dba)_3$ | 4 |

[a]Conversion values determined by LCMS with reference to caffeine as an internal standard.

With efforts to minimise catalyst loading seemingly complete, the remaining continuous variables were optimised using a design of experiments (DoE) approach.[282,283] While conventional reaction optimisation considers each variable separately, DoE assesses the influences that different variables may have on each other, in addition to their impact on overall reaction conversion. This can enable the identification of an optimal set of conditions that may otherwise have been overlooked (*Figure 2.2*).
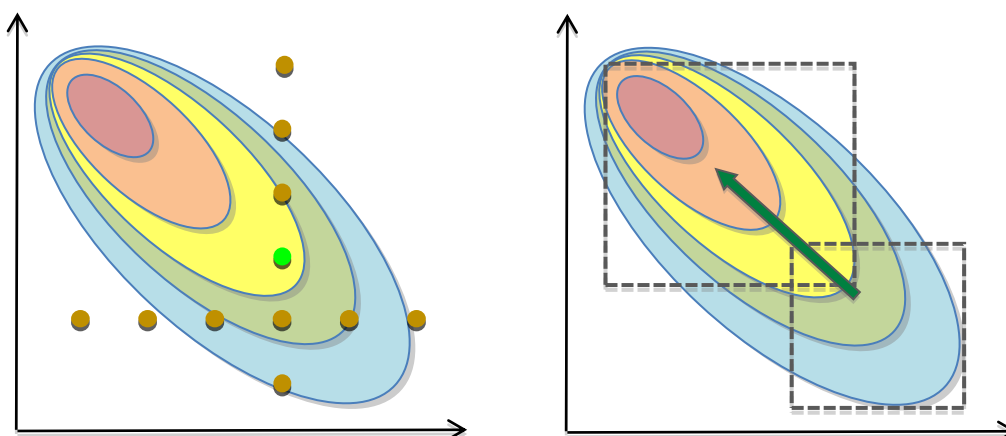


*Figure 2.2: An example of a linear optimisation approach (left) and an example of a DoE approach (right) in the optimisation of the same experiment*
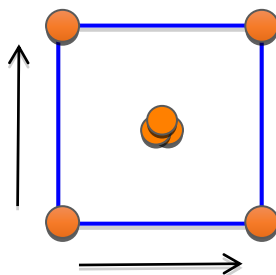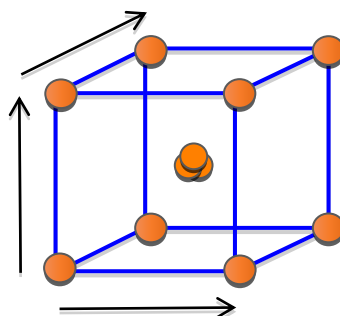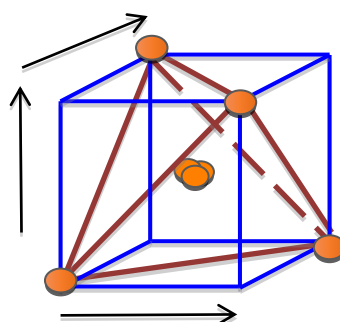
*Figure 2.3: a) A visual example of a two level optimisation with two variables, requiring 4 reactions plus centre-point reactions; b) A two level optimisation involving three variables (8 experiments plus centre-point reactions); c) A two level half-fractional optimisation, again involving three variables, but only requiring 4 reactions plus centre-point experiments*

To accommodate complete coverage of the variables incorporated within a two level DoE optimisation, a total of $2^k + x$ reactions must be performed, where $k$ is equivalent to the number of variables under study, and $x$ is the number of "centre point" reactions (typically 2-4). This total is comprised of reaction conditions that fully encompass all combinations of the minima and maxima of all variables under study. Centre point reaction conditions are composed of the intermediate values of every variable and are included to provide evidence of reproducibility and to enable an estimation of error. As the number of screening reactions required can rapidly expand as the number of variables under examination increases, half-

fractional designs are often employed to simplify the study. These eliminate the need for 50 % of the screening reactions by extrapolating the results already obtained, maintaining appropriate coverage of the minimum and maximum variable values (*Figure 2.3*). These DoE studies require a total of $\frac{2^k}{2} + x$ experiments for accurate results.

Half-fractional designs improve efficiency at the expense of accuracy. This is a consequence of the "aliasing" of results, where the influence of different reaction variables may be combined during the extrapolation portion of the calculation. Aliasing can become problematic during optimisations involving few variables, making interpretation of results challenging, however accuracy can be improved through the input of additional reactions.

Overall, the DoE approach is a highly efficient method of reaction optimisation, while concurrently minimising the number of reactions to be performed in the process. As part of this specific optimisation, a two-level, five-factor, half-fractional DoE protocol was undertaken as a means of optimising base, water and boronic acid stoichiometry, catalyst loading, and concentration. Gratifyingly, limited aliasing issues were encountered, with all main effects and two-factor interactions estimated with good accuracy.

The results of this study highlighted some unanticipated influences on the efficiency of the transformation (*Table 2.5*, *Graph 2.5*). While catalyst loading was unsurprisingly identified as a crucial variable, the significant impact of concentration was entirely unexpected. Upon further investigation, this dependency appeared to be a more complex manifestation of the impact of water stoichiometry. While relatively inconsequential at higher levels of dilution, the increased equivalents of water were found to have a substantial positive impact on conversion in concentrated samples (*Graph 2.6*).

*Table 2.5: Conversion values obtained from the DoE study*
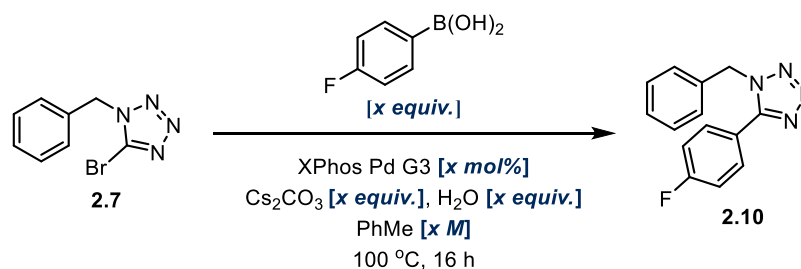


| Entry | Catalyst Loading (mol%) | Boronic Acid Stoichiometry (eq.) | Base Stoichiometry (eq.) | Water Stoichiometry (eq.) | Concentration (M) | Conversion (%)[a,b] |
|---|---|---|---|---|---|---|
| 1 | 10 | 2.5 | 1.1 | 100 | 0.1 | 49 |

| | | | | | | |
|---|---|---|---|---|---|---|
| 2 | 1 | 1.1 | 1.1 | 100 | 0.1 | **21** |
| 3 | 10 | 2.5 | 1.1 | 5 | 1 | **32** |
| 4 | 1 | 1.1 | 2.5 | 5 | 0.1 | **2** |
| 5 | 10 | 1.1 | 1.1 | 100 | 1 | **13** |
| 6 | 10 | 1.1 | 1.1 | 5 | 0.1 | **50** |
| 7 | 10 | 1.1 | 2.5 | 100 | 0.1 | **52** |
| 8 | 1 | 2.5 | 1.1 | 5 | 0.1 | **5** |
| 9 | 10 | 2.5 | 2.5 | 5 | 0.1 | **54** |
| 10 | 1 | 1.1 | 1.1 | 5 | 1 | **2** |
| 11 | 10 | 1.1 | 2.5 | 5 | 1 | **21** |
| 12 | 1 | 1.1 | 2.5 | 100 | 1 | **1** |
| 13 | 1 | 2.5 | 2.5 | 5 | 1 | **2** |
| 14 | 10 | 2.5 | 2.5 | 100 | 1 | **12** |
| 15 | 1 | 2.5 | 1.1 | 100 | 1 | **1** |
| 16 | 1 | 2.5 | 2.5 | 100 | 0.1 | **10** |
| 17 | 5.5 | 1.8 | 1.8 | 52.5 | 0.55 | **10**[c] |

[a]Conversions values determined by LCMS with reference to caffeine as an internal standard.

[b]Reported values are averages of two runs.

[c]Average of three runs.
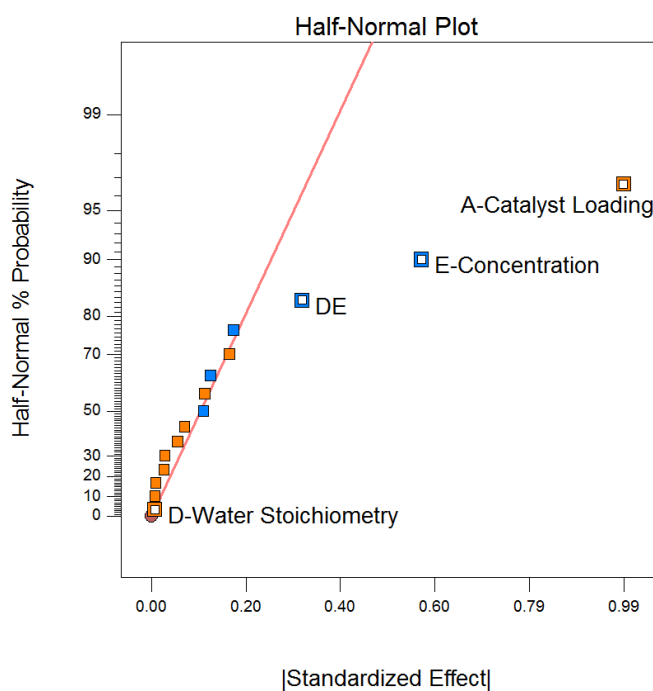


*Graph 2.5 A half-normal plot originating from the DoE study into the Pd-catalysed coupling of aryl bromide **2.7** and aryl boronic acids identified both catalyst loading and concentration as variables of interest*

Design-Expert® Software
Factor Coding: Actual
Original Scale
Conversion (%)
(adjusted for curvature)

54
1

X1 = E: Concentration
X2 = D: Water Stoichiometry

Actual Factors
A: Catalyst Loading = 9.75676
B: Boronic Acid Stoichiometry = 1.8
C: Base Stoichiometry = 1.8
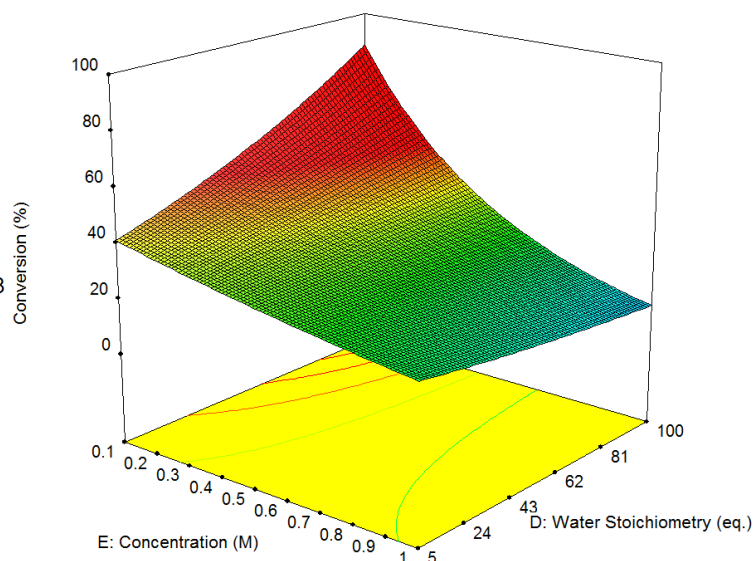
*Graph 2.6 A 3D response surface highlighting the relationship of concentration and water stoichiometry on the outcome of the reaction:*

As a consequence of this DoE study, an additional screen was conducted to investigate if increased equivalents of water in combination with a decreased catalyst loading could counteract the steep decline in conversion values that had previously been observed. Pleasingly, yields of tetrazole **2.10** were maintained at synthetically tractable levels of around 70 % at catalyst loadings of 2 and 3 mol% (*Table 2.6*). This represented a significant contrast to earlier results when only ten equivalents of water were used (*Table 2.3*).

Despite the length of this optimisation, the resulting conditions represented a robust alternative to the previous literature precedent. Firstly, the exchange of tetrakis for a more stable and versatile alternative in XPhos Pd G3 represented a considerable improvement in the longevity of the protocol, particularly as these catalysts remained equally proficient at similar loadings. Furthermore, the use of XPhos Pd G3 has the potential to broaden the scope of the reaction in comparison to tetrakis (for example, in the results of *Scheme 2.14*). The reaction time was also significantly reduced, with the completion of the newly developed methodology in only one sixth of the time required previously.

### 2.3.2.2 Optimisation of Hydrogenolysis Reaction

Following the discovery of reaction conditions to facilitate the synthesis of various 1-benzyl-5-aryl tetrazoles, work commenced on the development of a hydrogenolysis protocol to enable the debenzylation of these substrates. Limited precedent existed for this transformation, with only a single publication outlining the application of Rosenmund's catalyst ($Pd/BaSO_4$) as an efficient additive, although this optimisation was rather limited.[284]

Table 2.6: Decreased levels of catalyst loading maintained similar reaction conversions in the presence of superstoichiometric quantities of water, while concentration was shown to have little effect
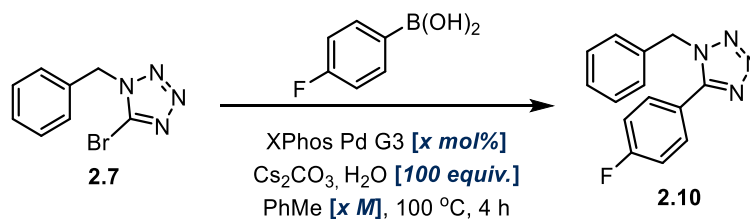


| Entry | Catalyst Loading (mol%) | Concentration (M) | Conversion (%)[a] |
|:-----:|:-----------------------:|:-----------------:|:-----------------:|
| 1 | 10 | 0.1 | 70 |
| 2 | 7 | 0.1 | 69 |
| 3 | 6 | 0.1 | 71 |
| 4 | 5 | 0.1 | 71 |
| 5 | 4 | 0.1 | 70 |
| 6 | 3 | 0.1 | 71 |
| 7 | 2 | 0.1 | 66 |
| 8 | 1 | 0.1 | 38 |
| 9 | 3 | 0.02 | 67 |

[a]Conversion values determined by LCMS with reference to caffeine as an internal standard.

It was decided that a more prudent approach would be an initial high-throughput screen, employing eight common industrial palladium on charcoal (Pd/C) catalysts from 3 commercial sources. While numerous hydrogenation catalysts are marketed under the moniker Pd/C, these species are non-equivalent, with unique properties such as charcoal nanostructure and method of palladium impregnation.[285,286] Such variations can result in significant differences in reactivity. Three solvents were also considered, given the importance of hydrogen solubility in such procedures.[286] Acetic acid has been shown to promote *N*-denzylation reactions,[287] and the role of this substance as an additive was also investigated (*Graph 2.7*).

Of the eight catalysts examined, five furnished almost quantitative conversion to the debenzylated product. Both ethanol and THF were suitable solvents, with ethanol selected for further assessment owing to its robust performance in previous Suzuki-hydrogenation studies within our laboratory.[272] The inclusion of acetic acid was found to be unnecessary, and in many cases proved detrimental to reaction conversion.
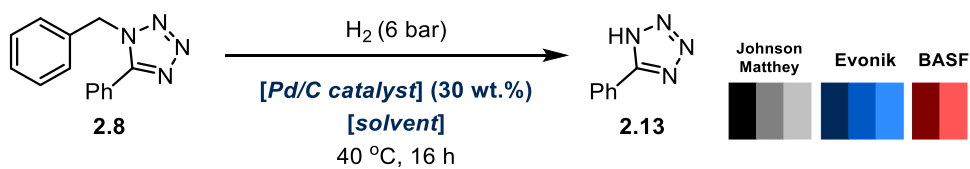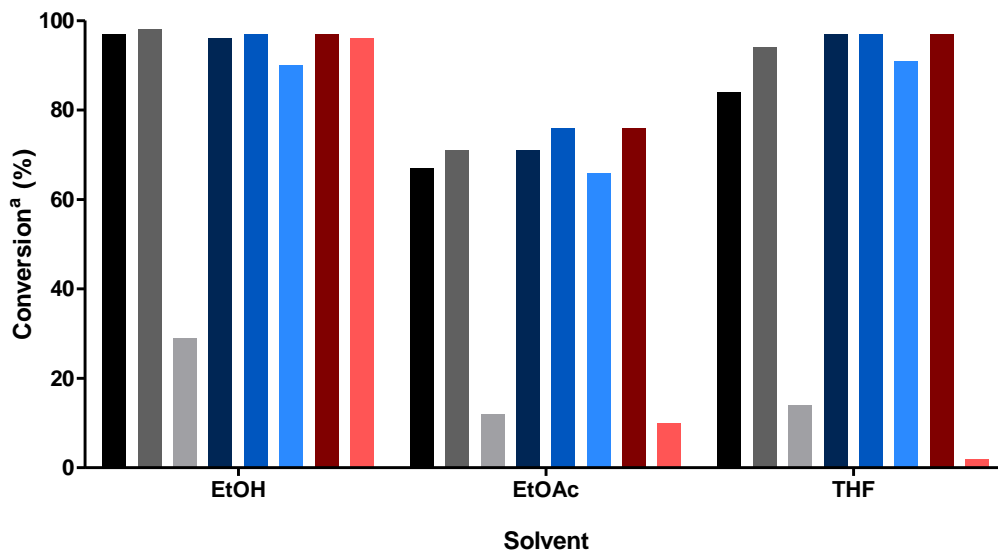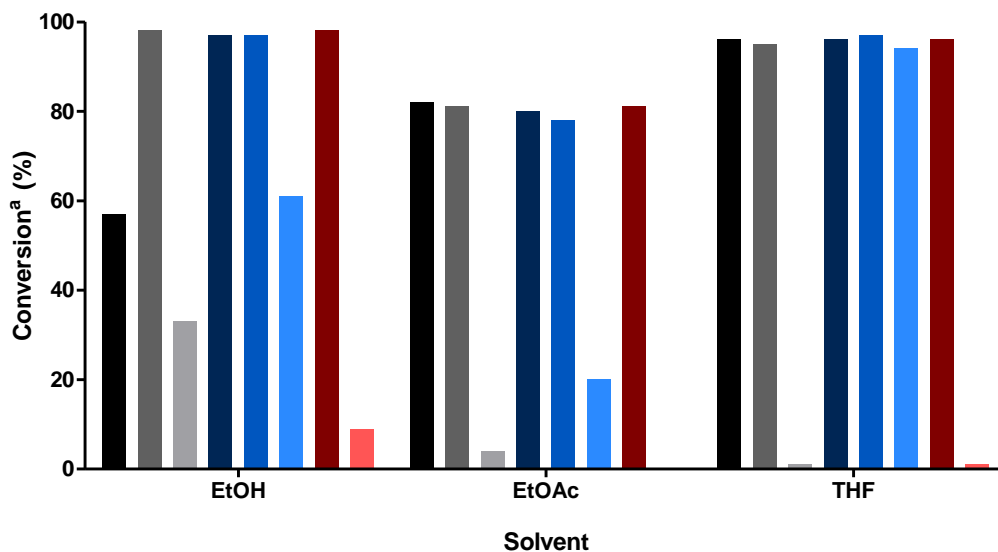
Graph 2.7: High-throughput screening of debenzylation conditions identified numerous suitable Pd/C catalysts, both in the absence (a) and presence (b) of acetic acid. [a]Conversions reported as a percentage of the total peak area of **2.8** and **2.13**

The five best-performing catalysts were reevaluated at reduced catalyst loadings, in order to differentiate between the high yields of the earlier results. The pressure of hydrogen was also decreased from 6 bar to 4 bar, in a continuing effort to identify the mildest debenzylation conditions available (*Table 2.7*).

*Table 2.7: Conversions obtained from lowering the loading of five potential Pd/C catalysts*
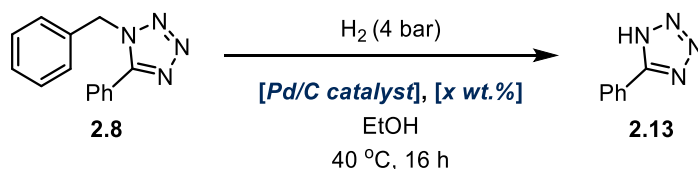


| Entry | Pd/C Catalyst | Catalyst Loading (wt. %) | Conversion (%)[a] |
|-------|---------------|--------------------------|-------------------|
| 1 | JM A405-028-5 | 20 | 38 |
| 2 | JM A503-032-5 | 20 | 33 |
| 3 | Evonik P1070 | 20 | 99 |
| 4 | Evonik P1071 | 20 | 98 |
| 5 | BASF 10318 | 20 | 99 |
| 6 | JM A405-028-5 | 10 | 24 |
| 7 | JM A503-032-5 | 10 | 20 |
| 8 | Evonik P1070 | 10 | 67 |
| 9 | Evonik P1071 | 10 (*2.5 mol%*) | 99 |
| 10 | BASF 10318 | 10 | 97 |

[a]Conversion values determined by LCMS with reference to caffeine as an internal standard.

The results of this screen identified Evonik P1071 and BASF 10318 as the optimal catalysts, with complete hydrogenolysis after 16 hours. The striking efficiency of this debenzylation is highlighted when considering that the application of 10 wt.% Pd/C is equivalent to only 2.5 mol% when expressed using more conventional units.

A final optimisation sought to lower the reaction temperature to room temperature, while simultaneously bringing the pressure of hydrogen gas to 1 bar. As shown in *Table 2.8*, this demonstrated the necessity of maintaining a temperature of 40 °C, with a decrease in conversion of more than 40 % in all cases. By contrast, the yield was relatively unaffected by the pressure of the hydrogen atmosphere.

Following the conclusion of this study, Evonik P1071 Pd/C (otherwise known as Noblyst® P1071) was selected as an appropriate debenzylation catalyst for incorporation within the Suzuki-hydrogenolysis one-pot protocol. Based on the results of the final screen (*Table 2.8*) a temperature of 40 °C was maintained for all future debenzylation reactions, with a H₂ pressure of 2 bar.

*Table 2.8: Attempts in further lowering the pressure and temperature of the debenzylation reaction conditions*
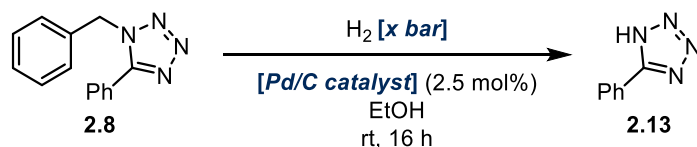


| Entry | Pd/C Catalyst | $H_2$ pressure (bar) | Conversion (%)[a] |
|-------|---------------|----------------------|-------------------|
| 1 | Evonik P1071 | 4 | 59 |
| 2 | Evonik P1071 | 3 | 56 |
| 3 | Evonik P1071 | 2 | 50 |
| 4 | Evonik P1071 | 1 | 47 |
| 5 | BASF 10318 | 4 | 53 |
| 6 | BASF 10318 | 3 | 50 |
| 7 | BASF 10318 | 2 | 44 |
| 8 | BASF 10318 | 1 | 42 |

[a]Conversion values determined by LCMS with reference to caffeine as an internal stanard.

### 2.3.2.3 Optimisation of One-Pot Suzuki-Hydrogenolysis

Prior to combining the two optimised reaction conditions, initial tests were conducted on the Suzuki reaction to assess whether the cross-coupling would be tolerant to the incorporation of Noblyst® P1071 Pd/C. The lowering of the boronic acid and base stoichiometry was also assessed, owing to the results of the earlier DoE study (*Table 2.5*). Gratifyingly, the decreased stoichiometry and incorporation of Pd/C was found to be compatible, with a conversion within five percent of the highest values obtained (*Table 2.9*).

Following this positive result, the two transformations were combined in a single pot for the first time (*Table 2.10*). With the robustness of the Suzuki protocol established, an initial screen examined the efficiency of the debenzylation conditions when exposed to the crude Suzuki reaction mixture. To avoid overcomplication, ethanol, the hydrogenolysis solvent, was added after the completion of the Suzuki reaction. Gratifyingly, $H_2$ pressure was found to be inconsequential to the conversions obtained, with improved or unchanged yields observed at the lower pressure of 2 bar. Unfortunately, the incorporation of the debenzylation protocol within the one-pot Suzuki-hydrogenolysis manifold necessitated a Pd/C loading of 10 mol% for adequate conversion (65 %). While not ideal, a loading of 10 mol% is typical of most debenzylation methodology, with a similar trend also observed as part of our group's previous research in this area.[272] This is likely a consequence of the poisoning of the Pd/C catalyst by the XPhos ligand of the Suzuki Pd species.

*Table 2.9: Investigating the incorporation of Pd/C within the Suzuki reaction manifold*

PhB(OH)$_2$ *[x equiv.]*

**2.7** → XPhos Pd G3 (3 mol %) / Cs$_2$CO$_3$ *[x equiv.]*, H$_2$O, PhMe / 100 °C, 16 h / *[+ additive]* → **2.8**
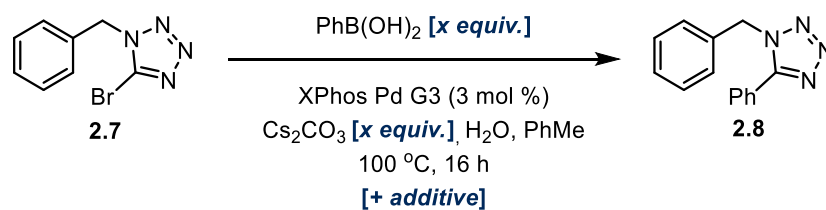
| Entry | Solvent | Boronic Acid Stoichiometry (eq.) | Base Stoichiometry (eq.) | Additive | Conversion (%)[a] |
|-------|---------|------|------|----------|-----------------|
| 1 | Toluene | 1.3 | 1.5 | - | 77 |
| 2 | Toluene | 1.3 | 1.5 | + Pd/C | 72 |
| 3 | Toluene | 1.5 | 2 | - | 76 |

[a]Conversions values determined by LCMS with reference to caffeine as an internal standard.

*Table 2.10: The initial incorporation of the Suzuki-debenzylation methodology within a one-pot manifold*

B(OH)$_2$

**2.7** → XPhos Pd G3 (3 mol%) / Noblyst P1071 Pd/C *[x mol%]* / Cs$_2$CO$_3$, H$_2$O, PhMe / 100 °C, 4 h / then H$_2$ *[x bar]*, EtOH / 40 °C, 20 h → **2.13**
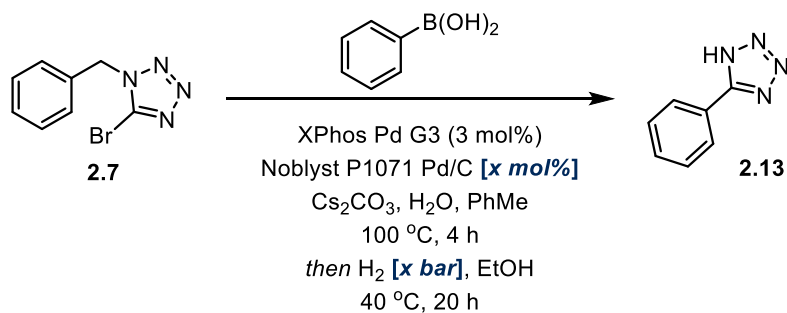
| Entry | Pd/C loading (mol%) | H$_2$ pressure (bar) | Conversion (%)[a] |
|-------|----------------------|----------------------|-------------------|
| 1 | 10 | 4 | 43 |
| 2 | 7.5 | 4 | 48 |
| 3 | 5 | 4 | 29 |
| 4 | 2.5 | 4 | 17 |
| 5 | 10 | 2 | 65 |
| 6 | 7.5 | 2 | 52 |
| 7 | 5 | 2 | 34 |
| 8 | 2.5 | 2 | 35 |

[a]Conversions values determined by LCMS with reference to caffeine as an internal standard.

While this experiment afforded relatively good conditions for further investigation, one final attempt was made to negate the need for solvent addition following completion of the Suzuki

74

reaction, through the addition of a co-solvent at the beginning of the protocol. While the ideal co-solvent for this procedure was ethanol, this required the lowering of the temperature of the Suzuki reaction to 70 °C in order to prevent evaporation. Consequently, *n*-butanol was also considered as a means of maintaining the temperature at 100 °C. The application of toluene as the sole solvent for both transformations was also investigated (*Table 2.11*).

*Table 2.11: Attempts at introducing the hydrogenolysis solvent from the beginning of the protocol were met with diminished yields*
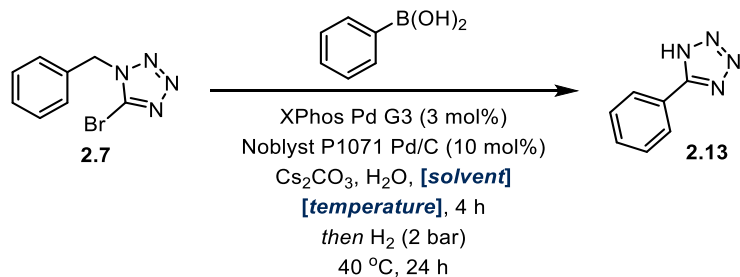


| Entry | Solvent | Suzuki Temperature (°C) | Conversion (%)[a] |
|:---:|:---:|:---:|:---:|
| 1 | PhMe | 100 | 24 |
| 2 | 4:1 (PhMe:*n*BuOH) | 100 | 24 |
| 3 | 3:2 (PhMe:*n*BuOH) | 100 | 4 |
| 4 | 1:1 (PhMe:*n*BuOH) | 100 | 34 |
| 5 | 4:1 (PhMe:EtOH) | 70 | 37 |
| 6 | 3:2 (PhMe:EtOH) | 70 | 22 |
| 7 | 1:1 (PhMe:EtOH) | 70 | 15 |

[a]Conversions values determined by LCMS with reference to caffeine as an internal standard.

Unfortunately, none of these modifications facilitated the inclusion of a co-solvent within the initial reaction mixture, with limited Suzuki or hydrogenolysis conversions obtained in all instances. Therefore, the conditions shown in *Scheme 2.15* were taken forward as the optimised protocol.
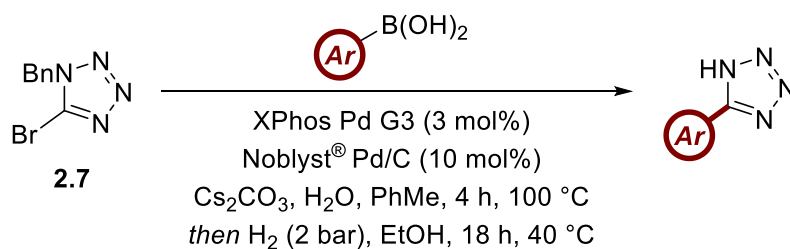


*Scheme 2.15: The optimised conditions identified in the novel arylation-debenzylation of 5-bromo tetrazole 2.7*

### 2.3.3  Scope of the Reaction

Following the identification of appropriate reaction conditions, the scope of the procedure was investigated. The boronic acids considered as part of this study were selected based on two criteria. Primarily, substrates encompassing a variety of electronic and steric characteristics were identified, while several others were based on their previous incorporation within key tetrazoles and NIs. It was intended that the inclusion of these substrates would further showcase the applicability of this protocol. It was determined that purification of the products by column chromatography should be avoided wherever possible. Such methods of compound isolation often require the investment of significant time and resources, and avoiding this represents a significant improvement in the overall practicality of the methodology. Purification was instead conducted through careful control of the pH of the reaction work-up, exploiting the natural acidity of the 1*H*-tetrazole product relative to all other components of the crude reaction mixture (*Scheme 2.16*).
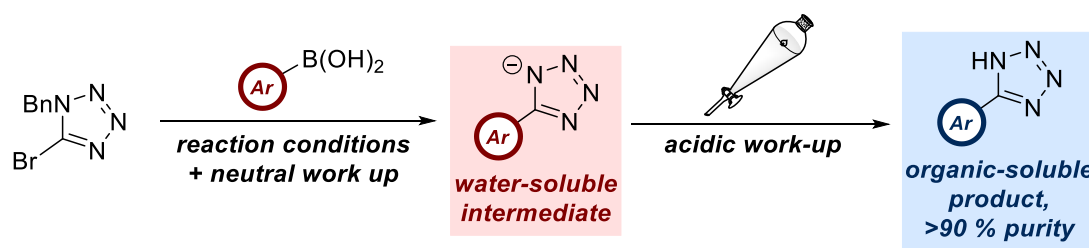


*Scheme 2.16: Control of pH during reaction work-up negates the need of purification by column chromatography*

The results of the substrate scope are shown in *Table 2.12*. While extensive, it was disappointing that no substrate exceeded the isolated yield of the model compound **2.13** (65 %). Nevertheless, additional species with differing electronic properties were shown to possess similar reactivity, with **2.14**, **2.15** and **2.16** isolated in good to moderate yields. The low conversion of methoxy derivative **2.20** was a surprising result, given the high yields observed for this substrate in the earlier optimisation of the Suzuki reaction (*Scheme 2.13*).

The poor performance of electron-rich substrates is also apparent in the failure of compounds **2.29** and **2.32**, which both exhibited substantial protodeboronation of the starting material. Electron-deficient systems, with the exception of **2.16**, are similarly incompatible, with the synthesis of **2.24**, **2.27** and **2.28** all unsuccessful. Gratifyingly, the reaction was reasonably tolerant of steric occlusion, with the isolation of *ortho*-tolyl substrate **2.18** in moderate yields. This did not extend to the 2,6-dimethyl species **2.23**, however, where no product formation was observed. The disparity in isolated yield between *meta*-substituted **2.17** and the corresponding *ortho* and *para* analogues remains unexplained but could be influenced by the purity of the boronic acid starting materials.

*Table 2.12: The scope of aryl and vinyl boronic acids investigated as part of the newly developed Suzuki-hydrogenolysis methodology*



**– Successful Substrates**



| | | | |
|---|---|---|---|
| **2.13** | **2.14** | **2.15** | **2.16** |
| *65 %* | *60 %* | *51 %* | *42 %* |
| **2.17** | **2.18** | **2.19** | **2.20** |
| *26 %* | *47 %* | *42 %* | *15 %* |
| **2.21** | **2.22**[a] | | |
| *23 %* | *22 %* | | |

**– Failed Substrates**



| | | | | |
|---|---|---|---|---|
| **2.23** | **2.24**[b] | **2.25** | **2.26** | **2.25**[c] |
| **2.27** | **2.28** | **2.29** | | |
| **2.30** | **2.31**[a,c] | **2.24**[b,c] | **2.20**[c] | **2.32** |
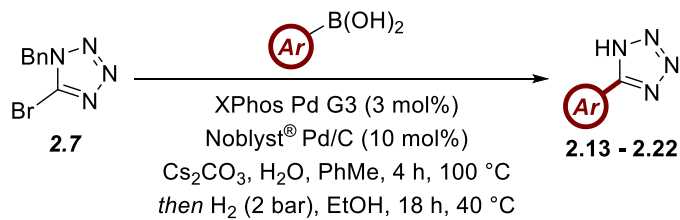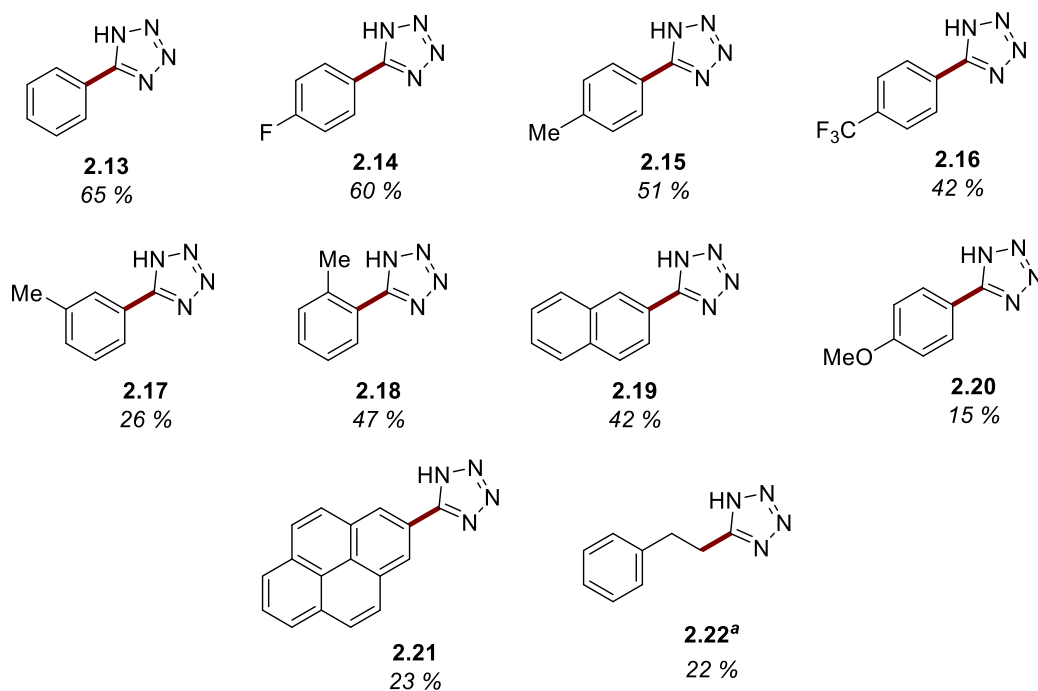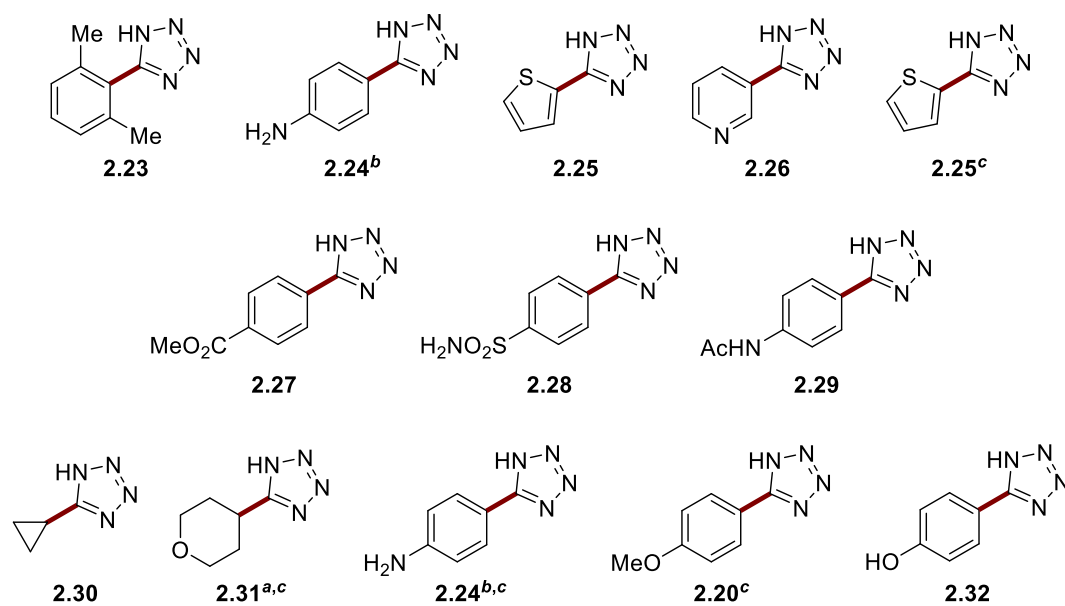
[a]from vinyl derivative, [b]from nitro derivative, [c]from BPin

77

Further attempts to incorporate the pinacol esters of some substrates were unsuccessful (**2.20**, **2.24**, **2.25**, and **2.31**). It is likely that the enhanced reactivity of the boronic acid motif is required to facilitate adequate transmetallation during the Suzuki component of the transformation. An example of a vinylboronic acid was successfully incorporated within the manifold, furnishing alkyl-substituted tetrazole **2.22** in low yields following hydrogenation of the olefin.

Specialised 2,5-diaryl tetrazole substituents prevalent in the literature including naphthyl,[88] pyrenyl[185] and thiophenyl[85] moieties are often incorporated as a means of raising the $\lambda_{max}$ required for NI generation. Consequently, efforts were made to introduce these motifs into this substrate scope. Both napthyl and pyrenyl substrates were amenable to the methodology, furnishing tetrazoles **2.19** and **2.21** in 42 and 23 % yields, respectively. The diminished yield of **2.21** can be attributed to the bulky *C*-substituent hindering effective surface adsorption during the hydrogenolysis phase. Unfortunately, 2-thienyl substrate **2.25** was incompatible. Given the propensity of the corresponding boronic acid to undergo protodeboronation,[288] it is likely that the harsh conditions promoted the decomposition of this material.

One common drawback that was observed during the investigation of this substrate scope was the limited hydrogenolysis of some intermediates following efficient Suzuki coupling. As mentioned above, it is possible that this drawback originates in the poisoning of the Pd/C catalyst by residual XPhos ligand employed during the Suzuki reaction. To expand the overall scope of the procedure, a handful of these substrates were investigated as part of a more conventional two-step protocol, with the initial Suzuki reaction products purified by column chromatography prior to their hydrogenolysis. While this is understandably less desirable from a practical perspective, it was deemed beneficial for substrates that were ineffective under the original conditions.

As an additional aspect of this investigation, a more accessible method of conducting the hydrogenolysis step was assessed. Thus far, all debenzylation reactions were performed within an automated reactor, employing pressurised vessels due to the necessity of a 2 bar hydrogen atmosphere. To make this procedure more cost-effective, it was performed using a 20 mL COware reaction vessel.[289] This enabled the generation of high pressures of reactive gases safely through the application of a two-chambered piece of glassware. In this example, the *ex situ* generation of hydrogen in chamber A facilitated the hydrogenolysis of the substrate, situated in chamber B (*Figure 2.4*).

Hyphenation of the established manifold enabled the improved isolation of a handful of substrates compared to the original conditions (*Table 2.13*). Both 4-methoxy derivative **2.20** and alkyl tetrazole **2.22** were isolated in yields more than 40 % higher, with the synthesis of **2.20** demonstrating applicability as a means of accessing pharmaceutically-relevant

compounds, such as the metabotropic glutamate (mGlu 2) receptor potentiator shown below.[290] Benzoate ester **2.27** was also accessed for the first time using this methodology in a 27 % yield, having previously failed to form. Two additional substrates, the 2-phenyl and 4-phenyl analogues **2.33** and **2.34** were also isolated. The incorporation of a bulky 2-phenyl moiety, albeit in low yields, provides further feedback on the tolerance of steric occlusion within this methodology. This motif is also present in the angiotensin receptor inhibitor losartan, a marketed pharmaceutical for the treatment of high blood pressure.[291]
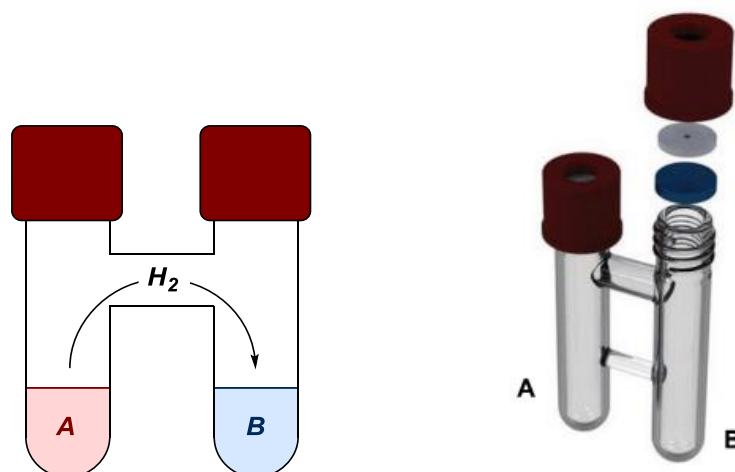


*Figure 2.4: A schematic outlining the COware reaction vessel*

### 2.3.4   The Modular Synthesis of 2,5-Diaryl Tetrazoles

With the development of a novel route towards a library of 5-substituted tetrazoles, the principal objective of the project could now be explored- a modular synthesis of a library of 2,5-diaryl tetrazoles. Four substrates from the above scope were selected to simulate the installation of various functional groups in the 5-position of the tetrazole. Following the large-scale syntheses of these four intermediates, a succession of copper-catalysed arylations utilising literature precedent would furnish a final matrix of sixteen 2,5-diaryl tetrazoles.[264] The objective of this study was to maximise the efficiency of the process, with only one chromatographic purification required for each substrate, and a total of 20 reactions affording the 16 target compounds.

The aromatic moieties selected to augment the tetrazole were carefully considered. Three of the four boronic acids adopted for the arylation of the *C*-position were maintained for subsequent arylation of the *N*-position. This would enable the synthesis of as many "match-pairs" as possible. For example, the synthesis of *N*-phenyl-*C*-naphthyl tetrazole and *N*-naphthyl-*C*-phenyl tetrazole would enable the determination of whether the *N*- or *C*-substituent exhibits greater influence on the $\lambda_{max}$ of the tetrazole.

Table 2.13: An additional scope of 5-substituted tetrazoles accessible through a two-pot approach
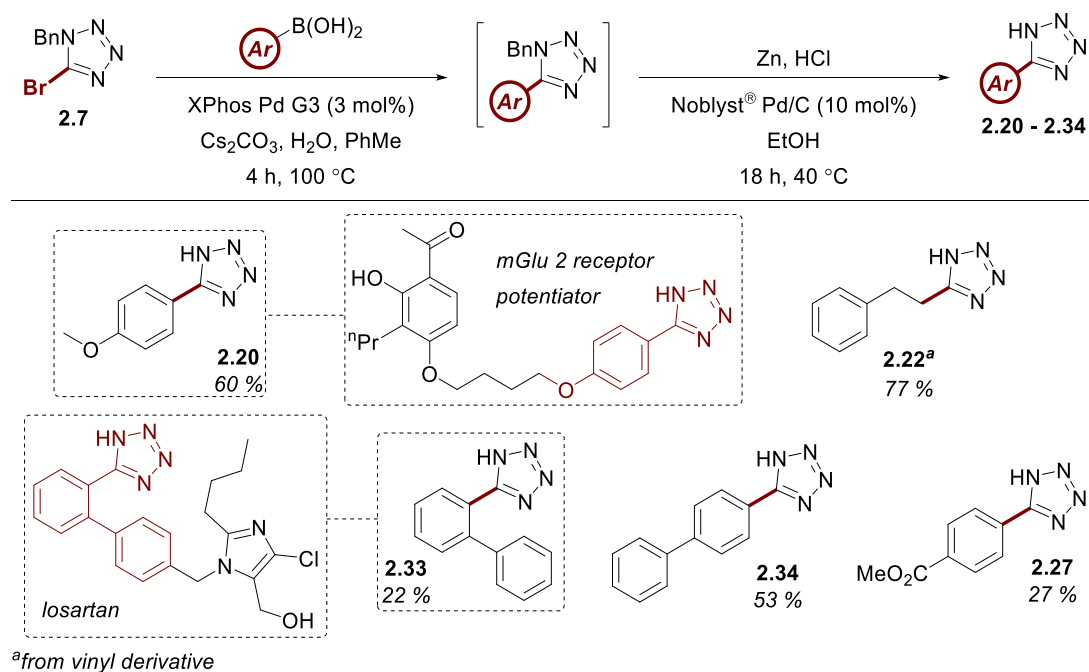


Naphthyl boronic acid was therefore selected as a substrate to investigate the impact of increased conjugation of the tetrazolyl π-system. *Ortho*-tolyl boronic acid was also investigated owing to recent reports on the application of sterically congested NIs in chemical biology.[222] Phenylboronic acid was included as a control substrate. 4-fluorophenylboronic acid was introduced as an example of a valuable *C*-aryl substituent, as the incorporation of a fluorine atom in this position provides a tremendously sensitive functional handle for the monitoring of NI reactivity (see *Section 3.3.1.2*, *3.3.2.1* and *4.3.2*). The final *N*-arylation substrate was 4-(acetamido)phenylboronic acid, to simulate the introduction of an easily modifiable, bioorthogonal functional handle (*Figure 2.5*).
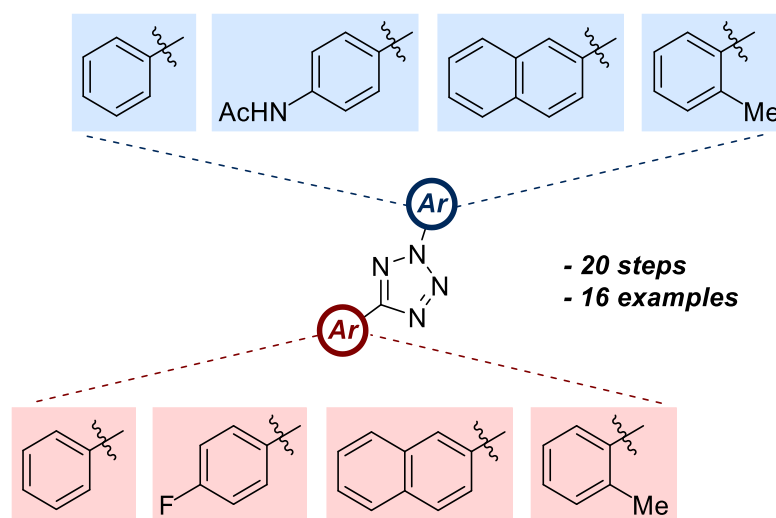


Figure 2.5: A summary of all functional groups considered in the modular synthesis of a library of 2,5-diaryl tetrazoles

To synthesise this library of 2,5-tetrazoles, it was necessary to generate the four desired 5-aryl tetrazoles on a larger scale. Translation of the existing methodology to a 2.5 mmol scale proceeded smoothly, with no detrimental impact on yield (*Table 2.14*). Indeed, two of the four substrates were isolated in improved yields relative to the 0.5 mmol scale previously employed (**2.18** and **2.19**). Consequently, a satisfactory excess of all four 5-aryl-1*H*-tetrazoles were obtained for application in the subsequent matrix. Gratifyingly, all were obtained in excess of 90 % purity without the need for column chromatography, with an isolation time of under one hour.

*Table 2.14: The scale-up synthesis of four 5-aryl tetrazoles for application in the array synthesis of 2,5-tetrazoles*
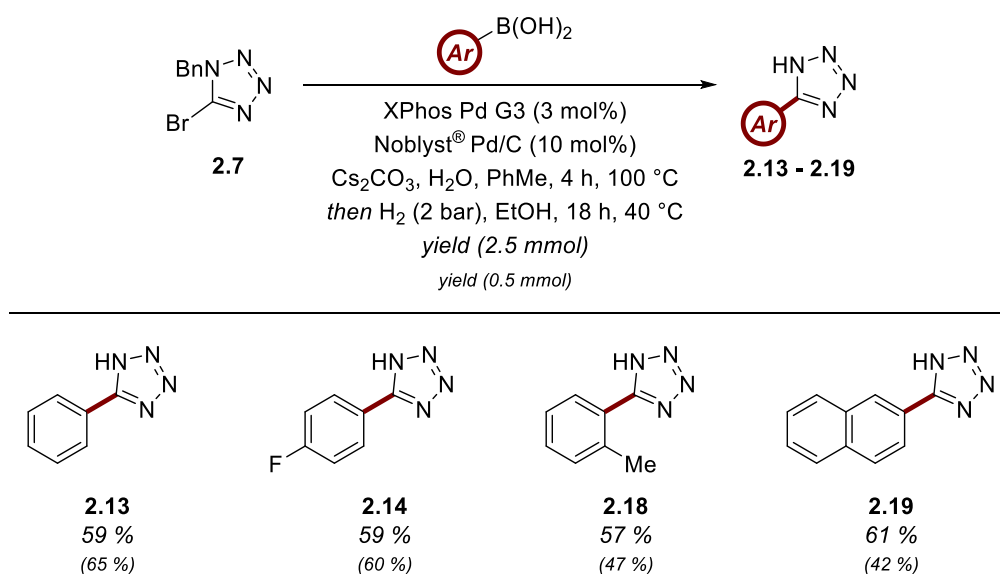


The outcome of this synthesis is shown in *Table 2.15*. The data obtained was extremely positive: fifteen of the sixteen tetrazoles were successfully furnished in synthetically tractable quantities. More than half of the *N*-arylation reactions afforded yields of >70 %, with overall yields of greater than 50 %. Most importantly, this modular approach towards these analogues drastically reduced the purification time that would have otherwise hindered their preparation. All reactions exhibited a relatively clean profile with no isolation difficulties, a substantial improvement over existing methodology.

Interesting trends in the reactivity of some substrates can also be immediately identified through this synthetic approach. For example, the inclusion of the naphthalene motif as either the *N*- or *C*-aryl group has a substantial influence on the stability of the heterocycle. It is likely that the increased conjugation of the π-electron system promotes the formation of the corresponding NI at lower temperatures. The high temperatures required by this protocol may facilitate premature formation of the 1,3-dipole, resulting in lower yields for these substrates. The incorporation of an *ortho* substituent in both the *C*- and *N*-aryl rings also has a small negative effect on the yield. This can be expected given the increased steric bulk of

the substrates, but the methodology remains competent and furnishes even the most congested analogue **2.50** in 36 % overall yield.

*Table 2.15: The modular, array-type synthesis of a library of 2,5-diaryl tetrazoles*



| Ar | (phenyl) | (4-NHAc-phenyl) | (2-naphthyl) | (2-Me-phenyl) |
|---|---|---|---|---|
| (phenyl) | **2.35** 83 % (54 %) | **2.36** 83 % (54 %) | **2.37** 84 % (55 %) | **2.38** 78 % (51 %) |
| (4-F-phenyl) | **2.39** 78 % (46 %) | **2.40** 71 % (42 %) | **2.41** 15 % (9 %) | **2.42** 81 % (48 %) |
| (2-naphthyl) | **2.43** 85 % (52 %) | **2.44** n.r. | **2.45** 16 % (10 %) | **2.46** 35 % (21 %) |
| (2-Me-phenyl) | **2.47** 68 % (39 %) | **2.48** 71 % (40 %) | **2.49** 30 % (17 %) | **2.50** 63 % (36 %) |
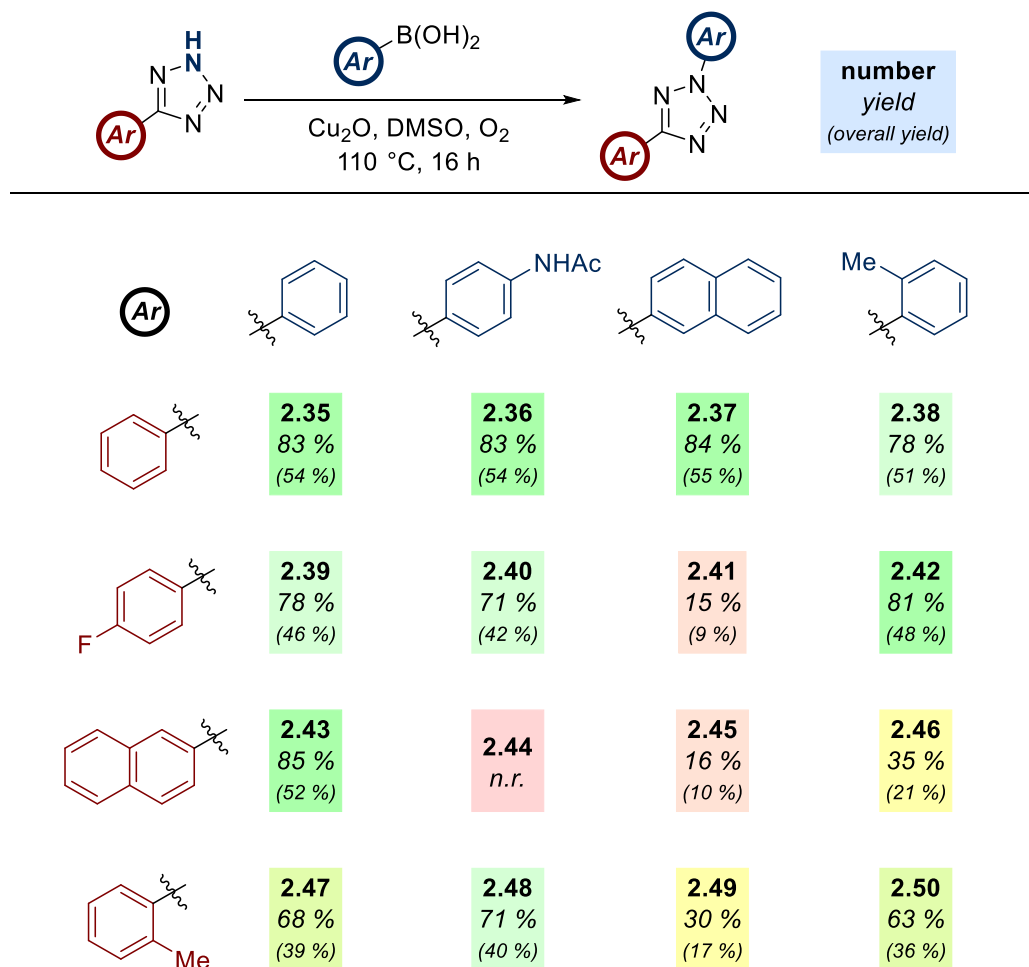
## 2.4 Conclusions and Outlook

As outlined in *Section 2.1.1*, while there are numerous protocols reported for the synthesis of 2,5-diaryl tetrazoles, none are compatible with a modular, array-type synthesis towards a library of these compounds. Given the enormous potential of this heterocycle as a traceless, light-activated precursor of the pleiotropic NI 1,3-dipole (*Section 1.4*), it is essential that greater efforts are made to further adapt the synthesis of 2,5-tetrazoles for application in the 21st century.

The study detailed above represents a significant advance on existing methods of accessing these motifs. The adoption of 5-bromo-1-benzyltetrazole as a lynchpin from which to construct a broad variety of NI precursors with minimal synthetic effort has substantial utility within this field. Furthermore, this valuable intermediate was accessed in excellent yields in just two steps from commercially available starting materials, while simultaneously negating the need for hazardous reagents in the formation of the heterocyclic ring itself.

While the optimisation of the protocol highlighted the challenges often associated with palladium-catalysed methodology, the resulting one-pot tandem Suzuki-hydrogenolysis of **2.7** and arylboronic acids enabled access to a range of different 5-aryltetrazoles in good yields. Most importantly, this procedure required no column chromatography in the purification of the product and was compatible with scale-up to synthetically useful levels (*Scheme 2.17*).
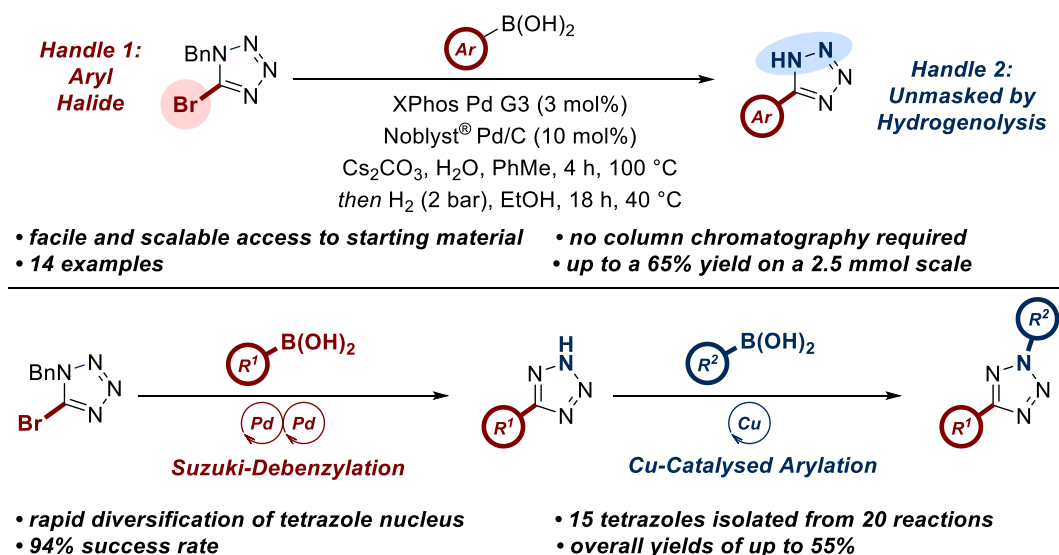


*Scheme 2.17: An overview of the principal findings of this chapter*

Furthermore, this reaction provided the rapid and facile synthesis of a library of fifteen 2,5-diaryl tetrazoles, with a 94 % success rate and more than half isolated in overall yields greater than 40 %. Given the increasing reports of 2,5-diaryl tetrazole application within the literature, it is anticipated that this reaction will enable increased diversification of these valuable heterocycles, indirectly facilitating greater understanding of the properties of the resulting NI 1,3-dipoles.

# 3  Metal-Free Coupling of Nitrile Imines and Boronic Acids

With a facile method of accessing NI precursors now in hand, further research shifted focus towards manipulation of the dipole itself. As discussed in *Section 1.3*, the properties of this species facilitate the exploitation of many transformations in comparison to most 1,3-dipoles. This promiscuous reactivity is at odds with the research output of this area, with much of the behaviour of this motif yet to be understood.

In accordance with our broader objectives of further understanding the nature of NI reactivity, we endeavoured to investigate the outcome of the combination of this 1,3-dipole with aryl boronic acids. Drawing mechanistic rationale from the Petasis reaction, it was proposed that this interaction may represent a route towards novel C-C bond formation through an unprecedented reactivity profile of the NI.

## 3.1  Introduction

### 3.1.1  The Petasis Borono-Mannich Reaction

First reported in 1993, the Petasis reaction is a multi-component reaction (MCR) between an amine, an aldehyde, and a boronic acid.[292–294] It proceeds *via* the formation of an imine or iminium moiety *in situ*, followed by the nucleophilic migration of the R group of the boronic acid, forming a substituted amine. The transformation is often referred to as the Petasis Borono-Mannich (PBM) reaction, owing to its similarities to the eponymous process which involves the nucleophilic attack of an electrophilic iminium centre.[295] In comparison to other MCRs such as the Ugi or Passerini, the PBM employs very mild conditions and is compatible with a range of different solvents.

In his initial publication, Petasis reported the condensation of a library of secondary amines with paraformaldehyde, furnishing a number of allyl amines upon combination with a vinyl boronic acid derivative (*Scheme 3.1*).[292] The reaction was generally high yielding across a variety of secondary amines, although examples were mainly limited to aliphatic motifs.
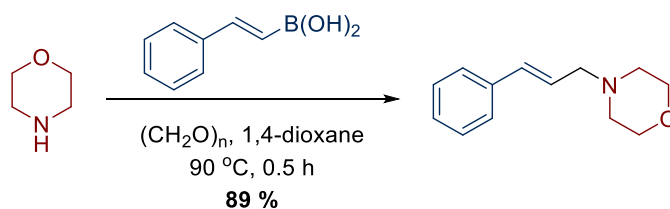


*Scheme 3.1: An example from Petasis' initial publication outlining the PBM reaction*

The scope of the process has been expanded significantly in recent years, particularly with respect to the amine component. The reaction is applicable with most primary and secondary species, with secondary amines and bulky primary amines affording superior yields.[296,297] These motifs form cationic iminium species, which exhibit substantially greater electrophilicity than the analogous imine and are therefore more susceptible to nucleophilic attack in the rate determining step of the reaction. Other amines such as anilines and amino acid derivatives are also compatible (*Scheme 3.2*).[297,298]
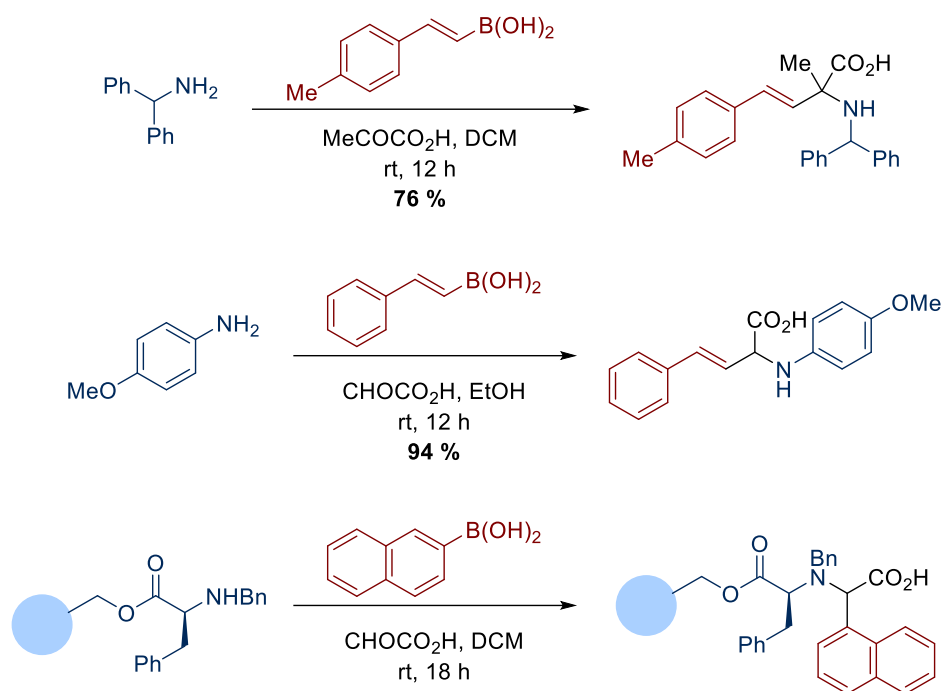


*Scheme 3.2: An assortment of compatible amines within the PBM reaction*

The scope of the carbonyl component of the PBM is considerably more restricted. While paraformaldehyde was employed in the initial study, almost all other examples involve aldehydes with adjacent alcohol or carboxylic acid moieties. This is due to the formation of a nucleophilic four-coordinate boronate as an intermediate within the reaction mechanism.[299] While Petasis' initial publication demonstrated that *in situ* boronate formation involving transient water or alcohols is possible, the reaction is accelerated significantly through the formation of an intramolecular boronate-imminium species

α-Hydroxy aldehydes, such as glycoaldehyde, and salicaldehyde derivatives are both common substrates. These follow a similar principle wherein the neighbouring alcohol moiety participates in the reaction *via* formation of a nucleophilic boronate complex (*Scheme 3.3*).[300,301] This protocol can also proceed with diastereoselectivity, typically yielding the *anti*-product relative to the boronic acid R-group and the α-hydroxy group.[302,303]
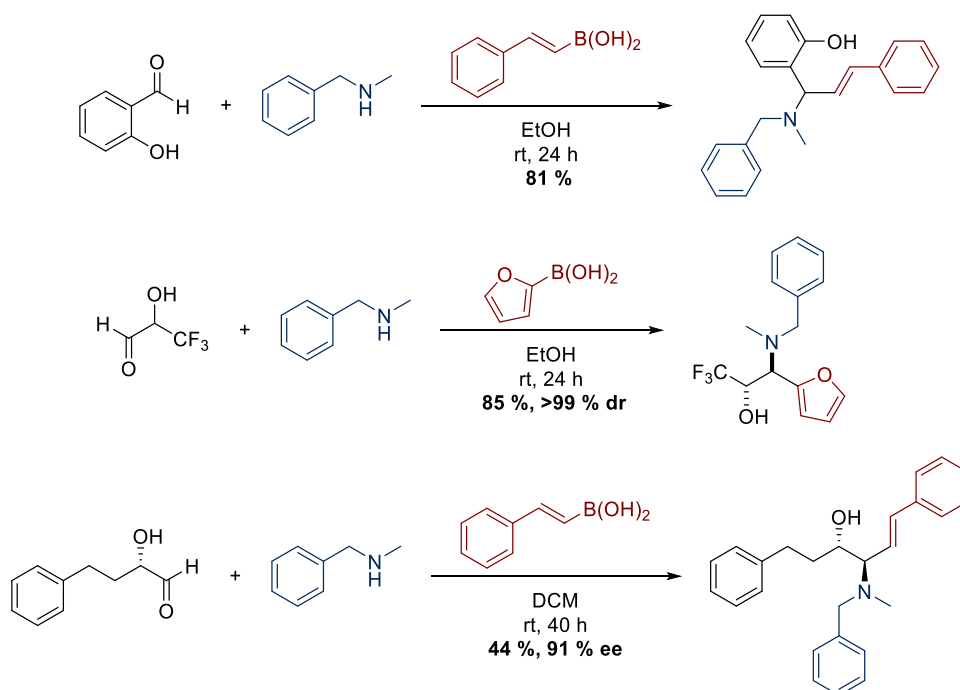
*Scheme 3.3: The application of salicaldehyde and glycoaldehyde derivatives within the PBM reaction*

The scope of the boronic acid component of the PBM is diverse, and most $sp^2$-hydridised boronic acids are compatible. Vinyl boronic acids exhibit superior activity in comparison to aryl boronic acids, with the reactivity of aryl compounds enhanced by electron-donating substituents (*Scheme 3.4*).[300,304–309]
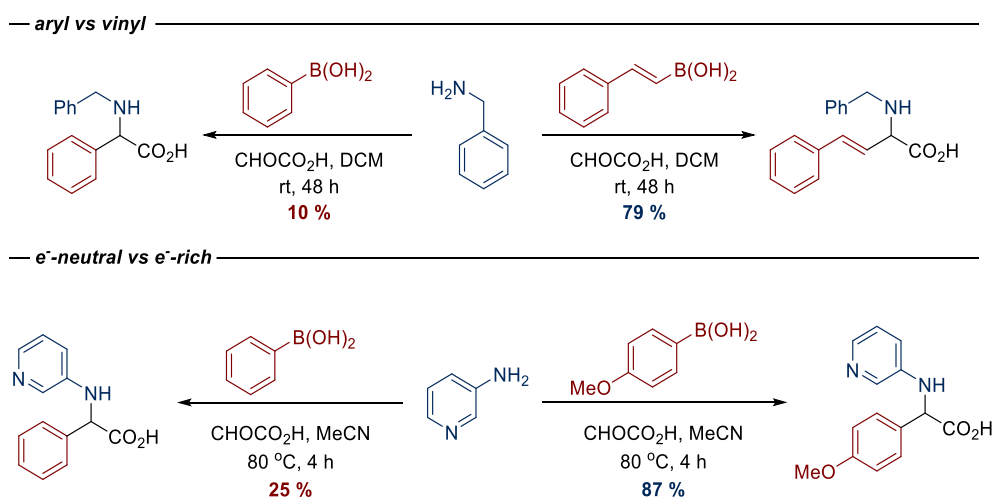


*Scheme 3.4: The increased reactivity of vinyl and electron-rich aryl boron species in the PBM reaction*

Other boron species can also participate in the PBM reaction. While relatively under-explored, boronic esters are able to furnish the desired products in comparable yields to the parent boronic acid.[296,309–311] However, while the system is tolerant of boronic esters, they are often significantly less reactive than the analogous boronic acids (*Scheme 3.5*). This has been hypothesised to be a consequence of their increased steric bulk, inhibiting the formation

of the key boronate complex and the migration of the boron-carbon bond into the iminium centre.[309]
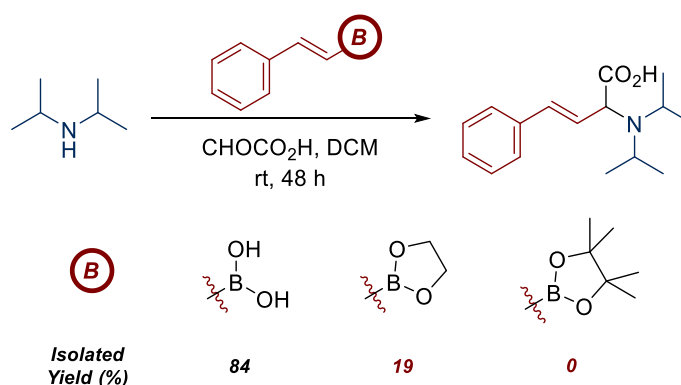


*Scheme 3.5: An example of the application of boronic esters under PBM conditions, highlighting their decreasing reactivity with increasing steric bulk*

Potassium tetrafluoroborate salts can also be introduced as boronic acid equivalents (*Scheme 3.6*).[312–314] While not particularly advantageous over the use of the boronic acids for most substrates, it does enable access to propargyl amines through the use of alkynyl tetrafluoroborate precursors,[313] however an acid catalyst is required to activate the reagent.
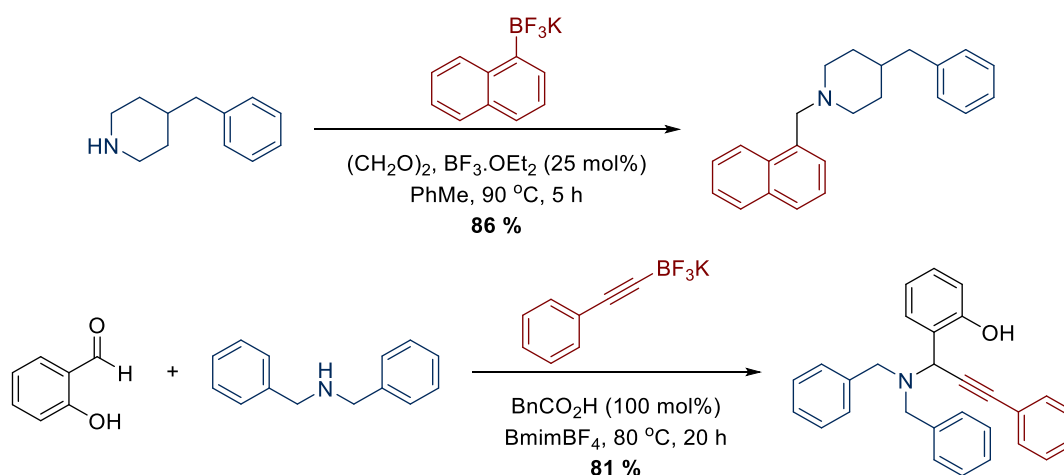


*Scheme 3.6: The application of BF₃K salts within the PBM reaction*

The mechanism of the PBM reaction has been a topic of continued research since the initial report in 1993.[292] A general overview is shown in *Scheme 3.7*, with formation of the nucleophilic "ate" complex and the generation of the electrophilic iminium species. This is followed by the irreversible migration of the vinyl or aryl group of the boronate. Numerous publications have identified this final carbon-carbon bond formation as the rate determining step.[307,308,315]

The formation of the boronic acid "ate" complex is one of the most significant aspects of the PBM. Neutral boronic acids are relatively inert in the presence of electrophiles, and formation of a boronate significantly increases the nucleophilicity of the species.[288] The formation of this key intermediate has been detected experimentally using ^{11}B NMR

spectroscopy.[316] The necessity of an α-hydroxyl or α-carboxyl moiety for the formation of this complex provides rationalisation for the limited scope of aldehydes in the reaction.
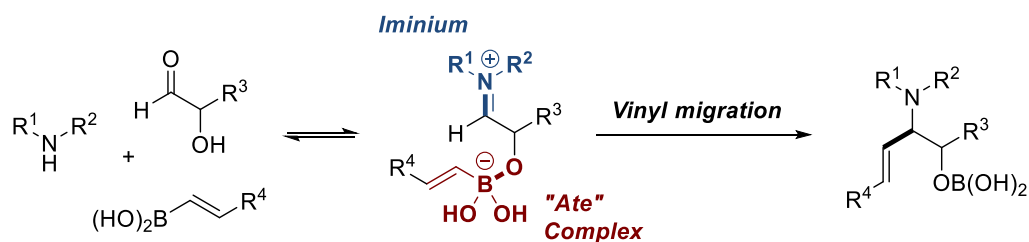


*Scheme 3.7: A general overview of the key steps of the PBM reaction*

One point of contention within the mechanism has been the order by which the iminium and "ate" complexes are formed. Two pathways were proposed in earlier reports, with either immediate condensation of the aldehyde and amine followed by coordination of the boron compound,[317] or rapid boronate complexation with slower generation of the iminium (*Scheme 3.8*).[316,318]
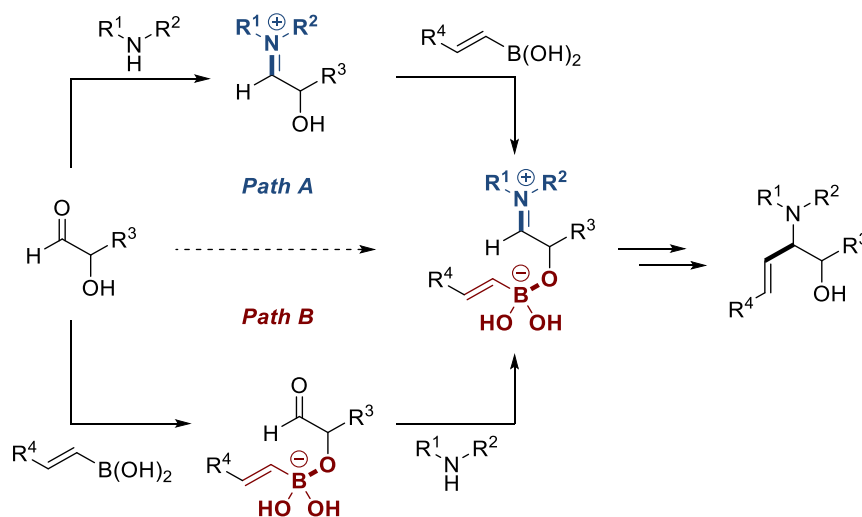


*Scheme 3.8: The two potential paths of "ate" complex formation*

Recent computational work has indicated that a slightly modified version of path A is the favoured mechanism.[315] The reaction proceeds *via* a zwitterionic iminium intermediate prior to the coordination of the boronic acid, which then forms the key "ate" complex (*Scheme 3.9*). While the starting aldehyde was indeed found to react with the boronic acid, this proceeded *via* a dehydrative mechanism, preventing the generation of a nucleophilic boronate species.

### 3.1.2   Applications to Nitrile Imine Chemistry

When considering the PBM mechanism, arguably the most important step is carbon-carbon bond formation *via* migration of the aryl or vinyl group of the boronic acid. The step is facilitated by the generation of two key intermediate functional groups; the electrophilic

iminium and the nucleophilic boronate complex. While the formation of the iminium is relatively facile, boronate generation requires the presence of a coordinating group adjacent to the electrophile, such as an acid or an alcohol. The intramolecularity of this "ate" complex is also important, as unsubstituted aldehydes are often incompatible.
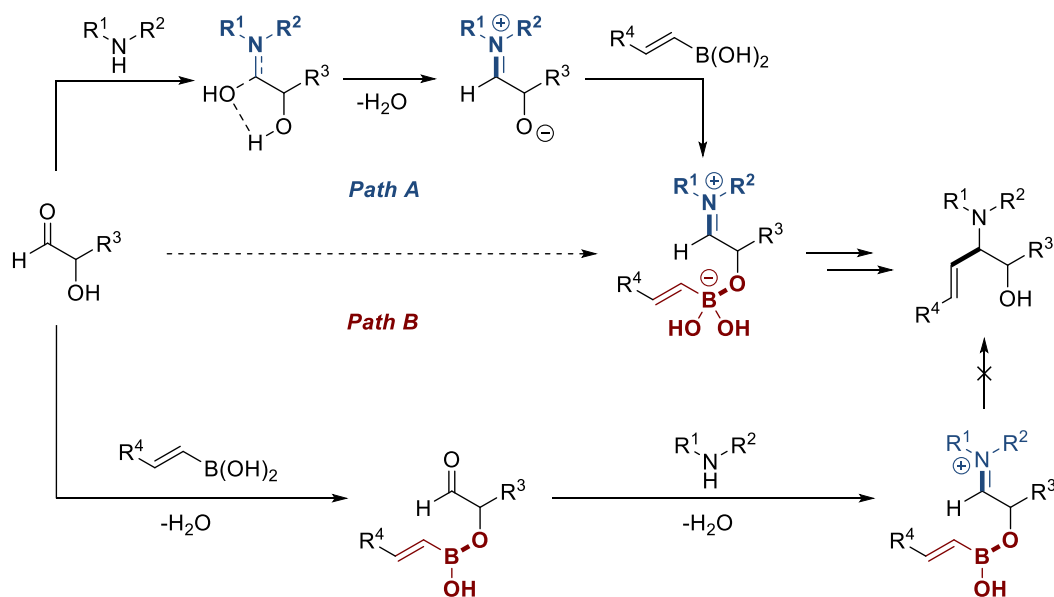


*Scheme 3.9: An updated mechanism of the formation of the key "ate" complex of the PBM reaction*

The similarities between this reaction profile and the properties of the NI dipole are extensive. Firstly, NIs possess a highly electrophilic *C*-terminus, the site of reaction with several simple nucleophiles such as amines and thiols. This is analogous to the electrophilic iminium species within the PBM reaction, which is also generated *in situ*. Secondly, the *N*-terminus of the NI possesses considerable electron density, potentially enabling formation of a nucleophilic boronate in a similar fashion to the "ate" complex of the PBM, mimicking the behaviour of a coordinating acid or alcohol. These two properties of the NI are also in close proximity, potentially enabling formation of the crucial intramolecular "ate" complex that is prominent within the PBM mechanism (*Scheme 3.10*).

The combination of these unique properties of the NI dipole, in conjunction with the knowledge of the PBM reaction mechanism, should facilitate a novel transformation between NIs and boronic acids, enabling access to a range of aryl hydrazone compounds without recourse to transition metal catalysis.

## 3.2 Aims

The aims of this chapter focus on the development of the hypothetical reactivity profile proposed in *Scheme 3.10* into a chemically tractable route towards C-C bond formation in the synthesis of aryl ketone hydrazones. This transformation would be highly favourable from a green chemistry perspective, as this represents a metal-free approach with the generation of minimal by-products.
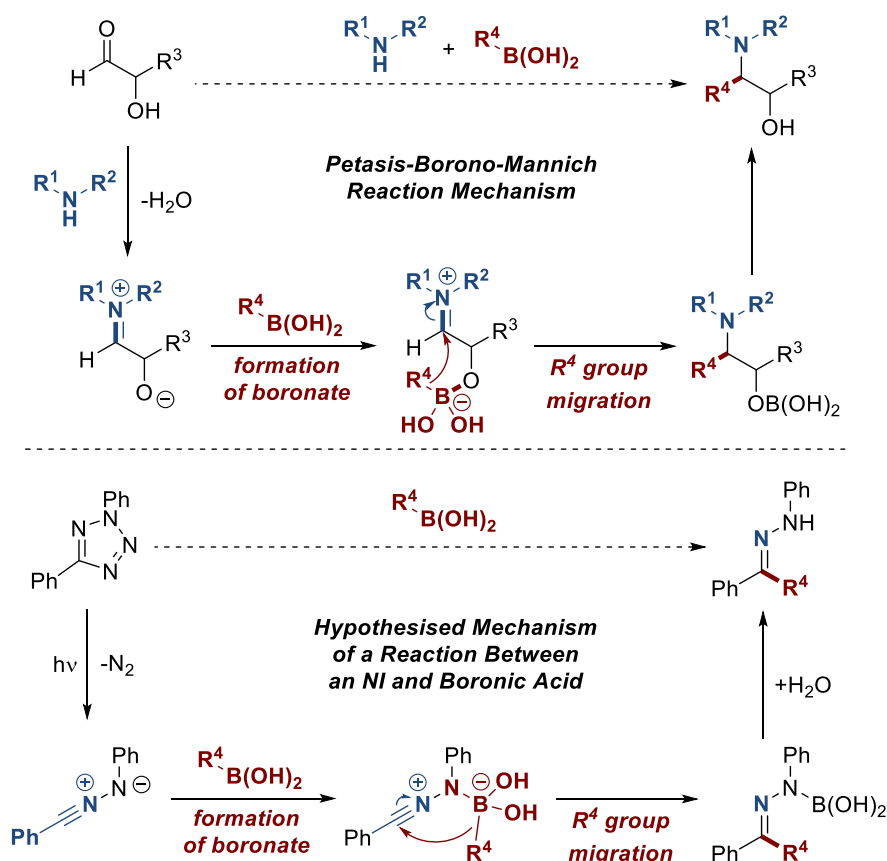
*Scheme 3.10: The application of the PBM reaction mechanism towards the novel reactivity of NIs and boronic acids*

Investigations will commence through an extensive assessment of potential reaction conditions, with both tetrazoles and hydrazonyl chlorides investigated as potential sources of the NI dipole, as both exhibit their own unique advantages. Ideally, complementary approaches involving both precursors will be developed (*Scheme 3.11*).
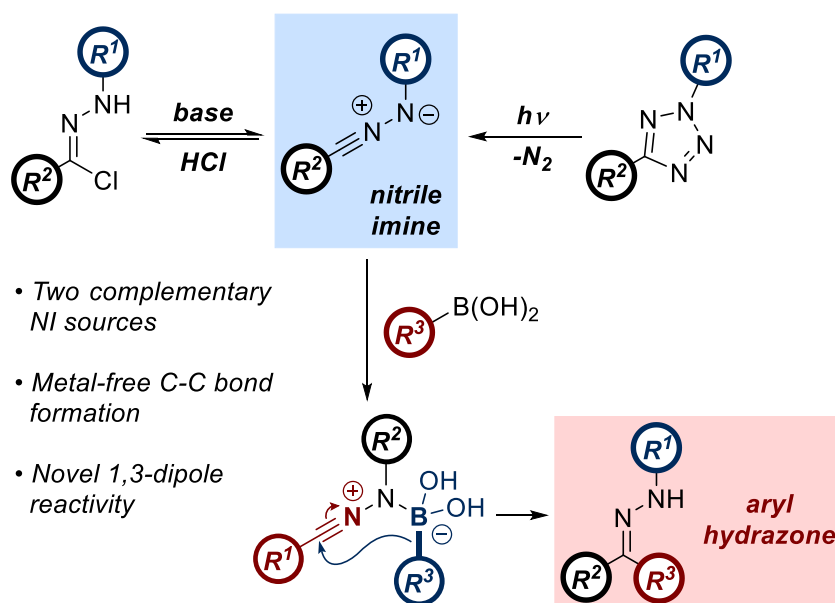


*Scheme 3.11: The general aims of this chapter*

The robustness of the procedure will then be assessed through evalution of the substrate scope. There will be particular emphasis on the influence of the boronic acid, owing to the proposed impact of its electronic properties on the propensity of the reaction. The inclusion of hydrazonyl chlorides as an NI source may also expand the reaction scope relative to 2,5-tetrazoles.

Finally, the potential applications of the methodology will be discussed, including its role in the metal-free synthesis of pharmaceutically relevant compounds, its incorporation within flow chemistry, and the further diversification of the aryl hydrazone products. The ligation of a tetrazole-modified biomolecule by a boronic acid will also be investigated to assess the affinity of this motif with the NI relative to other nucleophiles. Translation of the methodology into the closely related nitrile oxide (NO) 1,3-dipole will also be attempted owing to the similarity between the hydrazonyl chloride and hydroxamoyl chloride precursors, and their respective reactive intermediates. (*Scheme 3.12*).
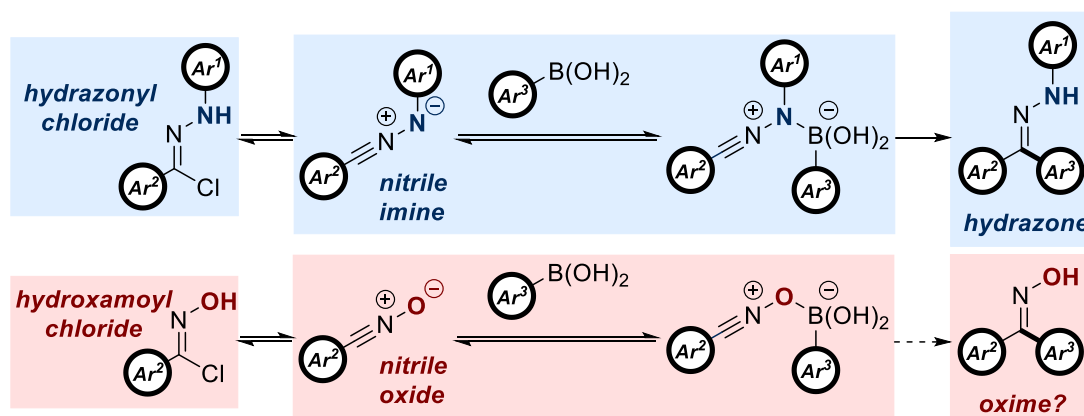


Scheme 3.12: The proposed adaption of the methodology from NI to NO dipoles

## 3.3    Results and Discussion

### 3.3.1   2,5-Tetrazoles as a Source of Nitrile Imine

Following on from the efforts of the previous chapter, 2,5-diaryl tetrazoles were introduced as the initial source of NI. Prior to beginning the investigation, some additional analogues were synthesised for application within the optimisation and scope (*Table 3.1*). The transformation discussed in the previous study was utilised in the synthesis of **3.1**, **3.2** and **3.3**.[264] The Kakehi synthesis was employed to access the remaining compounds.[258] The disparity in yields observed between these two approaches further emphasises the benefits of the more recently developed methodology.

*Table 3.1: The synthesis of additional tetrazole starting materials*
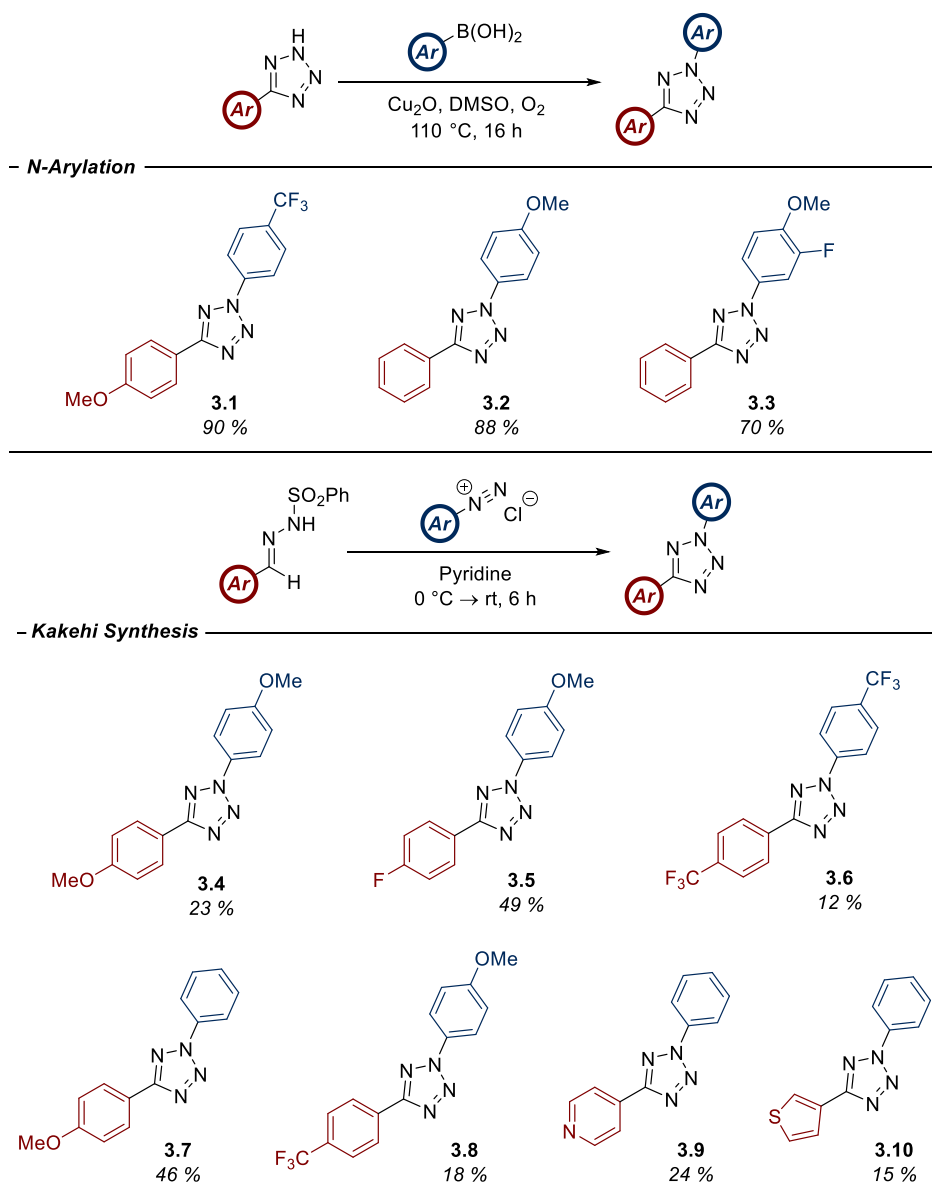
## 3.3.1.1 Proof of Concept Studies

As an initial proof of concept, 2,5-diaryl tetrazole **3.7** was irradiated with UV-B light in the presence of excess 4-methoxyphenylboronic acid. This substrate was selected as the electron-rich aromatic system was expected to enable the migration of the carbon-boron bond towards the *C*-terminus of the NI. Gratifyingly, this generated the desired product, hydrazone **3.11**, in a 46 % yield (*Scheme 3.13*). Around 44 % of tetrazole was also recovered, implying that the efficiency of the pathway was greater than the low conversion indicated, with initial NI generation hindered by a poor photolysis yield.

The procedure was then replicated using substrates which would generate a non-symmetric product. This was necessary due to the spectroscopic similarities of hydrazone **3.11** and the triazole by-product **3.12**, which may also have been generated.[205] The application of tetrazole **3.13** was expected to generate the non-symmetric hydrazone **3.14**, however the only product

isolated was identified as trace amounts of aryl ketone **3.15** (*Scheme 3.13*). This can be explained when considering the limited stability of hydrazones to even atmospheric quantities of water.[319] It is likely that the mildly acidic conditions of the silica gel employed in column chromatography promoted the hydrolysis of the hydrazone.
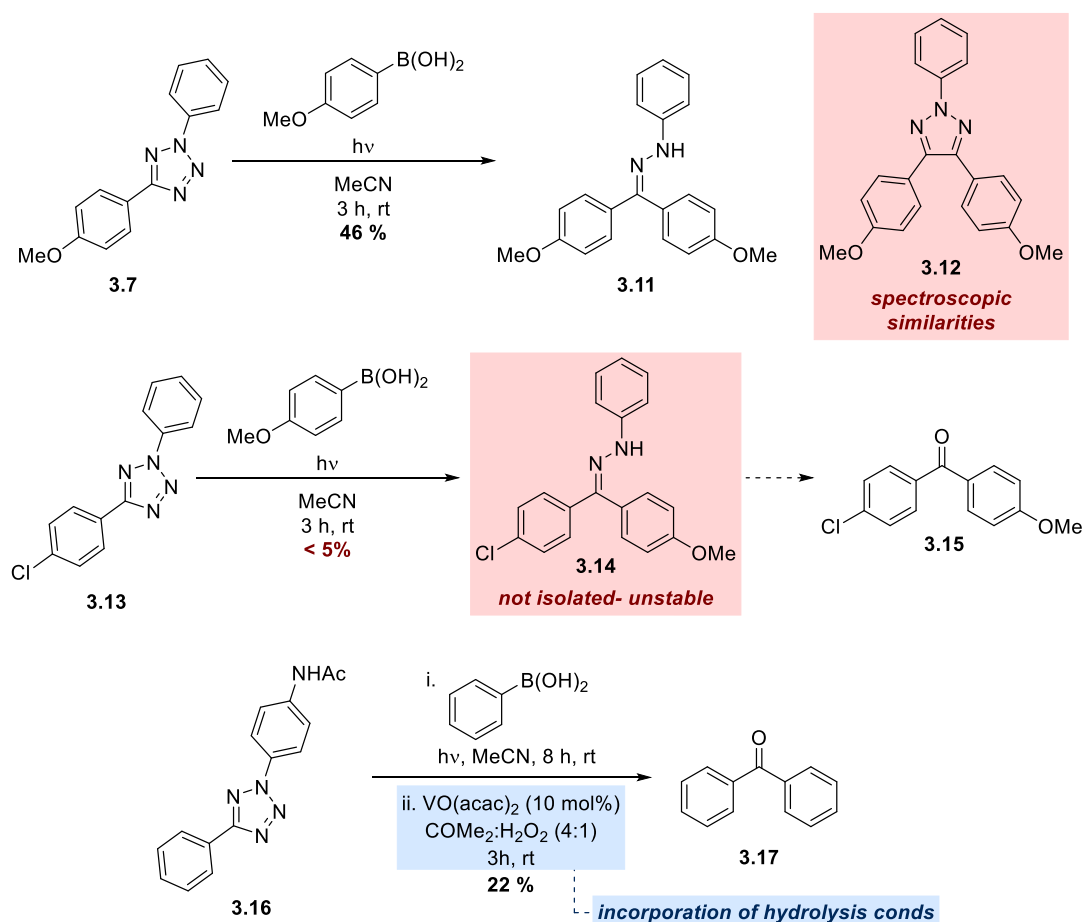


*Scheme 3.13: The initial proof of concept experiments between tetrazoles and aryl boronic acids*

Prior to commencing a full optimisation, the limited stability of the hydrazone products was addressed. It was reasoned that *in situ* hydrolysis to the ketone would enable an accurate determination of conversion, negating the need for dry conditions in the handling of the reaction mixture. Conditions obtained from the literature reported the oxidative cleavage of the C-N bond of the hydrazone using a vanadium(V) catalyst and hydrogen peroxide.[320] This work culminated in the final proof of concept reaction in which tetrazole **3.16** was photolysed in the presence of phenylboronic acid, with the hydrazone immediately oxidised *in situ*. The corresponding ketone was isolated in a 22 % yield (*Scheme 3.13*).

### 3.3.1.2 Optimisation of Reaction Conditions

The substrates chosen for the reaction optimisation were intended to be the simplest possible, using 2,5-diphenyl tetrazole (**3.18**) and phenyl boronic acid. However, limited photolysis of **3.18** during preliminary reactions hindered NI formation. This was thought to be related to the $\lambda_{max}$ of this precursor, with the opacity of the borosilicate flask at the required

wavelengths hindering its activation. To address this, tetrazole **3.2** was introduced, leading to greatly improved dipole generation (*Graph 3.1*).
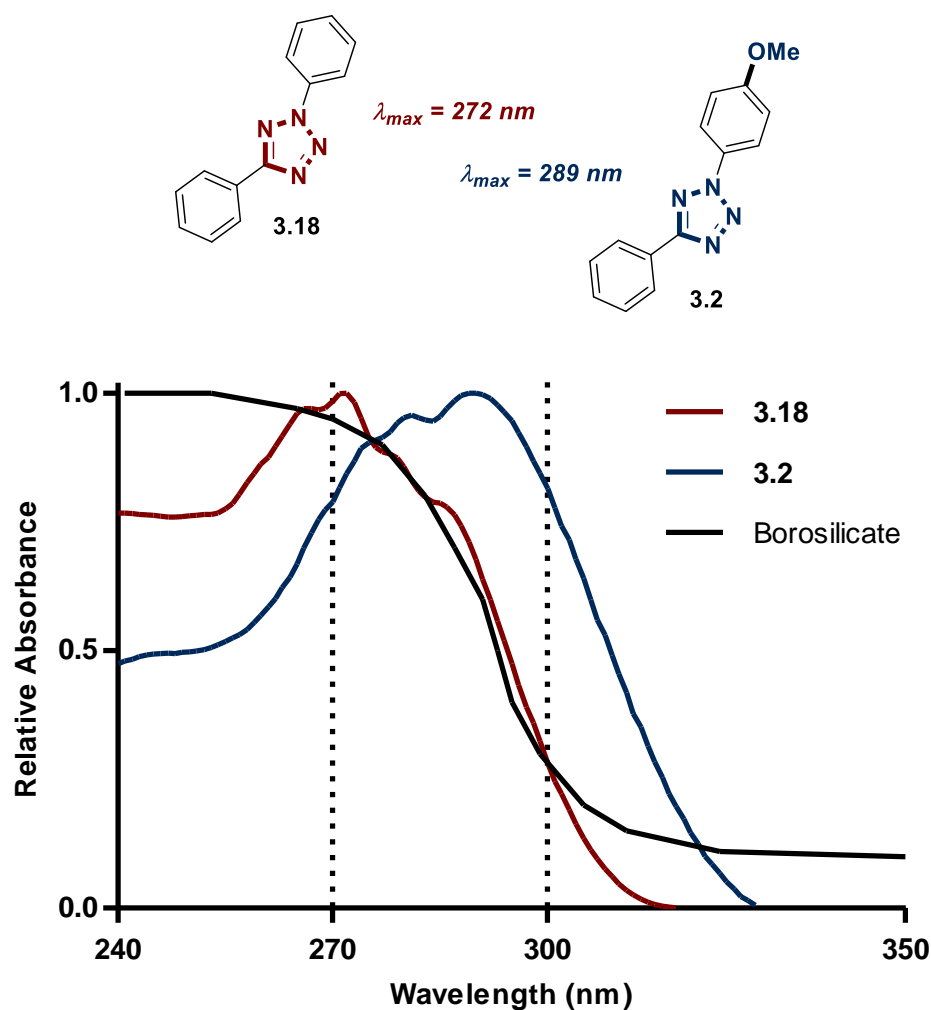


*Graph 3.1: The relative λmax values of tetrazoles 3.2 and 3.18, shown relative to the absorbance of 2.5 mm thick borosilicate glassware. Dashed lines indicate the primary transmission region of the UV light source.*

With the selection of appropriate reaction partners, a solvent screen was undertaken (*Table 3.2*). Unfortunately, conversions were found to be extremely low with acetone, ethyl acetate and THF all affording similar results. THF was taken forward due to the potential photosensitisation effects of solvents containing carbonyls. A 50:50 (v:v) mixture of 2-MeTHF and isopropyl alcohol was assessed due to its propensity in similar systems previously reported within our laboratory,[205] however this solvent only promoted NI dimerisation. The impact of different boron species was then investigated (*Table 3.3*), with any deviation from the boronic acid motif resulting in complete loss of reactivity. Variation of the boronic acid stoichiometry was also unsuccessful.

*Table 3.2: An initial solvent screen*



3.2                                                3.19
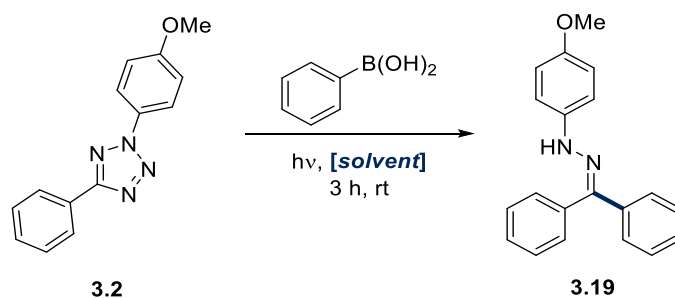
| Entry | Solvent | Conversion (%)[a] |
|-------|---------|-------------------|
| 1 | Acetone | 10 |
| 2 | THF | 9 |
| 3 | Acetonitrile | 7 |
| 4 | Ethyl Acetate | 10 |
| 5 | $^i$PrOH:2-MeTHF (1:1) | 2 |

[a]Conversion determined by HPLC with reference to caffeine as an internal standard

*Table 3.3: Investigation into the compatibility of different boron species within the reaction manifold*



3.2                                                3.19
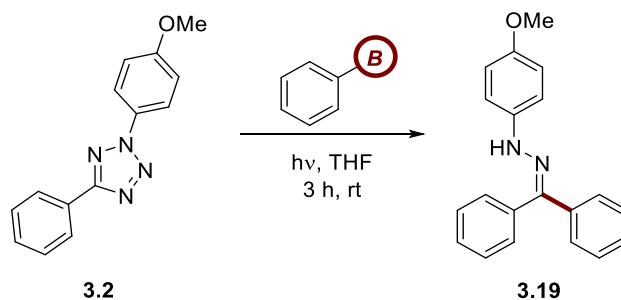
| Entry | B | Additive | B Stoichiometry | Conversion (%)[a] |
|-------|---|----------|-----------------|-------------------|
| 1 | B(OH)$_2$ | - | 2 | 9 |
| 2 | BPin | - | 2 | <1 |
| 3 | BF$_3$K | - | 2 | <1 |
| 4 | BF$_3$K | 18-crown-6 | 2 | <1 |
| 5 | B(OH)$_2$ | NaOH | 2 | <1 |
| 6 | B(OH)$_2$ | - | 1 | 6 |
| 7 | B(OH)$_2$ | - | 4 | 9 |

[a]Conversion determined by HPLC with reference to caffeine as an internal standard

While not helpful in the context of an optimisation, these results remain interesting from a mechanistic perspective. The failure of the corresponding pinacol ester seems to indicate that

the formation of a nucleophilic boronate is essential during the reaction. As BPin species are unable to form boronates,[321] the migration of the aryl group of the BPin cannot occur, eliminating the possibility of mechanistic pathway A in *Scheme 3.14*. This also represents a deviation from the PBM reaction mechanism, where boronic esters have demonstrated adequate compatibility.

The results of the trifluoroborate salt also offer some interesting mechanistic considerations. The BF$_3$K species is substantially more nucleophilic than the boronic acid,[322] yet is unable to facilitate hydrazone formation. This seems to indicate that the proximity of the two reactants is key to the migration of the aryl group. Coordination of a boron species with the NI simultaneously generates the boronate and brings it into the appropriate pose to facilitate intramolecular transfer of the aryl group. This can also rationalise why spiking the reaction mixture with sodium hydroxide led to no conversion. While the boronate was likely generated *in situ*, it would lack intramolecular coordination with the NI to enable aryl group migration, as with the BF$_3$K species. This data favours mechanistic route C in *Scheme 3.14*.

The impact of time and concentration were then assessed, with the results shown in *Table 3.4*. While an increased reaction time and dilution aided in more complete tetrazole photolysis (from approximately 30 % remaining to less than 10 %), neither variable was able to significantly improve conversion over what had been previously observed.
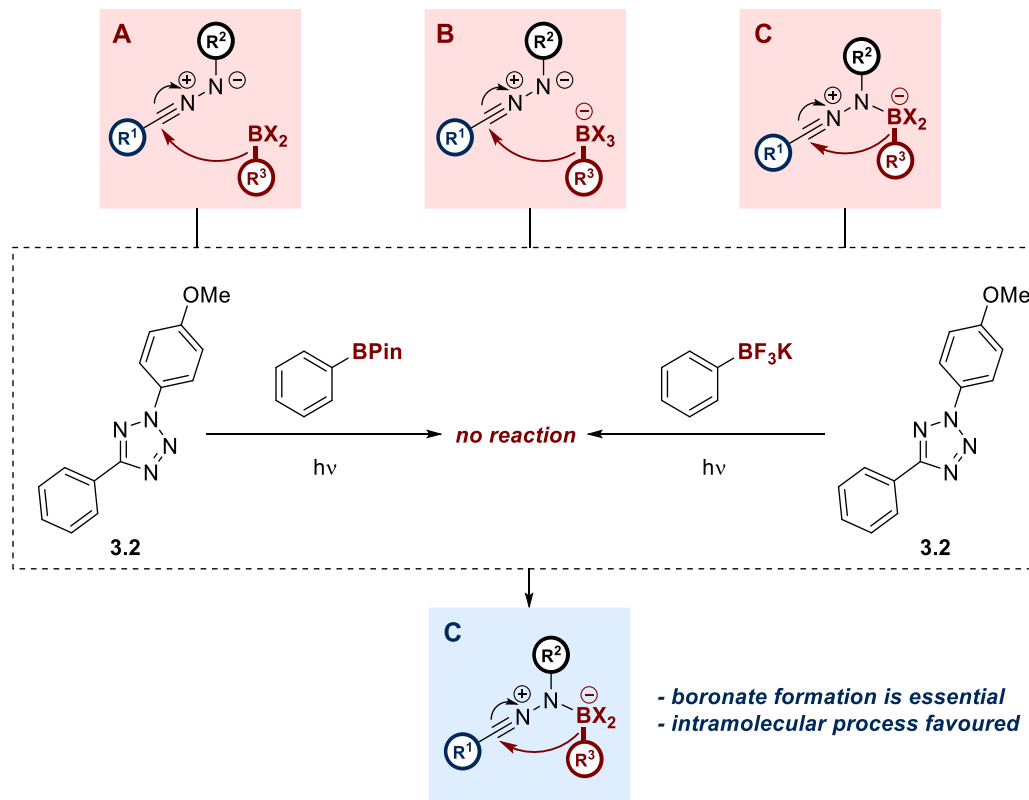


*Scheme 3.14: Insights into the mechanism of C-C bond formation in the reaction of NIs and boronic acids*

Table 3.4: The impact of concentration and time on reaction conversion
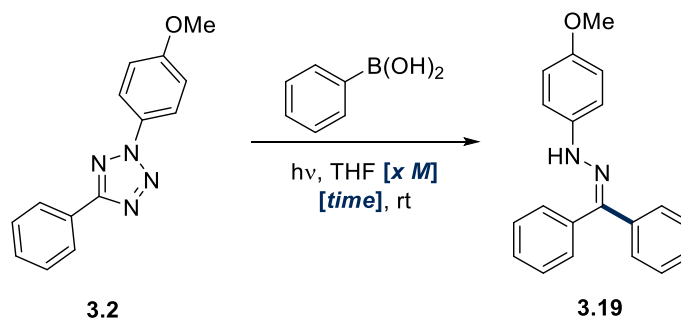


| Entry | Time (h) | Concentration (M) | Conversion (%)[a] |
|-------|----------|-------------------|-------------------|
| 1 | 1 | 0.08 | 4 |
| 2 | 2 | 0.08 | 5 |
| 3 | 3 | 0.08 | 9 |
| 4 | 7 | 0.08 | 9 |
| 5 | 3 | 0.04 | 6 |
| 6 | 3 | 0.16 | 9 |

[a]Conversion determined by HPLC with reference to caffeine as an internal standard

The results of these preliminary screens were puzzling. More complete photolysis of the tetrazole seldom led to an improved yield and generated a mass balance that failed to account for the fate of more than 80 % of the NI in some cases. This indicated one or more significant side reactions occurring during the procedure, and an examination of the HPLC chromatograms confirmed this, with a large unknown signal dominating the spectra (*Figure 3.1*).
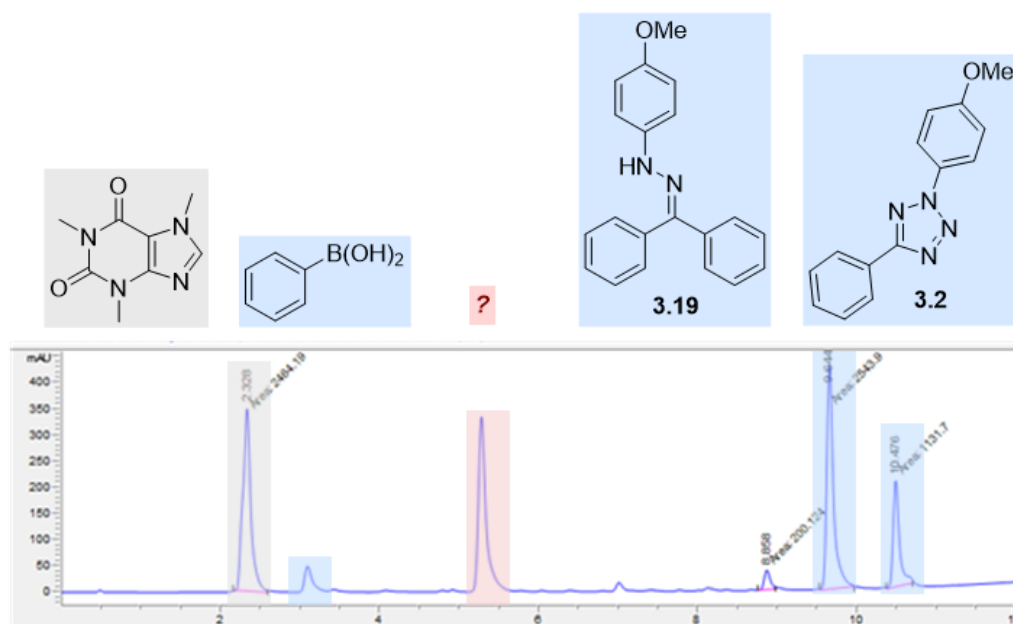


Figure 3.1: An example of an HPLC chromatogram from this optimisation, with a large unassigned elution at around 5.3 minutes

With efforts to isolate this species unsuccessful, control experiments were conducted to establish whether this unknown compound was a side product of the NI alone, or whether the boronic acid was implicated in its generation. Crucially, results suggested that both the boronic acid and NI were essential to its formation. To drive the reaction towards the desired ketone hydrazone, it was determined that introduction of the electron-rich substrate 4-methoxyphenylboronic acid may facilitate improved conversion through promotion of the critical C-B bond migration (*Scheme 3.10*). Previous mechanistic evidence from the PBM itself has also demonstrated the increased reactivity of electron-rich boronic acids (*Scheme 3.4*).

Oxidation of the hydrazone primary product into the ketone **3.20** was also reintroduced for this assay, due to difficulties in isolating the corresponding hydrazone. The reaction was performed using an NMR tube as opposed to round-bottom flasks to enable faster and more efficient tetrazole photolysis. The results of this screen are shown in *Table 3.5*.

*Table 3.5: The optimisation of reaction conditions when using 4-methoxyphenylboronic acid as a substrate*
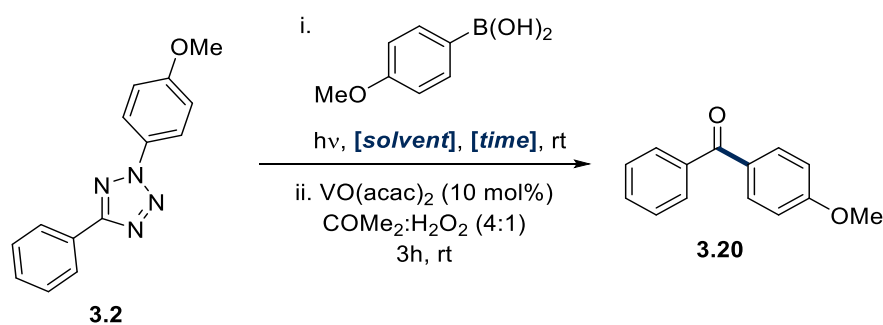


| Entry | Solvent | Time (h) | Concentration (M) | B(OH)$_2$ Stoichiometry | Conversion (%)[a] |
|-------|---------|----------|-------------------|-------------------------|-------------------|
| 1 | THF | 3 | 0.1 | 2 | 57 |
| 2 | MeCN | 3 | 0.1 | 2 | 53 |
| 3 | THF | 1 | 0.1 | 2 | 41 |
| 4 | THF | 2 | 0.1 | 2 | 48 |
| 5 | THF | 3 | 0.05 | 2 | 61 |
| 6 | THF | 3 | 0.2 | 2 | 57 |
| 7 | THF | 3 | 0.1 | 1 | 45 |
| 8 | THF | 3 | 0.1 | 3 | 69 |
| 9 | THF | 3 | 0.1 | 5 | 78 (75[b]) |

[a]Conversion determined by HPLC with reference to caffeine as an internal standard
[b]Isolated yield

Initial observations clearly showed that exchange of the boronic acid facilitated an improved conversion over previous attempts. Solvent again had little effect, as was also observed with

concentration and reaction time. However, boronic acid stoichiometry had a significant impact on reaction conversion. This was unexpected, as boronic acid stoichiometry was investigated as part of the initial optimisation involving phenylboronic acid (*Table 3.3*). It is likely that the increased reactivity of 4-methoxyphenylboronic acid makes the system more sensitive to its stoichiometry, leading to the pronounced increase in conversion.

Regardless of earlier results, the use of five equivalents of 4-methoxyphenylboronic acid generated a 75 % isolated yield of the corresponding ketone **3.20**, marking the first synthetically tractable yield of the campaign. However, multiple issues with the reaction remained. Firstly, the requirement of five equivalents of boronic acid severely limited the utility of the procedure. Secondly, the substrate scope had proven to be highly limited. Phenylboronic acid, an electronically neutral substrate, provided disappointingly low conversions, with introduction of a methoxy moiety in the *para* position of the aromatic ring necessary to facilitate improved yields. With a Hammett $\sigma_p$ value of -0.27,[279] this represents a considerable deviation from the neutral properties of an ideal optimisation. Finally, a substantial portion of the mass balance of earlier reactions remained unaccounted for. The identity of the unknown compound highlighted by HPLC remained elusive, despite establishing that both the boronic acid and the NI were required for its formation.

It was decided that a beneficial approach to tackling these problems would involve a switch from an HPLC assay to $^{19}F$ NMR spectroscopy. One of the principal advantages of NMR assays is that results are immediately quantifiable without calibration, as the integration of $^{19}F$ atoms are much more consistent than the 254 nm light absorbance between different organic molecules. NMR studies also avoid the degree of sample preparation required by HPLC. As HPLC assays traditionally employ reverse phase chromatography, the sample must be miscible in aqueous media. The reactivity of $H_2O$ means that any unstable intermediates, such as the NI or any side products, may be quenched by water prior to generation of the chromatogram. Furthermore, NMR allows the detection of multiple nuclei within the same spectra. This is particularly beneficial if $^{19}F$ atoms are incorporated into both reaction partners, as it permits identification of which compounds are responsible for the generation of each new species. This is more difficult to generate *via* HPLC and can only be assessed through further control experiments. $^{19}F$ NMR was selected over $^1H$ NMR to enable analysis without the need of a transfer into deuterated solvent.

The model reaction used in the previous optimisation work was modified incorporate multiple fluorine atoms. Preliminary experiments found that 5-(4-fluorophenyl)-2-(4-methoxyphenyl)-tetrazole (**3.5**) and 3-fluoro-4-methoxyphenylboronic acid enabled simple quantification of all species formed within the reaction mixture. 5-Phenyl-2-(3-fluoro-4-methoxyphenyl)-tetrazole (**3.3**) was used as a standard due to its near-identical $T_2$-relaxation

times, enabling the acquisition of accurate integration values. Replication of the reaction conditions used within the HPLC assay caused the yield to decrease from 78 % to 56 %. This was unsurprising, given the change in electronic properties of the alternative boronic acid. While the Hammett $\sigma_p$ value of the methoxy group is -0.27, the $\sigma_m$ value of fluorine is 0.34,[279] with the sum of these values rendering the substrate electron-deficient, and anticipated to be less reactive.

Initial screening addressed one of the key issues of the earlier optimisation through investigation of boronic acid stoichiometry (*Table 3.6*). It was found that conversion could be maintained when lowering the equivalents from five to three, while the use of any less resulted in a significant decrease in conversion. These results are similar to those observed during the earlier optimisation, where a relatively modest increase in yield (9 %) was observed when moving from 3 to 5 equivalents, with a significant increase of 24 % when moving from 1 equivalent to 3 (*Table 3.5*).

*Table 3.6: An investigation into the impact of boronic acid stoichiometry on conversion using $^{19}F$ NMR*
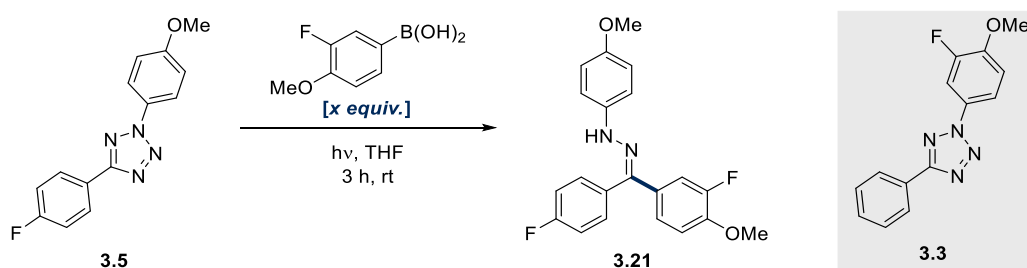


| Entry | B(OH)$_2$ Stoichiometry (equiv.) | Conversion (%)[a] |
|:-----:|:--------------------------------:|:-----------------:|
| 1 | 5 | 56 |
| 2 | 4 | 55 |
| 3 | 3 | 53 |
| 4 | 2 | 42 |
| 5 | 1 | 33 |

[a]Conversion determined by $^{19}F$ NMR with reference to **3.3** as an internal standard

The most important outcome of this study was additional information concerning the side reactions of the mixture. $^{19}F$ NMR data showed that the boronic acid was relatively benign, with its only side reaction involving oxidation to the phenol, and a substantial portion of starting material remaining following reaction completion. The NI, however, was much more promiscuous, generating several side products in addition to the desired hydrazone.

These results raised some interesting questions. Firstly, previous precedent indicated that in the absence of a reactive partner in solution, NIs would dimerise, forming the 1,2,3-triazole *via* the 1,2,3,4-tetrazine (*Section 1.3.3*). However, while detectable, neither the triazole nor

the tetrazine were ascribed to be a major side product. Secondly, earlier control experiments had shown that the presence of the boronic acid was essential in the formation of some unknown by-products, yet the species was not present in the final structure of any other compounds, as evidenced by the $^{19}$F NMR spectra.

A significant development was made during an investigation into the compatibility of alkyl boronic acids, where primary hydrazide **3.22** was unexpectedly isolated in 81 % yield (*Scheme 3.15*). This compound is a known hydration product of the intermediate NI, caused by nucleophilic attack of a water molecule into the neutral terminus of the dipole. However, in literature examples of this reaction, the process must be conducted at very high dilution using water as the solvent, as compensation for its limited nucleophilicity and due to competing dipole dimerisation. In the procedure above, no external source of water was added, save for that found in typical atmospheric conditions. A further control experiment excluding the boronic acid failed to replicate this exceptional result, indicating that the boronic acid is somehow necessary in the synthesis of this compound, corroborating earlier findings.
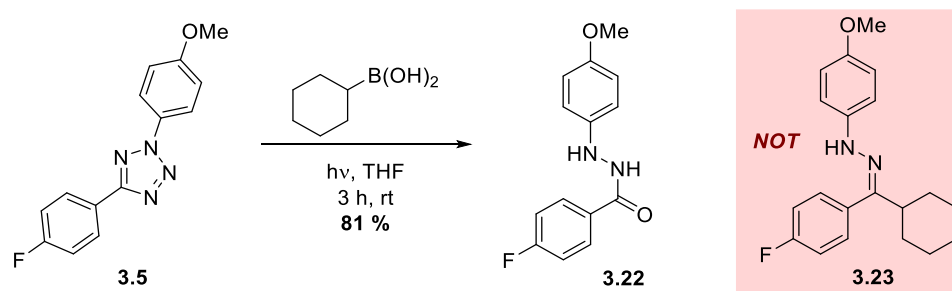


*Scheme 3.15: The unexpected isolation of primary hydrazide **3.22***

This can be rationalised when assuming rapid coordination of the boronic acid to the anionic terminus of the NI to form the hypothesised boronate complex. If the migration of the R group of the boronate is the rate limiting step of the procedure, then at this point the NI is susceptible to attack by another nucleophile, as it is no longer a conventional zwitterionic dipole, but rather an electrophilic pseudo-nitrillium ion (*Scheme 3.16*). This would justify why an NI in the presence of a boronic acid is more likely to be intercepted a nucleophile such as water, and could explain a key side reaction observed throughout the optimisation. The formation of **3.22** may also be exacerbated through the addition of super-stoichiometric portions of boronic acid, as the principal source of water is likely through the condensation of the boronic acid to form the corresponding boroxine. This would also explain the lack of triazole or tetrazine formation, as NI dimerisation relies on a concerted cycloaddition between two equivalents of the dipole, which would not be possible if the electronics of the original species had been distorted through coordination to the boronic acid.
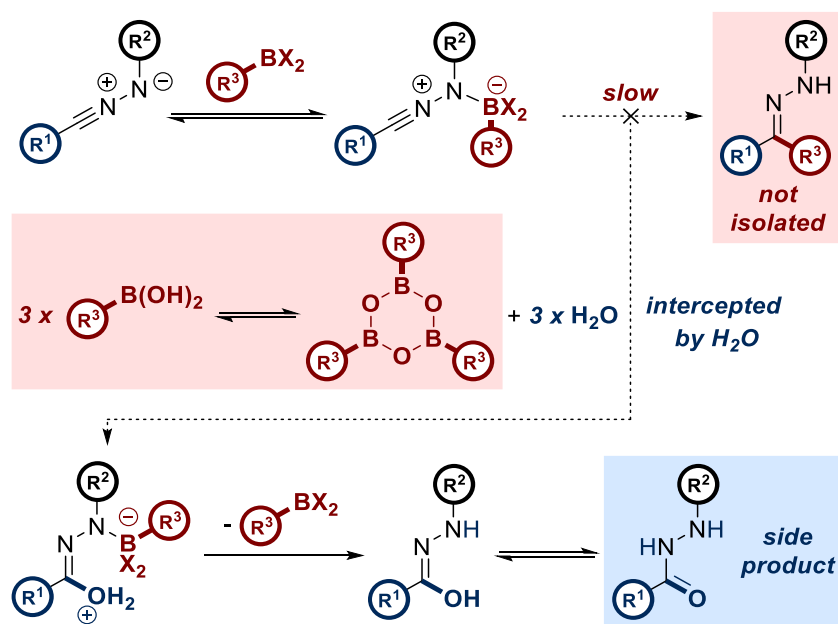
*Scheme 3.16: The hypothesised mechanism which facilitates the formation of primary hydrazide **3.22***

*Table 3.7: Elimination of the hydrazide by-product **3.22** from the reaction manifold*
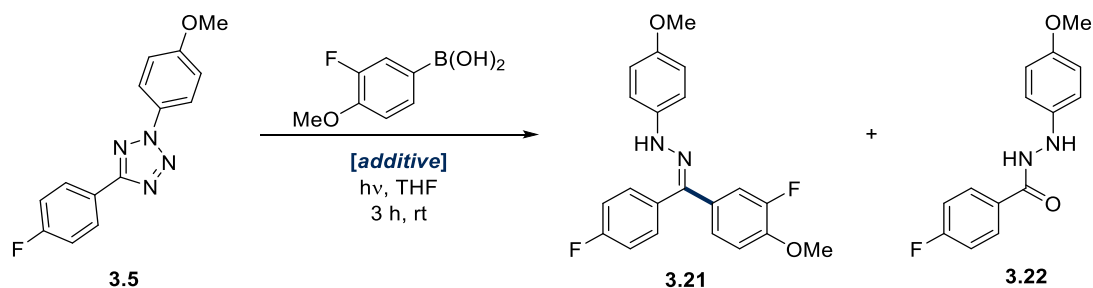


| Entry | Atmosphere | Additive | Conversion (%)[a] | |
|:---:|:---:|:---:|:---:|:---:|
| | | | 3.21 | 3.22 |
| 1 | - | - | 41 | 19 |
| 2 | $N_2$ | - | 45 | 18 |
| 3 | $N_2$ | 3 Å molecular sieves (400 gmol$^{-1}$) | 46 | 8 |
| 4 | $N_2$ | 3 Å molecular sieves (4000 gmol$^{-1}$) | 60 | 1 |
| 5 | $N_2$ | Trimethyl orthoformate (10 eq.) | 38 | 21 |
| 6 | $N_2$ | Trimethyl orthoformate (neat) | 11 | 31 |
| 7 | $N_2$ | 3 Å molecular sieves (400 gmol$^{-1}$)[b] | 61 | 2 |
| 8 | $N_2$ | 3 Å molecular sieves (4000 gmol$^{-1}$)[b] | 55 | <1 |

[a]Conversion determined by $^{19}F$ NMR with reference to **3.3** as an internal standard

[b]Crushed

Gratifyingly, analysis of **3.22** by $^{19}F$ NMR identified the compound as one of the most prominent by-products of the reaction. A focused optimisation was then conducted to remove water from the reaction mixture to minimise its formation (*Table 3.7*). Performing the reaction under nitrogen in an oven-dried flask did little to improve conversion, or to

diminish the yield of hydrazide. To combat the generation of $H_2O$ *via* boroxine formation, exogenous drying agents were added, while the oven-dried glassware and nitrogen atmosphere were maintained. Trimethylorthoformate was not capable of improving conversions, however success was achieved using 3 Å molecular sieves (MSs). While a relatively high loading was initially required to eliminate the hydrazide formation, this was reduced by a factor of 10 by crushing the sieves prior to their introduction.

These optimisation studies permitted the identification of highly efficient conditions for the novel reaction of NIs with aryl boronic acids, furnishing high yields in a reaction with no previous precedent prior to this research. This transformation represents an environmentally benign and economical approach towards C-C bond formation in the absence of any organometallic species, with only UV light and molecular sieves required as exogenous reagents (*Scheme 3.17*).
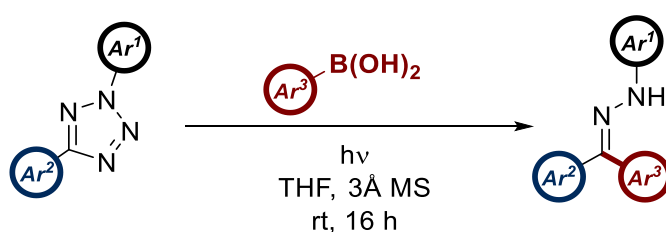


Scheme 3.17: The reaction conditions identified as part of the optimisation of the PBM-inspired reaction of NIs and aryl boronic acids

### 3.3.1.3 Scope of the Reaction

The studies outlined above facilitated a much better understanding of the reaction between NIs and aryl boronic acids, identifying robust conditions for investigation of the substrate scope. One of the only alterations made from the above conditions was the adoption of quartz round-bottom flasks as reaction vessels. This enabled the interrogation of a broader library of 2,5-diaryl tetrazoles (*e.g.* **3.18**) by maximising their exposure to incident light.

The most extensively examined substrate class were *para*-substituted aryl boronic acids, owing to the apparent influence of electronics on the outcome of the reaction. Substitution of the *para*-position was intended to minimise the impact of sterics while maximising electronic impact through direct conjugation of the substituent with the boron centre. The results of this study are shown in *Table 3.8*. A total of ten *para*-substituted examples were exposed to the optimised conditions using 2,5-diphenyl tetrazole as a reaction partner. It was immediately apparent that the electronics of the aromatic ring had a substantial influence on the isolated yield.

Beginning with compound **3.24**, a substrate for much of the optimisation, the reaction proceeded in very good yield. When this conversion is compared to the unsubstituted

product **3.30** (16 %), it is evident that the improved conversion of **3.24** can be attributed to the electron-rich properties of the boronic acid (*p*-MeO $\sigma_p$= -0.27[279]).

*Table 3.8: The scope of* para-*substitued aryl boronic acids*
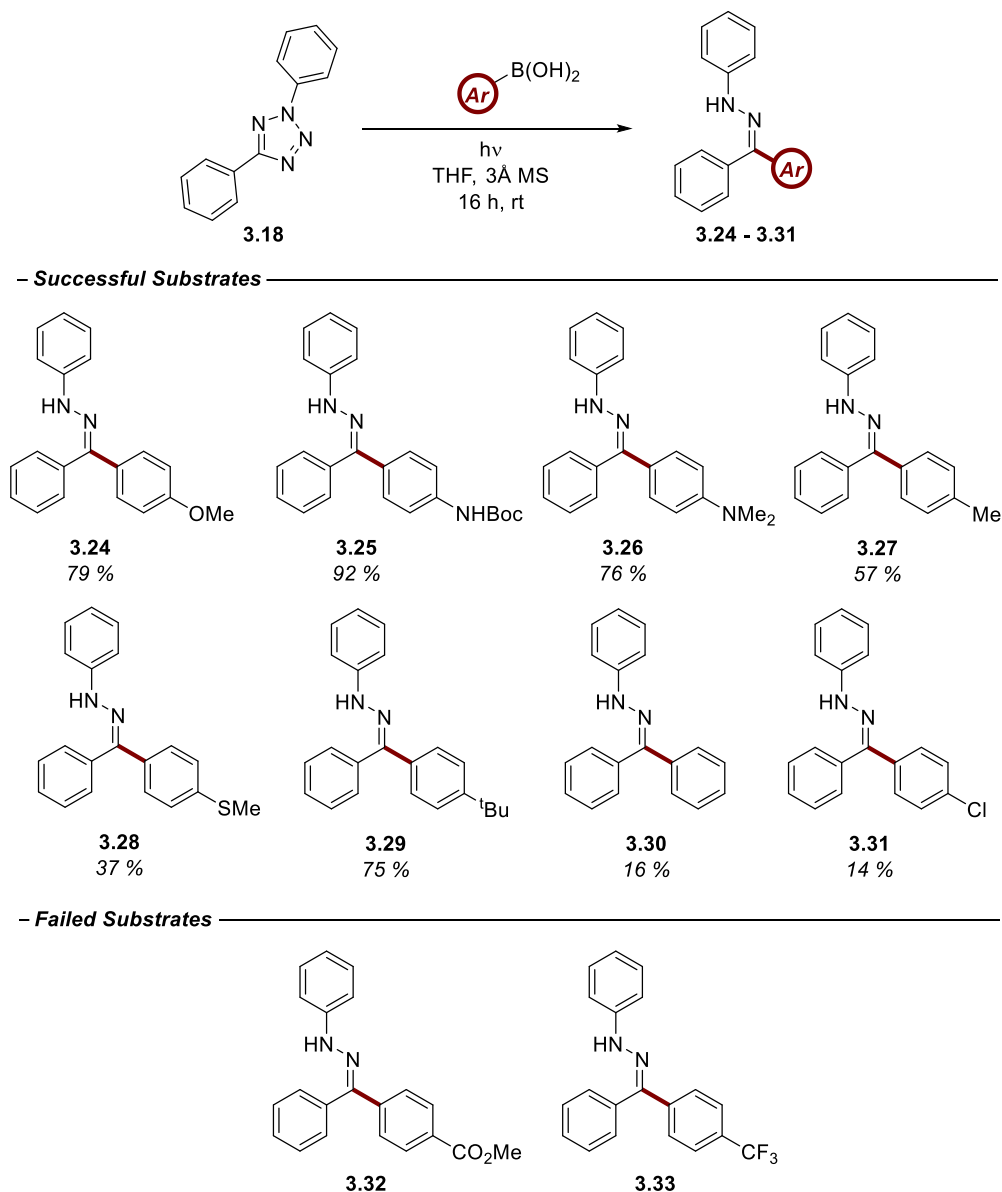


This trend is maintained in numerous other examples. In the case of electron-deficient boronic acids, such as 4-trifluoromethyl and 4-methoxycarbonyl ($\sigma_p$= 0.54 and 0.45, respectively[279]), the products did not form at all, with only NI decomposition observed. While a partial conversion of 14 % was observed for hydrazone **3.31**, this represented the lowest isolated yield and the only example of a formally electron deficient boronic acid (*p*-Cl $\sigma_p$= 0.23[279]).

By contrast, substitution of the aryl boronic acid with electron-donating groups afforded the desired hydrazones in good to excellent yields. Even mildly electron-donating moieties such as a methyl group had a significant impact on yield (comparing **3.27** to **3.30**). As a general

trend amongst electron-rich boronic acids, conversion increased with decreasing $\sigma_p$ value. One significant outlier was the conversion of hydrazone **3.25**, with an anomalously high yield of 92 % (*p*-NHCO$_2$R $\sigma_p$= -0.17[279]). While the reasons behind this excellent yield are not immediately apparent, it remains an encouraging example of the versatility of the protocol.

Following on from this investigation, the impact of steric factors was assessed through the incorporation of functional groups into the *meta* and *ortho* positions of the boronic acid. The scope was also broadened to include examples of heterocycles. Owing to the previous results, it was determined that the investigation of electron rich heterocycles such as thiophene and indazole would be of greater relevance.

*Table 3.9: The scope of heterocyclic and ortho and meta-substituted boronic acids*
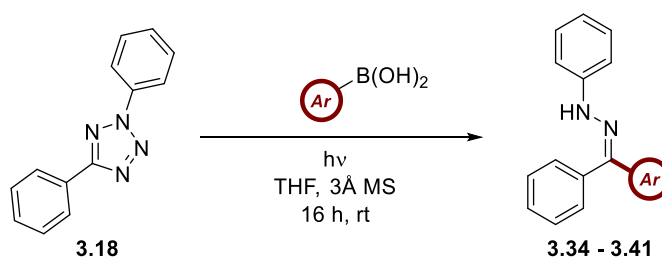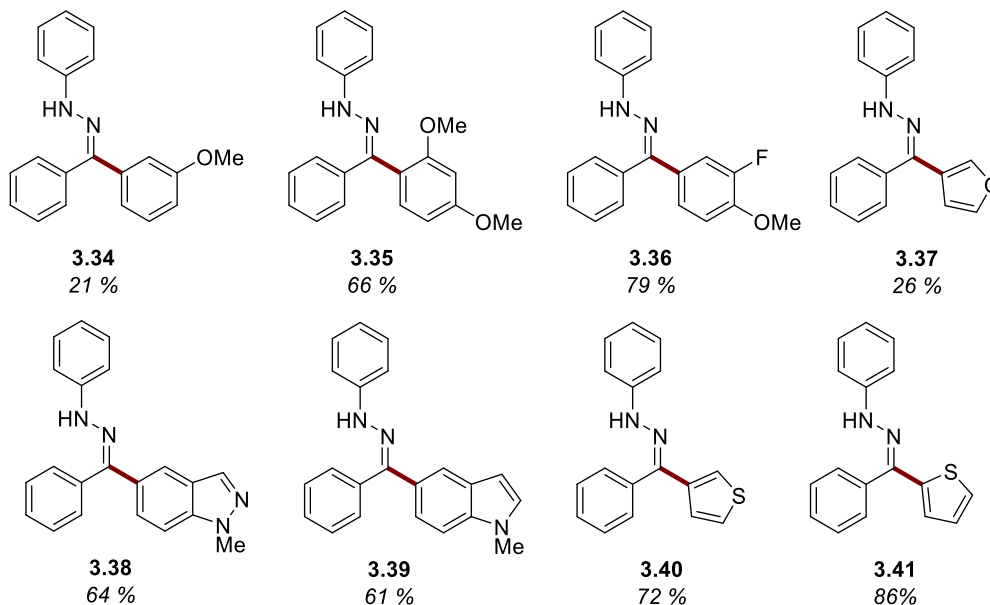


Pleasingly, the reaction manifold was highly tolerant of substitution of both the *meta* and *ortho* positions of the aryl boronic acid (*Table 3.9*). While hydrazone **3.34** was isolated in only a 21 % yield (*c.f.* the *para*-substituted regioisomer **3.24** isolated in a 79 % yield), this is due to the electronic impact of relocating the methoxy substituent, effectively inverting the electronic effects of the aromatic ring (*p*-MeO $\sigma_p$ = -0.27, *m*-MeO $\sigma_p$ = 0.12). The negligible impact of *meta*-substitution can be clearly observed in the isolated yield of hydrazone **3.36** (79 %). The retention of an "activating" methoxy group in the *para* position allows for an

accurate comparison with the *m*-H example **3.24**, with an identical yield obtained for both reactions.

*Ortho*-substituted boronic acids were also tolerated, with the isolation of hydrazone **3.35** in 66 % yield. While comparable to the yield of hydrazone **3.24** (79 %), the presence of an additional methoxy group constitutes further electronic activation of the boronic acid, meaning steric effects are not entirely detached from electronic influence in this comparison. Nevertheless, the minimal reduction in yield between the two substrates indicates that substitution in the *ortho*-position is well tolerated.

Five heterocyclic boronic acids also furnished the desired hydrazones, with good to excellent yields in most cases. All four heterocycles tested (thiophene, furan, indole and indazole) are electron-rich, meaning that these results remained consistent with those observed involving electron-rich boronic acids in the previous scope. The low yield of the furan-containing hydrazone **3.37** was initially surprising when compared to its closely related thienyl analogue **3.40** (26 % *vs.* 72 %). This can be explained by the propensity of furanyl boronic acids to undergo protodeboronation, meaning that this substrate may have been unstable under the reaction conditions.[288]

Overall, investigation of the boronic acid scope within this emerging process provided a satisfactory degree of diversity. The conditions were applicable to a wide number of electron-rich boronic acids, most of which were isolated in good to excellent yields. This also extended to heterocyclic boronic acids, as well as sterically encumbered examples. Unfortunately, electron-deficient species were generally incompatible, with only two examples furnishing the products, and in comparatively poor yields. This is likely based on the electronic contributions of the boronic acid substituents, with a comparison of conversion versus Hammett σ values displaying a clear trend of improved yields with increased electron density. However, the exact behaviour of these species cannot be explained through σ values alone. For example, two σ-neutral derivatives, **3.28** and **3.30**, generated yields that differ by over 20 %. Similarly, hydrazone **3.36**, which is defined by its σ value as electron-deficient, afforded a higher isolated yield than many electron-rich analogues.

Following examination of the boronic acid scope, modification of the NI dipole was also assessed. This required variation of the substituents of the 2,5-disubstituted tetrazoles employed in the reaction, which would in turn influence the behaviour of the NI following *in situ* generation of the dipole. Diversification of the NI was not as extensive as the investigation of boronic acids for a number of reasons. Firstly, the introduction of two sites of variation necessitated screening a much larger palette of substrates to achieve similar coverage. As 2,5-diaryl tetrazoles are not typically commercially available, the synthesis of an exhaustive scope of starting materials was not efficient nor practical, even through

application of the newly developed 2,5-tetrazole synthesis outlined above (*Section 2.3*). Secondly, the alteration of NI substituents was not anticipated to have such a significant influence on reaction yield as the properties of the boronic acid. Previous publications have shown that substantial alterations to the NI are necessary to meaningfully influence their properties.[31] Finally, changes to the 2,5-diaryl tetrazole could impact the efficiency of NI generation itself, rather than the subsequent reactivity of the NI. For example, as discussed above (*Section 1.2.3*), it has previously been demonstrated that certain substituents of 2,5-tetrazoles may inhibit NI formation entirely.[94] The inclusion of such a substrate within this scope could lead to a false negative result.

For these reasons, the NI substrates studied were limited to the following criteria. To investigate NI electronics, examples were included with electron-rich, electron-neutral, and electron-deficient groups in the *para* position of both aromatic rings, in all eight possible combinations. Methoxy and trifluoromethyl moieties were selected as the electron-donating and electron-withdrawing groups respectively, as both were known to have minimal impact on NI generation *via* photolysis. 4-Tolylboronic acid was selected as the boronic acid substrate, due to the comparatively modest yield of this compound in the initial scope above (57 %). This was intended to enable straightforward identification of any beneficial or detrimental impacts of the NI species on reaction yield, as the introduction of either phenylboronic acid or 4-methoxyphenylboronic acid may have resulted in deceptively low or high yields, respectively.

The results of this study are shown in *Table 3.10*. It was immediately apparent that the substituents of the NI have a significantly reduced influence on yield compared to the boronic acid. Firstly, all electron-deficient and electron-rich examples of substitution on the *N*-aryl ring afforded isolated yields within 10 % of the unsubstituted reference compound **3.27**. It was initially considered that boronate formation using the anionic terminus of the NI may have been affected by the electronic properties of this ring system, however the reaction yield remained unaffected. Modification of the *C*-aryl ring also proved to have a limited impact on reaction yield. This was exemplified by the yields of **3.44** and **3.45**, which both afforded moderate conversions despite possessing inverted electronic properties of the *C*-motif. Some examples did result in atypically low yields (*c.f.* **3.48** and **3.49**, 27 % and 16 %), however this is thought to be a consequence of isolation issues as opposed to substrate incompatibility.

One significant issue encountered during this scope was the partial hydrolysis of the hydrazones during column chromatography, as was observed during the early stages of the optimisation (*Scheme 3.13*). Compound **3.46** was isolated as the ketone derivative in a 47 % yield, representing an entirely metal-free procedure for the synthesis of aryl ketones using no

exogenous reagents other than silica. In other cases, partial hydrolysis resulted in unrepresentatively low reaction yields through continuous mechanical loss, such as compound **3.43**, which was eventually isolated as the ketone. Species containing an electron-rich *N*-aryl ring underwent ambient hydrolysis much more readily than any other hydrazones. The exact reason for this phenomenon remains unclear.

*Table 3.10: The scope of electronic modification of the NI component*
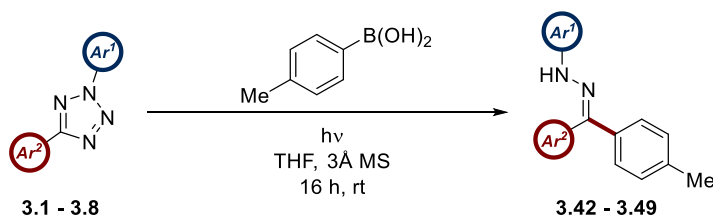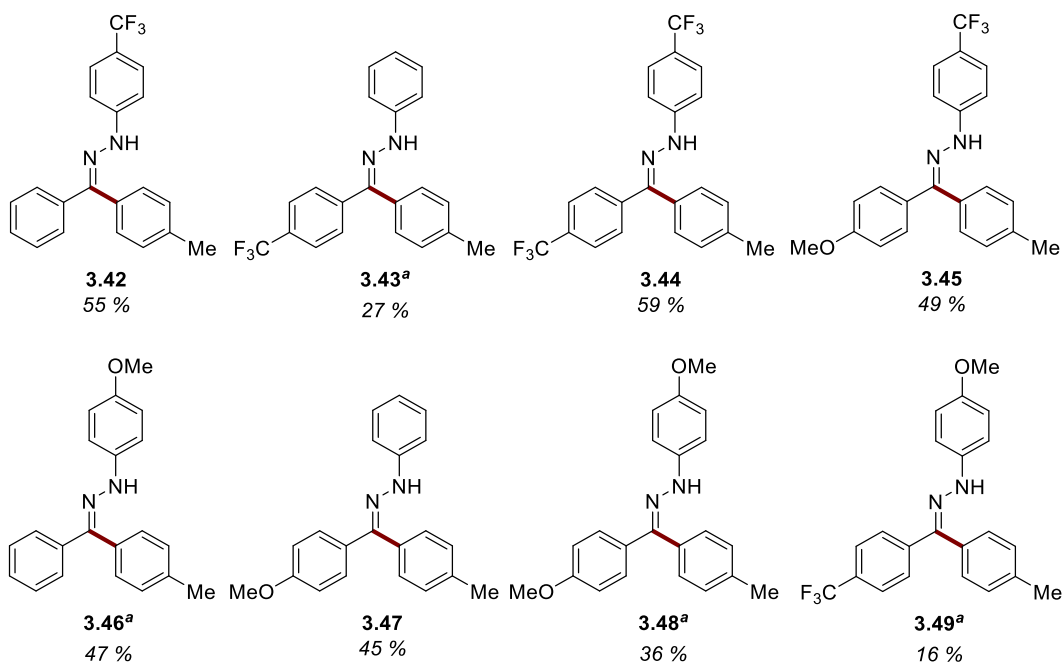


Due to the proximity of the *C*-aryl ring of the NI to the centre of the reaction, some additional parameters around this moiety were also probed (*Table 3.11*). These included both an electron-poor and electron-rich heterocycle, as well as the introduction of both a *m*-chloro and *o*-chloro moiety.

The reaction was tolerant of *ortho* and *meta* substitution as the synthesis of hydrazones **3.51** and **3.52** both proceeded smoothly. Steric occlusion of this ring could theoretically preclude the reaction by preventing aryl group migration onto the *C*-terminus of the NI. Gratifyingly, this was not observed in practice and all three chloro-substituted compounds were obtained in good yields. Only two heterocyclic substrates were investigated, with the electron-rich *C*-thiophenyl NI yielding the desired hydrazone **3.53** in an acceptable yield (36 %). Initial

concerns regarding the $\lambda_{max}$ value of the starting material due to the pronounced conjugative effects of the thiophene heterocycle were unfounded, and the tetrazole was fully consumed over the course of the photolysis.[323] The introduction of a pyridine ring on the *C*-terminus unfortunately resulted in no product formation. The complete consumption of the tetrazole indicated that generation of the NI was successful, however the dipole was evidently incompatible with the protocol. This may be due to the coordinating effect of the pyridine moiety, which may compete with the anionic terminus of the NI for complexation with the boronic acid.

*Table 3.11: Investigations into the impacts of steric and heterocyclic substitution of the C-aryl ring of the NI*



— **Successful Substrates** —



**3.50**[a]
*47 %*

**3.51**
*52 %*

**3.52**
*57 %*

**3.53**
*36 %*

— **Failed Substrates** —



**3.54**
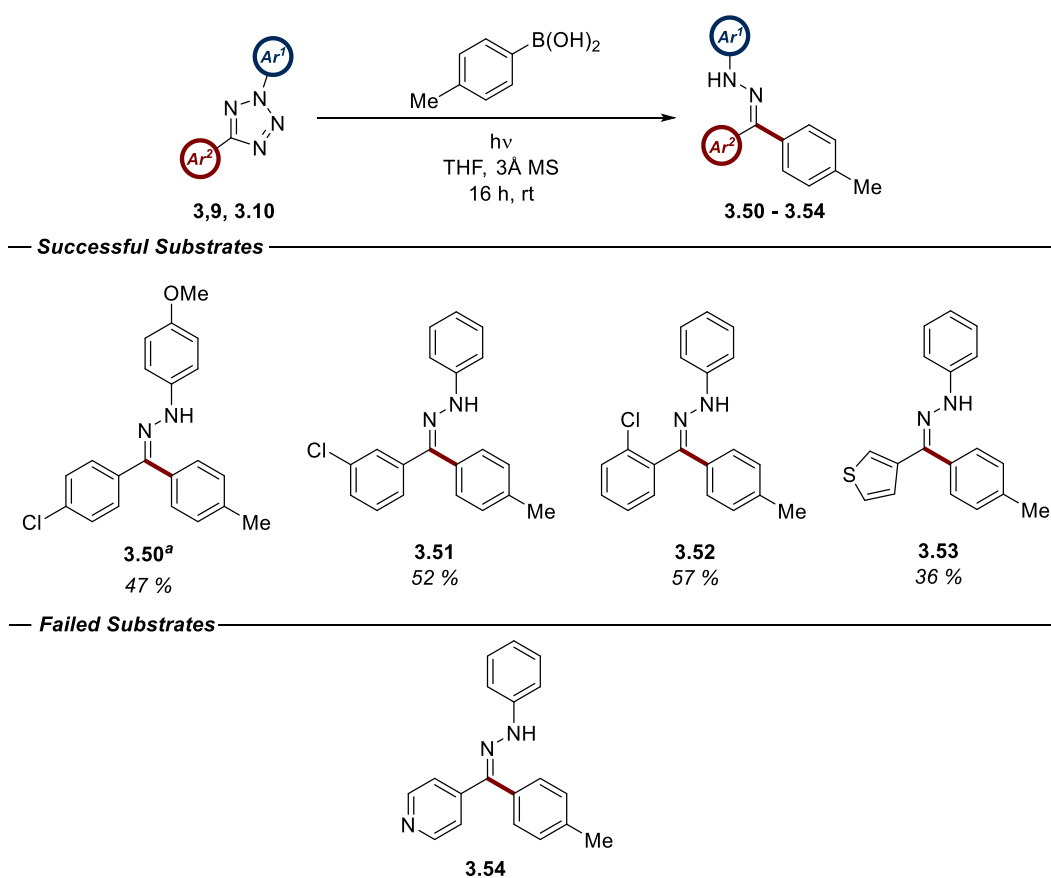
[a]*Isolated as the hydrolysed product*

Overall, the 2,5-diaryl tetrazole was significantly more tolerant to variation than the boronic acid. Both aromatic rings were amenable to substitution with electron-donating, electron-withdrawing, sterically congested and heterocyclic moieties, providing yields roughly equivalent to the unsubstituted tetrazole **3.18**. However, while the reaction was tolerant to several modifications, there were no substrates that significantly improved reaction yield. This was somewhat disappointing, as it underlines that the overall yield of the reaction remains largely dependent on the properties of the boronic acid. From a mechanistic perspective, this provides further evidence that initial formation of the proposed NI boronate complex is relatively facile, with the key step of the transformation likely to be the migration

of the aryl group of the boronate. Future experiments in this area may include NI substrates with more significant alterations to their *C* and *N*-termini, such as carbonyl groups, as this may have a more pronounced impact on the reaction outcome.

### *3.3.1.4 Further Applications*

To further demonstrate the versatility of this procedure, a number of subsequent investigations were conducted, exploring both the synthetic utility and orthogonality of the reaction.

One example of this was the adaption of the methodology for application in flow. Flow chemistry is a rapidly emerging field with enormous potential across a wide range of uses.[324] In contrast to conventional "batch" reactions, where compounds are stirred within a reaction vessel of a defined volume, flow chemistry capitalises on the unique properties of either turbulent or laminar flow within a length of tubing to mix reagents. This alternative approach to substrate interaction affords substantial enhancements to the efficiency of a process through rapid attainment of steady state conditions,[325] and is particularly advantageous when applying external stimuli to initiate the desired transformation.[326]

Flow photochemistry has already enjoyed widespread application throughout the literature.[327] One of main challenges associated with photochemical procedures is adaption to a larger scale, owing to the impracticality and significant energy consumption of larger light sources. The application of flow enables the reaction mixture to be steadily passed around a smaller bulb, facilitating reaction scale-up without requiring a larger light source. Furthermore, the application of flow tubing drastically increases the surface area of the reaction mixture exposed to the light source. This maximises the photon-uptake of the substrate by minimising energy loss through reflection and competing absorption that is commonly observed in analogous batch systems, and this typically enhances reaction rate significantly.

To assess the incorporation of the newly developed methodology within a flow reactor, tetrazole **3.55** and 4-methoxyphenylboronic acid were dissolved in THF and passed through a tubing system powered by a peristaltic pump. Photolysis was conducted by coiling the tubing around a UV light bulb (*Figure 3.2*). The reaction mixture was circulated through the system until complete consumption of starting material.

Pleasingly, the method was found to be readily compatible with this basic flow photochemistry system, affording an isolated yield of 71 % of **3.56** (*Scheme 3.18*). Furthermore, this was accomplished on a 0.75 mmol scale, three times larger than that employed in the previous substrate scope, in a reaction time of only six hours (*c.f.* 16 hours earlier). This represented the first reported photolytic generation of an NI in flow and

highlights the exceptional potential of flow photochemistry in the broader field of NI chemistry. The optimisation of this transformation certainly merits future work as a complementary alternative to the batch protocol.
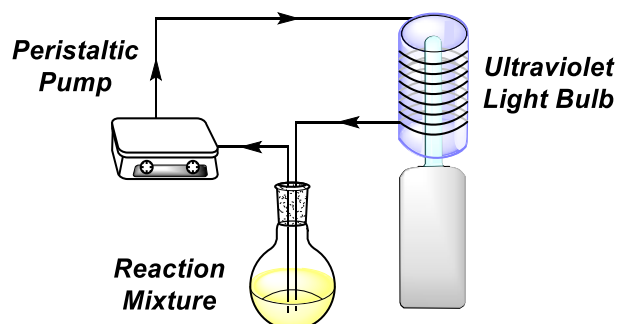


Figure 3.2: A schematic of the set-up employed during the photolysis of 2,5-tetrazoles in flow
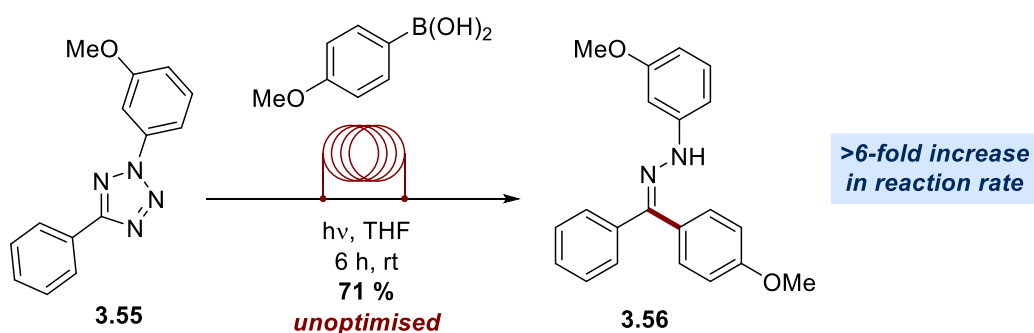


Scheme 3.18: The extremely efficient synthesis of hydrazone **3.56** in flow

The methodology was also used to improve upon an existing route towards an active pharmaceutical ingredient (API). Fenofibrate, also known as Tricor, is a hypolipidemic agent applied in the treatment of hypercholesterolemia.[328] An isopropyl ester, fenofibrate functions as a prodrug of fenofibric acid, which is a known peroxisome proliferator-activated receptor alpha (PPARα) agonist.[329] Industrial synthesis of fenofibrate relies on two disconnections. The oxygen-carbon bond of the alkyl ether moiety is typically formed using an $S_N1$ reaction, while the carbon-carbon bond of the diaryl ketone is most commonly synthesised using a Friedel-Crafts acylation (*Scheme 3.19*).[330]
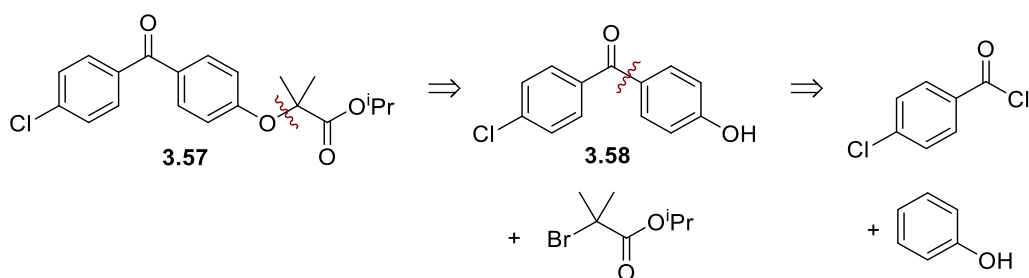


Scheme 3.19: Disconnection of Fenofibrate (**3.57**)

The synthesis of biaryl ketone **3.58** was identified as an ideal application of our emerging methodology. The prerequisite for an electron-rich species was fulfilled by the *para*-hydroxy

111

functionality, while the *para*-chlorophenyl moiety had already been shown to be well tolerated on the *C*-terminus of the NI (*Table 3.11*). The application of this methodology also represented a significant improvement over existing approaches. Formation of this bond as the final step of the synthesis requires the reaction between methyl ester **3.59** and 4-chlorobenzoic anhydride, as the isopropyl ester is incompatible.[331] Similarly, synthesis of ketone **3.58** itself requires the use of 4-chlorobenzoyl chloride and anisole, as the application of phenol would result in an esterification (*Scheme 3.20*).[332] Both of these approaches introduce an additional deprotection step into the synthesis of fenofibrate, requiring expenditure of additional resources and limiting overall reaction yield.
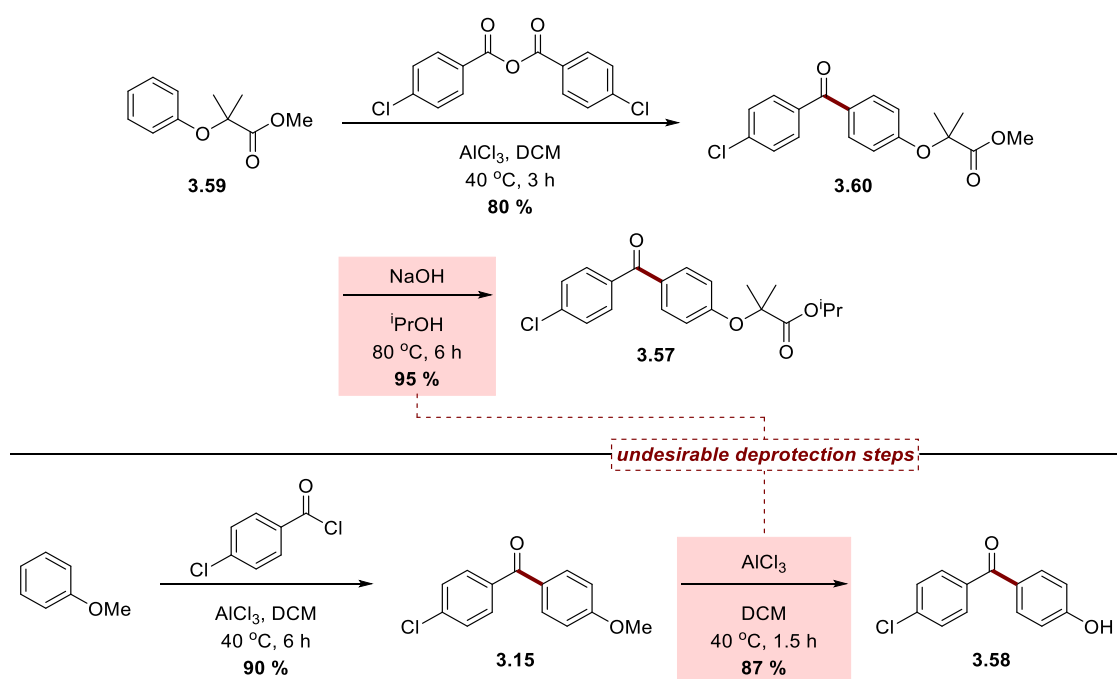


*Scheme 3.20: Two common approaches to forming the key carbon-carbon bond in fenofibrate synthesis*

By contrast, the application of hydrazone synthesis employing the appropriate coupling partners afforded key biaryl ketone intermediate **3.58** with only a solvent-switch required midway through the procedure, furnishing the compound in 66 % yield (*Scheme 3.21*). A further benefit of this approach is the lack of additional reactants. Only molecular sieves and HCl are required, both of which are easily removed *via* filtration and work-up, respectively. This portion of the procedure is also metal-free, which is important given the toxicity of even trace amounts of metals. The synthesis was then concluded using the $S_N1$ conditions already established (*Scheme 3.21*).[333]

As discussed above (*Section 1.4.1*), the traceless nature of NI generation through tetrazole photolysis is also highly attractive from a bioorthogonality perspective.[62] Boronic acids are also compatible within this environment, as this motif is not present in biological systems, relatively non-toxic and highly specific in its reactivity.[334] It was considered that the reaction

developed within this section may provide an opportunity for the site-selective labelling of a biomolecule using a NI-boronic acid pair.
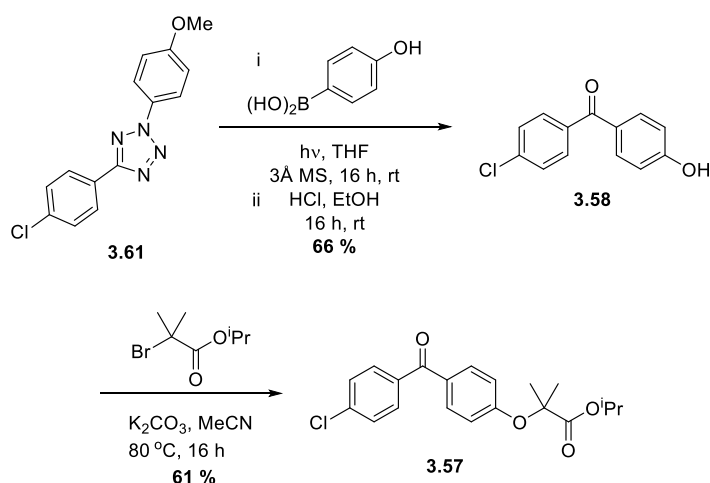


*Scheme 3.21: Transition metal-free, light-activated synthesis of fenofibrate*

To obtain proof-of-concept for this study, a small, tetrazole-containing peptide was synthesised, with the intention of modifying this with an aryl boronic acid. As the NI was previously shown to be much more reactive than the boronic acid (*Section 3.3.1.2*), the tetrazole was incorporated within the peptide, with the boronic acid acting as the covalent modifier. As reaction stoichiometry required that the boronic acid was present in excess, the incorporation of the NI within the biomolecule also enabled multiple equivalents of the boron species to be introduced. Superstoichiometric quantities of a ligation agent is common practice within chemical biology, as any excess reagent will be rapidly cleared by the organism or washed out following completion of the labelling procedure.
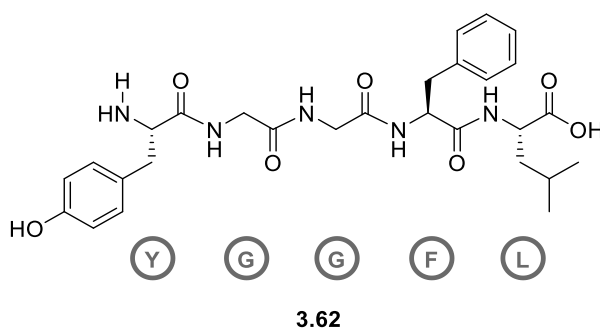


*Figure 3.3: The structure of Leu-enkaphalin*

The peptide identified as an ideal target for this preliminary investigation was a small pentamer known as Leu-enkaphalin (L-E) (**3.62**, *Figure 3.3*).[335] Composed of five amino acid residues, L-E is a naturally occurring species that acts as an opioid receptor ligand.[336] It was selected as a suitable candidate due to its low molecular weight, and has previously been extensively characterised. L-E also contains no nucleophilic residues, which is important when considering the promiscuous reactivity profile of the NI. While it was ultimately necessary to demonstrate NI selectivity over nucleophilic residues such as cysteine or

glutamic acid, their presence during a proof of concept experiment was undesirable. Finally, the hydrophobic nature of L-E enabled the continued application of THF as a solvent, facilitating replication of the reaction conditions from earlier studies.

L-E was synthesised using solid-phase peptide synthesis (SPPS) *via* a partially automated approach.[337] To most effectively simulate the natural substrate, the native carboxylate of the peptide's *C*-terminus was included, with Wang resin utilised as the solid-phase support.[338] Attachment of the tetrazole was facilitated through the preparation of compound **3.65** *via* the Kakehi synthesis (*Scheme 3.22*). A *para*-methoxy substituent was incorporated in the *N*-aryl ring to increase photolysis efficiency, with the *para*-carboxylate of the *C*-aryl ring enabling coupling of the tetrazole to L-E.
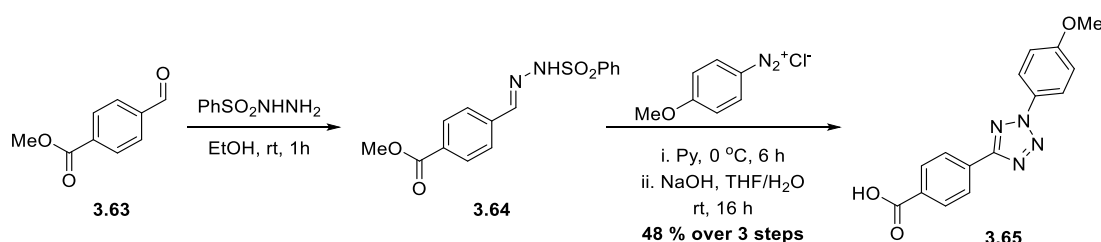


*Scheme 3.22: Synthesis of tetrazole **3.65***

The synthesis of the final functionalised peptide (compound **3.66**) was then accomplished through conventional SPPS manual coupling. Cleavage from the resin using acidic conditions furnished the desired peptide **3.66** after purification using preparative HPLC (*Scheme 3.23*). While the isolated yield appears disappointing from the perspective of small molecule chemistry, yields in this range are commonplace within SPPS due the multitude of individual reactions involved in the synthesis.
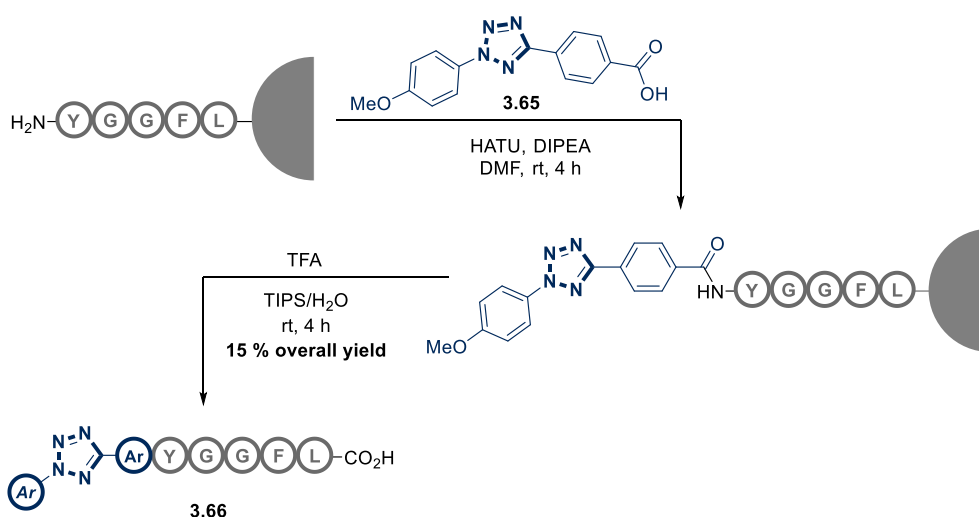


*Scheme 3.23: Synthesis of functionalised L-E species **3.66***

4-Methoxyphenylboronic acid was selected as an appropriate reaction partner due to its electron-rich nature, in addition to its prevalence within the earlier optimisation procedures

114

(*Section 3.3.1.2*). Unfortunately, photolysis of peptide **3.66** did not result in the generation of the desired product (**3.67**). LCMS analysis indicated the formation of hydrazide **3.68**, formed through the reaction of the NI and trifluoroacetic acid (TFA) (*Scheme 3.24*). This was a consequence of the preparative HPLC purification, which employed TFA as a 0.1 % modifier in the mobile phase. While solvent was removed from the peptide *via* freeze-drying, it is likely that residual TFA could nonetheless remain in sufficient quantities to out-compete the boronic acid in its reaction with the NI.
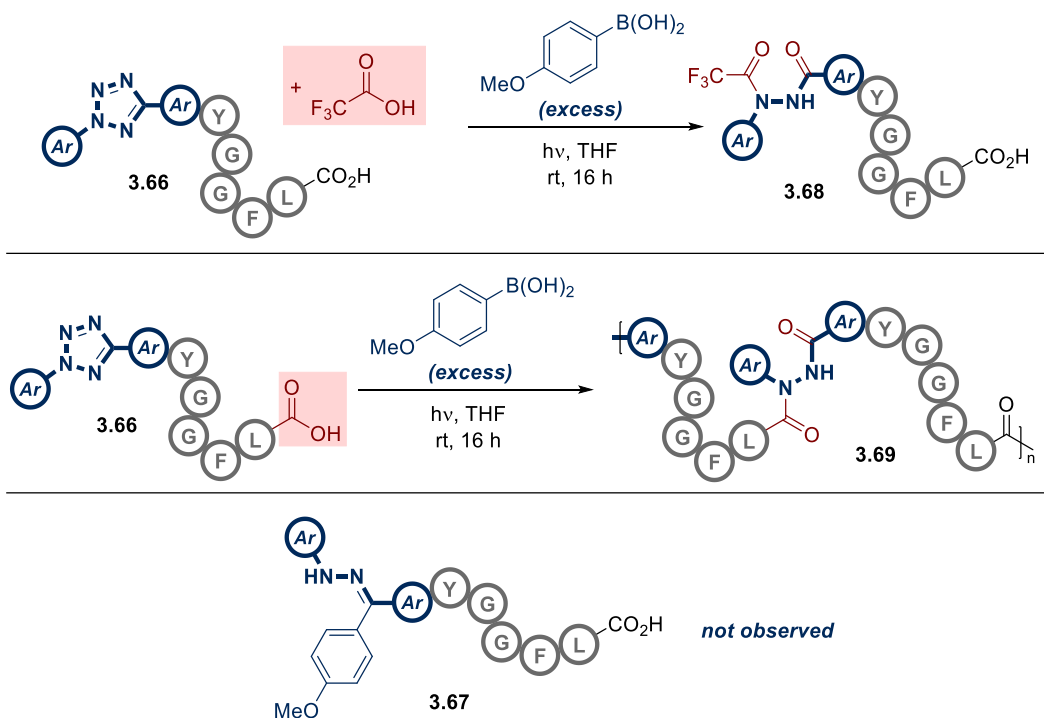


*Scheme 3.24: The interference of acidic residues in the attempt isolation of L-E adduct **3.67***

To prevent the formation of this by-product, the synthesis of **3.67** was reattempted using an ammonium hydroxide modifier during the purification of the starting material. However, photolysis of **3.66** on this occasion formed only a complex mixture. This may be rationalised by considering the free carboxylate of the *C*-terminus of the peptide. While the centre is too remote to trigger intramolecular cyclisation of the biomolecule, intermolecular reaction and subsequent polymerisation remains a possibility (*Scheme 3.24*). This result is indicative of the enhanced reactivity of the NI with carboxylic acids relative to boronic acids, inhibiting the desired pathway.

These experiments suggested that the pleiotropic reactivity of NIs with native chemical residues meant that the newly developed reaction could not be considered bioorthogonal. While disappointing, there is still significant scope for future work within this field. Incorporation of the NI within a biomolecular scaffold was relatively straightforward, which could enable the synthesis of numerous additional fragments. L-E also remains a useful

candidate for further study with a boronic acid reaction partner, if employing a solid support which does not furnish a carboxylate upon cleavage, such as the Rink amide resins.[339]

### 3.3.2    *Hydrazonyl Chlorides as a Source of Nitrile Imine*

While tetrazoles have several advantages as an NI source, including the lack of any exogenous reagents, facile synthesis, and precise control over time of activation, there are also a number of disadvantages. Most of these stem from the use of UV light, with 2,5-tetrazoles affording a slightly more limited substrate scope than alternative methods of NI generation. For example, substitution of either aromatic ring with a $NO_2$ functional group would inhibit the formation of the relevant NI, while the introduction of 2-alkyl tetrazoles produces a similar affect by decreasing the $\lambda_{max}$ of the substrate.[46] An additional aspect that should also be considered is the general safety of the protocol. The carcinogenic properties of UV light are extensively documented and may limit the accessibility of the methodology.[340] One further drawback is that tetrazole degradation is irreversible, due to the release of $N_2$ gas. This means that if the reaction partner is not particularly reactive, for example in the case of some boronic acids, conversion may be hindered through decomposition of the NI (see *Section 1.3.4*). Reversible generation of the NI has the advantage of creating a "depot" of the intermediate, where it may revert to a less reactive precursor when not required.

Through a survey of recent literature, it was decided that the best candidate for an alternative source of NI would be the hydrazonyl chlorides (*Scheme 3.25*, see *Section 1.2.1*). Treatment of these compounds with a tertiary organic base or an inorganic base leads to reversible generation of the NI intermediate. It was proposed that controlled release of the NI could lead to an increase in reaction yield, while the removal of UV light would broaden the substrate scope and render the transformation more amenable to scale-up.[65]
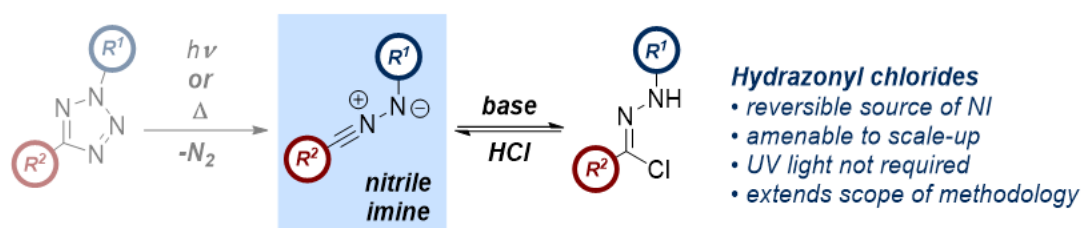


*Scheme 3.25: The introduction of hydrazonyl chlorides as an NI source*

In an analogous manner to *Section 3.3.1*, a series of hydrazonyl chlorides were first synthesised. This was accomplished through the chlorination of aryl hydrazones by dimethylsulfonium chloride, or the dehydration of alkyl hydrazines by triphenylphosphonium chloride (*Table 3.12*). The isolated yields of these reactions ranged

from good to moderate, but all were obtained in satisfactory quantities for the desired transformations.

Table 3.12: The synthesis of hydrazonyl chloride starting materials



**Chlorination**

| | | | |
|---|---|---|---|
| **3.70** | **3.71** | **3.72** | **3.73** |
| 42 % | 64 % | 23 % | 45 % |

**Dehydration**

| | |
|---|---|
| **3.74** | **3.75** |
| 51 % | 25 % |
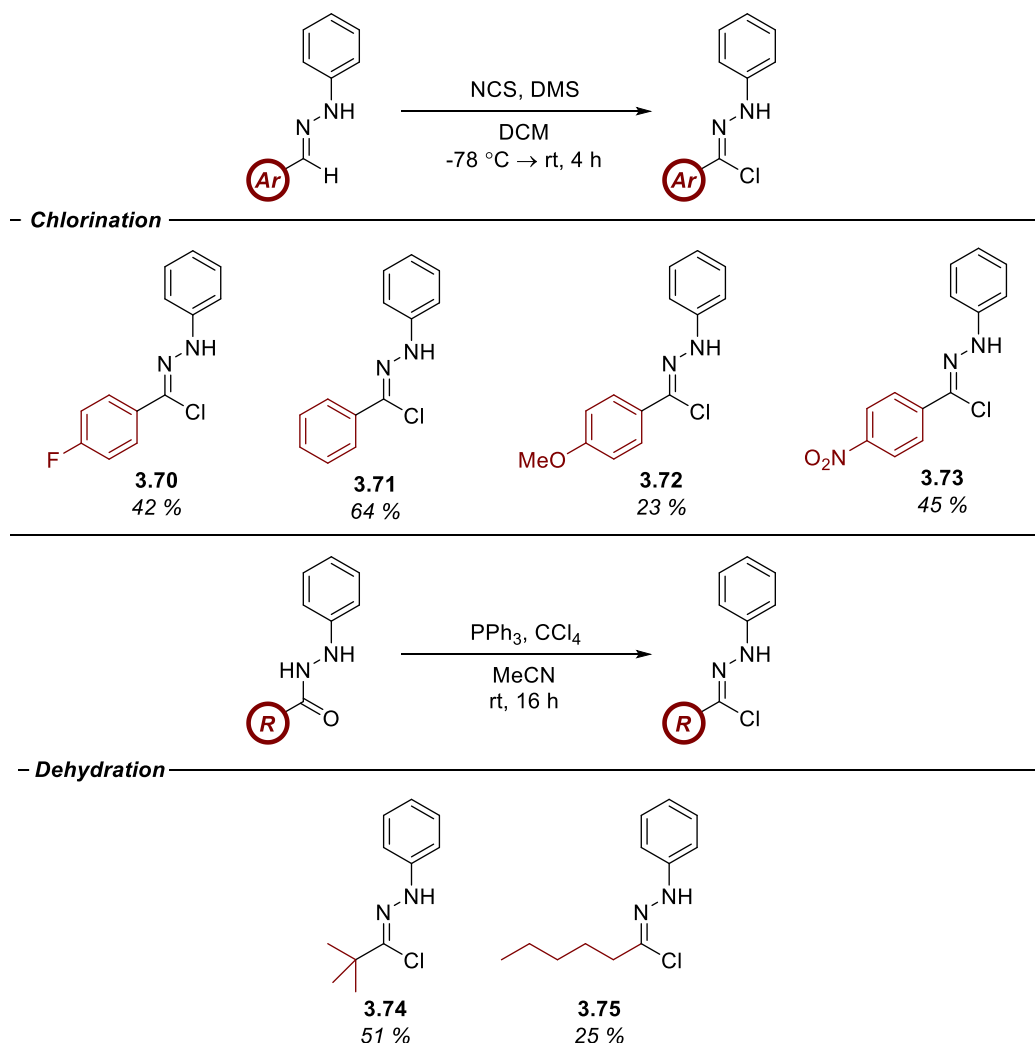
### 3.3.2.1 Optimisation of Reaction Conditions

Owing to the success of $^{19}$F NMR when investigating the use of tetrazoles, the same method of analysis was adopted throughout this optimisation. As an initial proof-of-concept, the substrates used in the previous optimisation were mirrored as closely as possible, employing 4-fluoro-*N*-phenylbenzohydrazonyl chloride (**3.70**) and 3-fluoro-4-methoxyphenylboronic acid, with triethylamine added to generate the NI. Unfortunately no conversion to the product was observed, and the reaction was repeated using 4-methoxyphenylboronic acid, owing to its higher reactivity (*Scheme 3.26*). This resulted in a 26 % conversion to the desired product, enabling this system to be carried forward as a model reaction. One slight disadvantage of this change was that the information that could be elucidated through the inclusion of the fluorine atom on the boronic acid was lost.

117
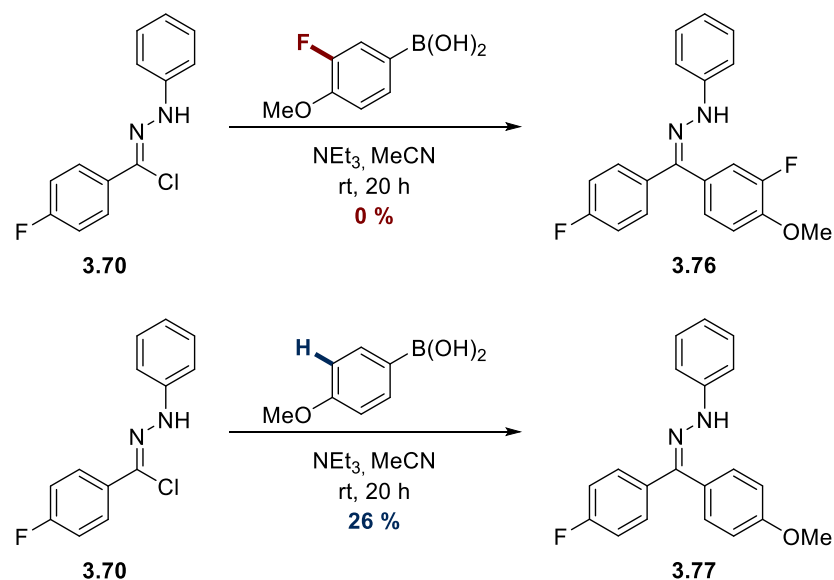
*Scheme 3.26: Initial proof of concept of the reaction between hydrazonyl chlorides and boronic acids in the presence of a base*

With the development of an appropriate assay, the choice of reaction solvent was addressed. Literature examples involving NI generation from hydrazonyl chlorides report a range of solvents,[149,176,341,342] therefore a large number were investigated, with the results shown in *Table 3.13*.

The most immediate trend was the superior performance of non-polar solvents in comparison to more polar systems, *e.g.* acetonitrile, THF and acetone in comparison to 1,4-dioxane, toluene and DCM. However, the trend of non-polar solvents generating more favourable conversions was not without exceptions (*e.g.* diethyl ether).

The promiscuity of the NI was problematic when using of solvents with nucleophilic or dipolarophilic character, where several side reactions were observed. This was particularly prevalent in protic solvents, with methanol, isopropanol, and water all failing to afford significant conversion of the desired product. In the case of water, this can be rationalised by considering the mechanism of primary hydrazide formation proposed within the previous section (*Section 3.3.1.2*). A similar process is also likely to operate when using an alcohol as the solvent, as has previously been demonstrated by Huisgen (*Section 1.3.2.1*).[12] Side reactions were also detected when DMSO, DMF, or acetone were employed, all of which are nucleophilic (in the latter case, *via* the enol tautomer), although the exact composition of these side products were never elucidated.

The outcome of this solvent screen was the selection of DCM for application in further optimisation studies, with toluene noted as a suitable alternative. While retaining the non-polar, aprotic properties of DCM, toluene is more environmentally benign and has a much higher boiling point, enabling more energy to be supplied to the system if necessary.

*Table 3.13: Selection of the optimal reaction solvent in the generation hydrazones from hydrazonyl chlorides*
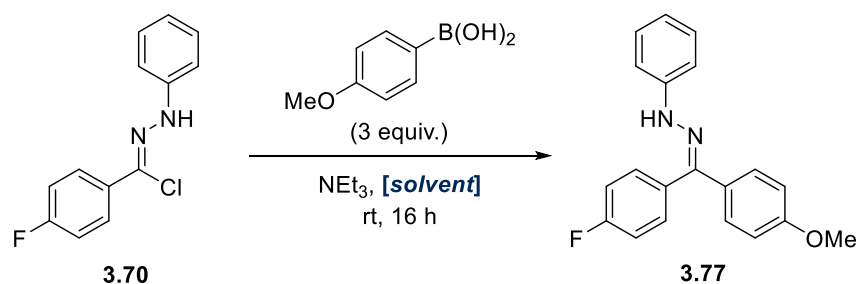


| Entry | Solvent | Conversion(%)[a, b] |
|:---:|:---:|:---:|
| 1 | MeCN | 32[c] |
| 2 | THF | 22 |
| 3 | DCM | 75 |
| 4 | Et$_2$O | 15 |
| 5 | MeOH | <1[c] |
| 6 | $^i$PrOH | <1[c] |
| 7 | 1,4-dioxane | 58 |
| 8 | DMSO | <1[c] |
| 9 | EtOAc | 48 |
| 10 | DMF | <1 |
| 11 | 2-MeTHF | 26 |
| 12 | PhMe | 50 |
| 13 | COMe$_2$ | 47[c] |
| 14 | H$_2$O | 13 |

[a] Conversion determined by $^{19}$F NMR with reference to an internal standard

[b] Average value of two experiments with a difference of <10 %

[c] Significant by-product formation observed

With judicious choice of solvent leading to a conversion of over 70 %, the stoichiometry of boronic acid was lowered from 3 to 1.1 equivalents for subsequent optimisation experiments to improve the overall atom economy of the transformation. This was first employed during screening of additional solvents based on the results of the initial screen. Two further chlorinated solvents, chloroform and dichloroethane (DCE) were assessed, along with the environmentally benign DCM replacement cyclopentylmethyl ether (CPME). The reduction in boronic acid stoichiometry lowered conversions, but synthetically tractable values of over 50 % were retained (*Table 3.14*). Chloroform and DCM both performed well, with chloroform considered an optimal replacement for DCM should the temperature need to be increased later in the optimisation.

An appropriate base was then evaluated. Triethylamine had been employed up until this point primarily due to its prevalence in the literature, but several factors needed to be considered including steric encumbrance, solubility and $pK_b$. Both organic and inorganic examples were screened across a range of $pK_b$ values, with the results displayed in *Table 3.15*. The trend between conversion and $pK_b$ was immediately apparent. Conversions steadily increased with increasing $pK_b$ to a value of around 12, at which point reactivity was lost. The identification of potassium phosphate enabled around a 20 % increase in conversion relative to the initial selection of triethylamine.

*Table 3.14: A screen of chlorinated and other related solvents*
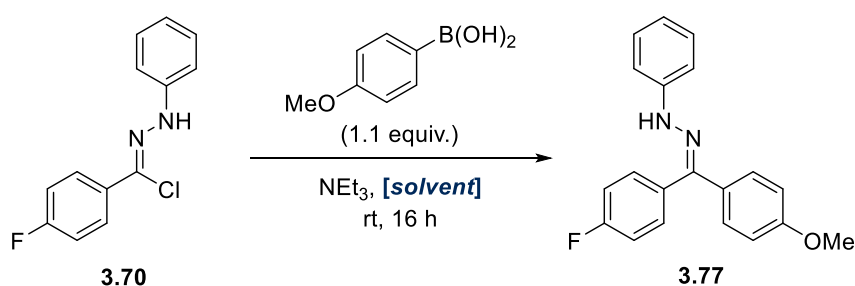


| Entry | Solvent | Conversion (%)[a, b] |
|-------|---------|------------------|
| 1 | DCM | 54 |
| 2 | DCE | 40 |
| 3 | CHCl₃ | 51 |
| 4 | CPME | 20 |

[a] Conversion determined by $^{19}$F NMR with reference to an internal standard

[b] Average value of two experiments with a difference of <10 %

Again, the reactivity of the NI hindered the application of some bases, owing to considerable side reactions. This typically occurred when using species with a higher $pK_b$, such as potassium hydroxide or the phosphazine base BEMP, but was also an issue with organic bases DABCO and DBU. The nucleophilicity of these species is again likely to be responsible (the reaction of NIs with amines is well documented[12,160,173]).

The comparison of organic and inorganic bases did not appear to have a significant impact upon reaction conversion. However, it is worth considering that the deprotonation of the hydrazonyl chloride may be hindered by a lack of solubility. This can rationalise the difference in performance between potassium carbonate relative to other bases of similar $pK_b$ values. The considerably lower conversion was perhaps due to its limited solubility (*Graph 3.2*). This argument is corroborated by the improved conversion of caesium carbonate, a species with an identical $pK_b$ but a more soluble counterion (*Graph 3.2*, *Table 3.16*).

*Table 3.15: Determining the suitability of various bases in their incorporation within the reaction manifold*

B(OH)$_2$

MeO

[*base*], DCM
16 h, rt

**3.70** → **3.77**
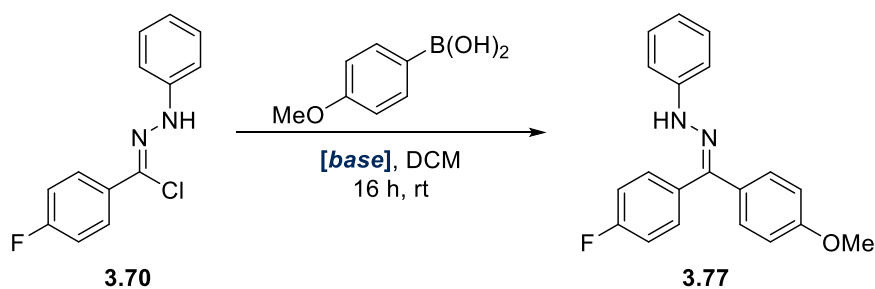
| Entry | Base | pK$_b$ Water (DMSO) | Conversion (%)[a, b] |
|---|---|---|---|
| 1 | KTFA | -0.25[343] | <1 |
| 2 | KOAc | 4.76 (12.3)[344] | <1 |
| 3 | Pyridine | 5.21 (3.4)[345] | <1 |
| 4 | Lutidine | 6.75 (4.46)[346] | 2 |
| 5 | NMM | 7.41[347] | 8 |
| 6 | Collidine | 7.48[348] | 10 |
| 7 | DABCO | 8.82 (8.93)[349] | <1[c] |
| 8 | K$_2$CO$_3$ | 10.33[350] | 20 |
| 9 | NEt$_3$ | 10.75 (9.0)[351] | 53 |
| 10 | DIPEA | 11.07[352] | 55 |
| 11 | DBU | 12-14[353] | 9[c] |
| 12 | K$_3$PO$_4$ | 12.32[354] | 71 |
| 13 | KF | 3.17 (15)[345] | 37 |
| 14 | KOH | 15.7 (31.4)[355] | 7[c] |
| 15 | KO$^t$Bu | 17.0 (32.2)[355] | 15[c] |
| 16 | BEMP | 27.6[d] | 6[c] |

[a] Conversion determined by $^{19}$F NMR with reference to an internal standard

[b] Average value of two experiments with a difference of <10 %

[c] Significant by-product formation observed

[d] Measured in MeCN

One further implication of base selection is the solubility of the salt produced upon deprotonation of the hydrazonyl chloride. This can impact the equilibrium between the precursor and the NI, with limited solubility of the conjugate acid accelerating dipole generation. As was observed in the tetrazole optimisation above, excessive amounts of the NI can lead to premature decomposition of the dipole with the overall effect of decreasing conversion to the hydrazone.
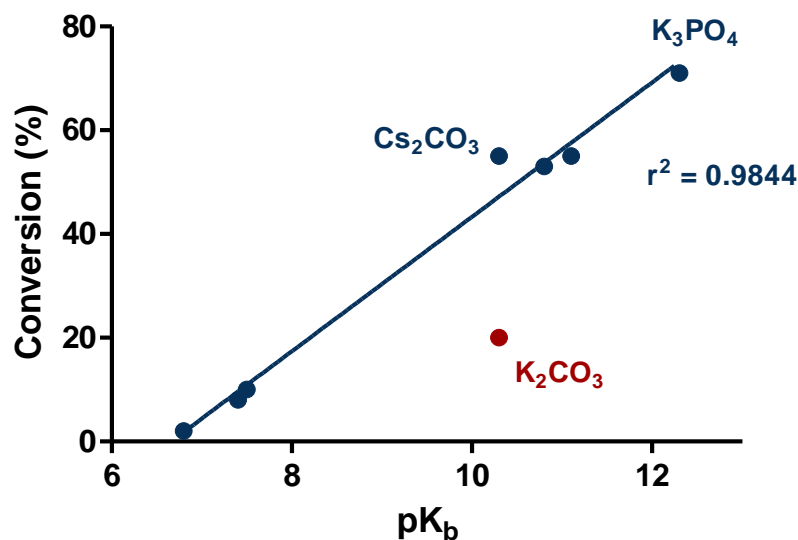
Due to the potential influence of base solubility, a screen of different counterions of both carbonate and phosphate bases was undertaken to determine the optimal base for use in the reaction. Phosphate was selected due to the superior performance of potassium phosphate in comparison to any organic base, while carbonate was included as an alternative. The results are shown in *Table 3.16*.

The results failed to identify any base superior to those that had already been investigated, however some of the hypotheses outlined above were corroborated. Beginning with the carbonate salts, the vast majority exhibited lower reactivity than potassium carbonate. Only one counterion, caesium, was shown to furnish improved conversions. This can again be rationalised through solubility, as the increased organic solubility of the caesium salts relative to other group I and II metals is well documented.[356]

The monobasic and dibasic forms of potassium phosphate were also assessed, however neither species generated any conversion. This was unsurprising, as the species have pK$_b$ values of 2.12 and 7.21, respectively,[354] well below the threshold identified to have a meaningful impact on reaction conversion. Disappointingly, a screen of counterions for the tribasic phosphate ion failed to identify any valid alternatives to potassium phosphate itself. This result was surprising given the complete lack of conversion of all other phosphates.

Nevertheless, the decision was made to progress to further stages of the optimisation using potassium phosphate as the base of choice in the generation of the NI. Both caesium carbonate and triethylamine were identified as potential alternatives owing to their favourable conversion values. As chloroform had shown similar conversion values as DCM at an earlier stage, the combination of potassium phosphate and chloroform was also investigated. Unfortunately, while initial conversion values appeared promising, rapid

decomposition of the product was observed upon reaction work-up. The exact reasons for this instability remain unclear but may be attributable to the increased acidity of the chloroform proton relative to DCM. With a pK$_a$ of 13.6,[357] chloroform is labile to deprotonation by phosphate, which may contribute to the decomposition of the hydrazone.

*Table 3.16: The screening of counterions of various carbonate and phosphate bases*
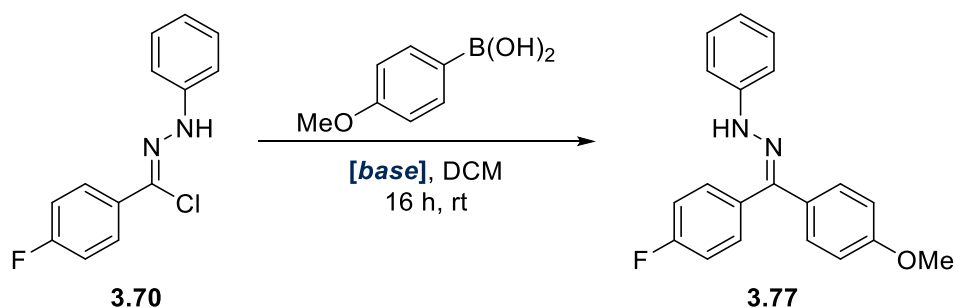


| Entry | Base | Conversion (%)[a, b] |
|-------|------|----------------------|
| 1 | (NH$_4$)$_2$CO$_3$ | <1 |
| 2 | Na$_2$CO$_3$ | <1 |
| 3 | CaCO$_3$ | <1 |
| 4 | K$_2$CO$_3$ | 20 |
| 5 | Cs$_2$CO$_3$ | 55 |
| 6 | KH$_2$PO$_4$ | <1 |
| 7 | K$_2$HPO$_4$ | <1 |
| 8 | K$_3$PO$_4$ | 70 |
| 9 | Na$_3$PO$_4$ | 3 |
| 10 | Ca$_3$(PO$_4$)$_2$ | <1 |
| 11 | Mg$_3$(PO$_4$)$_2$ | <1 |
| 12 | K$_3$PO$_4$[c] | 60[d] |

[a] Conversion determined by ^{19}F NMR with reference to an internal standard

[b] Average value of two experiments with a difference of <10 %

[c] CHCl$_3$ was used as reaction solvent

[d] Significant by-product formation observed

With an optimal solvent/base combination established, several continuous variables were then considered. It was decided that the most efficient method of optimising these variables would be through a DoE approach. Consequently, a two-level, five-factor, half-fractional experiment was conducted to optimise base and boronic acid stoichiometry, temperature, time, and concentration (*Table 3.17*). As with the DoE investigation in *Section 2.3.2.1*,

aliasing was found to be inconsequential in the estimation of two-factor interactions within this study.

*Table 3.17: Conversion values obtained from the DoE study*
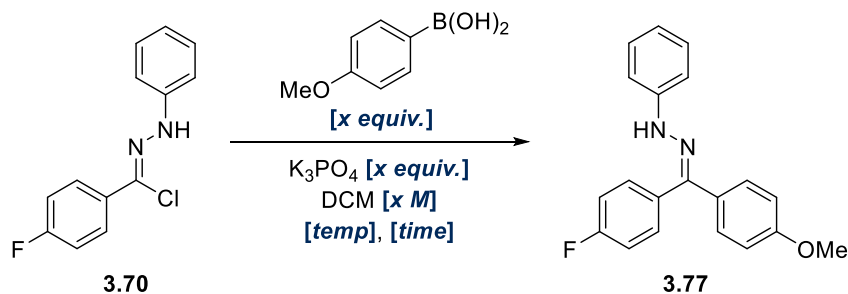


| Entry | Boronic Acid Stoichiometry (eq.) | Base Stoichiometry (eq.) | Concentration (M) | Time (h) | Temperature (° C) | Conversion (%)[a,b] |
|---|---|---|---|---|---|---|
| 1 | 1 | 1 | 0.01 | 16 | 20 | 25 |
| 2 | 1 | 1 | 0.1 | 16 | 40 | 48 |
| 3 | 1 | 1 | 0.1 | 3 | 20 | 23 |
| 4 | 1 | 1 | 0.01 | 3 | 40 | 34 |
| 5 | 1 | 3 | 0.1 | 16 | 20 | 2 |
| 6 | 1 | 3 | 0.01 | 16 | 40 | 22 |
| 7 | 1 | 3 | 0.01 | 3 | 20 | 1 |
| 8 | 1 | 3 | 0.1 | 3 | 40 | 19 |
| 9 | 3 | 1 | 0.1 | 16 | 20 | 63 |
| 10 | 3 | 1 | 0.01 | 16 | 40 | 82 |
| 11 | 3 | 1 | 0.01 | 3 | 20 | 12 |
| 12 | 3 | 1 | 0.1 | 3 | 40 | 78 |
| 13 | 3 | 3 | 0.01 | 16 | 20 | 63 |
| 14 | 3 | 3 | 0.1 | 16 | 40 | 82 |
| 15 | 3 | 3 | 0.1 | 3 | 20 | 60 |
| 16 | 3 | 3 | 0.01 | 3 | 40 | 75 |
| 17 | 2 | 2 | 0.06 | 9.5 | 30 | 65[c] |

[a] Conversion determined by $^{19}F$ NMR with reference to an internal standard

[b] Reported values are averages of three runs.

[c] Average of four runs.

124

Generation of a half-normal plot of the results facilitated the identification of the factors with the most significant impact upon conversion (*Graph 3.3*). Base stoichiometry was immediately shown to have a substantial influence, while temperature was also important. Perhaps the most interesting variable with an impact on reaction outcome was the ratio of boronic acid to base. This was a curious result, as it indicated that while an increase in boronic acid stoichiometry itself did not improve conversion, the stoichiometry of the boronic acid relative to the base had a significant impact.
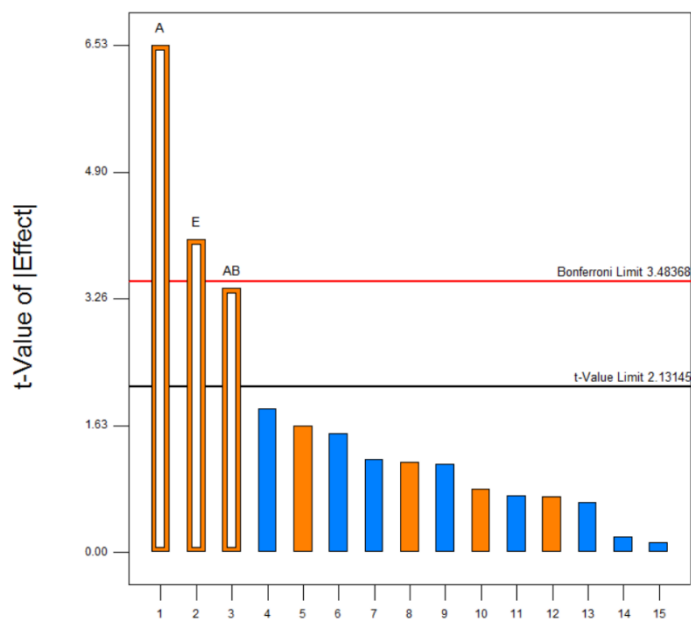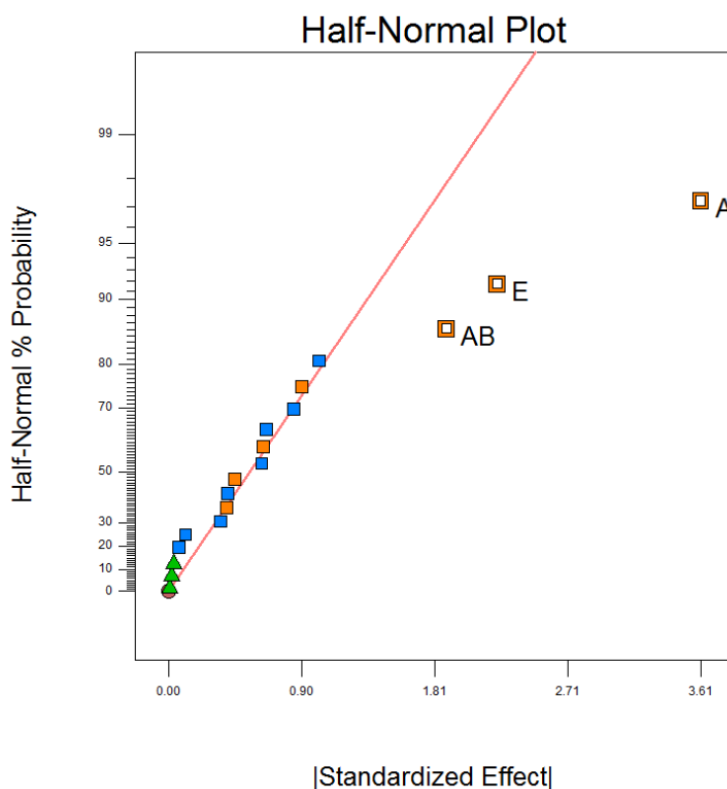


*Graph 3.3: Plot of the t-values of each variable (top) and the relevant half-normal plot (bottom)*

This result was visualised using the 3D surface shown in *Graph 3.4*. As would be expected, increasing base stoichiometry increased conversion. Considering only axis A, the use of one equivalent of potassium phosphate resulted in a conversion of around 10 %, while the introduction of 3 equivalents drove this value to around 80 %. However, this trend was not repeated with boronic acid stoichiometry. At lower stoichiometries of base, an increased loading of boronic acid was found to be detrimental to reaction conversion, whereas at maximum base loading, increasing the equivalents of boronic acid improved the yield. This inversion of influence depending on the stoichiometry of base is responsible for the generation of this unusual response surface.

This result indicated that the reaction proceeded more efficiently when the stoichiometry of base was greater than that of the boronic acid. This could be due to the boronic acid acting as a buffer. With a $pK_a$ of 9.24,[358] 4-methoxyphenylboronic acid is capable of quenching the phosphate, rendering it unable to deprotonate the hydrazonyl chloride. This effect can be diminished through the addition of further quantities of base.
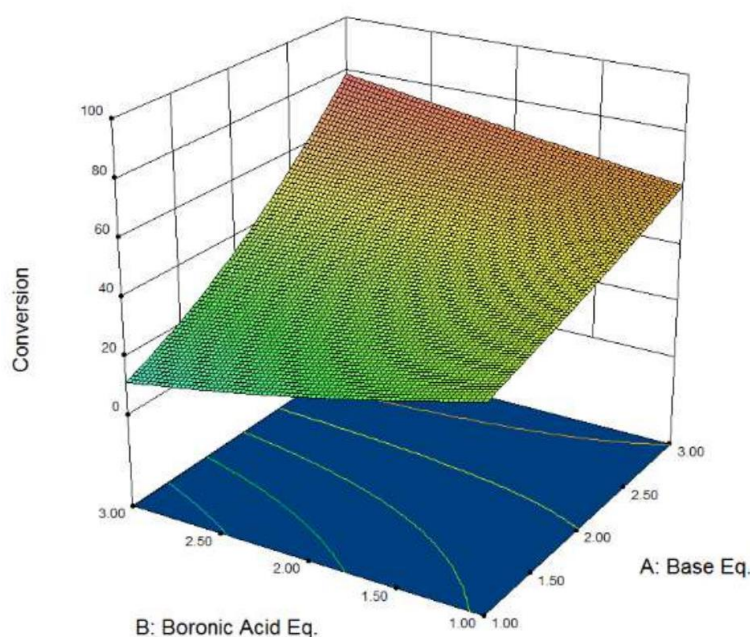


*Graph 3.4: Three-dimensional plot of the effects of base and boronic acid stoichiometry upon reaction yield*

The 3D response surface showing the correlation between temperature and base stoichiometry is more straightforward. As previously discussed, the equivalents of base showed a general correlation of increased conversion with increased loading. Temperature follows a similar trend, with increased values improving conversion. This leads to the correlation shown in *Graph 3.5*, with the maximum values of both variables leading to optimal conversion.

The results of this design of experiments optimisation did not greatly alter the conditions used, but rather offered justification for their selection. The equivalents of base and boronic

acid were maintained at 3 and 1.1, respectively, while temperature was raised to 40 °C, with the reaction complete within 3 hours. Concentration had a minimal impact on conversion, and as such the most concentrated variant (0.1 M) was taken forward for future work.
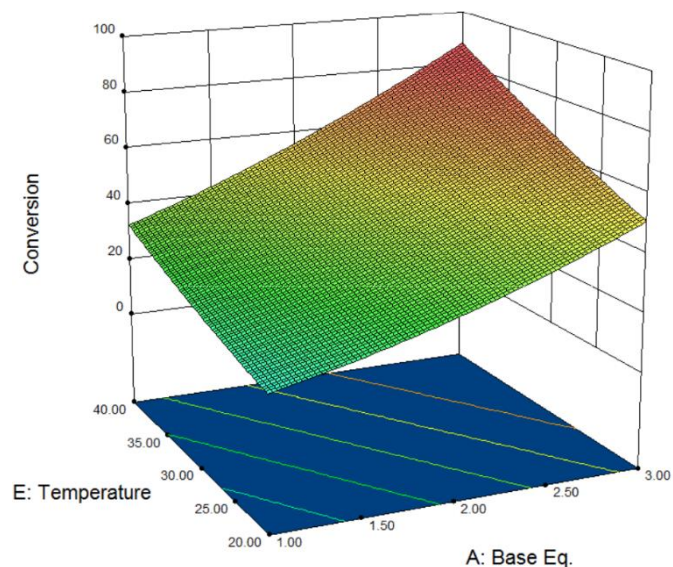


*Graph 3.5: A three-dimensional plot of the effects of base stoichiometry and temperature upon reaction yield*

The conditions developed above were then applied at a practical (0.25 mmol) scale, leading to the isolation of hydrazone **3.77** in an 80 % yield (*Scheme 3.27*). This represented an increase in conversion of almost 50 % compared to the initial conditions involving triethylamine and acetonitrile, and required only 1.1 equivalents of boronic acid. However, attempts in assessing the substrate scope immediately encountered difficulties when the boronic acid was exchanged with the 3-fluoro-4-methoxyphenyl derivative employed in the optimisation of the 2,5-diaryl tetrazole reaction manifold (*Section* 3.3.1.2). This reaction furnished only traces of the desired product **3.76**, leading to concerns that the transformation in its current form was limited to a single substrate.
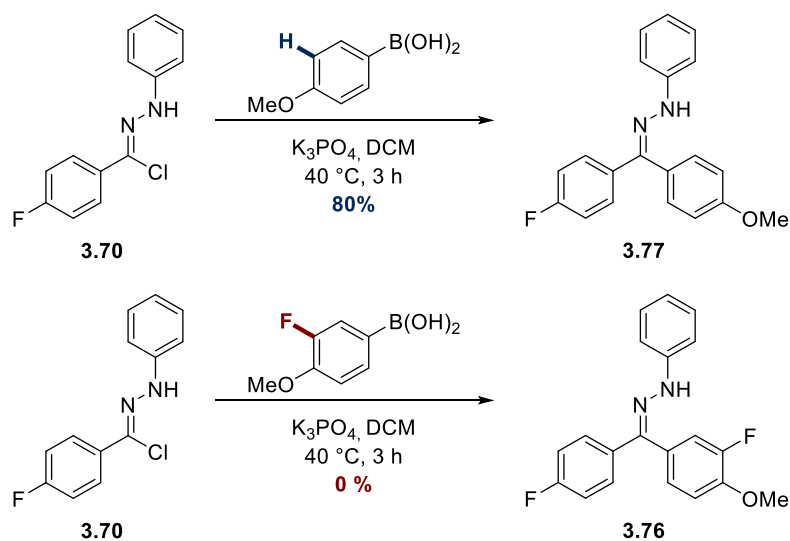


*Scheme 3.27: Attempts to synthesise hydrazones **3.76** and **3.77** using the updated conditions*

127

Owing to the results of the DoE optimisation, it was proposed that a further increase in the reaction temperature would facilitate an improved yield of more challenging substrates. Unfortunately, as DCM was already under reflux at 40 °C, this necessitated a change of solvent. While chloroform would have served as the initial alternative, the detrimental results of this solvent in conjunction with potassium phosphate led to the selection of toluene as a suitable replacement.

The procedure was first repeated in this solvent using 4-methoxyphenylboronic acid as a substrate (*Table 3.18*). Toluene produced a comparable yield of 75 % after just one hour of heating at 80 °C, at the expense of a slightly more complex reaction profile. While the isolated yield of the reaction performed in DCM improved when stirred overnight, the conversion decreased when stirred for a longer time in toluene. This indicated complete consumption of the starting material and partial thermal decomposition of the product, owing to the higher temperatures employed.

*Table 3.18: Investigations into the optimal time and temperature to facilitate the introduction of toluene into the reaction manifold*
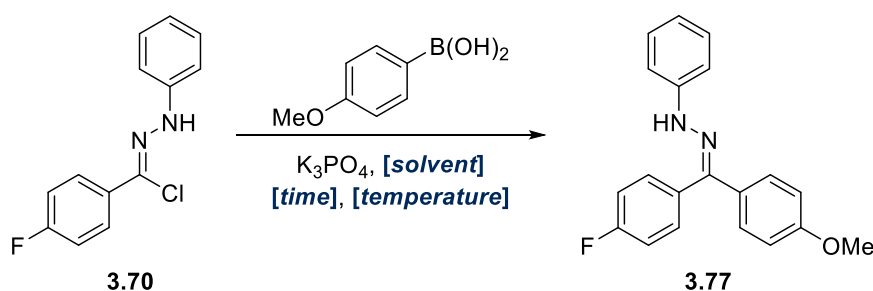


| Entry | Solvent | Temperature (°C) | Time (h) | Conversion (%)[a, b] | Isolated Yield (%) |
|-------|---------|------------------|----------|---------------------|--------------------|
| 1 | DCM | 40 | 3 | 85 | 80 |
| 2 | DCM | 40 | 16 | 86 | 85 |
| 3 | PhMe | 50 | 3 | 75 | 69 |
| 4 | PhMe | 80 | 1 | 81 | 75 |

[a] Conversion determined by $^{19}$F NMR with reference to an internal standard

[b] Average value of two experiments with a difference of <10 %

These conditions were reapplied with 3-fluoro-4-methoxyphenylboronic acid as a substrate, and a small optimisation was conducted. Gratifyingly, increasing the temperature did indeed result in an improved yield, with heating at 110 °C for 2 hours generating a conversion in excess of 30 % for the first time (*Table 3.19*). Furthermore, the use of a fluorinated compound as a substrate enabled a greater amount of information to be elucidated by $^{19}$F NMR. It was identified that the two major by-products of the reaction both originated from

the boronic acid, through protodeboronation and oxidation to the phenyl and phenol derivatives, respectively. The stoichiometry of boronic acid was first increased to limit the impact of these two side products. Unfortunately, as outlined above (*Section 3.3.1.2*), an increase in boronic acid equivalents relative to potassium phosphate may in fact inhibit the reaction. This was indeed the case, with a loss of 10 % conversion by increasing boronic acid stoichiometry from 1.1 to 2.

*Table 3.19: Optimisation of reaction conditions for electron deficient boronic acids*
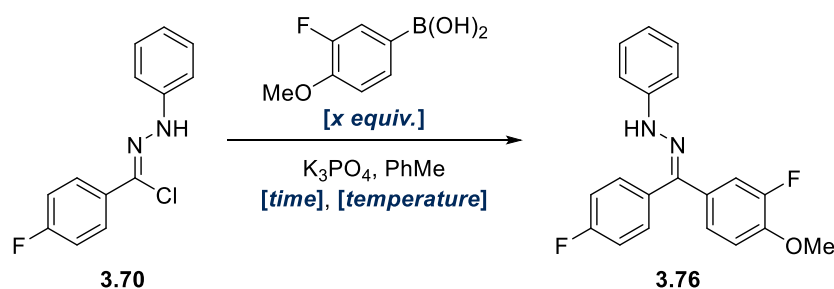


| Entry | Time (h) | Temperature (°C) | Equivalents of B(OH)$_2$ | Conversion (%)[a, b] |
|:---:|:---:|:---:|:---:|:---:|
| 1 | 2 | 60 | 1.1 | 2 |
| 2 | 2 | 80 | 1.1 | 17 |
| 3 | 2 | 110 | 1.1 | 34 |
| 4 | 2 | 60 | 2 | 3 |
| 5 | 2 | 110 | 2 | 24 |
| 6[c,d] | 2 | 80 | 1.1 | 4 |
| 7[c,d] | 2 | 80 | 2 | 2 |
| 8[c,d] | 2 | 110 | 2 | 30 |
| 9 | 16 | 110 | 1.1 | 23 |
| 10[c,d] | 16 | 110 | 1.1 | 41 |
| 11[c,d] | 16 | 110 | 2 | 42 |
| 12[c,d] | 16 | 110 | 3 | 48 |
| 13[c] | 16 | 110 | 1.1 | 35 |

[a] Conversion determined by $^{19}$F NMR with reference to an internal standard

[b] Average value of two experiments with a difference of <10 %

[c] Performed under an N$_2$ atmosphere

[d] 3 Å molecular sieves were added

As an alternative strategy, the reaction was performed under a nitrogen atmosphere and in the presence of molecular sieves. This was intended to eliminate the formation of either side product, by removing the source of oxygen and through the omission of water. This resulted in a slight increase in yield when combined with the longer reaction time of 16 hours,

furnishing 41 % conversion to the product. Curiously, increasing the stoichiometry of boronic acid was found to be no longer detrimental to the reaction yield. This could be rationalised by the absence of water, which may be necessary to facilitate proton transfer between the phosphate and boronic acid, which quenches the base.

This extended optimisation campaign enabled the identification of conditions which may be utilised in the synthesis of a wide range of aryl hydrazones, employing a diverse palette of boronic acid substrates (*Scheme 3.28*). These conditions can be considered complementary to those developed above using 2,5-tetrazoles as NI precursors.
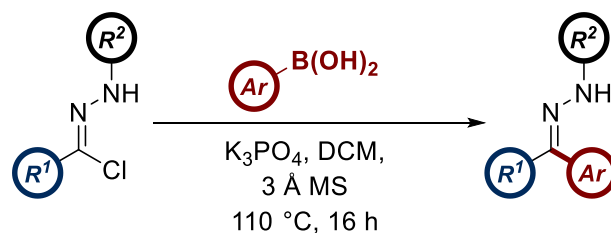


*Scheme 3.28: The optimised reaction conditions for the transition metal- and light-free C-C bond formation between an NI and an aryl boronic acid*

### 3.3.2.2 Scope of the Reaction

In an analogous manner to the investigation in *Section 3.3.1.3*, the compatibility of the optimised conditions was then assessed. To maintain consistency with the previous study, the boronic acid component was first investigated. The results of the earlier substrate scope and optimisation campaigns led to the conclusion that the electronic properties of the boronic acid would likely dictate the success of the reaction. A strategy similar to the previous investigation was developed, wherein *para*-substituted boronic acids were assigned as the main focus of the investigation to assess the impact of electronics on reaction yield. To enable a direct comparison, all boronic acids involved within this scope were also investigated as part of the earlier study employing 2,5-tetrazoles (*Section 3.3.1.3).*

The results of this study are shown in *Table 3.20*. As expected, the yield of the reaction once again strongly depended on the electronic properties of the boronic acid. The highest yields of this scope, **3.24** and **3.25** at 75 %, once again originated from the electronic-rich 4-methoxyphenylboronic acid and 4-Boc-aminophenylboronic acid ($\sigma_p$ values of -0.27 and -0.17, respectively[279]). These values were also reasonably consistent with the yields obtained as part of the previous scope in *Table 3.8*. One abnormal result was the failure of 4-dimethylaminophenylboronic acid, with the product obtained in 76 % yield using the previous conditions. This may be due to the relative insolubility of the species. More surprising disparities were encountered in some other electronically activated substrates. For example, 4-tolylboronic acid was markedly less efficient compared to the use of 2,5-diaryl tetrazoles (57 % to 28 %). This contrasted with the yields of **3.28** and **3.30**, both derived

from electronically neutral substrates. In these cases, there was a substantial improvement in isolated yield relative to the earlier conditions. These results seemed to indicate that the broader trend in boronic acid electronics identified within the previous scope was not quite as consistent here, with some variability in the conversions. This alternative protocol provided improved yields of electron-neutral boronic acids and diminished yields of electron-rich examples. This could be attributed to the higher temperatures of these conditions, which may impact the stability of the products. Regardless, this outcome was beneficial in satisfying the objective of developing a complimentary set of reaction conditions, where the yields of some substrates were improved relative to the substrate scope shown in *Table 3.8*.

*Table 3.20: The scope of para-substituted aryl boronic acids under the newly developed reaction conditions (the yields of the previous scope using tetrazoles as an NI source are also shown for comparison)*
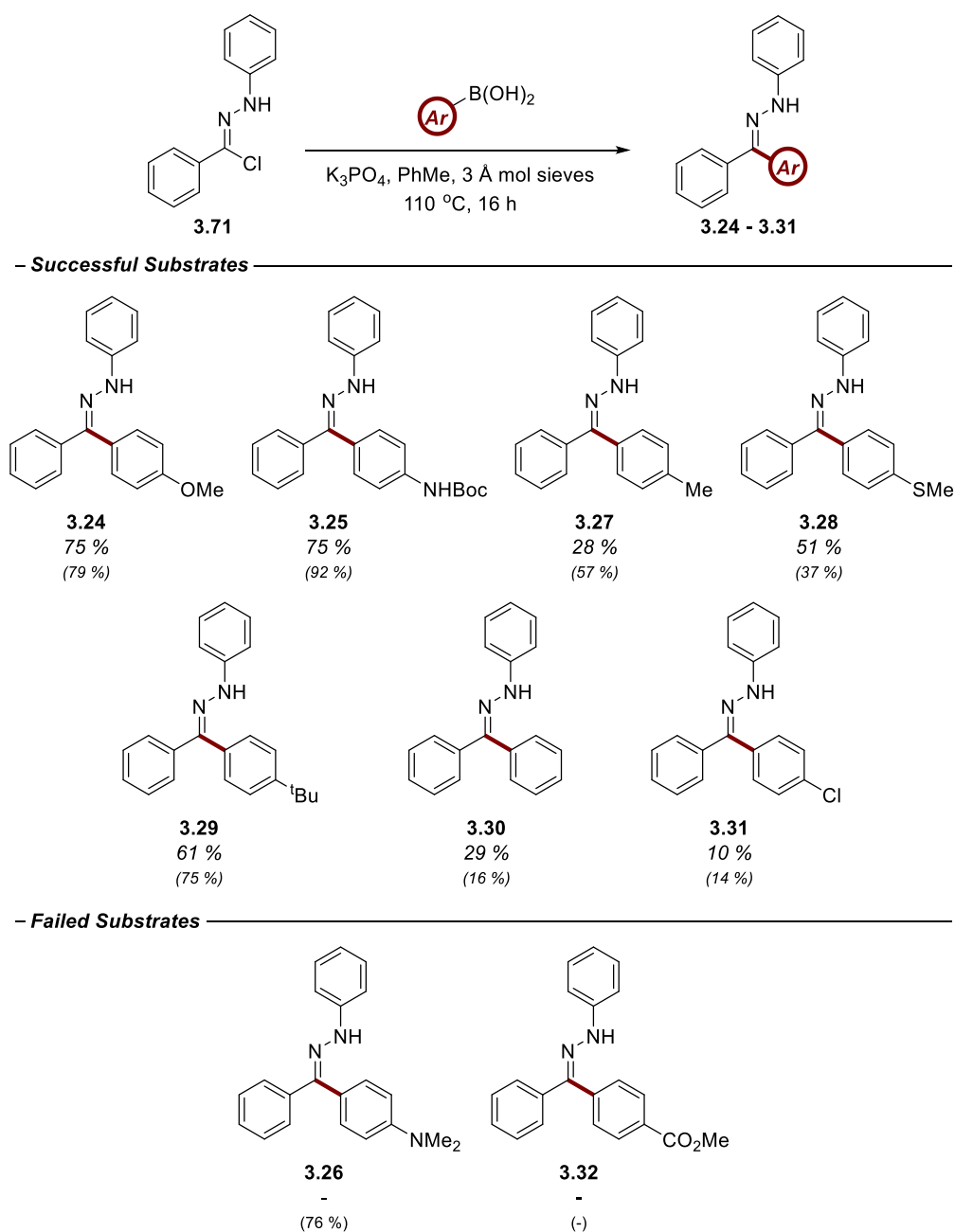
The compatibility of sterically encumbered and heterocyclic boronic acids is shown in *Table 3.21*. The introduction of sterically occluded substrates had a more significant impact on yield when employing hydrazonyl chlorides as the NI source, relative to previous conditions. While hydrazone **3.34** was formed in an almost identical yield, the use of 2,4-dimethoxyphenylboronic acid was incompatible with these conditions. This can be rationalised by considering the reversible nature of NI generation when employing hydrazonyl chlorides. In this instance the aryl ring migration of the boronic acid is competing with the nucleophilic attack of the chloride anion to reform the starting material. The consequence of this is that any factor which slows the rate of aryl ring migration, such as steric bulk, may favour the reformation of the starting material and the decomposition of the boronate complex.

*Table 3.21: The application of a variety of sterically occluded and heterocyclic boronic acids*
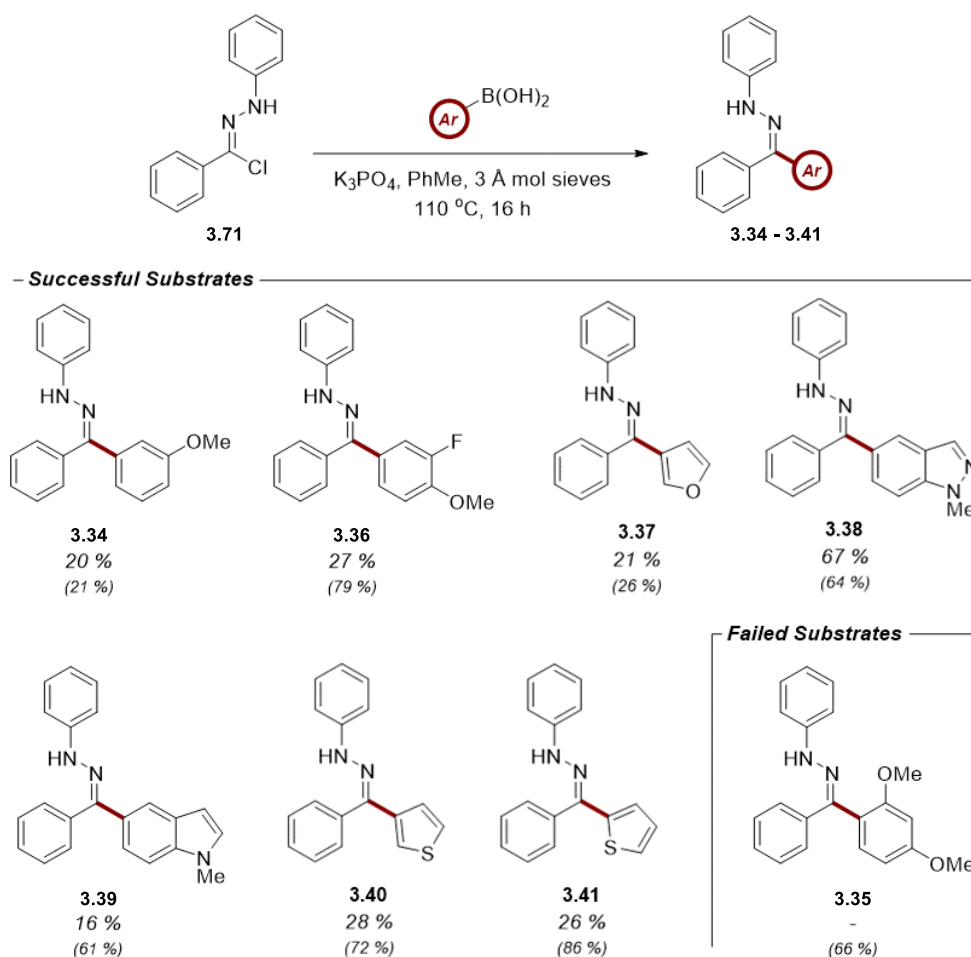


The application of electron-rich heterocycles was also investigated. Of the five examples obtained, only furan and indazole boronic acids retained a comparable yield to that obtained during application of 2,5-diaryl tetrazoles as NI sources. Both thiophene analogues and the methyl-indole species failed to replicate their previous levels of activity, albeit while still providing limited conversion to the desired products. In the case of these substrates,

protodeboronation will likely become a prevalent side reaction that will limit the success of hydrazone formation,[288] and is potentially exacerbated at higher temperatures.

Overall, the yields obtained in this substrate scope were broadly comparable to those obtained when employing tetrazoles as the NI source. Again, electron-rich boronic acids provided good to excellent yields, while less activated species afforded more moderate turnover. In general, the yields obtained when employing hydrazonyl chlorides were slightly lower than the tetrazole scope. This can be attributed to the higher reaction temperatures involved, which may induce partial decomposition of the product and could also influence the stability of the boronic acid starting material. One exception to this was the behaviour of electronically neutral substrates, which were isolated in improved yields. The impact of boronic acid sterics was also more pronounced when employing hydrazonyl chlorides, which is attributable to the reversible nature of NI formation.

While the investigation of boronic acid scope served as a method of comparing the efficiency of this methodology with the conditions developed in *Section 3.3.1*, an assessment of different hydrazonyl chlorides sought to exemplify the application of substrates that would not be tolerated when employing 2,5-tetrazoles. As a result, almost all NI precursors investigated as part of this scope represented compounds where the photolysis of the analogous tetrazole would be unsuccessful. These included aryl-nitro substituents, which would suffer from inefficient ISC following excitation, and *C-* and *N*-alkyl substituents, which would shift the $\lambda_{max}$ of the corresponding tetrazole to a higher energy due to the absence of $\pi$-system conjugation. Two *N*-tosyl examples were also investigated, owing to the diverse applications of *N*-tosyl hydrazones in organic synthesis through Bamford-Stevens and Shapiro-type chemistry.[359–361]

One disadvantage of this substrate library was the limited investigation on the impact of other aryl ring substituents, for example the 4-methoxyphenyl and 4-(trifluoromethyl)phenyl NIs from *Section 3.3.1.3* (*Table 3.10*). This was due to the substantial synthetic investment required in generating the starting materials, which individually require at least two transformations from commercially available ingredients. It was proposed that the small scope outlined above would provide an adequate overview of the generality of the process relative to the resources available for the execution of the study. Furthermore, the modification of these aryl substituents within the previous scope demonstrated little to no impact on the isolated yields. To corroborate that this was replicated within this additional scope, a hydrazonyl chloride incorporating a methoxy group within the *C*-aryl ring was included as a control.

The outcome of this investigation is shown in *Table 3.22*. In comparison with previous studies, the isolated yields were considerably lower, with many unanticipated results.

Nevertheless, a handful of substrates were shown to be compatible. Substitution of the *para* position of the *C*-aryl ring was tolerated, with hydrazones **3.11** and **3.78** isolated in good yields. This suggests that substitution of the aryl ring with other functional groups would also be tolerated. The application of phenylboronic acid highlighted an interesting difference between hydrazones **3.24** and **3.79**, with the electron-deficient example affording a yield almost five times greater than the former. This could occur through the promotion of aryl group migration onto the electrophilic *C*-terminus of the NI through the increased electron-withdrawing properties of the nitro group. However, the isolation of **3.80** in an identical yield with a much more activated nucleophile indicates that further investigation into the mechanism is required.

*Table 3.22: An investigation into the compatibility of various hydrazonyl chlorides under the reaction conditions*
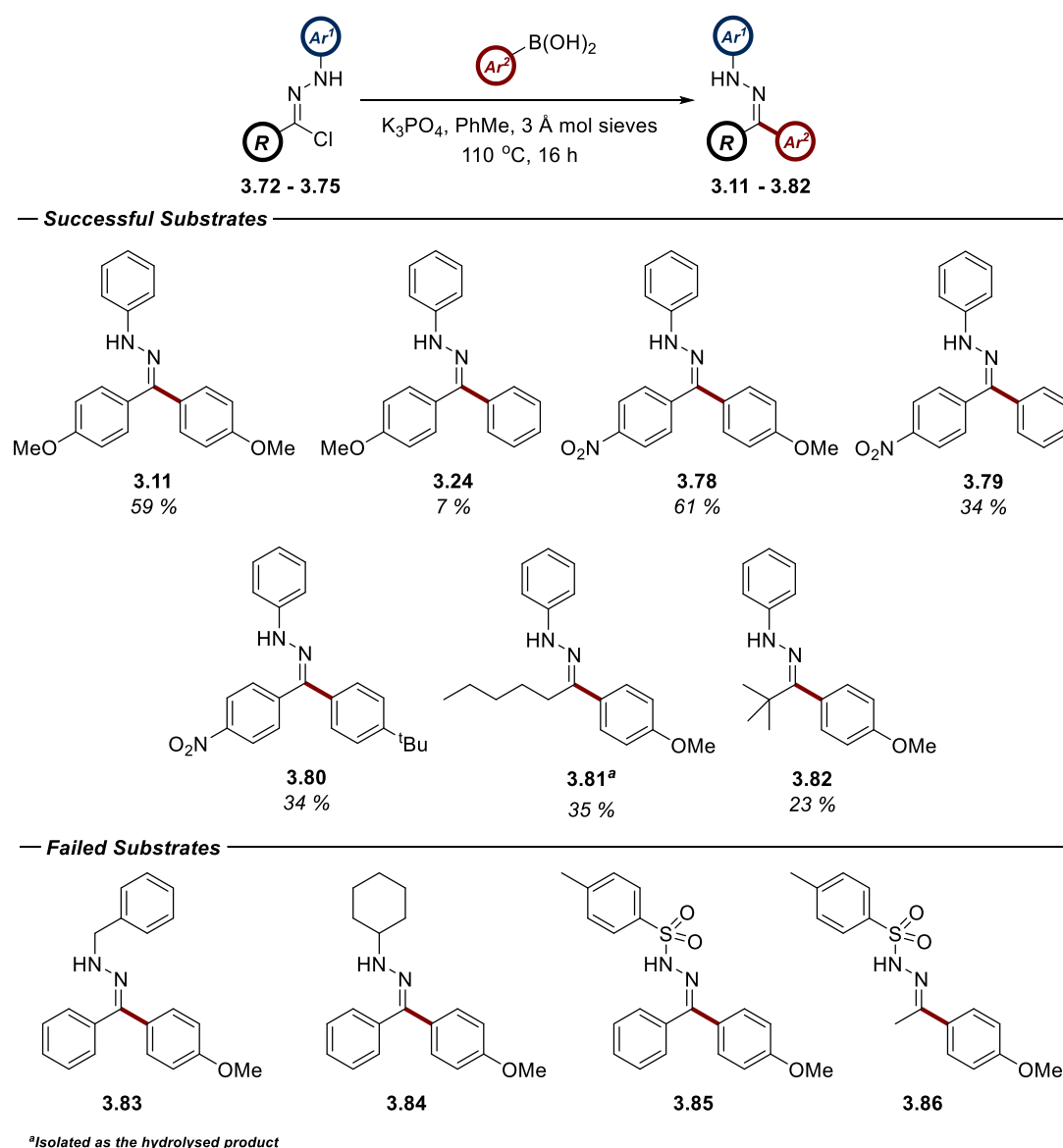


Alkyl substituents at the *C*-terminus of the NI dipole were also tolerated. Steric occlusion was relatively inconsequential (comparing the yields of **3.81** and **3.82**), however, the overall

yields were unfortunately very low. This incompatibility was exacerbated upon substitution of the *N*-terminus, with the removal of aromaticity unfeasible in all examples. The handling of these species and their precursors indicated that the removal of conjugation from around the NI motif significantly increased the reactivity of the dipole. In the cases of **3.83**, **3.84**, and **3.86**, the isolation of the analogous hydrazonyl chloride itself was unsuccessful (*Scheme 3.29*). The reduced stability of these compounds indicated that their compatibility with a reaction that required heating to over 100 °C was unlikely. When considering the properties of NIs (*Section 1.3.1.2*), it is unsurprising that the removal of resonance contributors would enhance their reactivity. This also verifies the more rapid decomposition of *N*-alkyl substrates, given the increased influence of the *N*-aryl ring over other aspects of NI chemistry.[121]
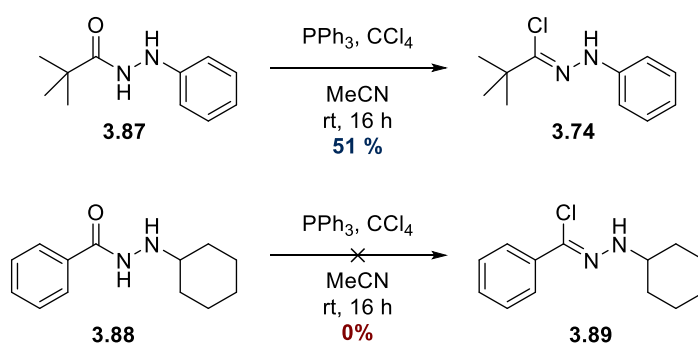


*Scheme 3.29: A comparison of the yields obtained in the synthesis of NI precursors when removing either the C- or N-aryl rings*

Despite the limited compatibility of alkyl NIs, this substrate scope still demonstrated the benefits of employing hydrazonyl chlorides as an NI source. While compounds such as **3.81** and **3.82** were isolated in low yields, this represents a robust improvement in the diversity of substrates in comparison to the photolysis of 2,5-tetrazoles. The facile incorporation of a nitro motif also broadens the scope of the reaction, and indicates that other functional groups incompatible with tetrazole photolysis, such as *N*-dimethylamine and anthracene,[94,362] can now be accommodated. Future work targeting the *in situ* generation of NIs directly from the corresponding hydrazones (*Section 1.2.2*) may yet facilitate the incorporation of *N*-alkyl substrates.

### 3.3.2.3 Application of Aryl Ketone Hydrazones in Synthesis

As a means of demonstrating the compatibility of the protocol, the synthesis of hydrazone **3.24** was increased to both 1 mmol and 5 mmol scales. This substrate was selected as one of the most high-yielding examples, meaning any substantial decrease in conversion would be immediately identifiable. The conditions selected corresponded to those identified in *Scheme 3.27*, employing DCM as the solvent and only 1.1 equivalents of the boronic acid. These conditions were selected to improve the atom economy of the procedure.

The results of increasing the scale are shown in *Scheme 3.30*. While a small decrease in yield was observed when transitioning to a 5 mmol scale, it was slightly increased when an intermediate scale of 1.2 mmol was applied. This increase was likely coincidental: the reaction time of nine hours was substantially longer than the three hours of the initial scope, and the mechanical loss associated with a 0.25 mmol scale would have a larger impact on yield, roughly proportional to the differences observed. The subsequent decrease from 89 % conversion to 72 % during the increase in scale from 1.2 mmol to 5 mmol demonstrated a small impact on the efficiency of the process. This may be a consequence of the heterogeneity of the reaction mixture, given the limited solubility of $K_3PO_4$ in DCM. The agitation of this suspension is likely to be less adequate at a larger scale, resulting in a slightly diminished yield. Despite this decrease, the result was extremely encouraging, as a 5 mmol scale required well in excess of 1 gram of starting material, with the isolation of more than 1 gram of product in a yield of more than 70 %, highlighting the applicability of the procedure. Furthermore, this represented a significant improvement over the maximum scale performed in *Section 3.3.1*, where 2,5-tetrazole photolysis was conducted on a 0.75 mmol scale at most.



$^a$reaction complete after 3 h
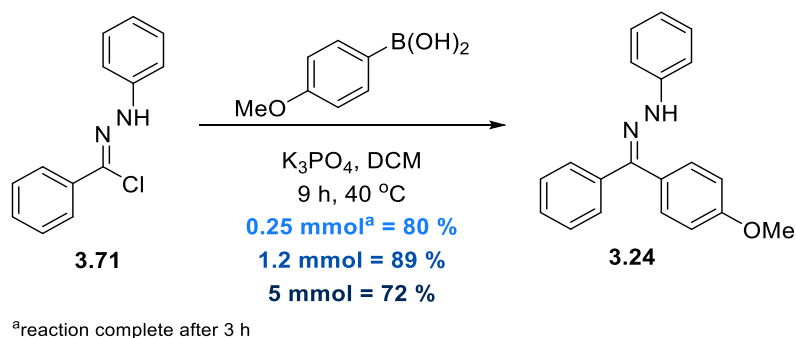
*Scheme 3.30: The differing yields in the synthesis of hydrazone **3.24** based on the scale of the reaction.*

In addition to their applications in molecular switches and other fields,[363] aryl hydrazones possess additional synthetic utility as valuable intermediates within organic chemistry. Given the acquisition of substantial quantities of hydrazone **3.24**, several further substrates were synthesised employing this hydrazone as a starting material to demonstrate this applicability.

In an initial investigation, the nucleophilicity of the compound was assessed through the methylation of the β-nitrogen of the hydrazone. This furnished the product **3.90** in good yields using relatively mild conditions. Furthermore, rapid access to this fully substituted hydrazone enabled its further modification *via* a [2+2] cycloaddition with a ketene, delivering the sterically congested β-lactam **3.91** in good yield (*Scheme 3.31*).[364] Heterocycles of this type are often viewed as important pharmacological targets.[365]
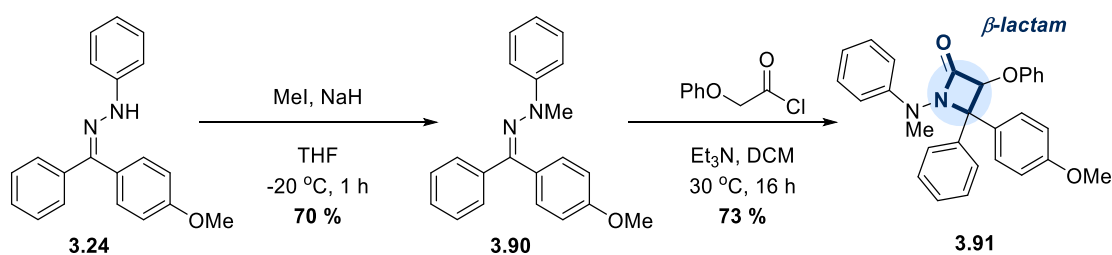
*Scheme 3.31: The methylation and subsequent cyclisation of biaryl ketone hydrazones*

As a follow-up into the generation of pharmaceutically relevant heterocycles, the synthesis of heavily substituted indazoles was exemplified through the oxidative ring-closure of the hydrazone and electron-deficient *C*-aryl ring (*Scheme 3.32*).[366] This procedure was highly effective as a transition metal-free approach towards these substrates, and proceeded with complete regioselectivity.
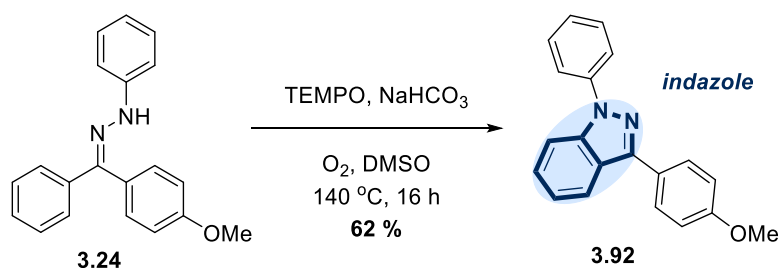


*Scheme 3.32: The metal-free synthesis of biaryl indazoles from hydrazones*

An additional heterocycle formation that may utilise these compounds is the Fischer indole synthesis.[367] While this involves a hydrazone with an enolisable proton, addition of an enolisable ketone to the reaction mixture enables hydrazine transfer from hydrazone **3.24**, forming the enolisable hydrazone *in situ*.[368] Demonstration of this process using butan-2-one furnished indole **3.93** in moderate yield (*Scheme 3.33*).
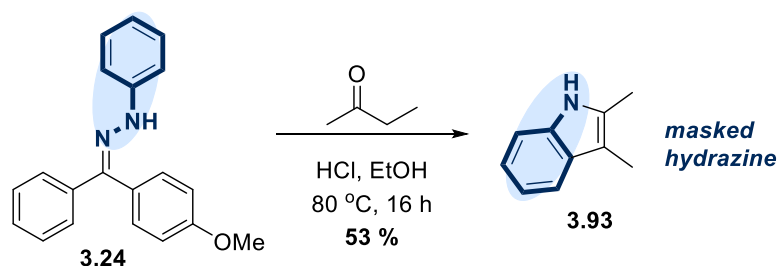


*Scheme 3.33: The synthesis of indoles using aryl ketone hydrazones*

Treatment of hydrazone **3.24** as a masked hydrazine can also facilitate the synthesis of aldehyde hydrazones. Due to their enhanced reactivity relative to biaryl ketones, the establishment of an equilibrium in the presence of an aldehyde will stimulate the migration of the hydrazine to the less-substituted carbonyl.[368] Exemplification of this protocol was performed using picolinaldehyde, which afforded the desired aldehyde hydrazone in good yield (*Scheme 3.34*).
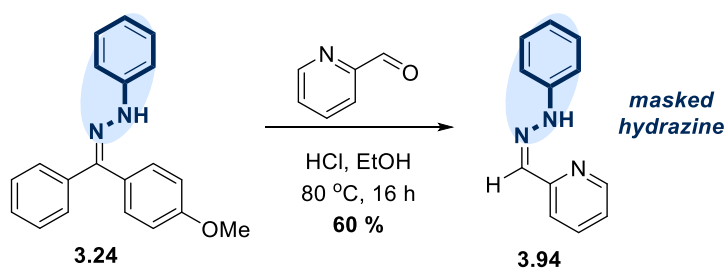
*Scheme 3.34: The application of biaryl ketone hydrazones as a hydrazine transfer agent*

While these hydrazones can be treated as hydrazine precursors, they can also be considered as masked biaryl ketones, as was demonstrated earlier in the chapter (*Section 3.3.1.2* and *Section 3.3.1.3*). To demonstrate the transformation of this particular substrate, hydrazone **3.24** was treated with $H_2O_2$ in the presence of catalytic $VO(acac)_2$ to furnish ketone **3.20** in excellent yield (*Scheme 3.35*).[369] These conditions were selected due to the efficiency of the process, however, **3.24** should be equally accommodating in the application of metal-free conditions such as those employed in *Table 3.10*.
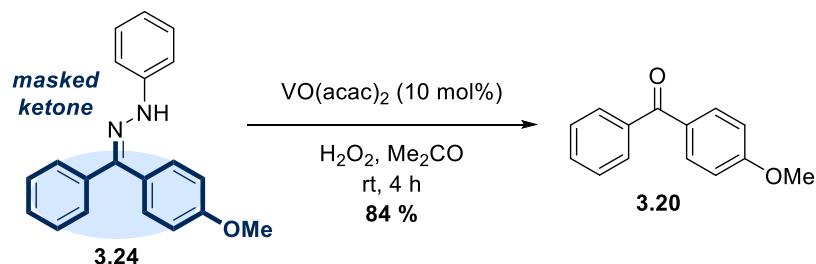


*Scheme 3.35: The deprotection of aryl ketone hydrazones to furnish aryl ketones*

One final synthetic application of ketone hydrazones that was considered was their role as a directing group in C-H activation chemistry. Hydrogen isotope exchange (HIE) was thought to offer the most appropriate exemplification of this reaction, owing to the numerous applications of deuterated and tritiated compounds within the pharmaceutical industry.[370,371] In accordance with literature precedent from Kerr and co-workers,[372] hydrazone **3.24** was stirred under a $D_2$ atmosphere in the presence of 5 mol% of an Ir(I) catalyst, resulting in moderate to good deuterium incorporation in the *ortho* positions of all three aryl rings surrounding the hydrazone (*Scheme 3.36*).
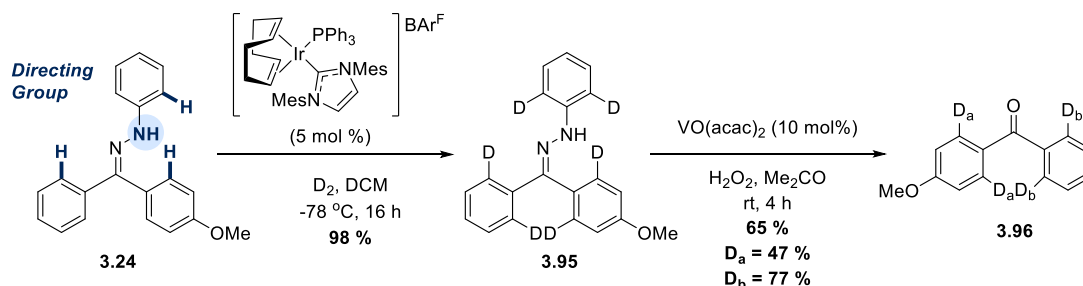


*Scheme 3.36: Hydrazones as a directing group in the Ir(III)-catalysed HIE of* ortho *protons*

Due to purification difficulties, it was deemed necessary to convert the initial product into the more stable biaryl ketone **3.96**, enabling accurate quantification of deuterium labelling by ^{1}H NMR spectroscopy. This species was obtained in good yield, with good levels of deuterium incorporation *meta* to the methoxy substituent. More complete deuteration of the phenyl ring was accomplished, at 77 %. This represents the first example of the site-selective labelling of a hydrazone motif *via* HIE, which, when combined with the other transformations outlined in this section, constitutes a powerful tool in the synthesis of several deuterated pharmaceutical precursors.

Overall, a total of seven additional reactions were conducted using the biaryl ketone hydrazone **3.24**, a product that is readily obtained in good to excellent yields through the application of the novel methodology outlined in this chapter. This further exemplifies the versatility of these hydrazones, and their applications in numerous, diverse chemical transformations.

### 3.3.2.4 Extension of the Methodology to the Nitrile Oxides

The development of hydrazonyl chlorides as an NI source also presents an additional opportunity. The corresponding oxime derivatives, the hydroxamoyl chlorides, represent a method of accessing the nitrile oxide (NO) 1,3-dipole, a close relative of the NI (*Scheme 3.37*).[373] Translation of the methodology into a second 1,3-dipole would represent a significant advance in the utility of the protocol.
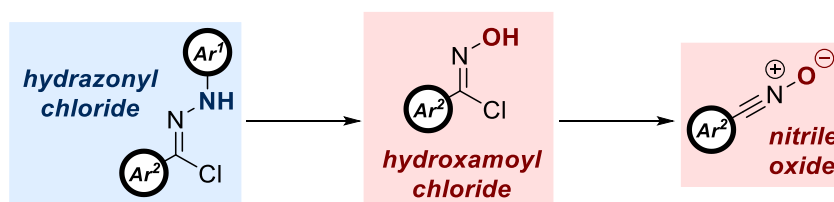


*Scheme 3.37: The similarity of the hydrazonyl chlorides and hydroxamoyl chlorides, which are in turn a source of the NO dipole*

NOs share several key properties with the closely related NIs. Aryl derivatives of both are highly reactive and exist as planar, propargylic structures that are typically generated *in situ*.[374,375] Electronically, aryl NOs possess an excess of electron density on the terminal oxygen atom, the anionic terminus, with an electrophilic nitrilium structure representing the neutral terminus.[375]

The stability of NOs is slightly greater than NIs, with more examples that are isolable at room temperature.[376,377] While relatively straightforward to prepare, these analogues require the incorporation of bulky substituents to shield the *C*-terminus from nucleophilic attack, and have limited synthetic applications (*Figure 3.4*). In contrast to the NO, only one example of

an NI stable at room temperature with no heteroatomic substituents has ever been disclosed, and required much more severe steric shielding of both termini.[378]
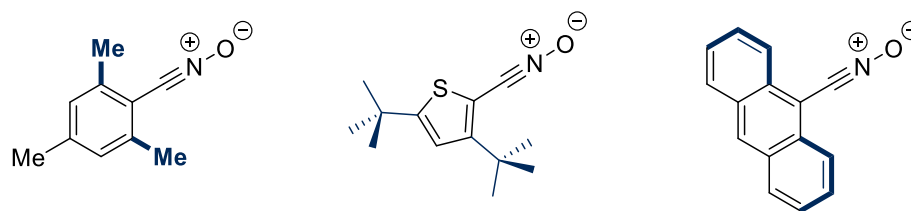


*Figure 3.4: Examples of bulky NOs that are stable at room temperature*

The most common source of NO employed within the literature is the hydroxamoyl chloride (*Scheme 3.37*). This precursor, or its brominated equivalent, is accessed from the corresponding aldoxime through the application of *N*-chloro or *N*-bromo succinimide (NCS or NBS).[379–381] In many examples this intermediate is not isolated, with sequential halogenation and dehydrohalogenation of the aldoxime liberating the NO in one pot (*Scheme 3.38*).[382–384] In parallel with NI generation, direct oxidation of the aldoxime is also possible using oxidising agents such as mercury(II) acetate,[385] iodobenzene dichloride,[386] and sodium hypobromite.[376]

An alternative approach towards the synthesis of NOs that is not shared by NIs is the dehydration of nitroalkanes by isocyanates.[387] This is most commonly employed in the generation of aliphatic NOs,[388] however, remains a convenient alternative in the synthesis of aryl analogues. Recent improvements to the reaction conditions have also enabled its application in flow and combinatorial chemistry.[389–391]
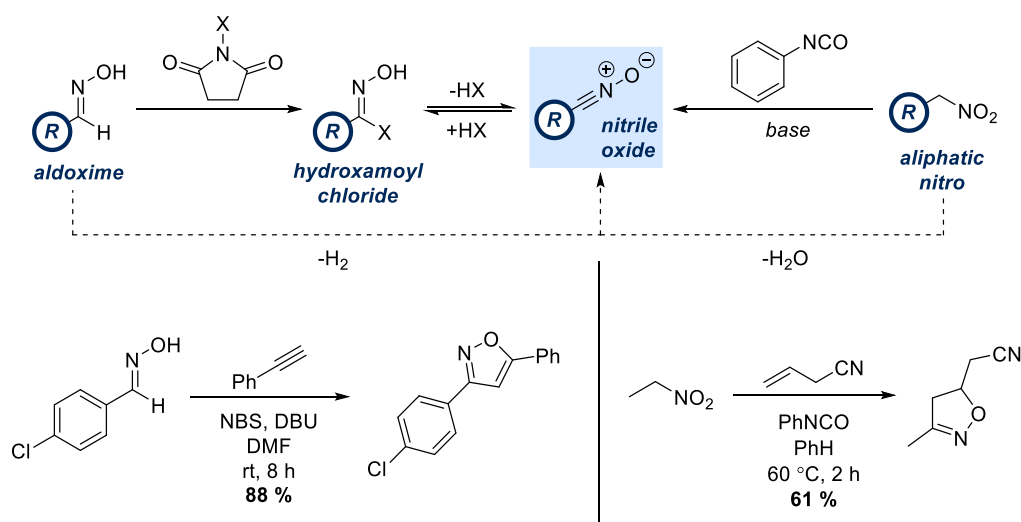


*Scheme 3.38: An overview of the most common sources of the NO dipole in the literature, with examples*

As with most 1,3-dipoles, the reactivity of NOs is dominated by 1,3-dipolar cycloaddition. Similarly to NIs, the vast majority of mono-substituted dipolarophiles afford 5-substituted isoxazolines or isoxazoles (*Scheme 3.39*).[373,390,392–394] Sterics are once again the primary

driver of regioselectivity, although 4-substituted products can be formed if employing electron-deficient substrates.[392] Interestingly, the degree of selectivity is slightly reduced when alkynes are employed as dipolarophiles in comparison to the analogous olefin.[392,395,396]
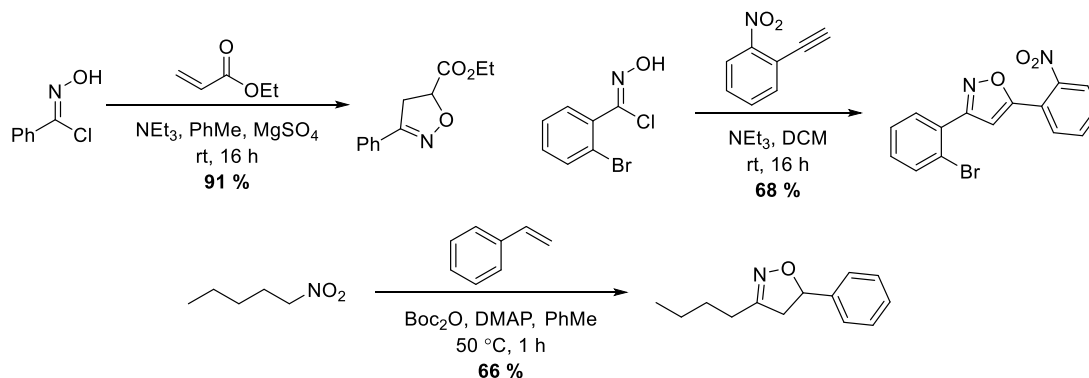


*Scheme 3.39: Examples of 1,3-dipolar cycloaddition involving NOs*

The energy difference between the two frontier molecular orbitals of NOs is slightly larger in comparison to NIs. While loosely defined as type II dipoles, the interaction of the NO LUMO and the dipolarophile HOMO is substantially more pronounced in the majority of cases, indicative of type III dipole reactivity.[105,106,118] These differences in orbital energies increase the reactivity of the NO towards electron-rich dipolarophiles relative to the NI, while lowering its reactivity with electron-deficient species. Cycloaddition rate can also be enhanced through the introduction of ring strain, particularly in the case of alkynes.[397]

The nucleophilic attack of NOs by several species has also been disclosed, with the 1,3-addition of heteroatomic nucleophiles similar to the reactivity observed with NIs. Both amines and thiols are competent substrates (*Scheme 3.40*), while oxygen-based nucleophiles are known but under-explored.[398–400] Reaction with acetates will undergo a further 1,4-rearrangement, analogous to the example involving NIs shown in *Section 1.3.2.4*, while hydration of the dipole furnishes the corresponding hydroxamic acid.[400,401]
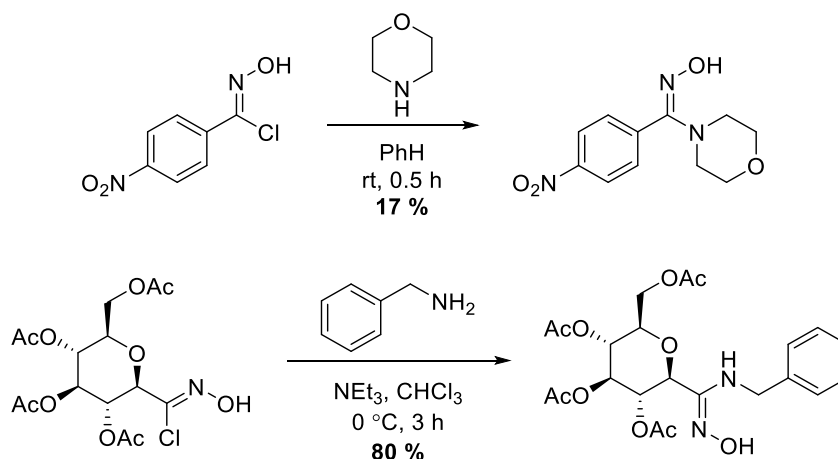


*Scheme 3.40: The application of some amines in the nucleophilic attack of NOs*

Where the reactivity of NOs with nucleophiles differs to NIs is in the formation of C-C bonds. While such transformations within NI chemistry are extremely scarce, underlining the importance of the methodology developed within this thesis, NOs can react with numerous carbon nucleophiles. Organometallics such Grignard reagents and organolithiums may undergo direct attack of the *C*-terminus,[402] while electron-rich heterocycles such as pyrrole have been shown to undergo electrophilic aromatic substitution (S$_E$Ar) reactions with the dipole (*Scheme 3.41*).[403] The reactivity of the NO with these substrates is further enhanced through the addition of a Lewis acid. Coordination to the *O*-terminus of the dipole forms an intermediate nitrilium species, which is more labile to nucleophilic attack. The introduction of acids such as aluminium trichloride and boron trifluoride enables nucleophilic addition of organozincates, and S$_E$Ar reaction with electron-rich benzene rings.[404,405] This form of reactivity is highly encouraging when considering the potential incorporation of the NO dipole into the methodology outlined in this section.
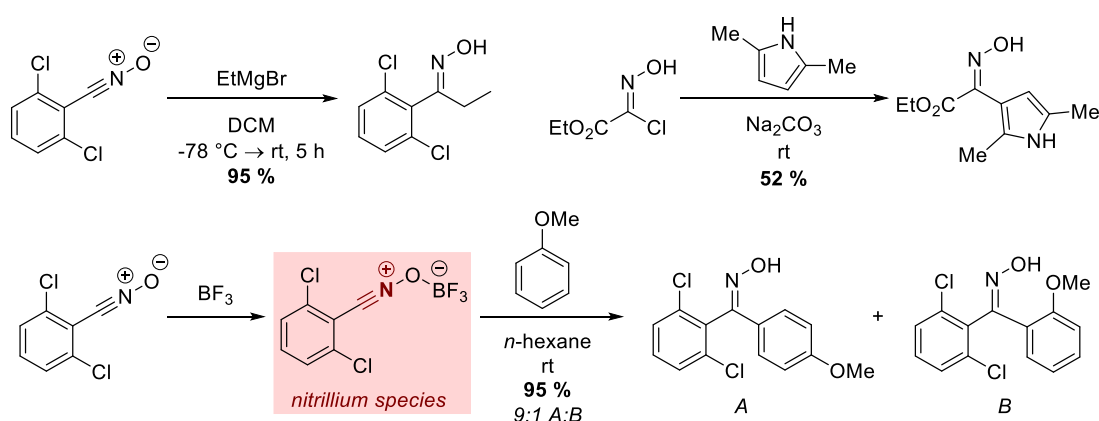


*Scheme 3.41: Examples of C-C bond formation using NOs and carbon-based nucleophiles*

As with NIs, in the absence of an appropriate reaction partner NOs may dimerise or isomerise, forming furoxans and isocyanates, respectively.[406] Dimerisation is highly favourable, and contributes to the fate of most NOs at room temperature. Unlike the NI, there is little ambiguity about the nature of this dimerisation, with a concerted cycloaddition between two equivalents of NO affording the furoxan.[407] Isomerisation to furnish the corresponding isocyanate is less common, but becomes more favourable at higher temperatures.[376]

While subtle differences in reactivity are apparent, the broader similarities between the NI and NO dipoles should facilitate the application of the newly developed methodology within this system. With this objective in mind, it was first necessary to synthesise the required starting materials and optimise the transformation. Hydroxamoyl chlorides **3.98** and **3.100** were easily obtained through chlorination of the corresponding oximes (*Scheme 3.43*). The

disparity in isolated yield between **3.98** and **3.100** can be attributed to the purification of **3.98** by column chromatography, as hydroxamoyl chlorides are unstable in the presence of silica.
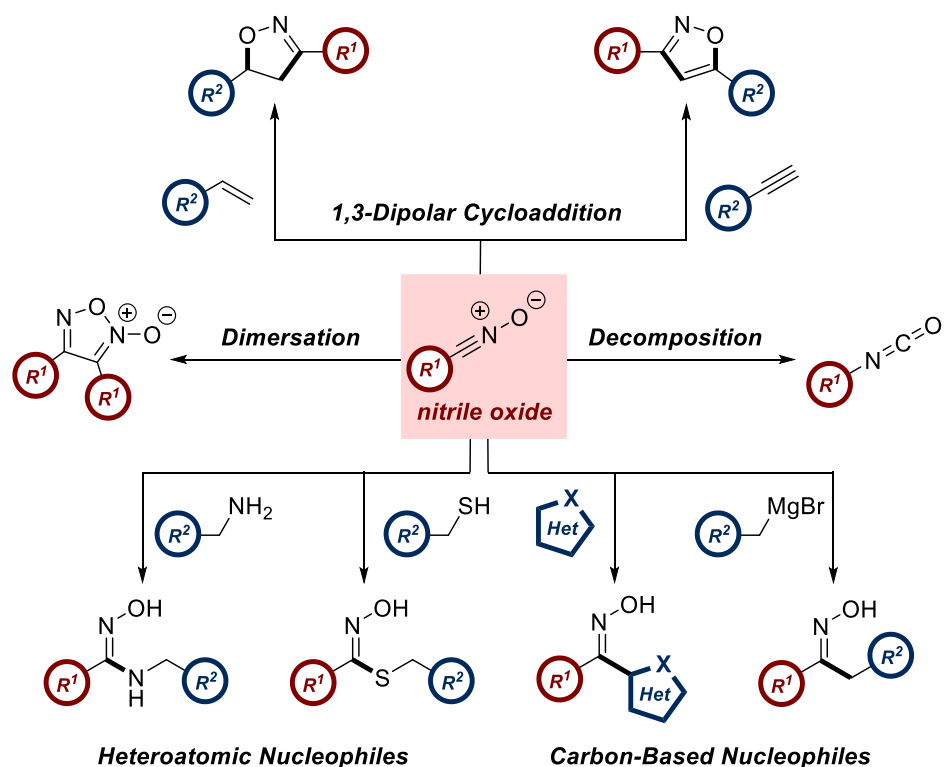


*Scheme 3.42: An overview of the reactivity of the NO 1,3-dipole*

With both analogues in hand, fluorinated substrate **3.98** was exposed to different bases in the presence of 4-methoxyphenylboronic acid or 4-(dimethylamino)phenylboronic acid (*Table 3.23*). Given the difference in $pK_a$ between hydrazonyl chlorides and hydroxamoyl chlorides, it was anticipated that this reaction may require a slightly weaker base than potassium phosphate. As expected, the replication of the conditions employed above (*Table 3.23*, entry 3) were unsuccessful with both boronic acids. More surprisingly, very little conversion to the desired product was observed over the entire screen when 4-methoxyphenylboronic acid was employed. Weaker bases such as $KH_2PO_4$ and $NaHCO_3$ were incompatible, with only caesium carbonate affording any conversion. These results were perplexing, given the isolation of other by-products. The introduction of pyridine furnished the corresponding 1,2,4,5-dioxadiazine **3.103**, a unique mode of NO dimerisation catalysed by weak heterocyclic bases (*Scheme 3.44*).[408] The application of DBU liberated the NO, however the only isolated product was the cycloaddition adduct of the dipole and the base (*Scheme 3.44*).
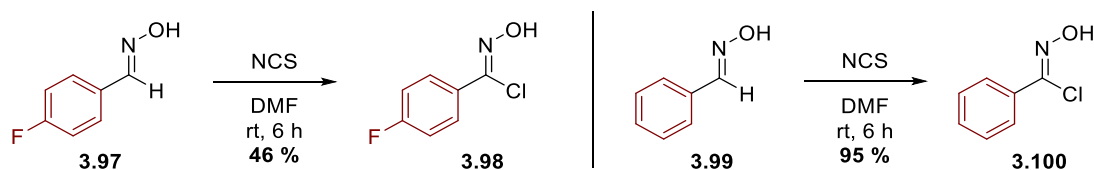


*Scheme 3.43: The synthesis of hydroxamoyl chloride starting materials*

Greater success was achieved when employing 4-(dimethylamino)phenylboronic acid, with four different bases affording ketoxime **3.102** in a tractable yield. Initial impressions indicated that the dependency of the reaction on the electronic properties of the boronic acid was exacerbated when applying NOs instead of NIs. The dimethylamino moiety possesses a much larger Hammet $\sigma_p$ value in comparison to the methoxy motif (-0.83 *vs*. -0.27),[279] and this substantial electron-donating capability was thought to be necessary to facilitate the reaction. However, the results of control experiments performed in the absence of base (*Table 3.23*, entry 9) resulted in an alternative proposal. The aryl dimethylamino moiety is weakly basic, with a $pK_b$ of around 5.1,[409] therefore it is possible that an excess of this boronic acid may perform a dual role as both a nucleophile and a base. The results of the control experiments were in agreement with this hypothesis, with 4-methoxyphenylboronic acid unable to furnish the ketoxime, and 4-(dimethylamino)phenylboronic acid affording a 46 % yield.

*Table 3.23: An investigation of different substrates and bases in the attempted synthesis of ketoximes from hydroxamoyl chlorides and aryl boronic acids*
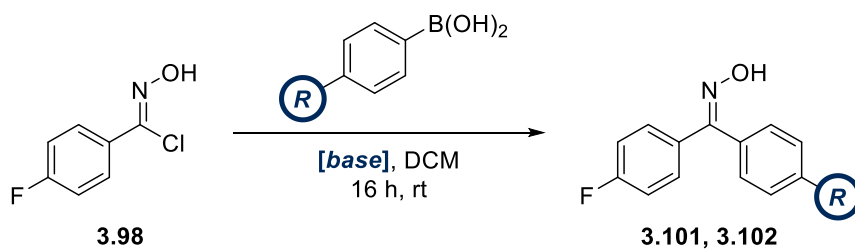


| Entry | Base | Conversion (%)[a] | |
|:-:|:-:|:-:|:-:|
| | | OMe (**3.101**) | NMe$_2$ (**3.102**) |
| 1 | KH$_2$PO$_4$ | <1 | 31 |
| 2 | K$_2$HPO$_4$ | <1 | 16 |
| 3 | K$_3$PO$_4$ | <1 | <1 |
| 4 | NaHCO$_3$ | <1 | 31 |
| 5 | Cs$_2$CO$_3$ | 17 | 11 |
| 6 | NEt$_3$ | <1 | <1 |
| 7 | Pyridine | <1[c] | <1[b] |
| 8 | DBU | <1[c] | <1[b] |
| 9 | - | <1 | 46 |

[a]Conversion determined by ^{19}F NMR with reference to an internal standard. [b]Significant by-product formation observed.

To further investigate this proposal, both caesium carbonate and *N,N'*-dimethylaniline (DMA) itself were advanced for further study (*Table 3.24*). Gratifyingly, DMA was found to function very well as a base, outperforming caesium carbonate. Five equivalents of DMA

and 3 equivalents of 4-methoxyphenylboronic acid afforded ketoxime **3.101** with a conversion of almost 60 %.
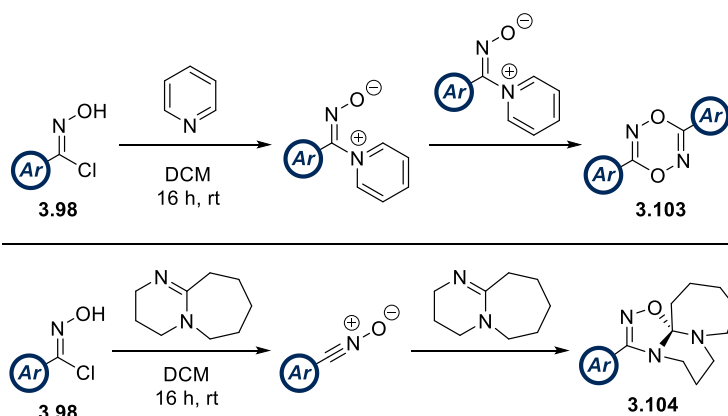


*Scheme 3.44: The unanticipated side reactions of pyridine and DBU with **3.98***

*Table 3.24: An investigation on the impact of reagent stoichiometry*
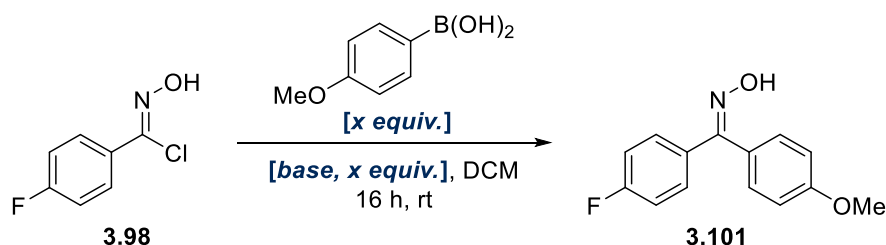


| Entry | Base | Base Stoichiometry (equiv.) | Boronic Acid Stoichiometry (equiv.) | Conversion (%)[a] |
|-------|------|-----------------------------|--------------------------------------|-------------------|
| 1 | $Cs_2CO_3$ | 5 | 3 | **30** |
| 2 | $Cs_2CO_3$ | 3 | 3 | **27** |
| 3 | $Cs_2CO_3$ | 3 | 1.5 | **17** |
| 4 | $Cs_2CO_3$ | 1.5 | 1.5 | **12** |
| 5 | DMA | 5 | 3 | **58** |
| 6 | DMA | 3 | 3 | **54** |
| 7 | DMA | 3 | 1.5 | **43** |
| 8 | DMA | 1.5 | 1.5 | **37** |

[a]Conversion determined by $^{19}F$ NMR with reference to an internal standard.

Given the success of increasing reaction temperature when employing hydrazonyl chlorides (*Graph 3.5*), a similar strategy was envisaged to further improve the conversions of this study. Due to the volatility of DCM, additional solvents were examined to identify alternatives with a higher boiling point (*Table 3.25*). The stoichiometries of boronic acid and base were also reduced to improve the overall atom economy of the process.

Acetonitrile and chloroform were found to be suitable alternatives, both affording conversions of 37 %. While this represented a slight decrease relative to DCM (43 %), both additional solvents exhibited significantly higher boiling points. Repeating these reaction conditions at near-reflux temperatures for all three solvents identified chloroform as a suitable reaction medium, with more than a 25 % increase in conversion upon heating at 60 °C.

*Table 3.25: Selection of the optimal solvent in the generation of oximes from hydroxamoyl chlorides*



| Entry | Solvent | Conversion (%)[a] |
|:---:|:---:|:---:|
| 1 | DCM | 43 |
| 2 | Toluene | <1 |
| 3 | 1,4-Dioxane | <1 |
| 4 | THF | <1 |
| 5 | MeCN | 37 |
| 6 | Acetone | 12 |
| 7 | CHCl$_3$ | 37 |
| 8 | 2-MeTHF | <1 |
| 9 | EtOAc | 3 |
| 10 | MeOH | 7 |
| 11 | DCM[c] | 52 |
| 12 | CHCl$_3$[d] | 63 |
| 13 | MeCN[e] | 57 |

[b]Conversion determined by ^{19}F NMR with reference to an internal standard. [c]Heated at 40 °C. [d]Heated at 60 °C. [e]Heated at 80 °C.

Having identified an appropriate solvent system, the stoichiometry of base and boronic acid were reassessed to identify the minimum quantities required for adequate conversion (*Table 3.26*). The application of two equivalents of boronic acid furnished satisfactory yields while remaining relatively economical, and also mirrored the stoichiometry employed in the optimised NI conditions above (*Scheme 3.28*). This enabled a direct comparison between the isolated yields under the two reaction conditions.

DMA stoichiometry had minimal impact on conversion, but isolation of ketoxime **3.101** from two reaction mixtures indicated that more equivalents of DMA generated a small increase in isolated yield. This is likely a consequence of increased DMA stoichiometry facilitating more straightforward purification of the product. Residual quantities of hydroxamoyl chloride **3.98** exhibited a similar polarity to **3.101**, leading to complications during column chromatography. Additional DMA aided in the consumption of this starting material, simplifying the isolation of the product. Given the inexpensive nature of this simple organic base, it was determined that the decreased atom economy incurred by employing five equivalents was inconsequential, given that this facilitated a 62 % isolated yield of the desired ketoxime. The transformation was also complete after only three hours, consistent with the findings from the NI optimisation, where increasing reaction temperature to 80 °C afforded the product in just one hour when employing 4-methoxyphenylboronic acid (*Table 3.18*). These rapid reaction times indicated that C-C bond formation between this boronic acid and the NI and NO dipoles was a highly efficient process.

*Table 3.26: A second investigation of reagent stoichiometry identified the optimised conditions for ketoxime synthesis*
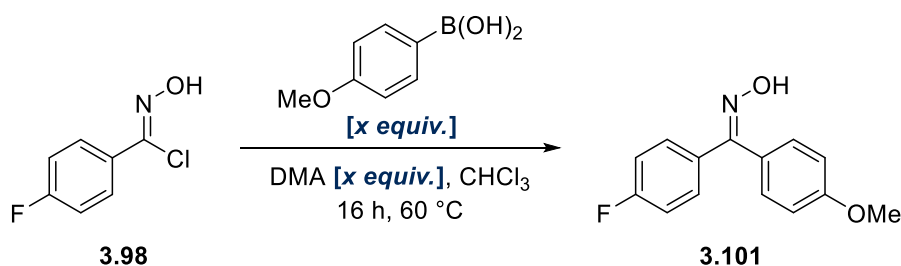


| Entry | Base Stoichiometry (equiv.) | Boronic Acid Stoichiometry (equiv.) | Conversion (%)[a] |
|-------|------------------------------|--------------------------------------|---------------------|
| 1 | 3 | 1.5 | **64** |
| 2 | 3 | 2 | **69 (54[b,c])** |
| 3 | 3 | 2.5 | **71** |
| 4 | 3 | 3 | **77** |
| 5 | 5 | 1.5 | **65** |
| 6 | 5 | 2 | **70 (62[b,c])** |
| 7 | 5 | 2.5 | **78** |

[a]Conversion determined by ^{19}F NMR with reference to an internal standard. [b]Isolated yield. [c]3 hours reaction time.

The conditions obtained through this optimisation campaign are outlined in *Scheme 3.45*. Overall, the behaviour of the NO dipole deviates considerably from the NI in some areas, yet the resulting conditions are nonetheless relatively similar to those obtained above (*Scheme 3.28*). The most significant difference is in the selection of base. DMA is considerably less

basic than potassium phosphate and forms a homogeneous reaction mixture, a substantial divergence from the previous study. Hydroxamoyl chloride **3.98** also appeared to be much more capricious in the properties of the base required to generate the NO. Whereas investigations into NI liberation furnished a linear trend of improved conversions with increasing $pK_b$ (*Graph 3.2*), no such correlation was observed here, with only two bases with drastically different properties shown to generate the desired ketoxime at all. This could be attributed to the increased reactivity of the NO, providing more alternative routes of dipole decomposition. Other variables, however, remained broadly consistent. Chloroform was found to be an acceptable solvent within the NI reaction manifold (when not used in conjunction with $K_3PO_4$, *Table 3.16*) and also found application in this procedure. Temperature was also shown to again have an important impact on conversion.
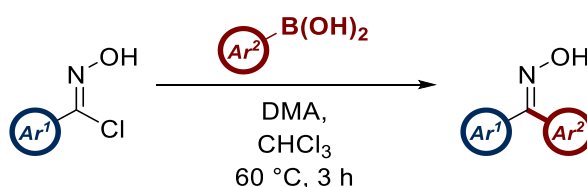


*Scheme 3.45: The optimised reaction conditions developed for the formation of ketoximes from NOs and boronic acids*

Following identification of these optimised conditions, a focused substrate scope was examined to assess the versatility of the protocol. All of the boronic acids employed were selected based on their previous reactivity with hydrazonyl chloride **3.71**, the direct analogue of NO precursor **3.100**. Despite the change in dipole, the boronic acids shared a strikingly similar reactivity profile with the earlier study (*Table 3.27*). Once again, electron-rich substrates **3.105** and **3.106** performed extremely well, with isolated yields of around 70 %. Removal of electron-donating groups induced a sharp decrease in yield, consistent with what was observed previously (**3.107** and **3.108**). One substantial difference was the compatibility of 4-(dimethylamino)phenylboronic acid, which was unsuccessful in the synthesis of the corresponding hydrazone (*Table 3.20*). The difference in reaction temperatures may account for this deviation, given that the NO transformation occurs 50 °C lower than the conditions employed above. The reactivity of heterocyclic boronic acids also translates well to the NO dipole. All three analogues investigated furnished yields within error of the values obtained in the previous scope, including an impressive yield of 65 % for ketoxime **3.110**. Unfortunately, *ortho*-substituted analogue **3.113** and electron-deficient species **3.114** both failed to afford the desired product, however this was not entirely unexpected given earlier results within *Sections 3.3.1.3* and *3.3.2.2*.

Overall, the consistency by which the results of NI reactivity are replicated within this NO study is remarkable. Of the eight substrates isolated, seven were obtained in yields within 10

% of those achieved through reaction with the NI dipole. These results are highly encouraging as part of the wider aim of developing a general protocol for application throughout several 1,3-dipoles.

*Table 3.27: An investigation of boronic acid scope in NO-mediated ketoxime formation (the isolated yields from the corresponding NI experiment are shown in brackets)*
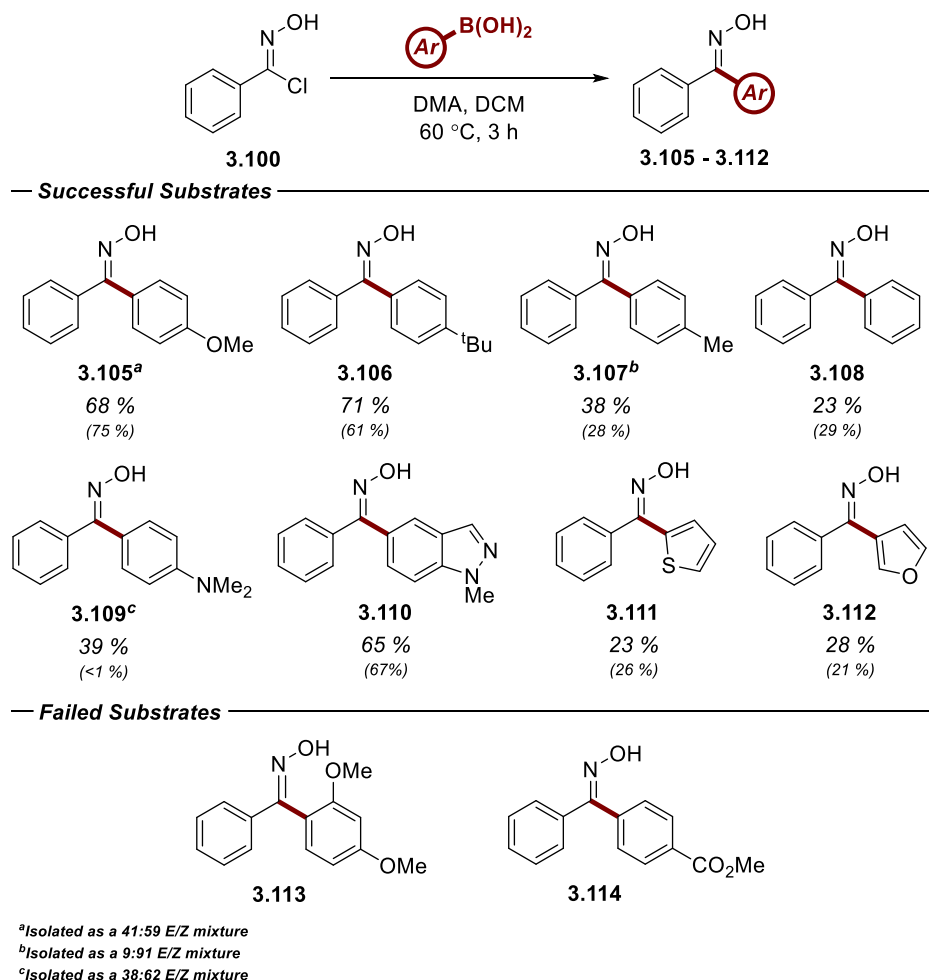


One additional interesting aspect of the coupling of NOs and boronic acids was its remarkable stereoselectivity, with the majority of compounds isolated solely as the *Z* isomer of the oxime. This selectivity was rarely observed during the earlier synthesis of ketone hydrazones, however this can likely be attributed to the reaction conditions. Heating at 110 °C likely promotes thermal isomerisation, and the photochemical isomerisation of hydrazones is well documented.[410] Nevertheless, the stereospecific nature of this ketoxime synthesis provides a further insight into the reaction mechanism. Isolation of the *Z*-isomer only, the thermodynamically disfavoured product, indicates that the oxygen moiety must be involved in the formation of the C-C bond on the *C*-terminus of the NO. This does not alter the proposed reaction mechanism whereby the boronic acid is first activated by the *O*-terminus of the dipole, but the *Z*-configuration of the product indicates that this process is indeed intramolecular, corroborating the results shown in *Scheme 3.14*. The reaction appears

to proceed *via* a pseudo-*syn*-addition of the boronic acid across the termini of the dipole. The generation of an X-ray crystal structure of the major component of ketoxime **3.105** confirmed that the Z-isomer was indeed the dominant product (*Scheme 3.46*).
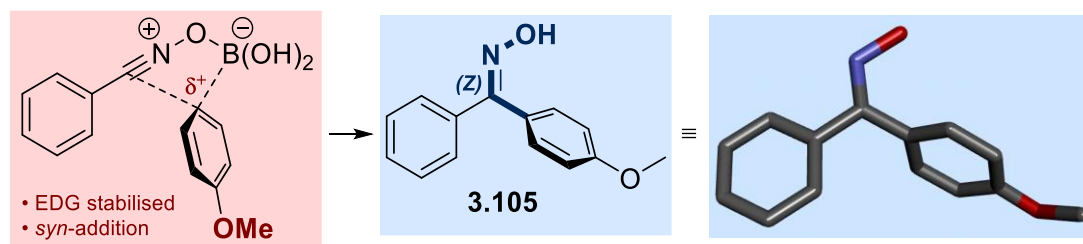


*Scheme 3.46: An X-Ray crystal structure of **3.105** provided conclusive evidence that the Z-isomer was the majority product*

## 3.4    Conclusions and Outlook

The extensive reactivity of the NI 1,3-dipole manifests itself as a broad spectrum of transformations with a range of different substrates. Given the limited exploration of its electrophilic properties, and only limited reports available on nucleophilic addition by acids, thiols and amines (*Section 1.3.2*), this chapter sought to investigate the reactivity of the NI with an alternative nucleophile, specifically aryl boronic acids. Mechanistic interrogation of the PBM reaction identified a proposed route towards aryl ketone hydrazones through nucleophilic attack by an intramolecularly-activated boronate complex.

The introduction of 2,5-diaryl tetrazoles as an NI source proved challenging, but eventually afforded isolated yields of 79 % from a model reaction system. Further mechanistic insight was gained through the isolation of primary hydrazide **3.22** as a side product, enabling improvement of the conditions by removing water from the reaction mixture. The protocol was compatible with 26 different combinations of aryl boronic acids and NIs, furnishing yields of up to 92 %. Electron-rich aryl and heterocyclic boronic acids performed well, with electron-poor and neutral analogues failing to exceed 40 % conversion in most cases. The methodology was also applied in the metal-free synthesis of an API and is compatible to scale-up through its straightforward incorporation within a flow chemistry manifold.

Initial studies into the relative reactivity of the boronic acid with the NI relative to other substrates suggested that it may be outcompeted by endogenous nucleophiles. While the application of the methodology in bioorthogonal chemistry was attempted through the synthesis of L-E modified with an NI, complications arising from the presence of carboxylic acids meant that the boronic acid motif was unable to function as a ligation handle.

Following the successful development of the protocol involving 2,5-tetrazoles (*Scheme 3.47*), the application of hydrazonyl chlorides was pursued to afford an alternative approach that avoided the use of UV light and expanded the substrate scope. Reaction optimisation

rapidly identified conditions that furnished yields in excess of 85 % using only 1.1 equivalents of boronic acid, however these were not general, and only compatible with electron-rich substrates. A DoE approach facilitated identification of a second set of more compatible conditions. Utilising this protocol, a diverse library of hydrazones were prepared in yields of up to 75 % (*Scheme 3.48*).
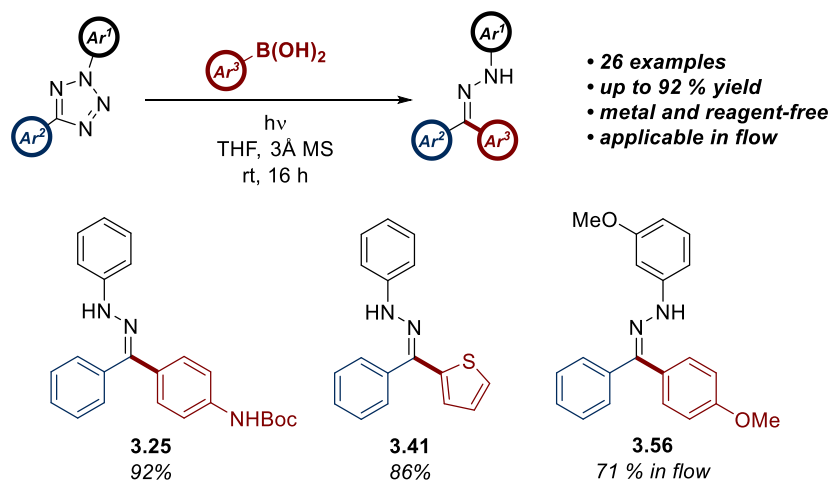


*Scheme 3.47: An overview of the principal discoveries of the first half of this chapter*

The newly developed conditions were also tolerant to a larger scale, with excellent yields at scales of more than 5 mmol. Substrate compatibility followed a similar trend to earlier compounds examined, with the additional incorporation of alkyl and aryl-nitro NIs owing to the absence of UV light. The protocol was also adapted for application within a second 1,3-dipole, with the metal-free coupling of NOs and boronic acids accomplished in good yields (*Scheme 3.48*). Future efforts in this area will involve development of a more general set of conditions, enabling the introduction of this methodology to several other 1,3-dipoles.
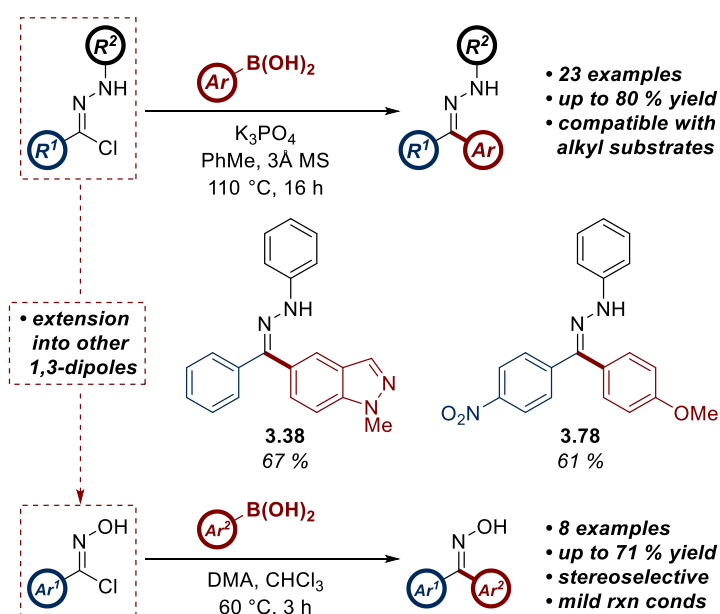


*Scheme 3.48: A summary of the newly developed methodology from the second half of this chapter*

# 4 The Quantification of Nitrile Imine Reactivity Profiles

While the research described thus far had contributed to understanding the generation, handling and reactivity of NI dipoles, little information regarding their relative reactivity with any of their cognate functional groups had been elucidated. Indeed, this is a broader concern within the wider scientific literature, with few reports documenting the relative reactivity of different nucleophiles and dipolarophiles with this 1,3-dipole. This final chapter is directed towards the quantitative profiling of the behaviour of the NI with several different substrates, with the objective of establishing a rank order of reactivity to facilitate more informed application of the dipole in chemical biology.

## 4.1 Introduction

### 4.1.1 The Relative Reactivity of Nitrile Imines

As mentioned in *Section 1.3*, the reactivity of NIs with both dipolarophiles and nucleophiles has been known for more than 60 years.[1] However, it was 54 years after these initial discoveries before a direct comparison between the reactivity of NIs with dipolarophiles and nucleophiles was discussed in detail. In this 2013 report, Zhao noted that the NI dipole was reactive towards several endogenous nucleophiles, including amino acids such as histidine and glycine.[160] Given the application of NIs as bioorthogonal probes in photoclick chemistry (*Section 1.4.1.1*), these findings were extremely significant. This extensive reactivity of the dipole with nucleophilic residues could potentially compromise the orthogonality of such a procedure. A further experiment also demonstrated that the nucleophilic addition of glycine was not entirely supressed during a competition experiment with the activated dipolarophile acrylamide (*Scheme 4.1a*).

Two years later, this purported lack of chemoselectivity was first observed in bioorthogonal ligation chemistry by Nallani.[411] Control experiments during the attempted photoclick conjugation of polyethyleneglycol (PEG) to bovine β-lactoglobulin (BLG) identified the unanticipated ligation of a 2,5-tetrazole to BLG in the absence of any apparent functional handle (*Scheme 4.1b*). The authors successfully replicated this reactivity with other native enzymes, such as horseradish peroxidase and lysozyme. The ubiquity of this transformation indicated that the NI must be reactive towards endogenous chemical motifs present within the biomolecular architecture. Nallani and coworkers tentatively assigned this to the 1,3-dipolar cycloaddition of the NI with the C2-C3 double bond of the tryptophan indole moiety, however more recent evidence indicates that this unanticipated ligation was mediated by the nucleophilic addition of a sulfur or carboxylate nucleophile, such as cysteine or aspartate.
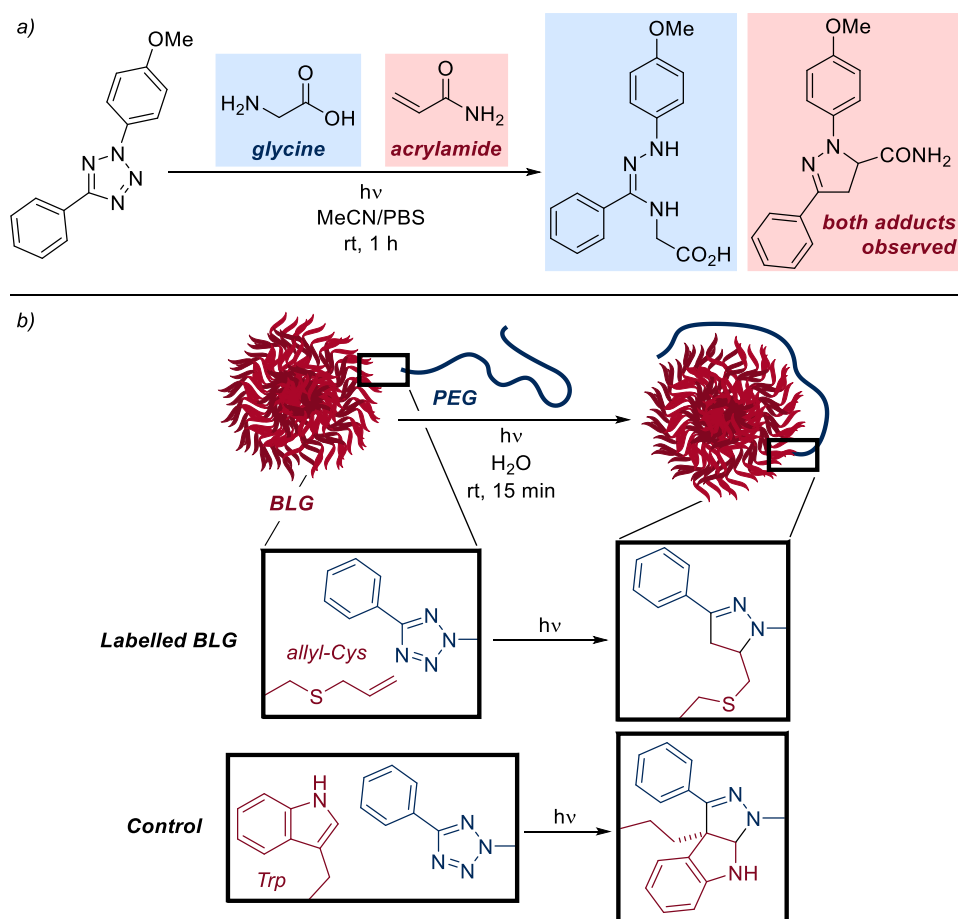
*Scheme 4.1: The preliminary studies that identified competitive reactivity between NIs and different functional groups within chemical biology*

Later that year, Yao provided conclusive evidence of this promiscuous reactivity of the NI through the introduction of what remains the most comprehensive set of reported NI competition experiments.[161] In the presence of an unactivated terminal alkene, NIs preferentially reacted with several examples of native nucleophiles. Acetic acid, alanine and even acetonitrile furnished the corresponding NI adducts in the presence of pent-4-en-1-ol (*Scheme 4.2*). This report also highlighted the pronounced reactivity of carboxylic acids relative to established dipolarophiles, with acetic acid and acrylamide shown to possess similar levels of reactivity with the 1,3-dipole.

This apparent lack of bioorthogonality was a concerning prospect when considering the potential applications of NI cycloaddition. However, despite intense literature activity working towards the rate enhancement of cycloaddition between NIs and dipolarophiles,[122–124,223,224,412] there remains no comprehensive investigation into the reactivity of any nucleophiles relative to these substrates. While Yao's report adequately demonstrated that pent-4-en-1-ol was not a suitable candidate for cycloaddition, it stopped short of providing a clearly defined point at which orthogonality was demonstrated and was almost entirely qualitative in its approach. Furthermore, the reactivities of nucleophilic substrates were never directly compared against each other, leaving a significant degree of ambiguity within these

findings. The report did generate a notable literature response in the identification of improved photoclick systems,[124,221,222] however, the true orthogonality of these analogues in the presence of pre-existing endogenous substrates remains completely untested.
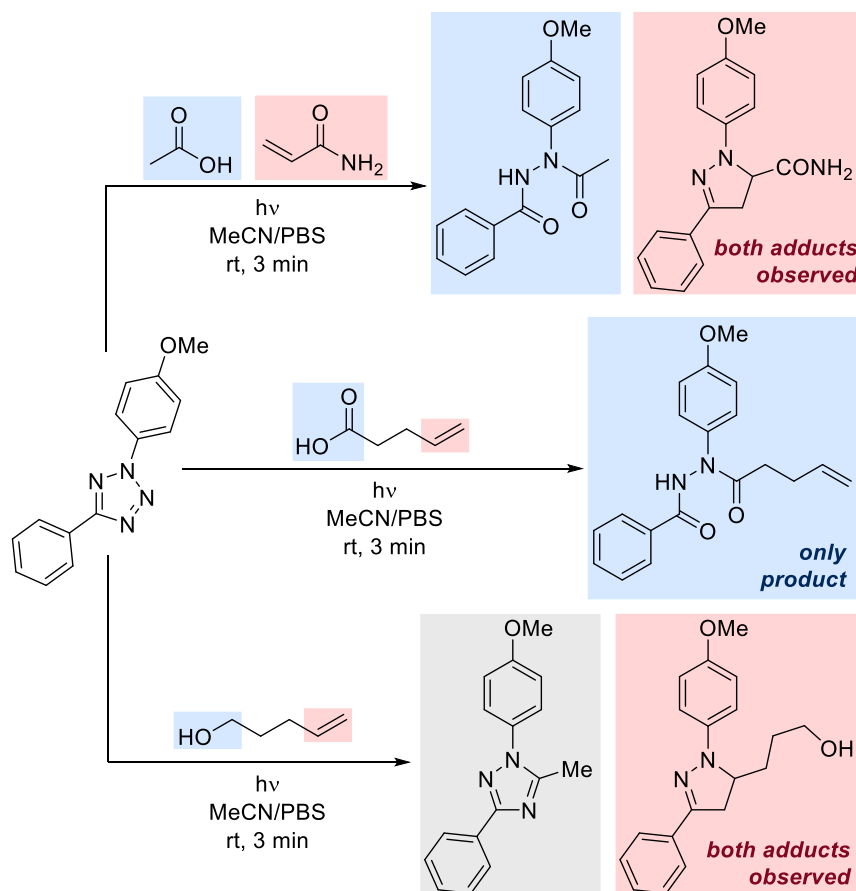


*Scheme 4.2: A summary of the outcomes obtained by Yao and co-workers in 2015*

## 4.1.2   The Design of Comprehensive Nitrile Imine Competition Experiments

Given this substantial gap in the literature, it is evident that there is an opportunity for the development of a more complete set of competition experiments between the NI and its numerous substrates. However, when considering the range of compatible compounds, it is essential that appropriate diligence is devoted to the design of this experiment.

The first consideration is the library of substrates to be examined, as it is important to include representative species from all potential NI reaction pathways. These can be categorised into two main classes- dipolarophiles and nucleophiles. The dipolarophile classification could be further distinguished by reference to alkene or alkyne motifs. The scope of nucleophilic reaction partners could also be sub-divided into substrates intended to mimic the nucleophilic residues found within amino acid side chains (*e.g.* aliphatic amines or carboxylic acids), and other exogenous systems, such as aryl thiols or aryl boronic acids (see *Section 3*).

Another factor is the development of an appropriate assay to quantitatively assess the outcome of the competition experiments. Due to the large number of substrates involved, the isolation of the product of every individual experiment would be impractical, meaning a high-throughput method of reaction monitoring is required. It is desirable to obtain a quantitative method of data collection, as previous literature competition experiments remain somewhat ambiguous due to only qualitative results being reported.[160]

A further aspect that must be considered is the species of NI to be employed within the competition experiments. The NI should originate from a 2,5-diaryl tetrazole precursor, as these compounds are employed as the source of the dipole in an overwhelming majority of literature examples. An additional desirable characteristic of this tetrazole is the incorporation of a functional handle, for example a carbonyl or methoxy group. The inclusion of this motif would further mirror the properties of NIs found in ligation chemistry, which are typically connected to either a biomolecule or labelling species using this type of linker. Any functional handle should also be relatively polar, to improve tetrazole solubility in the aqueous conditions necessitated by bioorthogonal transformations.

## 4.2    Aims

As alluded to in *Section 4.1.2*, the aims of this study centre on the development of a quantitative and comprehensive overview of the reactivity of the NI 1,3-dipole relative to all potential reaction partners within the context of bioorthogonal chemistry. This will be accomplished through a series of competition experiments between a total of nine potential dipolarophiles and nucleophiles, which have been designed to simulate every reactive moiety that the NI may encounter during a chemical ligation procedure. The library of substrates to be examined is shown in *Table 4.1*. Due to the previously reported negative results of pent-4-en-1-ol,[161] only electronically activated dipolarophiles were considered, with an alkene example (**4.1**) and one alkyne analogue (**4.2**). The attachment of electron withdrawing groups is known to improve the rate of NI cycloaddition relative to electron donating groups.[413] A range of exogenous and endogenous nucleophiles (herein referred to as "synthetic" and "native" nucleophiles, respectively), were also selected, with a particular interest on the influence of $pK_a$ on the reactivity of these matched pairs (*eg.* between thiols **4.4** and **4.7**). 4-Methoxyphenylboronic acid (**4.9**) was also included based on the results of *Section 3*. The native nucleophiles are made up of small molecule fragment mimics of the amino acids themselves to prevent any unnecessary complexity in the investigation. Owing to the known unreactivity of pent-4-en-1-ol, it was also deemed unnecessary to consider alcohol nucleophiles as candidates.

Table 4.1: A summary of the library of NI substrates under investigation as part of this study
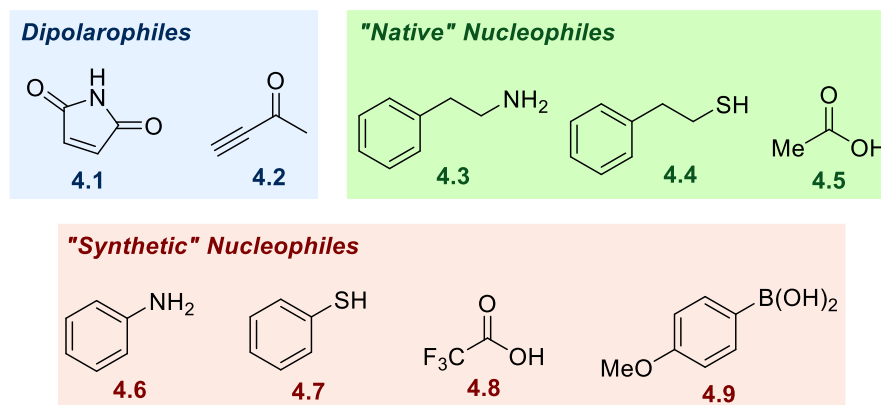
The photolysis of the tetrazole in the presence of two reaction partners will furnish the corresponding products, with the conversion of these two adducts obtained through $^{19}$F NMR spectroscopy. The integration of $^{19}$F resonances is easily accomplished through the addition of an internal standard, enabling quantification of reaction outcome. Furthermore, utilising $^{19}$F nuclei as opposed to $^{1}$H nuclei enables data collection in non-deuterated solvents, meaning that information can be rapidly obtained directly from the reaction mixture.

Tetrazole **4.10** was selected as the model NI precursor within the study (*Figure 4.1*). The incorporation of an acetamide motif provides an appropriate simulation of conjugation within a biomolecule and improves its aqueous solubility. Inclusion of fluorine atoms in the *meta* and *para* positions of the *N-* and *C*-aryl rings renders **4.10** compatible with the $^{19}$F NMR assay and minimises any interference through steric effects. Their contribution to the electronics of the 1,3-dipole cannot be prevented, but this is counteracted by the incorporation of the electron-donating acetamide. The presence of two fluorine atoms also facilitates the identification of any NI decomposition products, for example anilines or benzonitriles (*Section 1.3.4*).
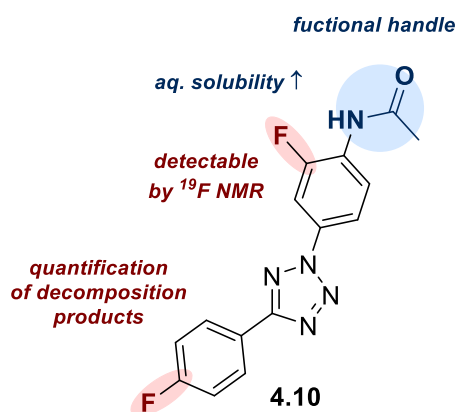


Figure 4.1: The structure of tetrazole **4.10**, the main substrate employed within this study

The individual competition experiments themselves involve NI generation in the presence of one equivalent of two different substrates. The ratio of products observed can then inform

upon the relative reactivity of these two species. These experiments can be sub-divided into six categories that are shown below (*Scheme 4.3*). The interrogation of this data will provide valuable information pertaining to the reactivity of the NI within certain subcategories of reaction partner. For example, the direct competition of all combinations of native nucleophiles will enable the identification of the most reactive example of this substrate within its class.

It is envisaged that rigorous adherence to the conditions and objectives outlined above will enable the development of the first authoritative and quantitative reactivity guide for the NI 1,3-dipole. If successful, this study will provide invaluable guidance relating to the effective application of the NI within the field of chemical biology.
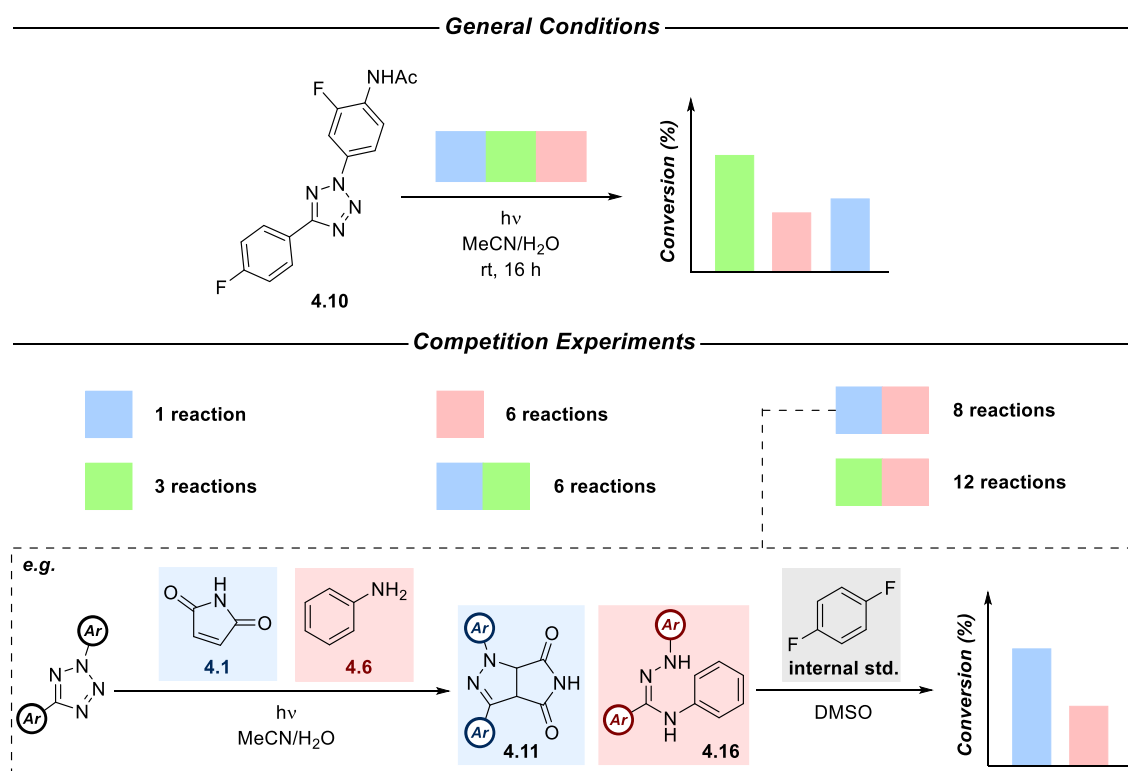


*Scheme 4.3: A summary of the methodology involved in the collection of data during this study into the relative reactivity of the NI dipole*

## 4.3 Results and Discussion

### 4.3.1 Synthesis of Starting Materials and Products

Prior to initiating the detailed competition experiments, it was necessary to separately synthesise all anticipated reaction products, to obtain authentic samples of the materials that would be quantified in the proposed assay. One additional synthetic effort required was the synthesis of 2,5-diaryl tetrazole **4.10**. Due to the extensive substitution of the *N*-aryl ring, the application of the methodology outlined in *Section* 2 was not feasible as the requisite boronic

acid was not available. Accordingly, the Kakehi synthesis was instead identified as an appropriate final step following synthesis of the appropriate precursors.[257,258] Initial preparation of the required hydrazone and aniline inputs **4.22** and **4.24** was straightforwardly accomplished prior to the generation of the tetrazole itself (*Scheme 4.4*). While this method was robust and high-yielding, the low solubility of tetrazole **4.10** in organic solvents made column chromatography of the compound extremely laborious and inefficient. Consequently, the order of steps was reversed. Initial formation of nitro-substituted tetrazole **4.26** enabled purification of this species by trituration from methanol, obviating the requirement for chromatographic purification. The efficiency of the subsequent reduction and acetylation steps enabled the completion of the synthesis while negating the necessity of column chromatography entirely. While the yield of this protocol was noticeably reduced, the expedient nature of this modified synthesis was such that the diminished conversion was not considered problematic.
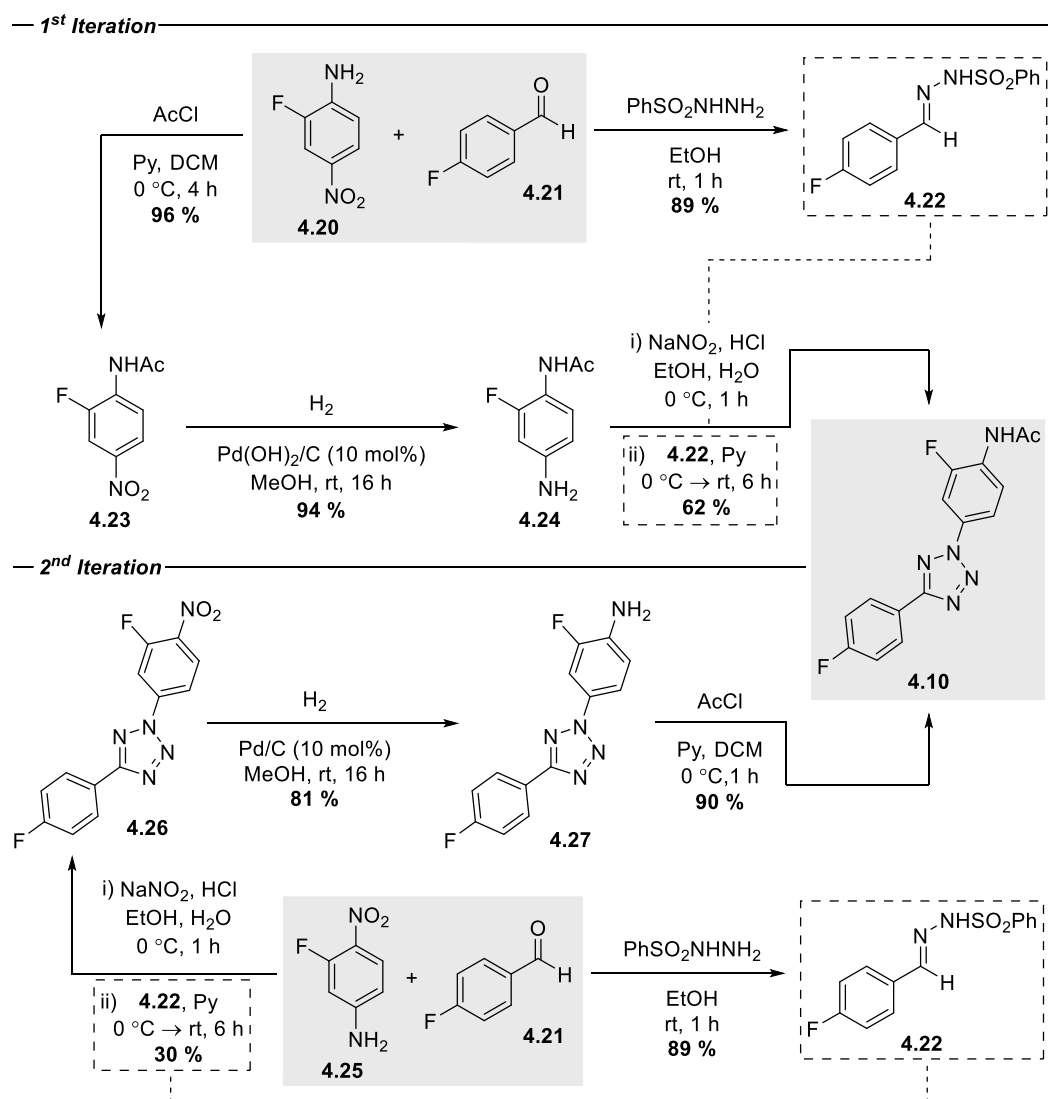


*Scheme 4.4: The synthesis of tetrazole **4.10***

With satisfactory quantities of tetrazole **4.10** obtained, attention turned to the isolation of the products through the combination of the reaction partners with NIs. To facilitate an accurate assessment of the substrates, the conditions were biased towards bioorthogonal compatibility, using a 9:1 acetonitrile:water solvent system. Ten equivalents of nucleophile or dipolarophile were employed, meaning that acceptable yields were expected to be observed for all suitable substrates. The exception was boronic acid **4.9**, which was employed using the conditions previously developed in *Section 3.3.1*.

Initial investigation of the dipolarophile substrates afforded an unusually low yield of pyrazoline **4.11** (68 %, *Table 4.2*). However, this was a consequence of isolation difficulties, as the product was extremely insoluble in most eluents, and the actual yield obtained remained synthetically tractable. No such problems were encountered when employing alkyne dipolarophile **4.2**, which furnished the desired pyrazole in excellent yield. Overall, both species were shown to represent suitable candidates for reactive NI ligation handles, meaning that any nucleophilic competition identified within the planned experiments would represent a genuine issue with respect to the bioorthogonality of the NI.

*Table 4.2: The reactivity profiles exhibited in the 1,3-dipolar cycloaddition with NIs*
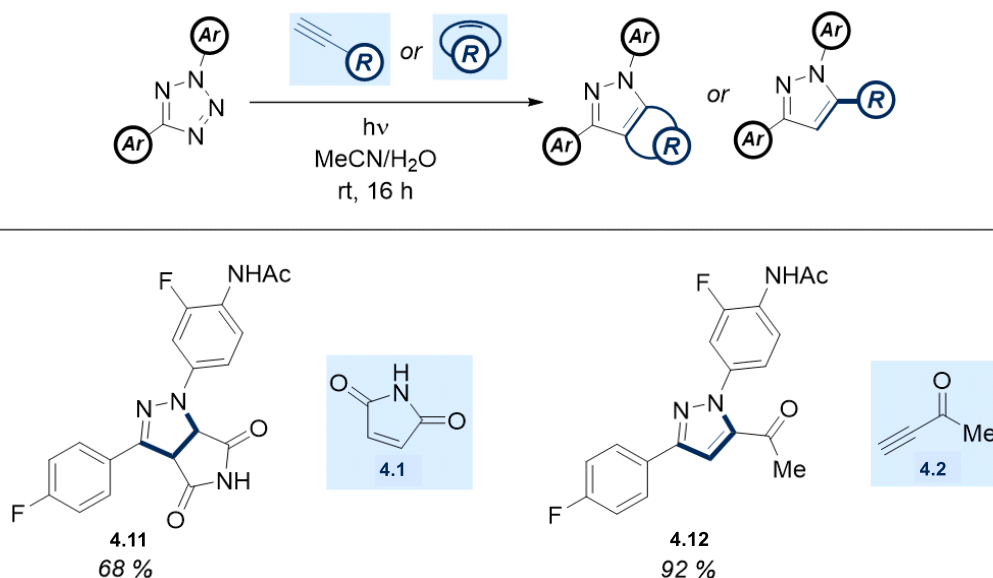


All three native nucleophiles were then introduced to the reaction mixture under the conditions described above, with the results shown in *Table 4.3*. All three candidates (**4.3**, **4.4**, and **4.5**) performed adequately and were advanced for application within the competition experiments. The inclusion of these substrates is particularly vital, with the aliphatic amine, thiol and carboxylic acid motifs constituting the vast majority of native nucleophilic residues in a protein environment. The slightly lower yield of phenethyl thiol (**4.4**) was surprising, given the propensity with which thiols have been shown to interact with NIs in recent literature.[221,251]
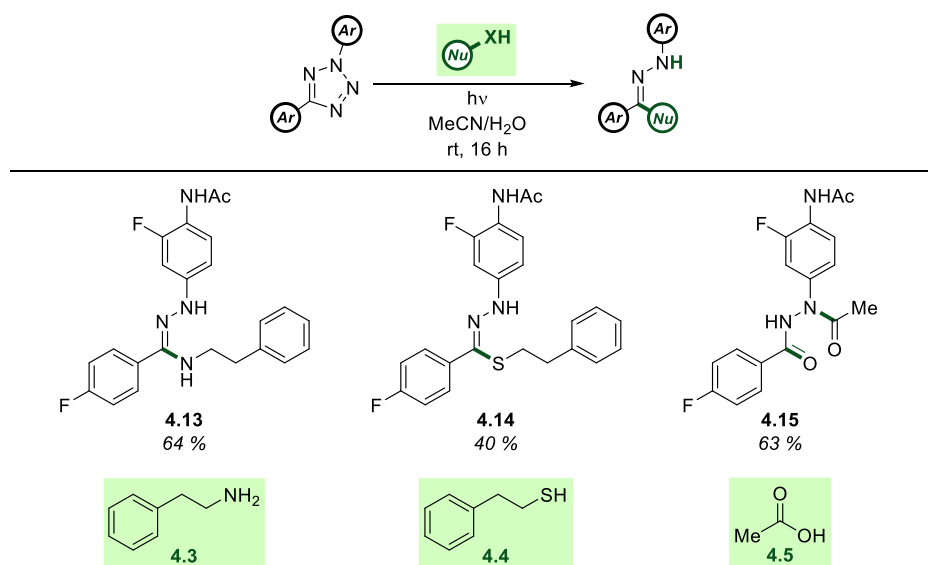
The final substrate class to be investigated were the synthetic nucleophiles, with the results obtained demonstrating considerable similarity with the results of the previous experiments (*Table 4.4*). Amine, thiol and carboxylic acid derivatives **4.6**, **4.7** and **4.8** were furnished in good to excellent yields. One interesting aspect of the shift to aryl amine and thiol nucleophiles was the increase in yield observed in each case. This may signify the importance of $pK_a$ in the reactivity of these substrates, however the similar yield obtained from trifluoroacetic acid (TFA) relative to acetic acid contradicts this argument. 4-Methoxyphenylboronic acid (**4.9**) afforded a yield of 34 % when employing modified conditions. While this conversion was slightly lower than anticipated, this was likely due to an electron-rich moiety on the *N*-aryl ring accelerating the hydrolysis of the compound, as was observed in *Section 3.3.1.3* (*Table 3.10*).

*Table 4.4: Non-native nucleophiles exhibit a range of reactivity towards NIs*
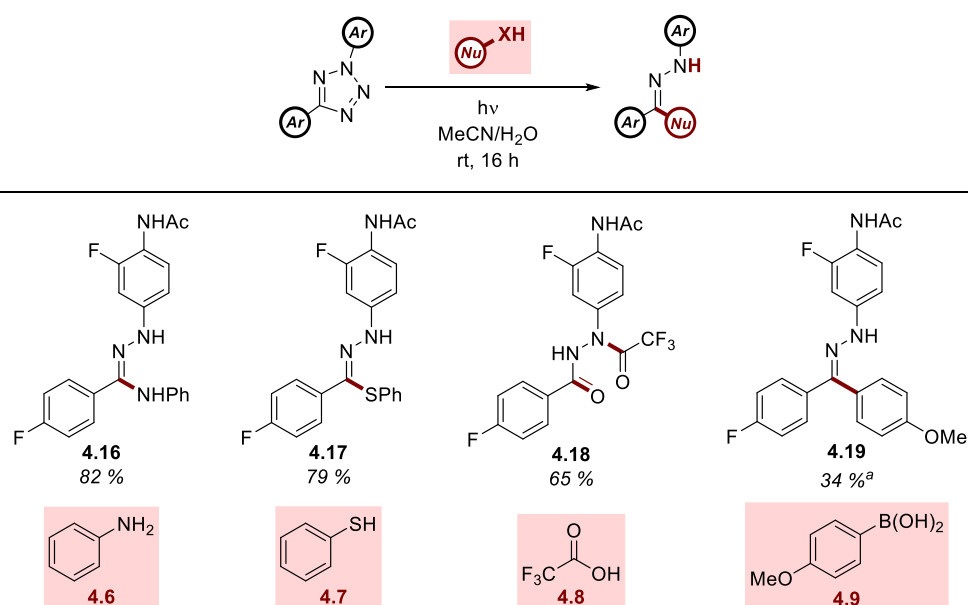


ªTHF used as a solvent, with 3 Å mol. seives

## 4.3.2 Competition Experiments

Following the successful preparation of all desired reaction products, these species were then subjected to direct one-to-one competition experiments in the presence of the NI, which was generated *in situ* from tetrazole precursor **4.10** (*Scheme 4.5*). The results of these individual experiments are first discussed, categorised into their respective sub-groups. The accumulated quantitative data is then discussed in detail and overall trends identified. All experiments were repeated a minimum of three times, with average conversions reported along with their associated error. In addition to the two intended reaction products, several by-products were also identified by ^{19}F NMR during these reactions. All of these corresponded to NI dimerisation or decomposition products, or their derivatives (*Sections 1.3.3* and *1.3.4, Scheme 4.5*) and were not investigated further in this study. Additionally, in most cases, the conversion values obtained for by-product formation were much lower than the yields of the two intended reactions.
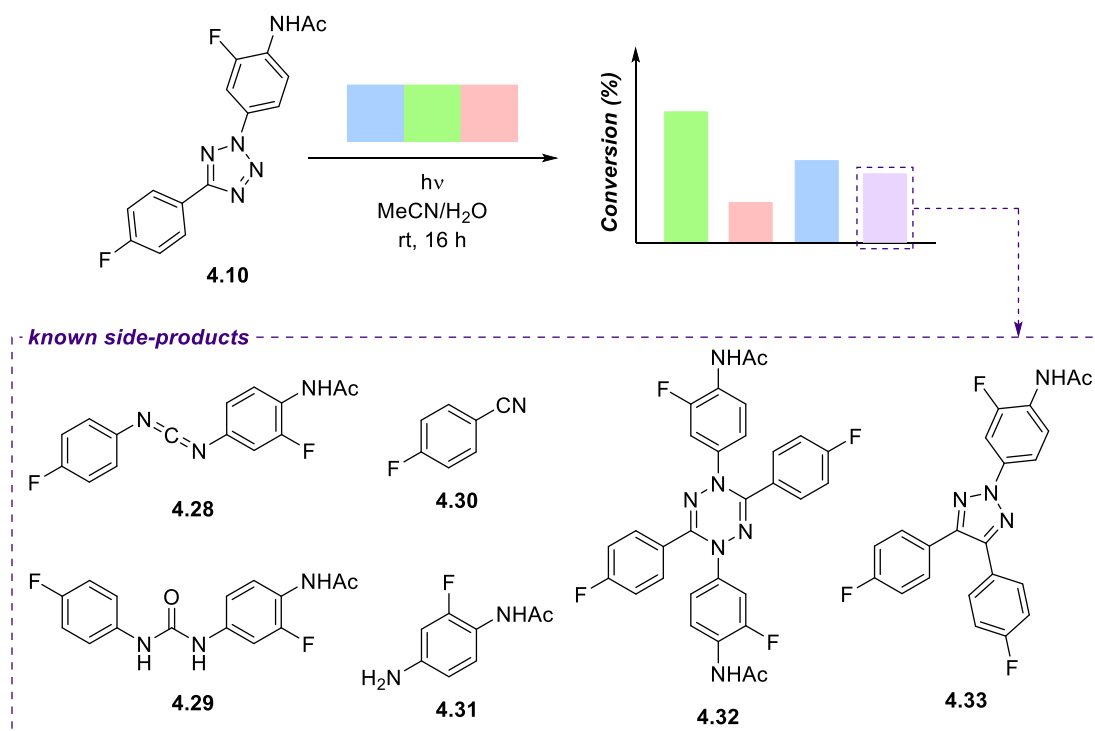


*Scheme 4.5: The general conditions employed in the subsequent competition experiments, and the identification of known by-products*

## 4.3.2.1 Individual Results

An initial competition experiment between the dipolarophiles **4.1** (maleimide) and **4.2** (butynone) exhibited remarkable selectivity for the alkene derivative, with a conversion of over 70 % (*Graph 4.1*). This is consistent with previous reports that highlight the increased reactivity of NIs with C-C double bonds in comparison to C-C triple bonds (*Section 1.3.1.2*).[8] **4.1** is also more electron-deficient, which may play an important role. The limited

formation of side-products is consistent with the high efficiency of the 1,3-dipolar cycloaddition process.
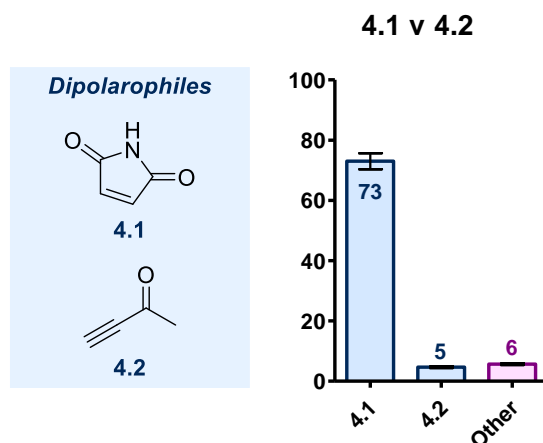


Graph 4.1: The results of a competition experiment between different dipolarophiles

The results of competition experiments between different endogenous nucleophiles were more diverse (*Graph 4.2*). Amine **4.3** and thiol **4.4** demonstrated modest reactivity towards the NI, with both achieving conversion values around 40 % when in direct competition. Acetic acid (**4.5**) was the most reactive, furnishing 59 % of the NI adduct in the presence of a thiol competitor. The limited formation of by-products again indicated the favourability of this procedure. However, competition between the amine and acid resulted in a complex reaction profile as deterimined by $^{19}$F NMR. Presumably, the formation of an ion pair between these two substrates inhibited their interaction with the NI, leading to increased levels of by-product formation.
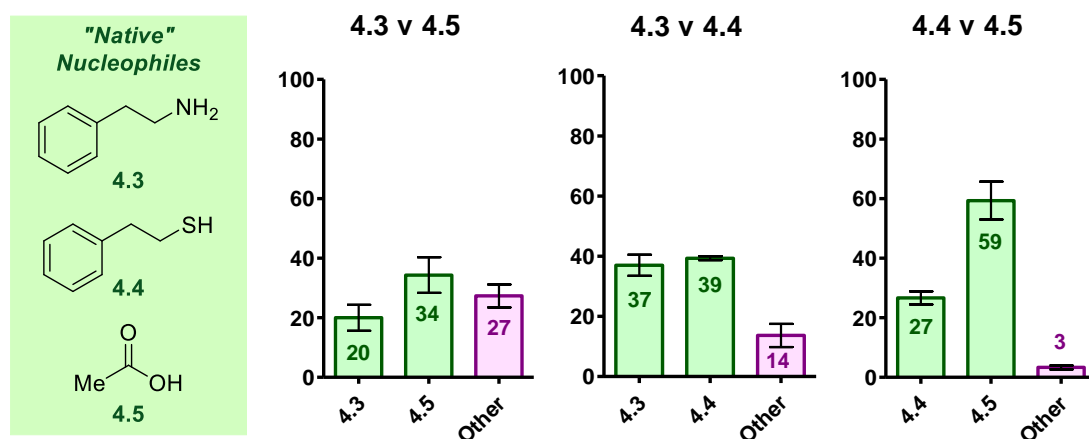


Graph 4.2: The results of competition experiments between different endogenous nucleophiles

A subsequent set of experiments investigated the relative reactivity of the alternative nucleophiles (*Graph 4.3*). Unfortunately, boronic acid **4.9** was found to be completely inactive, which may have been due to the aqueous reaction conditions employed.

Conversely, TFA (**4.8**) demonstrated remarkable reactivity, with conversion values of over 60 % in all three experiments. This was consistent with the data obtained in the previous study, with the carboxylic acid exhibiting enhanced reactivity relative to its thiol and amine counterparts. However, unlike the previous study, aryl thiol **4.7** was shown to outperform aryl amine **4.6**. The substantial difference in $pK_a$ between thiols **4.4** and **4.7** likely accounts for this disparity. Aryl amine **4.6** was generally very unreactive, only outcompeting the inactive boronic acid. Even in this example, significant by-product formation indicated that this reaction remained inefficient.

*"Synthetic" Nucleophiles*

**4.6v4.7** — 4.6: 26, 4.7: 62, Other: 2
**4.6v4.8** — 4.6: 2, 4.8: 62, Other: 11
**4.6v4.9** — 4.6: 58, 4.9: <1, Other: 30
**4.7v4.8** — 4.7: 2, 4.8: 81, Other: 12
**4.7v4.9** — 4.7: 64, 4.9: <1, Other: 13
**4.8v4.9** — 4.8: 66, 4.9: <1, Other: 12
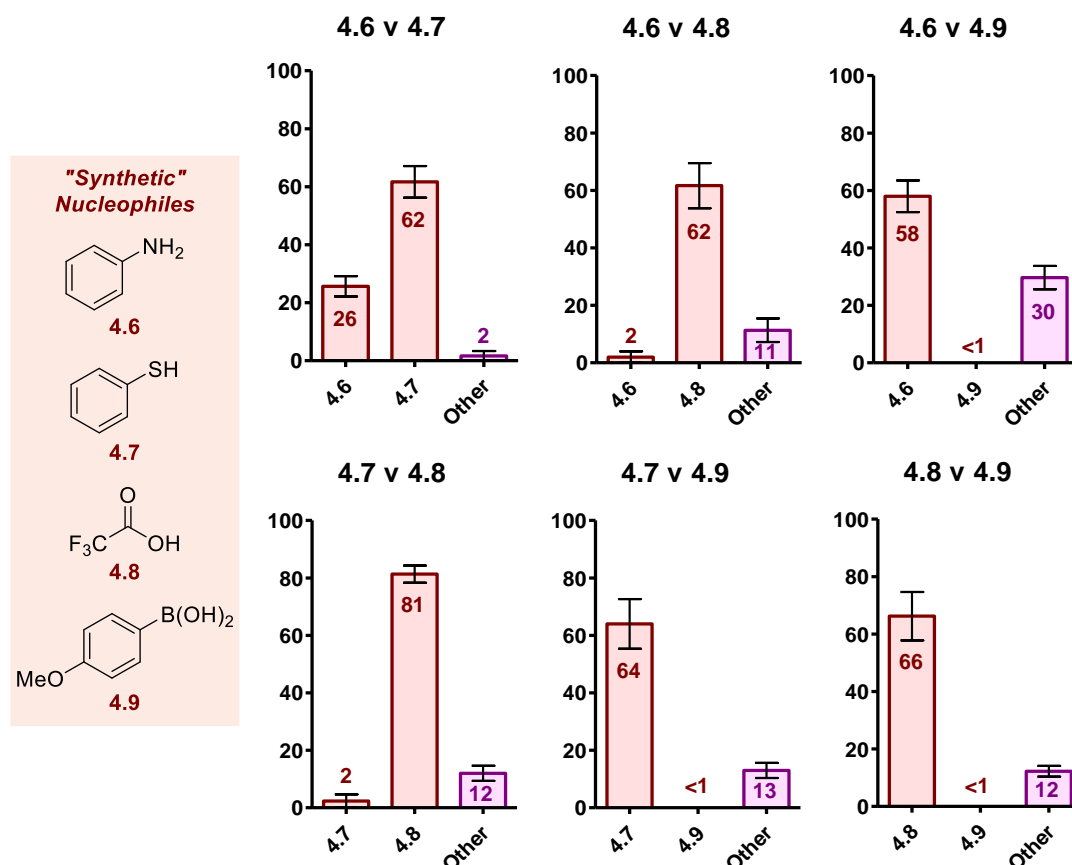
*Graph 4.3: The results of competition experiments between other nucleophiles*

The results outlined in *Graph 4.4* are of particular significance given that they document the relative reactivity of common dipolarophiles against native nucleophiles. To justify the bioorthogonality of NI cycloaddition, it was anticipated that dipolarophiles **4.1** and **4.2** should retain relatively high conversion values. As maleimide (**4.1**) and acetic acid (**4.5**) had been identified as the most reactive substrates within previous studies (*Graph 4.1* and *Graph 4.2*), the result of this experiment was viewed as especially significant. The convincing chemoselectivity demonstrated by maleimide (76 % to 9 %) signified the favourability of this cycloaddition. However, its competition against harder nucleophiles (amine **4.3** and thiol **4.4**) resulted in drastically reduced conversion values, which was likely a consequence of the removal of the dipolarophile by Michael addition.[414] The application of α,β-unsaturated

163

carbonyl systems in the labelling of nucleophilic amino acids is well known, although not particularly chemoselective.[415] While this result was inconclusive, the findings indicated that suitable activation of an olefin for 1,3-dipolar cycloaddition may provide orthogonal NI reactivity if off-site interactions can be avoided. Interestingly, Michael addition was also observed in the competition between alkyne **4.2** and amine **4.3**, but not between **4.2** and thiol **4.4**. This is likely due to the comparatively harder electronic nature of the alkyne relative to alkene **4.1**, rendering it inert to conjugation by the softer thiol. Unlike the alkene, **4.2** was shown to be incompatible as a bioorthogonal NI dipolarophile as it was convincingly outcompeted by carboxylic acid **4.5** (60 % vs 29 %).
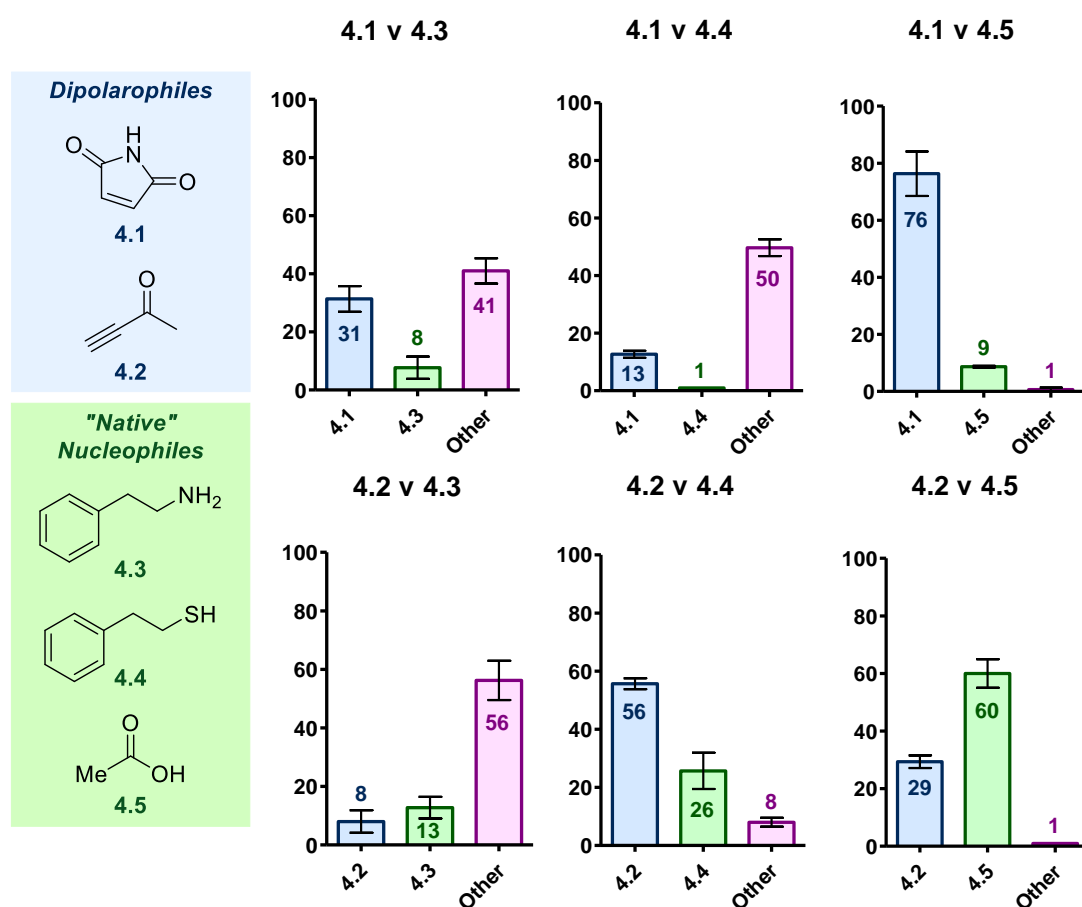


*Graph 4.4: The results of competition experiments between dipolarophiles and native nucleophiles*

The relative reactivity of these two dipolarophiles was further assessed by comparing their reactivity to synthetic nucleophiles **4.6** to **4.9** (*Graph 4.5*). Interestingly, while maleimide (**4.1**) was able to comfortably out-compete carboxylic acid **4.5**, its reactivity was almost completely suppressed upon exposure to TFA (**4.8**). This remarkable inversion of reactivity can be explained by the difference in pK$_a$ between the two acids, which revealed a hidden subtlety to NI reactivity that had never previously been considered. Carboxylic acid **4.8** also comfortably outperformed the alternative dipolarophile alkyne **4.2**, although this was expected given the results of the previous study. The strong performance of this carboxylic

acid could indicate a potential alternative to 1,3-dipolar cycloaddition as an orthogonal labelling agent in photoclick chemistry, as fluorinated carboxylates are not present in native biological systems.
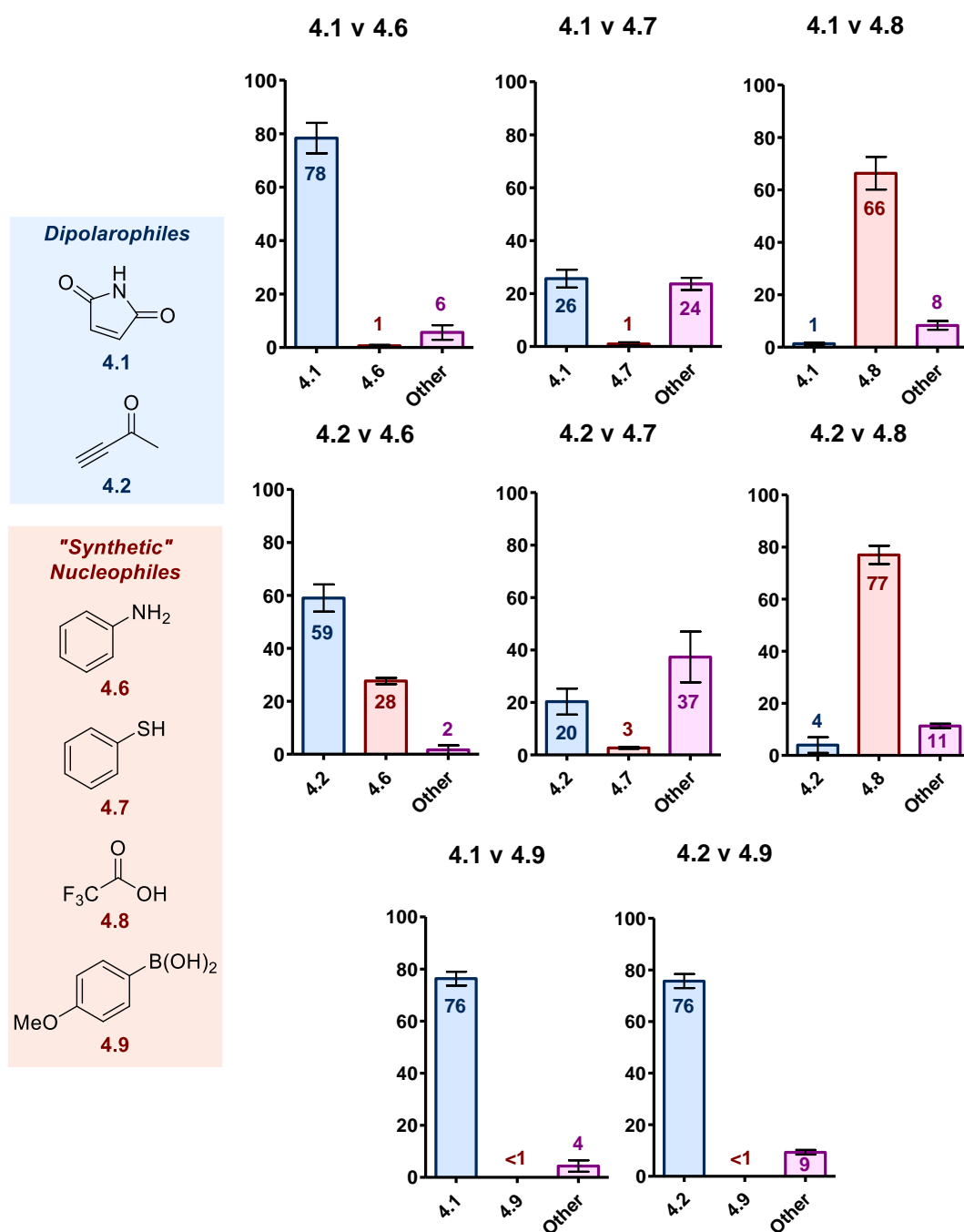


Graph 4.5: The results of competition experiments between dipolarophiles and alternative nucleophiles

Unlike its aliphatic analogue, aryl amine **4.6** was unable to undergo Michael addition with either dipolarophile, and was outcompeted by both species. The two α,β-unsaturated carbonyl systems were, however, neutralised by aryl thiol **4.7**, leading to substantial by-product formation in these cases. Unsuprisingly, both dipolarophiles were also fully selective over boronic acid substrate **4.9**.

165

The results of this study furnished an emerging correlation of NI reactivity to nucleophile $pK_a$, with fluorinated carboxylic acid derivatives such as TFA identified as potential alternative ligation agents within photoclick chemistry. Given these findings, the reactivity of these alternative nucleophiles relative to their endogenous analogues was of particular interest, with the results of these competition experiments shown in *Graph 4.6*. As was anticipated, lower $pK_a$ values were shown to enhance the reactivity of the substrate with the NI, with aryl thiol **4.7** outcompeting alkyl thiol **4.4**, and TFA (**4.8**) comfortably outperforming acetic acid (**4.5**). This reactivity initially appeared to be inverted in the case of amine substrates **4.3** and **4.6**, with the alkyl analogue proving to be much more reactive towards the NI. However, given that **4.6** is protonated at physiological pH, the direct comparison of $pK_a$ should be between the alkyl ammonium and the aryl amine motifs, meaning that the more acidic substrate is indeed more reactive.

Interestingly, the interaction of alkyl amine **4.3** with **4.8** was able to completely inhibit the reactivity of the carboxylic acid. A similar result was observed when acetic acid (**4.5**) was employed in the presence of **4.3** (*Graph 4.2*), and again it can be reasoned that ion-pair formation between the two substrates was responsible for this limited reactivity. This issue is exacerbated in the case TFA relative to acetic acid, due to the increased acidity of the former leading to a tighter ion pair. This is problematic if considering the development of fluorinated acids as an alternative NI reaction partner, given the abundance of basic residues in the architecture of most proteins.

Overall, the results of this study proved to be extremely informative over the relative reactivity of the NI 1,3-dipole. In the context of photoclick chemistry, potentially the most important finding was that alkene dipolarophiles may be electronically activated to the point that they may outcompete all native nucleophilic residues in reaction with the NI. However, a consequence of this enhanced reactivity is an increase in off-site reactivity through the 1,4-addition of nitrogen and sulfur-containing reactive groups. While alkyne **4.2** was also investigated as an alternative dipolarophile, this substrate was outperformed by the nucleophilic residues owing to its diminished reactivity with the NI.

The order of reactivity of the native nucleophilic residues with the NI 1,3-dipole remained consistent with previous results from the literature with carboxylic acids > thiols >> amines. While lysine mimic **4.3** was relatively unreactive towards the NI, it was extremely effective in neutralising other substrates, either through Michael addition or ion pair formation. Compounds **4.1**, **4.2**, **4.5**, **4.7**, and **4.8** all afforded noticeably lower conversion values when exposed to the NI in the presence of **4.3**.
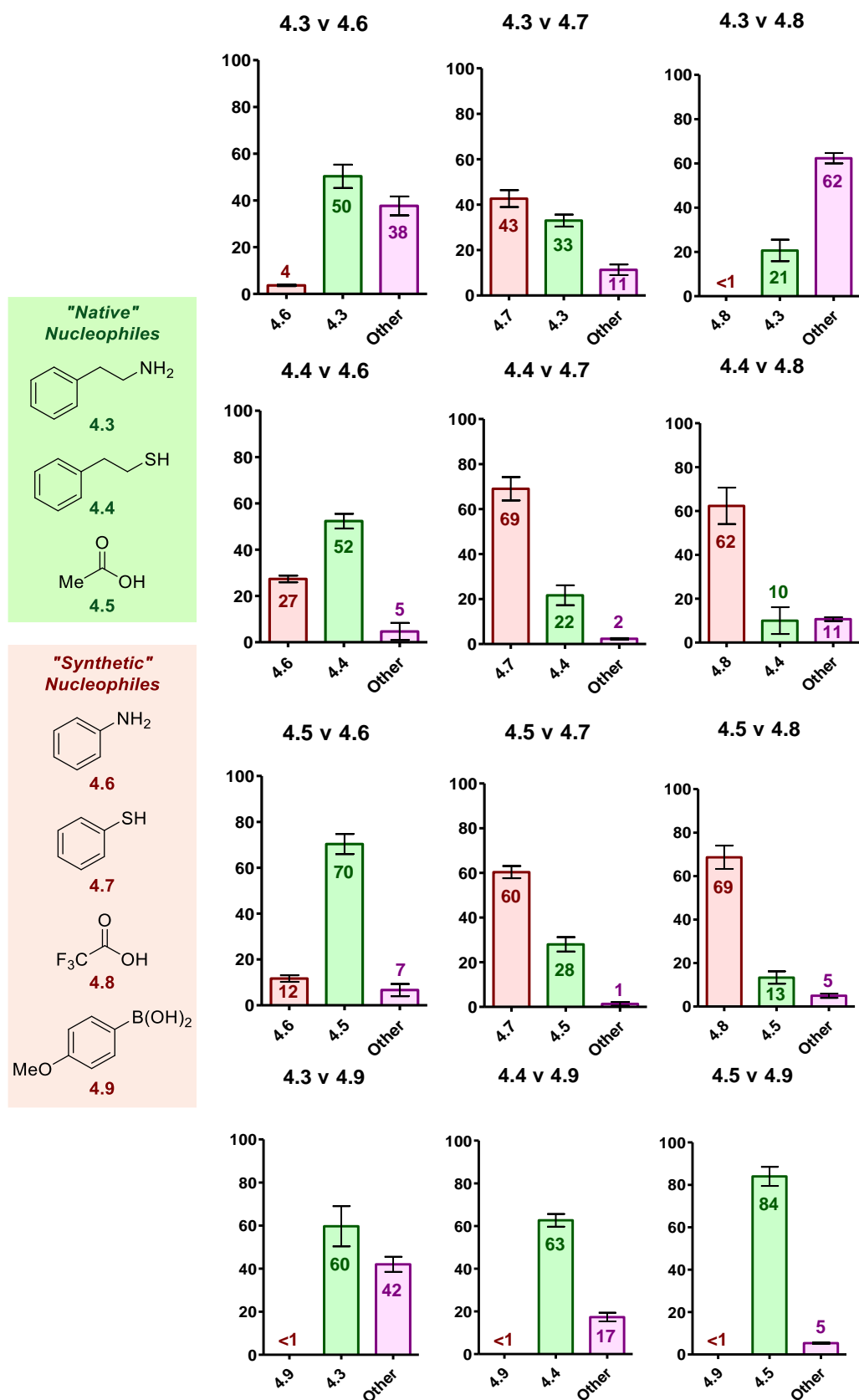
*Graph 4.6: The results of competition experiments between native nucleophiles and alternative synthetic nucleophiles*

The introduction of alternative nucleophiles into the study provided some interesting insights into the electrophilicity of the NI dipole, with both thiophenol (**4.7**) and TFA (**4.8**) shown to be highly effective ligation agents. With the exception of ion pair formation with amine **4.3**, carboxylic acid **4.8** was never outcompeted during the course of the study, furnishing conversion values of more than 60 % in all instances. One of the most striking results was the difference in reactivity of acetic and trifluoroacetic acid (**4.5** and **4.8**) when in competition with maleimide (**4.1**), highlighting the impact of the acidity of the nucleophile on its affinity with the NI dipole.

### 4.3.2.2 Comparative Results

The numerical data obtained from these competition experiments is shown in *Table 4.5*. As chemoselectivity data is commonly reported as a ratio, the relative reactivity of each competing pair was then calculated and is also displayed below.

In order to simplify this output, the average conversion values of all substrates were calculated, as well as the average conversion values of their competitors in each reaction. This enabled the determination of the average difference in conversion value between the substrate of interest and its competitors ($\Delta$, *Equation 4.1*).

$$\Delta = \overline{conversion\ of\ substrate} - \overline{conversion\ of\ competitor}$$

*Equation 4.1: The obtainment of the Δ value from the data in Table 4.5*

The interactions of different substrates during the above investigations considerably complicated this process. For example, while the reactivity of alkene **4.1** with thiol **4.4** was interesting from the perspective of bioorthogonal labelling, it was uninformative of the explicit relative reactivity of these substrates with the NI, as each species was inhibited by the other. In the interests of comparing relative NI reactivity exclusively, results with significant off-target activity were excluded from the calculation of these $\Delta$ values. The criteria for removal from this calculation were defined as results with a total conversion value of under 40 %, with by-product formation of more than 20 %. The introduction of this approach, combined with the application of $\Delta$, enabled a rank order of NI reactivity to be established (*Scheme 4.6*).

To provide additional context to these results, the average relative reactivity (*r*) of each substrate was also calculated by determining the ratio of each product relative to its competitor using these average conversion values (*Equation 4.2*).

$$r = \frac{\overline{conversion\ of\ substrate}}{\overline{conversion\ of\ competitor}}$$

*Equation 4.2: The obtainment of the r value from the data in Table 4.5*

Table 4.5: The quantitative data obtained through the competition experiments described above

**Dipolarophiles**

4.1    4.2

**"Native" Nucleophiles**

4.3    4.4    4.5

**"Synthetic" Nucleophiles**

4.6    4.7    4.8    4.9

4.10

hν
MeCN/H$_2$O
rt, 16 h
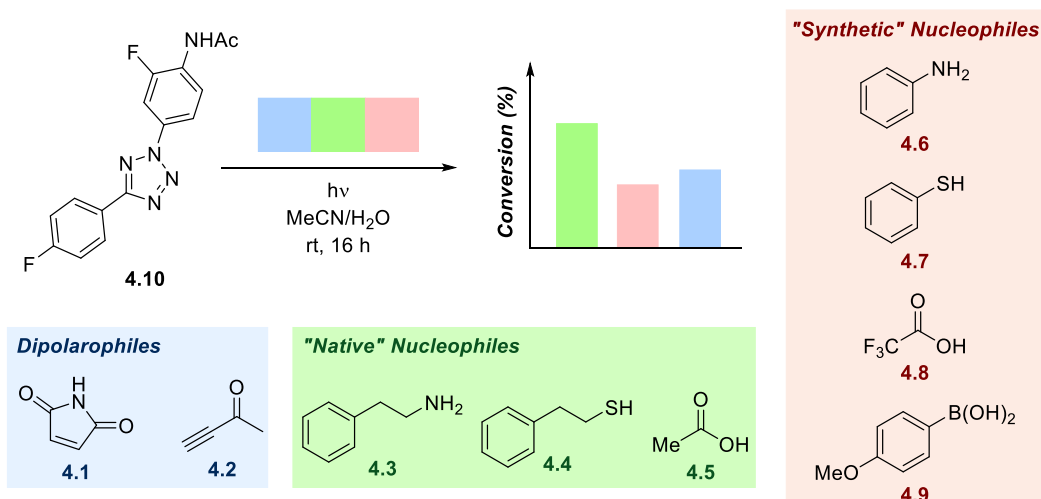
Conversion (%)

| Competitor | Substrate Conversion (%)[a] | | | | | | | | |
|---|---|---|---|---|---|---|---|---|---|
| | 4.1 | 4.2 | 4.3 | 4.4 | 4.5 | 4.6 | 4.7 | 4.8 | 4.9 |
| 4.1 | | 5 | 8[b] | 1[b] | 9 | 1 | 1[b] | 66 | <1 |
| 4.2 | 73 | | 13[b] | 26 | 60 | 28 | 3[b] | 77 | <1 |
| 4.3 | 31[b] | 8[b] | | 39 | 34 | 4 | 43 | <1[b] | <1 |
| 4.4 | 13[b] | 56 | 37 | | 59 | 27 | 69 | 62 | <1 |
| 4.5 | 76 | 29 | 20 | 27 | | 12 | 60 | 69 | <1 |
| 4.6 | 78 | 59 | 50 | 52 | 70 | | 62 | 62 | <1 |
| 4.7 | 26[b] | 20[b] | 33 | 22 | 28 | 26 | | 81 | <1 |
| 4.8 | 1 | 4 | 21[b] | 10 | 13 | 2 | 2 | | <1 |
| 4.9 | 76 | 76 | 60 | 63 | 84 | 58 | 64 | 66 | |

[a]Conversion values determined by $^{19}$F NMR with reference to 1,4-difluorobenzene as an internal standard. Each value is presented as an average of three experiments. [b]Significant by-product formation observed.

| Competitor | Factor of Product Formation Relative to Competitor | | | | | | | | |
|---|---|---|---|---|---|---|---|---|---|
| | 4.1 | 4.2 | 4.3 | 4.4 | 4.5 | 4.6 | 4.7 | 4.8 | 4.9 |
| 4.1 | | 0.1 | 0.3 | 0.1 | 0.1 | 0.0 | 0.0 | 66.0 | 0 |
| 4.2 | 14.6 | | 1.6 | 0.5 | 2.1 | 0.5 | 0.2 | 19.3 | 0 |
| 4.3 | 3.9 | 0.6 | | 1.1 | 1.7 | 0.1 | 1.3 | 0.0 | 0 |
| 4.4 | 13.0 | 2.2 | 0.9 | | 2.2 | 0.5 | 3.1 | 6.2 | 0 |
| 4.5 | 8.4 | 0.5 | 0.6 | 0.5 | | 0.2 | 2.1 | 5.3 | 0 |
| 4.6 | 78.0 | 2.1 | 12.5 | 1.9 | 5.8 | | 2.4 | 31.0 | 0 |
| 4.7 | 26.0 | 6.7 | 0.8 | 0.3 | 0.5 | 0.4 | | 40.5 | 0 |
| 4.8 | 0.0 | 0.1 | - | 0.2 | 0.2 | 0.0 | 0.0 | | 0 |
| 4.9 | - | - | - | - | - | - | - | - | |

An initial approach for calculating *r* involved determining the averages of the individual competition experiment ratios reported in *Table 4.5*, however minor differences in highly selective reactions significantly distorted the results of this dataset. For example, entries **4.1** vs. **4.6** and **4.8** vs. **4.7** exhibit substantially different *r* values (78.0 and 40.5), despite the similar conversions of these two experiments (78 % vs. 1 % and 81 % vs. 2 %). It was also necessary to exclude any results that had been compromised by off-target reactivity, as was the case with Δ. Consequently, *r* was derived as a ratio of the averaged conversion values employed during the calculation of Δ, and is also displayed in *Scheme 4.6*.

**4.8** F₃C–C(O)–OH  
Δ = +64%  
*r* = 13.8  
Avg. Conversion: 69%  
Competitor Conversion: 5%

**4.1** maleimide  
Δ = +45%  
*r* = 3.8  
Avg. Conversion: 61%  
Competitor Conversion: 16%

**4.7** Ph–SH  
Δ = +18%  
*r* = 1.6  
Avg. Conversion: 50%  
Competitor Conversion: 18%

**4.3** Ph–CH₂CH₂–NH₂  
Δ = +16%  
*r* = 1.7  
Avg. Conversion: 40%  
Competitor Conversion: 24%

**4.5** Me–C(O)–OH  
Δ = +8%  
*r* = 1.2  
Avg. Conversion: 46%  
Competitor Conversion: 39%

**4.2** butynone  
Δ = -6%  
*r* = 0.9  
Avg. Conversion: 38%  
Competitor Conversion: 44%

**4.4** Ph–CH₂CH₂–SH  
Δ = -10%  
*r* = 0.8  
Avg. Conversion: 34%  
Competitor Conversion: 44%

**4.6** aniline (Ph–NH₂)  
Δ = -34%  
*r* = 0.4  
Avg. Conversion: 20%  
Competitor Conversion: 54%

**4.9** MeO–C₆H₄–B(OH)₂  
Δ = -68%  
*r* = 0  
Avg. Conversion: <1%  
Competitor Conversion: 68%

Δ axis labels (top to bottom): 4.8, 4.1, 4.7, 4.3, 4.5, 0, 4.2, 4.4, 4.6, 4.9

*Scheme 4.6: The rank order of reactivity with the NI 1,3-dipole obtained from the competition experiments described above*

The results of this quantitative analysis of the data generally confirmed the trends identified within the previous section. TFA (**4.8**) was the most efficacious NI reaction partner, averaging a conversion 64 % greater than its competitor. It was also 13.8 times more likely than the competing substrate to react with the NI. Only maleimide (**4.1**) exhibited comparable reactivity with the dipole. These two results emphasised the favourability of 1,3-dipolar cycloaddition but also highlighted that alternative reactivity profiles of the NI can be

very efficient. Aryl thiol **4.7** also performed strongly and was the third most reactive NI substrate with a Δ value of +18 %, and an *r* value of 1.6.

The three native nucleophiles afforded mixed results, with Δ conversion values between +16 and -10 %. In most instances, these substrates were able to compete with other compounds, but never demonstrated substantial orthogonality, with *r* values of around 1. This is encouraging from the perspective of photoclick chemistry, as it suggests that the reaction of native nucleophiles with the NI can be outcompeted by employing an appropriately reactive ligation agent. Interestingly, despite the individual competition experiments (*Graph 4.2*) indicating the carboxylic acid **4.5** was the most reactive substrate, quantitative analysis suggested that aliphatic amine **4.3** exhibited the greatest affinity towards the 1,3-dipole. The *r* value of **4.3** was in fact greater than that of aryl thiol **4.7**, highlighting the surprisingly strong performance of the amine. This was an anomalous result and likely a false positive, as the extensive off-target reactivity of **4.3** made the determination of its relative reactivity towards the NI very challenging. In total, five of the eight competition experiments performed using this amine exhibited detrimental interactions between the two substrates, either through ion pair formation or 1,4-addition. The inconsistency of this species can be visualised by *Graph 4.7*. The average conversion values of **4.3** are substantially lower than would be expected relative to the correlation established by other substrates, due to the tendency of **4.3** to interact with its competitor rather than the NI. Extrapolation of this data would assign **4.3** a Δ value of around 0, more in line with the results displayed in *Graph 4.2*.
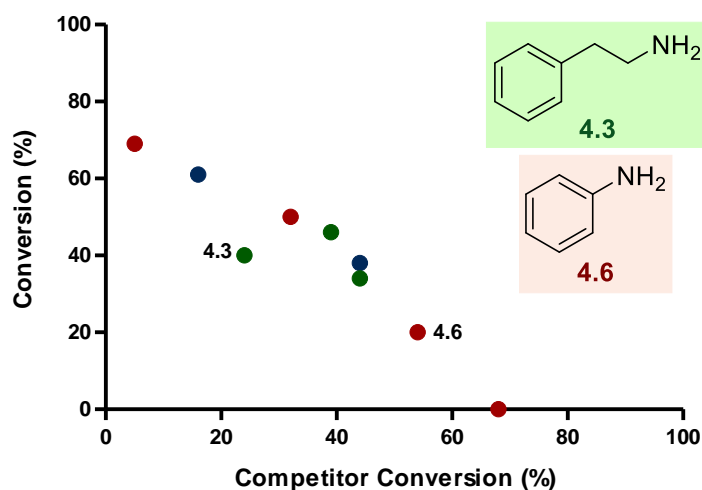


*Graph 4.7: A plot of average substrate conversion versus the average conversion of its competitor*

All other exogenous substrates examined during the study were shown to be ineffective reaction partners for NI ligation. While both alkyne **4.2** and aryl amine **4.6** performed extremely well in earlier substrate scopes in the absence of competitors (*Table 4.2* and *Table 4.4*), both were comfortably outperformed by other compounds within this assay. The result

of boronic acid **4.9** was the most disappointing, as it was completely inert towards the NI under the conditions employed ($r = 0$).

In general, both methods of quantification employed ($\Delta$ and $r$) were in agreement in the ranking of substrate reactivity. The relative reactivity ($r$) of carboxylic acid **4.8** accentuated the remarkable selectivity of this substrate, while the $\Delta$ values of both **4.8** and maleimide (**4.1**) demonstrated the enhanced reactivity of these two species relative to the other compounds examined.

While the above results afforded a much-improved understanding of the relative reactivity of the NI purely in terms of reactivity, questions remained concerning its bioorthogonality within photoclick chemistry. To simulate the suitability of different ligation agents for application in this field, further analysis was conducted on the above dataset using the results involving the competition of exogenous reagents and native nucleophiles (*Graph 4.4, Graph 4.6* and *Table 4.6*). Unlike the previous analysis, no data values were excluded due to off-target reactivity, as these concerns are particularly relevant to bioorthogonal chemistry. Again, averaged conversion values were obtained, and $\Delta$ was used to establish the relative reactivity of the substrates. Due to its poor performance in the previous analysis, boronic acid **4.9** was not included in this study. Ratios of relative reactivity were also not calculated, as the occurence of significant by-product formation was found to obfuscate the generation of accurate $r$ values.

The results of this investigation were broadly similar to the preceding analysis, but also included some significant differences (*Graph 4.8*). Again, alkene **4.1**, thiol **4.7** and fluorinated acid **4.8** were the top performing substrates, however in this instance all three afforded extremely similar $\Delta$ values of around +30 %. Interestingly, this indicated that both **4.1** and **4.8** were less orthogonal when compared exclusively to endogenous substrates. Conversely, aryl thiol **4.7** exhibited an increase in $\Delta$ conversion of more than 10 %. However, the interpretation of this data is not straightforward. While all three substrates appeared to be equally competent ligation agents, **4.1** and **4.8** are more effective in outcompeting the native nucleophiles in their reaction with the NI, but are also inhibited through Michael addition (**4.1**) and ion pair formation (**4.8**). Thiophenol **4.7** is unaffected by off-target reactivity but is not reactive enough towards the NI to exhibit greater selectivity. The overall outcome of these different reactivities is the same, with all three substrates demonstrating considerable aptitude towards NI ligation in the presence of native nucleophiles but falling short of the bioorthogonality required in a ligation handle. Further structural modification of compounds **4.1** or **4.8** would be required prior to applying them to photoclick chemistry.

Table 4.6: A truncated form of Table 4.5, highlighting the conversion values relevant to this further analysis
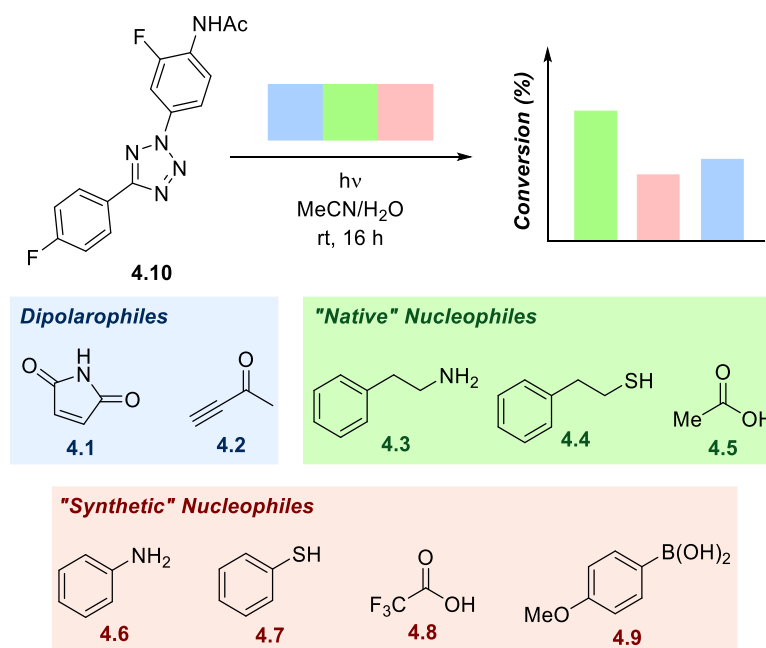
| Competitor | Substrate Conversion (%)[a] | | | | | | | |
|:---:|:---:|:---:|:---:|:---:|:---:|:---:|:---:|:---:|
| | 4.1 | 4.2 | 4.3 | 4.4 | 4.5 | 4.6 | 4.7 | 4.8 |
| 4.3 | 31[b] | 8[b] | | | | 4 | 43 | <1[b] |
| 4.4 | 13[b] | 56 | | | | 27 | 69 | 62 |
| 4.5 | 76 | 29 | | | | 12 | 60 | 69 |

[a]Conversion values determined by $^{19}$F NMR with reference to an internal standard. Each value is presented as an average of three experiments. [b]Significant by-product formation observed.

Alternative substrates **4.2** and **4.6** were also included within this smaller second study, however both demonstrated nearly identical performances to those observed during the initial analysis. Dipolarophile **4.2** remains the more promising of the two, capturing roughly the same quantity of the NI as its competitor, however this remains considerably below the minimum standard required for incorporation within a biochemical assay.

## 4.4  Conclusions and Outlook

Over the past decade, significant advances have been made in the application of the NI as a biorthogonal labelling agent in chemical biology, with the advent of photoclick chemistry developing this 1,3-dipolar cycloaddition into a genuine alternative to other established techniques. However, this drive towards further applications of the NI has often come at the expense of an improved understanding of its fundamental reactivity with both nucleophiles and dipolarophiles. The current study has made significant contributions towards rectifying this disparity, through completion of the first ever set of comprehensive competition experiments to obtain a quantitative reactivity profile of the dipole. This was accomplished

through the careful development of a high-throughput and informative $^{19}F$ NMR assay, with the results reinforced by the inclusion of a diverse range of substrates, including different dipolarophiles and nucleophiles. A scope conducted prior to the beginning of the competition experiments confirmed the competency of these substrates and enabled the characterisation of all reaction products.
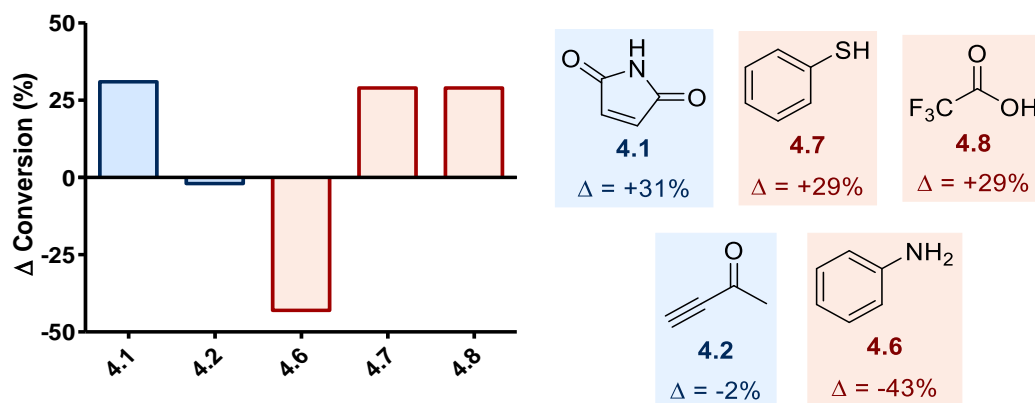


*Graph 4.8: The Δ values obtained when only considering the conversions obtained during endogenous nucleophile competition experiments*

The results of the competition experiments confirmed that 1,3-dipolar cycloaddition between the NI and an activated alkene is highly efficient, which can comfortably outcompete alkynes and most nucleophiles. However, the study also identified a hitherto undiscovered dependence of nucleophile $pK_a$ on NI reactivity. The most acidic substrate, TFA, was found to outcompete all other compounds including maleimide in its reactivity within the NI. This improved reactivity with the dipole was also evident using other acidic nucleophiles, such as thiophenol and acetic acid, which both performed strongly. The outcome of these studies was fully quantified, and subsequent analysis of the data enabled a rank order of NI reactivity to be established for the first time. These results mostly corroborated earlier qualitative observations, with the numerical assignments clearly outlining the dominance of maleimide and TFA. A second analysis focusing on the application of NIs for bioorthogonal labelling afforded more mixed results, with all three promising functional handles demonstrating only limited orthogonality when in competition with native nucleophiles. This was primarily a consequence of off-target reactivity and could certainly be addressed in a future study.

Based on these results, the outlook for continued application of photoclick chemistry is generally positive. 1,3-Dipolar cycloaddition was shown to be a feasible strategy of ligation that was still achievable in high yields even in the presence of several different competitors. However, substantial activation of the dipolarophile was also necessary, with only limited success when employing less reactive substrates, such as alkyne **4.2**. Acidic nucleophiles such as fluorinated carboxylic acids were also identified as a potential alternative ligation

handle for NIs. A future investigation to establish the reactivity of α,α-difluoroglutamate within a small peptide sequence would be a very informative study (*Scheme 4.7*).
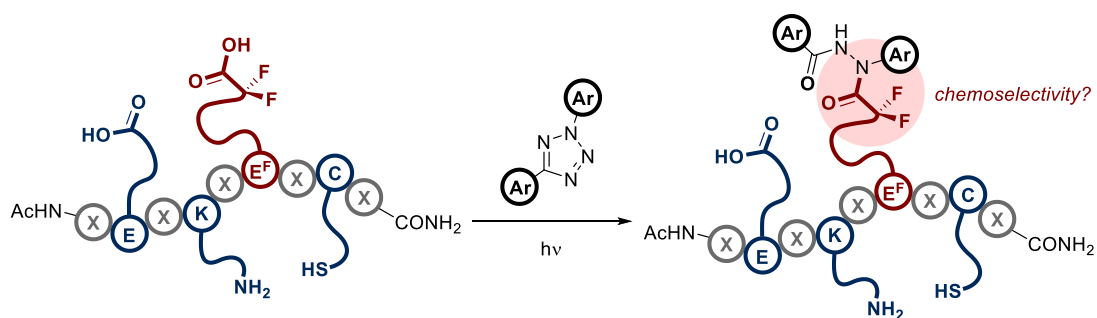


*Scheme 4.7: The potential chemoselective labelling of a fluorinated carboxylic acid within a small peptide sequence*

One of the additional benefits of this investigation was the identification of other factors that may be detrimental to orthogonality. While the affinity of the substrate for the NI must naturally be very high, in many cases problems instead originated from the excessive reactivity of the substrate with other compounds. This suggests that the design of an NI reaction partner should also consider methods of inhibiting these alternative pathways, in addition to promoting reactivity with the dipole. For example, while both maleimide and TFA demonstrated impressive affinity, neither would be suitable for immediate application due to extensive off-target reactivity.
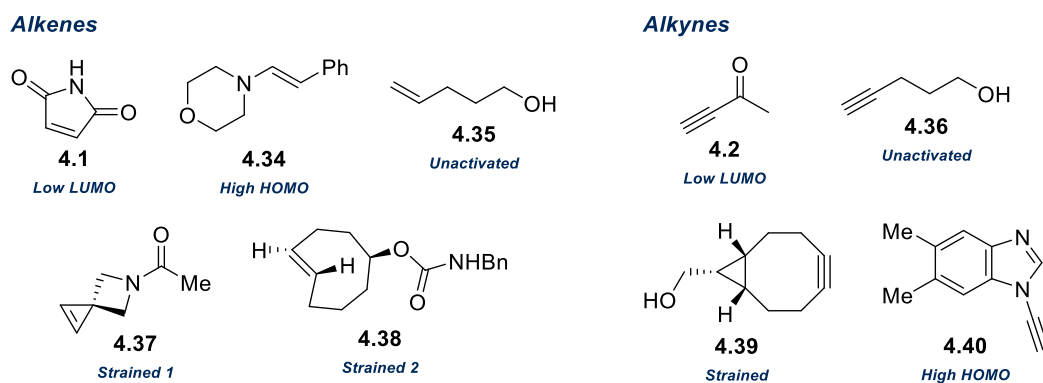


*Figure 4.2: Potential substrates for further competition experiments*

The development of these competition experiments has established a platform which will be used to conduct further studies in the near future. While different nucleophiles have been extensively investigated, the relative reactivity of NIs towards different dipolarophiles could still be probed in more detail. In particular, it would be prudent to include both strain- and electronically-activated examples that have recently been employed in bioorthogonal ligations within the literature, including cyclopropenes,[123,124,412] cyclooctenes,[122,223] ynamines,[416,417] and cyclooctynes (*Figure 4.2*).[122,224] These should also be supplememted with unactivated examples, such pent-4-en-1-ol from Yao's earlier study,[161] in order to

provide a comprehensive overview of the reactivity of NIs with dipolarophiles relative to competitive nucleophiles such as carboxylic acids and thiols.

# 5    Experimental

## 5.1    General Information

All reagents and solvents were obtained from commercial suppliers and were used without further purification unless otherwise stated. Purification was carried out according to standard laboratory methods.

### 5.1.1    Purification of Solvents and Reagents

Anhydrous THF, DCM, and toluene were obtained from a PureSolv SPS-400-5 solvent purification system. Solvents were transferred to and stored in septum-sealed oven-dried flasks over activated 4 Å molecular sieves and purged with and stored under nitrogen. Acetone, cyclohexane, dichloromethane, diethyl ether, ethyl acetate, methanol, *n*-hexane and petroleum ether 40–60 °C for purification purposes were used as obtained from suppliers without further modification. $K_3PO_4$ was stored in a vacuum oven at 60 ºC.

### 5.1.2    Experimental Details

All reactions were conducted using round-bottom flasks, microwave vials, HPLC vials or NMR tubes of appropriate volume. Reactions were carried out at elevated temperatures using a temperature-regulated hotplate/stirrer, while room temperature generally refers to ~ 20 ºC. Reactions requiring a reduced temperature were performed using an ice bath (0 °C) or a dry ice/actone slurry (-78 °C) and a temperature probe unless otherwise stated. Reactions requiring a UV lamp were conducted using either a Philips UV-B Broadband PLS 9W bulb, or a Philips UV-B Broadband TL 20W bulb (both 270 – 360 nm). Phase separation was conducted using IST Isolute Phase Separator Cartridges.

### 5.1.3    Purification of Products

Thin layer chromatography was carried out using Merck silica plates coated with fluorescent indicator UV254. These were analysed under 254 nm UV light or developed using potassium permanganate solution. Flash chromatography was carried out using ZEOprep 60 HYD 40-63 μm silica gel. Small scale centrifugation was conducted using an Eppendorf MiniSpin at 11 rpm for 3 minutes at room temperature. Large scale centrifugation was conducted using an Eppindorf 5804 centrifuge at 4000 rpm for 3 minutes at room temperature. Reverse-phase HPLC purification of peptides was conducted using a Gilson preparative HPLC system of 322 pumps coupled to a 151 UV/Vis 163 spectrometer, 234 Autoinjector and a GX-271 liquid handler using an Agilent Zorbax SB-C18 column (21.2 x 150 mm, 5 μm packing diameter) at room temperature. Purifications were performed using gradient methods ranging from 5-90 % MeCN in $H_2O$ over 30 minutes at a flow rate of 10 mL/min, with a 0.1 % TFA

modifier and UV monitoring at 214 nm. Analysis was conducted using Gilson Trilution v2.0 software. Freeze drying was conducted using a Christ Alpha 1-2 LD plus freeze drier

### 5.1.4 Analysis of Products

Fourier Transformed Infra-Red (FTIR) spectra were obtained using an A2 Technologies ATR 32 machine. $^1$H, $^{19}$F and $^{13}$C NMR spectra were obtained on a Bruker DRX 500 spectrometer at 500, 376 and 126 MHz, respectively, on a Bruker AV3 400 at 400, 471 and 101 MHz, respectively, or on a Bruker AVANCE 400 spectrometer at 400, 471 and 101 MHz, respectively. Chemical shifts are reported in ppm and coupling constants are reported in Hz with CDCl$_3$ referenced at 7.26 ($^1$H) and 77.16 ppm ($^{13}$C), DMSO-$d$6 referenced at 2.50 ($^1$H) and 39.52 ppm ($^{13}$C), acetone-$d$6 referenced at 2.05 ($^1$H) and 29.84 ppm ($^{13}$C) and methanol-$d$4 referenced at 3.31 ($^1$H) and 49.86 ppm ($^{13}$C). High-resolution mass spectra (HRMS) were obtained on a Thermofisher LTQ Orbitrap XL instrument at the EPSRC National Mass Spectrometry Service Centre (NMSSC), Swansea, or on a Waters XEVO G2-XS QTof instrument (100-1200 AMU) in positive ionization mode at GlaxoSmithKline Medicines Research Centre, Stevenage. Low-resolution mass spectra (LRMS) were obtained using an Agilent Technologies 1200 series LC-MS instrument with a 6130 single Quadropole, a ThermoQuest Finnigan LC duo coupled to a Razel syringe pump, and a Thermo DSQ (EI) with Trace GC. LC traces were recorded at a wavelength of 254 or 214 nm. Reverse phase HPLC data was obtained on an Agilent 1200 series HPLC using a Machery-Nagel Nucleodur C18 column. For some compounds detailed in *Section 2*, LCMS spectra were obtained using an Acquity UPLC CSH C18 column (50 mm x 2.1 mm i.d. 1.7 μm packing diameter) at 40 °C. The solvents employed were a 0.1 % v/v solution of formic acid in water, and a 0.1 % v/v solution of formic acid in acetonitrile. UV analysis was conducted using a Varian Cary 50 probe UV-visible spectrometer with spectral analysis conducted using the Varian Cary software. Crystallographic measurements were performed by Dr. Alan Kennedy at 150 K with an Oxford Diffraction Gemini S diffractometer and monochromated Cu radiation ($\lambda$ = 1.54184 Å). Programs from the SHELX suite were used for structure solution and refinement.[418] Refinement was to convergence against F$^2$ using all unique reflections. Non-H atoms were refined anisotropically. All H atoms bound to C were observed in difference maps but were included in the final model as riding atoms. The H atom bound to O was refined freely and isotropically.

### 5.1.5 Peptide Experimental Details

All Fmoc-protected amino acids were purchased from Novabiochem unless otherwise stated. HATU was purchased from Fluorochem, while triisopropyl silane, piperidine, and TFA were purchased from Alfa Aesar. Acetic anhydride and DIPEA were purchased from Sigma-Aldrich. All peptides were synthesised using Wang resin (1.1 mmol/g loading), which was

also purchased from Sigma Aldrich. All solvents were purchased from Sigma-Aldrich with the exception of DMF, which was purchased from Rathburn Chemicals Ltd. All manual couplings were performed in a Merrifield bubbler attached to a vacuum line, a nitrogen line and large round bottomed flask for waste. All automated couplings were carried out on a Protein Technologies Tribute automated synthesiser. The solvents attached to the synthesiser were DMF, DCM, 20 % piperidine in DMF, 0.5 M DIPEA in DMF and 15 % acetic anhydride in DMF.

### 5.1.6 Reverse Phase HPLC Methods

Reverse phase HPLC data was obtained on an Agilent 1200 series HPLC using a Machery-Nagel Nucleodur C18 column. Analysis was performed using a gradient method, eluting with 5 – 80 % MeCN/$H_2O$ over 16 minutes at a flow rate of 2 mL/min. Reactions using an internal standard required prior HPLC calibration using samples containing varying molarities of product and caffeine, allowing calculation of the response factor by substituting values into *Equation 5.1*. Screening reactions were then conducted using a known molarity of caffeine internal standard.

$$Response\ Factor = \frac{\left(\frac{Area}{Molarity}\right)Product}{\left(\frac{Area}{Molarity}\right)Standard}$$

*Equation 5.1: The calculation of response factors for HPLC calibration*

## 5.2    General Procedures

### 5.2.1    A Modular Protocol for the Synthesis of 2,5-Diaryl Tetrazoles

#### A:  Optimisation of Suzuki Reaction Using High-Throughput Screening

In a glovebox, a 24 or 96-well plate containing 1 mL or 250 uL vials was charged with a relevant Pd precatalyst (10 mol%). 1-benzyl-5-bromo-1*H*-tetrazole (1 equiv.) and an aryl boronic acid (1.5 equiv.) were then added as a solution/slurry in a specified solvent (0.1 M). An inorganic base (2 equiv.) was then added as a solution in water (20 % volume of solvent). The plate was then sealed, removed from the glovebox and stirred at 100 °C for 24 hours. The reaction mixtures were diluted to a concentration of around 4 mM with acetonitrile containing a known concentration of internal standard and analysed by HPLC.  Conversion values obtained were first normalised using the internal standard peak and reported as relative values of the most successful reaction mixture.

#### B:  Targeted Optimisation of Suzuki Reaction

1-benzyl-5-bromo-1*H*-tetrazole (1 equiv.) and an aryl boronic acid were added to either 0.5-2 mL microwave vials or 2 mL HPLC vials. The vessels were then charged with the relevant palladium precatalyst as a solution in the solvent. In the instances where a palladium source and ligand were employed, both catalyst and ligand were added as a solution in the solvent. In the instances where the palladium source was not soluble in the solvent, the catalyst was added as a solid prior to the solvent. Base was added as a solution in water, and the vessel was sealed and purged with nitrogen. In the instances where extremely low equivalents of water were used, the base was added as a solid after the addition of water. Following reaction completion, the reaction mixture was diluted with a solution of caffeine (0.5 equiv.) in acetonitrile. The mixture was further diluted to a concentration of around 4 mM, analysed by LCMS, and conversion values obtained.

#### C:  Optimisation of Hydrogenolysis Using High-Throughput Screening

To a 24 or 96-well plate containing 1 mL vials was added a palladium on carbon catalyst, which was weighed using a Mettler Toledo QX-96 automated weighing instrument. 1-benzyl-5-phenyl-1*H*-tetrazole (1 equiv.) was added as a solution in the relevant solvent (0.17 M), and in some specified cases, acetic acid (1 equiv.) was added at this stage. The vials were sealed using caps that had been pierced 5-10 times with a blunt needle and exposed to a hydrogen atmosphere of known pressure for 24 hours at either 40 °C or room temperature. Following reaction completion, the reaction mixtures were diluted to concentration of around 4 mM with acetonitrile and analysed by HPLC.  Conversion values were reported as a ratio of debenzylated product relative to remaining starting material.

## D: Targeted Optimisation of Hydrogenolysis

To eight HEL HP ChemScan reaction vessels was added a palladium on carbon catalyst. 1-benzyl-5-phenyl-1*H*-tetrazole (1 equiv.) was added as a solution in ethanol (0.1 M). The vessels are then sealed and exposed to a hydrogen atmosphere of a known pressure at room temperature for 16 hours. Following reaction completion, the reaction mixtures were diluted to a concentration of around 4 mM with acetonitrile and analysed by HPLC. Conversion values were reported as a ratio of debenzylated product relative to remaining starting material.

## E: Optimisation of One-Pot Suzuki-Hydrogenolysis

To eight Biotage Endeavor reaction vessels was added a solution of 1-benzyl-5-phenyl-1*H*-tetrazole (1 equiv.), phenylboronic acid (1.3 equiv.), and XPhos Pd G3 (3 mol%) as a solution in a known volume of solvent. Evonik Noblyst® P1071 20 % palladium on carbon was added to each vessel, before caesium carbonate (1.5 equiv.) was added as a solution in water (100 equiv.). The vessels were purged with nitrogen and heated at 100 °C for 4 hours. The vessels were then cooled to 40 °C, and in some instances, ethanol was added to the mixture at this stage. The reaction mixture was then stirred under a hydrogen atmosphere of a specified pressure at 40 °C for between 16 and 24 hours. Following reaction completion, the reaction mixture was diluted with a solution of caffeine (0.5 equiv.) in acetonitrile. The mixture was further diluted to a concentration of around 4 mM, analysed by LCMS, and conversion values obtained.

## F: One-Pot Synthesis of 5-Aryl Tetrazoles by Suzuki-Hydrogenolysis

To a 10 mL Biotage Endeavor reaction vessel was added Evonik Noblyst® P1071 20 % palladium on carbon (10 mol%). 1-benzyl-5-bromo-1*H*-tetrazole (1 equiv.), an aryl boronic acid (1.3 equiv.) and XPhos Pd G3 (3 mol%) were then added as a solution in toluene (0.1 M). To the resulting suspension was added caesium carbonate (1.5 equiv.) as a solution in water (100 equiv.), at which point the vessel was purged with nitrogen and stirred at 100 °C for 4 hours. Upon cooling to room temperature, ethanol (50 % volume of toluene) was added before the vessel was placed under a hydrogen atmosphere and heated at 40 °C for a further 18 hours. Upon reaction completion, the mixture was passed through celite and partitioned between ethyl acetate (30 mL) and water (30 mL). The organic phase was washed twice more with water (2 x 30 mL), before the aqueous phases were combined and acidified using 2M HCl solution (20 mL). The acidic aqueous phase was then washed three times with ethyl acetate (3 x 30 mL), before all organic layers were then combined, passed through a phase separator and concentrated under reduced pressure to yield the product.

### G:  Two-Step Protocol for the Synthesis of 5-Aryl Tetrazoles

To a microwave vial containing 1-benzyl-5-bromo-1*H*-tetrazole (1 equiv.), an aryl or vinyl boronic acid (1.5 equiv.) and XPhos Pd G3 (3 mol%) was added toluene (0.2 M). The vessel was purged with nitrogen, and caesium carbonate (2 equiv.) and water (10 equiv.) were added. The mixture was stirred at 100 °C for 2 hours, before being cooled to room temperature. The mixture was diluted with ethyl acetate (10 mL) and passed through a celite plug, which was then washed with a further portion of ethyl acetate (10 mL). The solution was concentrated under reduced pressure and purified by column chromatography. Isolation of the intermediate 1-benzyl-5-aryltetrazole was confirmed by ^{1}H NMR spectroscopy, before the species was added to chamber A of a 2 x 10 mL COware reaction vessel[289] as a solution in ethanol (0.1 M). Evonik Noblyst® P1071 20 % palladium on carbon (10 mol%) was also added to chamber A, while chamber B was charged with zinc powder (1.8 mmol, 118 mg) and 36 % hydrogen chloride solution (343 µL, 4 mmol). The vessel was sealed and stirred at 40 °C for 18 hours. The mixture was cooled to room temperature, diluted with ethyl acetate (10 mL) and passed through a celite plug, which was washed with a further portion of ethyl acetate (10 mL). This organic phase was washed twice with water (2 x 30 mL), before the aqueous phases were combined and acidified using 2M HCl solution (20 mL). The acidic aqueous phase was then washed three times with ethyl acetate (3 x 30 mL), before all organic layers were then combined, passed through a phase separator and concentrated under reduced pressure to yield the product.

### H:  The *N*-Arylation of 5-Aryl Tetrazoles

In accordance with previous literature precedent,[264] a solution of 5-phenyltetrazole (1 equiv.), aryl boronic acid (2 equiv.), and copper(I) oxide (0.05 equiv.) in DMSO (0.5 M) was stirred under an oxygen atmosphere at 110 °C until full consumption of the starting material was observed. The reaction mixture was cooled, diluted with DCM, and washed successively with 1M HCl and brine. The solution was passed through a phase separator, concentrated under vacuum and purified by column chromatography.

### *5.2.2   Metal-Free Coupling of Nitrile Imines and Boronic Acids*

### I:  Synthesis of 2,5-Tetrazole Starting Materials

In accordance with previous literature precedent,[257,258] a solution of the appropriate aldehyde (1 equiv.) and benzenesulfonohydrazide (1.1 equiv.) was stirred in ethanol (1 M) at room temperature for 1 hour. The reaction was quenched through the addition of water (0.05 M) and the resulting white solid was collected by filtration. Simultaneously, the relevant aniline (1 equiv.) was dissolved in a 2:2:1 solution of ethanol, $H_2O$, and HCl (0.5 M). To this solution was added $NaNO_2$ (1.1 equiv), dissolved in minimal $H_2O$, at 0 °C. The

corresponding mixture was stirred for 1 hour, before the benzensufonohydrazone obtained the first step was dissolved in pyridine (0.25 M) and slowly added to the reaction mixture at 0 °C. The resulting milieu was allowed to warm to room temperature and stirred for an additional 5 hours. The solution was diluted with DCM and washed successively with 1M HCl and brine. The solution was passed through a phase separator, concentrated under vacuum and purified by column chromatography.

### J: Optimisation of Reaction Conditions by HPLC

Tetrazole and a boron species were dissolved in the appropriate solvent and irradiated with UV light for a specified period of time. In some optimisation campaigns, the solution was diluted with acetone and 30 % hydrogen peroxide solution. VO(acac)$_2$ was added and the solution left to stir at room temperature for 4 hours.[320] The reaction mixture was then diluted with 50 mM solution of caffeine in MeCN, before being further diluted to concentration of around 4 mM with acetonitrile and water and analysed by HPLC.

### K: Optimisation of Reaction Conditions by $^{19}$F NMR

The 2,5-diaryl tetrazole **3.5** and 3-fluoro-4-methoxyphenylboronic acid were dissolved in the appropriate solvent and irradiated with UV light for a specified period of time. A solution of reaction standard 5-phenyl-2-(3-fluoro-4-methoxyphenyl)-tetrazole (**3.3**, 0.1 M in CDCl$_3$) was added to the reaction mixture, and the resulting solution was analysed by $^{19}$F NMR spectroscopy. Product peaks at -112.09, -115.17, -133.23 and -135.65 ppm were integrated against the peak of tetrazole **3.3** at -131.75 ppm. Conversion of primary hydrazide by-product **3.22** was also monitored at -106.65 ppm.

### L: UV Light-Mediated Coupling of Nitrile Imines and Boronic Acids

To an oven-dried quartz round-bottom flask (50 mL) equipped with a stirrer bar was added 3 Å molecular sieves (400 mgmmol$^{-1}$), tetrazole (1 equiv.), and boronic acid (3 equiv.). The mixture was dissolved in THF (0.1 M), purged with N$_2$ and irradiated under a UV lamp with stirring for 16 hours. The reaction mixture was diluted with ethyl acetate, filtered through Celite and rinsed with additional ethyl acetate. The crude solution was concentrated under vacuum and purified by column chromatography.

### M: Solid Phase Peptide Synthesis

SPPS of the desired peptides was accomplished using Wang resin, with the first amino acid residue of the sequence first converted into a symmetrical anhydride to enable loading onto the resin. The amino acid (1 equiv.) was dissolved in dry DCM (0.25 M), with a few drops of DMF necessary to ensure complete dissolution. Diisopropylcarbodiimide (DIC) (0.5 equiv.) was then dissolved in minimal dry DCM and added to the flask, and the mixture was stirred at 0 °C for 10 minutes, with additional DMF added to dissolve any precipitate. The solution

was allowed to warm to room temperature, stirred for an additional ten minutes, and the excess solvent removed using a rotary evaporator.

The symmetrical anhydride was then manually loaded onto the resin using a Merrifield bubbler (*Table 5.1*).

*Table 5.1: The procedure for the manual attachment of the first residue to Wang resin*

| Step | Solvent/Reagents | Volume (mL) | Time (min) | Mixing | Iterations |
|---|---|---|---|---|---|
| **Swell** | DCM | 5 | 10 | - | - |
| **Wash** | DMF | 5 | 0.5 | N$_2$ bubbling | 5 |
| **Esterification** | Amino acid anhydride (5 equiv.), DMAP (1 equiv.), DMF | 5 | 60 | N$_2$ bubbling | - |
| **Wash** | DMF | 5 | 0.5 | N$_2$ bubbling | 5 |
| **Wash** | DCM | 5 | 0.5 | N$_2$ bubbling | 5 |
| **Wash** | Diethyl ether | 5 | 0.5 | N$_2$ bubbling | 5 |
| **Vacuum Dry** | - | - | 10 | - | - |
| **Loading Test** | 20 % piperidine in DMF | 10 | 15 | Sonication | 2 |
| **Swell** | DCM | 5 | 10 | - | - |
| **Wash** | DMF | 5 | 0.5 | N$_2$ bubbling | 5 |
| **Capping** | Acetic anhydride (10 equiv.), Pyridine (1 equiv.), DMF | 5 | 30 | N$_2$ bubbling | - |
| **Wash** | DMF | 5 | 0.5 | N$_2$ bubbling | 5 |
| **Wash** | DCM | 5 | 0.5 | N$_2$ bubbling | 5 |
| **Wash** | Diethyl ether | 5 | 0.5 | N$_2$ bubbling | 5 |
| **Vacuum Dry** | - | - | 10 | - | - |

The extent of loading was assessed using the Fmoc loading test. A known weight of resin (~5-10 mg) was added to two 10 mL volumetric flasks, which were then filled with a solution of 20 % piperidine in DMF (10 mL) and sonicated for 15 minutes. The UV absorption of the samples at a wavelength of 302 nm was measured relative to a blank

solution of 20 % piperidine in DMF. The total loading of the resin was then derived from this information following derivation of the Beer-Lambert law (*Equation 5.2*).

$$Loading = \frac{A \times 10}{m \times 7.8}$$

*Equation 5.2: A derivation of the Beer-Lambert law required to ascertain the extent of amino acid loading on the solid support required for SPPS*

The two values obtained from this expression were then averaged to obtain the total loading of the resin. This loading value was employed to confirm the successful loading of the residue prior to capping the remaining hydroxyl groups of the Wang resin. It was also used to calculate the scale that would be required in the further synthesis of the peptide.

All subsequent residues were then loaded using an automated coupling process (*Table 5.2*, *Table 5.3*), which was terminated prior to the capping of the final residue (*Table 5.4*).

*Table 5.2: The procedure for the automated addition of the first amino to loaded resin*

| Step | Solvent/Reagents | Volume (mL) | Time (min) | Mixing | Iterations |
|---|---|---|---|---|---|
| Swell | DCM | 5 | 10 | - | - |
| Wash | DCM | 5 | 0.5 | Shaking | 5 |
| Wash | DMF | 5 | 0.5 | Shaking | 5 |
| Deprotection | 20 % piperidine in DMF | 5 | 5 | Shaking | - |
| Wash | DMF | 5 | 0.5 | Shaking | 5 |
| Coupling | Amino acid (5 equiv.), HATU, (5 equiv.), DIPEA (5 equiv.), DMF | 5 | 20 | Shaking | - |
| Wash | DMF | 5 | 0.5 | Shaking | 5 |

*Table 5.3: The procedure for the automated coupling of subsequent amino acids*

| Step | Solvent/Reagents | Volume (mL) | Time (min) | Mixing | Iterations |
|---|---|---|---|---|---|
| Deprotection | 20 % piperidine in DMF | 5 | 10 | Shaking | - |
| Wash | DMF | 5 | 0.5 | Shaking | 5 |

| Step | Solvent/Reagents | Volume (mL) | Time (min) | Mixing | Iterations |
|---|---|---|---|---|---|
| Coupling | Amino acid (5 equiv.), HATU, (5 equiv.), DIPEA (5 equiv.), DMF | 5 | 20 | Shaking | - |
| Wash | DMF | 5 | 0.5 | Shaking | 5 |

*Table 5.4: The procedure for the automated coupling of the final amino acid*

| Step | Solvent/Reagents | Volume (mL) | Time (min) | Mixing | Iterations |
|---|---|---|---|---|---|
| Deprotection | 20 % piperidine in DMF | 5 | 10 | Shaking | - |
| Wash | DMF | 5 | 0.5 | Shaking | 5 |
| Coupling | Amino acid (5 equiv.), HATU, (5 equiv.), DIPEA (5 equiv.), DMF | 5 | 20 | Shaking | - |
| Wash | DMF | 5 | 0.5 | Shaking | 5 |
| Wash | DCM | 5 | 0.5 | Shaking | 5 |
| Drain Dry | - | - | 10 | - | - |

The peptide was then capped with tetrazole **3.65** by employing the procedure outlined in *Table 5.5*.

*Table 5.5: The procedure for the capping of the peptide using tetrazole **3.65***

| Step | Solvent/Reagents | Volume (mL) | Time (min) | Mixing | Iterations |
|---|---|---|---|---|---|
| Swell | DCM | 5 | 10 | - | - |
| Wash | DMF | 5 | 0.5 | $N_2$ bubbling | 5 |
| Deprotection | 20 % piperidine in DMF | 5 | 10 | $N_2$ bubbling | - |
| Wash | DMF | 5 | 0.5 | $N_2$ bubbling | 5 |
| Coupling | Tetrazole **3.65** (2.5 equiv.), HATU, (2.5 equiv.), DIPEA (5 equiv.), DMF | 5 | 240 | $N_2$ bubbling | - |

| | | | | | | |
|---|---|---|---|---|---|---|
| **Wash** | DMF | 5 | 0.5 | N$_2$ bubbling | 5 |
| **Wash** | DCM | 5 | 0.5 | N$_2$ bubbling | 5 |
| **Wash** | Diethyl ether | 5 | 0.5 | N$_2$ bubbling | 5 |
| **Vacuum Dry** | - | - | 10 | - | - |

Recovery of the peptide from the resin was first performed on a trial scale (~15 mg). To this small mass of loaded resin was added ~250 µL of a solution of TFA:H$_2$O:TIPS (95:2.5:2.5 v/v). The solution was stirred for one hour at room temperature before it was decanted into cold diethyl ether (~1 mL) to precipitate the peptide. This suspension was centrifuged for 3 minutes, and the liquid phase discarded. The solid peptide was washed with further portions of cold ether and centrifuged two further times. The resulting crude peptide was dissolved in an acetonitrile/water mixture and analysed by LCMS.

Full-scale cleavage of the peptide from the resin was then accomplished using ~10 mL of the appropriate cleavage solution. A falcon tube containing diethyl ether was brought to 0 °C and used to precipitate the peptide product through drop-wise addition of the cleavage solution to the cold ether. The peptide was again washed by centrifugation (x3). Purification of the recovered crude was conducted using preparative HPLC and a solvent system of acetonitrile and water. Purified samples were isolated from solution *via* freeze drying.

## N: Synthesis of Aldehyde Hydrazones

Phenyl hydrazine hydrochloride (1 equiv.) was washed with 1M NaOH solution to generate the free phenyl hydrazine. This compound was dissolved and minimal EtOH and added dropwise to a solution of the relevant aryl aldehyde (1 equiv.) in EtOH (2.5 M). A few drops of H$_2$SO$_4$ were added to accelerate the reaction. The solution was stirred until consumption of the aldehyde starting material, and the mixture was filtered to isolate the product as a precipitate, which was used in the following steps without further purification. In the circumstances where the product would fail to precipitate, the reaction mixture was concentrated to dryness, and purified by column chromatography.

## O: Chlorination of Aldehyde Hydrazones

In accordance with previous literature precedent,[205] to an oven-dried flask under nitrogen was added *N*-chlorosuccinimde (1.7 equiv.) in DCM (1 M). Dimethylsulfide (3 equiv.) was added to the solution dropwise at 0 °C, maintaining a temperature of below 10 °C at all times. The reaction mixture was stirred for an additional 15 minutes, and then cooled to -78 °C. A solution of the relevant hydrazone (1 equiv.) was dissolved in minimal DCM and added dropwise to the reaction mixture. Stirring was maintained at -78 °C for 2 hours before being raised to room temperature. Following consumption of the hydrazone starting material,

the mixture was further diluted by DCM and washed successively with $H_2O$ and brine. The solution was passed through a phase separator, concentrated under vacuum and purified by column chromatography.

### P: Synthesis of Alkyl Hydrazides

To a solution of the relevant acid chloride (1 equiv.) and pyridine (10 equiv.) in DCM (1M) was added the relevant hydrazine (5 equiv.) at 0 °C. The reaction mixture was left to stir overnight at room temperature, before it was quenched using $H_2O$. The mixture was partitioned between DCM and $H_2O$, and the organic layer was washed successively with a further portion of $H_2O$ and brine. The solution was passed through a phase separator, concentrated under vacuum and purified by column chromatography.

### Q: Chlorination of Alkyl Hydrazides

In accordance with previous literature precedent,[419] to a solution of triphenylphosphine (1.2 equiv.) in MeCN (0.7 M) was added the relevant alkyl hydrazide (1 equiv.) and carbon tetrachloride (1.3 equiv.) at room temperature. The solution was stirred at this temperature overnight, before the reaction mixture was concentrated under vacuum. The resulting crude material was purified by column chromatography.

### R: Synthesis of Hydroxamoyl Chlorides

In accordance with previous literature precedent,[420] a solution of the relevant aldehyde (1 equiv.), hydroxylamine hydrochloride (2 equiv.), and sodium hydroxide (2 equiv.) in ethanol (0.8 M) was refluxed for 2 hours. The suspension was filtered, and the solid was washed with a further portion of ethanol. The filtrate was concentrated under vacuum and the residue dissolved in ethyl acetate. The organic layer was washed with water and brine, passed through a hydrophobic frit and concentrated under vacuum. The crude hydrazone was dissolved in DMF (0.7 M) and *N*-chlorosuccinimide (1.1 equiv.) was added in 8-10 portions to maintain the temperature below 40 °C. The reaction mixture was stirred at room temperature for 6 hours, when it was diluted with ethyl acetate. The organic layer was sequentially washed with 5 % lithium chloride solution, water, and brine, passed through a hydrophobic frit and concentrated under reduced pressure. The obtained residue was purified by column chromatography.

### S: Optimisation of Hydrazonyl Chloride Reaction Conditions

Hydrazonyl chloride **3.70** and 4-methoxyphenylboronic acid were added to the appropriate solvent. Base was added and the mixture was stirred at a specified temperature for the indicated period of time. Following reaction completion, a solution of compound **3.3** (0.2 M in DCM) was added to the reaction mixture. When using an inorganic base, the mixture was then filtered through celite to remove residual solids. The solution was spiked with $CDCl_3$

and analysed by $^{19}$F NMR spectroscopy. Product peaks at -112.31 and -115.01 ppm were integrated against the peak of reaction standard compound **3.3** at -132.21 ppm.

### T: Optimisation of Hydroxamoyl Chloride Reaction Conditions

Hydroxamoyl chloride **3.98** and the appropriate boronic acid were dissolved in a specified solvent. Base was added, and the reaction mixture was stirred at the specified temperature for the indicated period of time. Following reaction completion, a solution of 1,4-difluorobenzene (0.75 M in CDCl$_3$) was added to the reaction mixture. When using an inorganic base, the mixture was then filtered through celite to remove residual solids. The solution was analysed by $^{19}$F NMR spectroscopy. Product peaks at -111.76 and -111.94 ppm were integrated against the peak of reaction standard 1,4-difluorobenzene at -119.63 ppm.

### U: Base-Mediated Coupling of Hydrazonyl Chlorides and Aryl Boronic Acids

To an oven-dried 2-5 mL microwave vial was added 3 Å molecular sieves (400 mgmmol$^{-1}$), hydrazonyl chloride (1 equiv.), and boronic acid (2 equiv.). The mixture was dissolved in toluene (0.1 M), and K$_3$PO$_4$ (3 equiv.) was added to initiate the reaction. The solution was purged with N$_2$ and heated at 110 °C for 16 h. The reaction mixture was diluted with ethyl acetate, filtered through Celite and rinsed with additional ethyl acetate. The crude solution was concentrated under vacuum and purified by column chromatography.

### V: Base-Mediated Coupling of Hydroxamoyl Chlorides and Aryl Boronic Acids

To an oven-dried 5 mL microwave vial was added hydroxamoyl chloride (1 equiv.) and boronic acid (2 equiv.). The mixture was dissolved in chloroform (0.1 M), and *N,N'*-dimethylaniline (5 equiv.) was added to initiate the reaction. The solution was purged with N$_2$ and heated at 60 °C for 3 h. The reaction mixture was diluted with DCM and washed with 1M HCl solution. The organic phase was separated, washed with brine, passed through a phase separator and concentrated under vacuum. The crude residue was purified by column chromatography.

### 5.2.3 The Quantification of Nitrile Imine Reactivity Profiles

#### W: Synthesis of Reaction Products

Tetrazole **4.10** (1 equiv.) and the relevant substrate (10 equiv.) were dissolved in an acetonitrile and water mixture (9:1, 0.05 M) in a 50 mL quartz round-bottom flask. The mixture was stirred under the presence of UV light irradiation at room temperature for 16 hours, before the solvent was removed under reduced pressure. The crude residue was then purified by column chromatography.

### X: Competition Experiments

Tetrazole **4.10** (4.73 mg, 0.015 mmol) was added to a 2 mL HPLC vial. Both reaction partners were then added to the vial as 0.06 M standard solutions in a 9:1 acetonitrile and water mixture (250 μL each), and the resulting solution was stirred in the presence of UV light irradiation for 16 hours at room temperature. The reaction mixture was then spiked with 1,4-difluorobenzene (0.06 M in DMSO), and the solution was analysed using ^{19}F NMR spectroscopy. The diagnostic ^{19}F NMR shifts employed in the identification of specific compounds is detailed in *Table 5.6*.

*Table 5.6: ^{19}F NMR signals of interest in the subsequent competition experiments*
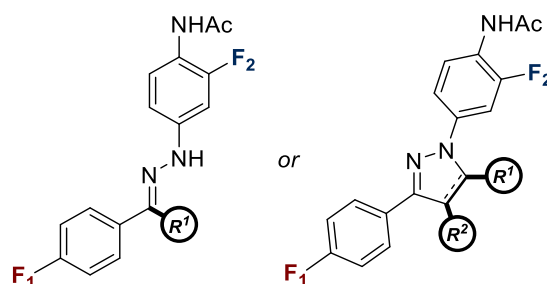


| Entry | Compound | Mass added to 10 mL MeCN:H₂O (0.6 mmol) | F₁ (ppm) | F₂ (ppm) |
|:---:|:---:|:---:|:---:|:---:|
| 1 | Standard | - | 120.00 | - |
| 2 | 4.10 | - | 110.06 | 122.36 |
| 3 | 4.1 | 58.2 mg | 111.82 | 122.98 |
| 4 | 4.2 | 46.9 μL | 113.94 | 124.54 |
| 5 | 4.3 | 76.9 μL | 113.47 | 123.66 |
| 6 | 4.4 | 80.4 μL | 114.05 | 123.30 |
| 7 | 4.5 | 34.3 μL | 107.63, 108.36 | 123.25, 123.93 |
| 8 | 4.6 | 54.8 μL | 113.82 | 123.42 |
| 9 | 4.7 | 61.2 μL | 114.13 | 123.18 |
| 10 | 4.8 | 45.9 μL | 106.90 | 123.14 |
| 11 | 4.9 | 91.2 mg | 113.00, 114.83 | 123.46 |

## 5.3    Optimisation of Reaction Conditions

### 5.3.1   A Modular Protocol for the Synthesis of 2,5-Diaryl Tetrazoles

#### 5.3.1.1 Optimisation of Suzuki Reaction

**Catalyst Screen with Phenyl Boronic Acid**
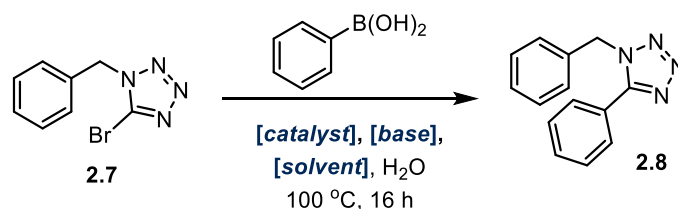


The screen was conducted as outlined in general procedure A using 24 x 250 μL vials, each containing 1-benzyl-5-bromo-1$H$-tetrazole (0.60 mg, 2.5 μmol), phenylboronic acid (0.46 mg, 3.75 μmol), XPhos, SPhos, DT$^n$BuP, AmPhos, DTBPF, or $^t$Bu$_3$P Pd G3 precatalysts (all 0.25 μmol), potassium carbonate (0.70 mg, 5 μmol) or potassium phosphate (1.06 mg, 5 μmol), toluene or dioxane (both 240 μL), and water (60 μL). The results obtained are detailed in *Table 5.7*.

*Table 5.7: Conversion values obtained from the above screen*

| Entry | Catalyst (μg) | Solvent (240 μL) | Base (mg) | Conversion[a] |
|:---:|:---:|:---:|:---:|:---:|
| 1 | XPhos (212 μg) | Toluene | K$_3$PO$_4$ (1.06 mg) | **0.36** |
| 2 | SPhos (195 μg) | Toluene | K$_3$PO$_4$ (1.06 mg) | **0.14** |
| 3 | DTnBuP (148 μg) | Toluene | K$_3$PO$_4$ (1.06 mg) | **0.03** |
| 4 | AmPhos (177 μg) | Toluene | K$_3$PO$_4$ (1.06 mg) | **0.01** |
| 5 | DTBPF (211 μg) | Toluene | K$_3$PO$_4$ (1.06 mg) | **0.09** |
| 6 | $t$Bu$_3$P (128 μg) | Toluene | K$_3$PO$_4$ (1.06 mg) | **0.02** |
| 7 | XPhos (212 μg) | Toluene | K$_2$CO$_3$ (0.70 mg) | **1.00** |
| 8 | SPhos (195 μg) | Toluene | K$_2$CO$_3$ (0.70 mg) | **0.17** |
| 9 | DTnBuP (148 μg) | Toluene | K$_2$CO$_3$ (0.70 mg) | **0.25** |
| 10 | AmPhos (177 μg) | Toluene | K$_2$CO$_3$ (0.70 mg) | **0.37** |
| 11 | DTBPF (211 μg) | Toluene | K$_2$CO$_3$ (0.70 mg) | **0.13** |
| 12 | $t$Bu$_3$P (128 μg) | Toluene | K$_2$CO$_3$ (0.70 mg) | **0.06** |
| 13 | XPhos (212 μg) | Dioxane | K$_3$PO$_4$ (1.06 mg) | **0.17** |
| 14 | SPhos (195 μg) | Dioxane | K$_3$PO$_4$ (1.06 mg) | **0.24** |

| 15 | DTnBuP (148 µg) | Dioxane | $K_3PO_4$ (1.06 mg) | **0.08** |
| 16 | AmPhos (177 µg) | Dioxane | $K_3PO_4$ (1.06 mg) | **0.05** |
| 17 | DTBPF (211 µg) | Dioxane | $K_3PO_4$ (1.06 mg) | **0.06** |
| 18 | $t$Bu$_3$P (128 µg) | Dioxane | $K_3PO_4$ (1.06 mg) | **0.03** |
| 19 | XPhos (212 µg) | Dioxane | $K_2CO_3$ (0.70 mg) | **0.18** |
| 20 | SPhos (195 µg) | Dioxane | $K_2CO_3$ (0.70 mg) | **0.16** |
| 21 | DTnBuP (148 µg) | Dioxane | $K_2CO_3$ (0.70 mg) | **0.15** |
| 22 | AmPhos (177 µg) | Dioxane | $K_2CO_3$ (0.70 mg) | **0.10** |
| 23 | DTBPF (211 µg) | Dioxane | $K_2CO_3$ (0.70 mg) | **0.03** |
| 24 | $t$Bu$_3$P (128 µg) | Dioxane | $K_2CO_3$ (0.70 mg) | **0.04** |

[a]Conversions determined by HPLC and reported relative to the highest recorded value with reference to an internal standard.

**Screen of XPhos Source**
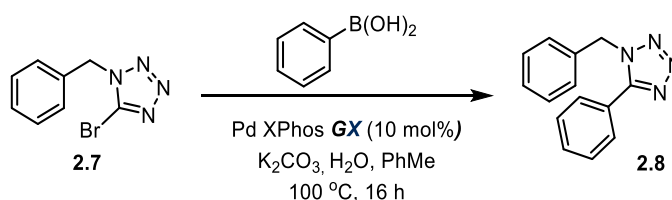


The screen was conducted as outlined in general procedure B using 5 x 2.5 mL microwave vials, each containing 1-benzyl-5-bromo-1*H*-tetrazole (12.0 mg, 50 µmol), phenylboronic acid (9.1 mg, 75 µmol), an XPhos precatalyst (5 µmol), potassium carbonate (14 mg, 100 µmol), toluene (500 µL), and water (9 µL, 500 µmol). In the instance where XPhos (2.7 mg, 5 µmol) was employed, palladium(II) acetate (1.1 mg, 5 µmol) was also added as a palladium source. The reaction was stirred at 100 °C for 3 hours. The results obtained are detailed in *Table 2.1* and *Table 5.8*

*Table 5.8: The conditions employed in the above screen*

| Entry | (Pre)catalyst (mg) | Conversion (%)[a] |
|---|---|---|
| 1 | XPhos (4.8 mg) + Pd(OAc)$_2$ (1.1 mg) | **50** |
| 2 | XPhos Pd G1 (3.7 mg) | **65** |
| 3 | XPhos Pd G2 (3.9 mg) | **66** |
| 4 | XPhos Pd G3 (4.2 mg) | **63** |
| 5 | XPhos Pd G4 (4.3 mg) | **70** |

[a]Conversion values determined by LCMS with reference to caffeine as an internal standard.
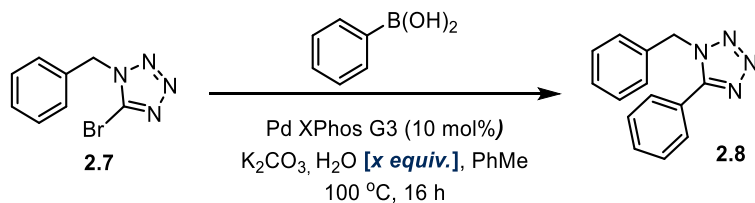
**Screen of Water Stoichiometry**



The screen was conducted as outlined in general procedure B using 5 x 2.5 mL microwave vials, each containing 1-benzyl-5-bromo-1*H*-tetrazole (12.0 mg, 50 μmol), phenylboronic acid (9.1 mg, 75 μmol), XPhos Pd G3 (4.2 mg, 5 μmol), potassium carbonate (14 mg, 100 μmol), toluene (500 μL), and water (1-50 equivalents). The reaction was stirred at 100 °C for 3 hours. The results obtained are detailed in *Table 2.2* and *Table 5.11*

*Table 5.9: The conditions employed in the above screen*

| Entry | Water (μL, mmol) | Conversion (%)[a] |
|:-----:|:----------------:|:-----------------:|
| 1 | 0.9 μL, 0.05 mmol | 64 |
| 2 | 4.5 μL, 0.25 mmol | 73 |
| 3 | 9.0 μL, 0.50 mmol | 76 |
| 4 | 18 μL, 1.00 mmol | 75 |
| 5 | 45 μL, 2.50 mmol | 70 |

[a]Conversion values determined by LCMS with reference to caffeine as an internal standard.

**Catalyst Screen with Other Boronic Acids**



The screen was conducted as outlined in general procedure A using 72 x 1 mL vials, each containing 1-benzyl-5-bromo-1*H*-tetrazole (2.40 mg, 10 μmol), 4-methoxyphenylboronic acid, 4-fluorophenylboronic acid, or 4-cyanophenylboronic acid (all 15 μmol), XPhos, SPhos, DT$^n$BuP, AmPhos, DTBPF, or $^t$Bu$_3$P Pd G3 precatalysts (all 1 μmol), potassium carbonate (2.50 mg, 20 μmol) or caesium carbonate (2.80 mg, 20 μmol), toluene or acetonitrile (both 960 μL), and water (240 μL). The results obtained are detailed in *Table 5.10*.

| Entry | ArB(OH)$_2$ (mg) | Catalyst (μg) | Solvent (960 μL) | Base (mg) | Conversion[a] |
|---|---|---|---|---|---|
| 1 | 4-methoxyphenyl (2.28 mg) | XPhos (848 μg) | MeCN | Cs$_2$CO$_3$ (2.8 mg) | **0.27** |
| 2 | 4-methoxyphenyl (2.28 mg) | SPhos (780 μg) | MeCN | Cs$_2$CO$_3$ (2.8 mg) | **0.19** |
| 3 | 4-methoxyphenyl (2.28 mg) | DTnBuP (592 μg) | MeCN | Cs$_2$CO$_3$ (2.8 mg) | **0.22** |
| 4 | 4-methoxyphenyl (2.28 mg) | AmPhos (708 μg) | MeCN | Cs$_2$CO$_3$ (2.8 mg) | **0.03** |
| 5 | 4-methoxyphenyl (2.28 mg) | DTBPF (844 μg) | MeCN | Cs$_2$CO$_3$ (2.8 mg) | **0.12** |
| 6 | 4-methoxyphenyl (2.28 mg) | $t$Bu$_3$P (512 μg) | MeCN | Cs$_2$CO$_3$ (2.8 mg) | **0.01** |
| 7 | 4-methoxyphenyl (2.28 mg) | XPhos (848 μg) | MeCN | K$_2$CO$_3$ (2.5 mg) | **0.30** |
| 8 | 4-methoxyphenyl (2.28 mg) | SPhos (780 μg) | MeCN | K$_2$CO$_3$ (2.5 mg) | **0.22** |
| 9 | 4-methoxyphenyl (2.28 mg) | DTnBuP (592 μg) | MeCN | K$_2$CO$_3$ (2.5 mg) | **0.31** |
| 10 | 4-methoxyphenyl (2.28 mg) | AmPhos (708 μg) | MeCN | K$_2$CO$_3$ (2.5 mg) | **0.03** |
| 11 | 4-methoxyphenyl (2.28 mg) | DTBPF (844 μg) | MeCN | K$_2$CO$_3$ (2.5 mg) | **0.02** |
| 12 | 4-methoxyphenyl (2.28 mg) | $t$Bu$_3$P (512 μg) | MeCN | K$_2$CO$_3$ (2.5 mg) | **0.04** |
| 13 | 4-methoxyphenyl (2.28 mg) | XPhos (848 μg) | Toluene | Cs$_2$CO$_3$ (2.8 mg) | **0.93** |
| 14 | 4-methoxyphenyl (2.28 mg) | SPhos (780 μg) | Toluene | Cs$_2$CO$_3$ (2.8 mg) | **0.73** |
| 15 | 4-methoxyphenyl (2.28 mg) | DTnBuP (592 μg) | Toluene | Cs$_2$CO$_3$ (2.8 mg) | **1.00** |
| 16 | 4-methoxyphenyl (2.28 mg) | AmPhos (708 μg) | Toluene | Cs$_2$CO$_3$ (2.8 mg) | **0.18** |

| | | | | | |
|---|---|---|---|---|---|
| 17 | 4-methoxyphenyl (2.28 mg) | DTBPF (844 µg) | Toluene | $Cs_2CO_3$ (2.8 mg) | **0.11** |
| 18 | 4-methoxyphenyl (2.28 mg) | $t$Bu$_3$P (512 µg) | Toluene | $Cs_2CO_3$ (2.8 mg) | **0.15** |
| 19 | 4-methoxyphenyl (2.28 mg) | XPhos (848 µg) | Toluene | $K_2CO_3$ (2.5 mg) | **0.67** |
| 20 | 4-methoxyphenyl (2.28 mg) | SPhos (780 µg) | Toluene | $K_2CO_3$ (2.5 mg) | **0.79** |
| 21 | 4-methoxyphenyl (2.28 mg) | DTnBuP (592 µg) | Toluene | $K_2CO_3$ (2.5 mg) | **0.61** |
| 22 | 4-methoxyphenyl (2.28 mg) | AmPhos (708 µg) | Toluene | $K_2CO_3$ (2.5 mg) | **0.18** |
| 23 | 4-methoxyphenyl (2.28 mg) | DTBPF (844 µg) | Toluene | $K_2CO_3$ (2.5 mg) | **0.11** |
| 24 | 4-methoxyphenyl (2.28 mg) | $t$Bu$_3$P (512 µg) | Toluene | $K_2CO_3$ (2.5 mg) | **0.20** |
| 25 | 4-fluorophenyl (2.10 mg) | XPhos (848 µg) | MeCN | $Cs_2CO_3$ (2.8 mg) | **0.22** |
| 26 | 4-fluorophenyl (2.10 mg) | SPhos (780 µg) | MeCN | $Cs_2CO_3$ (2.8 mg) | **0.16** |
| 27 | 4-fluorophenyl (2.10 mg) | DTnBuP (592 µg) | MeCN | $Cs_2CO_3$ (2.8 mg) | **0.23** |
| 28 | 4-fluorophenyl (2.10 mg) | AmPhos (708 µg) | MeCN | $Cs_2CO_3$ (2.8 mg) | **0.02** |
| 29 | 4-fluorophenyl (2.10 mg) | DTBPF (844 µg) | MeCN | $Cs_2CO_3$ (2.8 mg) | **0.02** |
| 30 | 4-fluorophenyl (2.10 mg) | $t$Bu$_3$P (512 µg) | MeCN | $Cs_2CO_3$ (2.8 mg) | **0.01** |
| 31 | 4-fluorophenyl (2.10 mg) | XPhos (848 µg) | MeCN | $K_2CO_3$ (2.5 mg) | **0.20** |
| 32 | 4-fluorophenyl (2.10 mg) | SPhos (780 µg) | MeCN | $K_2CO_3$ (2.5 mg) | **0.15** |
| 33 | 4-fluorophenyl (2.10 mg) | DTnBuP (592 µg) | MeCN | $K_2CO_3$ (2.5 mg) | **0.20** |
| 34 | 4-fluorophenyl | AmPhos | MeCN | $K_2CO_3$ | **0.06** |

| | | | | | |
|---|---|---|---|---|---|
| | (2.10 mg) | (708 µg) | | (2.5 mg) | |
| 35 | 4-fluorophenyl (2.10 mg) | DTBPF (844 µg) | MeCN | $K_2CO_3$ (2.5 mg) | 0.06 |
| 36 | 4-fluorophenyl (2.10 mg) | $t$Bu$_3$P (512 µg) | MeCN | $K_2CO_3$ (2.5 mg) | 0.01 |
| 37 | 4-fluorophenyl (2.10 mg) | XPhos (848 µg) | Toluene | $Cs_2CO_3$ (2.8 mg) | 1.00 |
| 38 | 4-fluorophenyl (2.10 mg) | SPhos (780 µg) | Toluene | $Cs_2CO_3$ (2.8 mg) | 0.95 |
| 39 | 4-fluorophenyl (2.10 mg) | DTnBuP (592 µg) | Toluene | $Cs_2CO_3$ (2.8 mg) | 0.38 |
| 40 | 4-fluorophenyl (2.10 mg) | AmPhos (708 µg) | Toluene | $Cs_2CO_3$ (2.8 mg) | 0.16 |
| 41 | 4-fluorophenyl (2.10 mg) | DTBPF (844 µg) | Toluene | $Cs_2CO_3$ (2.8 mg) | 0.08 |
| 42 | 4-fluorophenyl (2.10 mg) | $t$Bu$_3$P (512 µg) | Toluene | $Cs_2CO_3$ (2.8 mg) | 0.14 |
| 43 | 4-fluorophenyl (2.10 mg) | XPhos (848 µg) | Toluene | $K_2CO_3$ (2.5 mg) | 0.98 |
| 44 | 4-fluorophenyl (2.10 mg) | SPhos (780 µg) | Toluene | $K_2CO_3$ (2.5 mg) | 0.71 |
| 45 | 4-fluorophenyl (2.10 mg) | DTnBuP (592 µg) | Toluene | $K_2CO_3$ (2.5 mg) | 0.32 |
| 46 | 4-fluorophenyl (2.10 mg) | AmPhos (708 µg) | Toluene | $K_2CO_3$ (2.5 mg) | 0.15 |
| 47 | 4-fluorophenyl (2.10 mg) | DTBPF (844 µg) | Toluene | $K_2CO_3$ (2.5 mg) | 0.07 |
| 48 | 4-fluorophenyl (2.10 mg) | $t$Bu$_3$P (512 µg) | Toluene | $K_2CO_3$ (2.5 mg) | 0.10 |
| 49 | 4-cyanophenyl (2.20 mg) | XPhos (848 µg) | MeCN | $Cs_2CO_3$ (2.8 mg) | 0.33 |
| 50 | 4-cyanophenyl (2.20 mg) | SPhos (780 µg) | MeCN | $Cs_2CO_3$ (2.8 mg) | 0.00 |
| 51 | 4-cyanophenyl (2.20 mg) | DTnBuP (592 µg) | MeCN | $Cs_2CO_3$ (2.8 mg) | 0.00 |

| | | | | | |
|---|---|---|---|---|---|
| 52 | 4-cyanophenyl (2.20 mg) | AmPhos (708 μg) | MeCN | $Cs_2CO_3$ (2.8 mg) | **0.00** |
| 53 | 4-cyanophenyl (2.20 mg) | DTBPF (844 μg) | MeCN | $Cs_2CO_3$ (2.8 mg) | **0.19** |
| 54 | 4-cyanophenyl (2.20 mg) | $t$Bu₃P (512 μg) | MeCN | $Cs_2CO_3$ (2.8 mg) | **0.00** |
| 55 | 4-cyanophenyl (2.20 mg) | XPhos (848 μg) | MeCN | $K_2CO_3$ (2.5 mg) | **0.33** |
| 56 | 4-cyanophenyl (2.20 mg) | SPhos (780 μg) | MeCN | $K_2CO_3$ (2.5 mg) | **0.28** |
| 57 | 4-cyanophenyl (2.20 mg) | DTnBuP (592 μg) | MeCN | $K_2CO_3$ (2.5 mg) | **0.21** |
| 58 | 4-cyanophenyl (2.20 mg) | AmPhos (708 μg) | MeCN | $K_2CO_3$ (2.5 mg) | **0.07** |
| 59 | 4-cyanophenyl (2.20 mg) | DTBPF (844 μg) | MeCN | $K_2CO_3$ (2.5 mg) | **0.00** |
| 60 | 4-cyanophenyl (2.20 mg) | $t$Bu₃P (512 μg) | MeCN | $K_2CO_3$ (2.5 mg) | **0.17** |
| 61 | 4-cyanophenyl (2.20 mg) | XPhos (848 μg) | Toluene | $Cs_2CO_3$ (2.8 mg) | **1.00** |
| 62 | 4-cyanophenyl (2.20 mg) | SPhos (780 μg) | Toluene | $Cs_2CO_3$ (2.8 mg) | **0.56** |
| 63 | 4-cyanophenyl (2.20 mg) | DTnBuP (592 μg) | Toluene | $Cs_2CO_3$ (2.8 mg) | **0.73** |
| 64 | 4-cyanophenyl (2.20 mg) | AmPhos (708 μg) | Toluene | $Cs_2CO_3$ (2.8 mg) | **0.14** |
| 65 | 4-cyanophenyl (2.20 mg) | DTBPF (844 μg) | Toluene | $Cs_2CO_3$ (2.8 mg) | **0.58** |
| 66 | 4-cyanophenyl (2.20 mg) | $t$Bu₃P (512 μg) | Toluene | $Cs_2CO_3$ (2.8 mg) | **0.61** |
| 67 | 4-cyanophenyl (2.20 mg) | XPhos (848 μg) | Toluene | $K_2CO_3$ (2.5 mg) | **0.81** |
| 68 | 4-cyanophenyl (2.20 mg) | SPhos (780 μg) | Toluene | $K_2CO_3$ (2.5 mg) | **0.00** |
| 69 | 4-cyanophenyl | DTnBuP | Toluene | $K_2CO_3$ | **0.00** |

| | 4-cyanophenyl | | | (2.5 mg) | |
| | (2.20 mg) | (592 µg) | | | |
| 70 | 4-cyanophenyl | AmPhos | Toluene | K$_2$CO$_3$ | 0.00 |
| | (2.20 mg) | (708 µg) | | (2.5 mg) | |
| 71 | 4-cyanophenyl | DTBPF | Toluene | K$_2$CO$_3$ | 0.33 |
| | (2.20 mg) | (844 µg) | | (2.5 mg) | |
| 72 | 4-cyanophenyl | $t$Bu$_3$P | Toluene | K$_2$CO$_3$ | 0.12 |
| | (2.20 mg) | (512 µg) | | (2.5 mg) | |

ªConversions determined by HPLC and reported relative to the highest recorded value of each substrate with reference to an internal standard.

## Screen of Electron-Deficient Boronic Acids
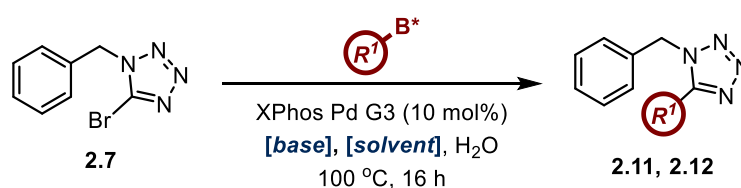


The screen was conducted as outlined in general procedure B using 24 x 2 mL HPLC vials, each containing 1-benzyl-5-bromo-1*H*-tetrazole (12.0 mg, 50 µmol), (4-(trifluoromethyl)phenyl)boronic acid (14.2 mg, 75 µmol), (4-cyanophenyl)boronic acid (11.0 mg, 75 µmol), (4-(trifluoromethyl)phenyl)boronic acid pinacol ester (20.4 mg, 75 µmol), or (4-cyanophenyl)boronic acid pinacol ester (17.2 mg, 75 µmol), XPhos Pd G3 (4.2 mg, 5.0 µmol), caesium carbonate (32.6 mg, 100 µmol), potassium phosphate (21.2 mg, 100 µmol) or potassium carbonate (13.8 mg, 100 µmol), toluene or *n*-butanol (both 500 µL), and water (45 µL, 2500 µmol). The reaction was stirred at 100 °C for 16 hours. The results obtained are detailed in *Table 5.11*.

*Table 5.11: Conversion values obtained from the above screen*

| Entry | Boron Species (mg) | Solvent (500 µL) | Base (mg) | Conversion(%)ª |
|---|---|---|---|---|
| 1 | (4-CF$_3$)PhB(OH)$_2$ (14.2 mg) | Toluene | K$_2$CO$_3$ (13.8 mg) | 54 |
| 2 | (4-CF$_3$)PhB(OH)$_2$ (14.2 mg) | Toluene | Cs$_2$CO$_3$ (32.6 mg) | 59 |
| 3 | (4-CF$_3$)PhB(OH)$_2$ (14.2 mg) | Toluene | K$_3$PO$_4$ (21.2 mg) | 52 |
| 4 | (4-CF$_3$)PhB(OH)$_2$ (14.2 mg) | *n*-Butanol | K$_2$CO$_3$ (13.8 mg) | 13 |

| | | | | |
|---|---|---|---|---|
| 5 | (4-CF$_3$)PhB(OH)$_2$ (14.2 mg) | $n$-Butanol | Cs$_2$CO$_3$ (32.6 mg) | **10** |
| 6 | (4-CF$_3$)PhB(OH)$_2$ (14.2 mg) | $n$-Butanol | K$_3$PO$_4$ (21.2 mg) | **9** |
| 7 | (4-CF$_3$)PhBPin (20.4 mg) | Toluene | K$_2$CO$_3$ (13.8 mg) | **4** |
| 8 | (4-CF$_3$)PhBPin (20.4 mg) | Toluene | Cs$_2$CO$_3$ (32.6 mg) | **9** |
| 9 | (4-CF$_3$)PhBPin (20.4 mg) | Toluene | K$_3$PO$_4$ (21.2 mg) | **15** |
| 10 | (4-CF$_3$)PhBPin (20.4 mg) | $n$-Butanol | K$_2$CO$_3$ (13.8 mg) | **15** |
| 11 | (4-CF$_3$)PhBPin (20.4 mg) | $n$-Butanol | Cs$_2$CO$_3$ (32.6 mg) | **11** |
| 12 | (4-CF$_3$)PhBPin (20.4 mg) | $n$-Butanol | K$_3$PO$_4$ (21.2 mg) | **12** |
| 13 | (4-CN)PhB(OH)$_2$ (11.0 mg) | Toluene | K$_2$CO$_3$ (13.8 mg) | **7** |
| 14 | (4-CN)PhB(OH)$_2$ (11.0 mg) | Toluene | Cs$_2$CO$_3$ (32.6 mg) | **6** |
| 15 | (4-CN)PhB(OH)$_2$ (11.0 mg) | Toluene | K$_3$PO$_4$ (21.2 mg) | **3** |
| 16 | (4-CN)PhB(OH)$_2$ (11.0 mg) | $n$-Butanol | K$_2$CO$_3$ (13.8 mg) | **11** |
| 17 | (4-CN)PhB(OH)$_2$ (11.0 mg) | $n$-Butanol | Cs$_2$CO$_3$ (32.6 mg) | **9** |
| 18 | (4-CN)PhB(OH)$_2$ (11.0 mg) | $n$-Butanol | K$_3$PO$_4$ (21.2 mg) | **5** |
| 19 | (4-CN)PhBPin (17.2 mg) | Toluene | K$_2$CO$_3$ (13.8 mg) | **9** |
| 20 | (4-CN)PhBPin (17.2 mg) | Toluene | Cs$_2$CO$_3$ (32.6 mg) | **27** |
| 21 | (4-CN)PhBPin | Toluene | K$_3$PO$_4$ | **21** |

|    | (17.2 mg) | | (21.2 mg) | |
|----|-----------|--|-----------|--|
| 22 | (4-CN)PhBPin <br> (17.2 mg) | *n*-Butanol | K$_2$CO$_3$ <br> (13.8 mg) | **11** |
| 23 | (4-CN)PhBPin <br> (17.2 mg) | *n*-Butanol | Cs$_2$CO$_3$ <br> (32.6 mg) | **6** |
| 24 | (4-CN)PhBPin <br> (17.2 mg) | *n*-Butanol | K$_3$PO$_4$ <br> (21.2 mg) | **6** |

ᵃConversion values determined by LCMS with reference to caffeine as an internal standard.
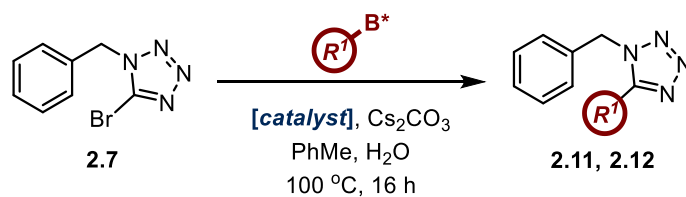
## Screen of Catalyst Loading
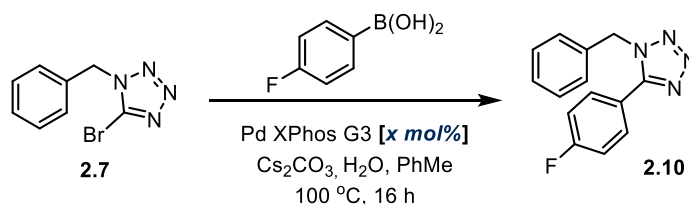


The screen was conducted as outlined in general procedure B using 5 x 2.5 mL microwave vials, each containing 1-benzyl-5-bromo-1*H*-tetrazole (12.0 mg, 50 μmol), 4-fluorophenylboronic acid (10.5 mg, 75 μmol), XPhos Pd G3 (0.5-10 mol%), caesium carbonate (32.6 mg, 100 μmol), toluene (500 μL), and water (9 μL, 500 μmol). The reaction was stirred at 100 °C for 16 hours. The results obtained are detailed in *Table 2.3* and *Table 5.12*.

*Table 5.12: The conditions employed in the above screen*

| Entry | Catalyst Loading (mg, mol%) | Conversion (%)ᵃ |
|-------|------------------------------|------------------|
| 1 | 4.2 mg, 10 mol% | **52** |
| 2 | 2.1 mg, 5 mol% | **47** |
| 3 | 1.1 mg, 2.5 mol% | **14** |
| 4 | 0.4 mg, 1 mol% | **6** |
| 5 | 0.2 mg, 0.5 mol% | **3** |

ᵃConversion values determined by LCMS with reference to caffeine as an internal standard.

## Screen of Bulky, Biaryl Ligands



The screen was conducted as outlined in general procedure B using 24 x 2 mL HPLC vials, each containing 1-benzyl-5-bromo-1$H$-tetrazole (12.0 mg, 50 µmol), (4-(trifluoromethyl)phenyl)boronic acid (14.2 mg, 75 µmol), (4-cyanophenyl)boronic acid (11.0 mg, 75 µmol), (4-(trifluoromethyl)phenyl)boronic acid pinacol ester (20.4 mg, 75 µmol), or (4-cyanophenyl)boronic acid pinacol ester (17.2 mg, 75 µmol), $^t$BuXPhos Pd G1 (1.7 mg, 2.5 µmol), RockPhos Pd G3 (2.1 mg, 2.5 µmol), BrettPhos Pd G3 (2.3 mg, 2.5 µmol), RuPhos Pd G3 (2.1 mg, 2.5 µmol), XPhos Pd G3 (2.1 mg, 2.5 µmol) or *tetrakis*(triphenylphosphine)palladium(0) (2.9 mg, 2.5 µmol), caesium carbonate (32.6 mg, 100 µmol), toluene (400 µL), and water (90 µL, 5000 µmol). The reaction was stirred at 100 °C for 16 hours. The results obtained are detailed in *Table 5.13*.

*Table 5.13: Conversion values obtained from the above screen*

| Entry | Catalyst (mg) | Boron Species (mg) | Conversion[a] |
|-------|---------------|--------------------|---------------|
| 1 | Pd(PPh$_3$)$_4$ (2.9 mg) | (4-CF$_3$)PhB(OH)$_2$ (14.2 mg) | 17 |
| 2 | Pd(PPh$_3$)$_4$ (2.9 mg) | (4-CF$_3$)PhBPin (20.4 mg) | 4 |
| 3 | Pd(PPh$_3$)$_4$ (2.9 mg) | (4-CN)PhB(OH)$_2$ (11.0 mg) | 18 |
| 4 | Pd(PPh$_3$)$_4$ (2.9 mg) | (4-CN)PhBPin (17.2 mg) | 22 |
| 5 | XPhos Pd G3 (2.1 mg) | (4-CF$_3$)PhB(OH)$_2$ (14.2 mg) | 31 |
| 6 | XPhos Pd G3 (2.1 mg) | (4-CF$_3$)PhBPin (20.4 mg) | 25 |
| 7 | XPhos Pd G3 (2.1 mg) | (4-CN)PhB(OH)$_2$ (11.0 mg) | 2 |
| 8 | XPhos Pd G3 (2.1 mg) | (4-CN)PhBPin (17.2 mg) | 29 |
| 9 | $^t$BuXPhos Pd G1 (1.7 mg) | (4-CF$_3$)PhB(OH)$_2$ (14.2 mg) | 2 |
| 10 | $^t$BuXPhos Pd G1 (1.7 mg) | (4-CF$_3$)PhBPin (20.4 mg) | 1 |
| 11 | $^t$BuXPhos Pd G1 (1.7 mg) | (4-CN)PhB(OH)$_2$ (11.0 mg) | 0 |
| 12 | $^t$BuXPhos Pd G1 (1.7 mg) | (4-CN)PhBPin (17.2 mg) | 1 |
| 13 | BrettPhos Pd G3 (2.3 mg) | (4-CF$_3$)PhB(OH)$_2$ (14.2 mg) | 20 |
| 14 | BrettPhos Pd G3 (2.3 mg) | (4-CF$_3$)PhBPin (20.4 mg) | 15 |

| 15 | BrettPhos Pd G3 (2.3 mg) | (4-CN)PhB(OH)$_2$ (11.0 mg) | 9 |
| 16 | BrettPhos Pd G3 (2.3 mg) | (4-CN)PhBPin (17.2 mg) | 17 |
| 17 | RockPhos Pd G3 (2.1 mg) | (4-CF$_3$)PhB(OH)$_2$ (14.2 mg) | 3 |
| 18 | RockPhos Pd G3 (2.1 mg) | (4-CF$_3$)PhBPin (20.4 mg) | 0 |
| 19 | RockPhos Pd G3 (2.1 mg) | (4-CN)PhB(OH)$_2$ (11.0 mg) | 0 |
| 20 | RockPhos Pd G3 (2.1 mg) | (4-CN)PhBPin (17.2 mg) | 0 |
| 21 | RuPhos Pd G3 (2.1 mg) | (4-CF$_3$)PhB(OH)$_2$ (14.2 mg) | 9 |
| 22 | RuPhos Pd G3 (2.1 mg) | (4-CF$_3$)PhBPin (20.4 mg) | 6 |
| 23 | RuPhos Pd G3 (2.1 mg) | (4-CN)PhB(OH)$_2$ (11.0 mg) | 9 |
| 24 | RuPhos Pd G3 (2.1 mg) | (4-CN)PhBPin (17.2 mg) | 14 |

[a]Conversion values determined by LCMS with reference to caffeine as an internal standard

## Screen of Different Palladium Sources
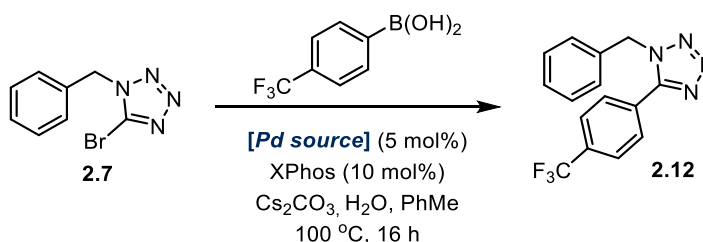


The screen was conducted as outlined in general procedure B using 6 x 2.5 mL microwave vials, each containing 1-benzyl-5-bromo-1*H*-tetrazole (12.0 mg, 50 μmol), 4-(trifluoromethyl)phenylboronic acid (14.2 mg, 75 μmol), (Pd(dppf)Cl$_2$ (1.8 mg, 2.5 µmol), palladium(II) chloride (0.4 mg, 2.5 µmol), palladium(II) acetate (0.6 mg, 2.5 µmol), Pd(PPh$_3$)$_2$Cl$_2$ (1.8 mg, 2.5 µmol), Pd$_2$(dba)$_3$ (1.1 mg, 1.25 µmol) or XPhos Pd G3 (2.1 mg, 2.5 µmol)), XPhos (2.4 mg, 5.0 µmol), caesium carbonate (32.6 mg, 100 µmol), toluene (500 μL), and water (90 μL, 5000 µmol). The reaction was stirred at 100 °C for 16 hours. The results obtained are detailed in *Table 2.4* and *Table 5.14*. Note that no XPhos was added to the reaction vessel where XPhos Pd G3 was used.

*Table 5.14: The conditions employed in the above screen*

| Entry | Palladium Source (mg) | Conversion (%)[a] |
|-------|-----------------------|-------------------|
| 1 | XPhos Pd G3 (2.1 mg) | 48 |
| 2 | PdCl$_2$ (0.4 mg) | 3 |
| 3 | Pd(OAc)$_2$ (0.6 mg) | 7 |

| 4 | Pd(PPh$_3$)$_2$Cl$_2$ (1.8 mg) | 0 |
| 5 | Pd(dppf)Cl$_2$ (1.8 mg) | 20 |
| 6 | Pd$_2$(dba)$_3$ (1.1 mg) | 4 |

[a]Conversion values determined by LCMS with reference to caffeine as an internal standard.
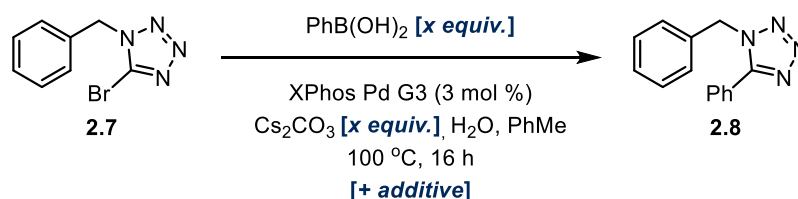
## Design of Experiments Study
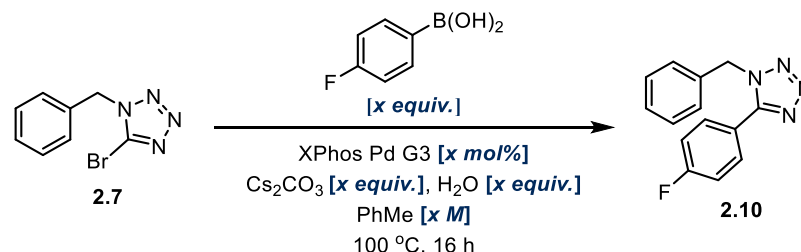


The screen was conducted as outlined in general procedure B using 35 x 2.5 mL microwave vials, each containing 1-benzyl-5-bromo-1*H*-tetrazole (12.0 mg, 50 µmol), 4-fluorophenylboronic acid (55 µmol – 125 µmol), XPhos Pd G3 (0.5 µmol – 5 µmol), caesium carbonate (55 µmol – 125 µmol), toluene (50 – 500 µL), and water (250 µmol - 5000 µmol). The reaction was stirred at 100 °C for 3 hours. The results obtained are detailed in *Table 2.5* and *Table 5.15*. Analysis was conducted on the results of this screen (*Graph 2.5* and *Graph 2.6*) using Design Expert[®] software by StatEase.[283]

*Table 5.15: The conditions employed in the above screen*

| Entry | Catalyst (mg, µmol) | ArB(OH)$_2$ (mg, µmol) | Base (mg, mmol) | Water (µL, mmol) | Toluene (µL) | Conversion (%)[a,b] |
|---|---|---|---|---|---|---|
| 1 | 4.2 mg 5.0 µmol | 17.5 mg 125 µmol | 17.9 mg 55 µmol | 90 µL 5.00 mmol | 500 µL | 49 |
| 2 | 0.4 mg 0.5 µmol | 7.7 mg 55 µmol | 17.9 mg 55 µmol | 90 µL 5.00 mmol | 500 µL | 21 |
| 3 | 4.2 mg 5.0 µmol | 17.5 mg 125 µmol | 17.9 mg 55 µmol | 4.5 µL 0.25 mmol | 50 µL | 32 |
| 4 | 0.4 mg 0.5 µmol | 7.7 mg 55 µmol | 40.7 mg 125 µmol | 4.5 µL 0.25 mmol | 500 µL | 2 |
| 5 | 4.2 mg 5.0 µmol | 7.7 mg 55 µmol | 17.9 mg 55 µmol | 90 µL 5.00 mmol | 50 µL | 13 |
| 6 | 4.2 mg 5.0 µmol | 7.7 mg 55 µmol | 17.9 mg 55 µmol | 4.5 µL 0.25 mmol | 500 µL | 50 |
| 7 | 4.2 mg | 7.7 mg | 40.7 mg | 90 µL | 500 µL | 52 |

| | | | | | | |
|---|---|---|---|---|---|---|
| | 5.0 µmol | 55 µmol | 125 µmol | 5.00 mmol | | |
| 8 | 0.4 mg, 0.5 µmol | 17.5 mg, 125 µmol | 17.9 mg, 55 µmol | 54.5 µL, 0.25 mmol | 500 µL | **5** |
| 9 | 4.2 mg, 5.0 µmol | 17.5 mg, 125 µmol | 40.7 mg, 125 µmol | 4.5 µL, 0.25 mmol | 500 µL | **54** |
| 10 | 0.4 mg, 0.5 µmol | 7.7 mg, 55 µmol | 17.9 mg, 55 µmol | 4.5 µL, 0.25 mmol | 50 µL | **2** |
| 11 | 4.2 mg, 5.0 µmol | 7.7 mg, 55 µmol | 40.7 mg, 125 µmol | 4.5 µL, 0.25 mmol | 50 µL | **21** |
| 12 | 0.4 mg, 0.5 µmol | 7.7 mg, 55 µmol | 40.7 mg, 125 µmol | 90 µL, 5.00 mmol | 50 µL | **1** |
| 13 | 0.4 mg, 0.5 µmol | 17.5 mg, 125 µmol | 40.7 mg, 125 µmol | 4.5 µL, 0.25 mmol | 50 µL | **2** |
| 14 | 4.2 mg, 5.0 µmol | 17.5 mg, 125 µmol | 40.7 mg, 125 µmol | 90 µL, 5.00 mmol | 50 µL | **12** |
| 15 | 0.4 mg, 0.5 µmol | 17.5 mg, 125 µmol | 17.9 mg, 55 µmol | 90 µL, 5.00 mmol | 50 µL | **1** |
| 16 | 0.4 mg, 0.5 µmol | 17.5 mg, 125 µmol | 40.7 mg, 125 µmol | 90 µL, 5.00 mmol | 500 µL | **10** |
| 17 | 2.3 mg, 2.8 µmol | 12.6 mg, 90 µmol | 29.3 mg, 90 µmol | 47 µL, 2.63 mmol | 275 µL | **10[c]** |

[a]Conversions values determined by LCMS with reference to caffeine as an internal standard.

[b]Reported values are averages of two runs.

[c]Average of three runs.

## Catalyst Loading Screen 2
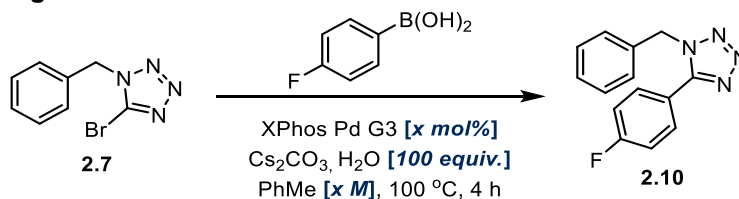


The screen was conducted as outlined in general procedure B using 9 x 2 mL HPLC vials, each containing 1-benzyl-5-bromo-1*H*-tetrazole (12.0 mg, 50 µmol), (4-fluorophenyl)boronic acid (9.1 mg, 65 µmol), XPhos Pd G3 (0.5 µmol – 5 µmol), caesium carbonate (24.4 mg, 75 µmol), toluene (500 µL - 2500 µL), and water (90 µL, 5000 µmol). The reaction was stirred at 100 °C for 4 hours. The results obtained are detailed in *Table 2.6* and *Table 5.16*

| Entry | Catalyst (mg, μmol) | Toluene (mL) | Conversion (%)[a] |
|-------|---------------------|--------------|-------------------|
| 1 | 4.2 mg, 5.0 μmol | 0.5 mL | **70** |
| 2 | 3.0 mg, 3.5 μmol | 0.5 mL | **69** |
| 3 | 2.5 mg, 3.0 μmol | 0.5 mL | **71** |
| 4 | 2.1 mg, 2.5 μmol | 0.5 mL | **71** |
| 5 | 1.7 mg, 2.0 μmol | 0.5 mL | **70** |
| 6 | 1.3 mg, 1.5 μmol | 0.5 mL | **71** |
| 7 | 0.8 mg, 1.0 μmol | 0.5 mL | **66** |
| 8 | 0.4 mg, 0.5 μmol | 0.5 mL | **38** |
| 9 | 1.3 mg, 1.5 μmol | 2.5 mL | **67** |

[a]Conversion values determined by LCMS with reference to caffeine as an internal standard.

**Compatibility Screen**



The screen was conducted as outlined in general procedure B using 3 x 2.5 mL microwave vials, each containing 1-benzyl-5-bromo-1*H*-tetrazole (12.0 mg, 50 μmol), phenylboronic acid (65 μmol or 75 μmol), XPhos Pd G3 (1.3 mg, 1.5 μmol), caesium carbonate (75 μmol or 100 μmol), toluene (500 μL), and water (90 μL, 5000 μmol). The reaction was stirred at 100 °C for 3 hours. The results obtained are detailed in *Table 2.9* and *Table 5.17*. Evonik Noblyst® P1071 20 % palladium on carbon (5.3 mg, 5 μmol) was also added to one of the vessels.

Table 5.17: The conditions employed in the above screen

| Entry | PhB(OH)$_2$ (mg, μmol) | Base (mg, μmol) | Pd/C (mg, μmol) | Conversion (%)[a] |
|-------|------------------------|-----------------|-----------------|-------------------|
| 1 | 7.9 mg, 65 μmol | 24 mg, 75 μmol | - | **77** |
| 2 | 7.9 mg, 65 μmol | 24 mg, 75 μmol | 5.3 mg, 5.0 μmol | **72** |
| 3 | 9.1 mg, 75 μmol | 32.6 mg, 100 μmol | - | **76** |

[a]Conversions values determined by LCMS with reference to caffeine as an internal standard.

## 5.3.1.2 Optimisation of Hydrogenolysis Reaction
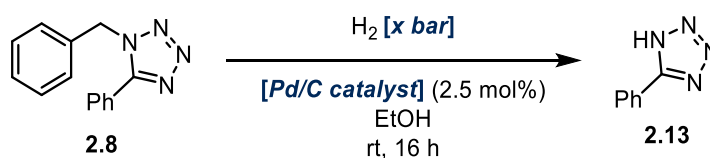
**General Conditions Screen**
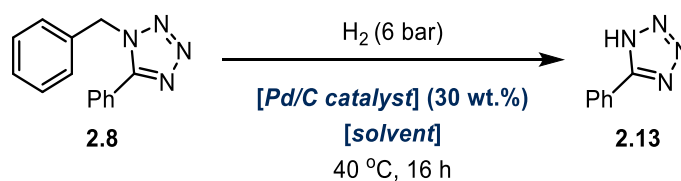


The screen was conducted as outlined in general procedure C using 48 x 1 mL vials, each containing 1-benzyl-5-phenyl-1*H*-tetrazole (15.0 mg, 63 μmol), a palladium on carbon catalyst (4.5 mg, 30 wt.%), and ethanol, ethyl acetate, or tetrahydrofuran (all 375 μL). Acetic acid (13 μL, 63 μmol) was added to half of the vessels. The reaction was stirred at 40 °C for 16 hours. The results obtained are detailed in *Table 5.18*.

Table 5.18: Conversion values obtained from the above screen

| Entry | Pd/C Catalyst (4.5 mg, 30 wt.%) | Solvent (375 μL) | Additive | Conversion (%)[a] |
|---|---|---|---|---|
| 1 | JM A405-028-5 | Ethanol | - | 97 |
| 2 | JM A405-032-5 | Ethanol | - | 98 |
| 3 | JM A503-032-5 | Ethanol | - | 29 |
| 4 | Evonik P1070 | Ethanol | - | 96 |
| 5 | Evonik P1071 | Ethanol | - | 97 |
| 6 | Evonik P1090 | Ethanol | - | 90 |
| 7 | BASF 10318 | Ethanol | - | 97 |
| 8 | BASF 10321 | Ethanol | - | 96 |
| 9 | JM A405-028-5 | Ethyl Acetate | - | 67 |
| 10 | JM A405-032-5 | Ethyl Acetate | - | 71 |
| 11 | JM A503-032-5 | Ethyl Acetate | - | 12 |
| 12 | Evonik P1070 | Ethyl Acetate | - | 71 |
| 13 | Evonik P1071 | Ethyl Acetate | - | 76 |
| 14 | Evonik P1090 | Ethyl Acetate | - | 66 |
| 15 | BASF 10318 | Ethyl Acetate | - | 76 |
| 16 | BASF 10321 | Ethyl Acetate | - | 10 |
| 17 | JM A405-028-5 | THF | - | 84 |
| 18 | JM A405-032-5 | THF | - | 94 |

| | | | | |
|---|---|---|---|---|
| 19 | JM A503-032-5 | THF | - | **14** |
| 20 | Evonik P1070 | THF | - | **97** |
| 21 | Evonik P1071 | THF | - | **97** |
| 22 | Evonik P1090 | THF | - | **91** |
| 23 | BASF 10318 | THF | - | **97** |
| 24 | BASF 10321 | THF | - | **2** |
| 25 | JM A405-028-5 | Ethanol | AcOH (13 µL) | **57** |
| 26 | JM A405-032-5 | Ethanol | AcOH (13 µL) | **98** |
| 27 | JM A503-032-5 | Ethanol | AcOH (13 µL) | **33** |
| 28 | Evonik P1070 | Ethanol | AcOH (13 µL) | **97** |
| 29 | Evonik P1071 | Ethanol | AcOH (13 µL) | **97** |
| 30 | Evonik P1090 | Ethanol | AcOH (13 µL) | **61** |
| 31 | BASF 10318 | Ethanol | AcOH (13 µL) | **98** |
| 32 | BASF 10321 | Ethanol | AcOH (13 µL) | **9** |
| 33 | JM A405-028-5 | Ethyl Acetate | AcOH (13 µL) | **82** |
| 34 | JM A405-032-5 | Ethyl Acetate | AcOH (13 µL) | **81** |
| 35 | JM A503-032-5 | Ethyl Acetate | AcOH (13 µL) | **4** |
| 36 | Evonik P1070 | Ethyl Acetate | AcOH (13 µL) | **80** |
| 37 | Evonik P1071 | Ethyl Acetate | AcOH (13 µL) | **78** |
| 38 | Evonik P1090 | Ethyl Acetate | AcOH (13 µL) | **20** |
| 39 | BASF 10318 | Ethyl Acetate | AcOH (13 µL) | **81** |
| 40 | BASF 10321 | Ethyl Acetate | AcOH (13 µL) | **0** |
| 41 | JM A405-028-5 | THF | AcOH (13 µL) | **96** |
| 42 | JM A405-032-5 | THF | AcOH (13 µL) | **95** |
| 43 | JM A503-032-5 | THF | AcOH (13 µL) | **1** |
| 44 | Evonik P1070 | THF | AcOH (13 µL) | **96** |
| 45 | Evonik P1071 | THF | AcOH (13 µL) | **97** |
| 46 | Evonik P1090 | THF | AcOH (13 µL) | **94** |
| 47 | BASF 10318 | THF | AcOH (13 µL) | **96** |
| 48 | BASF 10321 | THF | AcOH (13 µL) | **1** |

[a]Conversions reported as a percentage of total peak area of product and starting material.

**Further Catalyst Screen**
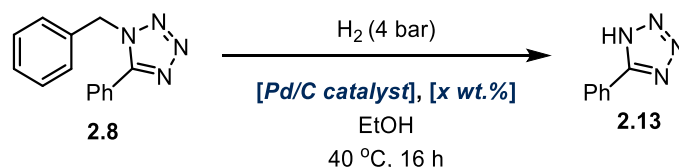


The screen was conducted as outlined in general procedure C using 10 x 1 mL vials, each containing 1-benzyl-5-phenyl-1*H*-tetrazole (30.0 mg, 127 µmol), a palladium on carbon catalyst (3.0 mg, 10 % wt. or 6.0 mg, 20 % wt.), and ethanol (750 µL). The reaction was stirred at 40 °C for 16 hours. The results obtained are detailed in *Table 2.7* and *Table 5.19*.

*Table 5.19: The conditions employed in the above screen*

| Entry | Pd/C Catalyst | Catalyst Loading (wt. %, mg) | Conversion (%)[a] |
|:-----:|:-------------:|:----------------------------:|:-----------------:|
| 1 | JM A405-028-5 | 20 wt. %, 6.0 mg | **38** |
| 2 | JM A503-032-5 | 20 wt. %, 6.0 mg | **33** |
| 3 | Evonik P1070 | 20 wt. %, 6.0 mg | **99** |
| 4 | Evonik P1071 | 20 wt. %, 6.0 mg | **98** |
| 5 | BASF 10318 | 20 wt. %, 6.0 mg | **99** |
| 6 | JM A405-028-5 | 10 wt. %, 3.0 mg | **24** |
| 7 | JM A503-032-5 | 10 wt. %, 3.0 mg | **20** |
| 8 | Evonik P1070 | 10 wt. %, 3.0 mg | **67** |
| 9 | Evonik P1071 | 10 wt. %, 3.0 mg | **99** |
| 10 | BASF 10318 | 10 wt. %, 3.0 mg | **97** |

[a]Conversion values determined by LCMS with reference to caffeine as an internal standard.

**Screen of Catalyst and H$_2$ Pressure**



The screen was conducted as outlined in general procedure D using 8 x 10 mL reaction vessels, each containing 1-benzyl-5-phenyl-1*H*-tetrazole (70.9 mg, 300 µmol), a palladium on carbon catalyst (7.5 µmol) and ethanol (3 mL). The reaction was stirred at room temperature for 16 hours. The results obtained are detailed in *Table 2.8* and *Table 5.20*.

| Entry | Pd/C Catalyst (mg) | H$_2$ pressure (bar) | Conversion (%)[a] |
|:---:|:---:|:---:|:---:|
| 1 | Evonik P1071 (8.0 mg) | 4 | 59 |
| 2 | Evonik P1071 (8.0 mg) | 3 | 56 |
| 3 | Evonik P1071 (8.0 mg) | 2 | 50 |
| 4 | Evonik P1071 (8.0 mg) | 1 | 47 |
| 5 | BASF 10318 (15.9 mg) | 4 | 53 |
| 6 | BASF 10318 (15.9 mg) | 3 | 50 |
| 7 | BASF 10318 (15.9 mg) | 2 | 44 |
| 8 | BASF 10318 (15.9 mg) | 1 | 42 |

[a]Conversion values determined by LCMS with reference to caffeine as an internal stanard.

### 5.3.1.3 *Optimisation of One-Pot Suzuki-Hydrogenolysis Reaction*

**Screen of Catalyst Loading**
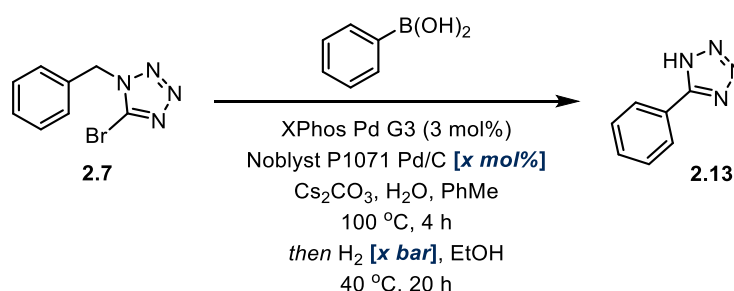


The screen was conducted as outlined in general procedure E using 8 x 10 mL reaction vessels, each containing 1-benzyl-5-phenyl-1*H*-tetrazole (120 mg, 500 μmol), phenylboronic acid (79 mg, 650 μmol), XPhos Pd G3 (12.7 mg, 15 μmol), Noblyst® P1071 20 % Pd/C (13 μmol - 50 μmol), caesium carbonate (244 mg, 750 μmol), water (901 μL, 50 mmol), toluene (5 mL) and ethanol (2.5 mL). The reaction was stirred at 100 °C under a nitrogen atmosphere for 4 hours, and at 40 °C under a hydrogen atmosphere of either 4 or 2 bar for 20 hours. The results obtained are detailed in *Table 2.10* and *Table 5.21*.

Table 5.21: The conditions employed in the above screen

| Entry | Pd/C loading (mol%, mg) | H$_2$ pressure (bar) | Conversion (%)[a] |
|:---:|:---:|:---:|:---:|
| 1 | 10 (53.2 mg) | 4 | 43 |
| 2 | 7.5 (39.9 mg) | 4 | 48 |

| 3 | 5 (26.6 mg) | 4 | **29** |
| 4 | 2.5 (13.3 mg) | 4 | **17** |
| 5 | 10 (53.2 mg) | 2 | **65** |
| 6 | 7.5 (39.9 mg) | 2 | **52** |
| 7 | 5 (26.6 mg) | 2 | **34** |
| 8 | 2.5 (13.3 mg) | 2 | **35** |

<sup>a</sup>Conversions values determined by LCMS with reference to caffeine as an internal standard.

## Solvent Screen
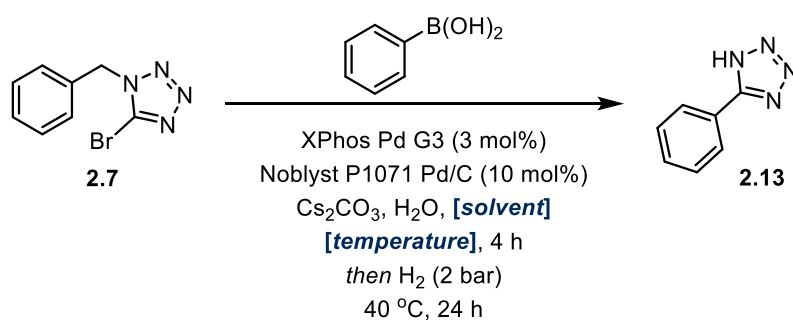


The screen was conducted as outlined in general procedure E using 7 x 10 mL reaction vessels, each containing 1-benzyl-5-phenyl-1*H*-tetrazole (120 mg, 500 µmol), phenylboronic acid (79 mg, 650 µmol), XPhos Pd G3 (12.7 mg, 15 µmol), Noblyst® P1071 20 % Pd/C (53.2 mg, 50 µmol), caesium carbonate (244 mg, 750 µmol), water (901 µL, 50 mmol), toluene (2.5 mL - 5 mL) and ethanol or *n*-butanol (both 1 - 2.5 mL). The reaction was stirred at a specified temperature under a nitrogen atmosphere for 4 hours, and at 40 °C under a hydrogen atmosphere of 2 bar for 24 hours. The results obtained are detailed in *Table 2.11* and *Table 5.22*.

*Table 5.22: The conditions employed in the above screen*

| Entry | Toluene (mL) | Co-solvent (mL) | Suzuki Temperature (°C) | Conversion (%)<sup>a</sup> |
|---|---|---|---|---|
| 1 | 5.0 mL | - | 100 | **24** |
| 2 | 4.0 mL | *n*BuOH (1.0 mL) | 100 | **24** |
| 3 | 3.0 mL | *n*BuOH (2.0 mL) | 100 | **4** |
| 4 | 2.5 mL | *n*BuOH (2.5 mL) | 100 | **34** |
| 5 | 4.0 mL | EtOH (1.0 mL) | 70 | **37** |
| 6 | 3.0 mL | EtOH (2.0 mL) | 70 | **22** |
| 7 | 2.5 mL | EtOH (2.5 mL) | 70 | **15** |

<sup>a</sup>Conversions values determined by LCMS with reference to caffeine as an internal standard.

### 5.3.2 Metal-Free Coupling of Nitrile Imines and Boronic Acids

*5.3.2.1 2,5-Diaryl Tetrazole Optimisation*

**Solvent Screen**
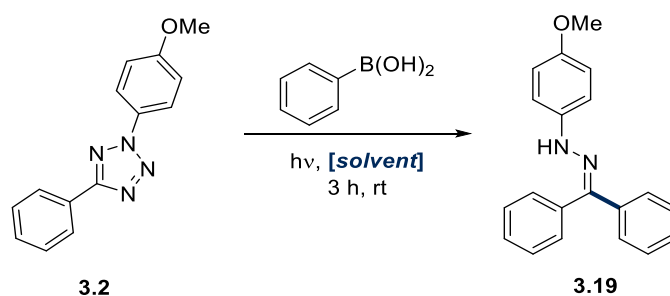


The screen was conducted as outlined in general procedure J using 5 x 5 mL round bottom flasks, each containing tetrazole **3.2** (11.1 mg, 0.05 mmol), phenylboronic acid (12.2 mg, 0.10 mmol), and either acetone, acetonitrile, THF, ethyl acetate, or *iso*propyl alcohol:2-MeTHF (1:1) (all 0.5 mL). The reaction was stirred under UV light irradiation at room temperature for 3 hours. The results obtained are detailed in *Table 3.2* and *Table 5.23*

*Table 5.23: The conditions employed in the above screen*

| Entry | Solvent (0.5 mL) | Conversion (%)[a] |
|:---:|:---:|:---:|
| 1 | Acetone | 10 |
| 2 | THF | 9 |
| 3 | Acetonitrile | 7 |
| 4 | Ethyl Acetate | 10 |
| 5 | *i*PrOH:2-MeTHF (1:1) | 2 |

[a]Conversion determined by HPLC with reference to caffeine as an internal standard

**Screen of Different Boron Species and Stoichiometries**
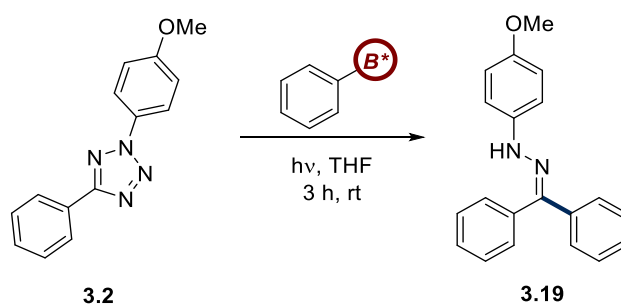


The screen was conducted as outlined in general procedure J using 6 x 5 mL round bottom flasks, each containing tetrazole **3.2** (11.1 mg, 0.05 mmol), either phenylboronic acid (0.05 mmol – 0.20 mmol), phenylboronic acid pinacol ester (20.4 mg, 0.10 mmol) or phenyl boronic acid trifluoroborate salt (18.4 mg, 0.10 mmol), and THF (0.5 mL). In specified cases, 18-crown-6 (26.4 mg, 0.10 mmol) or sodium hydroxide (10 mg, 0.25 mmol) were also

added to the reaction mixture. The reaction was stirred under UV light irradiation at room temperature for 3 hours. The results obtained are detailed in *Table 3.3* and *Table 5.24*

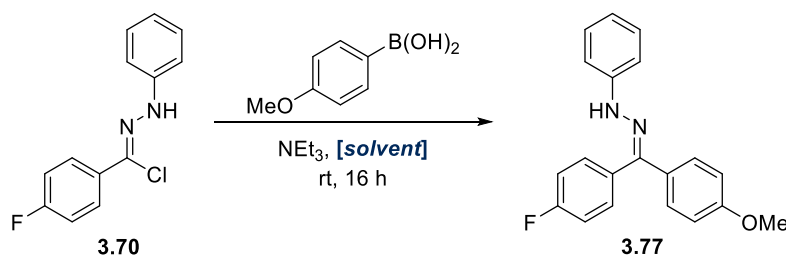*Table 5.24: The conditions employed in the above screen*

| Entry | B* (mg, mmol) | Additive (mg, mmol) | Conversion (%)[a] |
|-------|---------------|---------------------|-------------------|
| 1 | $B(OH)_2$ (12.2 mg, 0.10 mmol) | - | 9 |
| 2 | BPin (20.4 mg, 0.10 mmol) | - | <1 |
| 3 | $BF_3K$ (18.4 mg, 0.10 mmol) | - | <1 |
| 4 | $BF_3K$ (18.4 mg, 0.10 mmol) | 18-crown-6 (26.4 mg, 0.10 mmol) | <1 |
| 5 | $B(OH)_2$ (12.2 mg, 0.10 mmol) | NaOH (10.0 mg, 0.25 mmol) | <1 |
| 6 | $B(OH)_2$ (6.1 mg, 0.05 mmol) | - | 6 |
| 7 | $B(OH)_2$ (24.4 mg, 0.20 mmol) | - | 9 |

[a]Conversion determined by HPLC with reference to caffeine as an internal standard

**Screen of Discrete Variables**
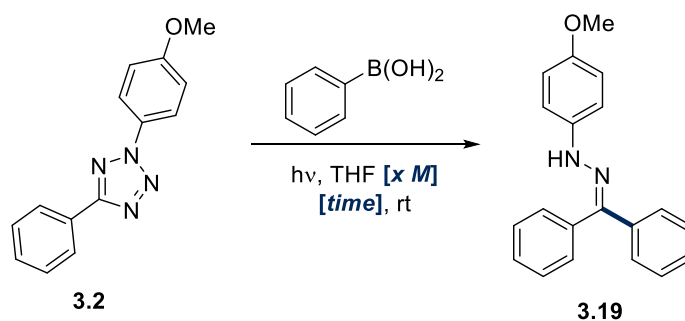


The screen was conducted as outlined in general procedure J using 6 x 5 mL round bottom flasks, each containing tetrazole **3.2** (11.1 mg, 0.05 mmol), phenylboronic acid (12.2 mg, 0.10 mmol), and THF (0.25 mL – 1.00 mL). The reaction was stirred under UV light irradiation at room temperature for 1 – 7 hours. The results obtained are detailed in *Table 3.4* and *Table 5.25*.

*Table 5.25: The conditions employed in the above screen*

| Entry | Time (h) | THF (mL) | Conversion (%)[a] |
|-------|----------|----------|-------------------|
| 1 | 1 | 0.50 mL | 4 |
| 2 | 2 | 0.50 mL | 5 |

| | | | | |
|---|---|---|---|---|
| 3 | 3 | 0.50 mL | | **9** |
| 4 | 7 | 0.50 mL | | **9** |
| 5 | 3 | 1.00 mL | | **6** |
| 6 | 3 | 0.25 mL | | **9** |

[a]Conversion determined by HPLC with reference to caffeine as an internal standard

## Further Screen of Discrete Variables



**3.2**

i. 4-methoxyphenylboronic acid B(OH)₂ / MeO

hv, [*solvent*], [*time*], rt

ii. VO(acac)₂ (10 mol%)
COMe₂:H₂O₂ (4:1)
3h, rt

**3.20**
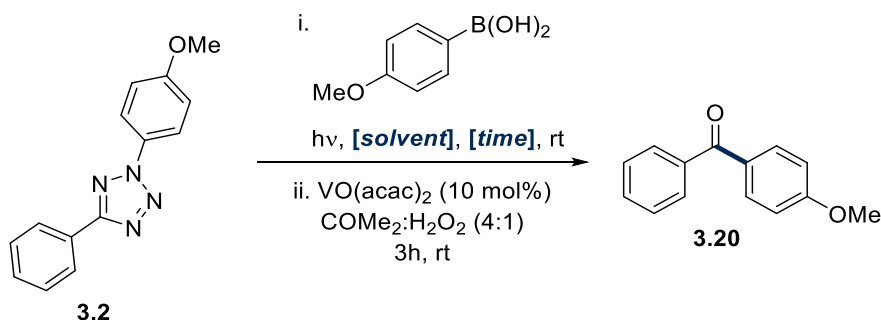
The screen was conducted as outlined in general procedure J using 9 x 5 mL round bottom flasks, each containing tetrazole **3.2** (11.1 mg, 0.05 mmol), phenylboronic acid (0.05 – 0.25 mmol), and THF (0.25 mL – 1.00 mL) or acetonitrile (0.50 mL). The reaction was stirred under UV light irradiation at room temperature for 1 – 3 hours, and then under ambient light conditions for a further 4 hours in the presence of VO(acac)₂ (1.33 mg, 0.005 mmol), H₂O₂ (0.1 mL) and acetone (0.5 mL). The results obtained are detailed in *Table 3.5* and *Table 5.26*.

*Table 5.26: The conditions employed in the above screen*

| Entry | Solvent (mL) | Time (h) | ArB(OH)₂ (mg, mmol) | Conversion (%)[a] |
|---|---|---|---|---|
| 1 | THF (0.50 mL) | 3 | 15.2 mg, 0.10 mmol | **57** |
| 2 | MeCN (0.50 mL) | 3 | 15.2 mg, 0.10 mmol | **53** |
| 3 | THF (0.50 mL) | 1 | 15.2 mg, 0.10 mmol | **41** |
| 4 | THF (0.50 mL) | 2 | 15.2 mg, 0.10 mmol | **48** |
| 5 | THF (1.00 mL) | 3 | 15.2 mg, 0.10 mmol | **61** |
| 6 | THF (0.25 mL) | 3 | 15.2 mg, 0.10 mmol | **57** |
| 7 | THF (0.50 mL) | 3 | 7.60 mg, 0.05 mmol | **45** |
| 8 | THF (0.50 mL) | 3 | 22.8 mg, 0.15 mmol | **69** |
| 9 | THF (0.50 mL) | 3 | 38.0 mg, 0.25 mmol | **78 (75[b])** |

[a]Conversion determined by HPLC with reference to caffeine as an internal standard
[b]Isolated yield

## Stoichiometry Screen Using ¹⁹F NMR
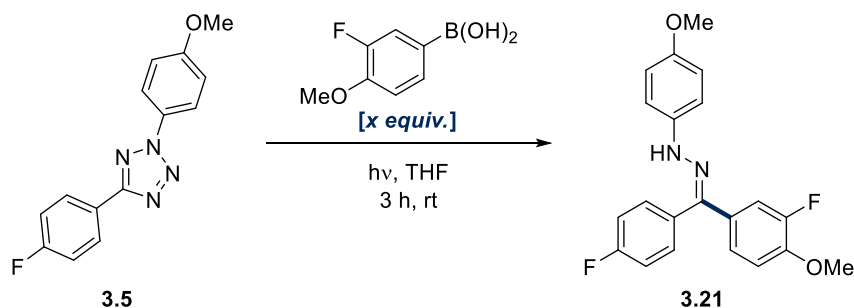


The screen was conducted as outlined in general procedure K using 5 NMR tubes, each containing tetrazole **3.5** (11.1 mg, 0.05 mmol), 3-fluoro-4-methoxyphenylboronic acid (0.05 – 0.25 mmol), and THF (0.5 mL). The reaction was irradiated with UV light at room temperature for 3 hours. The results obtained are detailed in *Table 3.6* and *Table 5.27*

*Table 5.27: The conditions employed in the above screen*

| Entry | ArB(OH)₂ (mg, mmol) | Conversion (%)[a] |
|:-----:|:-------------------:|:-----------------:|
| 1 | 42.5 mg, 0.25 mmol | 56 |
| 2 | 34.0 mg, 0.20 mmol | 55 |
| 3 | 25.5 mg, 0.15 mmol | 53 |
| 4 | 17.0 mg, 0.10 mmol | 42 |
| 5 | 8.50 mg, 0.05 mmol | 33 |

[a]Conversion determined by ¹⁹F NMR with reference to **3.3** as an internal standard

## Investigation of Different Drying Agents
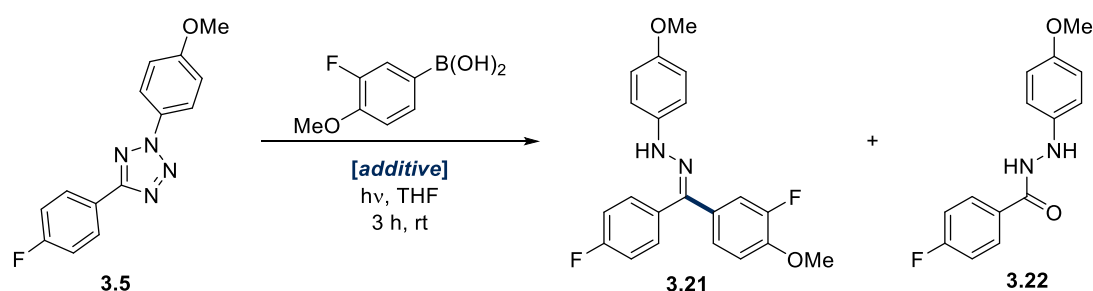


The screen was conducted as outlined in general procedure K using 8 NMR tubes, each containing tetrazole **3.5** (11.1 mg, 0.05 mmol), 3-fluoro-4-methoxyphenylboronic acid (25.5 mg, 0.15 mmol), and THF (0.5 mL). In specified cases, trimethylorthoformate (54.6 μL, 0.5 mmol) or 3Å molecular sieves (400 gmmol⁻¹ – 4000 gmmol⁻¹) were added. The reaction was irradiated with UV light at room temperature for 3 hours. The results obtained are detailed in *Table 3.7* and *Table 5.28*

*Table 5.28: The conditions employed in the above screen*

| Entry | Atmosphere | Additive | Conversion (%)[a] |
|:---:|:---:|:---:|:---:|
| 1 | - | - | 41 |
| 2 | $N_2$ | - | 45 |
| 3 | $N_2$ | 3 Å molecular sieves (20 mg, 400 gmol$^{-1}$) | 46 |
| 4 | $N_2$ | 3 Å molecular sieves (200 mg, 4000 gmol$^{-1}$) | 60 |
| 5 | $N_2$ | Trimethyl orthoformate (55 µL, 0.5 mmol) | 38 |
| 6 | $N_2$ | Trimethyl orthoformate (500 µL, 4.6 mmol) | 11 |
| 7 | $N_2$ | 3 Å molecular sieves (20 mg, 400 gmol$^{-1}$)[b] | 61 |
| 8 | $N_2$ | 3 Å molecular sieves (200 mg, 4000 gmol$^{-1}$)[b] | 55 |

[a]Conversion determined by $^{19}$F NMR with reference to **3.3** as an internal standard
[b]Crushed

### 5.3.2.2 Hydrazonyl Chloride Optimisation

**Solvent Screen**



The screen was conducted as outlined in general procedure S using 18 x 2 mL HPLC vials, each containing hydrazonyl chloride **3.70** (24.9 mg, 0.1 mmol), 4-methoxyphenylboronic acid (0.11 mmol - 0.3 mmol), triethylamine (41.8 µL, 0.3 mmol) and the specified solvent (1 mL). The reaction was stirred at room temperature for 16 hours. The results obtained are detailed in *Table 3.13, Table 3.14* and *Table 5.29*.

*Table 5.29: The conditions employed in the above screen*

| Entry | Solvent (1.00 mL) | ArB(OH)$_2$ (mg, mmol) | Conversion (%)[a, b] |
|:---:|:---:|:---:|:---:|
| 1 | MeCN | 45.6 mg, 0.30 mmol | 32[c] |
| 2 | THF | 45.6 mg, 0.30 mmol | 22 |
| 3 | DCM | 45.6 mg, 0.30 mmol | 75 |
| 4 | Et$_2$O | 45.6 mg, 0.30 mmol | 15 |
| 5 | MeOH | 45.6 mg, 0.30 mmol | <1[c] |
| 6 | $^i$PrOH | 45.6 mg, 0.30 mmol | <1[c] |
| 7 | 1,4-dioxane | 45.6 mg, 0.30 mmol | 58 |

| | | | |
|---|---|---|---|
| 8 | DMSO | 45.6 mg, 0.30 mmol | <1[c] |
| 9 | EtOAc | 45.6 mg, 0.30 mmol | 48 |
| 10 | DMF | 45.6 mg, 0.30 mmol | <1 |
| 11 | 2-MeTHF | 45.6 mg, 0.30 mmol | 26 |
| 12 | PhMe | 45.6 mg, 0.30 mmol | 50 |
| 13 | COMe$_2$ | 45.6 mg, 0.30 mmol | 47[c] |
| 14 | H$_2$O | 45.6 mg, 0.30 mmol | 13 |
| 15 | DCM | 16.7 mg, 0.11 mmol | 54 |
| 16 | DCE | 16.7 mg, 0.11 mmol | 40 |
| 17 | CHCl$_3$ | 16.7 mg, 0.11 mmol | 51 |
| 18 | CPME | 16.7 mg, 0.11 mmol | 20 |

[a] Conversion determined by $^{19}$F NMR with reference to an internal standard

[b] Average value of two experiments with a difference of <10 %

[c] Significant by-product formation observed

**Base Screen**
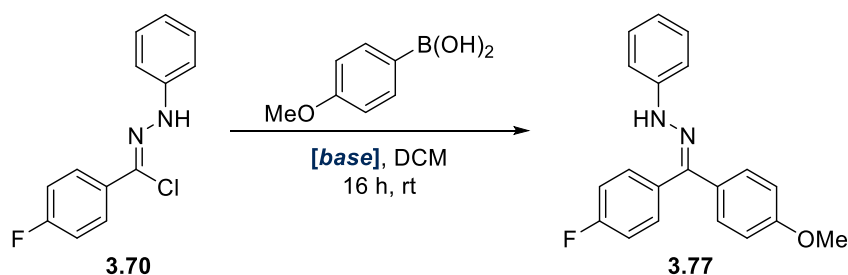


The screen was conducted as outlined in general procedure S using 16 x 2 mL HPLC vials, each containing hydrazonyl chloride **3.70** (24.9 mg, 0.1 mmol), 4-methoxyphenylboronic acid (16.7 mg, 0.11 mmol), the specified base (0.3 mmol) and DCM (1 mL). The reaction was stirred at room temperature for 16 hours. The results obtained are detailed in *Table 3.15* and *Table 5.30*.

*Table 5.30: The conditions employed in the above screen*

| Entry | Base (mg/µL) | Conversion (%)[a, b] |
|---|---|---|
| 1 | KTFA (45.6 mg) | <1 |
| 2 | KOAc (29.4 mg) | <1 |
| 3 | Pyridine (24.3 µL) | <1 |
| 4 | Lutidine (34.9 µL) | 2 |
| 5 | NMM (33.0 µL) | 8 |
| 6 | Collidine (39.8 µL) | 10 |
| 7 | DABCO (33.7 mg) | <1[c] |

| Entry | Base | Conversion |
|---|---|---|
| 8 | K₂CO₃ (41.5 mg) | **20** |
| 9 | NEt₃ (41.8 µL) | **53** |
| 10 | DIPEA (52.3 µL) | **55** |
| 11 | DBU (44.9 µL) | **9[c]** |
| 12 | K₃PO₄ (63.7 mg) | **71** |
| 13 | KF (17.4 mg) | **37** |
| 14 | KOH (16.8 mg) | **7[c]** |
| 15 | KOᵗBu (33.7 mg) | **15[c]** |
| 16 | BEMP (86.8 µL) | **6[c]** |

[a] Conversion determined by $^{19}F$ NMR with reference to an internal standard

[b] Average value of two experiments with a difference of <10 %

[c] Significant by-product formation observed

## Counterion Screen
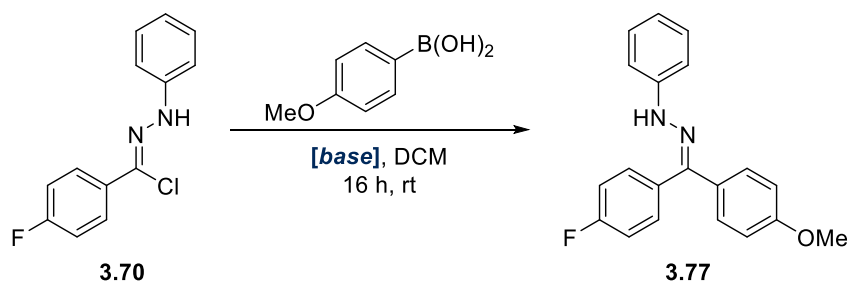


The screen was conducted as outlined in general procedure S using 12 x 2 mL HPLC vials, each containing hydrazonyl chloride **3.70** (24.9 mg, 0.1 mmol), 4-methoxyphenylboronic acid (16.7 mg, 0.11 mmol), the specified base (0.3 mmol) and DCM (1 mL). In one instance, chloroform (1 mL) was used instead of DCM. The reaction was stirred at room temperature for 16 hours. The results obtained are detailed in *Table 3.16* and *Table 5.31*.

*Table 5.31: The conditions employed in the above screen*

| Entry | Base (mg) | Conversion (%)[a, b] |
|---|---|---|
| 1 | (NH₄)₂CO₃ (28.8 mg) | **<1** |
| 2 | Na₂CO₃ (31.8 mg) | **<1** |
| 3 | CaCO₃ (30.0 mg) | **<1** |
| 4 | K₂CO₃ (41.5 mg) | **20** |
| 5 | Cs₂CO₃ (97.7 mg) | **55** |
| 6 | KH2PO₄ (40.8 mg) | **<1** |
| 7 | K₂HPO₄ (52.2 mg) | **<1** |
| 8 | K₃PO₄ (63.7 mg) | **70** |

| 9 | Na$_3$PO$_4$ (49.2 mg) | **3** |
| 10 | Ca$_3$(PO$_4$)$_2$ (93.1 mg) | **<1** |
| 11 | Mg$_3$(PO$_4$)$_2$ (122.1 mg) | **<1** |
| 12 | K$_3$PO$_4$[c] (63.7 mg) | **60[d]** |

[a] Conversion determined by $^{19}$F NMR with reference to an internal standard

[b] Average value of two experiments with a difference of <10 %

[c] CHCl$_3$ was used as reaction solvent

[d] Significant by-product formation observed

## Design of Experiments Study



**3.70**                      **3.77**
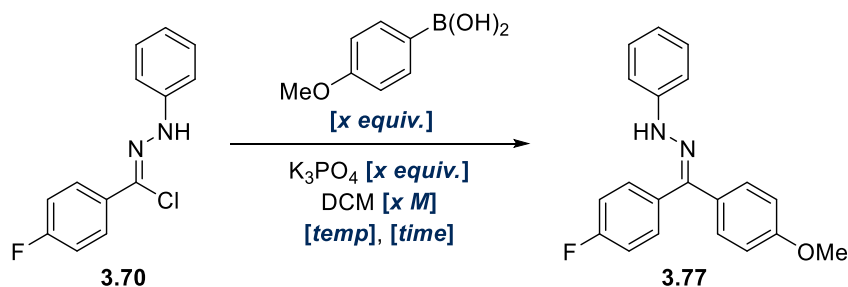
The screen was conducted as outlined in general procedure S using 52 x 2 mL HPLC vials, each containing hydrazonyl chloride **3.70** (24.9 mg, 0.1 mmol), 4-methoxyphenylboronic acid (0.11 mmol – 0.3 mmol), potassium phosphate (0.11 mmol – 0.3 mmol), and DCM (1 mL – 10 mL). The reaction was stirred at either room temperature, 30 °C or 40 °C for either 3, 9.5 or 16 hours. The results obtained are detailed in *Table 3.17* and *Table 5.32*. Analysis was conducted on the results of this screen (*Graph 3.3, Graph 3.4* and *Graph 3.5*) using Design Expert® software by StatEase.[283]

*Table 5.32: The conditions employed in the above screen*

| Entry | ArB(OH)$_2$ (mg, mmol) | Base (mg, mmol) | DCM (mL) | Time (h) | Temperature (° C) | Conversion[a,b] |
|---|---|---|---|---|---|---|
| 1 | 16.7 mg, 0.11 mmol | 23.3 mg, 0.11 mmol | 10.0 mL | 16 | 20 | **25** |
| 2 | 16.7 mg, 0.11 mmol | 23.3 mg, 0.11 mmol | 1.00 mL | 16 | 40 | **48** |
| 3 | 16.7 mg, 0.11 mmol | 23.3 mg, 0.11 mmol | 1.00 mL | 3 | 20 | **23** |
| 4 | 16.7 mg, 0.11 mmol | 23.3 mg, 0.11 mmol | 10.0 mL | 3 | 40 | **34** |
| 5 | 16.7 mg, 0.11 mmol | 63.7 mg, 0.30 mmol | 1.00 mL | 16 | 20 | **2** |

| | | | | | | |
|---|---|---|---|---|---|---|
| 6 | 16.7 mg, 0.11 mmol | 63.7 mg, 0.30 mmol | 10.0 mL | 16 | 40 | **22** |
| 7 | 16.7 mg, 0.11 mmol | 63.7 mg, 0.30 mmol | 10.0 mL | 3 | 20 | **1** |
| 8 | 16.7 mg, 0.11 mmol | 63.7 mg, 0.30 mmol | 1.00 mL | 3 | 40 | **19** |
| 9 | 45.6 mg, 0.30 mmol | 23.3 mg, 0.11 mmol | 1.00 mL | 16 | 20 | **63** |
| 10 | 45.6 mg, 0.30 mmol | 23.3 mg, 0.11 mmol | 10.0 mL | 16 | 40 | **82** |
| 11 | 45.6 mg, 0.30 mmol | 23.3 mg, 0.11 mmol | 10.0 mL | 3 | 20 | **12** |
| 12 | 45.6 mg, 0.30 mmol | 23.3 mg, 0.11 mmol | 1.00 mL | 3 | 40 | **78** |
| 13 | 45.6 mg, 0.30 mmol | 63.7 mg, 0.30 mmol | 10.0 mL | 16 | 20 | **63** |
| 14 | 45.6 mg, 0.30 mmol | 63.7 mg, 0.30 mmol | 1.00 mL | 16 | 40 | **82** |
| 15 | 45.6 mg, 0.30 mmol | 63.7 mg, 0.30 mmol | 1.00 mL | 3 | 20 | **60** |
| 16 | 45.6 mg, 0.30 mmol | 63.7 mg, 0.30 mmol | 10.0 mL | 3 | 40 | **75** |
| 17 | 31.2 mg, 0.21 mmol | 43.5 mg, 0.21 mmol | 5.50 mL | 9.5 | 30 | **65**[c] |

[a] Conversion determined by $^{19}F$ NMR with reference to an internal standard

[b] Reported values are averages of three runs.

[c] Average of four runs.

## The Introduction of Toluene as an Alternative Solvent
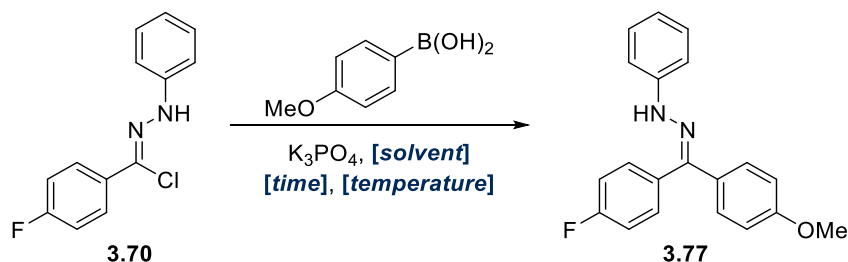


The screen was conducted as outlined in general procedure S using 4 x 2.5 mL microwave vials, each containing hydrazonyl chloride **3.70** (24.9 mg, 0.1 mmol), 4-methoxyphenylboronic acid (16.7 mg, 0.11 mmol), potassium phosphate (63.7 mg, 0.3 mmol) and DCM or toluene (1 mL). The reaction was stirred at 40 °C for 3 hours, 40 °C for 16 hours, 50 °C for 3 hours, or 80 °C for 1 hour. Following quantification, the mixture was evaporated to dryness and the crude residue was purified by column chromatography. The results obtained are detailed in *Table 3.18* and *Table 5.33*.

*Table 5.33: The conditions employed in the above screen*

| Entry | Solvent (mL) | Temperature (ºC) | Time (h) | Conversion (%)[a, b] | Isolated Yield (%) |
|---|---|---|---|---|---|
| 1 | DCM (1.00 mL) | 40 | 3 | **85** | **80** |
| 2 | DCM (1.00 mL) | 40 | 16 | **86** | **85** |
| 3 | PhMe (1.00 mL) | 50 | 3 | **75** | **69** |
| 4 | PhMe (1.00 mL) | 80 | 1 | **81** | **75** |

[a] Conversion determined by $^{19}$F NMR with reference to an internal standard

[b] Average value of two experiments with a difference of <10 %

## The Introduction of Electron-Deficient Boronic Acid Substrates
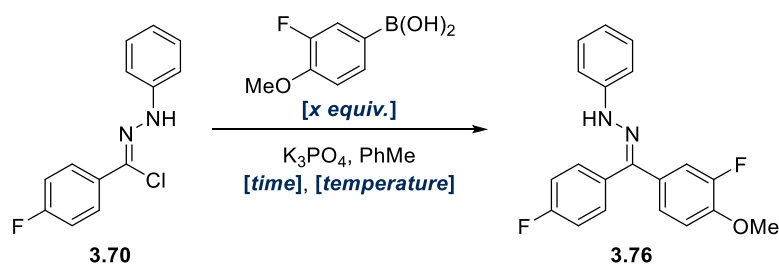


The screen was conducted as outlined in general procedure S using 13 x 2.5 mL microwave vials, each containing hydrazonyl chloride **3.70** (24.9 mg, 0.1 mmol), 3-fluoro-4-

methoxyphenylboronic acid (0.11 mmol – 0.3 mmol), potassium phosphate (63.7 mg, 0.3 mmol) and toluene (1.0 mL). The reaction was stirred at the appropriate temperature for the designated time period. The results obtained are detailed in *Table 3.19* and *Table 5.34*.

*Table 5.34: The conditions employed in the above screen*

| Entry | Time (h) | Temperature (°C) | ArB(OH)$_2$ (mg, mmol) | Conversion (%)[a, b] |
|:-----:|:--------:|:----------------:|:----------------------:|:-----------------:|
| 1 | 2 | 60 | 18.7 mg, 0.11 mmol | 2 |
| 2 | 2 | 80 | 18.7 mg, 0.11 mmol | 17 |
| 3 | 2 | 110 | 18.7 mg, 0.11 mmol | 34 |
| 4 | 2 | 60 | 34.0 mg, 0.20 mmol | 3 |
| 5 | 2 | 110 | 34.0 mg, 0.20 mmol | 24 |
| 6[c,d] | 2 | 80 | 18.7 mg, 0.11 mmol | 4 |
| 7[c,d] | 2 | 80 | 34.0 mg, 0.20 mmol | 2 |
| 8[c,d] | 2 | 110 | 34.0 mg, 0.20 mmol | 30 |
| 9 | 16 | 110 | 18.7 mg, 0.11 mmol | 23 |
| 10[c,d] | 16 | 110 | 18.7 mg, 0.11 mmol | 41 |
| 11[c,d] | 16 | 110 | 34.0 mg, 0.20 mmol | 42 |
| 12[c,d] | 16 | 110 | 51.0 mg, 0.30 mmol | 48 |
| 13[c] | 16 | 110 | 18.7 mg, 0.11 mmol | 35 |

[a] Conversion determined by $^{19}$F NMR with reference to an internal standard

[b] Average value of two experiments with a difference of <10 %

[c] Performed under an N$_2$ atmosphere

[d] 3 Å molecular sieves were added

### 5.3.2.3 Hydroxamoyl Chloride Optimisation

**Base Screen**
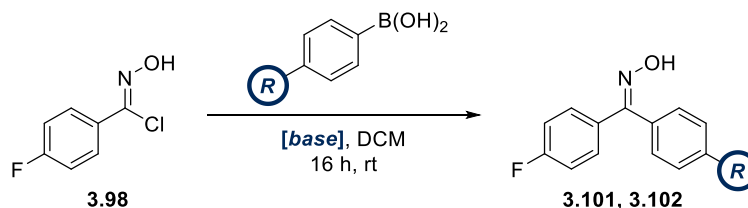


The screen was conducted as outlined in general procedure T using 18 x 2.5 mL microwave vials, each containing hydroxamoyl chloride **3.98** (17.4 mg, 0.1 mmol), 4-methoxyphenylboronic acid (45.6 mg, 0.3 mmol) or 4-(dimethylamino)phenylboronic acid (49.5 mg, 0.3 mmol), the specified base (0.5 mmol) and DCM (1 mL). The reaction was stirred at room temperature for 16 hours. The results obtained are detailed in *Table 3.23* and *Table 5.35*.

*Table 5.35: The conditions employed in the above screen*

| Entry | Base (mg/μL) | Conversion (%)[a] | |
|---|---|---|---|
| | | OMe | NMe$_2$ |
| 1 | KH$_2$PO$_4$ (68.0 mg) | <1 | 31 |
| 2 | K$_2$HPO$_4$ (87.0 mg) | <1 | 16 |
| 3 | K$_3$PO$_4$ (106 mg) | <1 | <1 |
| 4 | NaHCO$_3$ (42.0 mg) | <1 | 31 |
| 5 | Cs$_2$CO$_3$ (163 mg) | 17 | 11 |
| 6 | NEt$_3$ (70.1 μL) | <1 | <1 |
| 7 | Pyridine (40.0 μL) | <1[c] | <1[b] |
| 8 | DBU (75.0 μL) | <1[c] | <1[b] |
| 9 | - | <1 | 46 |

[a]Conversion determined by $^{19}$F NMR with reference to an internal standard. [b]Significant by-product formation observed.

## Base and Stoichiometry Screen
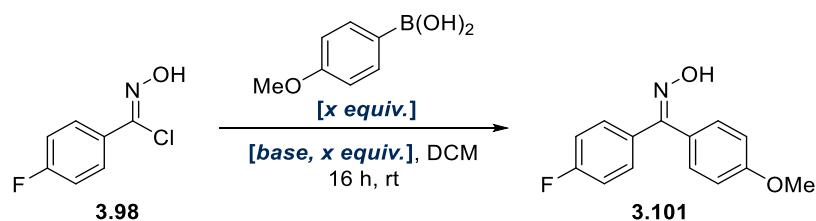


The screen was conducted as outlined in general procedure T using 8 x 2.5 mL microwave vials, each containing hydroxamoyl chloride **3.98** (17.4 mg, 0.1 mmol), 4-methoxyphenylboronic acid (0.15 mmol – 0.3 mmol), caesium carbonate or DMA (both 0.15 mmol – 0.5 mmol) and DCM (1 mL). The reaction was stirred at room temperature for 16 hours. The results obtained are detailed in *Table 3.24* and *Table 5.36*

*Table 5.36: The conditions employed in the above screen*

| Entry | Base (mg, mmol) | ArB(OH)$_2$ (mg, mmol) | Conversion (%)[a] |
|---|---|---|---|
| 1 | Cs$_2$CO$_3$ (163 mg, 0.50 mmol) | 45.6 mg, 0.30 mmol | 30 |
| 2 | Cs$_2$CO$_3$ (97.7 mg, 0.30 mmol) | 45.6 mg, 0.30 mmol | 27 |
| 3 | Cs$_2$CO$_3$ (97.7 mg, 0.30 mmol) | 22.8 mg, 0.15 mmol | 17 |
| 4 | Cs$_2$CO$_3$ | 22.8 mg, 0.15 mmol | 12 |

| | (48.9 mg, 0.15 mmol) | | |

| Entry | Solvent | | Conversion (%) |
|---|---|---|---|
| 5 | DMA (63.4 µL, 0.50 mmol) | 45.6 mg, 0.30 mmol | **58** |
| 6 | DMA (34.8 µL, 0.30 mmol) | 45.6 mg, 0.30 mmol | **54** |
| 7 | DMA (34.8 µL, 0.30 mmol) | 22.8 mg, 0.15 mmol | **43** |
| 8 | DMA (17.4 µL, 0.15 mmol) | 22.8 mg, 0.15 mmol | **37** |

<sup>a</sup>Conversion determined by <sup>19</sup>F NMR with reference to an internal standard.
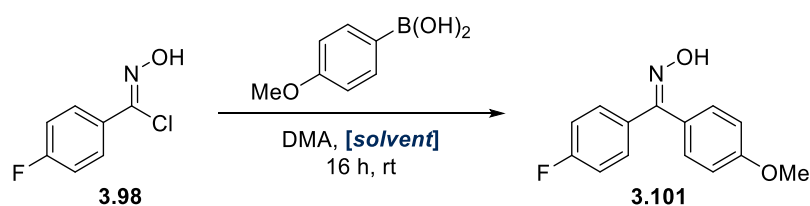
**Solvent Screen**



The screen was conducted as outlined in general procedure T using 13 x 2.5 mL microwave vials, each containing hydroxamoyl chloride **3.98** (17.4 mg, 0.1 mmol), 4-methoxyphenylboronic acid (22.8 mg, 0.15 mmol), DMA (24.0 µL, 0.3 mmol) and the specified solvent (1 mL). The reaction was stirred at room temperature for 16 hours. In some specific cases, the mixture was stirred for 16 hours at 40, 60 or 80 °C. The results obtained are detailed in *Table 3.25* and *Table 5.37*.

*Table 5.37: The conditions employed in the above screen*

| Entry | Solvent (1 mL) | Conversion (%)<sup>a</sup> |
|---|---|---|
| 1 | DCM | **43** |
| 2 | Toluene | **<1** |
| 3 | 1,4-Dioxane | **<1** |
| 4 | THF | **<1** |
| 5 | MeCN | **37** |
| 6 | Acetone | **12** |
| 7 | CHCl<sub>3</sub> | **37** |
| 8 | 2-MeTHF | **<1** |
| 9 | EtOAc | **3** |
| 10 | MeOH | **7** |
| 11 | DCM<sup>c</sup> | **52** |

| 12 | CHCl$_3$[d] | **63** |
| 13 | MeCN[e] | **57** |

**Further Stoichiometry Screen**



The screen was conducted as outlined in general procedure T using 7 x 2.5 mL microwave vials, each containing hydroxamoyl chloride **3.98** (17.4 mg, 0.1 mmol), 4-methoxyphenylboronic acid (0.15 mmol – 0.3 mmol), DMA (0.3 mmol – 0.5 mmol) and chloroform (1 mL). The reaction was stirred at 60 °C for 16 hours. In one specified instance, the reaction was instead stirred at 60 °C for 3 hours. The results obtained are detailed in *Table 3.26* and *Table 5.38*.

*Table 5.38: The conditions employed in the above screen*

| Entry | DMA (µL, mmol) | ArB(OH)$_2$ (mg, mmol) | Conversion (%)[a] |
|-------|----------------|------------------------|-------------------|
| 1 | 38.0 µL, 0.30 mmol | 22.8 mg, 0.15 mmol | **64** |
| 2 | 38.0 µL, 0.30 mmol | 30.4 mg, 0.20 mmol | **69 (54[b,c])** |
| 3 | 38.0 µL, 0.30 mmol | 38.0 mg, 0.25 mmol | **71** |
| 4 | 38.0 µL, 0.30 mmol | 45.6 mg, 0.30 mmol | **77** |
| 5 | 63.4 µL, 0.50 mmol | 22.8 mg, 0.15 mmol | **65** |
| 6 | 63.4 µL, 0.50 mmol | 30.4 mg, 0.20 mmol | **70 (62[b,c])** |
| 7 | 63.4 µL, 0.50 mmol | 38.0 mg, 0.25 mmol | **78** |

## 5.4    Characterisation of Compounds

### 5.4.1   A Modular Protocol for the Synthesis of 2,5-Diaryl Tetrazoles

#### 5.4.1.1 Starting Materials

#### *N*-benzylformamide (2.2)
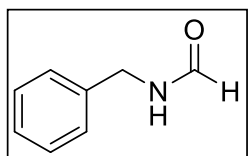
In accordance with previous literature precedent,[421] formic acid (671 μL, 17.5 mmol) was added to acetic anhydride (590 μl, 6.25 mmol) and the mixture was stirred at room temperature. After stirring for 15 minutes, a solution of benzylamine (547 μL, 5 mmol) in DCM (5 mL) was added dropwise, and the mixture was stirred at room temperature for 2 hours. The mixture was then diluted with DCM, washed with water and brine, and concentrated under reduced pressure to afford *N*-benzylformamide (629 mg, 3.86 mmol, 77 % yield) as a white solid. Limited analysis was conducted on this compound owing to the abandonment of the corresponding synthetic route.

**¹H NMR** (400 MHz, CDCl₃) δ 8.23 (s, 1H), 7.39 – 7.22 (m, 5H), 4.46 (d, $J$ = 5.5 Hz, 2H).

**¹³C NMR** (101 MHz, CDCl₃) δ 161.0, 128.8, 128.0, 127.7, 127.0, 42.2.

**LRMS** (ESI) calculated $m/z$ 134.1 for $C_8H_8NO$ [M-H]⁻, found 134.1.

Analytical data in agreement with the literature.[422]

#### *(Isocyanomethyl)benzene* (2.3)
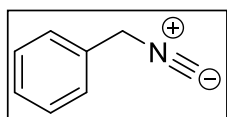
In accordance with previous literature precedent,[421] to a solution of *N*-benzylformamide (67.6 mg, 0.50 mmol) and triethylamine (174 μL, 1.25 mmol) in DCM (1 mL) was added POCl₃ (51.3 μL, 0.55 mmol) at 0 °C. Following complete addition, the reaction was allowed to warm to room temperature and stirred for 1 hour. The reaction mixture was made basic through the addition of an aqueous solution of 2M NaOH and extracted with ethyl acetate. The combined extracts were washed with brine, passed through a phase separator and concentrated under reduced pressure. The obtained residue was purified by silica gel column chromatography (0-100 % EtOAc in hexane) to afford (isocyanomethyl)benzene (34.1 mg, 0.25 mmol, 50.6 % yield) as a yellow oil. Limited analysis was conducted on this compound owing to the abandonment of the corresponding synthetic route.

**¹H NMR** (400 MHz, CDCl₃) δ 7.44 – 7.33 (m, 5H), 4.66 – 4.63 (m, 2H).

**LRMS** (ESI) calculated $m/z$ 117.1 for $C_8H_7N$ [M], found 117.0.

Analytical data in agreement with the literature.[423]

## 1-benzyl-1*H*-tetrazole (2.5)
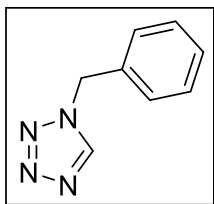
1. In accordance with previous literature procedure,[424] to a solution of 1*H*-tetrazole (0.45 M in MeCN, 11.1 mL, 5.0 mmol) and triethylamine (2.09 mL, 15 mmol) was added benzyl bromide (714 μL, 6 mmol) dropwise at room temperature. The solution was then stirred at 60 °C for 18 hours. The reaction mixture was passed through celite, and excess 2M NaOH solution was added to quench the excess benzyl bromide. The mixture was then concentrated under reduced pressure, re-dissolved in ethyl acetate and separated. The organic layer was washed with water and brine, before again being concentrated under reduced pressure. The obtained residue was purified by silica gel column chromatography (0-100 % EtOAc in hexane) to afford 1-benzyl-1*H*-tetrazole (313 mg, 1.94 mmol, 39 %) as a white solid. 2-benzyl-2*H*-tetrazole (**2.6**) (175 mg, 1.08 mmol, 22 %) was also isolated as a yellow liquid.

2. In accordance with previous literature procedure,[424] to a solution of 1*H*-tetrazole (0.45 M in MeCN, 100 mL, 45.0 mmol) and caesium carbonate (19.060 g, 58.5 mmol) was added benzyl bromide (5.89 mL, 49.5 mmol) dropwise at room temperature. The solution was then stirred at 60 °C for 18 hours. The reaction mixture was passed through celite, and excess 2M NaOH solution was added to the quench excess benzyl bromide. The mixture was then concentrated under reduced pressure, re-dissolved in ethyl acetate and separated. The organic layer was washed with water and brine, before again being concentrated under reduced pressure. The obtained residue was purified by silica gel column chromatography (0-100 % EtOAc in hexane) to afford 1-benzyl-1*H*-tetrazole (3.63 g, 22.2 mmol, 49 %) as a white solid. 2-benzyl-2*H*-tetrazole (**2.6**) (2.23 g, 12.8 mmol, 29 %) was also isolated as a yellow liquid.

**$^1$H NMR** (400 MHz, CDCl$_3$) δ 8.49 (s, 1H), 7.45 – 7.39 (m, 3H), 7.33 – 7.28 (m, 2H), 5.59 (s, 2H).

**$^{13}$C NMR** (101 MHz, CDCl$_3$) δ 142.5, 132.9, 129.6, 129.5, 128.4, 52.3.

**HRMS** (ESI) calculated *m/z* 161.8027 for C$_8$H$_9$N$_4$$^+$ [M+H]$^+$, found 161.8029.

**IR** ν$_{max}$ (neat): 3112, 1494, 1458, 1435, 1243, 1207, 1162, 1102 cm$^{-1}$.

Analytical data in agreement with the literature.[425]

## 2-benzyl-2*H*-tetrazole (2.6)
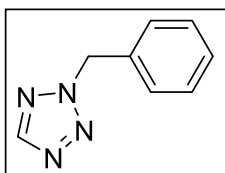
Isolated as a side product during the formation of **2.5**, as detailed above.

**¹H NMR** (400 MHz, CDCl₃) δ 8.49 (s, 1H), 7.38 – 7.31 (m, 5H), 5.78 (s, 2H).

**¹³C NMR** (101 MHz, CDCl₃) δ 153.3, 133.2, 129.1, 128.5, 56.8, one C not observed.

**HRMS** (ESI) calculated *m/z* 161.8027 for $C_8H_9N_4^+$ [M+H]⁺, found 161.8029.

**IR** $\nu_{max}$ (neat): 3140, 3035, 1607, 1497, 1457, 1342, 1281, 1187, 1124, 1077, 1026 cm⁻¹.

Analytical data in agreement with the literature.[426]

## 1-benzyl-5-bromo-1*H*-tetrazole (2.7)
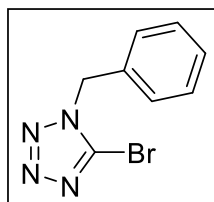


In accordance with previous literature procedure,[427] to a microwave vial was added 1-benzyl-1*H*-tetrazole (1.43 g, 8.93 mmol) and acetic acid (4.46 ml), followed by *N*-bromosuccinimide (1.91 g, 10.71 mmol). The resulting slurry was heated to 80 ℃ to give a homogeneous solution, which was stirred at this temperature for 6 hours. The reaction mixture was then cooled to room temperature, and slowly neutralised *via* dropwise addition of saturated sodium carbonate solution. The resulting precipitate was collected *via* filtration to yield 1-benzyl-5-bromo-1*H*-tetrazole (1.97 g, 8.17 mmol, 91 % yield) as a white solid.

**¹H NMR** (400 MHz, CDCl₃) δ 7.39 – 7.31 (m, 3H), 7.31 – 7.24 (m, 2H), 5.55 – 5.48 (m, 2H).

**¹³C NMR** (101 MHz, CDCl₃) δ 133.2, 132.5, 129.4, 129.3, 128.2, 52.1.

**HRMS** (ESI) calculated *m/z* 238.9854 for $C_8H_8^{79}BrN_4^+$ [M+H]⁺, found 238.9936.

**IR** $\nu_{max}$ (neat): 3028, 3002, 1559, 1496, 1455, 1430, 1404 cm⁻¹.

Analytical data in agreement with the literature.[427]

*5.4.1.2 5-Aryl Tetrazoles*

## 1-benzyl-5-phenyl-1*H*-tetrazole (2.8)
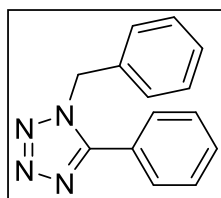


1. To a microwave vial containing 1-benzyl-5-bromo-1*H*-tetrazole (60 mg, 0.25 mmol), phenylboronic acid (45.7 mg, 0.38 mmol), and XPhos Pd G3 (21.2 mg, 0.025 mmol) was added toluene (2.0 mL). The vessel was purged with nitrogen, and potassium carbonate (69.1 mg, 0.5 mmol) was added as a solution in water (0.5 mL). The mixture was stirred at 100 °C for 3 hours, before being cooled to room temperature. The mixture was then diluted with ethyl acetate, passed through celite, and concentrated under reduced pressure. The obtained residue was purified by silica gel column chromatography (0-100 % EtOAc in hexane) to afford 1-benzyl-5-phenyl-1*H*-tetrazole (45.2 mg, 0.19 mmol, 76 % yield) as a colourless oil.

2. In accordance with previous literature precedent,[270] 1-benzyl-5-bromo-1$H$-tetrazole (239 mg, 1.00 mmol) phenylboronic acid (159 mg, 1.30 mmol), sodium carbonate (212 mg, 2.00 mmol) and tetrakis (34.7 mg, 0.03 mmol) were added to a round-bottom flask fitted with a findenser. The mixture was dissolved in a mixture of toluene (8 mL), ethanol (1 mL), and water (1 mL), and stirred at 110 °C for 17 hours. The crude reaction mixture was diluted with ethyl acetate, passed through celite, washed with water and brine, passed through a hydrophobic frit and concentrated under reduced pressure. The obtained residue was purified by silica gel column chromatography (0-100 % EtOAc in hexane) to afford 1-benzyl-5-phenyl-1H-tetrazole (179 mg, 0.75 mmol, 75 % yield) as a yellow oil.

**$^1$H NMR** (400 MHz, CDCl$_3$) δ 7.59 – 7.52 (m, 3H), 7.51 – 7.45 (m, 2H), 7.36 – 7.30 (m, 3H), 7.16 – 7.11 (m, 2H), 5.61 (s, 2H).

**$^{13}$C NMR** (101 MHz, CDCl$_3$) δ 154.8, 134.0, 131.4, 129.3, 129.2, 128.9, 128.8, 127.3, 123.9, 51.5.

**HRMS** (ESI) calculated *m/z* 237.1140 for C$_{14}$H$_{13}$N$_4$ [M+H]$^+$, found 237.1142.

**IR** ν$_{max}$ (neat): 3065, 3033, 2937, 2857, 1529, 1497, 1458, 1401 cm$^{-1}$.

Analytical data in agreement with the literature.[270]

### 1-benzyl-5-(4-methoxyphenyl)-1*H*-tetrazole (2.9)
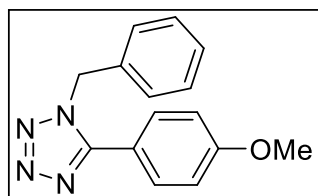


To a microwave vial containing 1-benzyl-5-bromo-1$H$-tetrazole (60 mg, 0.25 mmol), (4-methoxyphenyl)boronic acid (57.0 mg, 0.38 mmol), and XPhos Pd G3 (21.2 mg, 0.025 mmol) was added toluene (2.5 mL). The vessel was purged with nitrogen, and potassium carbonate (69.1 mg, 0.50 mmol) and water (0.045 mL, 2.50 mmol) were added. The mixture was stirred at 100 °C for 2 hours, before cooled to room temperature. The mixture was then diluted with ethyl acetate, passed through celite, and concentrated under reduced pressure. The obtained residue was purified by silica gel column chromatography (0-100 % EtOAc in hexane) to afford 1-benzyl-5-(4-methoxyphenyl)-1$H$-tetrazole (48.3 mg, 0.18 mmol, 72 % yield) as a yellow oil.

**$^1$H NMR** (400 MHz, CDCl$_3$) δ 7.52 (d, *J* = 8.0 Hz, 2H), 7.34 – 7.32 (m, 3H), 7.15 – 7.13 (m, 2H), 6.98 (d, *J* = 8.0 Hz, 2H), 5.60 (s, 2H), 3.84 (s, 3H).

**$^{13}$C NMR** (101 MHz, CDCl$_3$) δ 162.0, 154.6, 134.2, 130.5, 129.3, 128.8, 127.2, 115.9, 114.8, 55.6, 51.4.

**HRMS** (ESI) calculated *m/z* 267.1246 for C$_{15}$H$_{15}$ON$_4$ [M+H]$^+$, found 267.1250.

**IR** ν$_{max}$ (neat): 3081, 3027, 3006, 2958, 2937, 2841, 1611, 1581, 1477, 1446 cm$^{-1}$.

Analytical data in agreement with the literature.[428]

**1-benzyl-5-(4-fluorophenyl)-1*H*-tetrazole (2.10)**
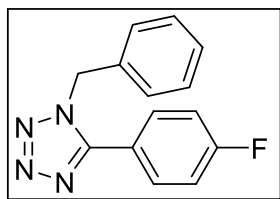


To a microwave vial containing 1-benzyl-5-bromo-1*H*-tetrazole (60 mg, 0.25 mmol), (4-fluorophenyl)boronic acid (52.5 mg, 0.38 mmol), and XPhos Pd G3 (21.2 mg, 0.025 mmol) was added toluene (2.5 mL). The vessel was purged with nitrogen, and potassium carbonate (69.1 mg, 0.50 mmol) and water (0.045 mL, 2.50 mmol) were added. The mixture was stirred at 100 °C for 2 hours, before cooled to room temperature. The mixture was then diluted with ethyl acetate, passed through celite, and concentrated under reduced pressure. The obtained residue was purified by silica gel column chromatography (0-100 % EtOAc in hexane) to afford 1-benzyl-5-(4-fluorophenyl)-1*H*-tetrazole (47.9 mg, 0.15 mmol, 60 % yield) as a colourless oil.

**¹H NMR** (400 MHz, CDCl₃) δ 7.61 – 7.54 (m, 2H), 7.37 – 7.31 (m, 3H), 7.21 – 7.09 (m, 4H), 5.61 (s, 2H).

**¹⁹F NMR** (376 MHz, CDCl₃) δ -107.44 – -107.60 (m).

**¹³C NMR** (101 MHz, CDCl₃) δ 164.6 (d, $^{1}J_{CF}$ = 253.2 Hz), 154.0, 133.9, 131.2 (d, $^{3}J_{CF}$ = 8.8 Hz), 129.4, 129.0, 127.2, 120.1 (d, $^{4}J_{CF}$ = 3.3 Hz), 116.7 (d, $^{2}J_{CF}$ = 22.2 Hz), 51.6.

**HRMS** (ESI) calculated *m/z* 255.1046 for $C_{14}H_{12}FN_4$ [M+H]⁺, found 255.1051.

**IR** $\nu_{max}$ (neat): 3070, 2964, 2932, 2857, 1606, 1539, 1473, 1450 cm⁻¹.

Analytical data in agreement with the literature.[270]

**1-benzyl-5-(4-(trifluoromethyl)phenyl)-1*H*-tetrazole (2.12)**
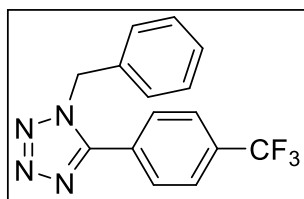


To a microwave vial containing 1-benzyl-5-bromo-1*H*-tetrazole (60 mg, 0.25 mmol), (4-(trifluoromethyl)phenyl)boronic acid (71.2 mg, 0.38 mmol), and XPhos Pd G3 (10.6 mg, 0.013 mmol) was added toluene (2.5 mL). The vessel was purged with nitrogen, and caesium carbonate (163 mg, 0.50 mmol) and water (0.450 mL, 25.0 mmol) were added. The mixture was stirred at 100 °C for 6 hours, before cooled to room temperature. The mixture was then diluted with ethyl acetate, passed through celite, and concentrated under reduced pressure. The obtained residue was purified by silica gel column chromatography (0-100 % EtOAc in hexane) to afford 1-benzyl-5-(4-(trifluoromethyl)phenyl)-1*H*-tetrazole (43.3 mg, 0.14 mmol, 56 % yield) as a colourless oil.

**¹H NMR** (400 MHz, CDCl₃) δ 7.77 (d, *J* = 8.3 Hz, 2H), 7.72 (d, *J* = 8.2 Hz, 2H), 7.39 – 7.35 (m, 3H), 7.17 – 7.13 (m, 2H), 5.64 (s, 2H).

**¹⁹F NMR** (376 MHz, CDCl₃) δ -63.17 (s).

$^{13}$**C NMR** (101 MHz, CDCl$_3$) δ 153.7, 133.7, 133.4 (q, $^2J_{CF}$ = 33.1 Hz), 129.50, 129.45, 129.1, 127.6, 127.2, 126.3 (q, $^3J_{CF}$ = 3.5 Hz), 123.6 (q, $^1J_{CF}$ = 272.6 Hz), 51.8.

**HRMS** (ESI) calculated *m/z* 305.1014 for C$_{15}$H$_{12}$F$_3$N$_4$ [M+H]$^+$, found 305.1018.

**IR** ν$_{max}$ (neat): 3075, 3038, 2964, 1624, 1539, 1497, 1449, 1426 cm$^{-1}$.

Analytical data in agreement with the literature.[428]

### 5-phenyl-1*H*-tetrazole (2.13)
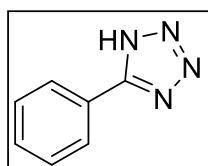


1. Synthesised in accordance with general procedure F using 1-benzyl-5-bromo-1*H*-tetrazole (120 mg, 0.50 mmol), phenylboronic acid (79 mg, 0.65 mmol), XPhos Pd G3 (12.7 mg, 15.0 μmol), Evonik P1071 Pd/C (53.2 mg, 50.0 μmol), caesium carbonate (244 mg, 0.75 mmol), water (901 μL, 50.0 mmol), toluene (5 mL) and ethanol (2.5 mL) to afford 5-phenyl-1*H*-tetrazole (47.7 mg, 0.32 mmol, 65 % yield) as a white solid.

2. Synthesised in accordance with general procedure F using 1-benzyl-5-bromo-1*H*-tetrazole (598 mg, 2.50 mmol), phenylboronic acid (396 mg, 3.75 mmol), XPhos Pd G3 (63.5 mg, 75 μmol), Evonik P1071 Pd/C (266 mg, 0.25 mmol), caesium carbonate (1.22 g, 3.75 mmol), water (4.50 mL, 250 mmol), toluene (25 mL) and ethanol (12.5 mL) to afford 5-phenyl-1*H*-tetrazole (216 mg, 1.47 mmol, 59 % yield) as a white solid.

$^1$**H NMR** (400 MHz, DMSO) δ 16.84 (br. s, 1H), 8.07 – 8.01 (m, 2H), 7.64 – 7.56 (m, 3H).

**13C NMR** (101 MHz, DMSO) δ 155.3, 131.2, 129.4, 126.9, 124.1.

**HRMS** (ESI) calculated *m/z* 147.0671 for C$_7$H$_7$N$_4$ [M+H]$^+$, found 147.0671.

**IR** ν$_{max}$ (neat): 3054, 2974, 2911, 2834, 1652, 1608, 1563, 1485, 1465, 1409 cm$^{-1}$.

Analytical data in agreement with the literature.[429]

### 5-(4-fluorophenyl)-1*H*-tetrazole (2.14)
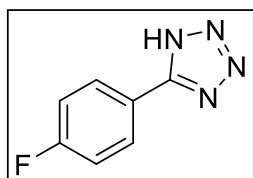


1. Synthesised in accordance with general procedure F using 1-benzyl-5-bromo-1*H*-tetrazole (120 mg, 0.50 mmol), 4-fluorophenylboronic acid (91 mg, 0.65 mmol), XPhos Pd G3 (12.7 mg, 15.0 μmol), Evonik P1071 Pd/C (53.2 mg, 50.0 μmol), caesium carbonate (244 mg, 0.75 mmol), water (901 μL, 50.0 mmol), toluene (5 mL) and ethanol (2.5 mL) to afford 5-(4-fluorophenyl)-1*H*-tetrazole (49.1 mg, 0.30 mmol, 59 % yield) as a white solid.

2. Synthesised in accordance with general procedure F using 1-benzyl-5-bromo-1*H*-tetrazole (598 mg, 2.50 mmol), 4-fluorophenylboronic acid (455 mg, 3.25 mmol), XPhos Pd G3 (63.5 mg, 75 μmol), Evonik P1071 Pd/C (266 mg, 250 μmol), caesium carbonate (1220 mg, 3.75

mmol), water (4.50 mL, 250 mmol), toluene (25 mL) and ethanol (12.5 mL) to afford 5-(4-fluorophenyl)-1*H*-tetrazole (245 mg, 1.48 mmol, 59 % yield) as a white solid.

**¹H NMR** (400 MHz, DMSO) δ 16.84 (br. s, 1H), 8.13 – 8.06 (m, 2H), 7.46 (app. t, *J* = 8.9 Hz, 2H).

**¹⁹F NMR** (376 MHz, DMSO) δ -108.98 (s).

**¹³C NMR** (101 MHz, DMSO) δ 163.6 (d, $^1J_{CF}$ = 249.0 Hz), 154.8, 129.4 (d, $^3J_{CF}$ = 9.0 Hz), 120.9, 116.5 (d, $^2J_{CF}$ = 22.3 Hz).

**HRMS** (ESI) calculated *m/z* 165.0576 for $C_7H_6FN_4$ [M+H]⁺, found 165.0579.

**IR** ν$_{max}$ (neat): 3070, 2985, 2916, 2841, 1609, 1498, 1446, 1410 cm⁻¹.

Analytical data in agreement with the literature.[430]

### 5-(*p*-tolyl)-1*H*-tetrazole (2.15)
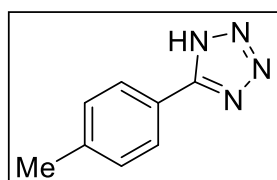


Synthesised in accordance with general procedure F using 1-benzyl-5-bromo-1*H*-tetrazole (120 mg, 0.50 mmol), *p*-tolylboronic acid (88 mg, 0.65 mmol), XPhos Pd G3 (12.7 mg, 15.0 μmol), Evonik P1071 Pd/C (53.2 mg, 50.0 μmol), caesium carbonate (244 mg, 0.75 mmol), water (901 μL, 50.0 mmol), toluene (5 mL) and ethanol (2.5 mL) to afford 5-(*p*-tolyl)-1*H*-tetrazole (41.2 mg, 0.26 mmol, 51 % yield) as a white solid.

**¹H NMR** (400 MHz, DMSO) δ 16.71 (br. s, 1H), 7.96 – 7.90 (m, 2H), 7.45 – 7.39 (m, 2H), 2.39 (s, 3H).

**¹³C NMR** (101 MHz, DMSO) δ 141.1, 129.9, 126.8, 121.3, 21.0, 1C not observed.

**HRMS** (ESI) calculated *m/z* 161.0827 for $C_8H_9N_4$ [M+H]⁺, found 161.0828.

**IR** ν$_{max}$ (neat): 3043, 2964, 2917, 2848, 1612, 1570, 1504, 1432, 1404 cm⁻¹.

Analytical data in agreement with the literature.[429]

### 5-(4-(trifluoromethyl)phenyl)-1*H*-tetrazole (2.16)
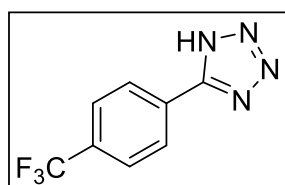


Synthesised in accordance with general procedure F using 1-benzyl-5-bromo-1*H*-tetrazole (120 mg, 0.50 mmol), (4-(trifluoromethyl)phenyl)boronic acid (123 mg, 0.65 mmol), XPhos Pd G3 (12.7 mg, 15.0 μmol), Evonik P1071 Pd/C (53.2 mg, 50.0 μmol), caesium carbonate (244 mg, 0.75 mmol), water (901 μL, 50.0 mmol), toluene (5 mL) and ethanol (2.5 mL) to afford 5-(4-(trifluoromethyl)phenyl)-1*H*-tetrazole (47.1 mg, 0.21 mmol, 42 % yield) as a white solid.

**¹H NMR** (400 MHz, DMSO) δ 17.08 (br. s, 1H), 8.26 (d, *J* = 7.9 Hz, 2H), 7.98 (d, *J* = 7.9 Hz, 2H).

**¹⁹F NMR** (376 MHz, DMSO) δ -61.53 (s).

**¹³C NMR** (101 MHz, DMSO) δ 155.3, 130.9 (q, $^2J_{CF}$ = 32.1 Hz), 128.4, 127.7, 126.3, 123.8 (q, $^1J_{CF}$ = 271.0 Hz).

**HRMS** (ESI) calculated *m/z* 215.0545 for $C_8H_6F_3N_4$ [M+H]$^+$, Found 215.0547.

**IR** ν$_{max}$ (neat): 3070, 2990, 2916, 2852, 1682, 1573, 1506, 1441 cm$^{-1}$.

Analytical data in agreement with the literature.[429]

### 5-(*m*-tolyl)-1*H*-tetrazole (2.17)
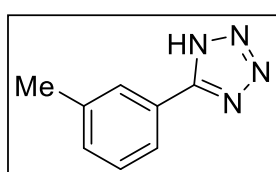
Synthesised in accordance with general procedure F using 1-benzyl-5-bromo-1*H*-tetrazole (120 mg, 0.50 mmol), *m*-tolylboronic acid (88 mg, 0.65 mmol), XPhos Pd G3 (12.7 mg, 15.0 μmol), Evonik P1071 Pd/C (53.2 mg, 50.0 μmol), caesium carbonate (244 mg, 0.75 mmol), water (901 μL, 50.0 mmol), toluene (5 mL) and ethanol (2.5 mL) to afford 5-(*m*-tolyl)-1*H*-tetrazole (21.3 mg, 0.13 mmol, 26 % yield) as a white solid.

**¹H NMR** (400 MHz, DMSO) δ 16.77 (br. s, 1H), 7.87 (s, 1H), 7.83 (d, *J* = 7.6 Hz, 1H), 7.48 (app. t, *J* = 7.6 Hz, 1H), 7.40 (d, *J* = 7.6 Hz, 1H), 2.41 (s, 3H).

**¹³C NMR** (101 MHz, DMSO) δ 155.3, 138.8, 131.8, 129.3, 127.4, 124.1, 20.9, 1C not observed.

**HRMS** (ESI) calculated *m/z* 161.0827 for $C_8H_9N_4$ [M+H]$^+$, found 161.0828.

**IR** ν$_{max}$ (neat): 3065, 2980, 2918, 2847, 1651, 1599, 1560, 1485, 1456, 1415, 1400 cm$^{-1}$.

Analytical data in agreement with the literature.[431]

### 5-(*o*-tolyl)-1*H*-tetrazole (2.18)
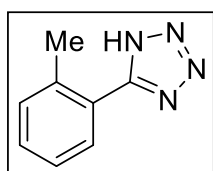
1. Synthesised in accordance with general procedure F using 1-benzyl-5-bromo-1*H*-tetrazole (120 mg, 0.50 mmol), *o*-tolylboronic acid (88.0 mg, 0.65 mmol), XPhos Pd G3 (12.7 mg, 15.0 μmol), Evonik P1071 Pd/C (53.2 mg, 50.0 μmol), caesium carbonate (244 mg, 0.75 mmol), water (901 μL, 50.0 mmol), toluene (5 mL) and ethanol (2.5 mL) to afford 5-(*o*-tolyl)-1*H*-tetrazole (37.8 mg, 0.23 mmol, 47 % yield) as a white solid.

2. Synthesised in accordance with general procedure F using 1-benzyl-5-bromo-1*H*-tetrazole (598 mg, 2.50 mmol), *o*-tolylboronic acid (442 mg, 3.25 mmol), XPhos Pd G3 (63.5 mg, 75.0 μmol), Evonik P1071 Pd/C (266 mg, 250 μmol), caesium carbonate (1.22 g, 3.75

mmol), water (4.50 mL, 250 mmol), toluene (25 mL) and ethanol (12.5 mL) to afford 5-(o-tolyl)-1*H*-tetrazole (229 mg, 1.41 mmol, 57 % yield) as a white solid.

**¹H NMR** (400 MHz, DMSO) δ 16.63 (br. s, 1H), 7.69 (d, *J* = 7.6 Hz, 1H), 7.52 − 7.36 (m, 3H), 2.48 (s, 3H).

**¹³C NMR** (101 MHz, DMSO) δ 155.2, 137.1, 131.3, 130.7, 129.3, 126.2, 123.8, 20.4.

**HRMS** (ESI) calculated *m/z* 161.0827 for $C_8H_9N_4$ [M+H]⁺, found 161.0827.

**IR** ν$_{max}$ (neat): 3065, 3027, 2964, 2921, 2847, 2714, 1654, 1606, 1561, 1484, 1464, 1404 cm⁻¹.

Analytical data in agreement with the literature.[429]

## 5-(naphthalen-2-yl)-1*H*-tetrazole (2.19)
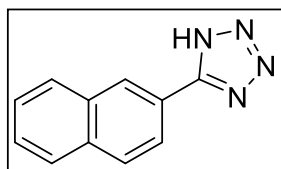


1. Synthesised in accordance with general procedure F using 1-benzyl-5-bromo-1*H*-tetrazole (120 mg, 0.50 mmol), naphthalen-2-ylboronic acid (112 mg, 0.65 mmol), XPhos Pd G3 (12.7 mg, 15.0 μmol), Evonik P1071 Pd/C (53.2 mg, 50.0 μmol), caesium carbonate (244 mg, 0.75 mmol), water (901 μL, 50.0 mmol), toluene (5 mL) and ethanol (2.5 mL) to afford 5-(naphthalen-2-yl)-1*H*-tetrazole (41.3 mg, 0.21 mmol, 42 % yield) as a white solid.

2. Synthesised in accordance with general procedure F using 1-benzyl-5-bromo-1*H*-tetrazole (598 mg, 2.50 mmol), naphthalen-2-ylboronic acid (559 mg, 3.25 mmol), XPhos Pd G3 (63.5 mg, 75.0 μmol), Evonik P1071 Pd/C (266 mg, 250 μmol), caesium carbonate (1.22 g, 3.75 mmol), water (4.50 mL, 50.0 mmol), toluene (25 mL) and ethanol (12.5 mL) to afford 5-(naphthalen-2-yl)-1*H*-tetrazole (331 mg, 1.53 mmol, 61 % yield) as a white solid.

**¹H NMR** (400 MHz, DMSO) δ 16.96 (br. s, 1H), 8.66 (d, *J* = 0.8 Hz, 1H), 8.17 − 8.07 (m, 3H), 8.05 − 8.01 (m, 1H), 7.69 − 7.61 (m, 2H).

**¹³C NMR** (101 MHz, DMSO) δ 133.9, 132.6, 129.2, 128.6, 127.8, 127.8, 127.2, 126.9, 123.6, 121.6, 1C not observed.

**HRMS** (ESI) calculated *m/z* 197.0827 for $C_{11}H_9N_4$ [M+H]⁺, found 197.0831.

**IR** ν$_{max}$ (neat): 3128, 3059, 2990, 2921, 2889, 2841, 1635, 1609, 1564, 1510, 1417 cm⁻¹.

Analytical data in agreement with the literature.[429]

## 5-(4-methoxyphenyl)-1*H*-tetrazole (2.20)
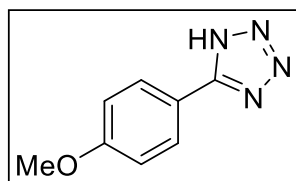
1. Synthesised in accordance with general procedure F using 1-benzyl-5-bromo-1*H*-tetrazole (120 mg, 0.50 mmol), 4-methoxyphenylboronic acid (99 mg, 0.65 mmol), XPhos Pd G3 (12.7 mg, 15.0 μmol), Evonik P1071 Pd/C (53.2 mg, 50.0 μmol), caesium carbonate (244 mg, 0.75 mmol), water (901 μL, 50.0 mmol), toluene (5 mL) and ethanol (2.5 mL) to afford 5-(4-methoxyphenyl)-1*H*-tetrazole (16.9 mg, 0.07 mmol, 15 % yield) as a white solid.

2. Synthesised in accordance with general procedure G using 1-benzyl-5-bromo-1*H*-tetrazole (120 mg, 0.50 mmol), 4-methoxyphenylboronic acid (114 mg, 0.75 mmol), XPhos Pd G3 (12.7 mg, 15.0 μmol), caesium carbonate (326 mg, 1.00 mmol), water (90.0 μL, 5.00 mmol), toluene (2.5 mL), Evonik P1071 Pd/C (36.3 mg, 34.0 μmol), and ethanol (2.5 mL) to afford 5-(4-methoxyphenyl)-1*H*-tetrazole (49.4 mg, 0.28 mmol, 60 % yield) as a white solid. Column chromatography (0-100 % ethyl acetate in petroleum ether) prior to the hydrogenolysis step was required for this substrate.

**¹H NMR** (400 MHz, DMSO) δ 7.98 (d, *J* = 8.9 Hz, 2H), 7.16 (d, *J* = 8.9 Hz, 2H), 3.84 (s, 3H) 1H not observed (exchangeable).

**¹³C NMR** (101 MHz, DMSO) δ 161.4, 128.6, 127.0, 116.3, 114.8, 55.4.

**HRMS** (ESI) calculated *m/z* 177.0776 for $C_8H_9ON_4$ [M+H]⁺, found 177.0770.

**IR** $\nu_{max}$ (neat): 3160, 3081, 3022, 2919, 2843, 1610, 1585, 1499, 1470, 1443, 1405 cm⁻¹.

Analytical data in agreement with the literature.[429]

## 5-(pyren-1-yl)-1*H*-tetrazole (2.21)
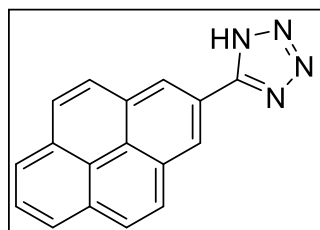
Synthesised in accordance with general procedure F using 1-benzyl-5-bromo-1*H*-tetrazole (120 mg, 0.50 mmol), pyren-1-ylboronic acid (160 mg, 0.65 mmol), XPhos Pd G3 (12.7 mg, 15.0 μmol), Evonik P1071 Pd/C (53.2 mg, 50.0 μmol), caesium carbonate (244 mg, 0.75 mmol), water (901 μL, 50.0 mmol), toluene (5 mL) and ethanol (2.5 mL) to afford 5-(pyren-1-yl)-1*H*-tetrazole (37.6 mg, 0.11 mmol, 23 % yield) as a white solid.

**¹H NMR** (400 MHz, DMSO) δ 17.12 (br. s, 1H), 8.95 (d, *J* = 9.3 Hz, 1H), 8.49 (s, 2H), 8.44 (d, *J* = 2.9 Hz, 1H), 8.42 (d, *J* = 2.9 Hz, 1H), 8.39 (d, *J* = 9.4 Hz, 1H), 8.36 (d, *J* = 8.9 Hz, 1H), 8.30 (d, *J* = 8.9 Hz, 1H), 8.21 − 8.15 (m, 1H).

**¹³C NMR** (101 MHz, DMSO) δ 132.5, 130.7, 130.1, 129.2, 129.1, 128.8, 128.5, 128.1, 127.3, 127.2, 126.9, 126.4, 126.1, 125.0, 124.2, 124.0, 123.4.

**HRMS** (ESI) calculated *m/z* 271.0984 for $C_{17}H_{11}N_4$ [M+H]$^+$, found 271.0988.

**IR** $\nu_{max}$ (neat): 3022, 2921, 2847, 1577, 1454, 1421 cm$^{-1}$.

Analytical data in agreement with the literature.[432]

## 5-phenethyl-1*H*-tetrazole (2.22)
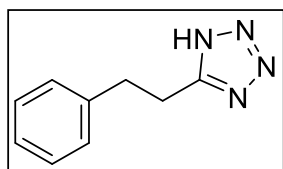


1. Synthesised in accordance with general procedure F using 1-benzyl-5-bromo-1*H*-tetrazole (120 mg, 0.50 mmol), (*E*)-styrylboronic acid (96 mg, 0.65 mmol), XPhos Pd G3 (12.7 mg, 15.0 µmol), Evonik P1071 Pd/C (53.2 mg, 50.0 µmol), caesium carbonate (244 mg, 0.75 mmol), water (901 µL, 50.0 mmol), toluene (5 mL) and ethanol (2.5 mL) to afford 5-phenethyl-1*H*-tetrazole (20.9 mg, 0.11 mmol, 22 % yield) as a brown gum.

2. Synthesised in accordance with general procedure G using 1-benzyl-5-bromo-1*H*-tetrazole (120 mg, 0.50 mmol), (*E*)-styrylboronic acid (111 mg, 0.75 mmol), XPhos Pd G3 (12.7 mg, 15.0 µmol), caesium carbonate (326 mg, 1.00 mmol), water (90.0 µL, 5.00 mmol), toluene (2.5 mL), Evonik P1071 Pd/C (29.6 mg, 28.0 µmol), and ethanol (2.5 mL) to afford 5-phenethyl-1*H*-tetrazole (48.9 mg, 0.28 mmol, 77 % yield) as a white solid. Column chromatography (0-100 % ethyl acetate in petroleum ether) prior to the hydrogenolysis step was required for this substrate.

**¹H NMR** (500 MHz, DMSO) δ 11.07 (br. s, 1H), 7.28 – 7.35 (m, 2H), 7.23 – 7.15 (m, 3H), 3.18 (t, *J* = 7.8 Hz, 2H), 3.06 (t, *J* = 7.7 Hz, 2H).

**¹³C NMR** (126 MHz, DMSO) δ 155.4, 140.0, 128.4, 128.3, 126.3, 32.7, 24.6.

**HRMS** (ESI) calculated *m/z* 175.0984 for $C_9H_{11}N_4$ [M+H]$^+$, found 175.0977.

**IR** $\nu_{max}$ (neat): 3030, 3007, 2992, 2972, 2922, 2857, 1560, 1491, 1454, 1425, 1408 cm$^{-1}$.

Analytical data in agreement with the literature.[433]

## Methyl 4-(1*H*-tetrazol-5-yl)benzoate (2.27)
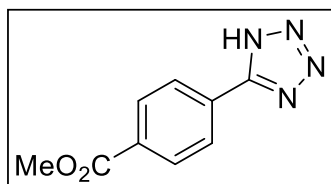


Synthesised in accordance with general procedure G using 1-benzyl-5-bromo-1*H*-tetrazole (120 mg, 0.50 mmol), (4-(methoxycarbonyl)phenyl)boronic acid (135 mg, 0.75 mmol), XPhos Pd G3 (12.7 mg, 15.0 µmol), caesium carbonate (326 mg, 1.00 mmol), water (90.0 µL, 5.00 mmol), toluene (2.5 mL), Evonik P1071 Pd/C (10.6 mg, 10.0 µmol), and ethanol (1.5 mL) to afford methyl 4-(1*H*-tetrazol-5-yl)benzoate (20.3 mg, 0.10 mmol, 27 % yield) as a yellow solid. Column chromatography (0-100 % ethyl acetate in petroleum ether) prior to the hydrogenolysis step was required for this substrate.

**¹H NMR** (400 MHz, DMSO) δ 8.19 (d, *J* = 8.6 Hz, 2H), 8.15 (d, *J* = 8.7 Hz, 2H), 3.89 (s, 3H).

**¹³C NMR** (101 MHz, DMSO) δ 165.6, 155.7, 145.3, 131.5, 130.1, 127.2, 52.4.

**HRMS** (ESI) calculated *m/z* 205.0720 for $C_9H_9N_4O_2$ [M+H]⁺, found 205.0720.

**IR** $v_{max}$ (neat): 3154, 3098, 3073, 3046, 3019, 2953, 2928, 2855, 1709, 1686, 1566, 1499, 1427 cm⁻¹.

Analytical data in agreement with the literature.[433]

### 5-([1,1'-biphenyl]-2-yl)-1*H*-tetrazole (2.33)
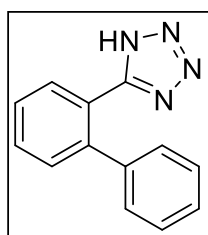
Synthesised in accordance with general procedure G using 1-benzyl-5-bromo-1*H*-tetrazole (120 mg, 0.50 mmol), [1,1'-biphenyl]-2-ylboronic acid (150 mg, 0.75 mmol), XPhos Pd G3 (12.7 mg, 15.0 μmol), caesium carbonate (326 mg, 1.00 mmol), water (90.0 μL, 5.00 mmol), toluene (2.5 mL), Evonik P1071 Pd/C (36.3 mg, 34.0 μmol), and ethanol (2.5 mL) to afford 5-([1,1'-biphenyl]-2-yl)-1*H*-tetrazole (24.1 mg, 0.11 mmol, 22 % yield) as a white solid. Column chromatography (0-100 % ethyl acetate in petroleum ether) prior to the hydrogenolysis step was required for this substrate.

**¹H NMR** (400 MHz, DMSO) δ 7.72 – 7.65 (m, 2H), 7.61 – 7.54 (m, 2H), 7.34 – 7.28 (m, 3H), 7.12 – 7.07 (m, 2H) 1H not observed (exchangeable).

**¹³C NMR** (101 MHz, DMSO) δ 141.5, 139.2, 131.1, 130.6, 128.7, 128.2, 127.7, 127.4, 123.4, 2C not observed.

**HRMS** (ESI) calculated *m/z* 223.0978 for $C_{13}H_{11}N_4$ [M+H]⁺, found 223.0979.

**IR** $v_{max}$ (neat): 3059, 2963, 2918, 2886, 2845, 2822, 1601, 1572, 1560, 1477, 1454, 1437 cm⁻¹.

Analytical data in agreement with the literature.[433]

### 5-([1,1'-biphenyl]-4-yl)-1*H*-tetrazole (2.34)
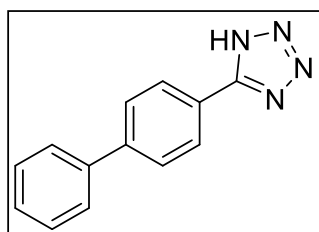
Synthesised in accordance with general procedure G using 1-benzyl-5-bromo-1*H*-tetrazole (120 mg, 0.50 mmol), [1,1'-biphenyl]-4-ylboronic acid (150 mg, 0.75 mmol), XPhos Pd G3 (12.7 mg, 15.0 μmol), caesium carbonate (326 mg, 1.00 mmol), water (90.0 μL, 5.00 mmol), toluene (2.5 mL), Evonik P1071 Pd/C (27.3 mg, 26.0 μmol), and ethanol (2.5 mL) to afford 5-([1,1'-biphenyl]-4-yl)-1*H*-tetrazole (56.7 mg, 0.26 mmol, 53 % yield) as a white solid. Column chromatography (0-

100 % ethyl acetate in petroleum ether) prior to the hydrogenolysis step was required for this substrate.

**¹H NMR** (500 MHz, DMSO) δ 8.15 (d, *J* = 8.3 Hz, 2H), 7.91 (d, *J* = 8.3 Hz, 2H), 7.76 (d, *J* = 7.5 Hz, 2H), 7.50 (app. t, *J* = 7.6 Hz, 2H), 7.43 – 7.40 (m, 1H).

**¹³C NMR** (126 MHz, DMSO) δ 155.0, 151.0, 142.7, 138.9, 129.1, 128.2, 127.6, 126.8, 123.1.

**HRMS** (ESI) calculated *m/z* 223.0978 for $C_{13}H_{11}N_4$ [M+H], found 223.0979.

**IR** $\nu_{max}$ (neat): 3092, 3059, 3003, 2982, 2922, 2851, 1614, 1560, 1522, 1501, 1483, 1452, 1425 cm⁻¹.

Analytical data in agreement with the literature.[429]

*5.4.1.3 2,5-Diaryl Tetrazoles*

**2,5-diphenyl-2*H*-tetrazole (2.35, 3.18)**
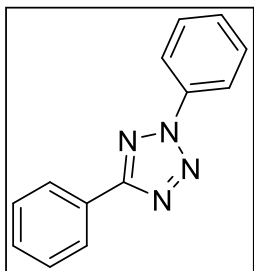


Synthesised in accordance with general procedure H using tetrazole **2.13** (29.0 mg, 0.20 mmol), phenylboronic acid (49.0 mg, 0.40 mmol), copper(I) oxide (1.40 mg, 10.0 μmol) and DMSO (2 mL) to afford 2,5-diphenyl-2*H*-tetrazole (36.7 mg, 0.17 mmol, 83 % yield) as a white solid.

**¹H NMR** (400 MHz, CDCl₃) δ 8.30 – 8.24 (m, 2H), 8.24 – 8.18 (m, 2H), 7.62 – 7.47 (m, 6H).

**¹³C NMR** (101 MHz, CDCl₃) δ 165.4, 137.1, 130.7, 129.8, 129.8, 129.1, 127.3, 127.2, 120.0.

**HRMS** (ESI) calculated *m/z* 223.0984 for $C_{13}H_{12}N_4$ [M+H]⁺, found 223.0986.

**IR** $\nu_{max}$ (neat): 3066, 1595, 1530, 1497, 1470, 1447 cm⁻¹.

Analytical data in agreement with the literature.[205]

**N*-(4-(5-phenyl-2*H*-tetrazol-2-yl)phenyl)acetamide (2.36, 3.16)**
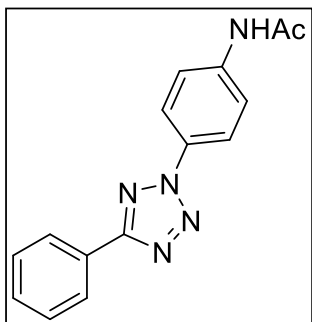


Synthesised in accordance with general procedure H using tetrazole **2.13** (29.0 mg, 0.20 mmol), (4-acetamidophenyl)boronic acid (72.0 mg, 0.40 mmol), copper(I) oxide (1.40 mg, 10.0 μmol) and DMSO (2 mL) to afford *N*-(4-(5-phenyl-2*H*-tetrazol-2-yl)phenyl)acetamide (49.7 mg, 0.18 mmol, 83 % yield) as a brown solid.

**¹H NMR** (400 MHz, DMSO) δ 10.32 (s, 1H), 8.18 – 8.13 (m, 2H), 8.09 (d, *J* = 9.0 Hz, 2H), 7.88 (d, *J* = 9.0 Hz, 2H), 7.63 – 7.58 (m, 3H), 2.11 (s, 3H).

**¹³C NMR** (101 MHz, MeOD) δ 162.4, 156.8, 132.3, 124.3, 122.3, 120.7, 118.9, 118.4, 112.1, 112.0, 14.5.

**HRMS** (ESI) calculated *m/z* 280.1193 for $C_{15}H_{14}N_5O$ [M+H]⁺, found 280.1196.

**IR** $v_{max}$ (neat): 3265, 3144, 3073, 2961, 2926, 1667, 1605, 1557, 1531, 1510, 1468, 1452, 1418 cm⁻¹.

Analytical data in agreement with the literature.[205]

### 2-(naphthalen-2-yl)-5-phenyl-2*H*-tetrazole (2.37)
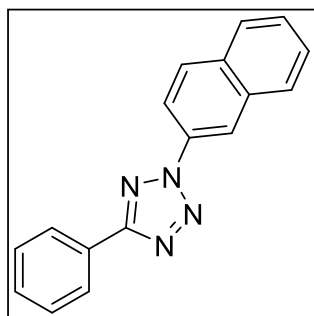
Synthesised in accordance with general procedure H using tetrazole **2.13** (29.0 mg, 0.20 mmol), 2-naphthylboronic acid (69.0 mg, 0.40 mmol), copper(I) oxide (1.40 mg, 10.0 μmol) and DMSO (2 mL) to afford 2-(naphthalen-2-yl)-5-phenyl-2*H*-tetrazole (46.0 mg, 0.17 mmol, 84 % yield) as a yellow solid.

**¹H NMR** (400 MHz, CDCl₃) δ 8.65 (d, *J* = 2.0 Hz, 1H), 8.34 – 8.28 (m, 3H), 8.02 (d, *J* = 8.9 Hz, 1H), 7.98 (dd, *J* = 6.5, 2.7 Hz, 1H), 7.91 (dd, *J* = 6.3, 2.9 Hz, 1H), 7.62 – 7.48 (m, 5H).

**¹³C NMR** (101 MHz, CDCl₃) δ 165.4, 134.4, 133.5, 133.2, 130.7, 130.0, 129.1, 128.8, 128.1, 127.6, 127.5, 127.3, 127.2, 118.3, 118.0.

**HRMS** (ESI) calculated *m/z* 273.1140 for $C_{17}H_{13}N_4$ [M+H]⁺, found 273.1143.

**IR** $v_{max}$ (neat): 3067, 3051, 2922, 1599, 1514, 1495, 1472, 1449 cm⁻¹.

### 5-phenyl-2-(*o*-tolyl)-2*H*-tetrazole (2.38)
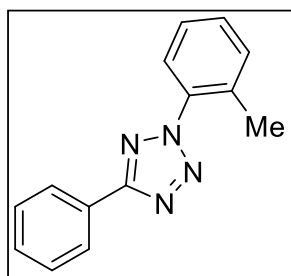
Synthesised in accordance with general procedure H using tetrazole **2.13** (29.0 mg, 0.20 mmol), *o*-tolylboronic acid (54.0 mg, 0.40 mmol), copper(I) oxide (1.40 mg, 10.0 μmol) and DMSO (2 mL) to afford 5-phenyl-2-(*o*-tolyl)-2*H*-tetrazole (37.0 mg, 0.16 mmol, 78 % yield) as an off-white solid.

**¹H NMR** (400 MHz, CDCl₃) δ 8.29 – 8.22 (m, 2H), 7.70 – 7.65 (m, 1H), 7.57 – 7.49 (m, 3H), 7.48 – 7.38 (m, 3H), 2.44 (s, 3H).

**¹³C NMR** (101 MHz, CDCl₃) δ 165.1, 136.7, 133.3, 132.1, 130.7, 130.5, 129.1, 127.4, 127.2, 127.1, 125.4, 18.9.

**HRMS** (ESI) calculated *m/z* 237.1140 for $C_{14}H_{13}N_4$ [M+H]⁺, found 237.1141.

**IR** $v_{max}$ (neat): 3051, 2959, 2920, 2853, 1585, 1530, 1497, 1468, 1450 cm⁻¹.

Analytical data in agreement with the literature.[434]

**5-(4-fluorophenyl)-2-phenyl-2*H*-tetrazole (2.39)**
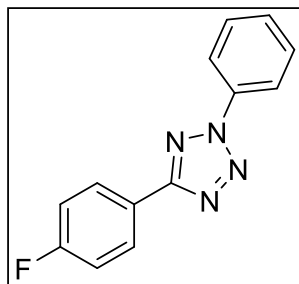


Synthesised in accordance with general procedure H using tetrazole **2.14** (39.0 mg, 0.24 mmol), phenylboronic acid (49.0 mg, 0.48 mmol), copper(I) oxide (1.70 mg, 12.0 μmol) and DMSO (2 mL) to afford 5-(4-fluorophenyl)-2-phenyl-2*H*-tetrazole (45.0 mg, 0.19 mmol, 78 % yield) as a white solid.

**$^1$H NMR** (400 MHz, CDCl$_3$) δ 8.28 – 8.21 (m, 2H), 8.20 – 8.15 (m, 2H), 7.61 – 7.54 (m, 2H), 7.53 – 7.47 (m, 1H), 7.24 – 7.17 (m, 2H).

**$^{19}$F NMR** (471 MHz, CDCl$_3$) δ -109.57 (tt, *J* = 8.6, 5.3 Hz).

**$^{13}$C NMR** (101 MHz, CDCl$_3$) δ 164.6, 164.4 (d, $^1J_{CF}$ = 250.9 Hz), 137.0, 129.9, 129.2 (d, $^3J_{CF}$ = 8.8 Hz), 123.6 (d, $^4J_{CF}$ = 3.1 Hz), 120, 116.2 (d, $^2J_{CF}$ = 22.0 Hz).

**HRMS** (ESI) calculated *m/z* 241.0889 for C$_{13}$H$_{10}$FN$_4$ [M+H]$^+$, found 241.0891.

**IR** ν$_{max}$ (neat): 3082, 3069, 3045, 3026, 2924, 1597, 1541, 1495, 1491, 1474, 1458, 1423 cm$^{-1}$.

Analytical data in agreement with the literature.[93]

**N-(4-(5-(4-fluorophenyl)-2*H*-tetrazol-2-yl)phenyl)acetamide (2.40)**
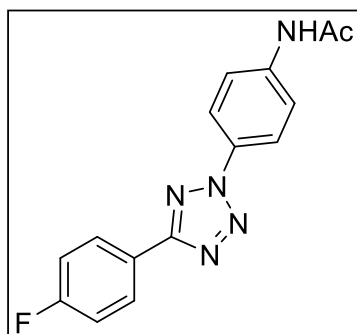


Synthesised in accordance with general procedure H using tetrazole **2.14** (32.8 mg, 0.20 mmol), (4-acetamidophenyl)boronic acid (71.6 mg, 0.40 mmol), copper(I) oxide (1.40 mg, 12.0 μmol) and DMSO (2 mL) to afford N-(4-(5-(4-fluorophenyl)-2*H*-tetrazol-2-yl)phenyl)acetamide (42.0 mg, 0.14 mmol, 71 % yield) as a white solid.

**$^1$H NMR** (400 MHz, DMSO) δ 10.31 (s, 1H), 8.20 (dd, *J* = 8.5, 5.6 Hz, 2H), 8.08 (d, *J* = 8.9 Hz, 2H), 7.87 (d, *J* = 8.9 Hz, 2H), 7.45 (app. t, *J* = 8.8 Hz, 2H), 2.10 (s, 3H).

**$^{19}$F NMR** (471 MHz, DMSO) δ -109.54 – -109.62 (m).

**$^{13}$C NMR** (101 MHz, CDCl$_3$) δ 168.8, 163.6 (d, $^1J_{CF}$ = 248.1 Hz), 163.5, 141.0, 131.0, 129.0 (d, $^3J_{CF}$ = 8.8 Hz), 123.1 (d, $^4J_{CF}$ = 2.9 Hz), 120.7 , 119.7, 116.5 (d, $^2J_{CF}$ = 22.0 Hz), 24.1.

**HRMS** (ESI) calculated *m/z* 298.1099 for C$_{15}$H$_{13}$FN$_5$O [M+H]$^+$, found 298.1101.

**IR** ν$_{max}$ (neat): 3310, 3277, 3208, 3150, 3088, 1665, 1609, 1541, 1508, 1466, 1423, 1414 cm$^{-1}$.

### 5-(4-fluorophenyl)-2-(naphthalen-2-yl)-2*H*-tetrazole (2.41)
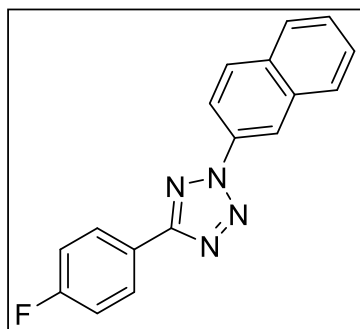
Synthesised in accordance with general procedure H using tetrazole **2.14** (39.2 mg, 0.24 mmol), 2-naphthylboronic acid (68.8 mg, 0.42 mmol), copper(I) oxide (1.70 mg, 12.0 µmol) and DMSO (2 mL) to afford 5-(4-fluorophenyl)-2-(naphthalen-2-yl)-2*H*-tetrazole (10.0 mg, 0.04 mmol, 15 % yield) as a yellow solid.

**$^1$H NMR** (400 MHz, CDCl$_3$) δ 8.66 (d, *J* = 2.0 Hz, 1H), 8.35 – 8.26 (m, 3H), 8.04 (d, *J* = 9.0 Hz, 1H), 8.02 – 7.98 (m, 1H), 7.96 – 7.91 (m, 1H), 7.65 – 7.56 (m, 2H), 7.24 (dd, *J* = 13.6, 4.9 Hz, 2H).

**$^{19}$F NMR** (471 MHz, CDCl$_3$) δ -109.41 – -109.65 (m).

**$^{13}$C NMR** (101 MHz, CDCl$_3$) δ 164.7, 163.4 (d, $^1J_{CF}$ = 250.8 Hz), 134.4, 133.6, 133.2, 130.1, 129.3 (d, $^3J_{CF}$ = 8.6 Hz), 128.8, 128.2, 127.7, 127.6, 123.6 (d, $^4J_{CF}$ = 4.2 Hz), 118.4, 118.0, 116.3 (d, $^2J_{CF}$ = 22.3 Hz).

**HRMS** (ESI) calculated *m/z* 291.1046 for C$_{17}$H$_{12}$FN$_4$ [M+H]$^+$, found 291.1046.

**IR** ν$_{max}$ (neat): 3061, 2953, 2922, 2851, 1607, 1603, 1539, 1510, 1476, 1460, 1447, 1423 cm$^{-1}$.

### 5-(4-fluorophenyl)-2-(*o*-tolyl)-2*H*-tetrazole (2.42)
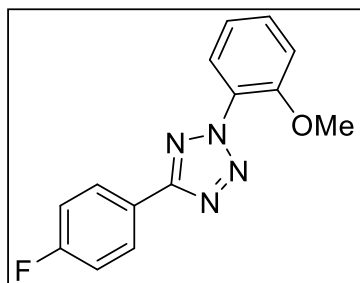
Synthesised in accordance with general procedure H using tetrazole **2.14** (32.8 mg, 0.20 mmol), *o*-tolylboronic acid (54.0 mg, 0.40 mmol), copper(I) oxide (1.40 mg, 10.0 µmol) and DMSO (2 mL) to afford 5-(4-fluorophenyl)-2-(*o*-tolyl)-2*H*-tetrazole (41.4 mg, 0.16 mmol, 81 % yield) as an off-white solid.

**$^1$H NMR** (400 MHz, CDCl$_3$) δ 8.27 – 8.21 (m, 2H), 7.66 (dd, *J* = 7.7, 1.1 Hz, 1H), 7.50 – 7.37 (m, 3H), 7.25 – 7.18 (m, 2H), 2.43 (s, 3H).

**$^{19}$F NMR** (471 MHz, CDCl$_3$) δ -109.70 (tt, *J* = 8.6, 5.3 Hz).

**$^{13}$C NMR** (101 MHz, CDCl$_3$) δ 164.33 (d, $^1J_{CF}$ = 250.7 Hz), 164.31, 136.6, 133.2, 132.1, 130.5, 129.2 (d, $^3J_{CF}$ = 8.6 Hz), 127.1 , 125.4, 123.7 (d, $^4J_{CF}$ = 2.9 Hz), 116.3 (d, $^2J_{CF}$ = 22.3 Hz), 18.9.

**HRMS** (ESI) calculated *m/z* 255.1046 for C$_{14}$H$_{12}$FN$_4$ [M+H]$^+$, found 255.1051.

**IR** ν$_{max}$ (neat): 3088, 2984, 2963, 2924, 2853, 1603, 1497, 1472, 1458, 1423 cm$^{-1}$.

## 5-(naphthalen-2-yl)-2-phenyl-2*H*-tetrazole (2.43)
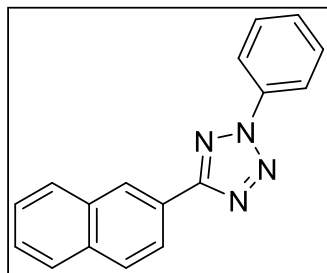
Synthesised in accordance with general procedure H using tetrazole **2.19** (39.2 mg, 0.20 mmol), phenylboronic acid (49.0 mg, 0.40 mmol), copper(I) oxide (1.40 mg, 10.0 μmol) and DMSO (2 mL) to afford 5-(naphthalen-2-yl)-2-phenyl-2*H*-tetrazole (46.4 mg, 0.17 mmol, 85 % yield) as a beige solid.

**¹H NMR** (500 MHz, CDCl₃) δ 8.80 (s, 1H), 8.32 (dd, *J* = 8.5, 1.6 Hz, 1H), 8.26 – 8.22 (m, 2H), 8.02 – 7.97 (m, 2H), 7.92 – 7.87 (m, 1H), 7.61 – 7.54 (m, 4H), 7.51 (app. t, *J* = 7.4 Hz, 1H).

**¹³C NMR** (126 MHz, CDCl₃) δ 165.5, 137.1, 134.5, 133.4, 129.81, 129.77, 128.93, 128.87, 128.0, 127.4, 127.1, 126.9, 124.6, 124.1, 120.0.

**HRMS** (ESI) calculated *m/z* 273.1140 for $C_{17}H_{13}N_4$ [M+H]⁺, found 273.1143.

**IR** ν_max (neat): 3051, 2930 2853, 1595, 1522, 1503, 1468, 1436 cm⁻¹.

## 2,5-di(naphthalen-2-yl)-2*H*-tetrazole (2.45)
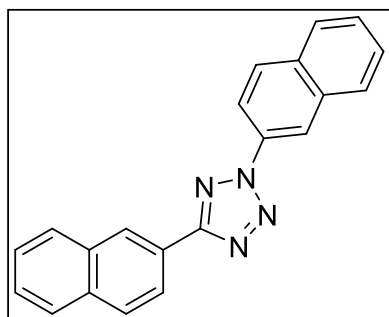
Synthesised in accordance with general procedure H using tetrazole **2.19** (39.2 mg, 0.20 mmol), 2-naphthylboronic acid (69.0 mg, 0.40 mmol), copper(I) oxide (1.40 mg, 10.0 μmol) and DMSO (2 mL) to afford 2,5-di(naphthalen-2-yl)-2*H*-tetrazole (10.2 mg, 0.03 mmol, 16 % yield) as a white solid.

**¹H NMR** (400 MHz, CDCl₃) δ 8.85 (s, 1H), 8.72 (d, *J* = 1.7 Hz, 1H), 8.39 (dd, *J* = 4.5, 1.8 Hz, 1H), 8.37 (dd, *J* = 4.1, 1.8 Hz, 1H), 8.07 (d, *J* = 9.0 Hz, 1H), 8.05 – 7.99 (m, 3H;), 7.97 – 7.90 (m, 2H;), 7.66 – 7.55 (m, 4H).

**¹³C NMR** (101 MHz, CDCl₃) δ 165.6, 134.6, 134.5, 133.6, 133.4, 133.3, 130.1, 129.0, 128.9, 128.85, 128.2, 128.1, 127.7, 127.6, 127.4, 127.2, 126.9, 124.6, 124.2, 118.5, 118.1.

**HRMS** (ESI) calculated *m/z* 323.1297 for $C_{21}H_{15}N_4$ [M+H]⁺, found 323.1299.

**IR** ν_max (neat): 3055, 3030, 1630, 1603, 1524, 1501, 1474, 1437 cm⁻¹.

### 5-(naphthalen-2-yl)-2-(*o*-tolyl)-2*H*-tetrazole (2.46)
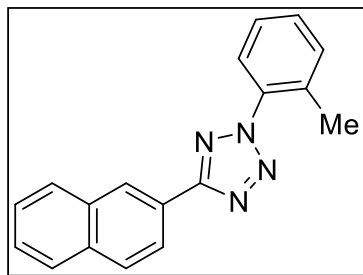


Synthesised in accordance with general procedure H using tetrazole **2.19** (39.2 mg, 0.20 mmol), *o*-tolylboronic acid (54.0 mg, 0.40 mmol), copper(I) oxide (1.40 mg, 10.0 µmol) and DMSO (2 mL) to afford 5-(naphthalen-2-yl)-2-(*o*-tolyl)-2*H*-tetrazole (20.0 mg, 0.07 mmol, 35 % yield) as a beige solid.

**¹H NMR** (500 MHz, CDCl₃) δ 8.80 (s, 1H), 8.32 (dd, *J* = 8.5, 1.6 Hz, 1H), 8.00 (d, *J* = 8.5 Hz, 1H), 8.00 – 7.97 (m, 1H), 7.93 – 7.88 (m, 1H), 7.71 (d, *J* = 7.9 Hz, 1H), 7.59 – 7.53 (m, 2H), 7.51 – 7.39 (m, 3H), 2.47 (s, 3H).

**¹³C NMR** (126 MHz, CDCl₃) δ 165.2, 136.7, 134.5, 133.4, 133.3, 132.1, 130.5, 129.0, 128.9, 128.0, 127.3, 127.07, 127.05, 126.9, 125.4, 124.7, 124.1, 19.0.

**HRMS** (ESI) calculated *m/z* 287.1297 for $C_{18}H_{15}N_4$ [M+H]⁺, found 287.1299.

**IR** ν_max (neat): 3061, 2924, 2853, 1605, 1522, 1493, 1464, 1435 cm⁻¹.

### 2-phenyl-5-(*o*-tolyl)-2*H*-tetrazole (2.47)
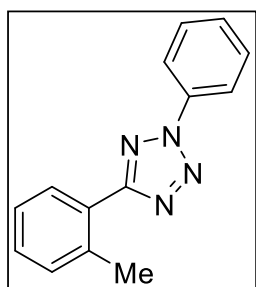


Synthesised in accordance with general procedure H using tetrazole **2.18** (32.0 mg, 0.20 mmol), phenylboronic acid (49.0 mg, 0.40 mmol), copper(I) oxide (1.40 mg, 10.0 µmol) and DMSO (2 mL) to afford 2-phenyl-5-(*o*-tolyl)-2*H*-tetrazole (32.0 mg, 0.14 mmol, 68 % yield) as an off-white solid.

**¹H NMR** (400 MHz, DMSO) δ 8.19 – 8.13 (m, 2H), 8.04 (dd, *J* = 7.6, 1.2 Hz, 1H), 7.73 – 7.66 (m, 2H), 7.64 – 7.59 (m, 1H), 7.50 – 7.36 (m, 3H), 2.64 (s, 3H).

**¹³C NMR** (101 MHz, DMSO) δ 164.9, 137.0, 136.2, 131.5, 130.4, 130.1, 129.2, 126.3, 125.6, 119.9, 21.2, 1C not observed.

**HRMS** (ESI) calculated *m/z* 237.1135 for $C_{14}H_{13}N_4$ [M+H]⁺, found 237.1134.

**IR** ν_max (neat): 3076, 3030, 2980, 2959, 2926, 1595, 1522, 1497, 1479, 1456, 1418 cm⁻¹.

### N-(4-(5-(o-tolyl)-2H-tetrazol-2-yl)phenyl)acetamide (2.48)
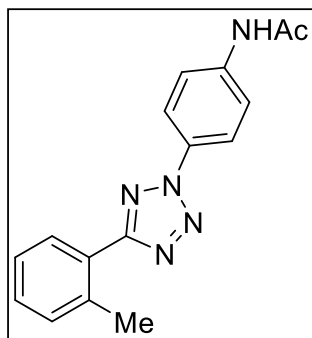


Synthesised in accordance with general procedure H using tetrazole **2.18** (32.0 mg, 0.20 mmol), (4-acetamidophenyl)boronic acid (71.6 mg, 0.40 mmol), copper(I) oxide (1.40 mg, 10.0 μmol) and DMSO (2 mL) to afford N-(4-(5-(o-tolyl)-2H-tetrazol-2-yl)phenyl)acetamide (41.2 mg, 0.14 mmol, 71 % yield) as a white solid.

**$^1$H NMR** (400 MHz, CDCl$_3$) δ 8.17 – 8.13 (m, 2H), 8.13 – 8.09 (m, 1H), 7.75 (d, $J$ = 8.9 Hz, 2H), 7.56 (br. s, 1H), 7.43 – 7.31 (m, 3H), 2.71 (s, 3H), 2.23 (s, 3H).

**$^{13}$C NMR** (101 MHz, CDCl$_3$) δ 168.6, 165.7, 139.3, 137.8, 133.0, 131.6, 130.3, 129.7, 126.3, 126.2, 120.7, 120.5, 24.8, 21.9.

**HRMS** (ESI) calculated $m/z$ 294.1349 for C$_{16}$H$_{16}$N$_5$O [M+H]$^+$, found 294.1351.

**IR** $\nu_{max}$ (neat): 3294, 3269, 3211, 3148, 3075, 2957, 2926, 1661, 1611, 1535, 1510, 1481, 1450, 1414 cm$^{-1}$.

### 2-(naphthalen-2-yl)-5-(o-tolyl)-2H-tetrazole (2.49)
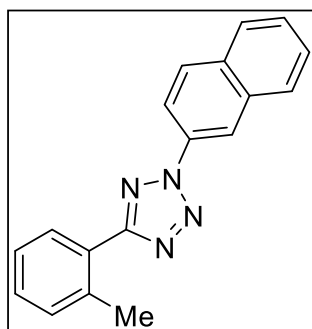


Synthesised in accordance with general procedure H using tetrazole **2.18** (32.0 mg, 0.20 mmol), 2-naphthylboronic acid (69.0 mg, 0.40 mmol), copper(I) oxide (1.40 mg, 10.0 μmol) and DMSO (2 mL) to afford 2-(naphthalen-2-yl)-5-(o-tolyl)-2H-tetrazole (17.3 mg, 0.06 mmol, 30 % yield) as an off-white solid.

**$^1$H NMR** (400 MHz, CDCl$_3$) δ 8.68 (d, $J$ = 2.0 Hz, 1H, 8.35 (dd, $J$ = 9.0, 2.2 Hz, 1H), 8.18 (dd, $J$ = 8.0, 1.5 Hz, 1H), 8.05 (d, $J$ = 9.0 Hz, 1H), 8.03 – 7.99 (m, 1H), 7.97 – 7.91 (m, 1H), 7.65 – 7.57 (m, 2H), 7.45 – 7.35 (m, 3H), 2.77 (s, 3H).

**$^{13}$C NMR** (101 MHz, CDCl$_3$) δ 165.9, 137.9, 134.5, 133.5, 133.3, 131.6, 130.3, 130.1, 129.8, 128.8, 128.2, 127.7, 127.5, 126.4, 126.3, 118.3, 118.0, 22.0.

**HRMS** (ESI) calculated $m/z$ 287.1291 for C$_{18}$H$_{15}$N$_4$ [M+H]$^+$, found 287.1288.

**IR** $\nu_{max}$ (neat): 3049, 3034, 2959, 2922, 2851, 1603, 1514, 1474, 1449 cm$^{-1}$.

**2,5-di-*o*-tolyl-2*H*-tetrazole (2.50)**
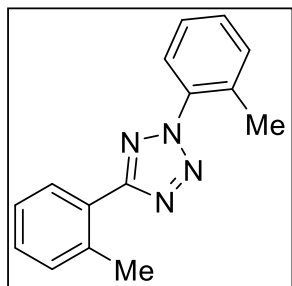
Synthesised in accordance with general procedure H using tetrazole **2.18** (32.0 mg, 0.20 mmol), *o*-tolylboronic acid (54.0 mg, 0.40 mmol), copper(I) oxide (1.40 mg, 10.0 μmol) and DMSO (2 mL) to afford 2,5-di-*o*-tolyl-2*H*-tetrazole (31.4 mg, 0.13 mmol, 63 % yield) as a yellow oil.

**¹H NMR** (500 MHz, CDCl$_3$) δ 8.19 – 8.16 (m, 1H), 7.71 (d, *J* = 7.9 Hz, 1H), 7.49 – 7.34 (m, 6H), 2.72 (s, 3H), 2.47 (s, 3H).

**¹³C NMR** (126 MHz, CDCl$_3$) δ 165.4, 137.7, 136.7, 133.0, 132.1, 131.6, 130.3, 130.2, 129.7, 127.1, 126.4, 126.2, 125.3, 22.0, 19.1.

**HRMS** (ESI) calculated *m/z* 251.1291 for C$_{15}$H$_{15}$N$_4$ [M+H]$^+$, found 251.1290.

**IR** ν$_{max}$ (neat): 3063, 3032, 2961, 2924, 1607, 1584, 1520, 1495, 1476, 1452 cm$^{-1}$.

*5.4.2.1 Starting Materials*

## 5-(4-methoxyphenyl)-2-(4-(trifluoromethyl)phenyl)-2*H*-tetrazole (3.1)
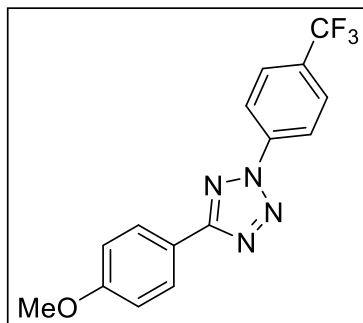


Synthesised in accordance with general procedure H using 5-(4-methoxyphenyl)-2*H*-tetrazole (64.0 mg, 0.37 mmol), boronic acid (141 mg, 0.74 mmol), Cu$_2$O (3.00 mg, 0.02 mmol), and DMSO (1.00 mL) to afford 5-(4-methoxyphenyl)-2-(4-(trifluoromethyl)phenyl)-2*H*-tetrazole (107 mg, 0.33 mmol, 90 % yield) as a white powder.

**$^1$H NMR** (400 MHz, CDCl$_3$) δ 8.35 (d, *J* = 8.4 Hz, 2H), 8.22 – 8.17 (m, 2H), 7.85 (d, *J* = 8.4 Hz), 7.08 – 7.03 (m, 2H), 3.90 (s, 3H).

**$^{19}$F NMR** (376 MHz, CDCl$_3$) δ -62.67 (s).

**$^{13}$C NMR** (101 MHz, CDCl$_3$) δ 165.7, 161.9, 139.3, 131.5 (q, $^2J_{CF}$ = 33.3 Hz), 128.9, 127.2, (q, $^3J_{CF}$ = 3.3 Hz), 123.7 (app. d, $^1J_{CF}$ = 272.3 Hz), 120.1, 119.4, 114.6, 55.6.

**HRMS** (ESI) calculated *m/z* 321.0958 for C$_{15}$H$_{12}$F$_3$N$_4$O [M+H]$^+$, found 321.0954.

**IR** ν$_{max}$ (neat): 3094, 3017, 2968, 2943, 2843, 1614, 1584, 1547, 1518, 1470, 1431 cm$^{-1}$.

## 5-(4-methoxyphenyl)-2-phenyl-2*H*-tetrazole (3.2)
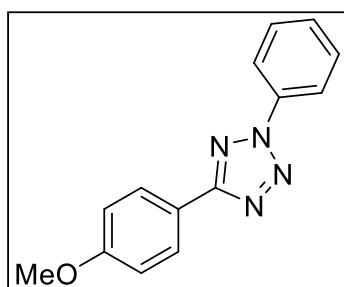


Synthesised in accordance with general procedure I using 4-methoxybenzaldehyde (1.36 g, 10.0 mmol), benzenesulfonohydrazide (1.89 g, 11.0 mmol), aniline (0.93 mL, 10.0 mmol), and sodium nitrite (759 mg, 11.0 mmol) to afford 5-(4-methoxyphenyl)-2-phenyl-2*H*-tetrazole (1.17 g, 4.64 mmol, 46 % yield) as a grey solid.

**$^1$H NMR** (500 MHz, CDCl$_3$) δ 8.19 (d, *J* = 8.9 Hz, 2H), 8.19 (d, *J* = 8.4 Hz, 2H), 7.58 - 7.55 (m, 2H), 7.50 - 7.47 (m, 1H), 7.04 (d, *J* = 8.9 Hz, 2H), 3.89 (s, 3H).

**$^{13}$C NMR** (101 MHz, CDCl$_3$) δ 165.2, 161.6, 137.1, 129.8, 129.6, 128.7, 120.0, 119.9, 114.5, 55.5.

**HRMS** (ESI) calculated *m/z* 253.1089 for C$_{14}$H$_{13}$N$_4$O [M+H]$^+$, found 253.1092.

**IR** ν$_{max}$ (neat): 3071, 3053, 3006, 2975, 2945, 2842, 1617, 1599, 1586, 1547, 1500, 1463 cm$^{-1}$.

Analytical data in agreement with the literature.[155]

## 2-(3-fluoro-4-methoxyphenyl)-5-phenyl-2*H*-tetrazole (3.3)
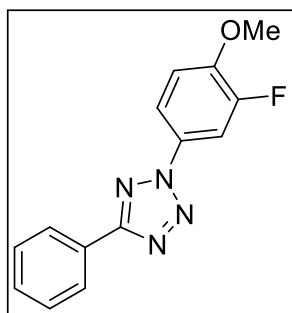
Synthesised in accordance with general procedure H using 5-phenyl-2*H*-tetrazole (1.81 g, 12.4 mmol), boronic acid (4.00 g, 23.5 mmol), Cu$_2$O (89.0 mg, 0.62 mmol), and DMSO (10.0 mL) to afford 2-(3-fluoro-4-methoxyphenyl)-5-phenyl-2*H*-tetrazole (2.35 g, 8.70 mmol, 70 % yield) as a white powder.

**$^1$H NMR** (400 MHz, CDCl$_3$) δ 8.26 – 8.20 (m, 2H), 7.99 – 7.92 (m, 2H), 7.55 – 7.47 (m, 3H), 7.15 – 7.08 (m, 1H), 3.97 (s, 3H).

**$^{19}$F NMR** (471 MHz, CDCl$_3$) δ -131.27 – -131.34 (m).

**$^{13}$C NMR** (101 MHz, CDCl$_3$) δ 165.3, 152.4 (d, $^1J_{CF}$ = 248.8 Hz), 149.0 (d, $^2J_{CF}$ = 10.5 Hz), 130.7, 130.1 (d, $^3J_{CF}$ = 9.1 Hz), 129.1, 127.2, 115.9 (d, $^3J_{CF}$ = 4.1 Hz), 113.7 (d, $^4J_{CF}$ = 1.9 Hz), 109.0 (d, $^2J_{CF}$ = 23.9 Hz), 56.7, one C not observed (coincident).

**HRMS** (ESI) calculated *m/z* 271.0990 for C$_{14}$H$_{12}$FN$_4$O [M+H]$^+$, found 271.0990.

**IR** ν$_{max}$ (neat): 3092, 3015, 2972, 2940, 2843, 1603, 1514, 1454 cm$^{-1}$.

## 2,5-*bis*(4-methoxyphenyl)-2*H*-tetrazole (3.4)
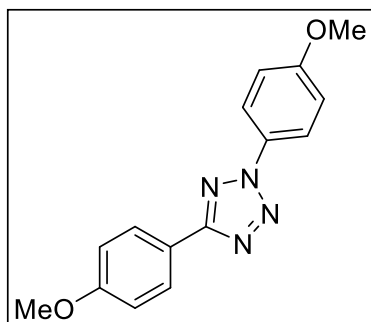
Synthesised in accordance with general procedure I using 4-methoxybenzaldehyde (365 uL, 3.00 mmol), benzenesulfonohydrazide (570 mg, 3.30 mmol), anisidine (370 mg, 3.00 mmol), and sodium nitrite (212 mg, 3.30 mmol) to afford 2,5-*bis*(4-methoxyphenyl)-2*H*-tetrazole (196 mg, 0.69 mmol, 23 % yield) as a yellow solid.

**$^1$H NMR** (500 MHz, CDCl$_3$) δ 8.17 (d, *J* = 8.7 Hz, 2H), 8.09 (d, *J* = 9.0 Hz, 2H), 7.07 - 7.01 (m, 4H), 3.885 (s, 3H), 3.879 (s, 3H).

**$^{13}$C NMR** (101 MHz, CDCl$_3$) δ 165.0, 161.5, 160.6, 130.7, 128.7, 121.5, 120.0, 114.8, 114.5, 55.8, 55.5.

**HRMS** (ESI) calculated *m/z* 283.1190 for C$_{15}$H$_{15}$N$_4$O$_2$ [M+H]$^+$, found 283.1189.

**IR** ν$_{max}$ (neat): 3005, 2930, 2837, 1609, 1595, 1582, 1508, 1466, 1433 cm$^{-1}$.

Analytical data in agreement with the literature.[205]

## 5-(4-fluorophenyl)-2-(4-methoxyphenyl)-2*H*-tetrazole (3.5)
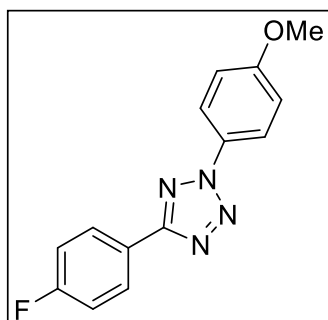
Synthesised in accordance with general procedure I using 4-fluorobenzaldehyde (3.72 g, 30.0 mmol), benzenesulfonohydrazide (5.68 g, 33.0 mmol), anisidine (3.70 g, 30.0 mmol), and sodium nitrite (2.28 g, 33.0 mmol) to afford 5-(4-fluorophenyl)-2-(4-methoxyphenyl)-2*H*-tetrazole (3.97 g, 14.7 mmol, 49 % yield) as a light yellow solid.

**$^1$H NMR** (500 MHz, CDCl$_3$) δ 8.21 (dd, $^2J_{HH}$ = 8.4 Hz, $^3J_{HF}$ = 5.8 Hz, 2H), 8.06 (d, $J$ = 8.8 Hz, 2H), 7.23 – 7.19 (m, 2H), 7.03 (d, $J$ = 8.8 Hz, 2H), 3.87 (s, 3H).

**$^{19}$F NMR** (471 MHz, CDCl$_3$) δ -109.80 - -109.88 (m).

**$^{13}$C NMR** (126 MHz, CDCl$_3$) δ 164.3, 164.2 (d, $^1J_{CF}$ = 250.5 Hz), 160.7, 130.5, 129.1 (d, $^3J_{CF}$ = 8.5 Hz), 123.7 (d, $^4J_{CF}$ = 3.1 Hz), 121.5, 116.2 (d, $^2J_{CF}$ = 22.0 Hz), 114.8, 55.8.

**HRMS** (ESI) calculated *m/z* 271.0995 for C$_{14}$H$_{12}$FN$_4$O [M+H]$^+$, found 271.0999.

**IR** ν$_{max}$ (neat): 3084, 2972, 2941, 2843, 1591, 1539, 1508, 1462, 1435 cm$^{-1}$.

## 2,5-*bis*(4-(trifluoromethyl)phenyl)-2*H*-tetrazole (3.6)
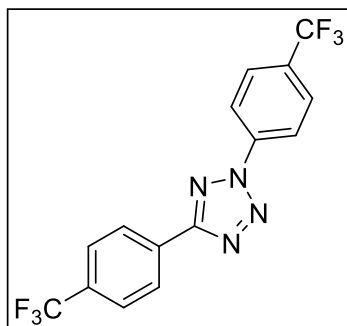
Synthesised in accordance with general procedure I using 4-(trifluoromethyl)benzaldehyde (273 uL, 2.00 mmol), benzenesulfonohydrazide (379 mg, 2.20 mmol), 4-(trifluoromethyl)aniline (250 mg, 2.00 mmol), and sodium nitrite (141 mg, 2.20 mmol) to afford 2,5-*bis*(4-(trifluoromethyl)phenyl)-2*H*-tetrazole (84.5 mg, 0.24 mmol, 12 % yield) as a white solid.

**$^1$H NMR** (500 MHz, CDCl$_3$) δ 8.40 (d, $J$ = 8.3 Hz, 2H), 8.38 (d, $J$ = 8.7 Hz, 2H), 7.88 (d, $J$ = 8.7 Hz, 2H), 7.82 (d, $J$ = 8.3 Hz, 2H).

**$^{19}$F NMR** (376 MHz, CDCl$_3$) δ -62.74 (s, 3F), -62.94 (s, 3F).

**$^{13}$C NMR** (126 MHz, CDCl$_3$) δ 164.6, 139.1, 132.8 (q, $^2J_{CF}$ = 33.0 Hz), 132.1 (q, $^2J_{CF}$ = 33.4 Hz), 130.3, 127.6, 127.3 (q, $^3J_{CF}$ = 3.6 Hz), 126.2 (q, $^3J_{CF}$ = 3.6 Hz), 124.0 (d, $^1J_{CF}$ = 272.6 Hz), 123.6 (d, $^1J_{CF}$ = 272.3 Hz), 120.3.

**HRMS** (ESI) calculated *m/z* 359.0732 for C$_{15}$H$_9$F$_6$N$_4$ [M+H]$^+$, found 359.0732.

**IR** ν$_{max}$ (neat): 3127, 3090, 3071, 1616, 1545, 1517, 1474, 1433 cm$^{-1}$.

## 2-(4-methoxyphenyl)-5-phenyl-2*H*-tetrazole (3.7)
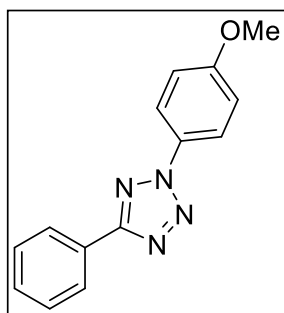


Synthesised in accordance with general procedure H using 5-phenyl-2*H*-tetrazole (1.00 g, 6.80 mmol), 4-methoxyphenyl boronic acid (2.08 g, 13.7 mmol), Cu$_2$O (49.0 mg, 0.34 mmol), and DMSO (10.0 mL) to afford 2-(4-methoxyphenyl)-5-phenyl-2*H*-tetrazole (1.51 g, 5.99 mmol, 88 % yield) as a white powder.

**$^1$H NMR** (500 MHz, MeOD-*d*4) δ 8.19 (d, *J* = 6.4 Hz, 2H), 8.09 (d, *J* = 8.7 Hz, 2H), 7.58 – 7.49 (m, 3H), 7.15 (d, *J* = 8.7 Hz, 2H), 3.89 (s, 3H).

**$^{13}$C NMR** (101 MHz, CDCl$_3$) δ 165.2, 160.7, 130.6, 129.1, 127.5, 127.1, 121.6, 119.7, 114.8, 55.8.

**HRMS** (ESI) calculated *m/z* 253.1084 for C$_{14}$H$_{13}$N$_4$O [M+H]$^+$, found 253.1083.

**IR** ν$_{max}$ (neat): 3017, 2844, 1610, 1597, 1515, 1452 cm$^{-1}$.

Analytical data in agreement with the literature.[435]

## 2-(4-methoxyphenyl)-5-(4-(trifluoromethyl)phenyl)-2*H*-tetrazole (3.8)
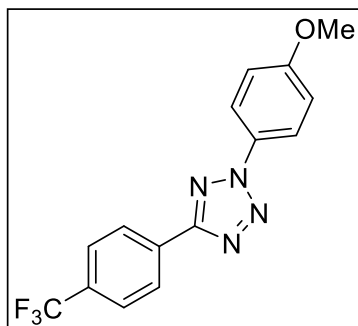


Synthesised in accordance with general procedure I using 4-(trifluoromethyl)-benzaldehyde (280 uL, 2.00 mmol), benzenesulfonohydrazide (379 mg, 2.20 mmol), anisidine (250 mg, 2.00 mmol), and sodium nitrite (141 mg, 2.20 mmol) to afford 2-(4-methoxyphenyl)-5-(4-(trifluoromethyl)phenyl)-2*H*-tetrazole (115 mg, 0.36 mmol, 18 % yield) as a yellow solid.

**$^1$H NMR** (500 MHz, CDCl$_3$) δ 8.37 (d, *J* = 8.2 Hz, 2H), 8.12 (d, *J* = 9.0 Hz, 2H), 7.79 (d, *J* = 8.2 Hz, 2H), 7.08 (d, *J* = 9.0 Hz, 2H), 3.91 (s, 3H).

**$^{19}$F NMR** (376 MHz, CDCl$_3$) δ -62.87 (s).

**$^{13}$C NMR** (101 MHz, CDCl$_3$) δ 164.0, 160.9, 132.4 (app. d, $^3J_{CF}$ = 32.3 Hz), 130.7 (app. d, $^2J_{CF}$ = 38.8 Hz), 127.4, 126.1 (q, $^4J_{CF}$ = 3.4 Hz), 124.1 (app. d, $^1J_{CF}$ = 272.3 Hz), 121.7, 114.9, 55.9, one C not observed (coincident).

**HRMS** (ESI) calculated *m/z* 321.0958 for C$_{15}$H$_{12}$F$_3$N$_4$O [M+H]$^+$, found 321.0960.

**IR** ν$_{max}$ (neat): 3016, 2922, 2847, 1624, 1609, 1595, 1543, 1512, 1470, 1458 cm$^{-1}$.

## 4-(2-phenyl-2*H*-tetrazol-5-yl)pyridine (3.9)
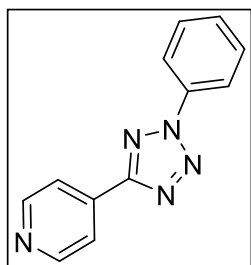


Synthesised in accordance with general procedure I using pyridine-4-carboxaldehyde (200 uL mg, 2.00 mmol), benzenesulfonohydrazide (379 mg, 2.20 mmol), aniline (183 uL, 2.00 mmol), and sodium nitrite (141 mg, 2.20 mmol) to afford 4-(2-phenyl-2*H*-tetrazol-5-yl)pyridine (108 mg, 0.48 mmol, 24 % yield) as a light brown solid.

**$^1$H NMR** (400 MHz, CDCl$_3$) δ 8.86 (app. br. s, 2H), 8.25 – 8.15 (m, 4H), 7.66 – 7.58 (m, 2H), 7.58 – 7.52 (m, 1H).

**$^{13}$C NMR** (101 MHz, CDCl$_3$) δ 163.2, 150.7, 136.8, 135.4, 130.4, 130.0, 121.4, 120.2.

**HRMS** (ESI) calculated *m/z* 224.0931 for C$_{12}$H$_{10}$N$_5$ [M+H]$^+$, found 224.0931.

**IR** ν$_{max}$ (neat): 3040, 3021, 2916, 1686, 1607, 1560, 1526, 1491, 1456, 1418 cm$^{-1}$.

Analytical data in agreement with the literature.[436]

## 2-phenyl-5-(thiophen-3-yl)-2*H*-tetrazole (3.10)
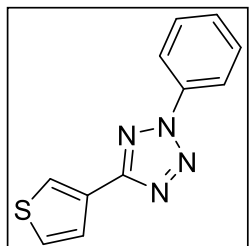


Synthesised in accordance with general procedure I using thiophene-3-carboxaldehyde (180 µL, 2.00 mmol), benzenesulfonohydrazide (379 mg, 2.20 mmol), aniline (183 µL, 2.00 mmol), and sodium nitrite (141 mg, 2.20 mmol) to afford 2-phenyl-5-(thiophen-3-yl)-2*H*-tetrazole (69.7 mg, 0.31 mmol, 15 % yield) as a yellow solid.

**$^1$H NMR** (400 MHz, CDCl$_3$) δ 8.20 – 8.15 (m, 3H), 7.80 (dd, *J* = 5.1, 1.2 Hz, 1H), 7.60 – 7.54 (m, 2H), 7.52 – 7.46 (m, 2H).

**$^{13}$C NMR** (101 MHz, CDCl$_3$) δ 162.0, 137.0, 129.8, 129.8, 128.7, 127.0, 126.5, 126.0, 120.0.

**HRMS** (ESI) calculated *m/z* 229.0542 for C$_{11}$H$_9$N$_4$S [M+H]$^+$, found 229.0541.

**IR** ν$_{max}$ (neat): 3200, 3092, 3065, 1701, 1597, 1522, 1508, 1477, 1447 cm$^{-1}$.

## 4-(2-(4-methoxyphenyl)-2*H*-tetrazol-5-yl)benzoic acid (3.65)
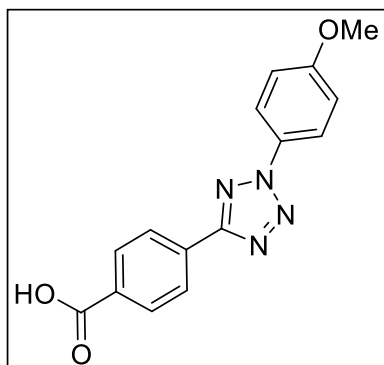


Synthesised in accordance with general procedure I using methyl 4-formylbenzoate (985 mg, 6.00 mmol), benzenesulfonylhydrazide (1.14 g, 6.60 mmol), anisidine (739 mg, 6.00 mmol), and NaNO$_2$ (629 mg, 9.00 mmol). Prior to work-up, the reaction mixture was treated with 4M sodium hydroxide solution (20.0 mL) and stirred for

an additional 16 hours at room temperature to afford 4-(2-(4-methoxyphenyl)-2*H*-tetrazol-5-yl)benzoic acid (847 mg, 2.88 mmol, 48 % yield) as a pale yellow solid.

**¹H NMR** (500 MHz, DMSO) δ 13.22 (s, 1H), 8.27 (d, *J* = 8.4 Hz, 2H), 8.15 (d, *J* = 8.4 Hz, 2H), 8.08 (d, *J* = 9.1 Hz, 2H), 7.22 (d, *J* = 9.1 Hz, 2H), 3.87 (s, 3H).
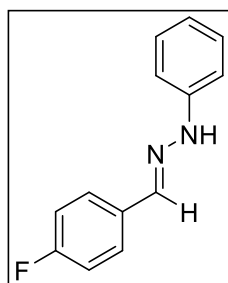
**¹³C NMR** (126 MHz, DMSO) δ 166.7, 163.5, 160.5, 132.6, 130.3, 130.2, 129.5, 126.7, 121.7, 115.1, 55.7.

**HRMS** (ESI) calculated *m/z* 295.0837 for $C_{15}H_{11}N_4O_3$ [M-H]⁻, found 295.0835.

**IR** $\nu_{max}$ (neat): 3088, 2995, 2967, 2839, 2671, 2538, 1694, 1618, 1599, 1576, 1537, 1512, 1422 cm⁻¹.

Analytical data in agreement with the literature.[161]

## 1-(4-fluorobenzylidene)-2-phenylhydrazine (5.1)



Synthesised in accordance with general procedure N using 4-fluorobenzaldehyde (5.27 mL, 50.0 mmol), phenylhydrazine hydrochloride (7.59 g, 52.5 mmol) and ethanol (20.0 mL) to afford 1-(4-fluorobenzylidene)-2-phenylhydrazine (9.04 g, 42.0 mmol, 84 % yield, >99:1 *E*:*Z* mixture) as a pink solid.

**¹H NMR** (400 MHz, CDCl₃) δ 7.66 − 7.61 (m, 3H), 7.32 − 7.25 (m, 2H), 7.15 − 7.02 (m, 4H), 6.89 (t, *J* = 7.3 Hz, 1H), exchangeable proton not observed.

**¹⁹F NMR** (376 MHz, CDCl₃) δ -112.72 (tt, $J_{HF}$ = 8.6, 5.5 Hz).

**¹³C NMR** (101 MHz, CDCl₃) δ 163.0 (d, $^1J_{CF}$ = 248.2 Hz), 144.8, 136.2, 131.7, 129.5, 127.9 (d, $^3J_{CF}$ = 8.0 Hz), 120.4, 115.8 (d, $^2J_{CF}$ = 22.0 Hz), 112.9.

**HRMS** (ESI) calculated *m/z* 215.0979 for $C_{13}H_{12}FN_2$ [M+H]⁺, found 215.0980.

**IR** $\nu_{max}$ (neat): 3310, 3053, 1595, 1574, 1524, 1502, 1487, 1445, 1226 cm⁻¹.

Analytical data in agreement with the literature.[437]

## 4-fluoro-*N*-phenylbenzohydrazonoyl chloride (3.70)
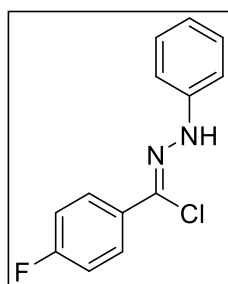


Synthesised in accordance with general procedure O using 4-fluorobenzaldehyde phenylhydrazone **5.1** (6.40 g, 30.0 mmol), *N*-chlorosuccinimide (6.80 g, 51.0 mmol), dimethyl sulfide (6.70 mL, 90.0 mmol) and DCM (30.0 mL) to afford 4-fluoro-*N*-phenylbenzohydrazonoyl chloride (3.10 g, 12.6 mmol, 42 % yield, >1:99 *E*:*Z* mixture) as a light yellow solid.

**¹H NMR** (400 MHz, CDCl₃) δ 7.99 (br. s, 1H), 7.94 – 7.87 (m, 2H), 7.35 – 7.28 (m, 2H), 7.20 – 7.14 (m, 2H), 7.14 – 7.06 (m, 2H), 6.95 (tt, $J$ = 7.4, 1.1 Hz, 1H).

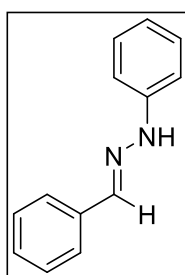**¹⁹F NMR** (471 MHz, CDCl₃) δ -111.77 - -111.86 (m).

**¹³C NMR** (101 MHz, CDCl₃) δ 163.5 (d, $^{1}J_{CF}$ = 249.8 Hz), 143.4, 130.8 (d, $^{4}J_{CF}$ = 3.6 Hz), 129.6, 128.4 (d, $^{3}J_{CF}$ = 8.1 Hz), 123.8, 121.4, 115.6 (d, $^{2}J_{CF}$ = 21.9 Hz), 113.6.

**HRMS** (ESI) calculated *m/z* 247.0433 for $C_{13}H_9ClFN_2$ [M-H]⁻, found 247.0430.

**IR** $v_{max}$ (neat): 3308, 3051, 1595, 1572, 1499, 1435, 1406, 1227 cm⁻¹.

Analytical data in agreement with the literature.[438]

### 1-benzylidene-2-phenylhydrazine (5.2)



Synthesised in accordance with general procedure N using benzaldehyde (2.65 mL, 25.0 mmol), phenylhydrazine hydrochloride (2.87 g, 25.0 mmol) and ethanol (10.0 mL) to afford 1-benzylidene-2-phenylhydrazine (4.11 g, 21.0 mmol, 84 % yield, >99:1 *E:Z* mixture) as an off-white solid.

**¹H NMR** (400 MHz, CDCl₃) δ 7.71 – 7.64 (m, 2H), 7.63 (s, 1H), 7.43 – 7.35 (m, 2H), 7.35 – 7.27 (m, 3H), 7.17 – 7.10 (m, 2H), 6.90 (tt, $J$ = 7.3, 1.1 Hz, 1H), exchangeable proton not observed.

**¹³C NMR** (101 MHz, CDCl₃) δ 144.8, 137.5, 135.5, 129.4, 128.7, 128.5, 126.3, 120.2, 112.9.

**HRMS** (ESI) calculated *m/z* 197.1073 for $C_{13}H_{13}N_2$ [M+H]⁺, found 197.1073.

**IR** $v_{max}$ (neat): 3310, 3055, 3024, 1591, 1564, 1522, 1493, 1483, 1440 cm⁻¹.

Analytical data in agreement with the literature.[437]

### *N*-phenylbenzohydrazonoyl chloride (3.71)
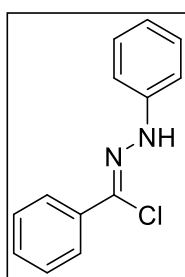


Synthesised in accordance with general procedure O using benzaldehyde phenylhydrazone **5.2** (4.90 g, 25.0 mmol), *N*-chlorosuccinimide (5.70 g, 43.0 mmol), dimethyl sulfide (5.50 mL, 75.0 mmol) and DCM (25.0 mL) to afford *N*-phenylbenzohydrazonoyl chloride (5.80 g, 25.4 mmol, 64 % yield, >1:99 *E:Z* mixture) as a light pink solid.

**¹H NMR** (400 MHz, CDCl₃) δ 8.05 (br. s, 1H), 7.98 – 7.90 (m, 2H), 7.45 – 7.36 (m, 3H), 7.35 – 7.29 (m, 2H), 7.22 – 7.17 (m, 2H), 6.95 (tt, $J$ = 7.4, 1.1 Hz, 1H).
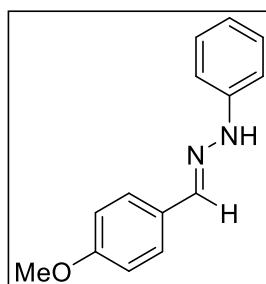
**¹³C NMR** (101 MHz, CDCl₃) δ 143.5, 134.6, 129.5, 129.4, 128.6, 126.6, 124.8, 121.3, 113.6.

**HRMS** (ESI) calculated *m/z* 229.0527 for $C_{13}H_{10}ClN_2$ [M-H]⁻, found 229.0525.

**IR** $v_{max}$ (neat): 3302, 3049, 2955, 2918, 1595, 1581, 1570, 1501, 1487, 1447 cm⁻¹.

Analytical data in agreement with the literature.[205]

## 1-(4-methoxybenzylidene)-2-phenylhydrazine (5.3)

Synthesised in accordance with general procedure N using 4-methoxybenzaldehyde (0.68 mL, 5.00 mmol), phenylhydrazine hydrochloride (795 mg, 5.50 mmol) and ethanol (2.00 mL), to afford 1-(4-methoxybenzylidene)-2-phenylhydrazine (756 mg, 3.35 mmol, 67 % yield, >99:1 *E:Z* mixture) as a pale yellow solid.

**1H NMR** (400 MHz, CDCl$_3$) δ 7.65 (s, 1H), 7.61 (d, *J* = 8.7 Hz, 2H), 7.33 – 7.23 (m, 2H), 7.14 – 7.07 (m, 2H), 6.92 (d, *J* = 8.7 Hz, 2H), 6.90 – 6.82 (m, 1H), 3.85 (s, 3H), 1H not observed (exchangeable).

**13C NMR** (101 MHz, CDCl$_3$) δ 160.2, 145.1, 137.5, 129.4, 128.3, 127.7, 120.0, 114.3, 112.8, 55.5.

**HRMS** (ESI) calculated *m/z* 227.1183 for C$_{14}$H$_{15}$N$_2$O [M+H]$^+$, found 227.1179.

**IR** $v_{max}$ (neat): 3314, 3024, 2955, 1593, 1528, 1497, 1464 cm$^{-1}$.

Analytical data in agreement with the literature.[439]

## 4-methoxy-*N*-phenylbenzohydrazonoyl chloride (3.72)
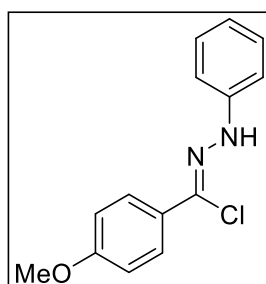
Synthesised in accordance with general procedure O using 4-methoxybenzaldehyde phenylhydrazone **5.3** (617 mg, 4.40 mmol), *N*-chlorosuccinimide (620 mg, 7.50 mmol), dimethyl sulfide (0.62 mL, 13.3 mmol) and DCM (5.00 mL) to afford 4-methoxy-*N*-phenylbenzohydrazonoyl chloride (165 mg, 0.74 mmol, 23 % yield, >1:99 *E:Z* mixture) as a white solid.

**1H NMR** (400 MHz, CDCl$_3$) δ 7.95 (br. s, 1H), 7.91 – 7.84 (m, 2H), 7.35 – 7.28 (m, 2H), 7.20 – 7.15 (m, 2H), 6.99 – 6.89 (m, 3H), 3.86 (s, 3H).
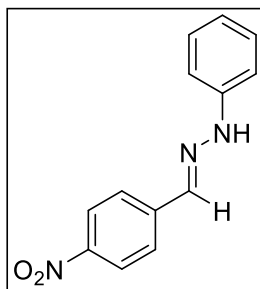
**13C NMR** (101 MHz, CDCl$_3$) δ 160.7, 143.7, 129.5, 128.0, 127.3, 124.9, 121.0, 113.9, 113.4, 55.5.

**HRMS** (ESI) calculated *m/z* 225.1023 for C$_{14}$H$_{14}$ClN$_2$O [M+H]$^+$, found 225.1022.

**IR** $v_{max}$ (neat): 3314, 3055, 3007, 2957, 2930, 2837, 1599, 1584, 1499, 1462, 1433 cm$^{-1}$.

Analytical data in agreement with the literature.[438]

## 1-(4-nitrobenzylidene)-2-phenylhydrazine (5.4)

Synthesised in accordance with general procedure N using 4-nitrobenzaldehyde (756 mg, 5.00 mmol), phenylhydrazine hydrochloride (795 mg, 5.50 mmol), and ethanol (2.00 mL) to afford 1-(4-nitrobenzylidene)-2-phenylhydrazine (953 mg, 3.94 mmol, 79 % yield, >99:1 *E:Z* mixture) as a red solid.

**¹H NMR** (500 MHz, CDCl₃) δ 8.22 (d, *J* = 8.9 Hz, 2H), 8.00 (br. s, 1H), 7.76 (d, *J* = 8.9 Hz, 2H), 7.68 (s, 1H), 7.36 – 7.29 (m, 2H), 7.15 (d, *J* = 7.6 Hz, 2H), 6.98 - 6.92 (m, 1H).

**¹³C NMR** (126 MHz, CDCl₃) δ 147.2, 143.7, 141.9, 133.9, 129.6, 126.4, 124.2, 121.4, 113.3.

**HRMS** (ESI) calculated *m/z* 242.0924 for $C_{13}H_{12}N_3O_2$ [M+H]⁺, found 242.0927.

**IR** ν$_{max}$ (neat): 3300, 3059, 3034, 1593, 1557, 1537, 1493, 1449, 1410, 1315, 1271 cm⁻¹.

Analytical data in agreement with the literature.[437]

## 4-nitro-*N*-phenylbenzohydrazonoyl chloride (3.73)
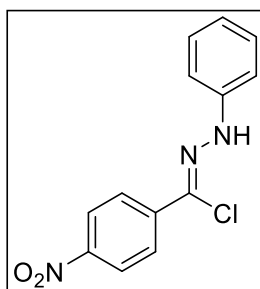
Synthesised in accordance with general procedure O using 4-nitrobenzaldehyde phenylhydrazone **5.4** (1.00 g, 4.10 mmol), *N*-chlorosuccinimide (940 mg, 7.10 mmol), dimethyl sulfide (0.92 mL, 12.5 mmol) and DCM (5.00 mL) to afford 4-nitro-*N*-phenylbenzohydrazonoyl chloride (512 mg, 1.86 mmol, 45 % yield, >1:99 *E:Z* mixture) as a red solid.

**¹H NMR** (400 MHz, CDCl₃) δ 8.31 – 8.22 (m, 3H), 8.10 – 8.04 (m, 2H), 7.38 – 7.32 (m, 2H), 7.24 – 7.19 (m, 2H), 7.06 – 6.98 (m, 1H).
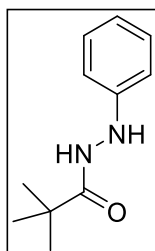
**¹³C NMR** (101 MHz, CDCl₃) δ 147.8, 142.6, 140.3, 129.7, 126.8, 123.9, 122.4, 122.3, 114.0.

**HRMS** (ESI) calculated *m/z* 276.0540 for $C_{13}H_{11}ClN_3O_2$ [M+H]⁺, found 276.0546.

**IR** ν$_{max}$ (neat): 3318, 3057, 2924, 1603, 1593, 1547, 1504, 1441, 1406, 1379, 1331 cm⁻¹.

Analytical data in agreement with the literature.[156]

## *N'*-phenylpivalohydrazide (3.87)

Synthesised in accordance with general procedure P using pivaloyl chloride (245 μL, 2.00 mmol), phenyl hydrazine (985 μL, 10.0 mmol), pyridine (177 μL, 2.20 mmol) and DCM (2.00 mL) to afford *N'*-phenylpivalohydrazide (367 mg, 1.91 mmol, 95 % yield) as a yellow solid.

**¹H NMR** (500 MHz, DMSO-*d₆*, 80 °C) δ 10.09 (s, 0.2H), 9.26 (s, 0.8H),

7.38 – 7.09 (m, 3H), 6.74 – 6.69 (m, 2H), 1.21 (s, 7.2H), 1.14 (s, 1.8H) (80:20 rotameric mixture).
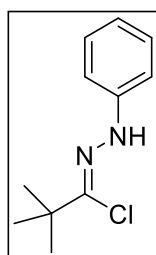
**$^{13}$C NMR** (126 MHz, DMSO-$d_6$, 80 °C) δ 176.6, 149.4, 128.1, 118.1, 112.1, 37.0, 26.9.

**HRMS** (ESI) calculated *m/z* 193.1341 for $C_{11}H_{17}N_2O$ [M+H]$^+$, found 193.1337.

**IR** $\nu_{max}$ (neat): 3260, 3252, 2968, 1657, 1597, 1537, 1493, 1481, 1435, 1400, 1358 cm$^{-1}$.

Analytical data in agreement with the literature.[440]

### *N*-phenylpivalohydrazonoyl chloride (3.74)

Synthesised in accordance with general procedure Q using hydrazide **3.87** (367 mg, 1.90 mmol), triphenylphosphine (600 mg, 2.30 mmol), carbon tetrachloride (250 μL, 2.50 mmol) and acetonitrile (2.70 mL) to afford *N*-phenylpivalohydrazonoyl chloride (203 mg, 0.97 mmol, 51 % yield, >1:99 *E*:*Z* mixture) as an orange liquid.

**$^1$H NMR** (500 MHz, CDCl$_3$) δ 7.63 (s, 1H), 7.26 (app. t, *J* = 7.9 Hz, 2H), 7.04 (d, *J* = 7.7 Hz, 2H), 6.88 (app. t, *J* = 7.3 Hz, 1H), 1.31 (s, 9H).

**$^{13}$C NMR** (126 MHz, CDCl$_3$) δ 144.3, 135.9, 129.4, 120.6, 113.2, 41.1, 28.5.

**HRMS** (ESI) calculated *m/z* 210.0924 for $C_{11}H_{15}ClN_2$ [M]$^+$, found 210.0925.

**IR** $\nu_{max}$ (neat): 3333, 2972, 2930, 2903, 2868, 1601, 1502, 1477, 1458, 1435 cm$^{-1}$.

### *N'*-phenylhexanehydrazide (5.5)
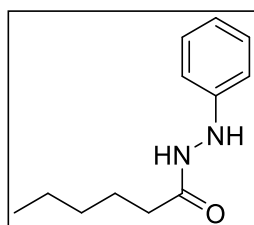
Synthesised in accordance with general procedure P using hexanoyl chloride (280 μL, 2.00 mmol), phenyl hydrazine (985 μL, 10.0 mmol), pyridine (177 μL, 2.20 mmol) and DCM (2.00 mL) to afford *N'*-phenylhexanehydrazide (116 mg, 0.56 mmol, 28 % yield) as a yellow solid.

**$^1$H NMR** (500 MHz, DMSO-$d_6$, 80 °C) δ 9.37 (s, 1H), 7.13 (t, *J* = 7.4 Hz, 2H), 6.75 – 6.67 (m, 3H), 2.17 (t, *J* = 7.2 Hz, 2H), 1.63 – 1.55 (m, 2H), 1.32 (app. s, 4H), 0.93 – 0.82 (m, 3H).

**$^{13}$C NMR** (126 MHz, DMSO-$d_6$, 80 °C) δ 171.5, 149.1, 128.1, 118.1, 112.0, 33.0, 30.5, 24.3, 21.3, 13.2.

**HRMS** (ESI) calculated *m/z* 207.1497 for $C_{12}H_{19}N_2O$ [M+H]$^+$, found 207.1502.

**IR** $\nu_{max}$ (neat): 3291, 3215, 3084, 3026, 2953, 2926, 2070, 2853, 1661, 1636, 1601, 1570, 1495, 1460, 1437 cm$^{-1}$.

### *N*-phenylhexanehydrazonoyl chloride (3.75)
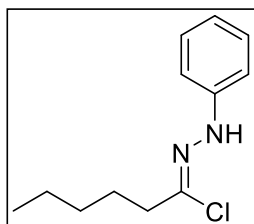
Synthesised in accordance with general procedure Q using hydrazide **5.5** (272 mg, 1.32 mmol), triphenylphosphine (416 mg, 1.58 mmol), carbon tetrachloride (166 μL, 1.72 mmol) and acetonitrile (1.90 mL) to afford *N*-phenylhexanehydrazonoyl chloride (75.0 mg, 0.33 mmol, 25 % yield, >1:99 *E*:*Z* mixture) as a yellow liquid.
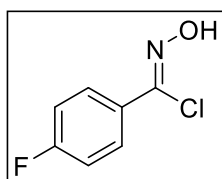
**$^1$H NMR** (500 MHz, CDCl$_3$) δ 7.62 (s, 1H), 7.29 (d, *J* = 7.9 Hz, 2H), 7.06 (d, *J* = 7.6 Hz, 2H), 6.91 (t, *J* = 7.3 Hz, 1H), 2.67 – 2.61 (m, 2H), 1.79 – 1.70 (m, 2H), 1.43 – 1.35 (m, 4H), 0.95 (t, *J* = 7.0 Hz, 3H).

**$^{13}$C NMR** (126 MHz, CDCl$_3$) δ 144.1, 129.4, 128.0, 120.6, 113.2, 38.9, 30.9, 26.5, 22.5, 14.1.

**HRMS** (ESI) calculated *m/z* 189.1392 for C$_{12}$H$_{17}$N$_2$ [M-HCl], found 189.1389.

**IR** ν$_{max}$ (neat): 3150, 3053, 3015, 2955, 2928, 2859, 1665, 1601, 1576, 1558, 1495, 1458 cm$^{-1}$.

### 4-fluoro-*N*-hydroxybenzimidoyl chloride (3.98)

Synthesised in accordance with general procedure R using 4-fluorobenzaldehyde (2.70 mL, 25.0 mmol), hydroxylamine hydrochloride (3.48 g, 50.0 mmol), sodium hydroxide (2.00 g, 50.0 mmol), ethanol (30.0 mL), *N*-chlorosuccinimide (1.80 g, 13.4 mmol) and DMF (15.0 mL) to afford 4-fluoro-*N*-hydroxybenzimidoyl chloride (1.97 g, 11.4 mmol, 46 % yield, >1:99 *E*:*Z* mixture) as a white solid.

**$^1$H NMR** (400 MHz, CDCl$_3$) δ 8.08 (s, 1H), 7.84 (dd, $^2J_{HH}$ = 8.7 Hz, $^3J_{HF}$ = 5.3, 2H), 7.10 (app. t, *J* = 8.7 Hz, 2H).

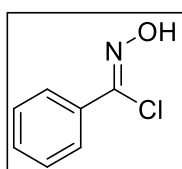**$^{19}$F NMR** (471 MHz, CDCl$_3$) δ -109.22 – -109.30 (m).

**$^{13}$C NMR** (126 MHz, CDCl$_3$) δ 164.4 (d, $^1J_{CF}$ = 251.9 Hz), 139.7, 129.4 (d, $^3J_{CF}$ = 8.6 Hz), 128.6 (d, $^4J_{CF}$ = 3.3 Hz), 115.8 (d, $^2J_{CF}$ = 22.2 Hz).

**HRMS** (ESI) calculated *m/z* 174.0122 for C$_7$H$_6$ClFNO [M+H]$^+$, found 174.0117.

**IR** ν$_{max}$ (neat): 3366, 3204, 3183, 3073, 3055, 1599, 1504, 1435, 1410, 1298, 1234 cm$^{-1}$.

Analytical data in agreement with the literature.[441]

### *N*-hydroxybenzimidoyl chloride (3.100)

Synthesised in accordance with general procedure R using benzaldehyde (2.55 mL, 25.0 mmol), hydroxylamine hydrochloride (3.48 g, 50.0 mmol),

sodium hydroxide (2.00 g, 50.0 mmol), ethanol (30.0 mL), *N*-chlorosuccinimide (3.67 g, 27.5 mmol), and DMF (35.0 mL) to afford N-hydroxybenzimidoyl chloride (3.70 g, 23.9 mmol, 95 % yield, >1:99 *E:Z* mixture) as a yellow solid.

**¹H NMR** (500 MHz, CDCl₃) δ 8.10 (s, 1H), 7.85 (d, *J* = 8.0 Hz, 2H), 7.49 – 7.39 (m, 3H).

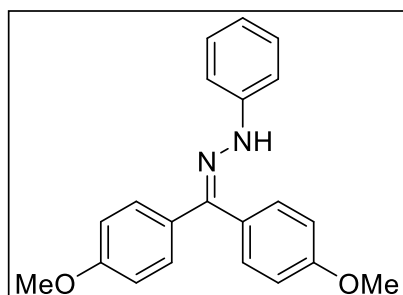**¹³C NMR** (126 MHz, CDCl₃) δ 140.5, 132.5, 130.9, 128.7, 127.4.

**HRMS** (ESI) calculated *m/z* 156.0216 for $C_7H_7ClNO$ [M+H]⁺, found 156.0217.

**IR** $v_{max}$ (neat): 3269, 3125, 3092, 3061, 3036, 2899, 1624, 1578, 1491, 1449 cm⁻¹.

Analytical data in agreement with the literature.[442]

*5.4.2.2 Hydrazones and Ketones*

**1-(*bis*(4-methoxyphenyl)methylene)-2-phenylhydrazine (3.11)**



1. Tetrazole **3.2** (20.0 mg, 0.08 mmol) and 4-methoxyphenylboronic acid (36 mg, 0.24 mmol) were dissolved in THF (3.00 mL). This mixture was then stirred under UV light irradiation at room temperature for 3 hours. Following reaction completion, the crude residue was concentrated under vacuum and purified by column chromatography (0-100 % ethyl acetate in petroleum ether) to afford 1-(*bis*(4-methoxyphenyl)methylene)-2-phenylhydrazine (12.2 mg, 0.04 mmol, 46 % yield) as a brown gum.

2. Synthesised in accordance with general procedure L using tetrazole **3.2** (63.1 mg, 0.25 mmol), 4-methoxyphenylboronic acid (114 mg, 0.75 mmol), and THF (2.50 mL) to afford 1-(*bis*(4-methoxyphenyl)methylene)-2-phenylhydrazine (58.4 mg, 0.18 mmol, 70 % yield) as a yellow oil.

3. Synthesised according to General Procedure U using hydrazonyl chloride **3.72** (65.2 mg, 0.25 mmol), 4-methoxyphenylboronic acid (76.0 mg, 0.50 mmol), and K₃PO₄ (159 mg, 0.75 mmol) to afford the product (49.3 mg, 0.15 mmol, 59 % yield) as a yellow oil.

**¹H NMR** (500 MHz, CDCl₃) δ 7.52 (d, *J* = 8.9 Hz, 2H), 7.44 (s, 1H), 7.27 – 7.19 (m, 4H), 7.10 – 7.02 (m, 4H), 6.84 (d, *J* = 8.9 Hz, 2H), 6.83 – 6.78 (m, 1H), 3.89 (s, 3H), 3.80 (s, 3H).
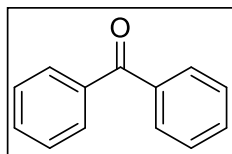
**¹³C NMR** (101 MHz, CDCl₃) δ 160.2, 159.9, 145.1, 144.4, 131.8, 130.7, 129.3, 128.1, 125.0, 119.8, 115.1, 113.7, 112.9, 55.51, 55.47.

**HRMS** (ESI) calculated *m/z* 333.1598 for $C_{21}H_{21}N_2O_2$ [M+H]⁺, found 333.1598.

**IR** $v_{max}$ (neat): 3320, 3051, 3003, 2954, 2932, 2909, 1643, 1599, 1499, 1456, 1441, 1416 cm⁻¹.

Analytical data in agreement with the literature.[443]

## Benzophenone (3.17)

Tetrazole **3.16** (126 mg, 0.50 mmol) and phenylboronic acid (305 mg, 2.50 mmol) were dissolved in acetonitrile (5.00 mL), and the mixture was stirred under UV light irradiation for 8 hours. Vanadium(V) acetoacetonate (13.2 mg, 0.05 mmol), 30 % w/w hydrogen peroxide solution (1.00 mL), and acetone (4.00 mL) were added, and the mixture was stirred at room temperature for a further 3 hours. Following reaction completion, the solution was diluted with DCM, washed with 10 % sodium metabisulfite solution and brine, passed through a phase separator and concentrated under vacuum. The crude product was purified by column chromatography (0-100 % ethyl acetate in petroleum ether) to afford benzophenone (20.0 mg, 0.11 mmol, 22 % yield) as a brown oil.

**$^1$H NMR** (500 MHz, CDCl$_3$) δ 7.81 (d, $J$ = 7.3 Hz, 4H), 7.62 - 7.56 (m, 2H), 7.52 – 7.46 (m, 4H).
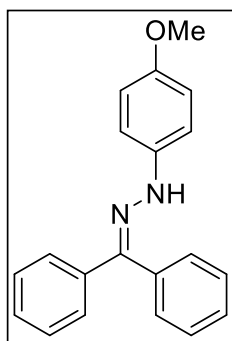
**$^{13}$C NMR** (126 MHz, CDCl$_3$) δ 196.9, 137.8, 132.6, 130.2, 128.4.

**HRMS** (ESI) calculated *m/z* 183.0800 for C$_{13}$H$_{11}$O [M+H]$^+$, found 183.0801.

**IR** ν$_{max}$ (neat): 3057, 2924, 2853, 1655, 1597, 1578, 1487, 1447 cm$^{-1}$.

Analytical data in agreement with the literature.[444]

## 1-(diphenylmethylene)-2-(4-methoxyphenyl)hydrazine (3.19)

This compound was prepared exclusively to serve as a reference peak as part of an HPLC optimisation assay. Synthesised in accordance with general procedure N using 4-methoxyphenyl hydrazine hydrochloride (500 mg, 2.86 mmol), benzophenone (497 mg, 2.73 mmol), and methanol (10.0 mL) to afford 1-(diphenylmethylene)-2-(4-methoxyphenyl)hydrazine (9 mg, 0.03 mmol, 1 % yield) as a yellow oil. The product was found to rapidly hydrolyse to the corresponding ketone under typical atmospheric conditions, and as such no additional characterisation was conducted.

## (4-methoxyphenyl)(phenyl)methanone (3.20)
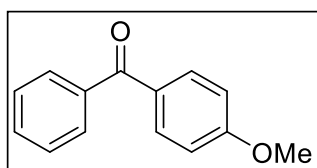
1. A solution of tetrazole **3.2** (126.1 mg, 0.5 mmol) and 4-methoxyphenylboronic acid (380 mg, 2.5 mmol) in THF (8 mL) was placed in a series of NMR tubes and irradiated with UV light at room temperature for 3 hours. Vanadium(V)

acetoacetonate (13.2 mg, 0.05 mmol), 30 % w/w hydrogen peroxide solution (1.00 mL), and acetone (4.00 mL) were added, and the mixture was stirred in a round-bottom flask at room temperature for a further 4 hours. Following reaction completion, the solution was diluted with DCM, washed with 10 % sodium metabisulfite solution and brine, passed through a phase separator and concentrated under vacuum. The crude product was purified by column chromatography (0-100 % ethyl acetate in petroleum ether) to afford (4-methoxyphenyl)(phenyl)methanone (80.0 mg, 0.38 mmol, 75 % yield) as an orange solid.

2. In accordance with previous literature precedent,[320] to a stirred mixture of hydrazone **3.24** (75.6 mg, 0.25 mmol) and VO(acac)$_2$ (6.60 mg, 0.03 mmol) in acetone (500 μL) was added H$_2$O$_2$ (125 μL) dropwise at room temperature. The reaction mixture was stirred for two hours and diluted with DCM. This solution was washed with 10 % sodium metabisulfite and brine, passed through a phase separator and concentrated under vacuum. The crude product was purified by column chromatography (0-100 % ethyl acetate in *n*-hexane) to furnish (4-methoxyphenyl)(phenyl)methanone (44.7 mg, 0.21 mmol, 84 % yield) as an off-white solid.

**$^1$H NMR** (500 MHz, CDCl$_3$) δ 7.83 (d, *J* = 8.7 Hz, 2H), 7.75 (d, *J* = 7.6 Hz, 2H), 7.59 − 7.53 (m, 1H), 7.50 − 7.44 (m, 2H), 6.96 (d, *J* = 8.7 Hz, 2H), 3.88 (s, 3H).
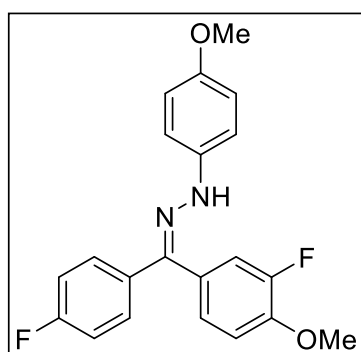
**$^{13}$C NMR** (126 MHz, CDCl$_3$) δ 195.7, 163.4, 138.4, 132.7, 132.0, 130.3, 129.8, 128.3, 113.7, 55.6.

**HRMS** (ESI) calculated *m/z* 213.0910 for C$_{14}$H$_{13}$O$_2$ [M+H]$^+$, found 213.0909.

**IR** ν$_{max}$ (neat): 3063, 3003, 2965, 2841, 1639, 1595, 1578, 1504, 1468, 1439, 1414 cm$^{-1}$.

Analytical data in agreement with the literature.[444]

## 1-((3-fluoro-4-methoxyphenyl)(4-fluorophenyl)methylene)-2-(4-methoxyphenyl)hydrazine (3.21)



Synthesised in accordance with general procedure L using tetrazole **3.5** (135 mg, 0.50 mmol), 3-fluoro-4-methoxyphenylboronic acid (276 mg, 1.50 mmol), and THF (5.00 mL), however, attempts at purification by column chromatography resulted in partial hydrolysis of the hydrazone. Complete hydrolysis was facilitated through stirring in a suspension of SiO$_2$, H$_2$O and MeOH with gentle heating to afford (3-fluoro-4-methoxyphenyl)(4-fluorophenyl)methanone (**5.6**) (38.2 mg, 0.15 mmol, 31 % yield) as a pale yellow solid. This compound was fully characterised:

**$^1$H NMR** (500 MHz, CDCl$_3$) δ 7.80 (dd, $^2J_{HH}$ = 8.4 Hz, $^3J_{HF}$ = 5.6 Hz, 2H), 7.62 − 7.55 (m, 2H), 7.20 − 7.13 (m, 2H), 7.06 − 7.00 (m, 1H), 3.98 (s, 3H).

$^{19}$**F NMR** (471 MHz, CDCl$_3$) δ -105.85 – -106.60 (m), -134.01 (dd, $J$ = 11.3, 8.5 Hz).

$^{13}$**C NMR** (126 MHz, CDCl$_3$) δ 193.2, 165.4 (d, $^1J_{CF}$ = 254.0 Hz), 152.0 (d, $^1J_{CF}$ = 248.4 Hz), 151.8 (d, $^2J_{CF}$ = 10.7 Hz), 134.0 (d, $^4J_{CF}$ = 3.2 Hz), 132.5 (d, $^3J_{CF}$ = 9.1 Hz), 130.4 (d, $^3J_{CF}$ = 5.1 Hz), 127.6 (d, $^4J_{CF}$ = 3.3 Hz), 117.9 (d, $^2J_{CF}$ = 19.2 Hz), 115.7 (d, $^2J_{CF}$ = 21.9 Hz), 112.5, 56.5.

**HRMS** (ESI) *m/z*: [M+H]$_+$ calculated for C$_{14}$H$_{11}$F$_2$O$_2$ 249.0727, found 249.0730.

**IR** ν$_{max}$ (neat): 3073, 2963, 2947, 1639, 1601, 1576, 1516, 1506, 1458, 1429, 1406 cm$^{-1}$.

In an effort to obtain hydrazone **3.21** without column chromatography, 4-methoxyphenylhydrazine (29.1 mg, 0.17 mmol) was added to a stirred solution of **5.6** (35.0 mg, 0.15 mmol) in ethanol (2.00 mL). A few drops of H$_2$SO$_4$ were added and the reaction was refluxed for 4 hours. H$_2$O (5 mL) was added to the reaction mixture and 1-((3-fluoro-4-methoxyphenyl)(4-fluorophenyl)methylene)-2-(4-methoxyphenyl)hydrazine (39.1 mg, 0.11 mmol, 70 % yield) was collected by filtration as an off-white solid. The product was found to rapidly hydrolyse to under atmospheric conditions, and as such full characterisation was not conducted.

$^{19}$**F NMR** (471 MHz, CDCl$_3$) δ -110.96 - -111.05 (m), -114.10 - -114.18 (m), -132.43 - -132.51 (m), -135.20 (dd, $J_{FH}$ = 13.0, 8.7 Hz) (mixture of stereoisomers).

### 1-((4-methoxyphenyl)(phenyl)methylene)-2-phenylhydrazine (3.24)
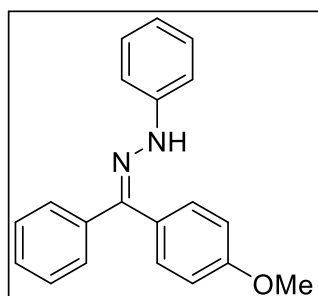


1. Synthesised in accordance with general procedure L using tetrazole **3.18** (55.6 mg, 0.25 mmol), 4-methoxyphenylboronic acid (114 mg, 0.75 mmol), and THF (2.50 mL) to afford 1-((4-methoxyphenyl)(phenyl)methylene)-2-phenylhydrazine (59.5 mg, 0.20 mmol, 79 % yield, 46:54 *E:Z* mixture) as a yellow oil.

2. Synthesised in accordance with general procedure U using hydrazonyl chloride **3.71** (57.7 mg, 0.25 mmol), 4-methoxyphenylboronic acid (76.0 mg, 0.50 mmol), K$_3$PO$_4$ (159 mg, 0.75 mmol) and toluene (2.50 mL) to afford 1-((4-methoxyphenyl)(phenyl)methylene)-2-phenylhydrazine (56.8 mg, 0.19 mmol, 75 % yield, 46:54 *E:Z* mixture) as a yellow oil.

3. Synthesised in accordance with general procedure U using hydrazonyl chloride **3.72** (65.2 mg, 0.25 mmol), phenylboronic acid (61.0 mg, 0.50 mmol), K$_3$PO$_4$ (159 mg, 0.75 mmol) and toluene (2.50 mL) to afford 1-((4-methoxyphenyl)(phenyl)methylene)-2-phenylhydrazine (5.5 mg, 0.02 mmol, 7 % yield, 46:54 *E:Z* mixture) as a yellow oil.

4. To an oven-dried 5 mL microwave vial was added hydrazonyl chloride **3.71** (57.7 mg, 0.25 mmol), and 4-methoxyphenylboronic acid (41.8 mg, 0.28 mmol). The mixture was

dissolved in DCM (2.50 mL), and $K_3PO_4$ (159 mg, 0.75 mmol) was added to initiate the reaction. The solution was stirred at 40 °C for 3 h. The reaction mixture was diluted with ethyl acetate, filtered through celite and rinsed with additional ethyl acetate. The crude solution was concentrated under vacuum and purified by column chromatography (0-100 % ethyl acetate in petroleum ether) to afford 1-((4-methoxyphenyl)(phenyl)methylene)-2-phenylhydrazine (60.2 mg, 0.20 mmol, 80 % yield, 46:54 *E*:*Z* mixture) as a yellow oil.

5. To an oven-dried 50 mL round-bottom flask was added hydrazonyl chloride **3.71** (275 mg, 1.2 mmol), and 4-methoxyphenylboronic acid (235 mg, 1.55 mmol). The mixture was dissolved in DCM (12.0 mL), and $K_3PO_4$ (764 mg, 3.60 mmol) was added. The solution was stirred at 40 °C for 9 h. The reaction mixture was diluted with ethyl acetate, filtered through celite and rinsed with additional ethyl acetate. The crude solution was concentrated under vacuum and purified by column chromatography to afford 1-((4-methoxyphenyl)(phenyl)methylene)-2-phenylhydrazine (322 mg, 1.06 mmol, 89 % yield, 44:56 *E*:*Z* mixture) as a yellow oil.

6. To an oven-dried 100 mL round-bottom flask was added hydrazonyl chloride **3.71** (1.15 g, 5 mmol), and 4-methoxyphenylboronic acid (836 mg, 5.50 mmol). The mixture was dissolved in DCM (50.0 mL), and $K_3PO_4$ (3.18 g, 15.0 mmol) was added. The solution was stirred at 40 °C for 9 h. The reaction mixture was diluted with ethyl acetate, filtered through celite and rinsed with additional ethyl acetate. The crude solution was concentrated under vacuum and purified by column chromatography to afford 1-((4-methoxyphenyl)(phenyl)methylene)-2-phenylhydrazine (1.09 g, 3.60 mmol, 72 % yield, 26:74 *E*:*Z* mixture) as a yellow oil.

**$^1$H NMR** (400 MHz, CDCl$_3$) δ 7.67 – 7.50 (m, 4H), 7.46 – 7.40 (br. s, 0.5 H), 7.40 – 7.24 (m, 5.5 H), 7.16 – 7.07 (m, 3H), 6.92 – 6.83 (m, 2H), 3.92 (s, 1.5 H), 3.84 (s, 1.5 H).

**$^{13}$C NMR** (101 MHz, CDCl$_3$) δ 160.2, 159.9, 145.0, 144.8, 144.4, 144.2, 138.9, 133.1, 131.4, 130.7, 129.7, 129.3, 129.2, 128.3, 128.1, 128.0, 126.7, 124.7, 120.1, 119.9, 115.2, 113.8, 113.0, 112.9, 55.5, 55.4.

**HRMS** (ESI) calculated *m/z* 303.1493 for $C_{20}H_{19}N_2O$ [M+H]$^+$, found 303.1492.

**IR** $\nu_{max}$ (neat): 3306, 3055, 3024, 2963, 2932, 1649, 1599, 1578, 1503, 1491, 1458, 1443 cm$^{-1}$.

Analytical data in agreement with the literature.[443]

### *tert*-butyl (4-(phenyl(2-phenylhydrazono)methyl)phenyl)carbamate (3.25)
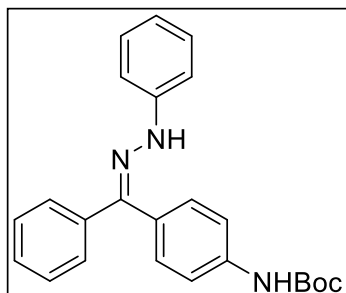
1. Synthesised in accordance with General Procedure L using tetrazole **3.18** (55.6 mg, 0.25 mmol), (4-((*tert*-butoxycarbonyl)amino)phenyl)boronic acid (178 mg, 0.75 mmol), and THF (2.50 mL) to afford *tert*-butyl (4-(phenyl(2-phenylhydrazono)methyl)phenyl)carbamate (88.8 mg, 0.23 mmol, 92 % yield, 55:45 *E*:*Z* mixture) as a yellow oil.
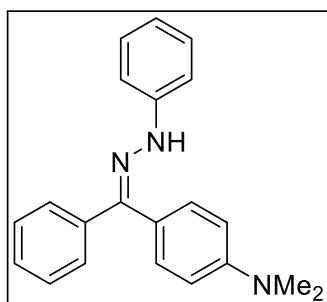
2. Synthesised in accordance with general procedure U using hydrazonyl chloride **3.71** (57.7 mg, 0.25 mmol), (4-((*tert*-butoxycarbonyl)amino)phenyl)boronic acid (119 mg, 0.50 mmol), $K_3PO_4$ (159 mg, 0.75 mmol) and toluene (2.5 mL) to afford *tert*-butyl (4-(phenyl(2-phenylhydrazono)methyl)phenyl)carbamate (72.6 mg, 0.19 mmol, 75 % yield, 48:52 *E*:*Z* mixture) as a yellow oil.

**$^1$H NMR** (500 MHz, CDCl$_3$) δ 7.64 − 7.49 (m, 5H), 7.47 − 7.43 (m, 0.6H), 7.36 − 7.23 (m, 6.4H), 7.13 − 7.06 (m, 2H), 6.86 (m, 1H), 6.76 (br. s, 0.6H), 6.60 (br. s, 0.4H), 1.60 − 1.57 (m, 5.1H), 1.56 − 1.53 (m, 3.9H).

**$^{13}$C NMR** (101 MHz, CDCl$_3$) δ 152.8, 152.7, 144.9, 144.8, 144.2, 144.0, 139.4, 138.7, 138.4, 133.4, 132.9, 130.2, 129.8, 129.34, 129.25, 128.3, 128.1, 127.4, 127.1, 126.7, 120.1, 120.0, 119.5, 118.2, 113.1, 113.0, 81.2, 80.8, 28.5.

**HRMS** (ESI) calculated *m/z* 388.2020 for $C_{24}H_{26}N_3O_2$ [M+H]$^+$, found 388.2011.

**IR** $v_{max}$ (neat): 3327, 3055, 2976, 2930, 1725, 1701, 1641, 1599, 1518, 1501, 1445, 1406 cm$^{-1}$.

### *N*,*N*-dimethyl-4-(phenyl(2-phenylhydrazono)methyl)aniline (3.26)

Synthesised in accordance with general procedure L using tetrazole **3.18** (55.6 mg, 0.25 mmol), 4-(dimethylamino)phenylboronic acid (124 mg, 0.75 mmol), and THF (2.50 mL) to afford *N*,*N*-dimethyl-4-(phenyl(2-phenylhydrazono)methyl)aniline (59.6 mg, 0.19 mmol, 76 % yield, 34:66 *E*:*Z* mixture) as a yellow oil.

**$^1$H NMR** (400 MHz, CDCl$_3$) δ 7.72 (br. s, 0.65H), 7.67 − 7.62 (m, 1.35H), 7.60 − 7.54 (m, 0.65H), 7.53 − 7.46 (m, 1H), 7.36 − 7.26 (m, 3.35H), 7.26 − 7.19 (m, 3H), 7.10 (app. dd, *J* = 8.6, 1.1 Hz, 1.3H), 7.06 (app. dd, *J* = 8.6, 1.1 Hz, 0.7H), 6.90 − 6.78 (m, 2.35H), 6.69 (d, *J* = 8.8 Hz, 0.65H), 3.07 (s, 3.9H), 2.98 (s, 2.1H).

**13C NMR** (101 MHz, CDCl₃) δ 150.7, 150.6, 145.4, 145.3, 145.09, 145.05, 139.4, 133.5, 130.3, 129.6, 129.30, 129.28, 129.25, 129.0, 128.2, 127.9, 127.7, 126.9, 119.74, 119.66, 119.6, 113.0, 112.8, 112.7, 112.0, 40.5, 40.4.

**HRMS** (ESI) calculated *m/z* 316.1808 for $C_{21}H_{22}N_3$ [M+H]⁺, found 316.1807.

**IR** $\nu_{max}$ (neat): 3310, 3265, 3053, 3026, 2922, 1661, 1639, 1597, 1543, 1514, 1501, 1491, 1443 cm⁻¹.

## 1-phenyl-2-(phenyl(*p*-tolyl)methylene)hydrazine (3.27)
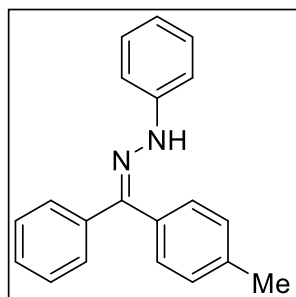


1. Synthesised in accordance with general procedure L using tetrazole **3.18** (55.6 mg, 0.25 mmol), *p*-tolylboronic acid (102 mg, 0.75 mmol), and THF (2.50 mL) to afford 1-phenyl-2-(phenyl(*p*-tolyl)methylene)hydrazine (41.0 mg, 0.14 mmol, 57 % yield, 44:56 *E:Z* mixture) as a yellow oil.

2. Synthesised in accordance with general procedure U using hydrazonyl chloride **3.71** (57.7 mg, 0.25 mmol), *p*-tolylboronic acid (68.0 mg, 0.50 mmol), K₃PO₄ (159 mg, 0.75 mmol), and toluene (2.50 mL) to afford 1-phenyl-2-(phenyl(*p*-tolyl)methylene)hydrazine (20.4 mg, 0.07 mmol, 28 %, 44:56 *E:Z* mixture) as a yellow oil.

**1H NMR** (400 MHz, CDCl₃) δ 7.67 – 7.50 (m, 4H), 7.48 (s, 0.5H), 7.41 (d, *J* = 7.7 Hz, 1H), 7.38 - 7.29 (m, 3H), 7.29 – 7.27 (m, 1.5H), 7.26 – 7.24 (m, 1H), 7.19 – 7.14 (m, 1H), 7.14 – 7.09 (m, 2H), 6.91 – 6.84 (m, 1H), 2.50 (s, 1.7H), 2.39 (s, 1.3H).

**13C NMR** (101 MHz, CDCl₃) δ 144.9, 144.8, 144.52, 144.48, 139.3, 138.7, 138.1, 135.8, 133.1, 130.5, 129.8, 129.32, 129.26, 129.2, 129.0, 128.3, 128.1, 126.7, 126.6, 120.1, 120.0, 113.03, 112.99, 112.96, 21.6, 21.4.

**HRMS** (ESI) calculated *m/z* 287.1543 for $C_{20}H_{19}N_2$ [M+H]⁺, found 287.1544.

**IR** $\nu_{max}$ (neat): 3318, 3053, 3024, 2980, 2920, 1736, 1710, 1655, 1601, 1578, 1555, 1487, 1441 cm⁻¹.

Analytical data in agreement with the literature.[445]

## 1-((4-(methylthio)phenyl)(phenyl)methylene)-2-phenylhydrazine (3.28)
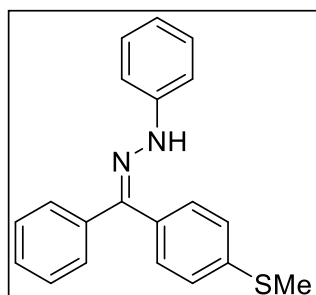


1. Synthesised in accordance with general procedure L using tetrazole **3.18** (55.6 mg, 0.25 mmol), 4-(methylthio)phenylboronic acid (126 mg, 0.75 mmol), and THF (2.50 mL) to afford 1-((4-(methylthio)phenyl)(phenyl)methylene)-2-phenylhydrazine (29.6 mg, 0.09 mmol, 37 % yield, 46:54 *E:Z* mixture) as a

yellow oil.

2. Synthesised in accordance with general procedure U using hydrazonyl chloride **3.71** (57.7 mg, 0.25 mmol), 4-(methylthio)phenylboronic acid (84.0 mg, 0.50 mmol), $K_3PO_4$ (159 mg, 0.75 mmol) and toluene (2.50 mL) to afford 1-((4-(methylthio)phenyl)(phenyl)methylene)-2-phenylhydrazine (40.9 mg, 0.13 mmol, 51 % yield, 44:56 *E:Z* mixture) as a yellow oil.

**¹H NMR** (500 MHz, CDCl₃) δ 7.60- 7.57 (m, 2H), 7.55 – 7.49 (m, 2H), 7.46 (br. s, 1H), 7.43 (d, *J* = 8.3 Hz, 1H), 7.32 (m, 2H), 7.29 – 7.22 (m, 3.5H), 7.20 (d, *J* = 8.6 Hz, 1H), 7.12 – 7.05 (m, 2H), 6.85 (td, *J* = 7.3, 4.3 Hz, 1H), 2.58 (s, 1.5H), 2.49 (s, 1.5H).

**¹³C NMR** (101 MHz, CDCl₃) δ 144.7, 144.0, 143.8, 140.5, 138.6, 138.5, 135.5, 132.8, 129.9, 129.8, 129.43, 129.37, 129.3, 129.1, 128.3, 128.2, 127.1, 127.0, 126.7, 126.3, 120.24, 120.19, 113.1, 113.0, 15.9, 15.4.

**HRMS** (ESI) calculated *m/z* 319.1263 for $C_{20}H_{19}N_2S$ [M+H]⁺, found 319.1260.

**IR** ν_max (neat): 3324, 3051, 3022, 2920, 2851, 1653, 1599, 1545, 1503, 1489, 1443 cm⁻¹.

### 1-((4-(*tert*-butyl)phenyl)(phenyl)methylene)-2-phenylhydrazine (3.29)
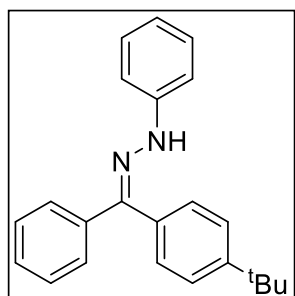


1. Synthesised in accordance with general procedure L using tetrazole **3.18** (55.6 mg, 0.25 mmol), 4-(*tert*-butyl)phenylboronic acid (134 mg, 0.75 mmol), and THF (2.50 mL) to afford 1-((4-(*tert*-butyl)phenyl)(phenyl)methylene)-2-phenylhydrazine (61.9 mg, 0.19 mmol, 75 % yield, 47:53 *E:Z* mixture) as a yellow oil.

2. Synthesised in accordance with general procedure U using hydrazonyl chloride **3.71** (57.7 mg, 0.25 mmol), 4-(*tert*-butyl)phenylboronic acid (89.0 mg, 0.50 mmol), $K_3PO_4$ (159.2 mg, 0.75 mmol) and toluene (2.50 mL) to afford 1-((4-(*tert*-butyl)phenyl)(phenyl)methylene)-2-phenylhydrazine (49.9 mg, 0.15 mmol, 61 % yield, 48:52 *E:Z* mixture) as a yellow oil.

**¹H NMR** (500 MHz, CDCl₃) δ 7.62 – 7.45 (m, 5H), 7.43 (br. s, 0.5H), 7.35 – 7.27 (m, 3H), 7.25 – 7.19 (m, 3.5H), 7.09 – 7.02 (m, 2H), 6.84 – 6.78 (m, 1H), 1.39 (s, 4.8H), 1.31 (s, 4.2H).

**¹³C NMR** (126 MHz, CDCl₃) δ 152.4, 151.3, 144.89, 144.87, 144.5, 138.8, 135.8, 133.1, 129.8, 129.7, 129.32, 129.28, 129.0, 128.3, 128.0, 126.71, 126.66, 126.4, 125.3, 120.1, 120.0, 113.08, 113.05, 113.0, 31.5, 31.4.

**HRMS** (ESI) calculated *m/z* 329.2012 for $C_{23}H_{25}N_2$ [M+H]⁺, found 329.2014.

**IR** ν_max (neat): 3325, 3057, 2961, 2866, 1655, 1601, 1578, 1501, 1491, 1445 cm⁻¹.

## 1-(diphenylmethylene)-2-phenylhydrazine (3.30)
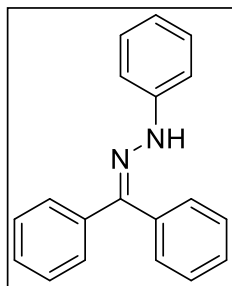
1. Synthesised in accordance with general procedure L using tetrazole **3.18** (55.6 mg, 0.25 mmol), phenylboronic acid (92.0 mg, 0.75 mmol), and THF (2.50 mL) to afford 1-(diphenylmethylene)-2-phenylhydrazine (11.1 mg, 0.04 mmol, 16 % yield) as a yellow oil.

2. Synthesised in accordance with general procedure U using hydrazonyl chloride **3.71** (57.7 mg, 0.25 mmol), phenylboronic acid (61.0 mg, 0.50 mmol), $K_3PO_4$ (159 mg, 0.75 mmol) and toluene (2.50 mL) to afford 1-(diphenylmethylene)-2-phenylhydrazine (19.4 mg, 0.07 mmol, 29 % yield) as a yellow oil.

**$^1$H NMR** (400 MHz, CDCl$_3$) δ 7.64 – 7.57 (m, 4H), 7.56-7.52 (m, 1H), 7.50 (br. s, 1H), 7.38 – 7.22 (m, 7H), 7.12 – 7.07 (m, 2H), 6.86 (tt, *J* = 7.4, 1.1 Hz, 1H).
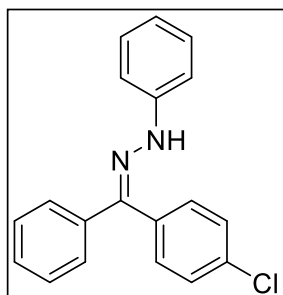
**$^{13}$C NMR** (101 MHz, CDCl$_3$) δ 144.8, 144.3, 138.5, 132.9, 129.8, 129.4, 129.3, 128.3, 128.1, 126.6, 120.2, 113.1, one C not observed (coincident).

**HRMS** (ESI) calculated *m/z* 273.1386 for $C_{19}H_{17}N_2$ [M+H]$^+$, found 273.1388.

**IR** ν$_{max}$ (neat): 3321, 3055, 2924, 1599, 1578, 1560, 1501, 1489, 1443 cm$^{-1}$.

Analytical data in agreement with the literature.[446]

## 1-((4-chlorophenyl)(phenyl)methylene)-2-phenylhydrazine (3.31)

1. Synthesised in accordance with general procedure L using tetrazole **3.18** (55.6 mg, 0.25 mmol), 4-chlorophenylboronic acid (117 mg, 0.75 mmol), and THF (2.50 mL) to afford 1-((4-chlorophenyl)(phenyl)methylene)-2-phenylhydrazine (10.9 mg, 0.04 mmol, 14 % yield, *E:Z* ratio not measured) as a yellow oil.

2. Synthesised in accordance with general procedure U using hydrazonyl chloride **3.71** (57.7 mg, 0.25 mmol), 4-chlorophenylboronic acid (78.2 mg, 0.50 mmol), $K_3PO_4$ (159 mg, 0.75 mmol) and toluene (2.50 mL) to afford 1-((4-chlorophenyl)(phenyl)methylene)-2-phenylhydrazine (7.30 mg, 0.02 mmol, 10 % yield, *E:Z* ratio not measured) as a yellow oil.

**$^1$H NMR** (400 MHz, CDCl$_3$) δ 7.63 – 7.41 (m, 6H), 7.35 – 7.26 (m, 5H), 7.26 – 7.22 (m, 1H), 7.12 – 7.05 (m, 2H), 6.91 – 6.83 (m, 1H).

**$^{13}$C NMR** (101 MHz, CDCl$_3$) δ 144.6, 144.5, 143.1, 138.2, 137.1, 133.9, 132.5, 131.3, 130.9, 130.2, 130.0, 129.6, 129.4, 129.2, 128.8, 128.5, 128.4, 128.3, 127.8, 126.5, 123.3, 120.5, 120.4, 113.2, 113.1.

**HRMS** (ESI) calculated *m/z* 307.0997 for $C_{19}H_{16}ClN_2$ [M+H]$^+$, found 307.1000.

**IR** $\nu_{max}$ (neat): 3059, 3034, 2924, 2853, 1659, 1585, 1485, 1447, 1398 cm$^{-1}$.

Analytical data in agreement with the literature.[445]

## 1-((3-methoxyphenyl)(phenyl)methylene)-2-phenylhydrazine (3.34)
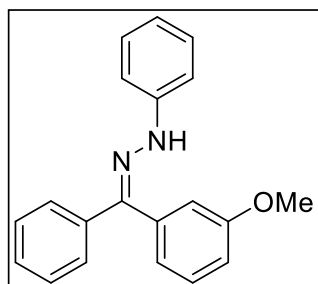
1. Synthesised in accordance with general procedure L using tetrazole **3.18** (55.6 mg, 0.25 mmol), 3-methoxyphenylboronic acid (128 mg, 0.75 mmol), and THF (2.50 mL) to afford 1-((3-methoxyphenyl)(phenyl)methylene)-2-phenylhydrazine (15.7 mg, 0.05 mmol, 21 % yield, 49:51 *E*:*Z* mixture) as a yellow oil.

2. Synthesised in accordance with general procedure U using hydrazonyl chloride **3.71** (57.7 mg, 0.25 mmol), 3-methoxyphenylboronic acid (85.0 mg, 0.50 mmol), K$_3$PO$_4$ (159 mg, 0.75 mmol) and toluene (2.50 mL) to afford 1-((3-methoxyphenyl)(phenyl)methylene)-2-phenylhydrazine (15.4 mg, 0.05 mmol, 20 % yield, 47:53 *E*:*Z* mixture) as a yellow oil.

**$^1$H NMR** (500 MHz, CDCl$_3$) δ 7.64 – 7.54 (m, 2H), 7.54 – 7.46 (m, 2H), 7.35 – 7.19 (m, 5.5H), 7.11 – 7.02 (m, 3H), 6.91 (d, *J* = 7.4 Hz, 0.5H), 6.88 – 6.77 (m, 2H), 3.83 (s, 1.5H), 3.82 (s, 1.5H).

**$^{13}$C NMR** (126 MHz, CDCl$_3$) δ 160.8, 159.7, 144.8, 144.7, 144.12, 144.08, 140.0, 138.3, 136.7, 134.2, 132.9, 131.0, 129.8, 129.40, 129.36, 129.3, 129.2, 128.3, 128.1, 126.6, 121.3, 120.3, 120.2, 119.6, 115.2, 114.3, 113.8, 113.1, 111.9, 55.5, 55.4.

**HRMS** (ESI) calculated *m/z* 303.1492 for C$_{20}$H$_{19}$N$_2$O [M+H]$^+$, found 303.1494.

**IR** $\nu_{max}$ (neat): 3325, 3298, 3055, 2955, 2926, 2853, 1655, 1597, 1578, 1504, 1485, 1447, 1431 cm$^{-1}$.

Analytical data in agreement with the literature.[447]

## 1-((2,4-dimethoxyphenyl)(phenyl)methylene)-2-phenylhydrazine (3.35)
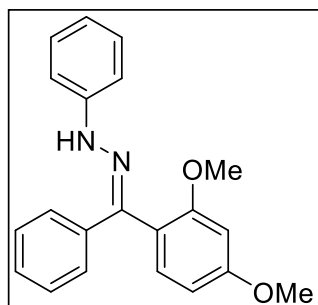
Synthesised in accordance with general procedure L using tetrazole **3.18** (55.6 mg, 0.25 mmol), 2,4-dimethoxyphenylboronic acid (137 mg, 0.75 mmol), and THF (2.50 mL) to afford 1-((2,4-dimethoxyphenyl)(phenyl)methylene)-2-phenylhydrazine (55.2 mg, 0.17 mmol, 66 % yield, >99:1 *E*:*Z* mixture) as a yellow oil.

**$^1$H NMR** (400 MHz, CDCl$_3$) δ 7.63 – 7.57 (m, 2H), 7.43 (br. s, 1H), 7.33 – 7.20 (m, 5H), 7.12 – 7.07 (m, 3H), 6.86 – 6.79 (m, 1H), 6.68 - 6.65 (m, 2H), 3.91 (s, 3H), 3.73 (s, 3H).

**13C NMR** (101 MHz, CDCl₃) δ 162.1, 158.6, 145.1, 141.8, 138.8, 131.6, 129.3, 128.2, 127.8, 126.3, 119.9, 113.6, 113.1, 105.8, 99.6, 55.9, 55.7.

**HRMS** (ESI) calculated $m/z$ 333.1598 for $C_{21}H_{21}N_2O_2$ [M+H]⁺, found 333.1600.

**IR** $\nu_{max}$ (neat): 3325, 3055, 3030, 2961, 2903, 2866, 1655, 1601, 1501, 1491, 1445 cm⁻¹.

## 1-((3-fluoro-4-methoxyphenyl)(phenyl)methylene)-2-phenylhydrazine (3.36)
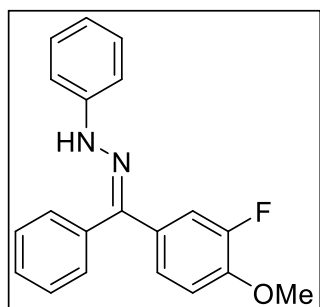


1. Synthesised in accordance with general procedure L using tetrazole **3.18** (55.6 mg, 0.25 mmol), 3-fluoro-4-methoxyphenylboronic acid (128 mg, 0.75 mmol), and THF (2.50 mL) to afford 1-((3-fluoro-4-methoxyphenyl)(phenyl)methylene)-2-phenylhydrazine (62.9 mg, 0.20 mmol, 79 % yield, 69:31 *E:Z* mixture) as a yellow oil.

2. Synthesised in accordance with general procedure U using hydrazonyl chloride **3.71** (57.7 mg, 0.25 mmol), (3-fluoro-4-methoxyphenyl)boronic acid (85.0 mg, 0.50 mmol), K₃PO₄ (159 mg, 0.75 mmol) and toluene (2.50 mL) to afford 1-((3-fluoro-4-methoxyphenyl)(phenyl)methylene)-2-phenylhydrazine (22.4 mg, 0.07 mmol, 27 % yield, *E:Z* ratio not measured) as a yellow oil.

**1H NMR** (400 MHz, CDCl₃) δ 7.64 – 7.49 (m, 4H), 7.46 (br. s, 0.7H), 7.39 – 7.24 (m, 3.9H), 7.18 – 7.05 (m, 3.7H), 6.92 – 6.83 (m, 1.7H), 4.00 (s, 0.9H), 3.90 (s, 2.1H).

**19F NMR** (376 MHz, CDCl₃) δ -132.53 (dd, $J_{FH}$ = 11.3, 7.8 Hz), -135.23 (ddd, $J_{FH}$ = 13.0, 8.7, 1.0 Hz).

**13C NMR** (101 MHz, CDCl₃) δ 153.1 (d, $^1J_{CF}$ = 249.5 Hz), 152.5 (d, $^1J_{CF}$ = 244.8 Hz), 148.5 (d, $^2J_{CF}$ = 10.5 Hz), 147.8 (d, $^2J_{CF}$ = 11.1 Hz), 144.7, 144.6, 143.1, 142.7, 138.4, 132.5, 132.2 (d, $^3J_{CF}$ = 6.8 Hz), 130.7, 129.9, 129.5, 129.3, 129.2, 128.4, 128.3, 128.2, 127.8, 126.6, 125.59, 125.55, 125.2, 125.1, 122.7 (d, $^4J_{CF}$ = 2.9 Hz), 120.3, 120.2, 117.3, 117.1, 114.4, 113.8 (d, $^3J_{CF}$ = 19.9 Hz), 113.1, 112.98, 112.97 (d, $^2J_{CF}$ = 29.8 Hz), 56.4.

**HRMS** (ESI) calculated $m/z$ 321.1398 for $C_{20}H_{18}FN_2O$ [M+H]⁺, found 321.1398.

**IR** $\nu_{max}$ (neat): 3331, 3057, 3024, 2960, 2934, 2841, 1649, 1599, 1578, 1501, 1491, 1431 cm⁻¹.

## 1-(furan-3-yl(phenyl)methylene)-2-phenylhydrazine (3.37)
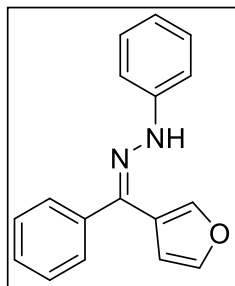


1. Synthesised in accordance with general procedure L using tetrazole **3.18** (55.6 mg, 0.25 mmol), furan-3-ylboronic acid (84.0 mg, 0.75 mmol), and THF (2.5 mL) to afford 1-(furan-3-yl(phenyl)methylene)-2-phenylhydrazine (16.9 mg, 0.06 mmol, 26 % yield, 50:50 *E:Z* mixture) as a yellow oil.

2. Synthesised in accordance with general procedure U using hydrazonyl chloride **3.71** (57.7 mg, 0.25 mmol), furan-3-ylboronic acid (55.9 mg, 0.50 mmol), $K_3PO_4$ (159 mg, 0.75 mmol), and toluene (2.50 mL) to afford 1-(furan-3-yl(phenyl)methylene)-2-phenylhydrazine (14.1 mg, 0.05 mmol, 21 % yield, 50:50 *E:Z* mixture) as a yellow oil.

**$^1$H NMR** (500 MHz, CDCl$_3$) δ 7.82 (s, 0.5H), 7.71 – 7.66 (m, 1.5H), 7.64 (s, 0.5H), 7.54 (t, *J* = 7.4 Hz, 1H), 7.51 – 7.43 (m, 1H), 7.42 – 7.36 (m, 1.5H), 7.34 (t, *J* = 7.4 Hz, 1H), 7.31 – 7.19 (m, 2.5H), 7.12 (d, *J* = 8.1 Hz, 1H), 7.08 (s, 0.5H), 7.02 (d, *J* = 8.1 Hz, 1H), 6.94 (s, *J* = 0.7 Hz, 0.5H), 6.86 (t, *J* = 7.3 Hz, 0.5H), 6.82 (t, *J* = 7.3 Hz, 0.5H), 6.50 (d, *J* = 0.6 Hz, 0.5H).

**$^{13}$C NMR** (101 MHz, CDCl$_3$) δ 144.8, 144.7, 144.6, 143.7, 142.4, 141.9, 138.6, 138.4, 136.7, 132.9, 129.7, 129.6, 129.4, 129.3, 128.6, 128.4, 128.3, 127.6, 126.6, 120.4, 120.0, 116.2, 113.2, 112.9, 111.1, 108.2.

**HRMS** (ESI) calculated *m/z* 263.1179 for $C_{17}H_{15}N_2O$ [M+H]$^+$, found 263.1182.

**IR** ν$_{max}$ (neat): 3323, 3138, 3053, 3024, 2924, 2853, 1647, 1599, 1558, 1541, 1493, 1445 cm$^{-1}$.

## 1-methyl-5-(phenyl(2-phenylhydrazono)methyl)-1*H*-indazole (3.38)
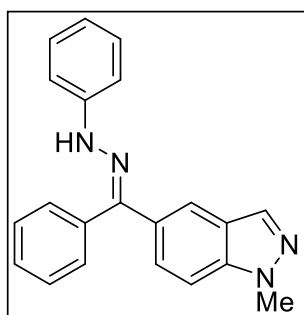


1. Synthesised in accordance with general procedure L using tetrazole **3.18** (55.6 mg, 0.25 mmol), (1-methyl-1*H*-indazol-5-yl)boronic acid (132 mg, 0.75 mmol), and THF (2.50 mL) to afford 1-methyl-5-(phenyl(2-phenylhydrazono)methyl)-1*H*-indazole (52.6 mg, 0.16 mmol, 64 % yield, 75:25 *E:Z* mixture) as a yellow oil.

2. Synthesised in accordance with general procedure U using hydrazonyl chloride **3.71** (57.7 mg, 0.25 mmol), (1-methyl-1*H*-indazol-5-yl)boronic acid (88.0 mg, 0.50 mmol), $K_3PO_4$ (159 mg, 0.75 mmol) and toluene (2.5 mL) to afford 1-methyl-5-(phenyl(2-phenylhydrazono)methyl)-1*H*-indazole (55.0 mg, 0.17 mmol, 67 % yield, 76:24 *E:Z* mixture) as a yellow oil.

**¹H NMR** (400 MHz, CDCl₃) δ 8.15 (dd, *J* = 8.9, 1.6 Hz, 0.25H), 8.07 (d, *J* = 0.9 Hz, 0.75H), 7.88 (d, *J* = 0.7 Hz, 0.25H), 7.76 – 7.74 (m, 0.75H), 7.65 – 7.53 (m, 4H), 7.48 – 7.44 (m, 0.5H), 7.42 – 7.35 (m, 1.5H), 7.35 – 7.28 (m, 3H), 7.27 – 7.21 (m, 1H), 7.09 (td, *J* = 8.6, 1.0 Hz, 2H), 6.88 – 6.82 (m, 1H), 4.17 (s, 2.25H), 4.08 (s, 0.75H).

**¹³C NMR** (101 MHz, CDCl₃) δ 144.91, 144.86, 144.8, 144.5, 139.9, 138.9, 133.6, 133.4, 133.1, 131.8, 129.9, 129.44, 129.36, 128.3, 128.1, 127.3, 126.7, 125.0, 124.9, 124.6, 122.4, 120.2, 120.1, 120.0, 113.1, 113.0, 110.7, 109.1, 35.9, 35.8.

**HRMS** (ESI) calculated *m/z* 327.1604 for $C_{21}H_{19}N_4$ [M+H]⁺, found 327.1604.

**IR** $v_{max}$ (neat): 3238, 3055, 2918, 2849, 1597, 1578, 1555, 1491, 1443 cm⁻¹.

### 1-methyl-5-(phenyl(2-phenylhydrazono)methyl)-1*H*-indole (3.39)
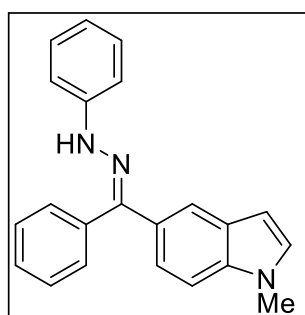


1. Synthesised in accordance with general procedure L using tetrazole **3.18** (55.6 mg, 0.25 mmol), (1-methyl-1*H*-indol-5-yl)boronic acid (131 mg, 0.75 mmol), and THF (2.50 mL) to afford 1-methyl-5-(phenyl(2-phenylhydrazono)methyl)-1*H*-indole (49.6 mg, 0.15 mmol, 61 % yield, 75:25 *E*:*Z* mixture) as a yellow oil.

2. Synthesised in accordance with general procedure U using hydrazonyl chloride **3.71** (57.7 mg, 0.25 mmol), (1-methyl-1*H*-indol-5-yl)boronic acid (87.3 mg, 0.50 mmol), K₃PO₄ (159 mg, 0.75 mmol) and toluene (2.5 mL) to afford 1-methyl-5-(phenyl(2-phenylhydrazono)methyl)-1*H*-indole (13.0 mg, 0.04 mmol, 16 %, 75:25 *E*:*Z* mixture) as a yellow oil.

**¹H NMR** (400 MHz, CDCl₃) δ 7.85 (dd, *J* = 8.7, 1.7 Hz, 0.25H), 7.69 – 7.58 (m, 3.5H), 7.54 – 7.50 (m, 1.25H), 7.41 – 7.37 (m, 0.75H), 7.34 – 7.27 (m, 2.75H), 7.25 – 7.05 (m, 5.25H), 7.02 (d, *J* = 3.1 Hz, 0.25H), 6.86 – 6.80 (m, 1H), 6.58 (dd, *J* = 3.1, 0.8 Hz, 0.75H), 6.42 (dd, *J* = 3.1, 0.7 Hz, 0.25H), 3.90 (s, 2.25H), 3.80 (s, 0.75H).

**¹³C NMR** (101 MHz, CDCl₃) δ 146.2, 145.8, 145.3, 145.0, 139.4, 136.9, 133.8, 130.4, 130.09, 130.06, 129.7, 129.4, 129.34, 129.30, 129.1, 128.21, 128.17, 127.9, 126.91, 126.87, 123.5, 122.4, 122.0, 120.5, 120.4, 119.8, 119.7, 113.0, 112.9, 110.7, 109.3, 101.9, 101.7, 33.2, 33.1.

**HRMS** (ESI) calculated *m/z* 326.1652 for $C_{22}H_{20}N_3$ [M+H]⁺, found 326.1654.

**IR** $v_{max}$ (neat): 3319, 3053, 2959, 2926, 1715, 1645, 1599, 1499, 1491, 1443 cm⁻¹.

## 1-phenyl-2-(phenyl(thiophen-3-yl)methylene)hydrazine (3.40)
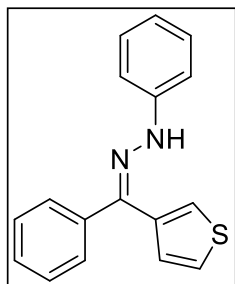
1. Synthesised in accordance with general procedure L using tetrazole **3.18** (33.5 mg, 0.15 mmol), thiophen-3-ylboronic acid (58.0 mg, 0.45 mmol), and THF (2.50 mL) to afford 1-phenyl-2-(phenyl(thiophen-3-yl)methylene)hydrazine (29.5 mg, 0.11 mmol, 72 % yield, 47:53 *E:Z* mixture) as a yellow oil.

2. Synthesised in accordance with general procedure U using hydrazonyl chloride **3.71** (57.7 mg, 0.25 mmol), thiophen-3-ylboronic acid (64.1 mg, 0.50 mmol), $K_3PO_4$ (159 mg, 0.75 mmol) and toluene (2.50 mL) to afford 1-phenyl-2-(phenyl(thiophen-3-yl)methylene)hydrazine (19.4 mg, 0.07 mmol, 28 % yield, 49:51 *E:Z* mixture) as a yellow oil.

**$^1$H NMR** (400 MHz, CDCl$_3$) δ 7.74 (br. s, 0.5H), 7.70 (dd, *J* = 5.1, 1.2 Hz, 0.5H), 7.66 – 7.56 (m, 2.5H), 7.55 – 7.50 (m, 0.5H), 7.46 (dd, *J* = 2.9, 1.2 Hz, 0.5H), 7.44 – 7.22 (m, 5.5H), 7.16 – 7.10 (m, 1.5H), 7.06 (dd, *J* = 8.6, 1.0 Hz, 1H), 6.93 – 6.82 (m, 1.5H).

**$^{13}$C NMR** (101 MHz, CDCl$_3$) δ 144.8, 144.7, 142.1, 141.5, 139.8, 138.6, 133.2, 132.8, 129.7, 129.5, 129.4, 129.3, 128.9, 128.4, 128.2, 128.1, 127.8, 126.6, 126.1, 125.84, 125.78, 123.3, 120.3, 120.1, 113.2, 113.0.

**HRMS** (ESI) calculated *m/z* 279.0950 for $C_{17}H_{15}N_2S$ [M+H]$^+$, found 279.0952.

**IR** $\nu_{max}$ (neat): 3321, 3098, 3051, 2924, 1597, 1578, 1560, 1499, 1489, 1443 cm$^{-1}$.

## 1-phenyl-2-(phenyl(thiophen-2-yl)methylene)hydrazine (3.41)
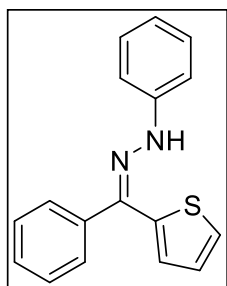
1. Synthesised in accordance with general procedure L using tetrazole **3.18** (55.6 mg, 0.25 mmol), thiophen-2-ylboronic acid (96.0 mg, 0.75 mmol), and THF (2.50 mL) to afford 1-phenyl-2-(phenyl(thiophen-2-yl)methylene)hydrazine (59.6 mg, 0.21 mmol, 86 % yield, 33:67 *E:Z* mixture) as a yellow oil.

2. Synthesised in accordance with general procedure U using hydrazonyl chloride **3.71** (57.7 mg, 0.25 mmol), thiophen-2-ylboronic acid (64.0 mg, 0.50 mmol), $K_3PO_4$ (159 mg, 0.75 mmol) and toluene (2.50 mL) to afford 1-phenyl-2-(phenyl(thiophen-2-yl)methylene)hydrazine (18.2 mg, 0.07 mmol, 26 % yield, *E:Z* ratio not measured) as a yellow oil.

**$^1$H NMR** (400 MHz, CDCl$_3$) δ 7.95 (br. s, 0.3H), 7.69 – 7.50 (m, 3H), 7.46 – 7.40 (m, 1.7H), 7.38 – 7.26 (m, 3H), 7.26 – 7.19 (m, 2H), 7.13 (dd, *J* = 8.6, 1.1 Hz, 1H), 7.05 (dd, *J* = 8.6, 1.0 Hz, 1H), 6.94 – 6.82 (m, 1.7H), 6.66 (dd, *J* = 3.6, 1.1 Hz, 0.3H).

**<sup>13</sup>C NMR** (101 MHz, CDCl₃) δ 144.8, 144.4, 140.9, 140.8, 138.9, 136.8, 132.2, 132.0, 129.8, 129.7, 129.5, 129.41, 129.36, 129.1, 128.33, 128.29, 128.0, 127.1, 126.7, 126.3, 126.1, 120.6, 120.3, 113.3, 113.1.

**HRMS** (ESI) calculated $m/z$ 279.0950 for $C_{17}H_{15}N_2S$ [M+H]⁺, found 279.0953.

**IR** $\nu_{max}$ (neat): 3320, 3100, 3053, 3030, 2959, 2924, 1597, 1557, 1499, 1487, 1441, 1425 cm⁻¹.

Analytical data in agreement with the literature.[448]

## 1-(phenyl(*p*-tolyl)methylene)-2-(4-(trifluoromethyl)phenyl)hydrazine (3.42)
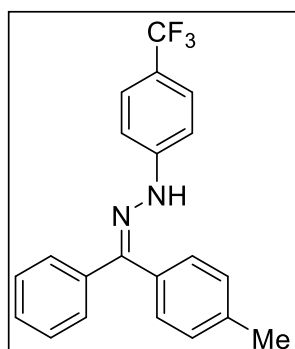
Synthesised in accordance with general procedure L using 5-phenyl-2-(4-(trifluoromethyl)phenyl)-2*H*-tetrazole (60.0 mg, 0.21 mmol), *p*-tolylboronic acid (84.4 mg, 0.62 mmol), and THF (2.50 mL) to afford 1-(phenyl(*p*-tolyl)methylene)-2-(4-(trifluoromethyl)phenyl)hydrazine (40.1 mg, 0.15 mmol, 55 % yield, 47:53 *E:Z* mixture) as a yellow oil.

**<sup>1</sup>H NMR** (500 MHz, CDCl₃) δ 7.76 − 7.66 (m, 1H), 7.63 − 7.57 (m, 2H), 7.54 (app. dd, $J$ = 8.7, 6.1 Hz, 0.5H), 7.49 (dd, $J$ = 8.0, 4.3 Hz, 3H), 7.41 (d, $J$ = 7.8 Hz, 1H), 7.36 − 7.31 (m, 2.5H), 7.23 (d, $J$ = 7.8 Hz, 1H), 7.18 − 7.09 (m, 3H), 2.49 (s, 1.7H), 2.37 (s, 1.3H).

**<sup>19</sup>F NMR** (376 MHz, CDCl₃) δ -61.21 − -61.27 (m).

**<sup>13</sup>C NMR** (101 MHz, CDCl₃) δ 147.33, 147.29, 146.6, 139.7, 138.8, 138.2, 135.4, 132.7, 131.1, 130.6, 129.9, 129.6, 129.4, 129.2, 129.1, 129.0, 128.6, 128.4, 126.94, 126.89, 126.8 (app. d, $^2J_{CF}$ = 19.7 Hz), 126.74, 126.70, 124.9 (app. d, $^1J_{CF}$ = 270.5 Hz), 121.8 (app. d, $^3J_{CF}$ = 5.2 Hz), 121.4 (app. d, $^3J_{CF}$ = 5.8 Hz), 112.6, 112.5, 21.6, 21.4.

**HRMS** (ESI) calculated $m/z$ 355.1417 for $C_{21}H_{18}F_3N_2$ [M+H]⁺, found 355.1415.

**IR** $\nu_{max}$ (neat): 3314, 3057, 3030, 2957, 2924, 1719, 1655, 1612, 1582, 1528, 1445 cm⁻¹.

## *p*-tolyl(4-(trifluoromethyl)phenyl)methanone (3.43)
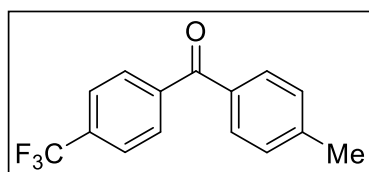
1. Synthesised in accordance with general procedure L using 2-phenyl-5-(4-(trifluoromethyl)phenyl)-2*H*-tetrazole (80.0 mg, 0.25 mmol), *p*-tolylboronic acid (102 mg, 0.75 mmol), and THF (2.50 mL), however attempts at purification by column chromatography resulted in partial hydrolysis of the hydrazone. Complete hydrolysis was facilitated through stirring in a suspension of SiO₂, H₂O and

MeOH with gentle heating to afford *p*-tolyl(4-(trifluoromethyl)phenyl)methanone (15.5 mg, 0.06 mmol, 27 % yield) as an off-white solid.

2. Synthesised in accordance with general procedure L using tetrazole **3.8** (80.0 mg, 0.25 mmol), *p*-tolylboronic acid (102 mg, 0.75 mmol), and THF (2.50 mL), however attempts at purification by column chromatography resulted in partial hydrolysis of the hydrazone. Complete hydrolysis was facilitated through stirring in a suspension of $SiO_2$, $H_2O$ and MeOH with gentle heating to afford *p*-tolyl(4-(trifluoromethyl)phenyl)methanone (10.6 mg, 0.04 mmol, 16 % yield) as an off-white solid.

**¹H NMR** (500 MHz, CDCl₃) δ 7.87 (d, *J* = 8.2 Hz, 2H), 7.75 (d, *J* = 8.2 Hz, 2H), 7.72 (d, *J* = 8.0 Hz, 2H), 7.31 (d, *J* = 8.0 Hz, 2H), 2.46 (s, 3H, CH₃).

**¹⁹F NMR** (471 MHz, CDCl₃) δ -62.98 (s).

**¹³C NMR** (126 MHz, CDCl₃) δ 195.4, 144.2, 141.3, 134.2, 133.7 (app. d, $^2J_{CF}$ = 32.7 Hz), 130.5, 130.2, 129.4, 125.4 (q, $^3J_{CF}$ = 3.6 Hz), 123.9 (app. d, $^1J_{CF}$ = 272.6 Hz), 21.9.

**HRMS** (ESI) calculated *m/z* 265.0840 for $C_{15}H_{12}F_3O$ [M+H]⁺, found 265.0839.

**IR** $\nu_{max}$ (neat): 2957, 2924, 2855, 1647, 1630, 1603, 1508, 1406 cm⁻¹.

Analytical data in agreement with the literature.[449]

## 1-(*p*-tolyl(4-(trifluoromethyl)phenyl)methylene)-2-(4-(trifluoromethyl)phenyl)hydrazine (3.44)
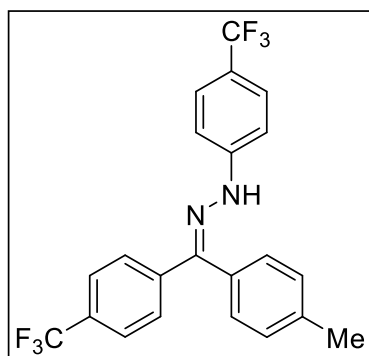


Synthesised in accordance with general procedure L using tetrazole **3.6** (70.0 mg, 0.20 mmol), *p*-tolylboronic acid (80.0 mg, 0.59 mmol), and THF (2.50 mL) to afford 1-(*p*-tolyl(4-(trifluoromethyl)phenyl)methylene)-2-(4-(trifluoromethyl)phenyl)hydrazine (48.5 mg, 0.11 mmol, 59 % yield, >99:1 *E:Z* mixture) as a yellow oil.

**¹H NMR** (500 MHz, CDCl₃) δ 7.79 (s, 1H), 7.70 (d, *J* = 8.3 Hz, 2H), 7.58 (d, *J* = 8.3 Hz, 2H), 7.50 (d, *J* = 8.5 Hz, 2H), 7.43 (d, *J* = 7.8 Hz, 2H), 7.22 (d, *J* = 7.8 Hz, 2H), 7.14 (d, *J* = 8.5 Hz, 2H), 2.50 (s, 3H).

**¹⁹F NMR** (471 MHz, CDCl₃) δ -61.36 (s), -62.54 (s).

**¹³C NMR** (101 MHz, CDCl₃) δ 147.1, 146.9, 144.90, 144.85, 141.6, 140.2, 139.2, 136.6, 134.7, 131.1, 130.9, 130.3, 130.0, 129.6 (app. d, $^2J_{CF}$ = 48.8 Hz), 129.0, 128.6, 127.0, 126.79, 126.75, 126.7, 125.3 (q, $^3J_{CF}$ = 3.9 Hz), 124.8 (app. d, $^1J_{CF}$ = 271.0 Hz), 124.4 (app. d, $^1J_{CF}$ = 271.9 Hz), 122.3 (q, $^2J_{CF}$ = 32.7 Hz), 120.5 (app. d, $^2J_{CF}$ = 45.5 Hz), 112.8, 112.7, 21.6, 21.4.

**HRMS** (ESI) calculated *m/z* 423.1290 for $C_{22}H_{17}F_6N_2$ [M+H]$^+$, found 423.1287.

**IR** $\nu_{max}$ (neat): 3339, 3054, 2955, 2926, 1647, 1614, 1557, 1526, 1512, 1408 cm$^{-1}$.

## 1-((4-methoxyphenyl)(*p*-tolyl)methylene)-2-(4-(trifluoromethyl)phenyl)hydrazine (3.45)
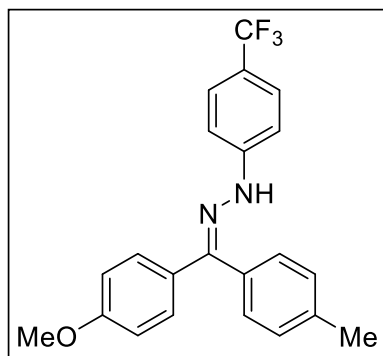
Synthesised in accordance with general procedure L using tetrazole **3.1** (80.1 mg, 0.25 mmol), *p*-tolylboronic acid (102 mg, 0.75 mmol), and THF (2.50 mL) to afford 1-((4-methoxyphenyl)(*p*-tolyl)methylene)-2-(4-(trifluoromethyl)phenyl)hydrazine (46.9 mg, 0.12 mmol, 49 % yield, 53:47 *E:Z* mixture) as a yellow oil.

**¹H NMR** (500 MHz, CDCl$_3$) δ 7.66 (br. s, 0.5H), 7.58 (br. s, 0.5H), 7.55 – 7.43 (m, 4H), 7.38 (d, *J* = 7.8 Hz, 1H), 7.27 – 7.24 (m, 1H) 7.21 (d, *J* = 7.9 Hz, 1H), 7.14 (d, *J* = 8.1 Hz, 1H), 7.12 – 7.07 (m, 3H), 6.86 (d, *J* = 8.8 Hz, 1H), 3.91 (s, 1.5H), 3.82 (s, 1.5H), 2.47 (s, 1.5H), 2.36 (s, 1.5H).

**¹⁹F NMR** (376 MHz, CDCl$_3$) δ -61.22 (s), -61.24 (s).

**¹³C NMR** (101 MHz, CDCl$_3$) δ 160.4, 160.3, 147.5, 147.4, 146.6, 146.5, 139.6, 138.7, 135.7, 131.1, 130.6, 130.5, 129.3 (app. d, $^2J_{CF}$ = 59.1 Hz), 129.1, 129.0, 128.3, 127.0, 126.7, 124.9 (app. d, $^1J_{CF}$ = 270.5 Hz), 124.5, 121.5 (app. d, $^3J_{CF}$ = 16.2 Hz), 121.2 (app. d, $^3J_{CF}$ = 15.8 Hz), 115.2, 113.8, 112.5, 112.4, 55.53, 55.48, 21.6, 21.4.

**HRMS** (ESI) calculated *m/z* 385.1522 for $C_{22}H_{20}F_3N_2O$ [M+H]$^+$, found 385.1521.

**IR** $\nu_{max}$ (neat): 3335, 3001, 2953, 2926, 2853, 1612, 1528, 1508, 1479, 1464, 1443, 1416 cm$^{-1}$.

## phenyl(*p*-tolyl)methanone (3.46)
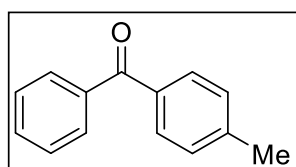
Synthesised in accordance with general procedure L using tetrazole **3.2** (41.0 mg, 0.16 mmol), *p*-tolylboronic acid (66.3 mg, 0.49 mmol), and THF (2.50 mL), however attempts at purification by column chromatography resulted in partial hydrolysis of the hydrazone. Complete hydrolysis was facilitated through stirring in a suspension of SiO$_2$, H$_2$O and MeOH with gentle heating to afford phenyl(*p*-tolyl)methanone (15.2 mg, 0.08 mmol, 47 % yield) as an off white solid.

**¹H NMR** (400 MHz, CDCl$_3$) δ 7.81 – 7.76 (m, 2H), 7.73 (d, *J* = 8.2 Hz, 2H), 7.61 – 7.55 (m, 1H), 7.49-7.45 (m, 2H), 7.29-7.27 (m, 2H), 2.44 (s, 3H).
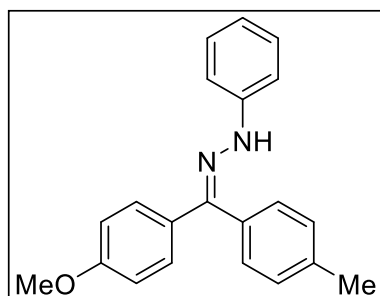
**¹³C NMR** (126 MHz, Acetone) δ 196.2, 144.0, 138.9, 135.9, 133.0, 130.8, 130.4, 129.9, 129.2, 21.6.

**HRMS** (ESI) calculated *m/z* 197.0961 for $C_{14}H_{13}O$ [M+H]⁺, found 197.0959.

**IR** $\nu_{max}$ (neat): 3057, 3026, 2920, 1653, 1605, 1445 cm⁻¹.

Analytical data in agreement with the literature.[444]

### 1-((4-methoxyphenyl)(*p*-tolyl)methylene)-2-phenylhydrazine (3.47)

Synthesised in accordance with general procedure L using tetrazole **3.7** (63.1 mg, 0.25 mmol), *p*-tolylboronic acid (102 mg, 0.75 mmol), and THF (2.50 mL) to afford 1-((4-methoxyphenyl)(*p*-tolyl)methylene)-2-phenylhydrazine (35.6 mg, 0.11 mmol, 45 % yield, 53:47 *E*:*Z* mixture) as a yellow oil.

**¹H NMR** (500 MHz, CDCl₃) δ 7.55 – 7.46 (m, 2.5H), 7.42 (s, 0.5H), 7.36 (d, *J* = 7.8 Hz, 1H), 7.25 – 7.18 (m, 4H), 7.12 (d, *J* = 8.1 Hz, 1H), 7.10 – 7.03 (m, 3H), 6.87 – 6.78 (m, 2H), 3.90 (s, 1.5H), 3.81 (s, 1.5H), 2.46 (s, 1.5H), 2.35 (s, 1.5H).

**¹³C NMR** (101 MHz, Acetone) δ 161.0, 160.7, 146.62, 146.55, 144.8, 144.7, 139.6, 138.3, 137.5, 132.9, 132.7, 131.4, 131.0, 130.5, 129.9, 129.8, 129.6, 128.5, 127.2, 126.1, 120.1, 120.0, 115.8, 114.4, 113.74, 113.66, 55.7, 55.6, 21.4, 21.2.

**HRMS** (ESI) calculated *m/z* 317.1648 for $C_{21}H_{21}N_2O$ [M+H]⁺, found 317.1646.

**IR** $\nu_{max}$ (neat): 3323, 3024, 2924, 2853, 1647, 1599, 1578, 1501, 1458, 1441, 1418 cm⁻¹.

### (4-methoxyphenyl)(*p*-tolyl)methanone (3.48)
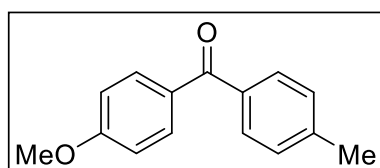
Synthesised in accordance with general procedure L using tetrazole **3.4** (70.6 mg, 0.25 mmol), *p*-tolylboronic acid (102 mg, 0.75 mmol), and THF (2.50 mL), however attempts at purification by column chromatography resulted in partial hydrolysis of the hydrazone. Complete hydrolysis was facilitated through stirring in a suspension of $SiO_2$, $H_2O$ and MeOH with gentle heating to afford (4-methoxyphenyl)(*p*-tolyl)methanone (20.2 mg, 0.09 mmol, 36 % yield) as an off-white solid.

**¹H NMR** (500 MHz, CDCl₃) δ 7.81 (d, *J* = 8.7 Hz, 2H), 7.68 (d, *J* = 8.0 Hz, 2H), 7.27 (d, *J* = 8.2 Hz, 2H), 6.96 (d, *J* = 8.7 Hz, 2H), 3.89 (s, 3H), 2.44 (s, 3H).
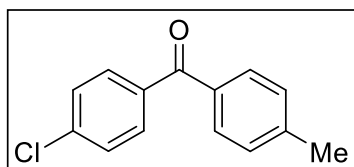
**¹³C NMR** (126 MHz, CDCl₃) δ 195.5, 163.2, 142.8, 135.7, 132.6, 130.7, 130.1, 129.0, 113.6, 55.6, 21.8.

**HRMS** (ESI) calculated *m/z* 227.1067 for $C_{15}H_{15}O_2$ [M+H]$^+$, found 227.1066.

**IR** $\nu_{max}$ (neat): 3009, 2955, 2918, 2847, 1682, 1641, 1593, 1504, 1462, 1447 cm$^{-1}$.

Analytical data in agreement with the literature.[450]

## (4-chlorophenyl)(*p*-tolyl)methanone (3.50)



Synthesised in accordance with general procedure L using 5-(4-chlorophenyl)-2-(4-methoxyphenyl)-2*H*-tetrazole (71.7 mg, 0.25 mmol), *p*-tolylboronic acid (102 mg, 0.75 mmol), and THF (2.50 mL), however attempts at purification by column chromatography resulted in partial hydrolysis of the hydrazone. Complete hydrolysis was facilitated through stirring in a suspension of SiO$_2$, H$_2$O and MeOH with gentle heating to afford (4-chlorophenyl)(*p*-tolyl)methanone product (28.2 mg, 0.12 mmol, 47 % yield) as an off-white solid.

**$^1$H NMR** (500 MHz, CDCl$_3$) δ 7.74 (d, *J* = 8.3 Hz, 2H), 7.69 (d, *J* = 7.9 Hz, 2H), 7.45 (d, *J* = 8.3 Hz, 2H), 7.29 (d, *J* = 7.9 Hz, 2H), 2.45 (s, 3H).
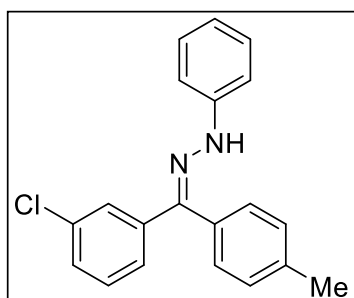
**$^{13}$C NMR** (101 MHz, CDCl$_3$) δ 195.4, 143.7, 138.8, 136.4, 134.7, 131.5, 130.3, 129.3, 128.7, 21.8.

**HRMS** (ESI) calculated *m/z* 231.0577 for $C_{14}H_{12}ClO$ [M+H]$^+$, found 231.0583.

**IR** $\nu_{max}$ (neat): 3030, 2960, 2916, 2853, 1643, 1605, 1584, 1510, 1481 cm$^{-1}$.

Analytical data in agreement with the literature.[450]

## 1-((3-chlorophenyl)(*p*-tolyl)methylene)-2-phenylhydrazine (3.51)



Synthesised in accordance with general procedure L using 5-(3-chlorophenyl)-2-phenyl-2*H*-tetrazole (64.2 mg, 0.25 mmol), *p*-tolylboronic acid (102 mg, 0.75 mmol), and THF (2.50 mL) to afford 1-((3-chlorophenyl)(*p*-tolyl)methylene)-2-phenylhydrazine (42.1 mg, 0.13 mmol, 52 % yield, 86:14 *E*:*Z* mixture) as a yellow oil.

**$^1$H NMR** (400 MHz, CDCl$_3$) δ 7.76 − 7.70 (m, 0.15H), 7.63 − 7.60 (m, 0.85H), 7.59 (br. s, 0.85H), 7.49 − 7.43 (m, 1.15H), 7.41 (app. d, *J* = 7.8 Hz, 1.85H), 7.35 − 7.33 (m, 0.15H), 7.30 − 7.19 (m, 5.6H), 7.15 (d, *J* = 8.0 Hz, 0.4H), 7.12 − 7.07 (m, 2H), 6.88 (tt, *J* = 7.4, 1.1 Hz, 1H), 2.49 (s, 2.5H), 2.37 (s, 0.5H).

**$^{13}$C NMR** (101 MHz, Acetone) δ 146.4, 146.0, 142.9, 142.2, 140.0, 138.6, 136.73, 136.66, 135.8, 134.7, 132.2, 132.0, 131.2, 130.7, 130.4, 130.0, 129.9, 129.8, 128.7, 128.2, 127.0, 126.5, 125.5, 120.7, 120.4, 114.0, 113.9, 21.5, 21.2.

**HRMS** (ESI) calculated *m/z* 321.1153 for $C_{20}H_{18}ClN_2$ [M+H]$^+$, found 321.1151.

**IR** $\nu_{max}$ (neat): 3324, 3065, 3026, 2920, 2855, 1719, 1647, 1601, 1566, 1501, 1420 cm$^{-1}$.

## 1-((2-chlorophenyl)(*p*-tolyl)methylene)-2-phenylhydrazine (3.52)
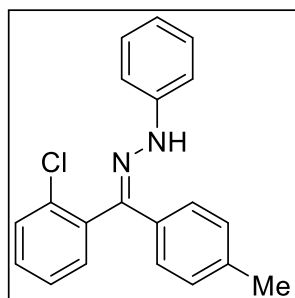


Synthesised in accordance with general procedure L using 5-(2-chlorophenyl)-2-phenyl-2*H*-tetrazole (64.2 mg, 0.25 mmol), *p*-tolylboronic acid (102 mg, 0.75 mmol), and THF (2.50 mL) to afford 1-((2-chlorophenyl)(*p*-tolyl)methylene)-2-phenylhydrazine (46.1 mg, 0.14 mmol, 57 % yield, >99:1 *E:Z* mixture) as a yellow oil.

**¹H NMR** (400 MHz, CDCl₃) δ 7.64 − 7.61 (m, 1H), 7.50 − 7.44 (m, 4H), 7.31 − 7.23 (m, 3H), 7.19 (br. s, 1H), 7.15 (dd, *J* = 8.5, 0.5 Hz, 2H), 7.11 (dd, *J* = 8.7, 1.1 Hz, 2H), 6.87 (tt, *J* = 7.5, 1.1 Hz, 1H), 2.37 (s, 3H).

**¹³C NMR** (101 MHz, CDCl₃) δ 144.7, 141.5, 138.2, 134.7, 133.9, 132.1, 131.2, 130.9, 130.7, 129.3, 129.2, 128.1, 126.0, 120.3, 113.2, 21.4.

**HRMS** (ESI) calculated *m/z* 321.1153 for $C_{20}H_{18}ClN_2$ [M+H]$^+$, found 321.1151.

**IR** $\nu_{max}$ (neat): 3329, 3051, 3024, 2955, 2920, 2853, 1722, 1655, 1601, 1578, 1553, 1499, 1435 cm$^{-1}$.

## 1-phenyl-2-(thiophen-3-yl(*p*-tolyl)methylene)hydrazine (3.53)
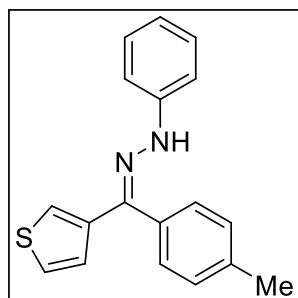


Synthesised in accordance with general procedure L using tetrazole **3.10** (47.8 mg, 0.21 mmol), *p*-tolylboronic acid (85.7 mg, 0.63 mmol), and THF (2.50 mL) to afford 1-phenyl-2-(thiophen-3-yl(*p*-tolyl)methylene)hydrazine (22.0 mg, 0.08 mmol, 36 % yield, 60:40 *E:Z* mixture) as a yellow oil.

**¹H NMR** (500 MHz, CDCl₃) δ 7.67 (d, *J* = 4.9 Hz, 1H), 7.59 (dd, *J* = 4.9, 2.9 Hz, 0.4H), 7.50 (d, *J* = 8.1 Hz, 1H), 7.44 (s, 1H), 7.37 (d, *J* = 7.8 Hz, 1H), 7.31 (dd, *J* = 5.0, 3.0 Hz, 0.6H), 7.29 − 7.20 (m, 3.4H), 7.17 − 7.08 (m, 2H), 7.05 (d, *J* = 8.1 Hz, 1H), 6.91 (d, *J* = 2.8 Hz, 0.6H), 6.87 − 6.80 (m, 1H), 2.47 (s, 1.8H), 2.36 (s, 1.2H).

**¹³C NMR** (101 MHz, CDCl₃) δ 144.8, 142.3, 141.7, 140.1, 139.4, 138.2, 135.9, 133.0, 130.4, 130.1, 129.4, 129.3, 129.1, 128.8, 128.1, 127.7, 126.5, 126.1, 125.9, 125.7, 123.3, 120.2, 120.0, 113.1, 113.0, 21.6, 21.4.

**HRMS** (ESI) calculated *m/z* 293.1107 for $C_{18}H_{17}N_2S$ [M+H]$^+$, found 293.1109.

**IR** $\nu_{max}$ (neat): 3323, 3102, 3049, 3024, 2918, 2853, 1641, 1599, 1499, 1410 cm$^{-1}$.

## 1-(3-methoxyphenyl)-2-((4-methoxyphenyl)(phenyl)methylene)hydrazine (3.56)
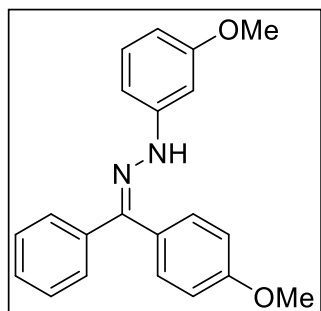
2-(3-methoxyphenyl)-5-phenyl-2*H*-tetrazole (193 mg, 0.75 mmol) and 4-methoxyphenyl boronic acid (342 mg, 2.30 mmol) were dissolved in THF (5.00 mL) and circulated through PTFE tubing around a UV light bulb enclosed in a quartz chamber for 4 hours using a peristaltic pump at a 2 mLmin$^{-1}$ flow rate (*Figure 3.2*). The reaction mixture was collected, concentrated under reduced pressure and purified by column chromatography (0-100 % ethyl acetate in petroleum ether) to afford 1-(3-methoxyphenyl)-2-((4-methoxyphenyl)(phenyl)methylene)hydrazine (177 mg, 0.53 mmol, 71 % yield, 43:57 *E:Z* mixture) as a yellow oil.

**¹H NMR** (500 MHz, CDCl₃) δ 7.60 – 7.52 (m, 2.4H), 7.52 – 7.48 (m, 1.2H), 7.36 (br. s, 0.4H), 7.33 – 7.22 (m, 3.8H), 7.14 – 7.04 (m, 2.2H), 6.84 (d, *J* = 8.9 Hz, 1H), 6.78 – 6.75 (m, 1H), 6.57 – 6.52 (m, 1H), 6.39 (td, *J* = 8.0, 2.2 Hz, 1H), 3.88 (s, 1.8H), 3.80 (s, 1.2H), 3.79 (s, 3H).

**¹³C NMR** (101 MHz, CDCl₃) δ 161.0, 160.2, 159.9, 146.3, 146.2, 144.5, 144.4, 138.8, 133.1, 131.3, 130.7, 130.1, 130.0, 129.7, 129.3, 129.2, 128.3, 128.1, 128.0, 126.7, 124.7, 115.2, 113.8, 105.8, 105.7, 105.5, 98.9, 98.7, 55.5, 55.4, 55.3.

**HRMS** (ESI) calculated *m/z* 333.1598 for $C_{21}H_{21}N_2O_2$ [M+H]⁺, found 333.1599.

**IR** ν$_{max}$ (neat): 3327, 3055, 2997, 2955, 2932, 2833, 1599, 1555, 1503, 1489, 1458, 1441 cm$^{-1}$.

## (4-chlorophenyl)(4-hydroxyphenyl)methanone (3.58)
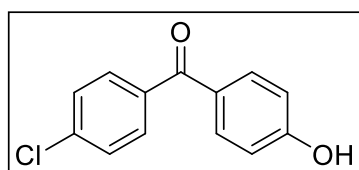
Synthesised in accordance with general procedure L using 5-(4-chlorophenyl)-2-(4-methoxyphenyl)-2*H*-tetrazole (72.0 mg, 0.25 mmol), 4-hydroxyphenylboronic acid (103 mg, 0.75 mmol), and THF (2.50 mL). Following complete conversion to the hydrazone, ethanol (2.50 mL) and concentrated hydrochloric acid (2.50 mL) were added, and the mixture was stirred at room temperature overnight. The resulting reaction mixture was passed through celite and partitioned between ethyl acetate and water. The organic layer was washed with a further portion of water and brine, passed through a phase separator and concentrated under vacuum. The crude residue was purified by column chromatography (0-100 % ethyl acetate in petroleum ether) to afford (4-chlorophenyl)(4-hydroxyphenyl)methanone (38.2 mg, 0.16 mmol, 66 % yield) as an off-white solid.

**¹H NMR** (500 MHz, CDCl₃) δ 7.76 (d, *J* = 8.7 Hz, 2H), 7.71 (d, *J* = 8.5 Hz, 2H), 7.46 (d, *J* = 8.5 Hz, 2H), 6.91 (d, *J* = 8.7 Hz, 2H), 5.51 (s, 1H).
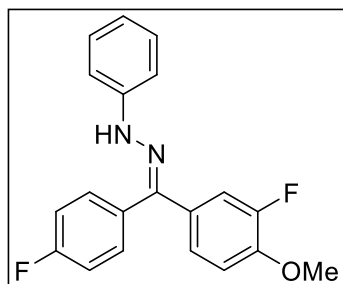
$^{13}$**C NMR** (101 MHz, CDCl$_3$) δ 194.5, 160.0, 138.6, 136.6, 132.9, 131.3, 130.2, 128.7, 115.4.

**HRMS** (ESI) calculated *m/z* 233.0369 for C$_{13}$H$_{10}$ClO$_2$ [M+H]$^+$, found 233.0373.

**IR** ν$_{max}$ (neat): 3316, 3067, 2955, 2922, 2853, 1641, 1597, 1560, 1508, 1485 cm$^{-1}$.

Analytical data in agreement with the literature.[451]

## 1-((3-fluoro-4-methoxyphenyl)(4-fluorophenyl)methylene)-2-phenylhydrazine (3.76)



Synthesised in accordance with general procedure U using hydrazonyl chloride **3.70** (62.0 mg, 0.25 mmol), (3-fluoro-4-methoxyphenyl)boronic acid (85.0 mg, 0.50 mmol), K$_3$PO$_4$ (159 mg, 0.75 mmol) and toluene (2.50 mL) to afford 1-((3-fluoro-4-methoxyphenyl)(4-fluorophenyl)methylene)-2-phenylhydrazine (18.2 mg, 0.05 mmol, 27 % yield, 88:12 *E*:*Z* mixture) as a yellow oil.

$^1$**H NMR** (400 MHz, CDCl$_3$) δ 7.57 − 7.52 (m, 2H), 7.49 (s, 1H), 7.29 − 7.23 (m, 2H), 7.17 (t, *J* = 8.4 Hz, 1H), 7.10 − 7.05 (m, 4H), 7.04 − 6.98 (m, 2H), 6.86 (tt, *J* = 7.5, 1.1 Hz, 1H), 4.00 (s, 3H).

$^{19}$**F NMR** (376 MHz, CDCl$_3$) δ -113.77 (tt, *J* = 8.5, 5.5 Hz), -132.29 − -132.40 (m).

$^{13}$**C NMR** (101 MHz, CDCl$_3$) δ 163.0 (d, $^1J_{CF}$ = 248.1 Hz), 153.2 (d, $^1J_{CF}$ = 249.4 Hz), 148.6 (d, $^2J_{CF}$ = 10.5 Hz), 144.6, 141.9, 134.6, 129.4, 128.3 (d, $^3J_{CF}$ = 7.9 Hz), 125.6 (d, $^3J_{CF}$ = 4.1 Hz), 125.0 (d, $^3J_{CF}$ = 5.7 Hz), 120.4, 117.2 (d, $^2J_{CF}$ = 18.5 Hz), 115.3 (d, $^2J_{CF}$ = 21.6 Hz), 114.5, 113.1, 56.5.

**HRMS** (ESI) calculated *m/z* 339.1303 for C$_{20}$H$_{17}$F$_2$N$_2$O [M+H]$^+$, found 339.1306.

**IR** ν$_{max}$ (neat): 3335, 3057, 2961, 2924, 2853, 1645, 1599, 1574, 1557, 1501, 1466, 1439, 1420, 1406 cm$^{-1}$.

## 1-((4-fluorophenyl)(4-methoxyphenyl)methylene)-2-phenylhydrazine (3.77)
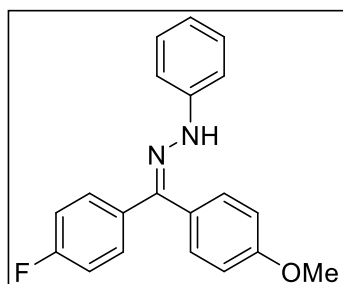


1. Triethylamine (168 μL, 1.20 mmol) was added to a solution of hydrazonyl chloride **3.70** (100 mg, 0.40 mmol) and 4- methoxyphenylboronic acid (182 mg, 1.20 mmol) in acetonitrile (5 mL). The mixture was stirred in a round-bottom flask at room temperature for 16 hours, before it was concentrated under vacuum and purified by column

chromatography (0-100 % ethyl acetate in petroleum ether) to afford 1-((4-fluorophenyl)(4-methoxyphenyl)methylene)-2-phenylhydrazine (32.9 mg, 0.10 mmol, 26 % yield, 35:65 *E*:*Z* mixture) as a yellow oil.

2. Hydrazonyl chloride **3.70** (57.7 mg, 0.25 mmol) and 4- methoxyphenylboronic acid (41.8 mg, 0.28 mmol) were dissolved in DCM (2.5 mL). $K_3PO_4$ (159 mg, 0.75 mmol) was added and the reaction mixture was stirred in a 5 mL microwave vial at 40 °C for 3 hours. Following reaction completion, the mixture was diluted with ethyl acetate, passed through celite and concentrated under reduced pressure. The crude residue was purified by column chromatography to afford 1-((4-fluorophenyl)(4-methoxyphenyl)methylene)-2-phenylhydrazine (60.2 mg, 0.20 mmol, 80 % yield, 46:54 *E*:*Z* mixture) as a yellow oil.

3. Hydrazonyl chloride **3.70** (57.7 mg, 0.25 mmol) and 4- methoxyphenylboronic acid (41.8 mg, 0.28 mmol) were dissolved in DCM (2.5 mL). $K_3PO_4$ (159 mg, 0.75 mmol) was added and the reaction mixture was stirred in a 5 mL microwave vial at 40 °C for 16 hours. Following reaction completion, the mixture was diluted with ethyl acetate, passed through celite and concentrated under reduced pressure. The crude residue was purified by column chromatography to afford 1-((4-fluorophenyl)(4-methoxyphenyl)methylene)-2-phenylhydrazine (64.2 mg, 0.21 mmol, 85 % yield, 46:54 *E*:*Z* mixture) as a yellow oil.

4. Hydrazonyl chloride **3.70** (57.7 mg, 0.25 mmol) and 4- methoxyphenylboronic acid (41.8 mg, 0.28 mmol) were dissolved in toluene (2.5 mL). $K_3PO_4$ (159 mg, 0.75 mmol) was added and the reaction mixture was stirred in a 5 mL microwave vial at 50 °C for 3 hours. Following reaction completion, the mixture was diluted with ethyl acetate, passed through celite and concentrated under reduced pressure. The crude residue was purified by column chromatography to afford 1-((4-fluorophenyl)(4-methoxyphenyl)methylene)-2-phenylhydrazine (52.0 mg, 0.17 mmol, 69 % yield, 45:55 *E*:*Z* mixture) as a yellow oil.

5. Hydrazonyl chloride **3.70** (57.7 mg, 0.25 mmol) and 4- methoxyphenylboronic acid (41.8 mg, 0.28 mmol) were dissolved in toluene (2.5 mL). $K_3PO_4$ (159 mg, 0.75 mmol) was added and the reaction mixture was stirred in a 5 mL microwave vial at 80 °C for 1 hour. Following reaction completion, the mixture was diluted with ethyl acetate, passed through celite and concentrated under reduced pressure. The crude residue was purified by column chromatography to afford 1-((4-fluorophenyl)(4-methoxyphenyl)methylene)-2-phenylhydrazine (57.0 mg, 0.19 mmol, 75 % yield, 45:55 *E*:*Z* mixture) as a yellow oil.

**^{1}H NMR** (400 MHz, CDCl_3) δ 7.61 – 7.55 (m, 2H), 7.54 (s, 1H), 7.29 – 7.23 (m, 4H), 7.13 – 7.07 (m, 4H), 7.02 (t, *J* = 8.8 Hz, 2H), 6.86 (tt, *J* = 7.5, 1.1 Hz, 1H), 3.91 (s, 3H).

**^{19}F NMR** (376 MHz, CDCl_3) δ -114.08 (tt, *J* = 8.5, 5.5 Hz).

$^{13}$**C NMR** (101 MHz, CDCl$_3$) δ 162.9 (d, $^1J_{CF}$ = 247.5 Hz), 160.3, 144.8, 143.3, 135.1, 130.6, 129.4, 128.3 (d, $^3J_{CF}$ = 7.9 Hz), 124.5, 120.1, 115.3, 115.2 (d, $^2J_{CF}$ = 19.4 Hz), 113.0, 55.5.

**HRMS** (ESI) calculated *m/z* 321.1403 for C$_{20}$H$_{18}$FN$_2$O [M+H]$^+$, found 321.1402.

**IR** ν$_{max}$ (neat): 3302, 3053, 3003, 2961, 2934, 2835, 1597, 1574, 1562, 1464, 1433, 1406 cm$^{-1}$.

### 1-((4-methoxyphenyl)(4-nitrophenyl)methylene)-2-phenylhydrazine (3.78)
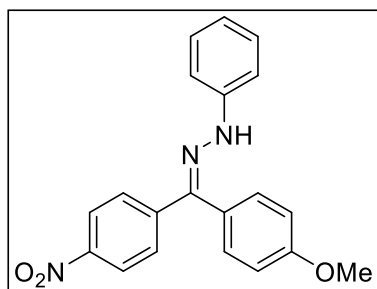


Synthesised in accordance with general procedure U using hydrazonyl chloride **3.73** (68.9 mg, 0.25 mmol), 4-methoxyphenylboronic acid (85.0 mg, 0.50 mmol), K$_3$PO$_4$ (159 mg, 0.75 mmol) and toluene (2.50 mL) to afford 1-((4-methoxyphenyl)(4-nitrophenyl)methylene)-2-phenylhydrazine (53.2 mg, 0.15 mmol, 61 % yield, 4:96 *E*:*Z* mixture) as a yellow oil.

$^1$**H NMR** (500 MHz, CDCl$_3$) δ 8.14 (d, *J* = 9.0 Hz, 2H), 7.78 (br. s, 1H), 7.71 (d, *J* = 9.0 Hz, 2H), 7.30 – 7.22 (m, 4H), 7.13 (d, *J* = 8.7 Hz, 2H), 7.10 (d, *J* = 7.8 Hz, 2H), 6.93 – 6.88 (m, 1H), 3.92 (s, 3H).

$^{13}$**C NMR** (126 MHz, CDCl$_3$) δ 160.7, 147.0, 145.0, 143.9, 141.6, 130.7, 129.5, 126.7, 123.7, 123.4, 121.2, 115.7, 113.5, 55.6.

**HRMS** (ESI) calculated *m/z* 348.1343 for C$_{20}$H$_{18}$N$_3$O$_3$ [M+H]$^+$, found 348.1344.

**IR** ν$_{max}$ (neat): 3306, 3291, 3057, 2997, 2926, 2841, 1641, 1591, 1549, 1504, 1487, 1466, 1439, 1404 cm$^{-1}$.

### 1-((4-nitrophenyl)(phenyl)methylene)-2-phenylhydrazine (3.79)
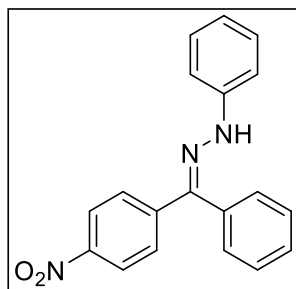


Synthesised in accordance with general procedure U using hydrazonyl chloride **3.73** (68.9 mg, 0.25 mmol), phenylboronic acid (61.0 mg, 0.50 mmol), K$_3$PO$_4$ (159 mg, 0.75 mmol) and toluene (2.50 mL) to afford 1-((4-nitrophenyl)(phenyl)methylene)-2-phenylhydrazine (26.9 mg, 0.08 mmol, 34 % yield, 90:10 *E*:*Z* mixture) as a yellow oil.

$^1$**H NMR** (400 MHz, CDCl$_3$) δ 8.49 – 8.44 (m, 0.2H), 8.18 – 8.13 (m, 1.8H), 7.74 – 7.69 (m, 2.8H), 7.66 – 7.50 (m, 3.2H), 7.34 – 7.26 (m, 4H), 7.13 – 7.09 (m, 2H), 6.92 (app. tt, *J* = 7.5, 1.1 Hz, 1H).
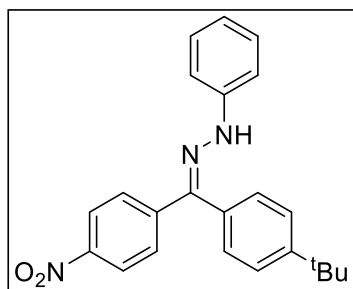
$^{13}$**C NMR** (101 MHz, CDCl$_3$) δ 147.0, 144.6, 143.8, 141.6, 131.6, 130.3, 130.0, 129.5, 129.2, 126.7, 123.8, 121.3, 113.5.

**HRMS** (ESI) calculated $m/z$ 318.1237 for $C_{19}H_{16}N_3O_2$ [M+H]$^+$, found 318.1239.

**IR** $\nu_{max}$ (neat): 3316, 3055, 2957, 2924, 2853, 1663, 1601, 1591, 1545, 1504, 1487, 1406 cm$^{-1}$.

Analytical data in agreement with the literature.[452]

### 1-((4-(*tert*-butyl)phenyl)(4-nitrophenyl)methylene)-2-phenylhydrazine (3.80)



Synthesised in accordance with general procedure U using hydrazonyl chloride **3.73** (68.9 mg, 0.25 mmol), (4-(*tert*-butyl)phenyl)boronic acid (89.0 mg, 0.50 mmol), $K_3PO_4$ (159 mg, 0.75 mmol) and toluene (2.50 mL) to afford 1-((4-(*tert*-butyl)phenyl)(4-nitrophenyl)methylene)-2-phenylhydrazine (31.3 mg, 0.08 mmol, 34 % yield, >99:1 *E*:*Z* mixture) as a yellow oil.

**$^1$H NMR** (500 MHz, CDCl$_3$) δ 8.16 (d, $J$ = 9.0 Hz, 2H), 7.81 (s, 1H), 7.72 (d, $J$ = 9.0 Hz, 2H), 7.63 (d, $J$ = 8.3 Hz, 2H), 7.30 − 7.26 (m, 2H), 7.25 (d, $J$ = 8.3 Hz, 2H), 7.12 (d, $J$ = 7.7 Hz, 2H), 6.91 (app. t, $J$ = 7.3 Hz, 1H), 1.43 (s, 9H).

**$^{13}$C NMR** (101 MHz, CDCl$_3$) δ 153.2, 147.0, 144.9, 143.9, 141.8, 129.5, 128.9, 128.5, 127.2, 126.8, 123.7, 121.2, 113.5, 35.1, 31.4.

**HRMS** (ESI) calculated $m/z$ 374.1869 for $C_{23}H_{24}N_3O_2$ [M+H]$^+$, found 374.1866.

**IR** $\nu_{max}$ (neat): 3321, 3053, 2959, 2926, 2864, 1599, 1543, 1504, 1487, 1404 cm$^{-1}$.

### 1-(4-methoxyphenyl)hexan-1-one (3.81)
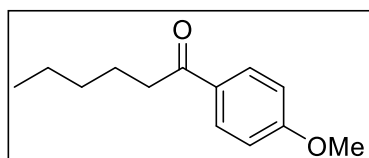


Synthesised in accordance with general procedure U using hydrazonyl chloride **3.75** (56.2  mg, 0.25 mmol), 4-methoxyphenylboronic acid (76.0 mg, 0.50 mmol), $K_3PO_4$ (159 mg, 0.75 mmol) and toluene (2.50 mL), however attempts at purification by column chromatography resulted in partial hydrolysis of the hydrazone. Complete hydrolysis was facilitated through stirring in a suspension of SiO$_2$, H$_2$O and MeOH with gentle heating to afford 1-(4-methoxyphenyl)hexan-1-one (18.0 mg, 0.09 mmol, 35 % yield) as a yellow oil.

**$^1$H NMR** (500 MHz, CDCl$_3$) δ 7.94 (d, $J$ = 8.9 Hz, 2H), 6.93 (d, $J$ = 8.8 Hz, 2H), 3.87 (s, 3H), 2.94 − 2.87 (m, 2H), 1.77 − 1.69 (m, 2H), 1.39 − 1.34 (m, 4H), 0.91 (t, $J$ = 7.0 Hz, 3H).

**$^{13}$C NMR** (126 MHz, CDCl$_3$) δ 199.4, 163.4, 130.4, 113.8, 55.6, 38.4, 31.7, 24.5, 22.7, 14.1, one C not observed.

**HRMS** (ESI) calculated $m/z$ 207.1385 for $C_{13}H_{19}O_2$ [M+H]$^+$, found 207.1383.

**IR** $\nu_{max}$ (neat): 3065, 3009, 2968, 2957, 2932, 2913, 2895, 2872, 2853, 2839, 1668, 1601, 1576, 1508, 1464, 1439, 1416, 1406 cm$^{-1}$.

## 1-(1-(4-methoxyphenyl)-2,2-dimethylpropylidene)-2-phenylhydrazine (3.82)
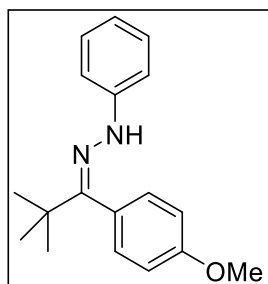
Synthesised in accordance with general procedure U using hydrazonyl chloride **3.74** (52.7 mg, 0.25 mmol), 4-methoxyphenylboronic acid (76.0 mg, 0.50 mmol), $K_3PO_4$ (159 mg, 0.75 mmol) and toluene (2.50 mL) to afford 1-(1-(4-methoxyphenyl)-2,2-dimethylpropylidene)-2-phenylhydrazine (16.2 mg, 0.06 mmol, 23 % yield, >99:1 *E:Z* mixture) as a yellow solid.

**$^1$H NMR** (500 MHz, CDCl$_3$) δ 7.18 (app. t, *J* = 7.9 Hz, 2H), 7.03 (app. q, *J* = 8.8 Hz, 4H), 6.92 (d, *J* = 7.7 Hz, 2H), 6.78 – 6.73 (m, 2H), 3.87 (s, 3H), 1.20 (s, 9H).
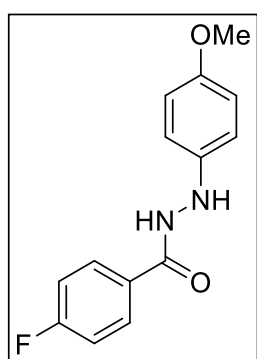
**$^{13}$C NMR** (126 MHz, CDCl$_3$) δ 159.7, 154.9, 145.7, 130.2, 129.2, 125.7, 119.3, 114.7, 112.7, 55.4, 38.4, 28.8.

**HRMS** (ESI) calculated *m/z* 281.1654 for C$_{18}$H$_{21}$N$_2$O [M-H]$^-$, found 281.1655.

**IR** $\nu_{max}$ (neat): 2957, 2928, 2870, 2857, 1724, 1665, 1601, 1574, 1508, 1476, 1460, 1443, 1416 cm$^{-1}$.

*5.4.2.3 Other Compounds*

## 4-fluoro-*N'*-(4-methoxyphenyl)benzohydrazide (3.22)

Synthesised in accordance with general procedure L using tetrazole **3.5** (108 mg, 0.40 mmol), cyclohexylboronic acid (154 mg, 2.00 mmol), and THF (5.00 mL), unexpectedly affording 4-fluoro-*N'*-(4-methoxyphenyl)benzohydrazide (53.0 mg, 0.20 mmol, 51 % yield) as a brown solid.

**$^1$H NMR** (500 MHz, CDCl$_3$) δ 8.14 (br. s, 1H), 7.83 (dd, $^2J_{HH}$ = 8.7 Hz, $^3J_{FH}$ = 5.3 Hz, 2H), 7.16 – 7.08 (m, 2H), 6.89 (d, *J* = 8.9 Hz, 2H), 6.83 – 6.77 (m, 2H), 6.31 (br. s, 1H), 3.75 (s, 3H).

**$^{19}$F NMR** (471 MHz, CDCl$_3$) δ -106.60 – -106.70 (m).

**$^{13}$C NMR** (126 MHz, CDCl$_3$) δ 166.9, 165.3 (d, $^1J_{CF}$ = 253.2 Hz), 155.1, 141.6, 129.7 (d, $^3J_{CF}$ = 9.0 Hz), 128.6 (d, $^4J_{CF}$ = 3.1 Hz), 116.1 (d, $^2J_{CF}$ = 21.9 Hz), 116.0, 114.8, 55.8.

**HRMS** (ESI) calculated *m/z* 261.1034 for C$_{14}$H$_{14}$FN$_2$O$_2$ [M+H]$^+$, found 261.1036.

**IR** $\nu_{max}$ (neat): 3337, 3235, 3071, 2997, 2953, 2932, 2833, 1645, 1601, 1528, 1503, 1460 cm$^{-1}$.

Analytical data in agreement with the literature.[453]

## isopropyl 2-(4-(4-chlorobenzoyl)phenoxy)-2-methylpropanoate (Fenofibrate, 3.57)
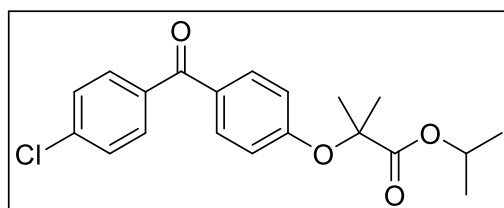


Aryl ketone **3.58** (30.0 mg, 0.13 mmol) and K$_2$CO$_3$ (53.5 mg, 0.39 mmol) were stirred in acetonitrile (5.00 mL) for 10 minutes, before isopropyl 2-bromo-2-methylpropanoate (27.0 µL, 0.16 mmol) was added. The reaction mixture was refluxed for 18 hours, quenched with 1M HCl solution and extracted twice with DCM. The combined organic phases were then washed with brine, passed through a phase separator and concentrated under vacuum. The crude product was purified using column chromatography (0-100 % ethyl acetate in petroleum ether) to afford isopropyl 2-(4-(4-chlorobenzoyl)phenoxy)-2-methylpropanoate (32.7 mg, 0.09 mmol, 61 % yield) as a pale yellow solid.

**$^1$H NMR** (500 MHz, CDCl$_3$) δ 7.72 (d, $J$ = 8.8 Hz, 2H), 7.69 (d, $J$ = 8.5 Hz, 2H), 7.44 (d, $J$ = 8.5 Hz, 2H), 6.86 (d, $J$ = 8.8 Hz, 2H), 5.08 (sept, $J$ = 6.3 Hz, 1H), 1.65 (s, 6H), 1.20 (d, $J$ = 6.3 Hz, 6H).

**$^{13}$C NMR** (126 MHz, CDCl$_3$) δ 194.4, 173.2, 159.9, 138.5, 136.6, 132.1, 131.3, 130.4, 128.7, 117.4, 79.6, 69.5, 25.5, 21.6.

**HRMS** (ESI) calculated $m/z$ 361.1201 for C$_{20}$H$_{22}$ClO$_4$ [M+H]$^+$, found 361.1204.

**IR** $\nu_{max}$ (neat): 3070, 2982, 2936, 1728, 1655, 1597, 1506, 1466, 1383 cm$^{-1}$.

Analytical data in agreement with the literature.[454]

## Leu-Enkaphalin-Tetrazole (3.66)
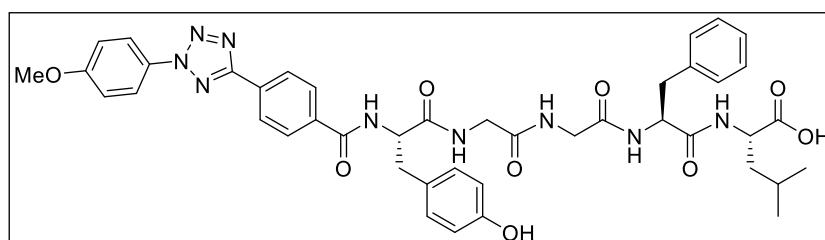


Synthesised in accordance with general procedure M using Wang resin (750 mg), Fmoc-Leu-OH (2912 mg, 8.25 mmol), Fmoc-Phe-OH (968 mg, 2.50 mmol), Fmoc-Gly-OH (743 mg, 2.50 mmol), Fmoc-Tyr(O$^t$Bu)-OH (1.15 g, 2.50 mmol), and tetrazole **3.65** (237 mg, 0.80 mmol), to afford the product (39.7 mg, 0.05 mmol, 15 %) as a white solid. Owing to the complexity of the compound, limited analysis was conducted.

**LRMS** (ESI) calculated $m/z$ 834.3 for C$_{43}$H$_{48}$N$_9$O$_9$ [M+H]$^+$, found 834.5.

*5.4.2.4 Derivatisation of 3.24*

## 2-((4-methoxyphenyl)(phenyl)methylene)-1-methyl-1-phenylhydrazine (3.90)
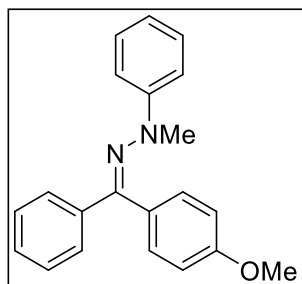


In accordance with previous literature precedent,[455] a 60 wt.% suspension of sodium hydride in mineral oil (240 mg, 6.00 mmol) was added to a solution of hydrazone **3.24** (75.6 mg, 0.25 mmol) in THF (1.00 mL) at -20 °C. The reaction mixture was stirred for 15 minutes, and methyl iodide (32.0 µL, 0.50 mmol) was added dropwise. The reaction mixture was allowed to warm to room temperature, stirred for an additional 3 hours, quenched with $H_2O$ and extracted twice with DCM. The combined organic phases were then washed with brine, passed through a phase separator and concentrated under vacuum. The crude product was purified using column chromatography (0-100 % ethyl acetate in *n*-hexane) to afford 2-((4-methoxyphenyl)(phenyl)methylene)-1-methyl-1-phenylhydrazine (55.2 mg, 0.17 mmol, 70 % yield, 34:66 *E:Z* mixture) as a yellow oil.

**¹H NMR** (500 MHz, Acetone-$d_6$) δ 7.59 (dd, *J* = 8.1, 1.4 Hz, 2H), 7.38 (m, 3H), 7.34 – 7.29 (m, 2H), 7.27 – 7.22 (m, 2H), 7.18 – 7.13 (m, 2H), 7.07 – 7.03 (m, 2H), 6.87 – 6.81 (m, 1H), 3.87 (s, 3H), 2.91 (s, 3H).

**¹³C NMR** (101 MHz, Acetone-$d_6$) δ 161.0, 157.7, 151.6, 140.9, 131.4, 130.4, 130.0, 129.5, 129.0, 128.9, 120.2, 115.3, 114.8, 55.7, 41.5.

**HRMS** (ESI) calculated *m/z* 317.1648 for $C_{21}H_{21}N_2O$ [M+H]⁺, found 317.1654.

**IR** $v_{max}$ (neat): 3057, 3024, 2953, 2924, 2852, 1597, 1493, 1460, 1443 cm⁻¹.

## 4-(4-methoxyphenyl)-1-(methyl(phenyl)amino)-3-phenoxy-4-phenylazetidin-2-one (3.91)
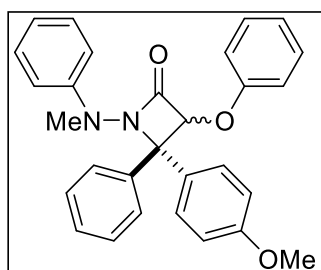


In accordance with previous literature precedent,[455] 2-phenoxyacetyl chloride (20.2 µL, 0.18 mmol), in DCM (1.00 mL) was added dropwise to a stirred solution of hydrazone **3.90** (50.3 mg, 0.17 mmol) and triethylamine (30.0 µL, 0.22 mmol) in DCM (1.00 mL) at 0 °C. The reaction mixture was stirred at room temperature for 6 hours, quenched with $NaHCO_3$ solution and extracted twice with DCM. The combined organic phases were then washed with brine, passed through a phase separator and concentrated under vacuum. The crude product was purified using column chromatography (0-100 % ethyl acetate in *n*-hexane) to afford 4-(4-methoxyphenyl)-1-(methyl(phenyl)amino)-3-phenoxy-4-phenylazetidin-2-one (54.7 mg, 0.12 mmol, 73 % yield, 58:42 diastereotopic mixture) as a white solid.

**¹H NMR** (500 MHz, CDCl₃) δ 7.41 – 7.37 (m, 1H), 7.33 – 7.13 (m, 10H), 7.01 – 6.94 (m, 2H), 6.91 (d, *J* = 7.8 Hz, 1.2H), 6.88 (d, *J* = 7.6 Hz, 0.8H), 6.86 - 6.82 (m, 2.4H), 6.81 - 6.77 (m, 1.6H), 5.79 (s, 0.6H), 5.77 (s, 0.4H), 3.78 (s, 1.8H), 3.77 (s, 1.2H), 3.17 (s, 1.2H), 3.15 (s, 1.8H).

**¹³C NMR** (126 MHz, CDCl₃) δ 166.5, 166.4, 159.6, 159.5, 157.61, 157.56, 148.8, 148.7, 139.1, 138.1, 131.3, 130.7, 129.8, 129.7, 129.61, 129.58, 129.5, 129.1, 129.0, 128.6, 128.4, 128.14, 128.09, 127.7, 122.9, 122.8, 121.7, 121.6, 117.2, 117.1, 116.1, 115.8, 114.0, 113.1, 85.1, 84.9, 77.3, 77.2, 55.4, 55.3, 42.5, 42.3.

**HRMS** (ESI) calculated *m/z* 451.2016 for C₂₉H₂₇N₂O₃ [M+H]⁺, found 451.2013.

**IR** νmax (neat): 3059, 3036, 2955, 2928, 2837, 1767, 1597, 1512, 1491, 1447, 1418 cm⁻¹.

## 6-methoxy-1,3-diphenyl-1*H*-indazole (3.92)
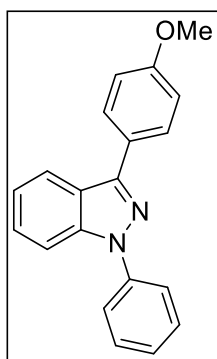


In accordance with previous literature precedent,[456] to a solution of hydrazone **3.24** (75.6 mg, 0.25 mmol) in DMSO (1.50 mL) was added TEMPO (11.7 mg, 0.08 mmol) and NaHCO₃ (21.0 mg, 0.25 mmol). The reaction was stirred at 140 °C under an oxygen atmosphere for 16 hours. The mixture was quenched with H₂O and extracted twice using DCM. The combined organic phases were then washed with brine, passed through a phase separator and concentrated under vacuum. The crude product was purified using column chromatography (0-100 % ethyl acetate in *n*-hexane) to afford 6-methoxy-1,3-diphenyl-1*H*-indazole (46.7 mg, 0.16 mmol, 62 % yield) as a white solid.

**¹H NMR** (500 MHz, CDCl₃) δ 8.04 – 8.00 (m, 2H), 7.94 (d, *J* = 8.9 Hz, 1H), 7.79 (d, *J* = 7.7 Hz, 2H), 7.57 (app. t, *J* = 7.7 Hz, 2H), 7.55 – 7.49 (m, 2H), 7.45 – 7.41 (m, 1H), 7.41 – 7.36 (m, 1H), 7.13 (d, *J* = 1.9 Hz, 1H), 6.95 (dd, *J* = 8.9, 1.9 Hz, 1H), 3.89 (s, 3H).
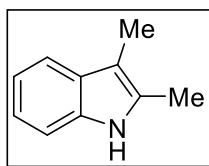
**¹³C NMR** (126 MHz, CDCl₃) δ 160.1, 146.3, 141.8, 140.4, 133.4, 129.6, 128.9, 128.4, 127.8, 126.8, 123.3, 122.5, 117.9, 113.7, 92.1, 55.8.

**HRMS** (ESI) calculated *m/z* 301.1335 for C₂₀H₁₇N₂O [M+H]⁺, found 301.1334.

**IR** νmax (neat): 3061, 3007, 2957, 2930, 2828, 1614, 1597, 1562, 1520, 1503, 1491, 1418, 1454, 1420, 1400 cm⁻¹.

Analytical data in agreement with the literature.[448]

## 2,3-dimethyl-1*H*-indole (3.93)

In accordance with previous literature precedent,[457] hydrazone **3.24** (75.6 mg, 0.25 mmol) was added to a solution of butan-2-one (45.0 μL, 0.50 mmol) in ethanol (5.00 mL) and concentrated HCl (100 μL). The reaction mixture was refluxed for 16 h, before the solution was concentrated under vacuum and quenched with water. The organic phase was twice extracted using DCM, washed with brine, passed through a phase separator and concentrated under vacuum. The crude product was purified using column chromatography (0-100 % ethyl acetate in *n*-hexane) to afford 2,3-dimethyl-1*H*-indole (19.1 mg, 0.13 mmol, 53 % yield) as a light brown solid.

**¹H NMR** (500 MHz, Acetone-$d_6$) δ 9.71 (br. s, 1H), 7.38 (d, $J$ = 7.6 Hz, 1H), 7.23 (d, $J$ = 7.7 Hz, 1H), 7.01 – 6.97 (m, 1H), 6.94 (td, $J$ = 7.6, 0.9 Hz, 1H), 2.34 (s, 3H), 2.18 (s, 3H).
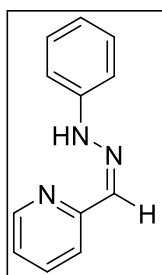
**¹³C NMR** (126 MHz, Acetone-$d_6$) δ 136.7, 131.9, 130.4, 121.0, 119.1, 118.3, 111.0, 106.6, 11.3, 8.5.

**HRMS** (ESI) calculated *m/z* 145.0891 for $C_{10}H_{12}N$ [M+H]⁺, found 145.0879.

**IR** $\nu_{max}$ (neat): 3393, 3051, 2914, 2857, 1649, 1609, 1584, 1522, 1483, 1462 cm⁻¹.

Analytical data in agreement with the literature.[368]

## 2-((2-phenylhydrazono)methyl)pyridine (3.94)

In accordance with previous literature precedent,[457] a mixture of hydrazone **3.24** (75.6 mg, 0.25 mmol) and picolinaldehyde (35.7 μL, 0.38 mmol) in ethanol (1.25 mL) and concentrated HCl (130 μL) was stirred at room temperature for 24 hours. The reaction mixture was concentrated under vacuum and purified by column chromatography (0-100 % ethyl acetate in *n*-hexane) to afford 2-((2-phenylhydrazono)methyl)pyridine (29.4 mg, 0.15 mmol, 60 % yield, >1:99 *E:Z* mixture) as a yellow solid.

**¹H NMR** (400 MHz, CDCl₃) δ 8.45 – 8.41 (m, 1H), 8.20 (s, 1H), 7.90 (d, $J$ = 8.1 Hz, 1H), 7.75 (s, 1H), 7.60 (app. td, $J$ = 7.9, 1.5 Hz, 1H), 7.22 – 7.15 (m, 2H), 7.10 – 7.03 (m, 3H), 6.81 (app. tt, $J$ = 7.4, 1.1 Hz, 1H).
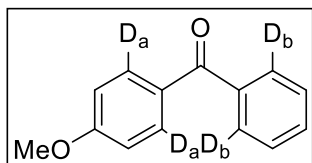
**¹³C NMR** (101 MHz, CDCl₃) δ 154.4, 148.5, 144.1, 136.9, 136.5, 129.5, 122.6, 121.0, 120.0, 113.2.

**HRMS** (ESI) calculated *m/z* 198.1031 for $C_{12}H_{12}N_3$ [M+H]⁺, found 198.1034.

**IR** $\nu_{max}$ (neat): 3223, 3183, 3125, 3057, 3022, 3003, 2945, 2891, 1597, 1566, 1493, 1466, 1450, 1435 cm⁻¹.

Analytical data in agreement with the literature.[368]

## (4-methoxyphenyl-2,6-*d*2)(phenyl-2,6-*d*2)methanone (3.96)

In accordance to previous literature precedent,[458] a flask bearing two stopcocks was flame dried and cooled under argon. Hydrazone **3.24** (65.0 mg, 0.22 mmol), [Ir(COD)(IMes)(PPh$_3$)][BAr$^F_4$] (18.6 mg, 1.10 μmol), and DCM (2.50 mL) were then added and the flask was cooled to -78 °C with stirring. The flask was evacuated and refilled with D$_2$ gas from a balloon. This vacuum and refilling cycle was repeated one further time. The stopcocks were then closed, and the flask was heated at 25 °C for 16 hours. The resulting mixture was concentrated under vacuum and the residue was passed through a silica plug using diethyl ether, to afford the corresponding hydrazone intermediate **3.95** (63.5 mg, 0.21 mmol, 98 % yield).

After significant decomposition of this hydrazone was observed, a portion of hydrazone (30.0 mg, 0.10 mmol) was dissolved in acetone (500 μL). To this mixture was added VO(acac)$_2$ (2.70 mg, 0.01 mmol), and H$_2$O$_2$ (125 μL) dropwise at room temperature. The reaction mixture was stirred for two hours and diluted with DCM. This solution was washed with 10 % sodium metabisulfite and brine, passed through a phase separator and concentrated under vacuum. The crude product was purified by column chromatography (0-100 % ethyl acetate in *n*-hexane) to afford (4-methoxyphenyl-2,6-*d*2)(phenyl-2,6-*d*2)methanone (13.8 mg, 0.06 mmol, 64 % yield) as an off-white solid.

The extent of deuteration was assessed by $^1$H NMR spectroscopy. The integrals were calibrated against a peak corresponding to a position not expected to be labelled. *Equation 5.3* was then used to calculate the extent of labelling:

$$\%D = 100 - \left[100 \times \left(\frac{Residual\ Integral}{Expected\ Inregral}\right)\right]$$

*Equation 5.3: The calculation of the extent of deuterium incorporation*

**$^1$H NMR** (400 MHz, Acetone-*d*$_6$) δ 7.83 – 7.78 (m, 2H$_a$), 7.76 – 7.71 (m, 2H$_b$), 7.63 (dd, *J* = 7.8, 7.0 Hz, 1H), 7.56 – 7.51 (m, 2H), 7.10 – 7.05 (m, 2H), 3.91 (s, 3H).

*Deuterium incorporation: D$_a$ = 44 %, D$_b$ = 77 %*

Labelling expected at signals at 7.80 ppm and 7.74 ppm respectively, measured against signal at 3.91 ppm.

**$^{13}$C NMR** (101 MHz, Acetone-*d*$_6$) δ 185.4, 154.5, 129.4, 129.3, 123.2, 122.9, 121.1, 120.4, 120.1, 119.9, 119.3, 119.2, 104.7, 104.6, 46.1, mixture of isotopes.

**HRMS** (ESI) calculated *m/z* 214.0972 for C$_{14}$H$_{12}$DO$_2$ [M$_{d1}$+H]$^+$, found 214.0972.

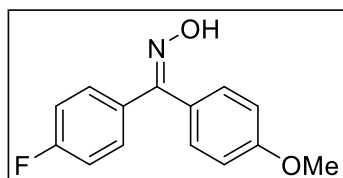Calculated *m/z* 215.1035 for C$_{14}$H$_{11}$D$_2$O$_2$ [M$_{d2}$+H]$^+$, found 215.1030.

Calculated $m/z$ 216.1098 for $C_{14}H_{10}D_3O_2$ $[M_{d3}+H]^+$, found 216.1084.

Calculated $m/z$ 217.1161 for $C_{14}H_9D_4O_2$ $[M_{d4}+H]^+$, found 217.1146.

**IR** $\nu_{max}$ (neat): 3053, 3005, 2965, 2943, 2914, 2839, 1639, 1582, 1504, 1466, 1435 cm$^{-1}$.

*5.4.2.5 Ketone Oximes*

## (4-fluorophenyl)(4-methoxyphenyl)methanone oxime (3.101)



1. To a 5 mL microwave vial was added hydroxamoyl chloride **3.98** (43.3 mg, 0.25 mmol) and (4-methoxyphenyl)boronic acid (76.0 mg, 0.50 mmol). The mixture was dissolved in chloroform (2.50 mL), and DMA (94.8 μl, 0.75 mmol) was added to initiate the reaction. The solution was purged with N$_2$ and heated at 60 °C for 3 h. The reaction mixture was diluted with DCM and washed with 1M HCl solution. The organic phase was separated, washed with brine, passed through a phase separator and concentrated under vacuum. The crude residue was purified by column chromatography (0-100 % diethyl ether in *n*-hexane) to afford (4-fluorophenyl)(4-methoxyphenyl)methanone oxime (33.2 mg, 0.14 mmol, 54 % yield, >1:99 *E*:*Z* mixture) as a white solid.

2. Synthesised in accordance with general procedure V using hydroxamoyl chloride **3.98** (43.3 mg, 0.25 mmol), (4-methoxyphenyl)boronic acid (76.0 mg, 0.50 mmol), DMA (158 μL, 1.25 mmol) and chloroform (2.50 mL) to afford (4-fluorophenyl)(4-methoxyphenyl)methanone oxime (38.0 mg, 0.16 mmol, 62 % yield, >1:99 *E*:*Z* mixture) as a white solid.

**$^1$H NMR** (500 MHz, CDCl$_3$) δ 9.25 (br. s, 1H), 7.52 − 7.42 (m, 4H), 7.10 − 6.99 (m, 4H), 3.90 (s, 3H).

**$^{19}$F NMR** (471 MHz, CDCl$_3$) δ -111.58 − -111.67 (m).

**$^{13}$C NMR** (126 MHz, CDCl$_3$) δ 163.7 (d, $^1J_{CF}$ = 249.6 Hz), 160.4, 156.9, 133.0 (d, $^4J_{CF}$ = 3.1 Hz), 131.3, 130.1 (d, $^3J_{CF}$ = 8.3 Hz), 129.4, 124.6, 115.5 (d, $^2J_{CF}$ = 21.6 Hz), 55.5.

**HRMS** (ESI) calculated $m/z$ 246.0930 for $C_{14}H_{13}FNO_2$ $[M+H]^+$, found 246.0934.

**IR** $\nu_{max}$ (neat): 3277, 3237, 3194, 3144, 3065, 3022, 3011, 2963, 2924, 1607, 1599, 1574, 1508, 1456, 1443, 1412 cm$^{-1}$.

Analytical data in agreement with the literature.[459]

## (4-methoxyphenyl)(phenyl)methanone oxime (3.105)
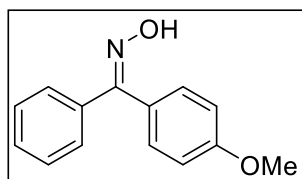
1. Synthesised in accordance with general procedure V using hydroxamoyl chloride **3.100** (38.9 mg, 0.25 mmol), (4-methoxyphenyl)boronic acid (76.0 mg, 0.50 mmol), DMA (158 μL, 1.25 mmol), and chloroform (2.5 mL) to afford (4-methoxyphenyl)(phenyl)methanone oxime (38.5 mg, 0.17 mmol, 68 % yield, 41:59 *E:Z* mixture) as a white solid.

2. Hydroxamoyl chloride **3.100** (1.50 g, 9.64 mmol) and (4-methoxyphenyl)boronic acid (2.93 g, 19.3 mmol) were added to a 250 mL round-bottom flask and dissolved in chloroform (96.0 mL). The vessel was purged with $N_2$ and DMA (6.10 mL, 48.2 mmol) was added to initiate the reaction. The mixture was heated at 60 °C for 6 hours, before being cooled to room temperature, diluted with DCM, and washed with 1M HCl solution and brine respectively. The resulting organic layers were passed through a phase separator, concentrated under vacuum and purified rapidly (~20 min from loading to elution) by column chromatography (0-100 % diethyl ether in *n*-hexane) to afford (4-methoxyphenyl)(phenyl)methanone oxime (1.59 g, 6.98 mmol 72 % yield, >1:99 *E:Z* mixture) as a purple solid.

**¹H NMR** (400 MHz, CDCl$_3$) δ 9.04 (br. s, 1H), 7.53 – 7.30 (m, 7H), 6.99 (d, $J$ = 8.8 Hz, 1.2H), 6.86 (d, $J$ = 8.9 Hz, 0.8H), 3.87 (s, 1.8H), 3.82 (s, 1.2H).

**¹³C NMR** (101 MHz, CDCl$_3$) δ 160.9, 160.3, 157.7, 157.7, 136.9, 133.1, 131.3, 129.5, 129.4, 129.3, 129.1, 128.9, 128.43, 128.35, 128.3, 124.8, 113.9, 113.7, 55.4.

**HRMS** (ESI) calculated *m/z* 228.1024 for $C_{14}H_{14}NO_2$ [M+H]$^+$, found 228.1029.

**IR** ν$_{max}$ (neat): 3173, 3100, 3084, 3075, 3049, 3011, 2957, 2930, 2930, 2899, 2893, 1605, 1574, 1514, 1452, 1433 cm$^{-1}$.

Analytical data in agreement with the literature.[459]

## (4-(*tert*-butyl)phenyl)(phenyl)methanone oxime (3.106)
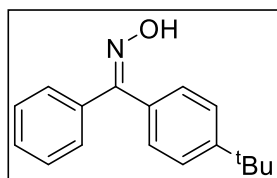
Synthesised in accordance with general procedure V using hydroxamoyl chloride **3.100** (38.9 mg, 0.25 mmol), (4-(*tert*-butyl)phenyl)boronic acid (89.0 mg, 0.50 mmol), DMA (158 μL, 1.25 mmol) and chloroform (2.50 mL) to afford (4-(*tert*-butyl)phenyl)(phenyl)methanone oxime (44.8 mg, 0.18 mmol, 71 % yield, , >1:99 *E:Z* mixture) as a white solid.

**¹H NMR** (500 MHz, CDCl$_3$) δ 9.19 (br. s, 1H), 7.51 – 7.47 (m, 4H), 7.41 (d, $J$ = 8.3 Hz, 2H), 7.37 (d, $J$ = 6.9 Hz, 1H), 7.35 – 7.32 (m, 2H), 1.38 (s, 9H).
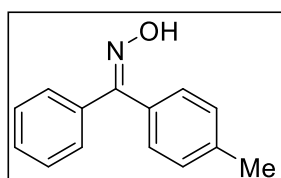
**13C NMR** (126 MHz, CDCl₃) δ 158.1, 152.3, 136.7, 129.7, 129.5, 129.3, 128.4, 128.2, 125.3, 34.9, 31.4.

**HRMS** (ESI) calculated *m/z* 254.1545 for C₁₇H₂₀NO [M+H]⁺, found 254.1549.

**IR** ν_max (neat): 3279, 3225, 3208, 3194, 3132, 3086, 3080, 3055, 2961, 2932, 2905, 2866, 1609, 1508, 1495, 1449, 1439 cm⁻¹.

## phenyl(*p*-tolyl)methanone oxime (3.107)



Synthesised in accordance with general procedure V using hydroxamoyl chloride **3.100** (38.9 mg, 0.25 mmol), *p*-tolylboronic acid (68.0 mg, 0.50 mmol), DMA (158 μL, 1.25 mmol) and chloroform (2.50 mL) to afford phenyl(*p*-tolyl)methanone oxime (20.1 mg, 0.10 mmol, 38 % yield, 9:91 *E*:*Z* mixture) as a white solid.

**1H NMR** (500 MHz, CDCl₃) δ 8.66 (br. s, 1H), 7.46 (d, *J* = 7.9 Hz, 2H), 7.38 – 7.24 (m, 7H), 2.41 (s, 2.7H), 2.35 (s, 0.3H).

**13C NMR** (126 MHz, CDCl₃) δ 158.2, 139.3, 136.6, 129.8, 129.6, 129.4, 129.1, 128.4, 128.1, 21.6.

**HRMS** (ESI) calculated *m/z* 212.1075 for C₁₄H₁₄NO [M+H]⁺, found 212.1075.

**IR** ν_max (neat): 3258, 3215, 3190, 3169, 3134, 3103, 3084, 3051, 3024, 2918, 1609, 1512, 1493, 1447, 1402 cm⁻¹.

Analytical data in agreement with the literature.[459]

## diphenylmethanone oxime (3.108)
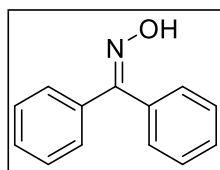


Synthesised in accordance with general procedure V using hydroxamoyl chloride **3.100** (38.9 mg, 0.25 mmol), phenylboronic acid (61.0 mg, 0.50 mmol), and DMA (158 μL, 1.25 mmol) to afford diphenylmethanone oxime (13.5 mg, 0.07 mmol, 23 % yield) as a white solid.

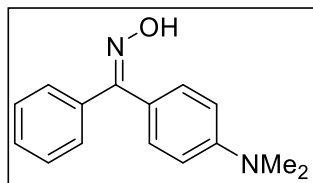**1H NMR** (400 MHz, CDCl₃) δ 8.78 (br. s, 1H), 7.53 – 7.40 (m, 7H), 7.40 – 7.30 (m, 3H).

**13C NMR** (126 MHz, CDCl₃) δ 158.2, 136.4, 132.8, 129.7, 129.4, 129.3, 128.5, 128.4, 128.0.

**HRMS** (ESI) calculated *m/z* 198.0919 for C₁₃H₁₂NO [M+H]⁺, found 198.0917.

**IR** ν_max (neat): 3211, 3188, 3177, 3132, 3057, 3026, 2953, 2922, 2887, 1491, 1445, 1429 cm⁻¹.

Analytical data in agreement with the literature.[459]

## (4-(dimethylamino)phenyl)(phenyl)methanone oxime (3.109)

Synthesised in accordance with general procedure V using hydroxamoyl chloride **3.100** (38.9 mg, 0.25 mmol), (4-(dimethylamino)phenyl)boronic acid (82.5 mg, 0.50 mmol), DMA (158 μL, 1.25 mmol) and chloroform (2.50 mL) to afford (4-(dimethylamino)phenyl)(phenyl)methanone oxime (23.1 mg, 0.10 mmol, 39 % yield, 38:62 *E*:*Z* mixture) as a white solid.

**¹H NMR** (500 MHz, CDCl₃) δ 8.17 (s, 0.6H), 7.94 (s, 0.4H), 7.55 – 7.28 (m, 7H), 6.75 (d, *J* = 8.0 Hz, 1.2H), 6.64 (d, *J* = 8.0 Hz, 0.8H), 3.02 (s, 3.6H), 2.98 (s, 2.4H).

**¹³C NMR** (101 MHz, CDCl₃) δ 158.5, 158.3, 151.4, 150.9, 137.5, 133.5, 131.3, 129.2, 128.9, 128.8, 128.6, 128.3, 123.9, 119.7, 111.8, 111.4, 40.4.

**HRMS** (ESI) calculated *m/z* 241.1341 for $C_{15}H_{17}N_2O$ [M+H]⁺, found 241.1341.

**IR** ν$_{max}$ (neat): 3211, 3186, 3167, 3156, 3140, 3130, 3113, 3073, 3024, 3003, 2992, 2893, 2812, 1607, 1526, 1485, 1445, 1425, 1412 cm⁻¹.

## (1-methyl-1*H*-indazol-5-yl)(phenyl)methanone oxime (3.110)
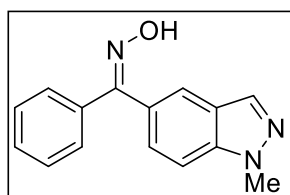
Synthesised in accordance with general procedure V using hydroxamoyl chloride **3.100** (38.9 mg, 0.25 mmol), (1-methyl-1*H*-indazol-5-yl)boronic acid (88.0 mg, 0.50 mmol), DMA (158 μL, 1.25 mmol) and chloroform (2.50 mL) to afford (1-methyl-1*H*-indazol-5-yl)(phenyl)methanone oxime (41.0 mg, 0.16 mmol, 65 % yield, >1:99 *E*:*Z* mixture) as a white solid.

**¹H NMR** (500 MHz, CDCl₃) δ 9.36 (br. s, 1H), 8.04 (s, 1H), 7.85 (s, 1H), 7.55 – 7.45 (m, 4H), 7.42 – 7.30 (m, 3H), 4.13 (s, 3H).

**¹³C NMR** (126 MHz, CDCl₃) δ 158.1, 139.9, 136.9, 133.6, 129.6, 128.5, 128.2, 127.9, 125.2, 123.8, 123.0, 108.8, 35.8.

**HRMS** (ESI) calculated *m/z* 250.0980 for $C_{15}H_{12}N_3O$ [M-H]⁻, found 250.0988.

**IR** ν$_{max}$ (neat): 3204, 3181, 3169, 3136, 3059, 3026, 2974, 2965, 2941, 2913, 2903, 2845, 1626, 1506, 1493, 1452, 1443 cm⁻¹.

## phenyl(thiophen-2-yl)methanone oxime (3.111)
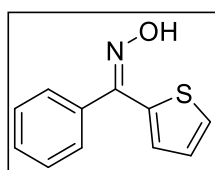
Synthesised in accordance with general procedure V using hydroxamoyl chloride **3.100** (38.9 mg, 0.25 mmol), thiophen-2-ylboronic acid (64.0 mg, 0.50 mmol), DMA (158 μL, 1.25 mmol) and chloroform (2.50 mL) to afford phenyl(thiophen-2-yl)methanone oxime

(11.8 mg, 0.06 mmol, 23 % yield, >1:99 *E:Z* mixture) as a white solid.

**¹H NMR** (500 MHz, CDCl₃) δ 9.76 (br. s, 1H), 7.61 (d, *J* = 5.1 Hz, 1H), 7.55 (d, *J* = 7.7 Hz, 2H), 7.48 – 7.41 (m, 3H), 7.24 (d, *J* = 3.8 Hz, 1H), 7.06 (app. t, *J* = 4.4 Hz, 1H).

**¹³C NMR** (126 MHz, CDCl₃) δ 152.0, 136.3, 133.0, 132.3, 131.3, 129.44, 129.42, 128.5, 125.8.

**HRMS** (ESI) calculated *m/z* 204.0483 for C₁₁H₁₀NOS [M+H]⁺, found 204.0479.

**IR** ν$_{max}$ (neat): 3086, 3057, 3026, 2980, 2953, 2924, 2816, 2772, 2756, 1607, 1591, 1576, 1497, 1437, 1414 cm⁻¹.

Analytical data in agreement with the literature.[460]

### furan-3-yl(phenyl)methanone oxime (3.112)
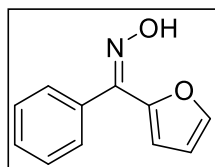


Synthesised in accordance with general procedure V using hydroxamoyl chloride **3.100** (38.9 mg, 0.25 mmol), furan-3-ylboronic acid (55.9 mg, 0.50 mmol), DMA (158 μL, 1.25 mmol) and chloroform (2.50 mL) to afford furan-3-yl(phenyl)methanone oxime (12.9 mg, 0.07 mmol, 28 % yield, >1:99 *E:Z* mixture) as a white solid.

**¹H NMR** (500 MHz, CDCl₃) δ 9.66 (br. s, 1H), 8.16 (s, 1H), 7.54 (d, *J* = 7.8 Hz, 2H), 7.48 – 7.39 (m, 4H), 6.60 (s, 1H).

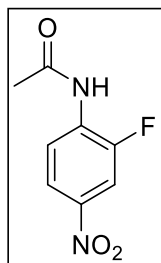**¹³C NMR** (126 MHz, CDCl₃) δ 150.9, 147.5, 142.1, 136.2, 129.4, 128.8, 128.5, 117.3, 111.8.

**HRMS** (ESI) calculated *m/z* 188.0712 for C₁₁H₁₀NO₂ [M+H]⁺, found 188.0708.

**IR** ν$_{max}$ (neat): 3265, 3179, 3165, 3156, 3129, 3105, 3075, 3057, 3030, 2918, 1562, 1508, 1491, 1445 cm⁻¹.

## 5.4.3 The Quantification of Nitrile Imine Reactivity Profiles

### 5.4.3.1 Starting Materials

#### *N*-(2-fluoro-4-nitrophenyl)acetamide (4.23)

In accordance with previous literature precedent,[461] acetyl chloride (7.80 mL, 110 mmol) was added dropwise to a solution of 2-fluoro-4-nitroaniline (15.6 g, 100 mmol) and pyridine (8.07 mL, 200 mmol) in DCM (100 mL) at 0 °C. The solution was left to warm to room temperature and stirred for a further hour. The resulting precipitate was collected *via* filtration and washed with methanol to afford *N*-(2-fluoro-4-nitrophenyl)acetamide (19.0 g, 95.9 mmol, 96 % yield) as an orange solid.

**¹H NMR** (500 MHz, DMSO-*d*6) δ 10.25 (s, 1H), 8.41 (app. t, $J$ = 8.5 Hz, 1H), 8.16 (dd, $^2J_{HF}$ = 11.0 Hz, $^3J_{HH}$ = 2.3 Hz, 1H), 8.09 (d, $J$ = 9.1 Hz, 1H), 2.19 (s, 3H).

**¹⁹F NMR** (376 MHz, DMSO-*d*6) δ -122.57 (s).

**¹³C NMR** (126 MHz, DMSO-*d*6) δ 169.7, 151.1 (d, $^1J_{CF}$ = 248.8 Hz), 142.2 (d, $^3J_{CF}$ = 8.3 Hz), 133.4 (d, $^2J_{CF}$ = 11.1 Hz), 121.6 (d, $^4J_{CF}$ = 1.9 Hz), 120.5 (d, $^3J_{CF}$ = 3.0 Hz), 111.4 (d, $^2J_{CF}$ = 24.7 Hz), 23.9.

**IR** $\nu_{max}$ (neat): 3262, 3217, 3154, 3130, 3119, 3088, 3030, 1684, 1618, 1605, 1553, 1491, 1418 cm⁻¹.

Analytical data in agreement with the literature.[462]

#### *N*-(4-amino-2-fluorophenyl)acetamide (4.24)
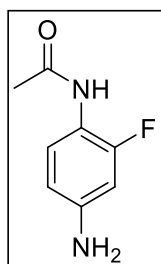
*N*-(2-fluoro-4-nitrophenyl)acetamide (**4.23**, 4.40 g, 22.2 mmol) and Pd(OH)₂/C (20 wt.%, 1.18 g, 10 mol%) were added to an 100 mL round-bottom flask. The flask was purged with nitrogen, and methanol (45.0 mL) was added. The mixture was then stirred under a hydrogen atmosphere at room temperature for 16 hours. Upon reaction completion, the solution was diluted with ethyl acetate and passed through celite. The resulting solution was concentrated under vacuum to afford *N*-(4-amino-2-fluorophenyl)acetamide (3.49 g, 20.8 mmol, 94 % yield) as a violet solid.

**¹H NMR** (500 MHz, DMSO-*d*6) δ 9.19 (s, 1H), 7.16 (app. t, $J$ = 8.8 Hz, 1H), 6.35 (dd, $^2J_{HF}$ = 13.0 Hz, $^3J_{HH}$ = 2.2 Hz, 1H), 6.31 (dd, $J$ = 8.5, 2.1 Hz, 1H), 5.23 (s, 2H), 1.97 (s, 3H).
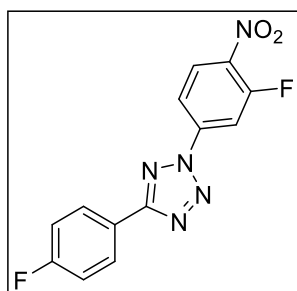
**¹⁹F NMR** (471 MHz, DMSO-*d*6) δ -123.50 - -123.77 (m).

**$^{13}$C NMR** (126 MHz, DMSO-*d*6) δ 168.2, 156.0 (d, $^{1}J_{CF}$ = 242.1 Hz), 147.7 (d, $^{3}J_{CF}$ = 10.8 Hz), 127.0 (d, $^{3}J_{CF}$ = 3.4 Hz), 113.7 (d, $^{2}J_{CF}$ = 12.9 Hz), 109.2 (d, $^{4}J_{CF}$ = 2.2 Hz), 100.3 (d, $^{2}J_{CF}$ = 22.8 Hz), 22.9 (s).

**IR** $\nu_{max}$ (neat): 3431, 3304, 3252, 3038, 1661, 1638, 1626, 1593, 1514, 1445 cm$^{-1}$.

Analytical data in agreement with the literature.[462]

### 2-(3-fluoro-4-nitrophenyl)-5-(4-fluorophenyl)-2*H*-tetrazole (4.26)



Synthesised in accordance with general procedure I using 4-fluorobenzaldehyde (52.7 mL, 25.5 mmol), benzenesulfonohydrazide (4.82 g, 28.0 mmol), 2-fluoro-4-nitroaniline (4.37 g, 28.0 mmol) and sodium nitrite (1.79 g, 28.0 mmol) to afford 2-(3-fluoro-4-nitrophenyl)-5-(4-fluorophenyl)-2*H*-tetrazole (2.34 g, 7.72 mmol, 30 % yield) as a grey solid.

**$^{1}$H NMR** (500 MHz, CDCl$_3$) δ 7.40 (app. t, *J* = 8.4 Hz, 1H), 7.33 (dd, $^{2}J_{HH}$ = 8.6 Hz, $^{3}J_{HF}$ = 5.4 Hz, 2H), 7.28 (app. d, *J* = 2.4 Hz, 1H), 7.26 (app. s, 1H), 6.34 - 6.28 (m, 2H).

**$^{19}$F NMR** (471 MHz, CDCl$_3$) δ -107.93 - -108.09 (m), -111.94 - -112.09 (m).

**$^{13}$C NMR** (101 MHz, CDCl$_3$) δ 165.5, 164.8 (d, $^{1}J_{CF}$ = 252.3 Hz), 156.4 (d, $^{1}J_{CF}$ = 267.8 Hz), 140.9 (d, $^{2}J_{CF}$ = 10.2 Hz), 137.4 (d, $^{3}J_{CF}$ = 7.2 Hz), 129.6 (d, $^{3}J_{CF}$ = 9.0 Hz), 128.2, 122.5 (d, $^{4}J_{CF}$ = 3.5 Hz), 116.6 (d, $^{2}J_{CF}$ = 22.0 Hz), 115.3 (d, $^{3}J_{CF}$ = 4.4 Hz), 110.1 (d, $^{2}J_{CF}$ = 26.9 Hz).

**HRMS** (ESI) calculated *m/z* 304.0641 for C$_{13}$H$_8$F$_2$N$_5$O$_2$ [M+H]$^+$, found 304.0637.

### 2-fluoro-4-(5-(4-fluorophenyl)-2*H*-tetrazol-2-yl)aniline (4.27)
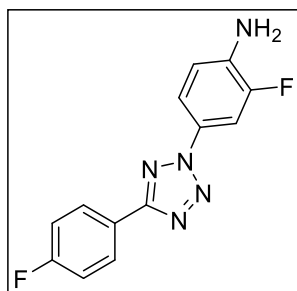


Aryl nitro compound **4.26** (1.17 g, 3.90 mmol) and Pd/C (5 wt.%, 822 mg, 10 mol%) were added to a 100 mL round-bottom flask. The flask was purged with nitrogen, and methanol (10.0 mL) was added. The mixture was then stirred under a hydrogen atmosphere at room temperature for 16 hours. Upon reaction completion, the solution was diluted with ethyl acetate and passed through celite. The resulting solution was concentrated under vacuum to afford 2-fluoro-4-(5-(4-fluorophenyl)-2*H*-tetrazol-2-yl)aniline (853 mg, 3.12 mmol, 81 % yield) as a yellow solid.

**$^{1}$H NMR** (500 MHz, DMSO-*d*6) δ 8.18 (dd, $^{2}J_{HH}$ = 8.9 Hz, $^{3}J_{HF}$ = 5.4 Hz, 2H), 7.78 (dd, $^{2}J_{HF}$ = 11.7 Hz, $^{3}J_{HH}$ = 2.4 Hz, 1H), 7.73 - 7.65 (m, 1H), 7.44 (app. t, *J* = 8.9 Hz, 2H), 6.97 (app. t, *J* = 9.0 Hz, 1H), 5.84 (s, 2H).

**$^{19}$F NMR** (471 MHz, DMSO-*d*6) δ -109.56 - -110.14 (m), -132.89 (t, *J* = 10.6 Hz).

<superscript>13</superscript>**C NMR** (126 MHz, DMSO-*d*6) δ 163.5 (d, $^1J_{CF}$ = 248.3 Hz), 163.2, 149.4 (d, $^1J_{CF}$ = 239.5 Hz), 138.7 (d, $^2J_{CF}$ = 12.8 Hz), 128.9 (d, $^3J_{CF}$ = 8.7 Hz), 124.5 (d, $^3J_{CF}$ = 9.1 Hz), 123.2 (d, $^4J_{CF}$ = 3.3 Hz), 116.9 (d, $^4J_{CF}$ = 2.6 Hz), 116.4 (d, $^2J_{CF}$ = 22.2 Hz), 115.8 (d, $^3J_{CF}$ = 5.6 Hz), 107.9 (d, $^2J_{CF}$ = 23.8 Hz).

**HRMS** (ESI) calculated *m/z* 274.0899 for $C_{13}H_9F_2N_5$ [M+H]$^+$, found 274.0900.

### *N*-(2-fluoro-4-(5-(4-fluorophenyl)-2*H*-tetrazol-2-yl)phenyl)acetamide (4.10)
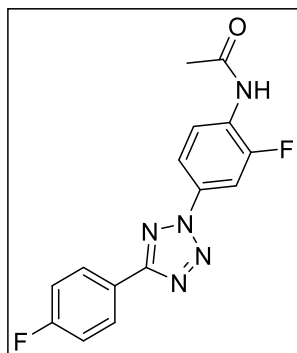


1. Synthesised in accordance with general procedure I using 4-fluorobenzaldehyde (**4.21**, 0.53 mL, 5.00 mmol), benzenesulfonohydrazide (878 mg, 5.10 mmol), *N*-(4-amino-2-fluorophenyl)acetamide (**4.23**, 1.05 g, 6.30 mmol) and sodium nitrite (402 mg, 6.30 mmol) to afford *N*-(2-fluoro-4-(5-(4-fluorophenyl)-2*H*-tetrazol-2-yl)phenyl)acetamide (1.03 g, 3.27 mmol, 62 % yield) as a yellow solid.

2. Aniline **4.27** (1.71 g, 6.25 mmol) and pyridine (1.00 mL, 12.5 mmol) were dissolved in DCM (12.5 mL). The solution was cooled to 0 °C, and acetyl chloride (500 µL, 6.87 mmol) was added dropwise under stirring. Following complete addition, the mixture was allowed to warm to room temperature and stirred for 1 hour. The reaction mixture was then filtered, and the filtrand washed with methanol to afford *N*-(2-fluoro-4-(5-(4-fluorophenyl)-2*H*-tetrazol-2-yl)phenyl)acetamide (1.77 g, 5.63 mmol, 90 % yield) as a white solid.

**¹H NMR** (500 MHz, DMSO-*d*6) δ 9.80 (s, 1H), 8.27 (app. t, *J* = 8.5 Hz, 1H), 8.21 (dd, $^2J_{HH}$ = 8.2 Hz, $^3J_{HF}$ = 5.6 Hz, 2H), 8.00 (dd, $^2J_{HF}$ = 11.1, $^3J_{HH}$ = 1.7 Hz, 1H), 7.94 (d, *J* = 8.9 Hz, 1H), 7.42 (app. t, *J* = 8.7 Hz, 2H), 2.16 (s, 3H).

**¹⁹F NMR** (471 MHz, DMSO-*d*6) δ -109.53 (s), -121.43 (s).

**¹³C NMR** (126 MHz, DMSO-*d*6) δ 168.6, 163.5, 163.3 (d, $^1J_{CF}$ = 248.9 Hz), 152.7 (d, $^1J_{CF}$ = 247.7 Hz), 131.6 (d, $^3J_{CF}$ = 9.8 Hz), 128.8 (d, $^3J_{CF}$ = 8.8 Hz), 128.0 (d, $^2J_{CF}$ = 11.4 Hz), 124.1 (d, $^4J_{CF}$ = 2.3 Hz), 122.7 (d, $^3J_{CF}$ = 3.1 Hz), 115.9 (d, $^2J_{CF}$ = 22.3 Hz), 115.7 (d, $^4J_{CF}$ = 3.4 Hz), 107.6 (d, $^2J_{CF}$ = 25.6 Hz), 23.1.

**HRMS** (ESI) calculated *m/z* 316.1004 for $C_{15}H_{12}F_2N_5O$ [M+H]$^+$, found 316.1009.

**IR** $\nu_{max}$ (neat): 3256, 3204, 3040, 2924, 1668, 1609, 1535, 1508, 1445 cm$^{-1}$.

## *N*-(2-fluoro-4-(3-(4-fluorophenyl)-4,6-dioxo-4,5,6,6a-tetrahydropyrrolo[3,4-*c*]pyrazol-1(3*H*)-yl)phenyl)acetamide (4.11)
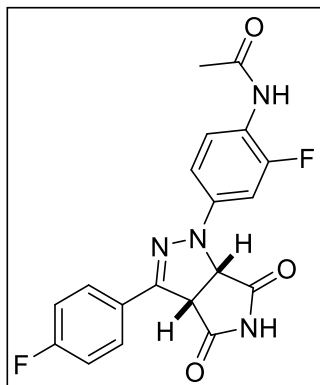
Synthesised in accordance with general procedure W using tetrazole **4.10** (78.8 mg, 0.25 mmol), maleimide (243 mg, 2.50 mmol), acetonitrile (4.50 mL) and water (500 μL) to afford *N*-(2-fluoro-4-(3-(4-fluorophenyl)-4,6-dioxo-4,5,6,6a-tetrahydropyrrolo[3,4-*c*]pyrazol-1(3*H*)-yl)phenyl)acetamide (65.4 mg, 0.17 mmol, 68 % yield) as a white solid. Owing to the insolubility of this compound, it was collected by filtration without requiring column chromatography.

**¹H NMR** (500 MHz, DMSO-*d*6) δ 11.92 (s, 1H), 9.55 (s, 1H), 8.03 (dd, $^2J_{HH}$ = 8.6 Hz, $^3J_{HF}$ = 5.6 Hz, 2H), 7.63 (app. t, *J* = 8.8 Hz, 1H), 7.32 (app. t, *J* = 8.8 Hz, 2H), 7.28 (dd, $^2J_{HF}$ = 13.1 Hz, $^3J_{HH}$ = 2.2 Hz, 1H), 7.21 (dd, $^2J_{HH}$ = 8.9 Hz, $^4J_{HF}$ = 1.7 Hz, 1H), 5.32 (d, *J* = 10.7 Hz, 1H), 5.17 (d, *J* = 10.6 Hz, 1H), 2.04 (s, 3H).

**¹⁹F NMR** (471 MHz, DMSO-*d*6) δ -111.29 (s), -122.08 - -122.90 (m).

**¹³C NMR** (126 MHz, DMSO-*d*6) δ 174.9, 173.8, 168.4, 162.7 (d, $^1J_{CF}$ = 247.7 Hz), 154.8 (d, $^1J_{CF}$ = 243.5 Hz), 143.9, 142.3 (d, $^3J_{CF}$ = 10.4 Hz), 129.4 (d, $^3J_{CF}$ = 8.4 Hz), 127.0 (d, $^4J_{CF}$ = 2.7 Hz), 126.0 (d, $^3J_{CF}$ = 2.6 Hz), 118.6 (d, $^2J_{CF}$ = 12.6 Hz), 115.5 (d, $^2J_{CF}$ = 21.9 Hz), 109.2 (d, $^4J_{CF}$ = 1.6 Hz), 101.2 (d, $^2J_{CF}$ = 25.7 Hz), 66.7, 55.1, 23.1.

**HRMS** (ESI) calculated *m/z* 385.1107 for $C_{19}H_{15}F_2N_4O_3$ [M+H]⁺, found 385.1108.

**IR** ν$_{max}$ (neat): 3248, 3051, 3038, 2972, 2934, 2754, 1775, 1721, 1616, 1601, 1508, 1449 cm⁻¹.

## *N*-(4-(5-acetyl-3-(4-fluorophenyl)-1*H*-pyrazol-1-yl)-2-fluorophenyl)acetamide (4.12)
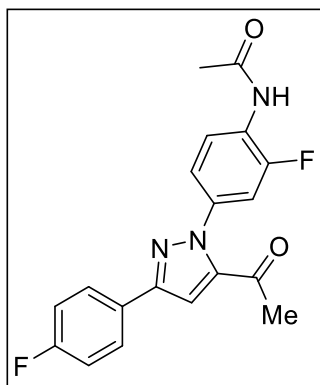
Synthesised in accordance with general procedure W using tetrazole **4.10** (78.8 mg, 0.25 mmol), 3-butyn-2-one (195 μL, 2.50 mmol), acetonitrile (4.50 mL) and water (500 μL) to afford *N*-(4-(5-acetyl-3-(4-fluorophenyl)-1*H*-pyrazol-1-yl)-2-fluorophenyl)acetamide (82.1 mg, 0.23 mmol, 92 % yield) as a white solid. Owing to the insolubility of this compound, it was collected by filtration without requiring column chromatography.

**¹H NMR** (500 MHz, DMSO-*d6*) δ 9.89 (s, 1H), 8.00 (app. t, *J* = 8.8 Hz, 1H), 7.96 (dd, $^2J_{HH}$ = 8.6 Hz, $^3J_{HF}$ = 5.6 Hz, 2H), 7.86 (s, 1H), 7.48 (dd, $^2J_{HF}$ = 11.5 Hz, $^3J_{HH}$ = 2.1 Hz, 1H), 7.34 - 7.27 (m, 3H), 2.58 (s, 3H), 2.13 (s, 3H).

**¹⁹F NMR** (471 MHz, DMSO-*d6*) δ -113.21 - -113.41 (m), -124.01 (t, *J* = 9.6 Hz).

**¹³C NMR** (101 MHz, DMSO) δ 188.1, 168.8, 162.2 (d, $^1J_{CF}$ = 245.5 Hz), 152.4 (d, $^1J_{CF}$ = 245.5 Hz), 149.7, 141.1, 136.4 (d, $^3J_{CF}$ = 9.9 Hz), 128.3 (d, $^3J_{CF}$ = 2.5 Hz), 127.5 (d, $^3J_{CF}$ = 8.4 Hz), 126.3 (d, $^2J_{CF}$ = 11.7 Hz), 123.2, 121.6 (d, $^4J_{CF}$ = 2.4 Hz), 115.8 (d, $^2J_{CF}$ = 21.6 Hz), 113.4 (d, $^2J_{CF}$ = 23.1 Hz), 110.7, 28.7, 23.5.

**HRMS** (ESI) calculated *m/z* 356.1205 for $C_{19}H_{16}F_2N_3O_2$ [M+H]⁺, found 356.1208.

**IR** $\nu_{max}$ (neat): 3235, 3188, 3127, 3036, 2955, 2922, 2853, 1680, 1661, 1609, 1537, 1508, 1435, 1420 cm⁻¹.

### *N*-(2-fluoro-4-(2-((4-fluorophenyl)(phenethylamino)methylene)hydrazinyl)phenyl)acetamide (4.13)
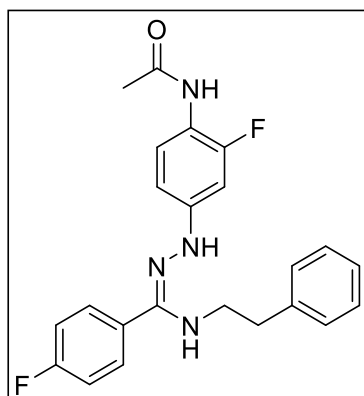


Synthesised in accordance with general procedure W using tetrazole **4.10** (78.8 mg, 0.25 mmol), phenethylamine (314 μL, 2.50 mmol), acetonitrile (4.50 mL) and water (500 μL) to afford *N*-(2-fluoro-4-(2-((4-fluorophenyl)(phenethylamino)methylene)hydrazinyl)phenyl)acetamide (65.3 mg, 0.16 mmol, 64 % yield, 86:14 *E:Z* mixture) as a brown oil.

**¹H NMR** (500 MHz, DMSO-*d6*) δ 9.35 (s, 0.9H), 9.26 (s, 0.1H), 8.75 (s, 0.1H), 8.57 (s, 0.9H), 7.47 – 7.15 (m, 8.3H), 7.07 (d, *J* = 7.1 Hz, 1.7H), 6.74 (dd, $^2J_{HF}$ = 13.1, $^3J_{HH}$ = 2.0 Hz, 0.9H), 6.69 – 6.63 (m, 1H), 6.53 (d, *J* = 8.8 Hz, 0.1H), 3.47 (s, 0.3H), 3.27 – 3.20 (m, 1.7H), 2.96 (t, *J* = 7.4 Hz, 0.3H), 2.71 (t, *J* = 7.3 Hz, 1.7H), 2.01 (s, 2.5H), 1.98 (s, 0.5H).

**¹⁹F NMR** (471 MHz, DMSO-*d6*) δ -112.94 (s), -123.05 (s).

**¹³C NMR** (126 MHz, DMSO-*d6*) δ 168.2, 162.4 (d, $^1J_{CF}$ = 244.6 Hz), 155.6 (d, $^1J_{CF}$ = 242.6 Hz), 145.8 (d, $^3J_{CF}$ = 9.6 Hz), 138.8, 130.6 (d, $^3J_{CF}$ = 8.7 Hz), 130.2 (d, $^3J_{CF}$ = 8.3 Hz), 128.7, 128.3, 126.4, 126.2, 126.0, 115.4 (d, $^2J_{CF}$ = 21.4 Hz), 115.1 (d, $^2J_{CF}$ = 21.7 Hz), 107.8, 99.0 (d, $^2J_{CF}$ = 23.8 Hz), 45.9, 36.9, 23.1.

**HRMS** (ESI) calculated *m/z* 381.1521 for $C_{23}H_{23}F_2N_4O$ [M+H]⁺, found 381.1521.

## phenethyl-*N*-(4-acetamido-3-fluorophenyl)-4-fluorobenzohydrazonothioate (4.14)
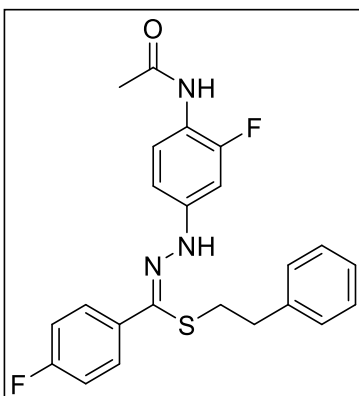
Synthesised in accordance with general procedure W using tetrazole **4.10** (78.8 mg, 0.25 mmol), phenethylmercaptan (335 μL, 2.50 mmol), acetonitrile (4.50 mL) and water (500 μL) to afford phenethyl-*N*-(4-acetamido-3-fluorophenyl)-4-fluorobenzohydrazonothioate (45.6 mg, 0.11 mmol, 40 % yield, >1:99 *E:Z* mixture) as a brown solid.

**¹H NMR** (500 MHz, CDCl₃) δ 8.61 (s, 1H), 8.13 (app. t, $J$ = 8.7 Hz, 1H), 7.87 (dd, $^2J_{HH}$ = 8.6 Hz, $^3J_{HF}$ = 5.5 Hz, 2H), 7.32 - 7.26 (m, 4H), 7.15 (app. t, $J$ = 8.6 Hz, 2H), 7.09 (d, $J$ = 6.9 Hz, 2H), 7.03 (dd, $^2J_{HF}$ = 12.8 Hz, $^3J_{HH}$ = 2.1 Hz, 1H), 6.76 (d, $J$ = 8.7 Hz, 1H), 3.02 (t, $J$ = 7.3 Hz, 2H), 2.83 (t, $J$ = 7.3 Hz, 2H), 2.25 (s, 3H).

**¹⁹F NMR** (471 MHz, CDCl₃) δ -112.80 - -112.91 (m), -128.53 - -128.64 (m).

**¹³C NMR** (126 MHz, CDCl₃) δ 168.2, 163.2 (d, $^1J_{CF}$ = 248.9 Hz), 154.0 (d, $^1J_{CF}$ = 242.0 Hz), 141.4 (d, $^3J_{CF}$ = 10.4 Hz), 139.2, 135.4, 132.8 (d, $^3J_{CF}$ = 2.9 Hz), 129.2 (d, $^3J_{CF}$ = 8.1 Hz), 128.69, 128.68, 126.9, 123.5, 119.1 (d, $^2J_{CF}$ = 11.1 Hz), 115.6 (d, $^2J_{CF}$ = 21.8 Hz), 108.9 (d, $^4J_{CF}$ = 2.6 Hz), 100.5 (d, $^2J_{CF}$ = 24.8 Hz), 36.5, 34.4, 24.5.

**HRMS** (ESI) calculated *m/z* 426.1446 for $C_{23}H_{22}F_2N_3OS$ [M+H]⁺, found 426.1446.

**IR** $\nu_{max}$ (neat): 3258, 3026, 2926, 1665, 1626, 1599, 1518, 1499, 1454, 1429, 1404 cm⁻¹.

## *N*-(4-(1-acetyl-2-(4-fluorobenzoyl)hydrazineyl)-2-fluorophenyl)acetamide (4.15)
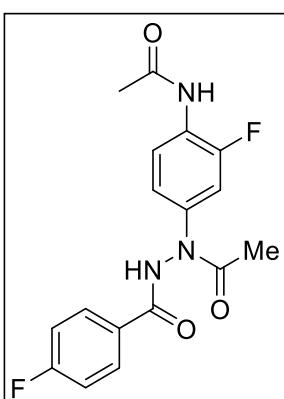
Synthesised in accordance with general procedure W using tetrazole **4.10** (78.8 mg, 0.25 mmol), acetic acid (142 μL, 2.50 mmol), acetonitrile (4.50 mL) and water (500 μL) to afford *N*-(4-(1-acetyl-2-(4-fluorobenzoyl)hydrazineyl)-2-fluorophenyl)acetamide (54.4 mg, 0.16 mmol, 63 % yield) as an orange solid.

**¹H NMR** (500 MHz, DMSO-*d*6, 80 °C) δ 11.28 (s, 1H), 9.48 (s, 1H), 8.09 - 7.91 (m, 2H), 7.82 (app. t, $J$ = 8.4 Hz, 1H), 7.39 (d, $^2J_{HF}$ = 12.5 Hz, 1H), 7.34 (app. t, $J$ = 8.7 Hz, 2H), 7.25 (d, $J$ = 8.7 Hz, 1H), 2.13 (s, 3H), 2.08 (s, 3H).

**¹⁹F NMR** (471 MHz, DMSO-*d*6, 80 °C) δ -107.47 (s), -123.15 (s).

$^{13}$**C NMR** (126 MHz, DMSO-$d6$, 80 °C) δ 168.2, 164.3, 164.2 (d, $^1J_{CF}$ = 250.6 Hz), 152.8 (d, $^1J_{CF}$ = 245.2 Hz), 138.1 (s), 129.95 (d, $^3J_{CF}$ = 9.2 Hz), 128.0, 123.8, 119.1, 115.2 (d, $^2J_{CF}$ = 22.0 Hz), 111.2, 22.8, 21.2, two C not observed.

**HRMS** (ESI) calculated $m/z$ 348.1154 for $C_{17}H_{16}F_2N_3O_3$ [M+H]$^+$, found 348.1157.

**IR** $\nu_{max}$ (neat): 3258, 3196, 3144, 3009, 2994, 1663, 1622, 1603, 1524, 1499, 1427 cm$^{-1}$.

### *N*-(2-fluoro-4-(2-((4-fluorophenyl)(phenylamino)methylene)hydrazineyl)phenyl)acetamide (4.16)
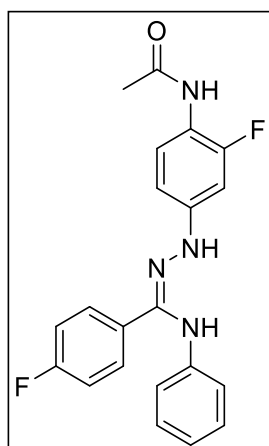


Synthesised in accordance with general procedure W using tetrazole **4.10** (78.8 mg, 0.25 mmol), aniline (228 μL, 2.50 mmol), acetonitrile (4.50 mL) and water (500 μL) to afford *N*-(2-fluoro-4-(2-((4-fluorophenyl)(phenylamino)methylene)hydrazineyl)phenyl)acetamide (78.3 mg, 0.21 mmol, 82 % yield, >1:99 *E*:*Z* mixture) as a yellow solid.

$^1$**H NMR** (500 MHz, CDCl₃) δ 7.95 (app. t, $J$ = 8.7 Hz, 1H), 7.67 (dd, $^2J_{HH}$ = 7.9 Hz, $^3J_{HF}$ = 5.6 Hz, 2H), 7.49 (s, 1H), 7.23 (app. t, $J$ = 7.6 Hz, 2H), 7.13 (s, 1H), 7.06 - 6.99 (m, 3H), 6.92 (t, $J$ = 7.3 Hz, 1H), 6.72 - 6.62 (m, 3H), 5.74 (s, 1H), 2.17 (s, 3H).

$^{19}$**F NMR** (471 MHz, CDCl₃) δ -112.02 (s), -128.50 (s).

$^{13}$**C NMR** (126 MHz, CDCl₃) δ 168.3, 163.5 (d, $^1J_{CF}$ = 249.3 Hz), 154.3 (d, $^1J_{CF}$ = 242.2 Hz), 142.9 (d, $^3J_{CF}$ = 10.4 Hz), 141.2, 137.7, 130.8, 129.7, 128.7 (d, $^3J_{CF}$ = 8.3 Hz), 123.8, 121.4, 118.3, 116.5, 115.7 (d, $^2J_{CF}$ = 21.8 Hz), 108.9, 100.5 (d, $^2J_{CF}$ = 24.7 Hz), 24.5 (s).

**HRMS** (ESI) calculated $m/z$ 381.1521 for $C_{21}H_{19}F_2N_4O$ [M+H]$^+$, found 381.1521.

**IR** $\nu_{max}$ (neat): 3250, 3231, 3217, 3184, 3100, 3051, 3022, 2959, 2924, 1661, 1626, 1599, 1520, 1499, 1433 cm$^{-1}$.

### phenyl-*N*-(4-acetamido-3-fluorophenyl)-4-fluorobenzohydrazonothioate (4.17)
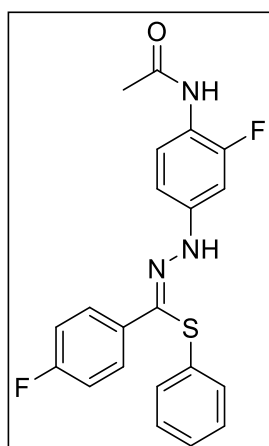


Synthesised in accordance with general procedure W using tetrazole **4.10** (74.0 mg, 0.23 mmol), thiophenol (255 μL, 2.30 mmol), acetonitrile (4.50 mL) and water (500 μL) to afford phenyl-*N*-(4-acetamido-3-fluorophenyl)-4-fluorobenzohydrazonothioate (73.7 mg, 0.19 mmol, 79 % yield, >1:99 *E*:*Z* mixture) as a yellow solid.

**¹H NMR** (500 MHz, CDCl₃) δ 8.82 (s, 1H), 8.07 (app. t, $J$ = 8.5 Hz, 1H), 7.97 - 7.90 (m, 2H), 7.25 - 7.14 (m, 6H), 7.04 (app. t, $J$ = 12.3 Hz, 3H), 6.75 (d, $J$ = 8.4 Hz, 1H), 2.19 (s, 3H).

**¹⁹F NMR** (471 MHz, CDCl₃) δ -112.92 (s), -128.37 (s).

**¹³C NMR** (126 MHz, CDCl₃) δ 168.2, 163.2 (d, $^1J_{CF}$ = 248.9 Hz), 153.9 (d, $^1J_{CF}$ = 242.4 Hz), 140.9 (d, $^3J_{CF}$ = 10.4 Hz), 133.4 (d, $^3J_{CF}$ = 3.0 Hz), 131.8, 131.5, 129.7, 128.9 (d, $^3J_{CF}$ = 8.2 Hz), 128.3, 127.0, 123.6, 119.5 (d, $^2J_{CF}$ = 11.1 Hz), 115.6 (d, $^2J_{CF}$ = 21.9 Hz), 109.2 (d, $^4J_{CF}$ = 2.6 Hz), 100.8 (d, $^2J_{CF}$ = 24.9 Hz), 24.5.

**HRMS** (ESI) calculated $m/z$ 398.1133 for $C_{21}H_{18}F_2N_3OS$ [M+H]⁺, found 398.1132.

**IR** $\nu_{max}$ (neat): 3335, 3252, 2922, 1684, 1667, 1636, 1601, 1582, 1535, 1518, 1499, 1481, 1429, 1404 cm⁻¹.

### *N*-(2-fluoro-4-(2-(4-fluorobenzoyl)-1-(2,2,2-trifluoroacetyl)hydrazineyl)phenyl)acetamide (4.18)
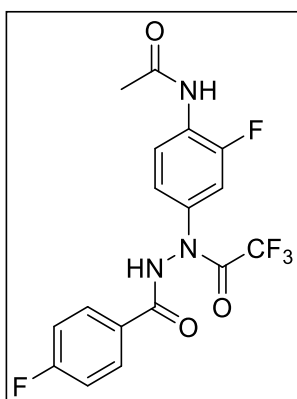


Synthesised in accordance with general procedure W using tetrazole **4.10** (78.8 mg, 0.25 mmol), TFA (191 μL, 2.50 mmol), acetonitrile (4.50 mL) and water (500 μL) to afford *N*-(2-fluoro-4-(2-(4-fluorobenzoyl)-1-(2,2,2-trifluoroacetyl)hydrazineyl)phenyl)acetamide (64.6 mg, 0.16 mmol, 65 % yield) as an orange solid.

**¹H NMR** (500 MHz, DMSO-*d*6) δ 12.00 (s, 1H), 9.86 (s, 1H), 8.02 - 7.92 (m, 3H), 7.53 - 7.32 (m, 4H), 2.09 (s, 3H).

**¹⁹F NMR** (376 MHz, DMSO-*d*6) δ -70.05 (s), -106.27 (s), -122.26 - -122.53 (m).

**¹³C NMR** (101 MHz, DMSO-*d*6) δ 168.85, 165.4, 164.8 (d, $^1J_{CF}$ = 251.0 Hz), 156.5 (q, $^2J_{CF}$ = 35.5 Hz), 152.7 (d, $^1J_{CF}$ = 246.2 Hz), 135.7 (d, $^3J_{CF}$ = 8.9 Hz), 130.6 (d, $^3J_{CF}$ = 9.4 Hz), 127.3 (d, $^3J_{CF}$ = 2.5 Hz), 126.0 (d, $^2J_{CF}$ = 11.8 Hz), 124.1, 119.8 (d, $^4J_{CF}$ = 2.7 Hz), 116.0 (d, $^2J_{CF}$ = 22.2 Hz), 115.9 (q, $^1J_{CF}$ = 288.7 Hz), 111.7 (d, $^2J_{CF}$ = 23.6 Hz), 23.4.

**HRMS** (ESI) calculated $m/z$ 419.1137 for $C_{17}H_{16}F_5N_4O_3$ [M+NH₄]⁺, found 419.1355.

**IR** $\nu_{max}$ (neat): 3291, 3281, 3192, 3179, 3169, 3156, 2984, 2978, 1724, 1692, 1667, 1605, 1526, 1504, 1435, 1408 cm⁻¹.

### *N*-(2-fluoro-4-(2-((4-fluorophenyl)(4-methoxyphenyl)methylene)hydrazinyl)phenyl)acetamide (4.19)
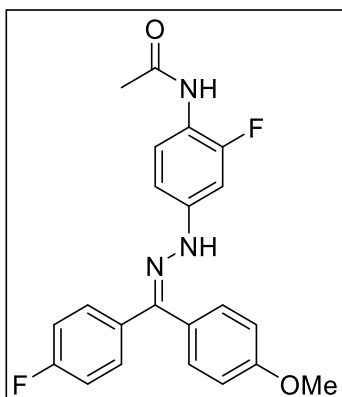


Synthesised in accordance with general procedure L using tetrazole **4.10** (78.8 mg, 0.25 mmol), 4-methoxyphenylboronic acid (114 mg, 0.75 mmol), and THF (2.50 mL) to afford *N*-(2-fluoro-4-(2-((4-fluorophenyl)(4-methoxyphenyl)methylene)hydrazinyl)phenyl)acetamide (33.2 mg, 0.08 mmol, 34 % yield, 64:36 *E*:*Z* mixture) as a yellow oil.

**$^1$H NMR** (500 MHz, CDCl$_3$) δ 7.97 (t, *J* = 8.6 Hz, 1H), 7.56 – 7.43 (m, 3H), 7.34 – 7.18 (m, 3H), 7.11 – 6.96 (m, 4H), 6.85 (d, *J* = 8.6 Hz, 1H), 6.59 (d, *J* = 8.6 Hz, 1H), 3.89 (s, 1.9H), 3.81 (s, 1.1H), 2.17 (s, 3H).

**$^{19}$F NMR** (471 MHz, CDCl$_3$) δ -110.74 – -111.09 (m), -113.38 – -113.77 (m), -128.38 – -128.82 (m).

**$^{13}$C NMR** (126 MHz, CDCl$_3$) δ 168.3, 163.2 (d, $^1J_{CF}$ = 249.9 Hz), 163.1 (d, $^1J_{CF}$ = 248.3 Hz), 160.4, 160.2, 154.2 (d, $^1J_{CF}$ = 241.9 Hz), 144.3, 142.4 (d, $^3J_{CF}$ = 10.7 Hz), 135.9, 134.8, 132.5, 131.2 (d, $^3J_{CF}$ = 8.1 Hz), 131.0, 130.9, 130.5, 129.0, 128.7 (d, $^4J_{CF}$ = 3.2 Hz), 128.5 (d, $^3J_{CF}$ = 8.0 Hz), 128.0, 125.7, 124.2, 123.6, 118.3 (d, $^2J_{CF}$ = 11.0 Hz), 117.1 (d, $^2J_{CF}$ = 21.6 Hz), 115.3, 115.2, 113.9, 113.8, 108.5 (d, $^4J_{CF}$ = 2.4 Hz), 100.0 (d, $^2J_{CF}$ = 24.9 Hz), 55.52, 55.47, 24.5.

**HRMS** (ESI) calculated *m/z* 396.1518 for C$_{22}$H$_{19}$F$_2$N$_3$O$_2$ [M+H]$^+$, found 396.1520.

## 5.5 Competition Experiment Data

The following tables detail the individual conversion values recorded during the competition experiments outlined in *Section 4.3.2*. All experiments were performed in triplicate in accordance with general procedure X. In some instances, reactions were repeated a fourth time to minimise the experimental error. Graphic interpretation of the data was acquired using Prism 5 software.[463]

*Table 5.39:* **4.1** *vs* **4.2**
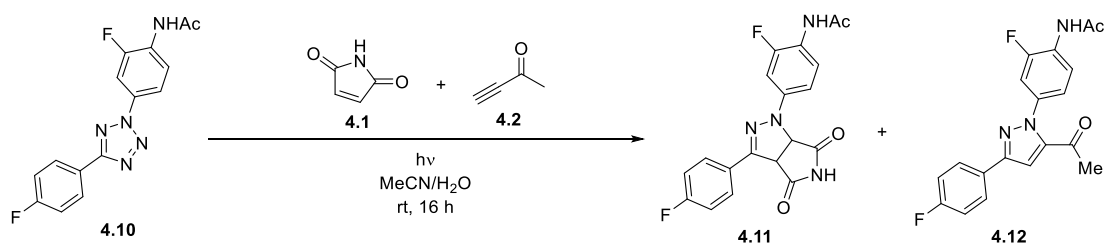


| Entry | Conversion (%)[a] | |
| --- | --- | --- |
| | **4.11** | **4.12** |
| 1 | 77 | 4 |
| 2 | 68 | 5 |
| 3 | 74 | 5 |
| **Average** | **73.0 ± 2.6** | **4.7 ± 0.3** |

[a]Conversion determined by ^{19}F NMR with reference to 1,4-difluorobenzene an internal standard

*Table 5.40:* **4.1** *vs* **4.3**
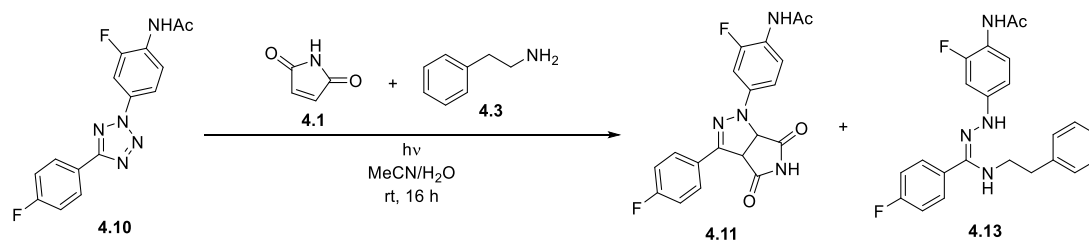


| Entry | Conversion (%)[a] | |
| --- | --- | --- |
| | **4.11** | **4.13** |
| 1 | 23 | 2 |
| 2 | 33 | 15 |
| 3 | 38 | 6 |
| **Average** | **31.3 ± 4.4** | **7.7 ± 3.8** |

[a]Conversion determined by ^{19}F NMR with reference to 1,4-difluorobenzene an internal standard

*Table 5.41: **4.1** vs **4.4***
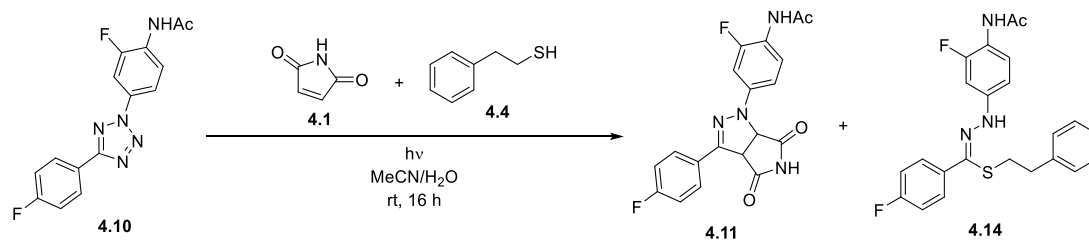


| Entry | Conversion (%)[a] | |
| :---: | :---: | :---: |
| | **4.11** | **4.14** |
| 1 | 11 | 1 |
| 2 | 12 | 1 |
| 3 | 15 | 1 |
| **Average** | **12.7 ± 1.2** | **1.0 ± 0.0** |

[a]Conversion determined by ^{19}F NMR with reference to 1,4-difluorobenzene an internal standard

*Table 5.42: **4.1** vs **4.5***
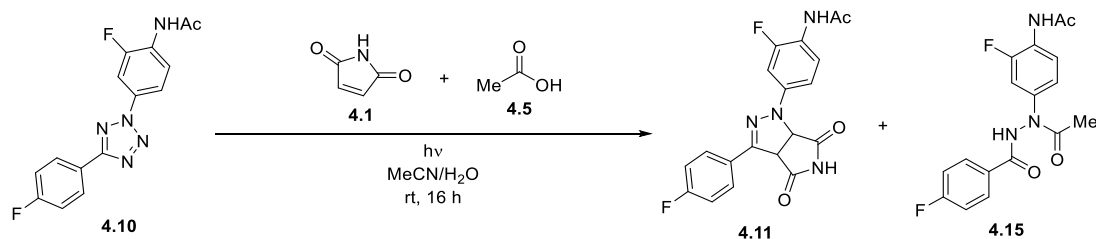


| Entry | Conversion (%)[a] | |
| :---: | :---: | :---: |
| | **4.11** | **4.15** |
| 1 | 63 | 9 |
| 2 | 90 | 8 |
| 3 | 76 | 9 |
| **Average** | **76.3 ± 7.8** | **8.7 ± 0.3** |

[a]Conversion determined by ^{19}F NMR with reference to 1,4-difluorobenzene an internal standard

*Table 5.43: **4.1** vs **4.6***
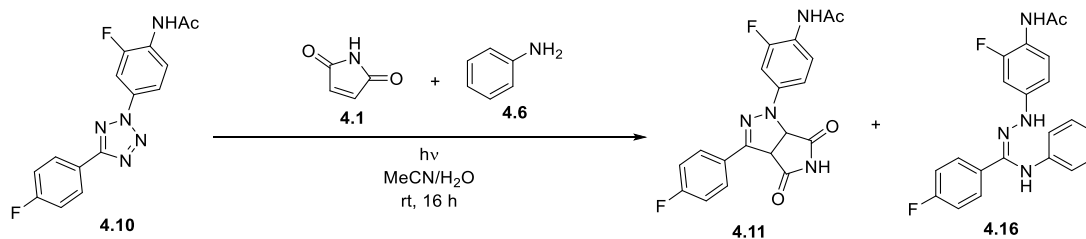


| Entry | Conversion (%)[a] | |
| :---: | :---: | :---: |
| | 4.11 | 4.16 |
| 1 | 67 | 1 |
| 2 | 85 | <1 |
| 3 | 83 | 1 |
| **Average** | **78.3 ± 5.7** | **0.7 ± 0.3** |

[a]Conversion determined by $^{19}$F NMR with reference to 1,4-difluorobenzene an internal standard

*Table 5.44: **4.1** vs **4.7***
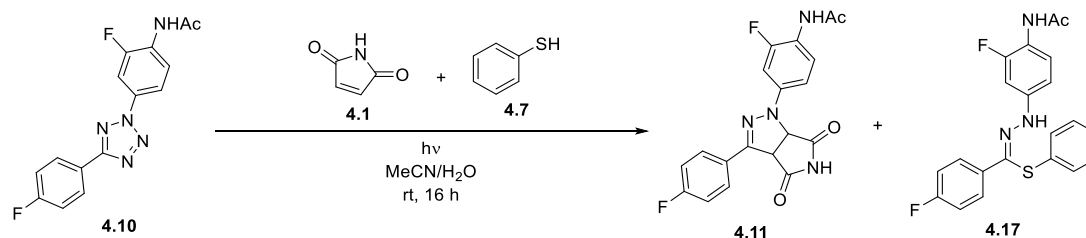


| Entry | Conversion (%)[a] | |
| :---: | :---: | :---: |
| | 4.11 | 4.17 |
| 1 | 30 | 1 |
| 2 | 19 | 0 |
| 3 | 28 | 2 |
| **Average** | **25.7 ± 3.4** | **1.0 ± 0.6** |

[a]Conversion determined by $^{19}$F NMR with reference to 1,4-difluorobenzene an internal standard

*Table 5.45:* **4.1** *vs* **4.8**
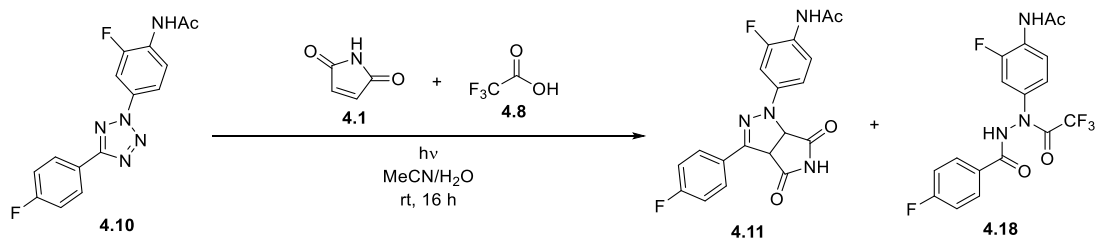


| Entry | Conversion (%)[a] | |
|:---:|:---:|:---:|
| | **4.11** | **4.18** |
| 1 | 2 | 71 |
| 2 | 1 | 74 |
| 3 | 1 | 54 |
| **Average** | **1.3 ± 0.3** | **66.3 ± 6.2** |

[a]Conversion determined by $^{19}$F NMR with reference to 1,4-difluorobenzene an internal standard

*Table 5.46:* **4.1** *vs* **4.9**
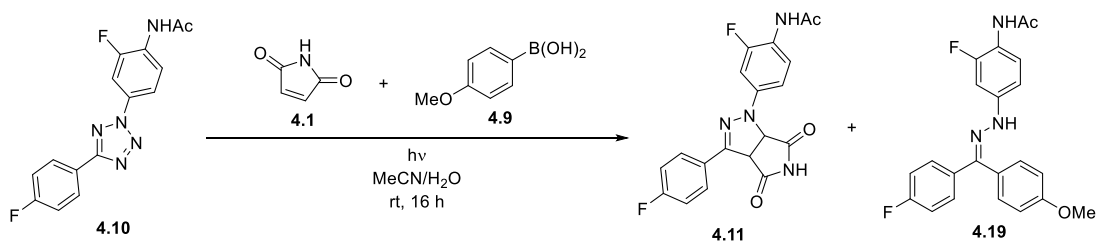


| Entry | Conversion (%)[a] | |
|:---:|:---:|:---:|
| | **4.11** | **4.19** |
| 1 | 71 | <1 |
| 2 | 79 | <1 |
| 3 | 79 | <1 |
| **Average** | **76.3 ± 2.7** | **<1** |

[a]Conversion determined by $^{19}$F NMR with reference to 1,4-difluorobenzene an internal standard

304

*Table 5.47: **4.2** vs **4.3***
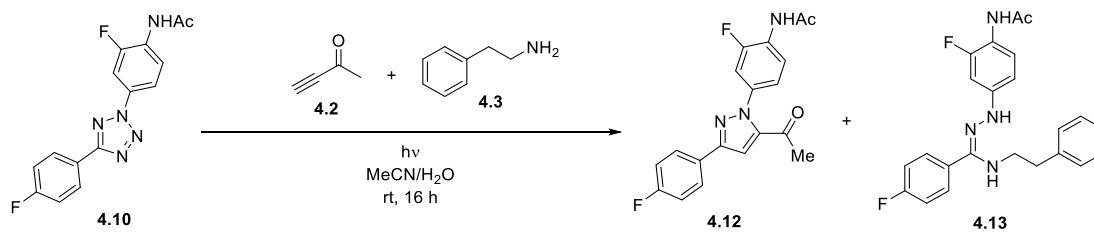


| Entry | Conversion (%)[a] | |
| :---: | :---: | :---: |
| | **4.12** | **4.13** |
| 1 | 19 | 15 |
| 2 | 1 | 22 |
| 3 | 6 | 9 |
| 4 | 6 | 5 |
| **Average** | **8.0 ± 3.9** | **12.8 ± 3.7** |

[a]Conversion determined by $^{19}$F NMR with reference to 1,4-difluorobenzene an internal standard

*Table 5.48: **4.2** vs **4.4***
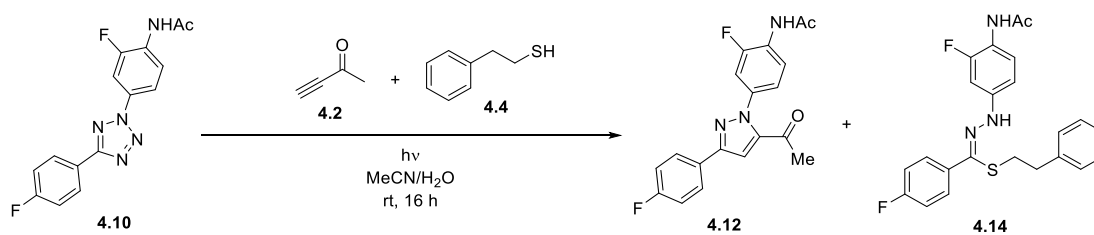


| Entry | Conversion (%)[a] | |
| :---: | :---: | :---: |
| | **4.12** | **4.14** |
| 1 | 57 | 38 |
| 2 | 58 | 18 |
| 3 | 52 | 21 |
| **Average** | **55.7 ± 1.9** | **25.7 ± 6.2** |

[a]Conversion determined by $^{19}$F NMR with reference to 1,4-difluorobenzene an internal standard
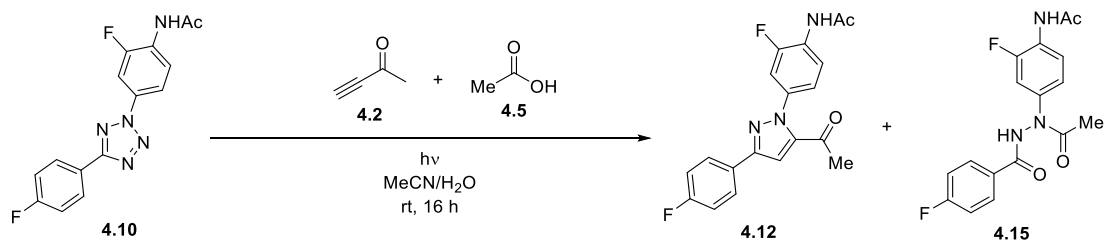
| Entry | Conversion (%)[a] | |
|:---:|:---:|:---:|
| | **4.12** | **4.15** |
| 1 | 32 | 52 |
| 2 | 31 | 69 |
| 3 | 25 | 59 |
| **Average** | **29.3 ± 2.2** | **60.0 ± 4.9** |

[a]Conversion determined by $^{19}$F NMR with reference to 1,4-difluorobenzene an internal standard

*Table 5.50:* **4.2** *vs* **4.6**
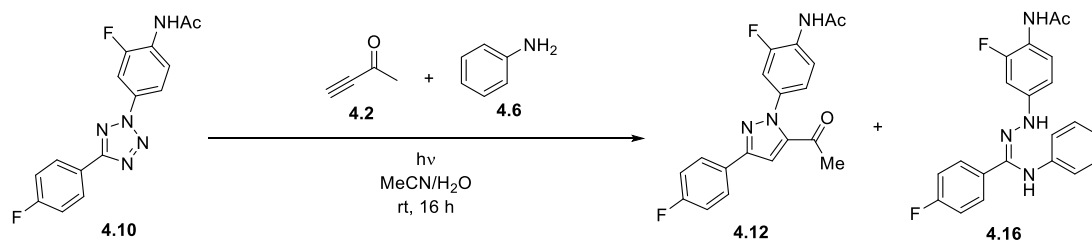


| Entry | Conversion (%)[a] | |
|:---:|:---:|:---:|
| | **4.12** | **4.16** |
| 1 | 52 | 27 |
| 2 | 56 | 26 |
| 3 | 69 | 30 |
| **Average** | **59.0 ± 5.1** | **27.7 ± 1.2** |

[a]Conversion determined by $^{19}$F NMR with reference to 1,4-difluorobenzene an internal standard

*Table 5.51: **4.2** vs **4.7***
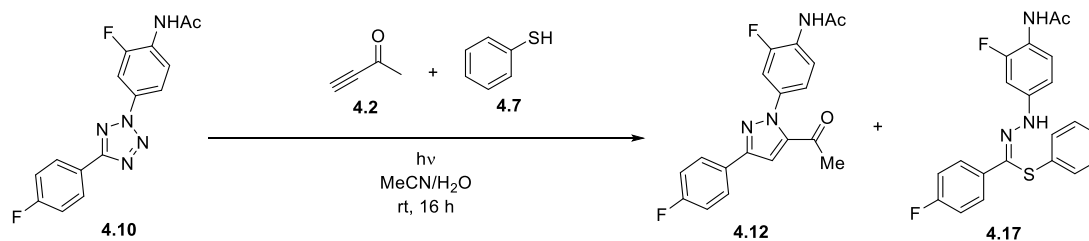


| Entry | Conversion (%)[a] | |
| :---: | :---: | :---: |
| | **4.12** | **4.17** |
| 1 | 28 | 3 |
| 2 | 22 | 2 |
| 3 | 11 | 3 |
| **Average** | **20.3 ± 5.0** | **2.7 ± 0.3** |

[a]Conversion determined by $^{19}$F NMR with reference to 1,4-difluorobenzene an internal standard

*Table 5.52: **4.2** vs **4.8***
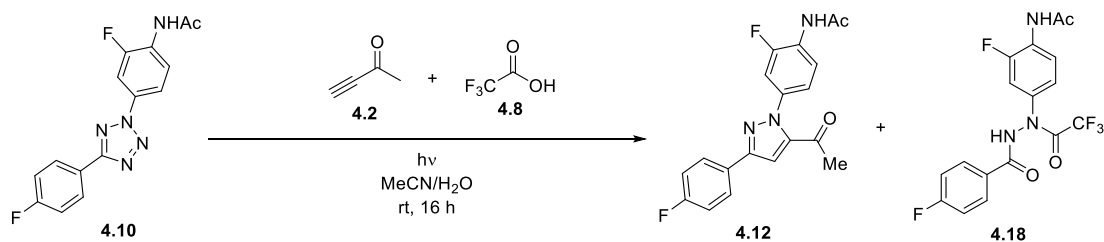


| Entry | Conversion (%)[a] | |
| :---: | :---: | :---: |
| | **4.12** | **4.18** |
| 1 | 1 | 84 |
| 2 | 1 | 74 |
| 3 | 10 | 73 |
| **Average** | **4.0 ± 3.0** | **77.0 ± 3.5** |

[a]Conversion determined by $^{19}$F NMR with reference to 1,4-difluorobenzene an internal standard

*Table 5.53: **4.2** vs **4.9***
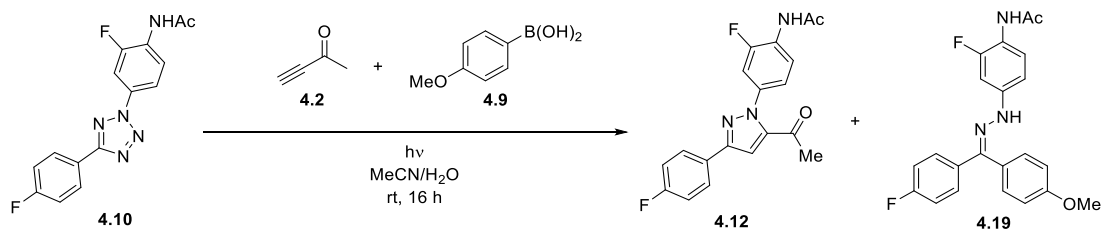


| Entry | Conversion (%)[a] | |
| --- | --- | --- |
| | **4.12** | **4.19** |
| 1 | 74 | <1 |
| 2 | 81 | <1 |
| 3 | 72 | <1 |
| **Average** | **75.7 ± 2.7** | **<1** |

[a]Conversion determined by ^{19}F NMR with reference to 1,4-difluorobenzene an internal standard

*Table 5.54: **4.3** vs **4.4***
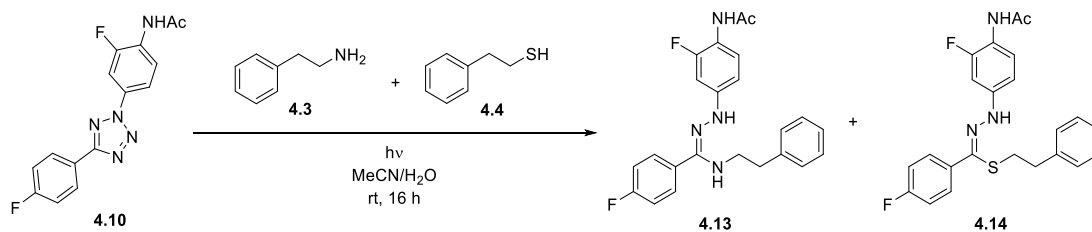


| Entry | Conversion (%)[a] | |
| --- | --- | --- |
| | **4.13** | **4.14** |
| 1 | 30 | 38 |
| 2 | 40 | 40 |
| 3 | 41 | 40 |
| **Average** | **37.0 ± 3.5** | **39.3 ± 0.7** |

[a]Conversion determined by ^{19}F NMR with reference to 1,4-difluorobenzene an internal standard

*Table 5.55: **4.3** vs **4.5***
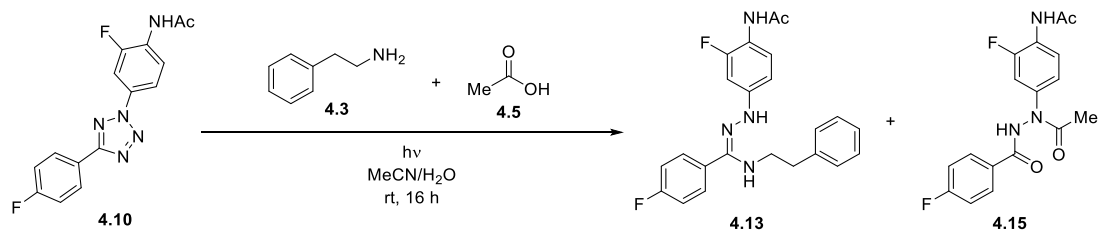


| Entry | Conversion (%)[a] | |
|:---:|:---:|:---:|
| | **4.13** | **4.15** |
| 1 | 19 | 26 |
| 2 | 28 | 31 |
| 3 | 13 | 46 |
| **Average** | **20.0 ± 4.4** | **34.3 ± 6.0** |

[a]Conversion determined by ^{19}F NMR with reference to 1,4-difluorobenzene an internal standard

*Table 5.56: **4.3** vs **4.6***
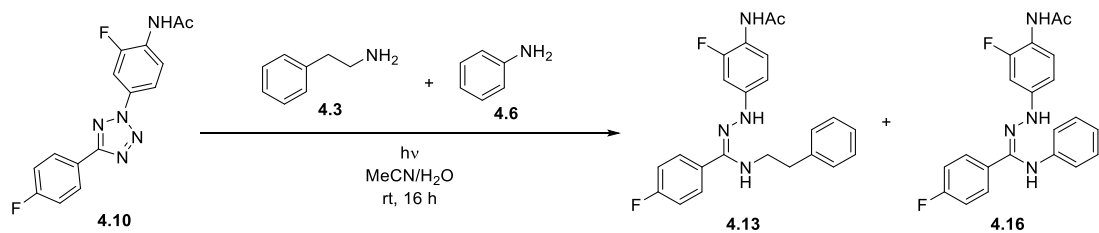


| Entry | Conversion (%)[a] | |
|:---:|:---:|:---:|
| | **4.13** | **4.16** |
| 1 | 41 | 4 |
| 2 | 58 | 3 |
| 3 | 52 | 4 |
| **Average** | **50.3 ± 5.0** | **3.7 ± 0.3** |

[a]Conversion determined by ^{19}F NMR with reference to 1,4-difluorobenzene an internal standard

*Table 5.57: **4.3** vs **4.7***
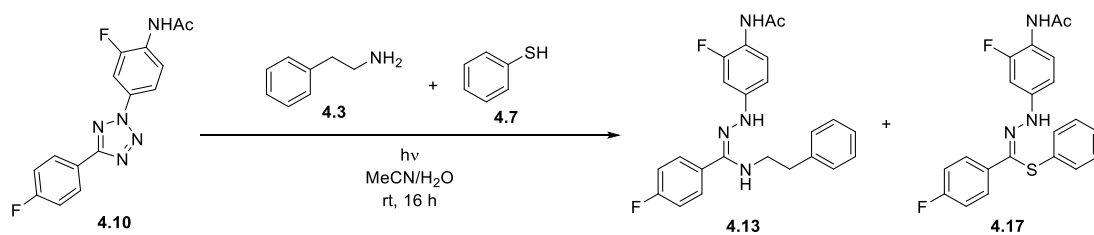


| Entry | Conversion (%)[a] | |
|:---:|:---:|:---:|
| | **4.13** | **4.17** |
| 1 | 34 | 36 |
| 2 | 37 | 43 |
| 3 | 28 | 49 |
| **Average** | **33.0 ± 2.6** | **42.7 ± 3.8** |

[a]Conversion determined by $^{19}$F NMR with reference to 1,4-difluorobenzene an internal standard

*Table 5.58: **4.3** vs **4.8***
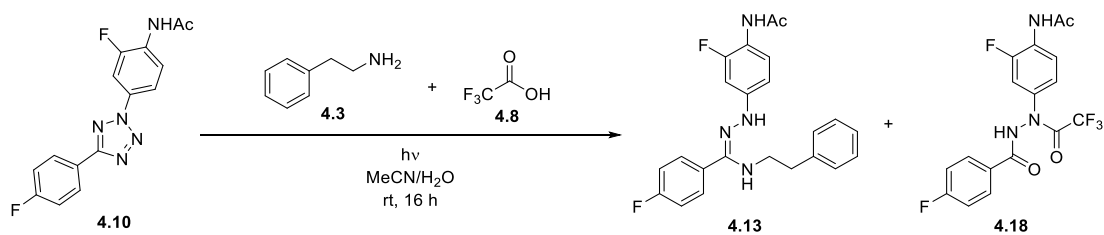


| Entry | Conversion (%)[a] | |
|:---:|:---:|:---:|
| | **4.13** | **4.18** |
| 1 | 26 | <1 |
| 2 | 25 | <1 |
| 3 | 11 | <1 |
| **Average** | **20.7 ± 4.8** | **<1** |

[a]Conversion determined by $^{19}$F NMR with reference to 1,4-difluorobenzene an internal standard

*Table 5.59:* **4.3** *vs* **4.9**
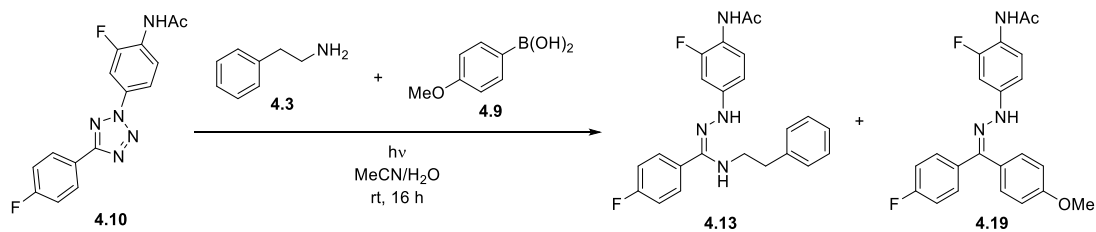


| Entry | Conversion (%)[a] | |
|:---:|:---:|:---:|
| | **4.13** | **4.19** |
| 1 | 45 | <1 |
| 2 | 77 | <1 |
| 3 | 57 | <1 |
| **Average** | **59.7 ± 9.3** | **<1** |

[a]Conversion determined by $^{19}$F NMR with reference to 1,4-difluorobenzene an internal standard

*Table 5.60:* **4.4** *vs* **4.5**
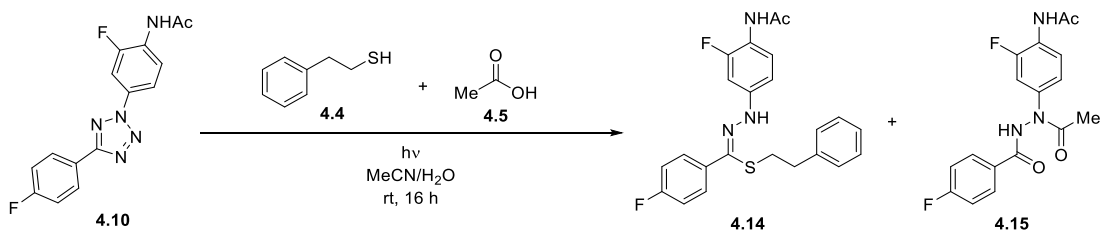


| Entry | Conversion (%)[a] | |
|:---:|:---:|:---:|
| | **4.14** | **4.15** |
| 1 | 31 | 53 |
| 2 | 24 | 72 |
| 3 | 25 | 53 |
| **Average** | **26.7 ± 2.2** | **59.3 ± 6.3** |

[a]Conversion determined by $^{19}$F NMR with reference to 1,4-difluorobenzene an internal standard

*Table 5.61: 4.4 vs 4.6*
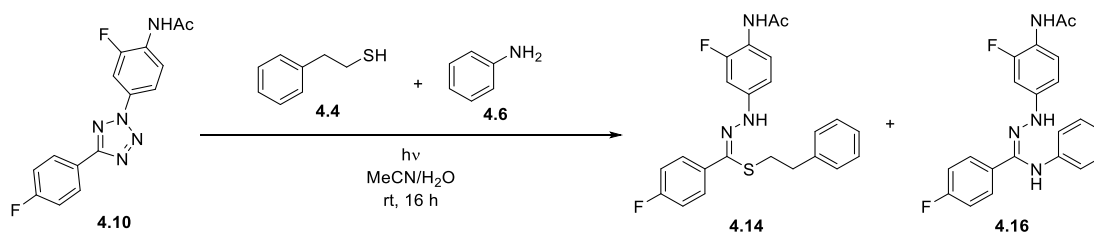


| Entry | Conversion (%)[a] | |
|---|---|---|
| | **4.14** | **4.16** |
| 1 | 46 | 25 |
| 2 | 56 | 30 |
| 3 | 55 | 27 |
| **Average** | **52.3 ± 3.2** | **27.3 ± 1.5** |

[a]Conversion determined by ^{19}F NMR with reference to 1,4-difluorobenzene an internal standard

*Table 5.62: 4.4 vs 4.7*
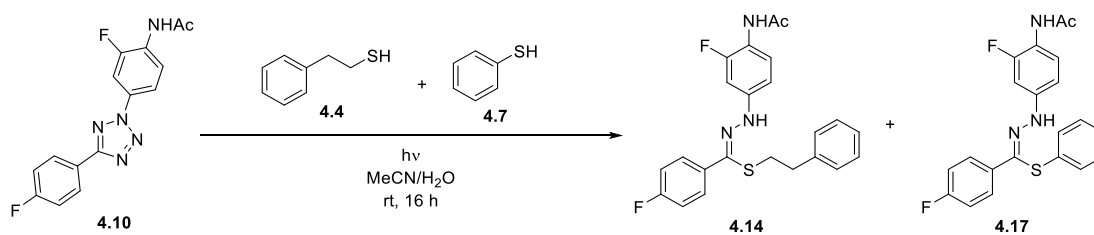


| Entry | Conversion (%)[a] | |
|---|---|---|
| | **4.14** | **4.17** |
| 1 | 30 | 60 |
| 2 | 20 | 69 |
| 3 | 15 | 78 |
| **Average** | **21.7 ± 4.4** | **69 ± 5.2** |

[a]Conversion determined by ^{19}F NMR with reference to 1,4-difluorobenzene an internal standard

*Table 5.63: **4.4** vs **4.8***
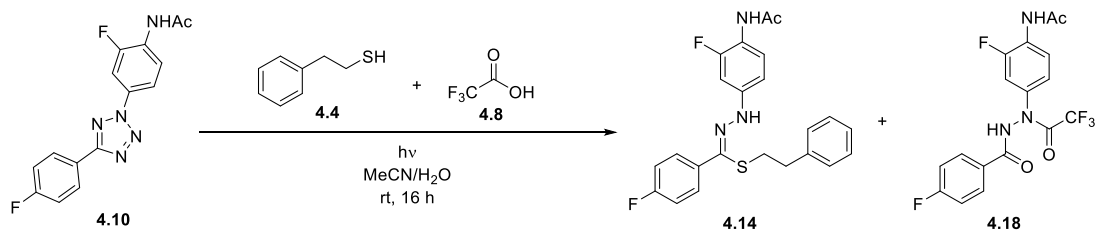


| | Conversion (%)[a] | |
|:---:|:---:|:---:|
| Entry | **4.14** | **4.18** |
| 1 | 22 | 46 |
| 2 | 6 | 68 |
| 3 | 2 | 73 |
| **Average** | **10.0 ± 6.1** | **62.3 ± 8.3** |

[a]Conversion determined by $^{19}$F NMR with reference to 1,4-difluorobenzene an internal standard

*Table 5.64: **4.4** vs **4.9***
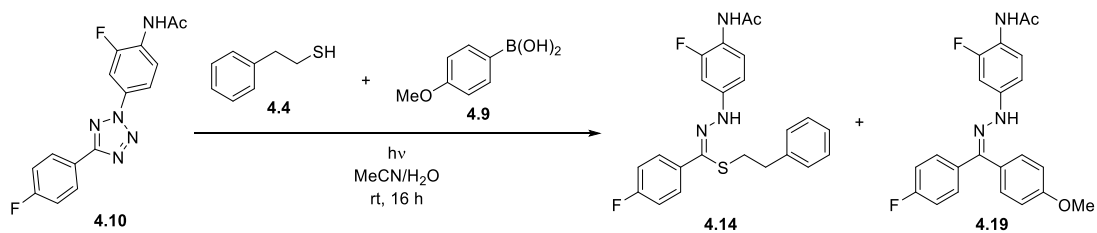


| | Conversion (%)[a] | |
|:---:|:---:|:---:|
| Entry | **4.14** | **4.19** |
| 1 | 64 | <1 |
| 2 | 67 | <1 |
| 3 | 57 | <1 |
| **Average** | **62.7 ± 3.0** | **<1** |

[a]Conversion determined by $^{19}$F NMR with reference to 1,4-difluorobenzene an internal standard

*Table 5.65: **4.5** vs **4.6***
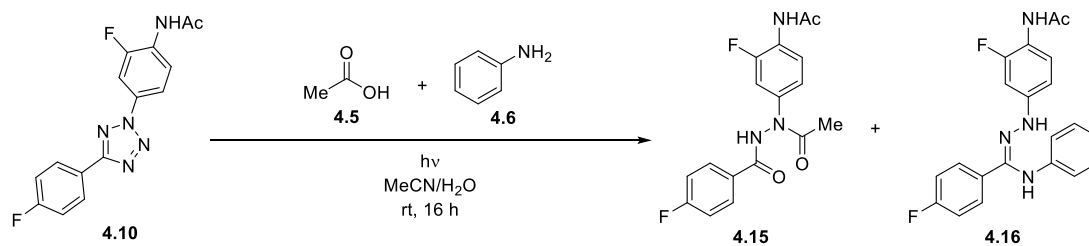


| Entry | Conversion (%)[a] | |
|:---:|:---:|:---:|
| | **4.15** | **4.16** |
| 1 | 62 | 14 |
| 2 | 77 | 12 |
| 3 | 72 | 9 |
| **Average** | **70.3 ± 4.4** | **11.7 ± 1.5** |

[a]Conversion determined by ^{19}F NMR with reference to 1,4-difluorobenzene an internal standard

*Table 5.66: **4.5** vs **4.7***
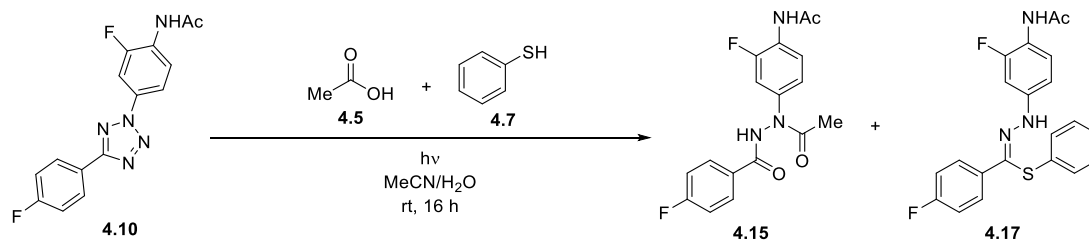


| Entry | Conversion (%)[a] | |
|:---:|:---:|:---:|
| | **4.15** | **4.17** |
| 1 | 27 | 62 |
| 2 | 34 | 55 |
| 3 | 23 | 64 |
| **Average** | **28.0 ± 3.2** | **60.3 ± 2.7** |

[a]Conversion determined by ^{19}F NMR with reference to 1,4-difluorobenzene an internal standard

*Table 5.67: **4.5** vs **4.8***
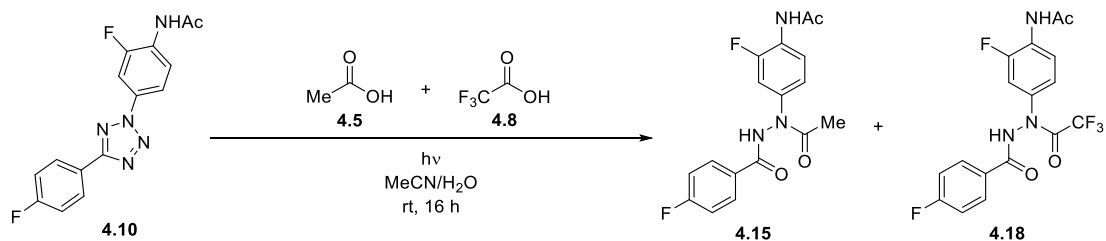


| Entry | Conversion (%)[a] | |
|:---:|:---:|:---:|
| | **4.15** | **4.18** |
| 1 | 19 | 61 |
| 2 | 10 | 79 |
| 3 | 11 | 66 |
| **Average** | **13.3 ± 2.8** | **68.7 ± 5.4** |

[a]Conversion determined by $^{19}$F NMR with reference to 1,4-difluorobenzene an internal standard

*Table 5.68: **4.5** vs **4.9***
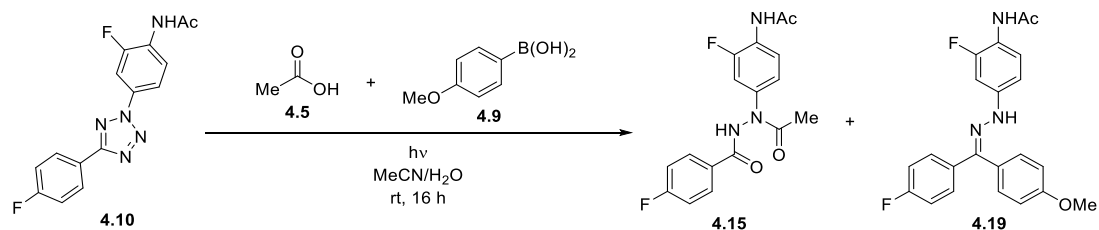


| Entry | Conversion (%)[a] | |
|:---:|:---:|:---:|
| | **4.15** | **4.19** |
| 1 | 75 | <1 |
| 2 | 89 | <1 |
| 3 | 88 | <1 |
| **Average** | **84.5 ± 4.5** | **<1** |

[a]Conversion determined by $^{19}$F NMR with reference to 1,4-difluorobenzene an internal standard

315

*Table 5.69:* **4.6** *vs* **4.7**
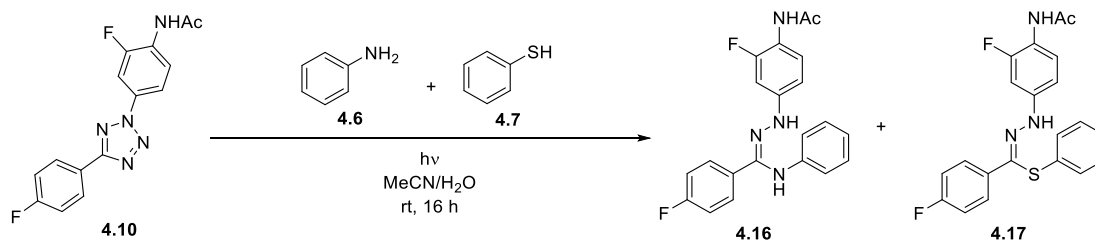


| Entry | Conversion (%)[a] | |
| :---: | :---: | :---: |
| | **4.16** | **4.17** |
| 1 | 27 | 51 |
| 2 | 31 | 65 |
| 3 | 19 | 69 |
| **Average** | **25.7 ± 3.5** | **61.7 ± 5.5** |

[a]Conversion determined by $^{19}$F NMR with reference to 1,4-difluorobenzene an internal standard

*Table 5.70:* **4.6** *vs* **4.8**
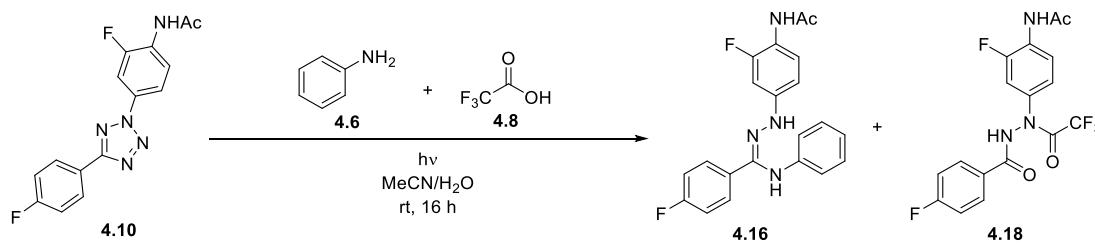


| Entry | Conversion (%)[a] | |
| :---: | :---: | :---: |
| | **4.16** | **4.18** |
| 1 | <1 | 71 |
| 2 | 6 | 68 |
| 3 | <1 | 46 |
| **Average** | **2.0 ± 2.0** | **61.7 ± 7.9** |

[a]Conversion determined by $^{19}$F NMR with reference to 1,4-difluorobenzene an internal standard

*Table 5.71: 4.6 vs 4.9*
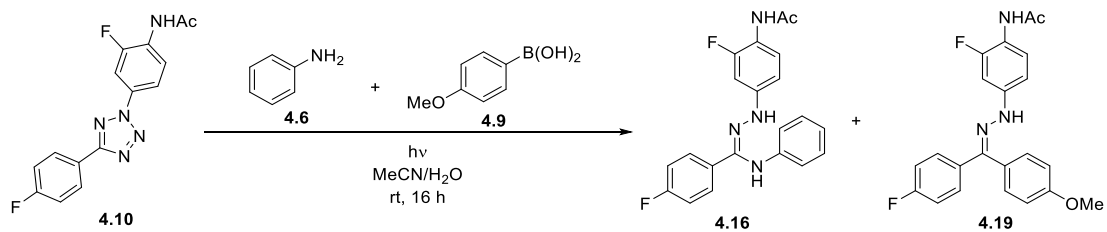


| Entry | Conversion (%)[a] | |
| --- | --- | --- |
| | 4.16 | 4.19 |
| 1 | 47 | <1 |
| 2 | 63 | <1 |
| 3 | 64 | <1 |
| Average | 58.0 ± 5.5 | <1 |

[a]Conversion determined by $^{19}$F NMR with reference to 1,4-difluorobenzene an internal standard

*Table 5.72: 4.7 vs 4.8*
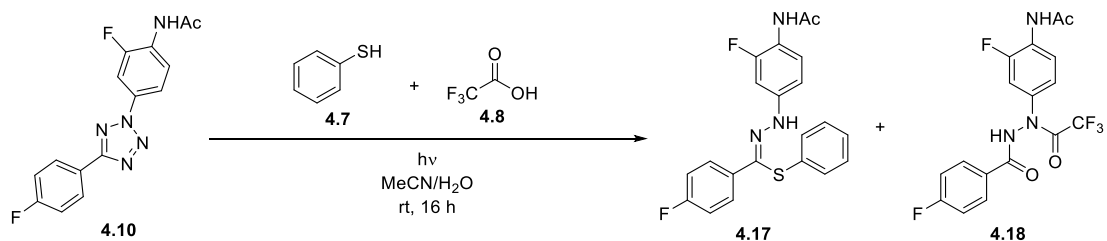


| Entry | Conversion (%)[a] | |
| --- | --- | --- |
| | 4.17 | 4.18 |
| 1 | <1 | 87 |
| 2 | 7 | 80 |
| 3 | <1 | 77 |
| Average | 2.3 ± 2.3 | 81.3 ± 3.0 |

[a]Conversion determined by $^{19}$F NMR with reference to 1,4-difluorobenzene an internal standard

*Table 5.73:* **4.7** *vs* **4.9**
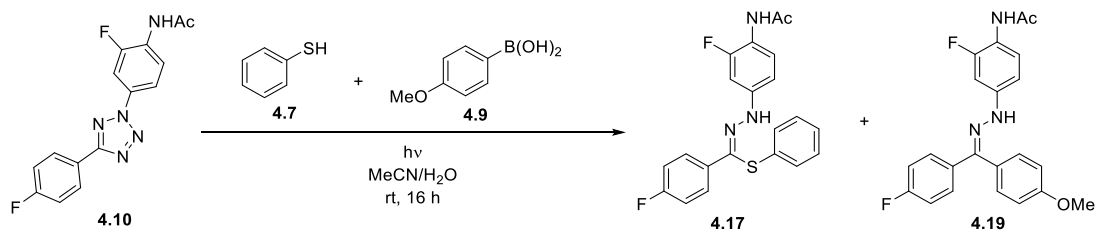


| Entry | Conversion (%)[a] | |
|:---:|:---:|:---:|
| | **4.17** | **4.19** |
| 1 | 47 | <1 |
| 2 | 70 | <1 |
| 3 | 75 | <1 |
| **Average** | **64.0 ± 8.6** | **<1** |

[a]Conversion determined by $^{19}$F NMR with reference to 1,4-difluorobenzene an internal standard

*Table 5.74:* **4.8** *vs* **4.9**
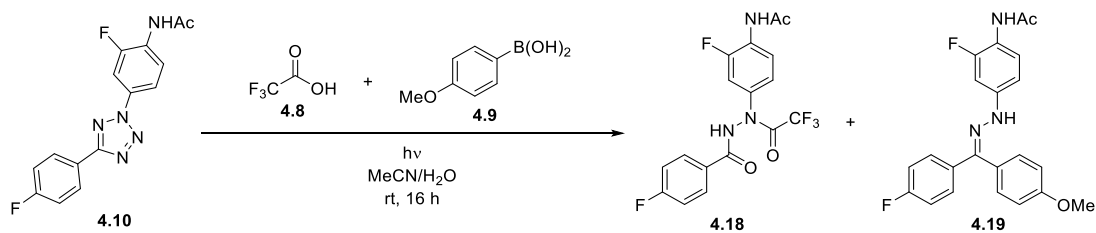


| Entry | Conversion (%)[a] | |
|:---:|:---:|:---:|
| | **4.18** | **4.19** |
| 1 | 42 | <1 |
| 2 | 81 | <1 |
| 3 | 71 | <1 |
| 4 | 71 | <1 |
| **Average** | **66.3 ± 8.4** | **<1** |

[a]Conversion determined by $^{19}$F NMR with reference to 1,4-difluorobenzene an internal standard

## Appendix 1: X-Ray Crystallography *(provided by Dr. Alan Kennedy)*

The final model is shown in *Figure 5.1* and selected crystallographic and refinement parameters are given in *Table 5.75*. CCDC 1987300 contains the supplementary crystallographic data for this structure. These data can be obtained free of charge from the Cambridge Crystallographic Data Centre via www.ccdc.cam.ac.uk/data_request/cif.
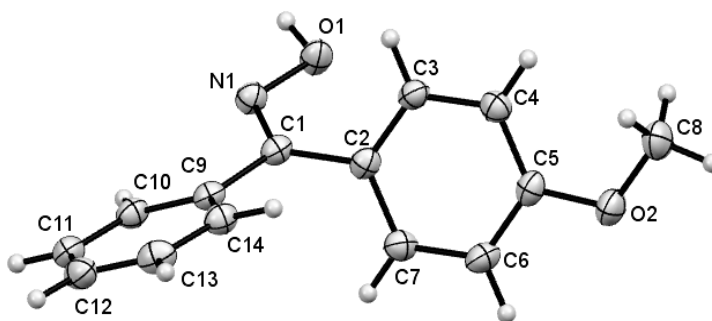


*Figure 5.1: Molecular structure of compound **3.105** with non-H atoms shown as 50 % probability ellipsoids and H atoms as small spheres of arbitrary size*

*Table 5.75: Selected crystallographic and refinement parameters*

| | | | |
|---|---|---|---|
| **Compound** | 3.105 | **Z** | 4 |
| **Formula** | $C_{14}H_{13}NO_2$ | **Refls. Collected** | 3911 |
| **Molecular Weight** | 227.25 | **Refls. Independant** | 2095 |
| **Crystal system** | Monoclinic | **Refls. Observed** | 1880 |
| **Space Group** | $P2_1/c$ | **Rint** | 0.0191 |
| **λ Å** | 1.54184 | **No. Parameters** | 160 |
| **$a$ Å** | 9.9101(3) | **Goodness of Fit** | 1.043 |
| **$b$ Å** | 9.4677(3) | **R[I>2σ(I)], $F$** | 0.0410 |
| **$c$ Å** | 12.2514(4) | **Rw, $F^2$** | 0.1166 |
| **$\beta$ °** | 94.841(3) | **Residual $e$ density Max. e$Å^{-3}$** | 0.217 |
| **Volume $Å^3$** | 1145.40(6) | **Residual $e$ density Min. e$Å^{-3}$** | -0.291 |
| **Temp. $K$** | 150(2) | **Extinction coeff.** | 0.0132(13) |

# 6    References

1    R. Huisgen, M. Seidel, J. Sauer, J. McFarland and G. Wallbillich, *J. Org. Chem.*, 1959, **24**, 892–893.

2    R. Huisgen, J. Sauer and H. J. Sturm, *Angew. Chem.*, 1958, **70**, 272–273.

3    R. Huisgen, R. Grashey, E. Aufderhaar and R. Kunz, *Chem. Ber.*, 1965, **98**, 642–649.

4    R. Huisgen, E. Aufderhaar and G. Wallbillich, *Chem. Ber.*, 1965, **98**, 1476–1486.

5    R. Huisgen, H. Knupfer, R. Sustmann, G. Wallbillich and V. Weberndörfer, *Chem. Ber.*, 1967, **100**, 1580–1592.

6    J. S. Clovis, A. Eckell, R. Huisgen, R. Sustmann, G. Wallbillich and V. Weberndörfer, *Chem. Ber.*, 1967, **100**, 1593–1601.

7    R. Huisgen, R. Sustmann and G. Wallbillich, *Chem. Ber.*, 1967, **100**, 1786–1801.

8    A. Eckell, R. Huisgen, R. Sustmann, G. Wallbillich, D. Grashey and E. Spindler, *Chem. Ber.*, 1967, **100**, 2192–2213.

9    R. Huisgen and V. Weberndörfer, *Chem. Ber.*, 1967, **100**, 71–78.

10   J. S. Clovis, A. Eckell, R. Huisgen and R. Sustmann, *Chem. Ber.*, 1967, **100**, 60–70.

11   R. Huisgen, J. Sauer, H. J. Sturm and J. H. Markgraf, *Chem. Ber.*, 1960, **93**, 2106–2124.

12   R. Huisgen, J. Sauer and M. Seidel, *Chem. Ber.*, 1961, **94**, 2503–2509.

13   R. Huisgen, J. Sauer and M. Seidel, *Chem. Ber.*, 1960, **93**, 2885–2891.

14   R. Huisgen, H. J. Sturm and M. Seidel, *Chem. Ber.*, 1961, **94**, 1555–1562.

15   R. Huisgen, R. Grashey, M. Seidel, H. Knupfer and R. Schmidt, *Justus Liebigs Ann. Chem.*, 1962, **658**, 169–180.

16   R. Huisgen, M. Seidel, G. Wallbillich and H. Knupfer, *Tetrahedron*, 1962, **17**, 3–29.

17   R. Huisgen, R. Grashey, M. Seidel, G. Wallbillich, H. Knupfer and R. Schmidt, *Justus Liebigs Ann. Chem.*, 1962, **653**, 105–113.

18   R. Huisgen, R. Grashley, H. Knupfer, R. Kunz and M. Seidel, *Chem. Ber.*, 1964, **97**, 1085–1095.

19   L. M. Oh, *Tetrahedron Lett.*, 2006, **47**, 7943–7946.

20    R. K. V. Lim and Q. Lin, *Acc. Chem. Res.*, 2011, **44**, 828–839.

21    G. Delaittre, A. S. Goldmann, J. O. Mueller and C. Barner-Kowollik, *Angew. Chem. Int. Ed.*, 2015, **54**, 11388–11403.

22    R. Huisgen, *Angew. Chem. Int. Ed.*, 1963, **2**, 565–598.

23    P. Caramella and K. N. Houk, *J. Am. Chem. Soc.*, 1976, **98**, 6397–6399.

24    H. Bock, R. Dammel, S. Fischer and C. Wentrup, *Tetrahedron Lett.*, 1987, **28**, 617– 620.

25    M. W. Wong and C. Wentrup, *J. Am. Chem. Soc.*, 1993, **115**, 7743–7746.

26    P. Caramella and K. N. Houk, *J. Am. Chem. Soc.*, 1976, **98**, 6397–6399.

27    D. Bégué, G. G. Qiao and C. Wentrup, *J. Am. Chem. Soc.*, 2012, **134**, 5339–5350.

28    P. Caramella, R. W. Gandour, J. A. Hall, C. G. Deville and K. N. Houk, *J. Am. Chem. Soc.*, 1977, **99**, 385–392.

29    M. Granier, A. Baceiredo, V. Huch, M. Veith and G. Bertrand, *Inorg. Chem.*, 1991, **30**, 1161–1162.

30    D. Bégué and C. Wentrup, *J. Org. Chem.*, 2014, **79**, 1418–1426.

31    C. M. Nunes, I. Reva, M. T. S. Rosado and R. Fausto, *Eur. J. Org. Chem.*, 2015, 7484–7493.

32    W. Sieber, P. Gilgen, S. Chaloupka, H.-J. Hansen and H. Schmid, *Helv. Chim. Acta*, 1973, **56**, 1679–1690.

33    H. Meier, Hansruedi; Heinzelmann, Willy; Heimgartner, *Chimia (Aarau).*, 1980, **34**, 504–506.

34    H. Meier, Hansruedi; Heinzelmann, Willy; Heimgartner, *Chimia (Aarau).*, 1980, **34**, 506–508.

35    N. H. Toubro and A. Holm, *J. Am. Chem. Soc.*, 1980, **102**, 2093–2094.

36    C. Csongár, P. Leihkauf, V. Lohse and G. Tomaschewski, *Zeitschrift für Chemie*, 1984, **24**, 96–97.

37    C. Csongár, P. Leihkauf, V. Lohse, M. Siegmund and G. Tomaschewski, *Zeitschrift für Chemie*, 1985, **25**, 106–107.

38    C. Csongár, P. Leihkauf, V. Lohse and G. Tomaschewski, *J. für Prakt. Chemie*, 1985, **327**, 96–102.

39    P. Leihkauf, V. Lohse, C. Csongár, M. Siegmund and G. Tomaschewski, *Zeitschrift für Chemie*, 1987, **27**, 371–372.

40    P. Leihkauf, V. Lohse, C. Csongár and G. Tomaschewski, *Zeitschrift für Chemie*, 1985, **25**, 266–267.

41    K. Bhattacharyya, D. Ramalah, P. K. Das and M. V. George, *J. Photochem.*, 1987, **36**, 63–84.

42    C. Wentrup and R. Flammang, *J. Phys. Org. Chem.*, 1998, **11**, 350–355.

43    C. Wentrup, S. Fischer, A. Maquestiau and R. Flammang, *Angew. Chem. Int. Ed. Engl.*, 1985, **24**, 56–57.

44    C. M. Nunes, C. Araujo-Andrade, R. Fausto and I. Reva, *J. Org. Chem.*, 2014, **79**, 3641–3646.

45    K. H. von Locquenghien, R. Réau and G. Bertrand, *J. Chem. Soc., Chem. Commun.*, 1991, 1192–1193.

46    S.-L. Zheng, Y. Wang, Z. Yu, Q. Lin and P. Coppens, *J. Am. Chem. Soc.*, 2009, **131**, 18036–18037.

47    F. Castan, A. Baceiredo, D. Bigg and G. Bertrand, *J. Org. Chem.*, 1991, **56**, 1801–1807.

48    G. Bertrand and C. Wentrup, *Angew. Chem. Int. Ed. Engl.*, 1994, **33**, 527–545.

49    N. Emig, F. P. Gabbaï, H. Krautscheid, R. Réau and G. Bertrand, *Angew. Chem. Int. Ed.*, 1998, **37**, 989–992.

50    C. Leue, R. Reau, B. Neumann, H.-G. Stammler, P. Jutzi and G. Bertrand, *Organometallics*, 1994, **13**, 436–438.

51    W. Uhl, F. Hannemann, W. Saak and R. Wartchow, *Eur. J. Inorg. Chem.*, 1999, **1999**, 771–776.

52    G. Sicard, A. Baceiredo and G. Bertrand, *J. Am. Chem. Soc.*, 1988, **110**, 2663–2664.

53    A. S. Shawali and M. A. N. Mosselhi, *J. Heterocycl. Chem.*, 2003, **40**, 725–746.

54    A. S. Shawali, N. M. Elwan and A. M. Awad, *J. Chem. Res.*, 1997, 268–269.

55    A. F. Hegarty, M. P. Cashman and F. L. Scott, *J. Chem. Soc. D Chem. Commun.*, 1971, 684.

56    A. F. Hegarty, M. P. Cashman and F. L. Scott, *J. Chem. Soc. Perkin Trans. 2*, 1972,

44.

57     S. R. Donohue, C. Halldin and V. W. Pike, *Tetrahedron Lett.*, 2008, **49**, 2789–2791.

58     G. Zecchi, L. Garanti and G. Molteni, *Heterocycles*, 1995, **40**, 777.

59     G. Molteni, *ARKIVOC*, 2007, 224–246.

60     K. Anderson, E. Butler, D. Anderson and E. Woolley, *J. Phys. Chem.*, 1967, **71**, 3566–3569.

61     G. Molteni, M. Orlandi and G. Broggini, *J. Chem. Soc., Perkin Trans. 1*, 2000, 3742–3745.

62     C. P. Ramil and Q. Lin, *Curr. Opin. Chem. Biol.*, 2014, **21**, 89–95.

63     J. Azizian, S. Soozangarzadeh and K. Jadidi, *Synth. Commun.*, 2001, **31**, 1069–1073.

64     R. Atir, S. Mallouk, K. Bougrin, M. Soufiaoui and A. Laghzizil, *Synth. Commun.*, 2006, **36**, 111–120.

65     R. S. Tewari and P. Parihar, *J. Chem. Eng. Data*, 1981, **26**, 418–420.

66     P. Wolkoff, *Can. J. Chem.*, 1975, **53**, 1333–1335.

67     H. Wamhoff and M. Zahran, *Synthesis*, 1987, 876–879.

68     K. M. L. Rai and A. Hassner, *Synth. Commun.*, 1989, 2799–2807.

69     J. J. Oviedo, P. de la Cruz, J. Garin, J. Orduna and F. Langa, *Tetrahedron Lett.*, 2005, **46**, 4781–4784.

70     W. A. F. Gladstone, J. B. Aylward and R. O. C. Norman, *J. Chem. Soc. C Org.*, 1969, 2587.

71     K. M. Lokanatha Rai and N. Linganna, *Synth. Commun.*, 1997, **27**, 3737–3744.

72     D. W. Chen and Z. C. Chen, *Synth. Commun.*, 1995, **25**, 1617–1626.

73     D. V. Sowmya, G. Lakshmi Teja, A. Padmaja, V. Kamala Prasad and V. Padmavathi, *Eur. J. Med. Chem.*, 2018, **143**, 891–898.

74     S. Ningaiah, S. D. Doddaramappa, Chandra, M. Madegowda, S. Keshavamurthy and U. K. Bhadraiah, *Synth. Commun.*, 2014, **44**, 2222–2231.

75     P. Scheiner and W. M. Litchman, *J. Chem. Soc. Chem. Commun.*, 1972, 781.

76     L. M. T. Frija, M. L. S. Cristiano, A. Gómez-Zavaglia, I. Reva and R. Fausto, *J. Photochem. Photobiol. C Photochem. Rev.*, 2014, **18**, 71–90.

77      J. E. Baldwin and S. Y. Hong, *Chem. Commun.*, 1967, 1136a.

78      S.-Y. Hong and J. E. Baldwin, *Tetrahedron*, 1968, **24**, 3787–3794.

79      M. Feist, L. Alder and C. Csongár, *J. Therm. Anal.*, 1988, **33**, 1201–1206.

80      C. Csongár, M. Feist and G. Tomaschewski, *Zeitschrift für Chemie*, 1987, **27**, 99–100.

81      International Organization for Standardization, *Space environment (natural and artificial) — Process for determining solar irradiances*, 2007.

82      Yizhong Wang, A. Claudia I. Rivera Vera and Q. Lin, *Org. Lett.*, 2007, **9**, 4155–4158.

83      R. P. Rastogi, Richa, A. Kumar, M. B. Tyagi and R. P. Sinha, *J. Nucleic Acids*, 2010, **2010**, 592980.

84      Y. Wang, W. J. Hu, W. Song, R. K. V. Lim and Q. Lin, *Org. Lett.*, 2008, **10**, 3725–3728.

85      P. An, Z. Yu and Q. Lin, *Chem. Commun.*, 2013, **49**, 9920.

86      Z. Yu, L. Y. Ho, Z. Wang and Q. Lin, *Bioorg. Med. Chem. Lett.*, 2011, **21**, 5033–6.

87      P. Lederhose, K. N. R. Wüst, C. Barner-Kowollik and J. P. Blinco, *Chem. Commun.*, 2016, **52**, 5928–5931.

88      Z. Yu, T. Y. Ohulchanskyy, P. An, P. N. Prasad and Q. Lin, *J. Am. Chem. Soc.*, 2013, **135**, 16766–16769.

89      R. R. Batchelor, E. Blasco, K. N. R. Wuest, H. Lu, M. Wegener, C. Barner-Kowollik and M. H. Stenzel, *Chem. Commun.*, 2018, **54**, 2436–2439.

90      J. P. Menzel, F. Feist, B. Tuten, T. Weil, J. P. Blinco and C. Barner-Kowollik, *Angew. Chem. Int. Ed.*, 2019, **58**, 7470–7474.

91      P. Lederhose, D. Abt, A. Welle, R. Müller, C. Barner-Kowollik and J. P. Blinco, *Chem. Eur. J.*, 2018, **24**, 576–580.

92      E. Sato, Y. Kanaoka and A. Padwa, *J. Org. Chem.*, 1982, **47**, 4256–4260.

93      V. Lohse, P. Leihkauf, C. Csongar and G. Tomaschewski, *J. für Prakt. Chemie*, 1988, **330**, 406–414.

94      E. Blasco, Y. Sugawara, P. Lederhose, J. P. Blinco, A.-M. Kelterer and C. Barner-Kowollik, *ChemPhotoChem*, 2017, **1**, 159–163.

95    J. P. Menzel, B. B. Noble, A. Lauer, M. L. Coote, J. P. Blinco and C. Barner-Kowollik, *J. Am. Chem. Soc.*, 2017, **139**, 15812–15820.

96    M. Maus, W. Rettig, D. Bonafoux and R. Lapouyade, *J. Phys. Chem. A*, 1999, **103**, 3388–3401.

97    D. L. Browne and J. P. A. Harrity, *Tetrahedron*, 2010, **66**, 553–568.

98    R. Huisgen, R. Grashey, H. Gotthardt and R. Schmidt, *Angew. Chem. Int. Ed. Engl.*, 1962, **1**, 48–49.

99    R. Huisgen, R. Grashey and H. Gotthardt, *Angew. Chem. Int. Ed. Engl.*, 1962, **1**, 49.

100   P. Claus, T. Doppler, N. Gakis, M. Georgarakis, H. Giezendanner, P. Gilgen, H. Heimgartner, B. Jackson, M. Märky, N. S. Narasimhan, H. J. Rosenkranz, A. Wunderli, H.-J. Hansen and H. Schmid, *Pure Appl. Chem.*, 1973, **33**, 339–362.

101   Y. Huseya, A. Chinone and M. Ohta, *Bull. Chem. Soc. Jpn.*, 1971, **44**, 1667–1668.

102   M. Märky, H. Meier, A. Wunderli, H. Heimgartner, H. Schmid and H.-J. Hansen, *Helv. Chim. Acta*, 1978, **61**, 1477–1510.

103   A. Strauss and H.-H. Otto, *Helv. Chim. Acta*, 1997, **80**, 1823–1830.

104   R. Sustmann, *Tetrahedron Lett.*, 1971, **12**, 2717–2720.

105   K. N. Houk, J. Sims, C. R. Watts and L. J. Luskus, *J. Am. Chem. Soc.*, 1973, **95**, 7301–7315.

106   K. N. Houk, J. Sims, R. E. Duke, R. W. Strozier and J. K. George, *J. Am. Chem. Soc.*, 1973, **95**, 7287–7301.

107   K. N. Houk, *Acc. Chem. Res.*, 1975, **8**, 361–369.

108   A. K. Chandra and M. Tho Nguyen, *J. Comput. Chem.*, 1998, **19**, 195–202.

109   G. Molteni and A. Ponti, *Molecules*, 2017, **22**, 202.

110   A. Ponti and G. Molteni, *J. Org. Chem.*, 2001, **66**, 5252–5255.

111   M. Ríos-Gutiérrez and L. R. Domingo, *Tetrahedron*, 2019, **75**, 1961–1967.

112   T. Shimizu, Y. Hayashi, T. Nishio and K. Teramura, *Bull. Chem. Soc. Jpn.*, 1984, **57**, 787–790.

113   M. Chiericato, P. Dalla Croce, G. Carganico and S. Maiorana, *J. Heterocycl. Chem.*, 1979, **16**, 383–384.

114    B. Green and K. Sheu, *Steroids*, 1994, **59**, 479–484.

115    J. Z. Chandanshive, P. B. González, W. Tiznado, B. F. Bonini, J. Caballero, C. Femoni and M. Comes Franchini, *Tetrahedron*, 2012, **68**, 3319–3328.

116    G. Molteni and A. Ponti, *Tetrahedron*, 2003, **59**, 5225–5229.

117    S. Emamiam, *J. Mol. Graph. Model.*, 2015, **60**, 155–161.

118    R. Sustmann, *Pure Appl. Chem.*, 1974, **40**, 569–593.

119    P. Leihkauf, V. Lohse, C. Csongar and G. Tomaschewski, *J. für Prakt. Chemie*, 1989, **331**, 789–798.

120    P. Leihkauf, V. Lohse, C. Csongár and G. Tomaschewski, *Zeitschrift für Chemie*, 1990, **30**, 29–30.

121    Y. Wang, W. Song, W. J. Hu and Q. Lin, *Angew. Chem. Int. Ed.*, 2009, **48**, 5330–3.

122    Y. Kurra, K. A. Odoi, Y.-J. Lee, Y. Yang, T. Lu, S. E. Wheeler, J. Torres-Kolbus, A. Deiters and W. R. Liu, *Bioconjug. Chem.*, 2014, **25**, 1730–1738.

123    Z. Yu and Q. Lin, *J. Am. Chem. Soc.*, 2014, **136**, 4153–4156.

124    P. An, H.-Y. Wu, T. M. Lewandowski and Q. Lin, *Chem. Commun.*, 2018, **54**, 14005–14008.

125    X. S. Wang, Y.-J. Lee and W. R. Liu, *Chem. Commun.*, 2014, **50**, 3176.

126    K. Tanaka, S. Maeno and K. Mitsuhashi, *Chem. Lett.*, 1982, **11**, 543–546.

127    K. A. Baruah, D. Prajapati and J. S. Sandhu, *Tetrahedron*, 1988, **44**, 1241–1246.

128    M. Barzaghi, P. L. Beltrame, P. Dalla Croce, P. Del Buttero, E. Licandro, S. Maiorana and G. Zecchi, *J. Org. Chem.*, 1983, **48**, 3807–3810.

129    V. Padmavathi, B. J. M. Reddy, B. C. O. Reddy and A. Padmaja, *Tetrahedron*, 2005, **61**, 2407–2411.

130    R. Fusco, L. Garanti and G. Zecchi, *Tetrahedron Lett.*, 1974, **15**, 269–272.

131    L. Garanti, A. Sala and G. Zecchi, *J. Org. Chem.*, 1977, **42**, 1389–1392.

132    M. P. Winters, C. A. Teleha and Z. Sui, *Tetrahedron Lett.*, 2014, **55**, 2150–2153.

133    L. Basolo, E. M. Beccalli, E. Borsini, G. Broggini, M. Khansaa and M. Rigamonti, *Eur. J. Org. Chem.*, 2010, 1694–1703.

134    O. Tsuge, K. Ueno and S. Kanemasa, *Chem. Lett.*, 1984, **13**, 285–288.

135  D. Pla, D. S. Tan and D. Y. Gin, *Chem. Sci.*, 2014, **5**, 2407–2415.

136  G. L'abbé, S. Emmers, W. Dehaen and L. K. Dyall, *J. Chem. Soc., Perkin Trans. 1*, 1994, 2553–2558.

137  T. Sasaki and K. Kanematsu, *J. Chem. Soc. C Org.*, 1971, 2147.

138  H. Meier, H. Heimgartner and H. Schmid, *Helv. Chim. Acta*, 1977, **60**, 1087–1090.

139  K.-H. Pfoertner and J. Foricher, *Helv. Chim. Acta*, 1980, **63**, 653–657.

140  A. Agócs, A. Bényei, L. Somogyi and P. Herczegh, *Tetrahedron: Asymmetry*, 1998, **9**, 3359–3363.

141  J. Barluenga, F. Fernández-Marí, E. Aguilar, A. L. Viado and B. Olano, *Tetrahedron Lett.*, 1998, **39**, 4887–4890.

142  P. Del Buttero, G. Molteni and T. Pilati, *Tetrahedron Lett.*, 2003, **44**, 1425–1427.

143  L. De Benassuti, L. Garanti and G. Molteni, *Tetrahedron*, 2004, **60**, 4627–4633.

144  G. Broggini, L. Garanti, G. Molteni and G. Zecchi, *Tetrahedron: Asymmetry*, 1999, **10**, 487–492.

145  G. Broggini, L. Garanti, G. Molteni, T. Pilati, A. Ponti and G. Zecchi, *Tetrahedron: Asymmetry*, 1999, **10**, 2203–2212.

146  G. Broggini, G. Casalone, L. Garanti, G. Molteni, T. Pilati and G. Zecchi, *Tetrahedron: Asymmetry*, 1999, **10**, 4447–4454.

147  G. Broggini, G. Molteni and T. Pilati, *Tetrahedron: Asymmetry*, 2000, **11**, 1975–1983.

148  G. Molteni and T. Pilati, *Tetrahedron: Asymmetry*, 1999, **10**, 3873–3876.

149  M. P. Sibi, L. M. Stanley and C. P. Jasperse, *J. Am. Chem. Soc.*, 2005, **127**, 8276.

150  M. P. Sibi, L. M. Stanley and T. Soeta, *Adv. Synth. Catal.*, 2006, **348**, 2371–2375.

151  G. Wang, X. Liu, T. Huang, Y. Kuang, L. Lin and X. Feng, *Org. Lett.*, 2013, **15**, 76–79.

152  A. L. Gerten, M. C. Slade, K. M. Pugh and L. M. Stanley, *Org. Biomol. Chem.*, 2013, **11**, 7834.

153  K. Tanaka, H. Masuda and K. Mitsuhashi, *Bull. Chem. Soc. Jpn.*, 1986, **59**, 3901–3904.

154 K. Brahma, A. K. Sasmal and C. Chowdhury, *Org. Biomol. Chem.*, 2011, **9**, 8422.

155 R. Remy and C. G. Bochet, *European J. Org. Chem.*, 2018, **2018**, 316–328.

156 V. V. Voronin, M. S. Ledovskaya, E. G. Gordeev, K. S. Rodygin, V. P. Ananikov and N. D. Zelinsky, *J. Org. Chem.*, 2018, **83**, 3819–3828.

157 C. Spiteri, S. Keeling and J. E. Moses, *Org. Lett.*, 2010, **12**, 3368–3371.

158 Y. Zhang, X. Ma, Y. Chen, X. Chen, L. Guo, W. Cao, J. Chen and M. S. Wong, *Eur. J. Org. Chem.*, 2013, **2013**, 3005–3012.

159 S. Morrocchi, A. Ricca and A. Zanarotti, *Tetrahedron Lett.*, 1970, **11**, 3215–3218.

160 Y. Zhang, W. Liu and Z. Zhao, *Molecules*, 2013, **19**, 306–315.

161 Z. Li, L. Qian, L. Li, J. C. Bernhammer, H. V. Huynh, J.-S. Lee and S. Q. Yao, *Angew. Chem. Int. Ed.*, 2015, **55**, 2002–2006.

162 C. Csongár, L. Grubert and G. Tomaschewski, *Zeitschrift für Chemie*, 1988, **28**, 24–25.

163 J. B. Aylward and F. L. Scott, *J. Chem. Soc. C Org.*, 1970, 968.

164 A. S. Shawali and H. M. Hassaneen, *Tetrahedron Lett.*, 1972, **13**, 1299–1300.

165 A. S. Shawali, M. Sami, S. M. Sherif and C. Párkányi, *J. Heterocycl. Chem.*, 1980, **17**, 877–880.

166 M. M. El-Abadelah, M. Z. Nazer, N. S. El-Abadlah and H. Meier, *J. für Prakt. Chemie/Chemiker-Zeitung*, 1997, **339**, 90–91.

167 B. A. Abu Thaher, J. A. Zahra and M. M. El-Abadelah, *J. Heterocycl. Chem.*, 2002, **39**, 901–904.

168 B. Abu Thaher, J. A. Zahra, M. M. El-Abadelah and H.-H. Otto, *Monatsh. Chem.*, 2004, **135**, 435–439.

169 N. I. Hindawi, J. A. Zahra, M. M. El-Abadelah, B. A. Abu Thaher and K.-P. Zeller, *Monatsh. Chem.*, 2006, **137**, 1349–1355.

170 H. M. Dalloul, *ARKIVOC*, 2008, **14**, 243–241.

171 H. M. M. Dalloul, *Phosphorus. Sulfur. Silicon Relat. Elem.*, 2011, **186**, 1876–1884.

172 M. S. Mustafa, M. M. El-Abadelah, M. S. Mubarak, I. Chibueze, D. Shao and R. U. Agu, *Int. J. Chem.*, 2011, **3**, 89.

173    H. M. M. Dalloul, *Tetrahedron*, 2009, **65**, 8722–8726.

174    P. Sharma, S. V. Bhat, M. R. R. Prabhath, A. Molino, E. Nauha, D. J. D. Wilson and J. E. Moses, *Org. Lett.*, 2018, **20**, 4263–4266.

175    B. A. Thaher and H.-H. Otto, *Monatsh. Chem.,* 2002, **133**, 1011–1016.

176    J. A. Zahra, B. A. Abu Thaher, M. M. El-Abadelah and R. Boese, *Org. Biomol. Chem.*, 2003, **1**, 822–825.

177    J. A. Zahra, B. A. Thaher, M. M. El-Abadelah and H.-H. Otto, *Monatsh. Chem.*, 2005, **136**, 567–570.

178    J. A. Zahra, B. A. Abu Thaher, M. M. El-Abadelah and R. Boese, *Org. Biomol. Chem.*, 2005, **3**, 2599.

179    L. Bruché, L. Garanti and G. Zecchi, *J. Chem. Soc., Perkin Trans. 1*, 1981, 2245–2249.

180    L. Bruché, L. Garanti and G. Zecchi, *J. Chem. Soc., Perkin Trans. 1*, 1984, 2535–2539.

181    H. Meier and H. Heimgartner, *Helv. Chim. Acta*, 1985, **68**, 1283–1300.

182    S. Zhao, J. Dai, M. Hu, C. Liu, R. Meng, X. Liu, C. Wang and T. Luo, *Chem. Commun.*, 2016, **52**, 4702–4705.

183    A. Herner, J. Marjanovic, T. M. Lewandowski, V. Marin, M. Patterson, L. Miesbauer, D. Ready, J. Williams, A. Vasudevan and Q. Lin, *J. Am. Chem. Soc.*, 2016, **138**, 14609–14615.

184    C. Heiler, J. T. Offenloch, E. Blasco and C. Barner-Kowollik, *ACS Macro Lett.*, 2017, **6**, 56–61.

185    W. Konrad, C. Fengler, S. Putwa and C. Barner-Kowollik, *Angew. Chem. Int. Ed.*, 2019, **58**, 7133–7137.

186    E. M. Awad, N. M. Elwan, H. M. Hassaneen, A. Linden and H. Heimgartner, *Helv. Chim. Acta*, 2001, **84**, 1172–1180.

187    W.-S. Miao, F. Xiong, M.-X. Wang and Z.-T. Huang, *Synth. Commun.*, 2000, **30**, 3255–3265.

188    C. Altug, Y. Dürüst and M. C. Elliott, *Tetrahedron Lett.*, 2009, **50**, 7392–7394.

189    C. Altuğ, Y. Dürüst, M. C. Elliott, B. M. Kariuki, T. Rorstad and M. Zaal, *Org. Biomol. Chem.*, 2010, **8**, 4978.

190    A. H. M. Elwahy, A. F. Darweesh and M. R. Shaaban, *J. Heterocycl. Chem.*, 2012, **49**, 1120–1125.

191    D. J. P. Pinto, M. J. Orwat, S. Koch, K. A. Rossi, Richard S. Alexander, A. Smallwood, P. C. Wong, A. R. Rendina, J. M. Luettgen, R. M. Knabb, K. He, B. Xin, R. R. Wexler and P. Y. S. Lam, *J. Med. Chem.*, 2007, **50**, 5339–5356.

192    L. M. Oh, H. Wang, S. C. Shilcrat, R. E. Herrmann, D. B. Patience, P. G. Spoors and J. Sisko, *Org. Process Res. Dev.*, 2007, **11**, 1032–1042.

193    A. C. Donohue, S. Pallich and T. D. McCarthy, *J. Chem. Soc. Perkin Trans. 1*, 2001, **0**, 2817–2822.

194    H. M. E. Hassaneen, H. M. Hassaneen and M. H. Elnagdi, *Zeitschrift für Naturforsch. B*, 2004, **59**, 1132–1136.

195    G. Utecht, A. Fruziński and M. Jasiński, *Org. Biomol. Chem.*, 2018, **16**, 1252–1257.

196    D. Y. Curtin and N. E. Alexandrou, *Tetrahedron*, 1963, **19**, 1697–1703.

197    C. Wintner, *Tetrahedron Lett.*, 1970, **11**, 2275–2276.

198    J. H. Markgraf, S. H. Brown, M. W. Kaplinsky and R. G. Peterson, *J. Org. Chem.*, 1964, **29**, 2629–2632.

199    J. K. Stille and F. W. Harris, *J. Polym. Sci. Part B Polym. Lett.*, 1966, **4**, 333–336.

200    J. K. Stille and F. W. Harris, *J. Polym. Sci. Part A-1 Polym. Chem.*, 1968, **6**, 2317–2330.

201    M. V. George and C. S. Angadiyavar, *J. Org. Chem.*, 1971, **36**, 1589–1594.

202    R. R. Fraser, Gurudata and K. E. Haque, *J. Org. Chem.*, 1969, **34**, 4118–4120.

203    P. Scheiner and J. F. Dinda, *Tetrahedron*, 1970, **26**, 2619–2629.

204    S. Fischer and C. Wentrup, *J. Chem. Soc., Chem. Commun.*, 1980, 502–503.

205    S. Stewart, R. Harris and C. Jamieson, *Synlett*, 2014, **25**, 2480–2484.

206    G. Maier, J. Eckwert, A. Bothur, H. P. Reisenauer and C. Schmidt, *Liebigs Ann.*, 1996, 1041–1053.

207    D. Bégué, G. G. Qiao and C. Wentrup, *J. Am. Chem. Soc.*, 2012, **134**, 5339–5350.

208    A. Ismael, R. Fausto and M. L. S. Cristiano, *J. Org. Chem.*, 2016, **81**, 11656–11663.

209    P. Conti, S. J. di Ventimiglia, A. Pinto, L. Tamborini, F. S. Menniti, J. T. Lazzaro and

C. De Micheli, *Chem. Biodivers.*, 2008, **5**, 657–663.

210   J. A. Pfefferkorn, C. Choi, S. D. Larsen, B. Auerbach, R. Hutchings, W. Park, V. Askew, L. Dillon, J. C. Hanselman, Z. Lin, G. H. Lu, A. Robertson, C. Sekerke, M. S. Harris, A. Pavlovsky, G. Bainbridge, N. Caspers, M. Kowala and B. D. Tait, *J. Med. Chem.*, 2008, **51**, 31–45.

211   S. Manyem, M. P. Sibi, G. H. Lushington, B. Neuenswander, F. Schoenen and J. Aubé, *J. Comb. Chem.*, 2006, **9**, 20–28.

212   H. C. Kolb, M. G. Finn and K. B. Sharpless, *Angew. Chem. Int. Ed.*, 2001, **40**, 2004–2021.

213   R. K. V. Lim and Q. Lin, *Chem. Commun.*, 2010, **46**, 1589.

214   R. K. V Lim and Q. Lin, *Acc. Chem. Res.*, 2011, **44**, 828–39.

215   A. Herner and Q. Lin, *Top. Curr. Chem.*, 2016, **374**, 1.

216   W. Song, Y. Wang, J. Qu and Q. Lin, *J. Am. Chem. Soc.*, 2008, **130**, 9654–9655.

217   W. Song, Y. Wang, J. Qu, M. M. Madden and Q. Lin, *Angew. Chem. Int. Ed.*, 2008, **47**, 2832–2835.

218   J. Wang, W. Zhang, W. Song, Y. Wang, Z. Yu, J. Li, M. Wu, L. Wang, J. Zang and Q. Lin, *J. Am. Chem. Soc.*, 2010, **132**, 14812–14818.

219   Y.-J. Lee, B. Wu, J. E. Raymond, Y. Zeng, X. Fang, K. L. Wooley and W. R. Liu, *ACS Chem. Biol.*, 2013, **8**, 1664–1670.

220   Y. Wang and Q. Lin, *Org. Lett.*, 2009, **11**, 3570–3573.

221   P. An, T. Lewandowski, T. G. Erbay, P. Liu and Q. Lin, *J. Am. Chem. Soc.*, 2018, **140**, 4860–4868.

222   P. An and Q. Lin, *Org. Biomol. Chem.*, 2018, **16**, 5241–5244.

223   L. Zhang, X. Zhang, Z. Yao, S. Jiang, J. Deng, B. Li and Z. Yu, *J. Am. Chem. Soc.*, 2018, **140**, 7390–7394.

224   X. Zhang, X. Wu, S. Jiang, J. Gao, Z. Yao, J. Deng, L. Zhang and Z. Yu, *Chem. Commun.*, 2019, **55**, 7187–7190.

225   Y. Tian, M. P. Jacinto, Y. Zeng, Z. Yu, J. Qu, W. R. Liu and Q. Lin, *J. Am. Chem. Soc.*, 2017, **139**, 6078–6081.

226   Y. Tian and Q. Lin, *Chem. Commun.*, 2018, **54**, 4449–4452.

227    Z. Li, K. Cheng, J.-S. Lee, S. Q. Yao and K. Ding, *Angew. Chem. Int. Ed.*, 2017, **56**, 15044–15048.

228    Z. Yu, L. Y. Ho and Q. Lin, *J. Am. Chem. Soc.*, 2011, **133**, 11912–11915.

229    T. T. Zengeya, J. M. Garlick, R. A. Kulkarni, M. Miley, A. M. Roberts, Y. Yang, D. R. Crooks, C. Sourbier, W. M. Linehan and J. L. Meier, *J. Am. Chem. Soc.*, 2016, **138**, 15813–15816.

230    R. A. Kulkarni, C. A. Briney, D. R. Crooks, S. E. Bergholtz, C. Mushti, S. J. Lockett, A. N. Lane, T. W. -M. Fan, R. E. Swenson, W. Marston Linehan and J. L. Meier, *ChemBioChem*, 2019, **20**, 360–365.

231    P. An, T. M. Lewandowski and Q. Lin, *ChemBioChem*, 2018, **19**, 1326–1333.

232    Y. Iwakura, S. Shiraishi and M. Akiyama, *Die Makromol. Chemie*, 1966, **97**, 278–281.

233    J. K. Stille and L. D. Gotter, *J. Polym. Sci. Part B Polym. Lett.*, 1968, **6**, 11–14.

234    D. Estupiñán, T. Gegenhuber, J. P. Blinco, C. Barner-Kowollik and L. Barner, *ACS Macro Lett.*, 2017, **6**, 229–234.

235    J. K. Stille and L. D. Gotter, *Macromolecules*, 1969, **2**, 465–468.

236    J. O. Mueller, D. Voll, F. G. Schmidt, G. Delaittre and C. Barner-Kowollik, *Chem. Commun.*, 2014, **50**, 15681–15684.

237    C. J. Dürr, P. Lederhose, L. Hlalele, D. Abt, A. Kaiser, S. Brandau and C. Barner-Kowollik, *Macromolecules*, 2013, **46**, 5915–5923.

238    Hiltebrandt Kai; Pauloehrl Thomas; Blinco James P; Linkert Katharina; Borner Hans G; Barner-Kowollik Christopher, *Angew. Chem. Int. Ed.*, 2015, **54**, 2838–43.

239    A. Rudin, P. Choi, A. Rudin and P. Choi, *Free-Radical Polymerization*, Academic Press, Cambridge, 3rd edn., 2013.

240    J. K. Stille and L. D. Gotter, *Macromolecules*, 1969, **2**, 468–474.

241    J. K. Stille and A. T. Chen, *Macromolecules*, 1972, **5**, 377–384.

242    R. Darkow, M. Yoshikawa, T. Kitao, G. Tomaschewski and J. Schellenberg, *J. Polym. Sci. Part A Polym. Chem.*, 1994, **32**, 1657–1664.

243    R. Darkow, U. Hartmann and G. Tomaschewski, *React. Funct. Polym.*, 1997, **32**, 195–207.

244    J. O. Mueller, N. K. Guimard, K. K. Oehlenschlaeger, F. G. Schmidt and C. Barner-Kowollik, *Polym. Chem.*, 2014, **5**, 1447–1456.

245    A. Hufendiek, A. Carlmark, M. A. R. Meier and C. Barner-Kowollik, *ACS Macro Lett.*, 2016, **5**, 139–143.

246    D. Estupiñán, C. Barner-Kowollik and L. Barner, *Angew. Chem. Int. Ed.*, 2018, **57**, 5925–5929.

247    H.-P. M. de Hoog, M. Nallani and B. Liedberg, *Polym. Chem.*, 2012, **3**, 302–306.

248    M. Dietrich, G. Delaittre, J. P. Blinco, A. J. Inglis, M. Bruns and C. Barner-Kowollik, *Adv. Funct. Mater.*, 2012, **22**, 304–312.

249    S. F. M. van Dongen, H.-P. M. de Hoog, R. J. R. W. Peters, M. Nallani, R. J. M. Nolte and J. C. M. van Hest, *Chem. Rev.*, 2009, **109**, 6212–6274.

250    C. Rodriguez-Emmenegger, C. M. Preuss, B. Yameen, O. Pop-Georgievski, M. Bachmann, J. O. Mueller, M. Bruns, A. S. Goldmann, M. Bastmeyer and C. Barner-Kowollik, *Adv. Mater.*, 2013, **25**, 6123–6127.

251    B. Vonhören, O. Roling, C. Buten, M. Körsgen, H. F. Arlinghaus and B. J. Ravoo, *Langmuir*, 2016, **32**, 2277–2282.

252    C. Buten, S. Lamping, M. Körsgen, H. F. Arlinghaus, C. Jamieson and B. J. Ravoo, *Langmuir*, 2018, **34**, 2132–2138.

253    C. Wendeln and B. J. Ravoo, *Langmuir*, 2012, **28**, 5527–5538.

254    E. Blasco, M. Piñol, L. Oriol, B. V. K. J. Schmidt, A. Welle, V. Trouillet, M. Bruns and C. Barner-Kowollik, *Adv. Funct. Mater.*, 2013, **23**, 4011–4019.

255    D. Abt, B. V. K. J. Schmidt, O. Pop-Georgievski, A. S. Quick, D. Danilov, N. Y. Kostina, M. Bruns, W. Wenzel, M. Wegener, C. Rodriguez-Emmenegger and C. Barner-Kowollik, *Chem. Eur. J.*, 2015, **21**, 13186–13190.

256    L. Delafresnaye, N. Zaquen, R. P. Kuchel, J. P. Blinco, P. B. Zetterlund and C. Barner-Kowollik, *Adv. Funct. Mater.*, 2018, **28**, 1800342.

257    S. Ito, Y. Tanaka and A. Kakehi, *Bull. Chem. Soc. Jpn.*, 1976, **49**, 762–766.

258    S. Ito, Y. Tanaka, A. Kakehi and K. Kondo, *Bull. Chem. Soc. Jpn.*, 1976, **49**, 1920–1923.

259    M. Ramanathan, Y.-H. Wang and S.-T. Liu, *Org. Lett.*, 2015, **17**, 5886–5889.

260    A. Y. Fedorov and J.-P. Finet, *Tetrahedron Lett.*, 1999, **40**, 2747–2748.

261 I. P. Beletskaya, D. V. Davydov and M. S. Gorovoy, *Tetrahedron Lett.*, 2002, **43**, 6221–6223.

262 D. V. Davydov, I. P. Beletskaya, B. B. Semenov and Y. I. Smushkevich, *Tetrahedron Lett.*, 2002, **43**, 6217–6219.

263 T. Zhou and Z.-C. Chen, *J. Chem. Res.*, 2004, **2004**, 404–405.

264 Y. Li, L.-X. Gao and F.-S. Han, *Chem. Commun.*, 2012, **48**, 2719.

265 C.-Y. Liu, Y. Li, J.-Y. Ding, D.-W. Dong and F.-S. Han, *Chem. Eur. J.*, 2014, **20**, 2373–81.

266 T. Onaka, H. Umemoto, Y. Miki, A. Nakamura and T. Maegawa, *J. Org. Chem.*, 2014, **79**, 6703–6707.

267 CN 106749067, 2017, 1–7.

268 J. Roh, K. Vávrová and A. Hrabálek, *European J. Org. Chem.*, 2012, **2012**, 6101–6118.

269 S. Wiedemann, M. Bio, L. Brown, K. Hansen and N. Langille, *Synlett*, 2012, **23**, 2231–2236.

270 K. Y. Yi and S. Yoo, *Tetrahedron Lett.*, 1995, **36**, 1679–1682.

271 R. Patouret and T. M. Kamenecka, *Tetrahedron Lett.*, 2016, **57**, 1597–1599.

272 P. S. Campbell, C. Jamieson, I. Simpson and A. J. B. Watson, *Chem. Commun.*, 2018, **54**, 46–49.

273 T. Jin, S. Kamijo and Y. Yamamoto, *Tetrahedron Lett.*, 2004, **45**, 9435–9437.

274 K. Y. Yi and S. Yoo, *Tetrahedron Lett.*, 1995, **36**, 1679–1682.

275 N. C. Bruno, M. T. Tudge and S. L. Buchwald, *Chem. Sci.*, 2013, **4**, 916–920.

276 C. Amatore, A. Jutand and A. Thuilliez, *Organometallics*, 2001, **20**, 3241–3249.

277 A. J. J. Lennox and G. C. Lloyd-Jones, *Chem. Soc. Rev.*, 2014, 43, 412–443.

278 S. F. Rach and F. E. Kuhn, *Chem. Rev.*, 2009, **109**, 2061–2080.

279 C. Hansch, A. Leo and R. W. Taft, *Chem. Rev.*, 1991, **91**, 165–195.

280 D. S. Surry and S. L. Buchwald, *Chem. Sci.*, 2011, **2**, 27–50.

281 B. T. Ingoglia, C. C. Wagen and S. L. Buchwald, *Tetrahedron*, 2019, **75**, 4199–4211.

282 R. Carlson, *Design and optimization in organic synthesis*, Elsevier, 1992.

283  P. M. Murray, F. Bellany, L. Benhamou, D.-K. Bučar, A. B. Tabor and T. D. Sheppard, *Org. Biomol. Chem.*, 2016, **14**, 2373–2384.

284  M. Seki, *Synthesis*, 2014, **46**, 3249–3255.

285  J. C. Chaston and E. J. Sercombe, *Platin. Met. Rev.*, 1961, **5**, 122.

286  S. Nishimura, *Handbook of Heterogeneous Catalytic Hydrogenation for Organic Synthesis. Wiley-VCH:*, 2001, vol. 5.

287  H. Ji, Q. Jing, J. Huang and R. B. Silverman, *Tetrahedron*, 2012, **68**, 1359–1366.

288  G. Noonan and A. G. Leach, *Org. Biomol. Chem.*, 2015, **13**, 2555–2560.

289  S. D. Friis, A. T. Lindhardt and T. Skrydstrup, *Acc. Chem. Res.*, 2016, **49**, 594–605.

290  A. B. Pinkerton, J.-M. Vernier, H. Schaffhauser, B. A. Rowe, U. C. Campbell, D. E. Rodriguez, D. S. Lorrain, C. S. Baccei, L. P. Daggett and L. J. Bristow, *J. Med. Chem.*, 2004, **47**, 4595–4599.

291  J. V. Duncia, P. B. M. W. M. Timmermans, A. T. Chiu, D. J. Carini, G. B. Gregory, A. L. Johnson, W. A. Price, G. J. Wells, P. C. Wong and J. C. Calabrese, *J. Med. Chem.*, 1990, **33**, 1312–1329.

292  N. A. Petasis and I. Akritopoulou, *Tetrahedron Lett.*, 1993, **34**, 583–586.

293  N. R. Candeias, F. Montalbano, P. M. S. D. Cal and P. M. P. Gois, *Chem. Rev.*, 2010, **110**, 6169–6193.

294  P. Wu, M. Givskov and T. E. Nielsen, *Chem. Rev.*, 2019, **119**, 11245–11290.

295  F. F. Blicke in *Organic Reactions*, John Wiley & Sons, Inc., Hoboken, NJ, USA, 2011, pp. 303–341.

296  N. A. Petasis and I. A. Zavialov, *J. Am. Chem. Soc.*, 1997, **119**, 445–446.

297  N. A. Petasis, A. Goodman and I. A. Zavialov, *Tetrahedron*, 1997, **53**, 16463–16470.

298  S. R. Klopfenstein, J. J. Chen, A. Golebiowski, M. Li, S. X. Peng and X. Shao, *Tetrahedron Lett.*, 2000, **41**, 4835–4839.

299  R. Y. Souza, G. A. Bataglion, D. A. C. Ferreira, C. C. Gatto, M. N. Eberlin and B. A. D. Neto, *RSC Adv.*, 2015, **5**, 76337–76341.

300  N. J. McLean, H. Tye and M. Whittaker, *Tetrahedron Lett.*, 2004, **45**, 993–995.

301  N. A. Petasis and S. Boral, *Tetrahedron Lett.*, 2001, **42**, 539–542.

302    C. W. G. Au and S. G. Pyne, *J. Org. Chem.*, 2006, **71**, 7097–7099.

303    G. K. S. Prakash, M. Mandal, S. Schweizer, N. A. Petasis and G. A. Olah, *Org. Lett.*, 2000, **2**, 3173–3176.

304    A. Mieczkowski, W. Koźmiński and J. Jurczak, *Synthesis*, 2010, **2010**, 221–232.

305    M. Follmann, F. Graul, T. Schäfer, S. Kopec and P. Hamley, *Synlett*, 2005, **2005**, 1009–1011.

306    M. Shevchuk, A. Sorochinsky, V. Khilya, V. Romanenko and V. Kukhar, *Synlett*, 2010, **2010**, 73–76.

307    N. R. Candeias, L. F. Veiros, C. A. M. Afonso and P. M. P. Gois, *Eur. J. Org. Chem.*, 2009, **2009**, 1859–1863.

308    N. R. Candeias, P. M. S. D. Cal, V. André, M. T. Duarte, L. F. Veiros and P. M. P. Gois, *Tetrahedron*, 2010, **66**, 2736–2745.

309    T. J. Southwood, M. C. Curry and C. A. Hutton, *Tetrahedron*, 2006, **62**, 236–242.

310    T. Koolmeister, M. Södergren and M. Scobie, *Tetrahedron Lett.*, 2002, **43**, 5965–5968.

311    H. Jourdan, G. Gouhier, L. Van Hijfte, P. Angibaud and S. R. Piettre, *Tetrahedron Lett.*, 2005, **46**, 8027–8031.

312    S. Stas and K. A. Tehrani, *Tetrahedron*, 2007, **63**, 8921–8931.

313    G. W. Kabalka, B. Venkataiah and G. Dong, *Tetrahedron Lett.*, 2004, **45**, 729–731.

314    J.-P. Tremblay-Morin, S. Raeppel and F. Gaudette, *Tetrahedron Lett.*, 2004, **45**, 3471–3474.

315    J. Tao and S. Li, *Chin. J. Chem.*, 2010, **28**, 41–49.

316    N. Schlienger, M. R. Bryce and T. K. Hansen, *Tetrahedron*, 2000, **56**, 10023–10030.

317    N. A. Petasis and S. Boral, *Tetrahedron Lett.*, 2001, **42**, 539–542.

318    A. S. Voisin, A. Bouillon, J.-C. Lancelot, A. Lesnard, H. Oulyadi and S. Rault, *Tetrahedron Lett.*, 2006, **47**, 2165–2169.

319    J. Kalia and R. T. Raines, *Angew. Chem. Int. Ed.*, 2008, **47**, 7523–6.

320    S. Kanta De, *Synth. Commun.*, 2004, **34**, 4409–4415.

321    J. Takagi, K. Takahashi, T. Ishiyama and N. Miyaura, *J. Am. Chem. Soc.*, 2002, **124**,

8001–8006.

322    G. Berionni, B. Maji, P. Knochel and H. Mayr, *Chem. Sci.*, 2012, **3**, 878–882.

323    P. An, Z. Yu and Q. Lin, *Org. Lett.*, 2013, **15**, 5496–5499.

324    M. B. Plutschack, B. Pieber, K. Gilmore and P. H. Seeberger, *Chem. Rev.*, 2017, 117, 11796–11893.

325    F. M. Akwi and P. Watts, *Chem. Commun.*, 2018, **54**, 13894–13928.

326    J. C. Robertson, M. L. Coote and A. C. Bissember, *Nat. Rev. Chem.*, 2019, 3, 290–304.

327    F. Politano and G. Oksdath-Mansilla, *Org. Process Res. Dev.*, 2018, **22**, 1045–1062.

328    L. P. H. Yang and G. M. Keating, *Am. J. Cardiovasc. Drugs*, 2009, **9**, 401–409.

329    B. Staels, J. Dallongeville, J. Auwerx, K. Schoonjans, E. Leitersdorf and J. C. Fruchart, *Circulation*, 1998, **98**, 2088–93.

330    R. Vardanyan and V. Hruby in *Synthesis of Best-Seller Drugs*, Elsevier, 2016, pp. 419–458.

331    European Patent Office, EP0002151, 1979, 3–5.

332    European Patent Office, FR2342723, 1977, 12–13.

333    European Patent Office, EP0245156 (A1), 1987, 4–6.

334    D. G. Hall and B. Akgun, *Angew. Chem. Int. Ed.*, 2018, **57**, 13028–13044.

335    J. Hughes, T. W. Smith, H. W. Kosterlitz, L. A. Fothergill, B. A. Morgan and H. R. Morris, *Nature*, 1975, **258**, 577–579.

336    M. Noda, Y. Teranishi, H. Takahashi, M. Toyosato, M. Notake, S. Nakanishi and S. Numa, *Nature*, 1982, **297**, 431–434.

337    R. B. Merrifield, *J. Am. Chem. Soc.*, 1963, **85**, 2149–2154.

338    S.-S. Wang, *J. Am. Chem. Soc.*, 1973, **95**, 1328–1333.

339    F. Albericio, N. Kneib-Cordonier, S. Biancalana, L. Gera, R. I. Masada, D. Hudson and G. Barany, *J. Org. Chem.*, 1990, **55**, 3730–3743.

340    S. E. Mancebo and S. Q. Wang, *Rev. Environ. Health*, 2014, **29**, 265–273.

341    L. Bruché and G. Zecchi, *Tetrahedron*, 1989, **45**, 7427–7432.

342    G. Broggini, L. Garanti, G. Molteni and G. Zecchi, *J. Chem. Soc. Perkin Trans. 1*,

1998, 4103–4106.

343   J. F. J. Dippy, S. R. C. Hughes and A. Rozanski, *J. Chem. Soc.*, 1959, 2492.

344   F. G. Bordwell and D. Algrim, *J. Org. Chem.*, 1976, **41**, 2507–2508.

345   F. G. Bordwell, *Acc. Chem. Res.*, 1988, **21**, 456–463.

346   E. A. Braude and F. C. Nachod, *Determination of organic structures by physical methods.*, Academic Press, 1955.

347   H. K. Hall, *J. Am. Chem. Soc.*, 1957, **79**, 5441–5444.

348   K. Clarke and K. Rothwell, *J. Chem. Soc.*, 1960, 1885.

349   R. L. Benoit, D. Lefebvre and M. Fréchette, *Can. J. Chem.*, 1987, **65**, 996–1001.

350   J. Meier and G. Schwarzenbach, *Helv. Chim. Acta*, 1957, **40**, 907–917.

351   I. M. Kolthoff, M. K. Chantooni and S. Bhowmik, *J. Am. Chem. Soc.*, 1968, **90**, 23–28.

352   J. A. Riddick, W. B. Bunger and T. K. Sakano, *Organic solvents: physical properties and methods of purification. Fourth edition*, John Wiley and Sons, New York, 1986.

353   K. Kaupmees, A. Trummal and I. Leito, *Croat. Chem. Acta*, 2014, **87**, 385–395.

354   W. D. Kumler and J. J. Eiler, *J. Am. Chem. Soc.*, 1943, **65**, 2355–2361.

355   W. N. Olmstead, Z. Margolin and F. G. Bordwell, *J. Org. Chem.*, 1980, **45**, 3295–3299.

356   G. Dijkstra, W. H. Kruizinga and R. M. Kellogg, *J. Org. Chem.*, 1987, **52**, 4230–4234.

357   P. Scharlin, *Acta Chem. Scand.*, 1986, **40A**, 207–209.

358   M. A. Martínez-Aguirre, R. Villamil-Ramos, J. A. Guerrero-Alvarez and A. K. Yatsimirsky, *J. Org. Chem.*, 2013, **78**, 4674–4684.

359   W. R. Bamford and T. S. Stevens, *J. Chem. Soc.*, 1952, 4735.

360   R. H. Shapiro and M. J. Heath, *J. Am. Chem. Soc.*, 1967, **89**, 5734–5735.

361   Y. Xia and J. Wang, *Chem. Soc. Rev.*, 2017, 46, 2306–2362.

362   K. Livingstone and C. Jamieson, *unpublished results*.

363   I. Aprahamian, *Chem. Commun.*, 2017, **53**, 6674–6684.

364    S. D. Sharma and S. B. Pandhi, *J. Org. Chem.*, 1990, **55**, 2196–2200.

365    K. F. Kong, L. Schneper and K. Mathee, *APMIS*, 2010, 118, 1–36.

366    J. Hu, H. Xu, P. Nie, X. Xie, Z. Nie and Y. Rao, *Chem. Eur. J.*, 2014, **20**, 3932–3938.

367    E. Fischer and F. Jourdan, *Berichte der Dtsch. Chem. Gesellschaft*, 1883, **16**, 2241–2245.

368    W. Wu, X.-H. Fan, L.-P. Zhang and L.-M. Yang, *RSC Adv.*, 2014, **4**, 3364–3367.

369    S. Kanta De, *Synth. Commun.*, 2004, **34**, 4409–4415.

370    M. Larance and A. I. Lamond, *Nat. Rev. Mol. Cell Biol.*, 2015, **16**, 269–280.

371    J. Atzrodt, V. Derdau, W. J. Kerr and M. Reid, *Angew. Chem. Int. Ed.*, 2018, **57**, 3022–3047.

372    W. J. Kerr, M. Reid and T. Tuttle, *Angew. Chem. Int. Ed.*, 2017, **56**, 7808–7812.

373    L. I. Belenkii, in *Nitrile Oxides, Nitrones, and Nitronates in Organic Synthesis*, ed. H. Feuer, John Wiley & Sons, Inc., Hoboken, NJ, USA, 2nd edn., 2007, pp. 1–127.

374    M. Christl and R. Huisgen, *Chem. Ber.*, 1973, **106**, 3345–3367.

375    D. K. Mandal, in *Pericyclic Chemistry*, Elsevier, Amsterdam, 2018, pp. 107–190.

376    C. Grundmann and J. M. Dean, *J. Org. Chem.*, 1965, **30**, 2809–2812.

377    M. M. Krayushkin, A. A. Loktionov and L. I. Belenkii, *Chem. Heterocycl. Compd.*, 1988, **24**, 850–856.

378    R. Réau, G. Veneziani, F. Dahan and G. Bertrand, *Angew. Chem. Int. Ed. Engl.*, 1992, **31**, 439–440.

379    M. Tóth, S. Kun, É. Bokor, M. Benltifa, G. Tallec, S. Vidal, T. Docsa, P. Gergely, L. Somsák and J.-P. Praly, *Bioorg. Med. Chem.*, 2009, **17**, 4773–4785.

380    A. Dondoni and P. P. Giovannini, *Synthesis*, 2002, **2002**, 1701–1706.

381    B. H. Kim, Y. J. Chung, G. Keum, J. Kim and K. Kim, *Tetrahedron Lett.*, 1992, **33**, 6811–6814.

382    A. G. Tyrkov and E. A. Yurtaeva, *Russ. J. Org. Chem.*, 2019, **55**, 978–982.

383    S. Mohammed, R. A. Vishwakarma and S. B. Bharate, *RSC Adv.*, 2015, **5**, 3470–3473.

384    Y. J. Shang and Y. G. Wang, *Synthesis*, 2002, **2002**, 1663–1668.

385    K. M. Lokanatha Rai, N. Linganna, A. Hassner and C. Anjanamurthy, *Org. Prep. Proced. Int.*, 1992, **24**, 91–93.

386    A. S. Radhakrishna, K. Sivaprakash and B. B. Singh, *Synth. Commun.*, 1991, **21**, 1625–1629.

387    T. Mukaiyama and T. Hoshino, *J. Am. Chem. Soc.*, 1960, **82**, 5339–5342.

388    Z. Gombos, J. Nyitrai, P. Kolonits and M. Kajtár-Peredy, *J. Chem. Soc. Perkin Trans. 1*, 1989, 1915–1921.

389    Y. Basel and A. Hassner, *Synthesis*, 1997, **1997**, 309–312.

390    M. Brasholz, S. Saubern and G. P. Savage, *Aust. J. Chem.*, 2011, **64**, 1397.

391    S. Chandrasekhar, A. Raza, M. Venkat Reddy and J. S. Yadav, *J. Comb. Chem.*, 2002, **4**, 652–655.

392    D. K. Mandal, in *Pericyclic Chemistry*, Elsevier, 2018, pp. 107–190.

393    R. P. Litvinovskaya and V. A. Khripach, *Usp. Khim.*, 2001, **70**, 483–485.

394    W. M. Gołębiewski and M. Gucma, *J. Heterocycl. Chem.*, 2006, **43**, 509–513.

395    K. Bast, M. Christ, R. Huisgen, W. Mack and R. Sustmann, *Chem. Ber.*, 1973, **106**, 3258–3274.

396    B. Iddon, H. Suschitzky, A. W. Thompson, B. J. Wakefield and D. J. Wright, *J. Chem. Res.*, 1978, 2038.

397    F. Heaney, *European J. Org. Chem.*, 2012, 3043–3058.

398    M. Blanc-Muesse, H. Driguez, B. Joseph, M. C. Viaud and P. Rollin, *Tetrahedron Lett.*, 1990, **31**, 3867–3868.

399    K. W. J. Baker, K. S. Horner, S. A. Moggach, R. M. Paton and I. A. S. Smellie, *Tetrahedron Lett.*, 2004, **45**, 8913–8916.

400    K. J. Dignam, A. F. Hegarty and P. L. Quain, *J. Chem. Soc. Perkin Trans. 2*, 1977, 1457–1462.

401    K. J. Dignam, A. F. Hegarty and P. L. Quain, *J. Org. Chem.*, 1978, **43**, 388–393.

402    J. N. Kim, H. R. Kim and E. K. Ryu, *Tetrahedron Lett.*, 1993, **34**, 5117–5120.

403    T. L. Gilchrist and A. Lemos, *J. Chem. Soc. Perkin Trans. 1*, 1993, 1391–1396.

404    S. Auricchio, A. Bini, E. Pastormerlo, A. Ricca and A. M. Truscello, *Tetrahedron*,

1994, **50**, 7589–7596.

405    J. N. Kim and E. K. Ryu, *Tetrahedron Lett.*, 1993, **34**, 3567–3570.

406    R. M. Paton, in *Comprehensive Heterocyclic Chemistry*, Elsevier Inc., 1984, vol. 6–7, pp. 393–426.

407    G. Bianchi, C. De Micheli and R. Gandolfi, *The chemistry of double-bonded functional groups*, Wiley, London, 1977.

408    F. De Sarlo, *J. Chem. Soc. Perkin Trans. 1*, 1974, 1951.

409    W. M. Haynes, *CRC Handbook of Chemistry and Physics*, CRC Press LLC, Boca Raton, 94th edn., 2013.

410    X. Su and I. Aprahamian, *Chem. Soc. Rev.*, 2014, 43, 1963–1981.

411    W. Siti, A. K. Khan, H.-P. M. de Hoog, B. Liedberg and M. Nallani, *Org. Biomol. Chem.*, 2015, **13**, 3202–3206.

412    Z. Yu, Y. Pan, Z. Wang, J. Wang and Q. Lin, *Angew. Chem. Int. Ed.*, 2012, **51**, 10600–10604.

413    P. Leihkauf, V. Lohse, C. Csongar and G. Tomaschewski, *J. für Prakt. Chemie*, 1989, **331**, 789–798.

414    A. Michael, *J. für Prakt. Chemie*, 1887, **35**, 349–356.

415    M. Aslam and A. Dent, *Bioconjugation : protein coupling techniques for the biomedical sciences*, Macmillan Reference, London, 1998.

416    M. Z. C. Hatit, J. C. Sadler, L. A. McLean, B. C. Whitehurst, C. P. Seath, L. D. Humphreys, R. J. Young, A. J. B. Watson and G. A. Burley, *Org. Lett.*, 2016, **18**, 1694–1697.

417    C. P. Seath, G. A. Burley and A. J. B. Watson, *Angew. Chem. Int. Ed.*, 2017, **56**, 3314–3318.

418    G. M. Sheldrick, *Acta Crystallogr. A*, 2015, **71**, 3–8.

419    Z. Guo, H. Jia, H. Liu, Q. Wang, J. Huang and H. Guo, *Org. Lett.*, 2018, **20**, 2939–2943.

420    M. Tóth, S. Kun, É. Bokor, M. Benltifa, G. Tallec, S. Vidal, T. Docsa, P. Gergely, L. Somsák and J. P. Praly, *Bioorg. Med. Chem.*, 2009, **17**, 4773–4785.

421    W. K. C. Park, M. Auer, H. Jaksche and C. H. Wong, *J. Am. Chem. Soc.*, 1996, **118**,

10150–10155.

422    M. Suchý, A. A. H. Elmehriki and R. H. E. Hudson, *Org. Lett.*, 2011, **13**, 3952–3955.

423    I. Dias-Jurberg, F. Gagosz and S. Z. Zard, *Org. Lett.*, 2010, **12**, 416–419.

424    WO2015001024A1, 2014.

425    A. Khalafi-Nezhad and S. Mohammadi, *RSC Adv.*, 2013, **3**, 4362.

426    M. Begtrup, P. Larsen and U. Edlund, *Acta Chem. Scand.*, 1990, **44**, 1050–1057.

427    S. Wiedemann, M. Bio, L. Brown, K. Hansen and N. Langille, *Synlett*, 2012, **23**, 2231–2236.

428    G. Aridoss and K. K. Laali, *European J. Org. Chem.*, 2011, **2011**, 6343–6355.

429    A. Vignesh, N. S. P. Bhuvanesh and N. Dharmaraj, *J. Org. Chem.*, 2017, **82**, 887–892.

430    R. Ranjan Chakraborty and P. Ghosh, *Tetrahedron Lett.*, 2018, **59**, 3616–3619.

431    M.-S. Xie, X. Cheng, Y.-G. Chen, X.-X. Wu, G.-R. Qu and H.-M. Guo, *Org. Biomol. Chem.*, 2018, **16**, 6890–6894.

432    S. S. Bag, S. Talukdar and S. J. Anjali, *Bioorg. Med. Chem. Lett.*, 2016, **26**, 2044–2050.

433    K. Ishihara, M. Kawashima, T. Shioiri and M. Matsugi, *Synlett*, 2016, **27**, 2225–2228.

434    Y. Li, L.-X. Gao and F.-S. Han, *Chem. Commun.*, 2012, **48**, 2719–21.

435    X. Shang, R. Lai, X. Song, H. Li, W. Niu and J. Guo, *Bioconjug. Chem.*, 2017, **28**, 2859–2864.

436    T. Onaka, H. Umemoto, Y. Miki, A. Nakamura and T. Maegawa, *J. Org. Chem.*, 2014, **79**, 6703–6707.

437    B. Török, A. Sood, S. Bag, R. Tulsan, S. Ghosh, D. Borkin, A. R. Kennedy, M. Melanson, R. Madden, W. Zhou, H. LeVine and M. Török, *Biochemistry*, 2013, **52**, 1137–1148.

438    G. Wang, X. Liu, T. Huang, Y. Kuang, L. Lin and X. Feng, *Org. Lett.*, 2013, **15**, 76–79.

439    X. Deng and N. S. Mani, *J. Org. Chem.*, 2008, **73**, 2412–2415.

440   M. J. Kornet, T. T. Tita and A. P. Thio, *Synth. Commun.*, 1986, **16**, 1261–1274.

441   C. Peifer, M. Abadleh, J. Bischof, D. Hauser, V. Schattel, H. Hirner, U. Knippschild and S. Laufer, *J. Med. Chem.*, 2009, **52**, 7618–7630.

442   A. V. Dubrovskiy and R. C. Larock, *Org. Lett.*, 2010, **12**, 1180–1183.

443   R. Fusco and F. Sannicolo, *J. Org. Chem.*, 1981, **46**, 83–89.

444   K. O. Jeon, J. H. Jun, J. S. Yu and C. K. Lee, *J. Heterocycl. Chem.*, 2003, **40**, 763–771.

445   W. Wei, Z. Wang, X. Yang, W. Yu and J. Chang, *Adv. Synth. Catal.*, 2017, **359**, 3378–3387.

446   C. Mauger and G. Mignani, *Synth. Commun.*, 2006, **36**, 1123–1129.

447   T. Zhang and W. Bao, *J. Org. Chem.*, 2013, **78**, 1317–1322.

448   J. Yu, J. W. Lim, S. Y. Kim, J. Kim and J. N. Kim, *Tetrahedron Lett.*, 2015, **56**, 1432–1436.

449   C. Wang, L. Huang, F. Wang and G. Zou, *Tetrahedron Lett.*, 2018, **59**, 2299–2301.

450   H. Li, Y. Xu, E. Shi, W. Wei, X. Suo and X. Wan, *Chem. Commun.*, 2011, **47**, 7880.

451   G. K. S. Prakash, C. Panja, T. Mathew and G. A. Olah, *Catal. Letters*, 2007, **114**, 24–29.

452   M. G. B. Drew and G. R. Willey, *J. Chem. Soc., Perkin Trans. 2*, 1986, 215–220.

453   W. Wang, T. Zhang, L. Duan, X. Zhang and M. Yan, *Tetrahedron*, 2015, **71**, 9073–9080.

454   K. Škoch, I. Císařová and P. Štěpnička, *Organometallics*, 2016, **35**, 3378–3387.

455   S. D. Sharma and S. B. Pandhi, *J. Org. Chem.*, 1990, **55**, 2196–2200.

456   J. Hu, H. Xu, P. Nie, X. Xie, Z. Nie and Y. Rao, *Chem. Eur. J.*, 2014, **20**, 3932–3938.

457   W. Wu, X. H. Fan, L. P. Zhang and L. M. Yang, *RSC Adv.*, 2014, **4**, 3364–3367.

458   W. J. Kerr, D. M. Lindsay, P. K. Owens, M. Reid, T. Tuttle and S. Campos, *ACS Catal.*, 2017, **7**, 7182–7186.

459   W. Zhang, S. Yang, Q. Lin, H. Cheng and J. Liu, *J. Org. Chem.*, 2019, **84**, 851–859.

460   A. Sasse, H. Stark, X. Ligneau, S. Elz, S. Reidemeister, C. R. Ganellin, J. C. Schwartz and W. Schunack, *Bioorg. Med. Chem.*, 2000, **8**, 1139–1149.

461     US Patent Office, US9776968B2, 2016.

462     B. Schmidt, N. Elizarov, N. Riemer and F. Hölter, *Eur. J. Org. Chem.*, 2015, **2015**, 5826–5841.

463     Graphpad, 2018.